Catalytic enantioselective synthesis of O- and N-substituted quaternary carbon stereogenic centers : 1. AL-catalyzed alkylations of α-ketoesters with dialkylzinc reagents. 2. AG-catalyzed vinylogous Mannich-type reactions of α-ketoimine esters with siloxyfurans

Author: Laura Caroline Wieland

Boston College
The Graduate School of Arts and Sciences
Department of Chemistry

CATALYTIC ENANTIOSELECTIVE SYNTHESIS OF *O*- AND *N*-SUBSTITUTED QUATERNARY CARBON STEREOGENIC CENTERS: 1. AL-CATALYZED ALKYLATIONS OF α-KETOESTERS WITH DIALKYLZINC REAGENTS. 2. AG-CATALYZED VINYLOGOUS MANNICH-TYPE REACTIONS OF α-KETOIMINE ESTERS WITH SILOXYFURANS.

A dissertation

by

LAURA CAROLINE WIELAND

submitted in partial fulfillment of the requirements
for the degree of
Doctor of Philosophy
August 2008

Acknowledgements

I feel privileged to have completed my graduate studies in the chemistry department of Boston College. I have found this to be an incredibly open group of people, and have benefited from many helpful conversations with graduate students, post-docs, and professors throughout the department.

I would especially like to thank professor Amir Hoveyda, my thesis advisor and mentor, for his undying enthusiasm and support of all of the work going on in his group. He is an inspiring teacher and advisor, and I hope to benefit from his example throughout my career. When I joined the Hoveyda group, I was given the opportunity to work on a project which was started by Dr. Hongbo Deng. Hongbo, along with Dr. Kerry Benenato (Murphy) Dr. Alex Hird, and Dr. Laura Akullian patiently taught me the nuances of working with dialkylzinc reagents, and their guidance was critical in my development as a scientist. As my time in the group progressed, I had the pleasure of working alongside many incredibly talented graduate students and post-docs in the Hoveyda group, and I thank every single one of them. I was lucky enough to work directly with Ms. Erika Vieira on my second project, and I'd like to especially thank her for her tireless efforts in elucidating catalyst structure, and for her willingness to 'just do it again' whenever necessary.

I would like to thank the members of the peptide project, and especially 'team Mannich,' Nate, Emma, Hiroki, Peng, Drew, Dan and Erika, for their helpful discussions and experimental assistance throughout my time at BC. As a member of the peptide group, I had the benefit of regular meetings with Professor Marc Snapper and several members of the Snapper group, and I am indebted to them for their countless invaluable suggestions.

The following document was proofread by Dr. Pamela Lombardi, Ms. Erika Vieira, and Mr. Kevin Brown in the Hoveyda group, and by my dissertation committee; professors

Amir Hoveyda, Marc Snapper, and Jason Kingsbury. I truly appreciate the time they invested on the improvement of this document.

I am grateful to Ms. Kyoko Mandai, Mr. Steven Malcolmson, Dr. Richard Staples, and Dr. Peter Muller for their assistance in securing X-ray crystal structures. This certainly could not have been accomplished without their expertise.

Finally, I would like to thank my family and friends for their continuing support throughout my graduate career. While they did not contribute directly to the creation of this document, they have enhanced my quality of life through long runs, bike rides, coffee walks, nights out, happy hours, and dance parties in the lab. My parents, Jeanne and Paul, have encouraged my scientific endeavors from an early age, and have been incredibly supportive throughout my entire life. My grandma, Viola, opened her door to me (and many of my friends) at a moment's notice for much-needed 36 hour retreats in New Hampshire. My brother, Mark, has always been my role model and, along with his wife Carrie and their son Ben, continues to inspire me in all aspects of life. I have been blessed with wonderful friends, both within the Hoveyda group and outside of it, and I thank all of them for making my time thus far in Boston unforgettable. I especially would like to thank my classmate, Kevin Brown, for always being the person that I consulted first whenever I had a new project idea, and for simply being there for me in every way possible over the past six years. He is an amazing scientist and friend, and I look forward to watching his career progress.

In loving memory of Arnold Torkelson, Ph.D.

CATALYTIC ENANTIOSELECTIVE SYNTHESIS OF *O*- AND *N*-SUBSTITUTED QUATERNARY CARBON STEREOGENIC CENTERS: 1. AL-CATALYZED ALKYLATIONS OF α-KETOESTERS WITH DIALKYLZINC REAGENTS. 2. AG-CATALYZED VINYLOGOUS MANNICH-TYPE REACTIONS OF α-KETOIMINE ESTERS WITH SILOXYFURANS.

Laura Caroline Wieland

Thesis Advisor: Professor Amir H. Hoveyda

Abstract

Chapter 1: We disclose an Al-catalyzed enantioselective method for additions of Me_2Zn and Et_2Zn to α-ketoesters bearing aromatic alkenyl, and alkyl substituents. These transformations are promoted in the presence of a readily available amino acid-based ligand, and afforded the desired products in excellent yields and in up to 95% ee. In addition, we discovered a remarkable enhancement of efficiency and selectivity in the presence of an achiral phosphoramidate additive.

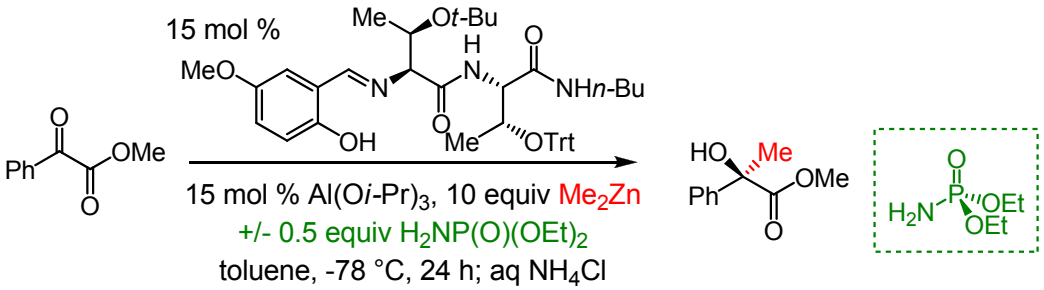

without additive: 92% conv, 67% ee

with 50 mol % $H_2NP(O)(OEt)_2$: 97% yield, 95% ee

Chapter 2: An efficient diastereo- and enantioselective Ag-catalyzed method for additions of a commercially available siloxyfuran to α-ketoimine esters is disclosed. Catalytic transformations require an inexpensive metal salt (AgOAc) and an air stable chiral ligand that is readily prepared in three steps from commercially available materials in 42% overall yield. Aryl- as well as heterocyclic substituted ketoimines can be used effectively in the Ag-catalyzed process. Additionally, two examples regarding reactions of alkyl-substituted ketoimines are presented. An electronically modified N-aryl group is introduced that is responsible for high reaction efficiency (>98% conversion, 72–95% yields after purification), diastereo- (up to >98:2 dr) and enantioselectivity (up to 97:3 er or 94% ee). The new N-aryl unit is also crucial for conversion of the asymmetric vinylogous Mannich products to the unprotected amines in high yields. Spectroscopic and X-ray data are among the physical evidence provided that shed light on the identity of the Ag-based chiral catalysts and some of the mechanistic subtleties of this class of enantioselective C–C bond forming processes.

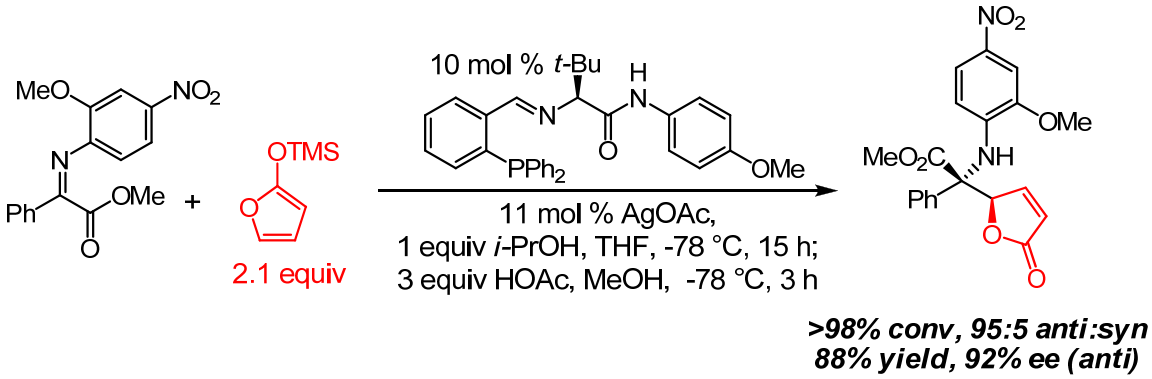

>98% conv, 95:5 anti:syn
88% yield, 92% ee (anti)

Table of Contents

Chapter 1. **Al-Catalyzed Enantioselective Alkylations of α-Ketoesters with Dialkylzinc Reagents**[1]

1.1 *Introduction and background*

Catalytic, asymmetric additions of alkylmetal reagents to aldehydes to form secondary alcohols have been well studied.[2] However, the related catalytic alkylations of ketones leading to the formation of tertiary alcohols[3] remain significantly less developed, despite the prevalence of tertiary alcohols in natural products and medicinally relevant compounds (examples shown in Figure 1.1). Ketones represent a much more challenging substrate class than aldehydes, as they are less reactive than aldehydes, and steric differentiation around the prochiral carbon becomes more difficult when there is not a proton substituent. One approach to overcoming the lower reactivity of ketones relative to aldehydes[4] is the study of activated ketones, such as α-ketoesters. The alkylation products of this type of substrate have a highly functionalizable ester group α- to the newly formed chiral tertiary alcohol.

---

(1) "Al-Catalyzed Enantioselective Alkylation of α-Ketoesters by Dialkylzinc Reagents. Enhancement of Enantioselectivity and Reactivity by an Achiral Lewis Base Additive," Wieland, L. C.; Deng, H.; Snapper, M. L.; Hoveyda, A. H. *J. Am. Chem. Soc.* **2005**, *127*, 15453-15456.

(2) For a review on asymmetric organozinc additions to carbonyls, see: "Catalytic Asymmetric Organozinc Additions to Carbonyl Compounds," Pu, L.; Yu, H. -B. *Chem. Rev.* **2001**, *101,* 757-824.

(3) For reviews on asymmetric synthesis of quaternary carbon stereogenic centers, see: (a) "The Catalytic Enantioselective Construction of Molecules with Quaternary Carbon Stereocenters," Corey, E. J.; Guzman-Perez, A. *Angew. Chem. Int. Ed.* **1998**, *37*, 388-401. (b) "Enantioselective Construction of Quaternary Stereocenters," Christoffers, J.; Mann, A. *Angew. Chem. Int. Ed.* **2001**, *40*, 4591-4597. (c) "Stereoselective Formation of Quaternary Carbon Centers and Related Functions," Barriault, L.; Denissova, I. *Tetrahedron*, **2003**, *59*, 10105-10146. (d) "Stereoselective Construction of Quaternary Stereocenters," Christoffers, J.; Baro, A. *Adv. Synth. Catal*. **2005**, *347*, 1473-1482. (e) "Enantioselective Catalytic Formation of Quaternary Stereogenic Centers," Cozzi, P. G.; Hilgraf, R.; Zimmermann, N. *Eur. J. Org. Chem*. **2007**, 5969-5994.

(4) For reviews on nucleophilic additions to ketones, see: (a) "Asymmetric Catalysis for the Construction of Quaternary Carbon Centers: Nucleophilic Addition on Ketones and Ketimines," Riant, O.; Hannedouche, *J. Org. Biomol. Chem.* **2007**, *5*, 873-888. (b) "Asymmetric Addition to Ketones: Enantioselective Formation of Tertiary Alcohols," García, C.; Martín, V. S. *Curr. Org. Chem.* **2006**, *10*, 1849-1889.

Figure 1.1: Natural products and biologically-important molecules that contain a chiral tertiary alcohol or derivative

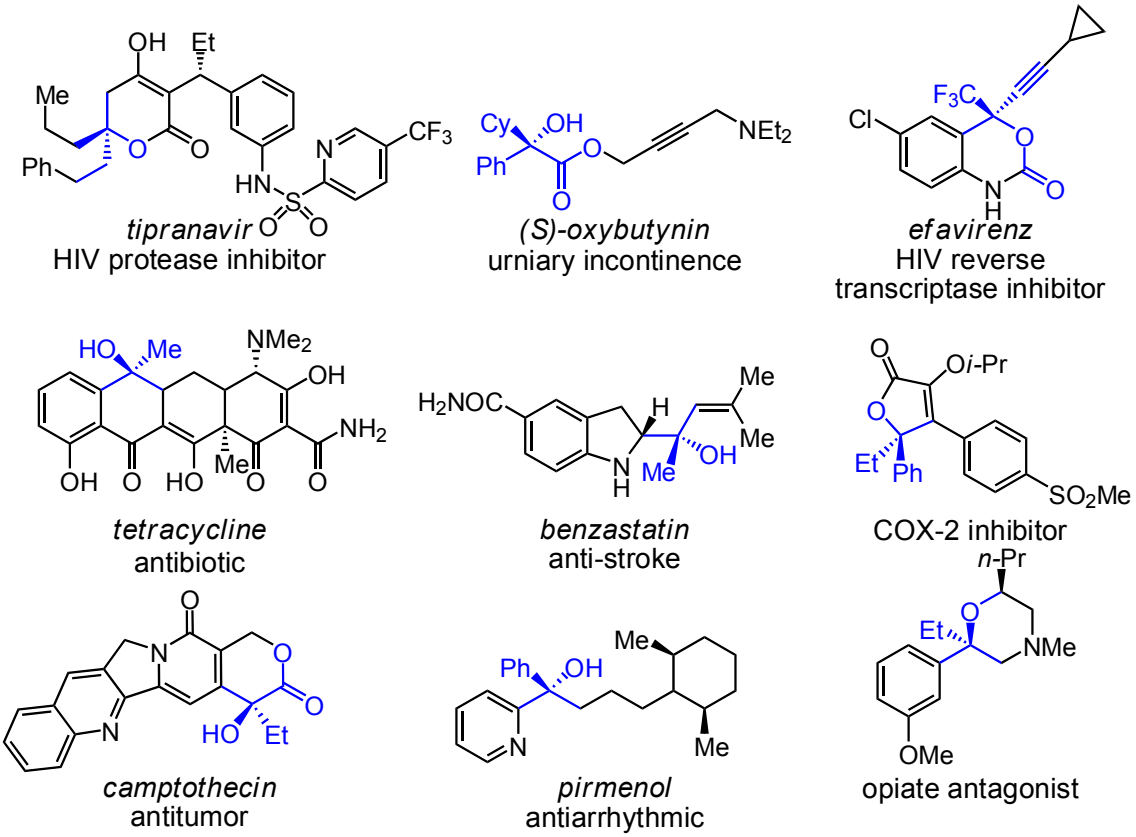

There are currently five reports of catalytic asymmetric dialkylzinc additions to α-ketoesters (including the work described herein). The first report was disclosed by Kozlowski and coworkers, who demonstrated the enantioselective addition of Et_2Zn to aromatic α-ketoesters catalyzed by bifunctional chiral Ti-salen complex **1.3** with enantioselectivities up to 78% ee (Scheme 1.1).[5] Hydrolysis of the alkylation product, followed by recrystallization, afforded the corresponding chiral acid in 70% yield and

(5) (a) "The First Catalytic Asymmetric Addition of Dialkylzincs to α-Ketoesters," DiMauro, E.; Kozlowski, M. *Org. Lett*. **2002**, *4*, 3781-3784. (b) "Development of Bifunctional Salen Catalysts: Rapid, Chemoselective Alkylations of α-Ketoesters," DiMauro, E.; Kozlowski, M. *J. Am. Chem. Soc.*, **2002**, *124*, 12668-12669. (c) "Mechanism and Scope of Salen Bifunctional Catalysts in Asymmetric Aldehyde and α-Ketoester Alkylation," Fennie, M. W.; DiMauro, E. F.; O'Brien, E. M.; Annamalai, V.; Kozlowski, M. C. *Tetrahedron* **2005**, *61*, 6249–6265.

98% ee (data not shown). The addition of dialkyzinc reagents other than Et_2Zn was not discussed. We can presume that the high reactivity of Et_2Zn compared with related dialkylzinc nucleophiles was required for reactivity and/or selectivity. Reagent specificity is a common drawback in reactions with dialkylzinc reagents, and will be discussed in greater detail in section 1.8.a .

Scheme 1.1: Ti-catalyzed addition of Et_2Zn to α-ketoesters by Kozlowski and coworkers

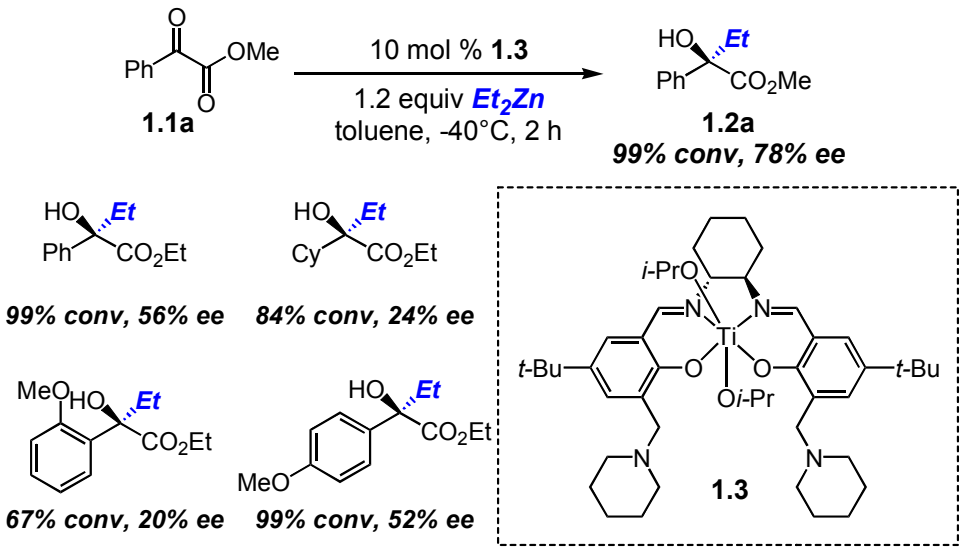

The Shibasaki group has shown that the addition of Me_2Zn to aromatic α-ketoesters catalyzed by chiral hydroxyproline-based catalyst **1.5** proceeds with enantioselectivities up to 96% ee (Scheme 1.2).[6] In this report, the less reactive (relative to Et_2Zn) Me_2Zn was utilized exclusively. Relatively high temperatures (-20 °C) and catalyst loadings (10-20 mol %) were required in order to obtain good levels of reactivity; however non-catalyzed background reactions can also occur at these 'elevated' temperatures. Slow addition of Me_2Zn over 30 h was required to overcome these undesired side reactions. As with the Kozlowski protocol (10 mol % Ti-salen complex **1.3**, 1.2 equiv Et_2Zn, toluene, -40 ºC, 2 h), only one dialkylzinc reagent was reported,

(6) "Multicenter Strategy for the Development of Catalytic Enantioselective Nucleophilic Alkylation of Ketones: Me_2Zn Addition to α-Ketoesters," Funabashi, K.; Jachmann, M.; Kanai, M.; Shibasaki, M. *Angew. Chem. Int. Ed.* **2003**, *42,* 5489-5492.

presumably because the large difference in reactivity between Et_2Zn and Me_2Zn renders methods developed for one reagent incompatible with the other.

The authors report an interesting effect with the addition of *i*-PrOH. In the absence of this achiral additive, there was a positive nonlinear effect, however the nonlinearity disappears in the presence of 27 mol % *i*-PrOH. The authors propose that *i*-PrOH (ZnO*i*-Pr in the reaction mixture) breaks up aggregates and drives the catalyst equilibrium towards a monomeric species.

Scheme 1.2: Amino alcohol-catalyzed enantioselective addition of Me_2Zn to α-ketoesters by Shibasaki and coworkers

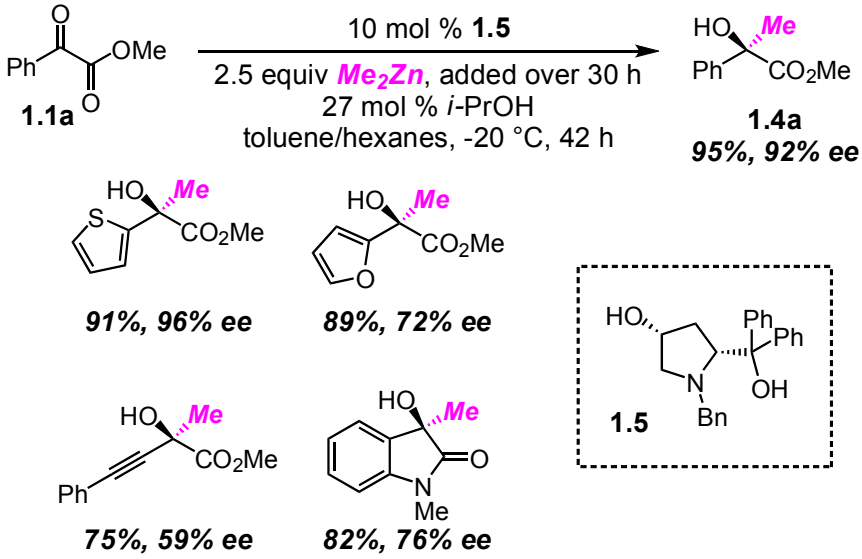

Subsequent to our report, Pedro and co-workers disclosed a mandelamide-catalyzed addition of Me_2Zn to α-ketoesters (Scheme 1.3).[7] In the presence of 20 mol % amino alcohol **1.8** and 6.0 equiv Me_2Zn, moderate to good enantioselectivities were obtained for a variety of electron-rich and electron-poor aryl substrates, as well as heteroaromatic substrates (56-87% yield, 63-90% ee). Unfortunately, enantioselectivity

(7) (a) "Catalytic Asymmetric Addition of Dimethylzinc to α-Ketoesters, Using Mandelamides as Ligands," Blay, G.; Fernández, I.; Marco-Aleixandre, A.; Pedro, J. R. *Org. Lett*. **2006**, 1287-1290. (b) "Enantioselective Addition of Dimethylzinc to α-Keto Esters," Blay, G.; Fernández, I.; Marco-Aleixandre, A.; Pedro, J. R. *Synthesis* **2007**, *23*, 3754-3757.

suffered significantly in the case of aliphatic substrates (35% ee), and reactions with other dialkylzinc reagents were not disclosed.

Scheme 1.3: Enantioselective addition of Me_2Zn to α-ketoesters by Pedro and coworkers

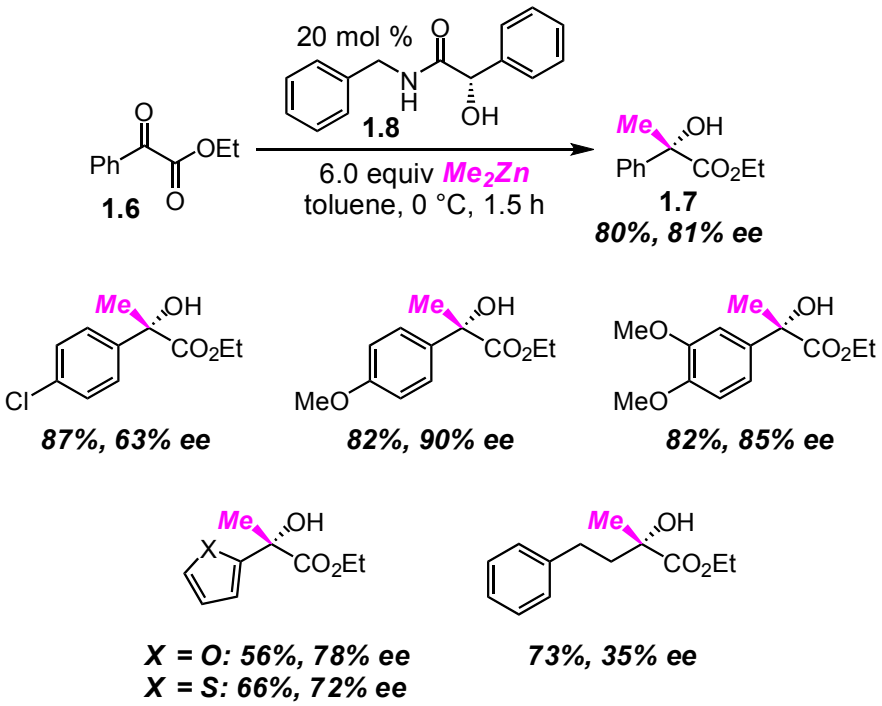

A study from Jiang and co-workers shows the enantioselective addition of di*alkynyl*zinc reagents, generated *in situ* from terminal alkynes and $Zn(OTf)_2$, to α-ketoesters (Scheme 1.4).[8] This process was promoted by 22 mol % aminoalcohol **1.10**, and the derived alkynyl-alcohols were obtained in up to 94% ee (70 °C, toluene). Aryl and heteroaromatic substrates underwent efficient alkynylation, as did a variety of substituted terminal alkynes. The alkynylation product of methyl pyruvate was obtained in high enantioselectivity, however in very low yield (**(-)-1.9c**, 11% yield, 92% ee). This was likely due to side reactions caused by adventitious enolization of methyl pyruvate under the reaction conditions.

(8) "Highly Enantioselective Alkynylation of α-Keto Ester: An Efficient Method for Constructing a Chiral Tertiary Carbon Center," Jiang, B.; Chen, Z.; Tang, X. *Org. Lett*. **2002**, 3451-3453.

Scheme 1.4: Alkynylation of α-ketoesters by Jiang and coworkers

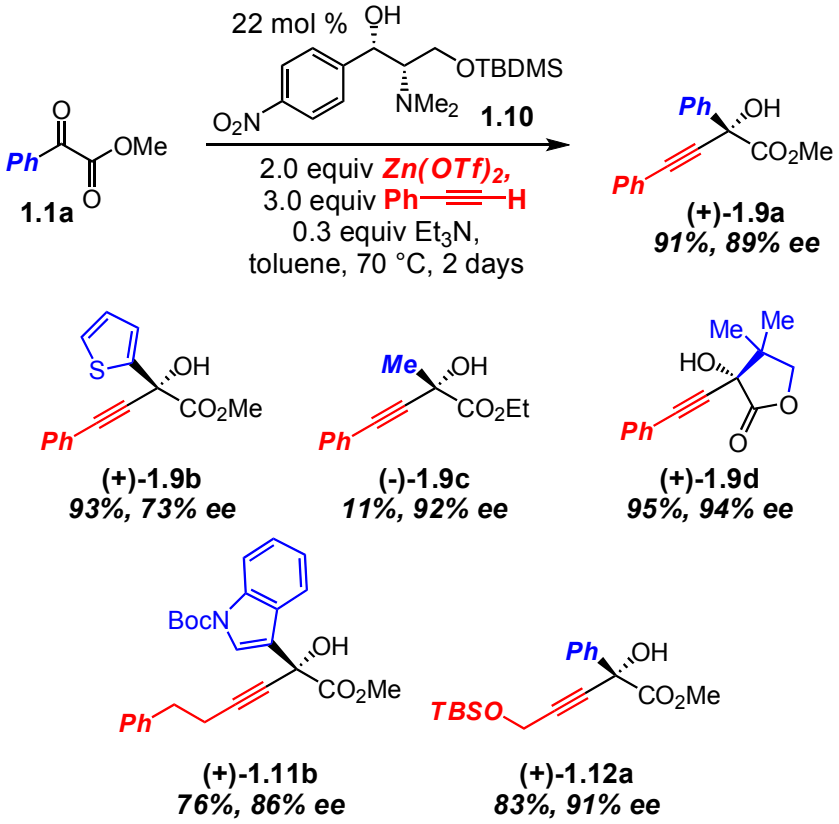

Currently, several other methods exist for enantioselective additions of carbon-based nucleophiles other than dialkylzinc reagents to α-ketoesters which will not be

discussed here. These methods include aldol addition,[9] nitroaldol addition,[10] ene reactions,[11] Rh-catalyzed alkynylations and dienylations,[12] arylations,[13] and allylations.[14]

1.2 *Initial screens and optimization studies for the Al-catalyzed enantioselective alkylation of α-ketoesters with Et_2Zn*

1.2.a Identification of a general catalytic system for enantioselective additions of Et_2Zn to α-ketoesters with chiral peptide-based ligands

Peptide-based ligands of the type outlined in Figure 1.2 have proven to be a versatile and powerful class of chiral ligands for a variety of metal-catalyzed C-C bond forming reactions.[15] This class of ligands is easily synthesized from commercially

---

(9) (a) "A Chiral Ag-Based Catalyst for Practical, Efficient, and Highly Enantioselective Additions of Enolsilanes to α-Ketoesters," Akullian, L. C.; Snapper, M. L.; Hoveyda, A. H. *J. Am. Chem. Soc*. **2006**, *128*, 6532-6533. (b) "C_1-Symmetric Oxazolinyl Sulfoximines as Ligands in Copper-Catalyzed Asymmetric Mukaiyama Aldol Reactions," Sedelmeier, J.; Hammerer, T.; Bolm, C. *Org. Lett*. **2008**, *10*, 917-920. (c) "Asymmetric Direct Aldol Reaction of Functionalized Ketones Catalyzed by Amine Organocatalysts Based on Bispidine," Liu, J.; Yang, Z.; Wang, Z.; Wang, F.; Chen, X.; Liu, X.; Feng, X.; Su, Z.; Hu, C. *J. Am. Chem. Soc.* **2008**, *130*, 5654-5655.

(10) (a) "Enantioselective Nitroaldol Reaction of α-Ketoesters Catalyzed by Cinchona Alkaloids," Li, H.; Wang, B.; Deng, L. *J. Am. Chem. Soc.* **2006**, *128*, 732-733. (b) "Highly Enantioselective Henry (Nitroaldol) Reaction of Aldehydes and α-Ketoesters Catalyzed by *N,N'*-Dioxide-Copper(I) Complexes," Qin, B.; Xiao, X.; Liu, X.; Huang, J.; Wen, Y.; Feng X. *J. Org. Chem.* **2007**, *72*, 9323-9328. (c) "Asymmetric Organocatalytic Nitroaldol Reaction of α-Ketoesters: Stereoselective Construction of Chiral Tertiary Alcohols at Subzero Temperature," Takada, K.; Takemura, N.; Cho, K.; Sohtome, Y.; Nagasawa, K. *Tetrahedron Lett*. **2008**, *49*, 1623-1626.

(11) "Enantioselective Catalysis of Ketoester-ene Reaction of Silyl Enol Ether to Construct Quaternary Carbons by Chiral Dicationic Palladium(II) Complexes," Mikami, K.; Kawakami, Y.; Akiyama, K., Aikawa, K. *J. Am. Chem. Soc.* **2007**, *129*, 12950-12951.

(12) (a) "Highly Enantioselective Direct Reductive Coupling of Conjugated Alkynes and α-Ketoesters via Rhodium-Catalyzed Asymmetric Hydrogenation," Kong, J.-R.; Ngai, M.-Y. Krische, M. J. *J. Am. Chem. Soc.* **2006**, *128*, 718-719. (b) "Catalytic Carbonyl *Z*-Dienylation via Multicomponent Reductive Coupling of Acetylene to Aldehydes and α-Ketoesters Mediated by Hydrogen: Carbonyl Insertion into Cationic Rhodacyclopentadienes," Kong, J. R.; Krische, M. J. *J. Am. Chem. Soc*. **2006**, *128*, 16040-16041.

(13) "Enantioselective Rhodium-Catalyzed Addition of Arylboronic Acids to α-Ketoesters," Duan, H.-F.; Xie, J.-H.; Qiao, X.-C.; Wang, L.-X.; Zhou, Q.-L. *Angew. Chem. Int. Ed*. **2008**, *47*, 4351-4353.

(14) "Highly Enantioselective Allylation of α-Ketoesters Catalyzed by *N,N'*-Dioxide-In(III) Complexes," Zheng, K.; Qin, B.; Liu, Q.; Feng, X. *J. Org. Chem*. **2007**, *72*, 8478-8483.

(15) For representative examples, see (a) "Al-Catalyzed Asymmetric Alkylations of Pyridyl-Substituted Alkynyl Ketones with Dialkylzinc Reagents," Friel, D. K.; Snapper, M. L.; Hoveyda, A. H. *J. Am. Chem. Soc.* **2008,** *130,* 9942-9951. (b) "Catalytic Asymmetric Alkylations of Ketoimines. Enantioselective Synthesis of *N*-Substituted Quaternary Carbon Stereogenic Centers by Zr-Catalyzed Additions of Dialkylzinc Reagents to Aryl-, Alkyl- and Trifluoroalkyl-Substituted Ketoimines," Fu, P.; Snapper, M. L.; Hoveyda, A. H. *J. Am. Chem. Soc.* **2008**, *130,* 5530-5541. (c) "Asymmetric Synthesis of Acyclic Amines Through Zr- and Hf-Catalyzed Enantioselective Addition of Alkylzinc Reagents to Imines," Akullian, L. C.; Porter, J. R.; Traverse, J. F.; Snapper, M. L.; Hoveyda, A. H. *Adv. Synth. Catal*. **2005**, *347,* 417-425. (d)

available starting materials using standard peptide-coupling methods, and the source of chirality is readily modified by altering the identity of the amino acids of the backbone. In addition, the metal-binding portions (*N*-terminus and *C*-terminus) can be easily tuned for specific reactivity.

Figure 1.2: General scaffold of amino acid-based chiral ligands

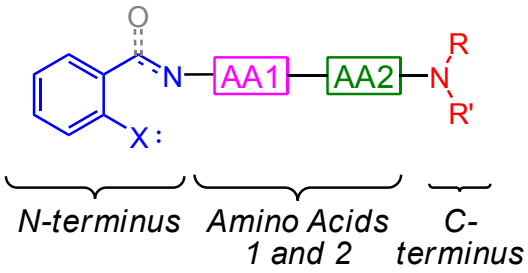

We set out to identify a new peptide-based chiral ligand system for the development of the first generally effective addition of dialkylzinc reagents to α-ketoesters. We began by identifying an effective Lewis acid-ligand combination for the alkylation of methyl benzoylformate (**1.1a**) with Et_2Zn. As shown in Figure 1.3, we tested fifteen metal salts in combination with nine unique ligand scaffolds, each of which incorporated a different metal binding site at the *N*-terminus. Through these initial screens, we discovered that the combination of $Al(O\textit{i}\text{-}Pr)_3$ and salicyl imine-derived peptide ligand **1.13** provided the desired product (**1.2a**) in 92% conv and 29% ee (Eq 1).[16]

"Small Peptides as Ligands for Catalytic Asymmetric Alkylations of Olefins. Rational Design of Catalysts or of Searches that Lead to Them?," Hoveyda, A. H.; Hird, A. W.; Kacprzynski, M. A. *Chem. Commun.* **2004**, *16*, 1779-1785.

(16) Initial screens shown in Figure 1.3 were carried out by Dr. Hongbo Deng.

Figure 1.3: Ligands and Lewis acids included in initial screens

Imine, Amine, and Amide N-Termini Included in Initial Screens:

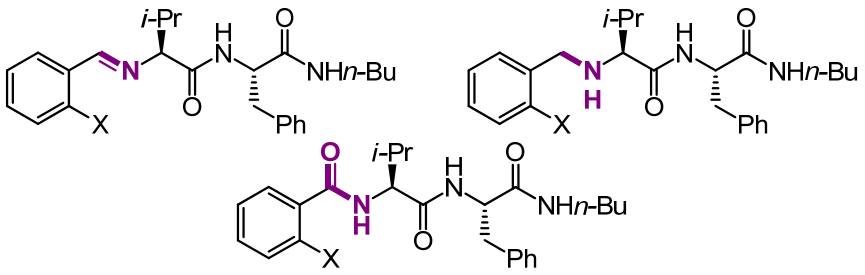

Chelation Sites Included in Initial Screens:

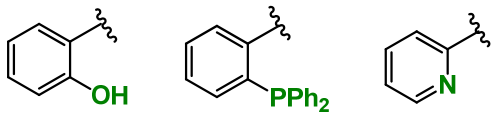

Lewis Acids Included in Initial Screens:

$Ti(O\textit{i}\text{-}Pr)_4$, $Zr(O\textit{i}\text{-}Pr)_4$, $Hf(O\textit{i}\text{-}Pr)_4$, $Al(O\textit{i}\text{-}Pr)_3$, $Sr(O\textit{i}\text{-}Pr)_2$, $Sc(O\textit{i}\text{-}Pr)_3$, $Yb(O\textit{i}\text{-}Pr)_3$, $Yb(OTf)_3$, $Zn(O\textit{t}\text{-}Bu)_2$, $Zn(OTf)_2$, $Sm(O\textit{i}\text{-}Pr)_3$, $(CuOTf)_2.C_6H_6$, $Cu(OTf)_2$, $Cu(O\textit{i}\text{-}Pr)_2$, $MgBr_2$

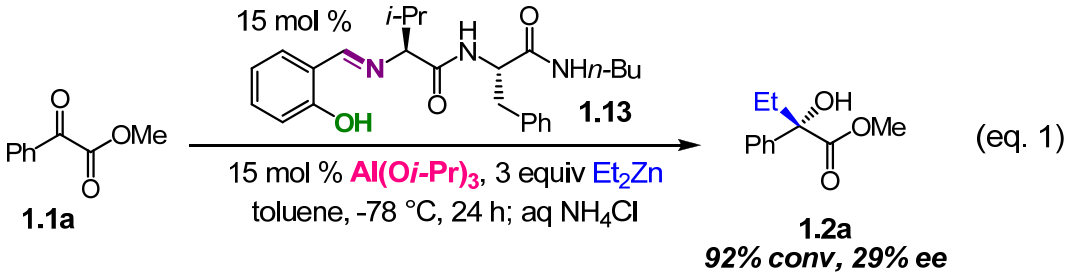

1.2.b Positional screening as a method for the identification of an effective ligand for Al-catalyzed enantioselective alkylations of α-ketoesters with Et_2Zn

Our next goal was to improve the selectivity and efficiency of the Al-catalyzed process shown in Eq. 1. We thought to accomplish this task by application of an iterative positional screening strategy first introduced by Houghten in 1993 for the discovery of

new synthetic peptides for opiod receptor ligands [17] and developed within these laboratories in the context of asymmetric catalysis.[18] When employing this screening strategy, one assumes that the observed changes in enantioselectivity or efficiency which result upon modification at each position on the ligand are additive. Thus, we can screen a large number of amino acids at each position, and we can also make Schiff base and *C*-terminus modifications, without having to synthesize every possible combination.

1.2.b.1 *Amino acid screens*

Our initial screen involved the AA1 portion of the ligand **1.13**, with AA2 = Phe.[19] Results from our AA1 screen are shown in Figure 1.4. We discovered that the substitution of Thr(O*t*-Bu) for Val at AA1 (**1.14**) led to the greatest improvement in enantioselectivity (>98% conv, 43% ee with **1.14** vs. 92% conv, 29% ee with **1.13**).

---

(17) "The Use of Positional Scanning Synthetic Peptide Combinatorial Libraries for the Rapid Determination of Opiod Receptor Ligands," Dooley, C. T.; Houghten, R. A. *Life Sciences* **1993,** *52,* 1509-1517.

(18) "Chiral Catalyst Discovery Through Ligand Diversity. Ti-Catalyzed Enantioselective Addition of TMSCN to *meso* Epoxides," Cole, B. M.; Shimizu, K. D.; Krueger, C. A.; Harrity, J. P. A.; Snapper, M. L.; Hoveyda, A. H. *Angew. Chem., Int. Ed*. **1996**, *35*, 1668-1671.

(19) We generally screen the AA1 position first, followed by the AA2 position due to ease of synthesis.

Figure 1.4: Results from amino acid screen at the AA1 position of chiral ligand **1.13**

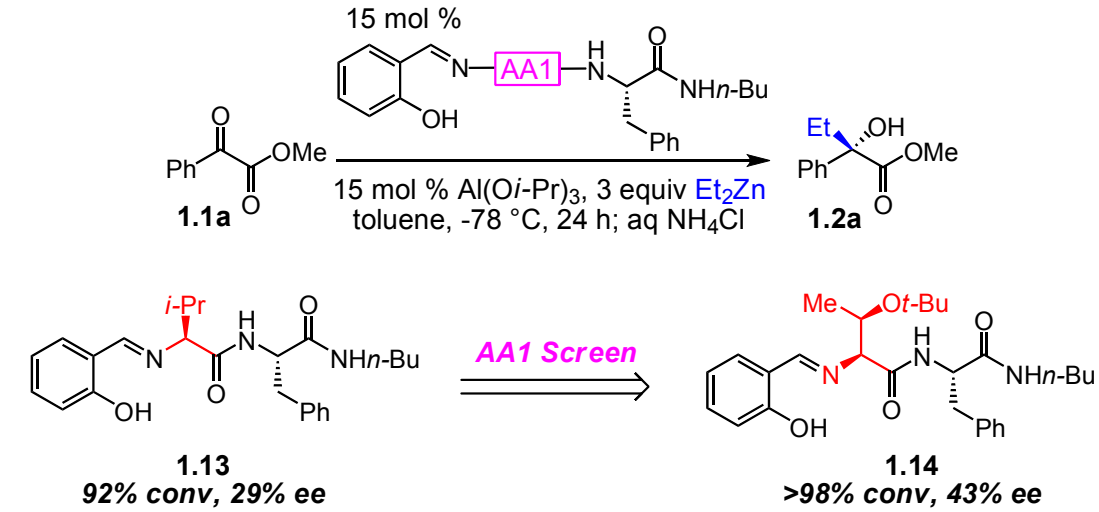

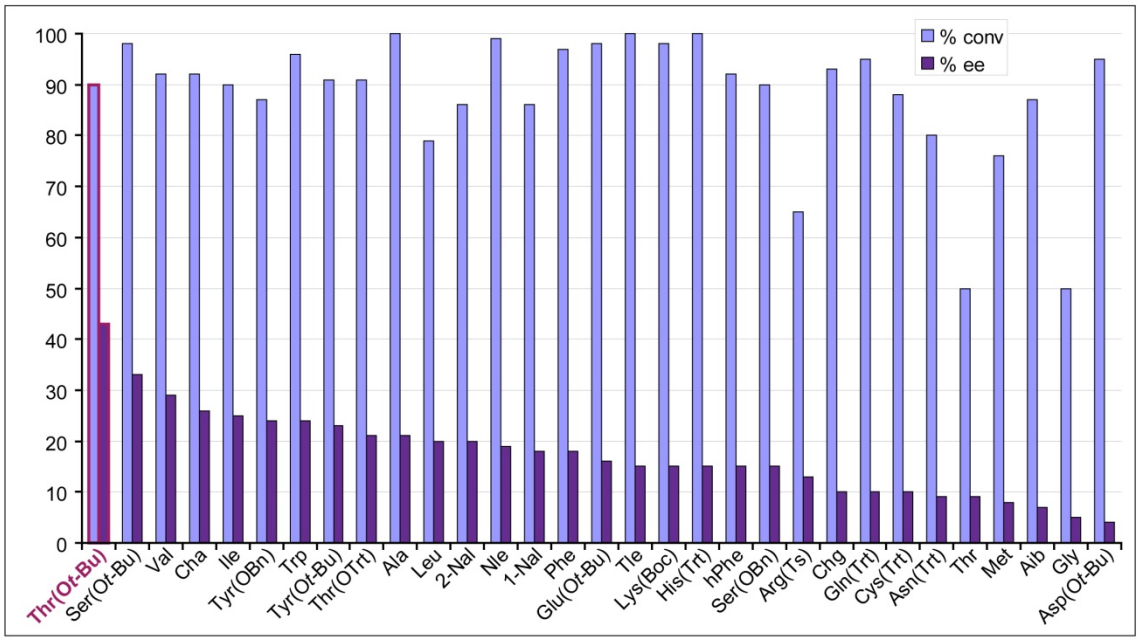

We continued our optimization studies with an AA2 screen, incorporating Thr(O*t*-Bu) as AA1. We found that a Thr-derived amino acid was optimal at this position as well, however in this case a trityl protecting group was required (**1.15**, Figure 1.5). With 15 mol % dipeptide ligand **1.15**, we were then able to obtain the desired tertiary alcohol **1.2a** in >98% conv and 72% ee.

Figure 1.5: Results from amino acid screen at the AA2 position of chiral ligand **1.14**

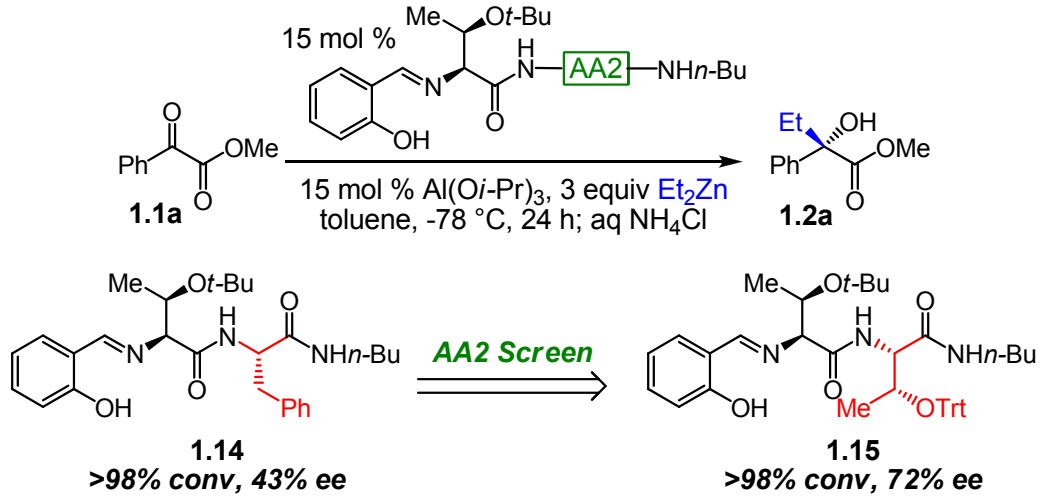

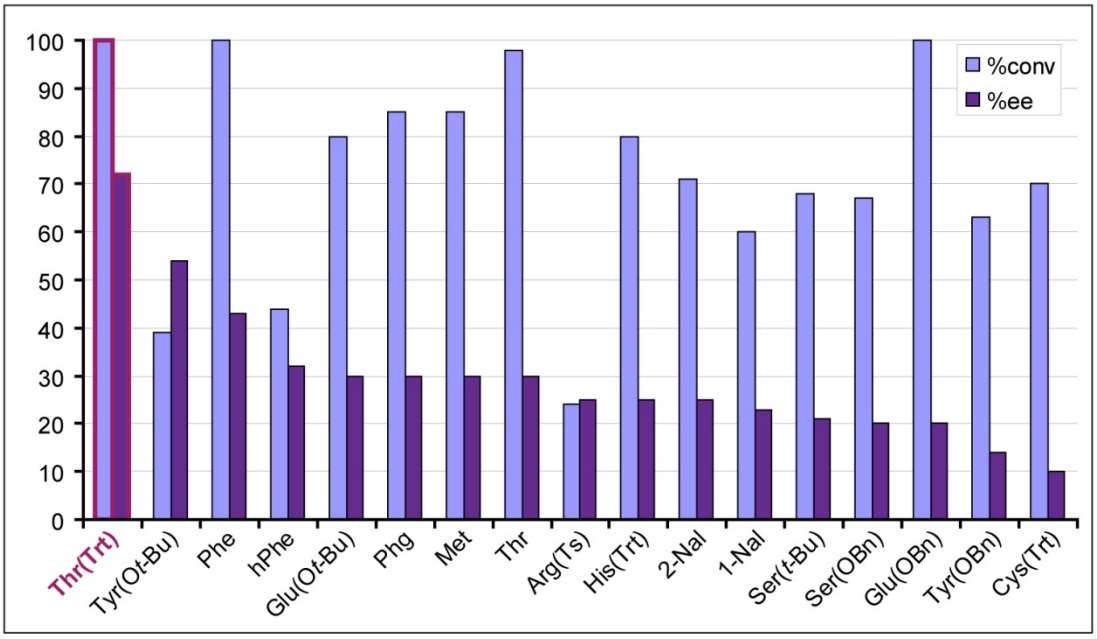

At this point, we decided to test our original assumption that observed increases in enantioselectivity resulting from amino acid modifications are additive. In other words, we wanted to confirm that each amino acid functions independently rather than acting in a cooperative manner. We selected a diverse set of amino acids and re-screened AA1 with Thr(OTrt) as AA2. As expected, the highest levels of selectivity were obtained with Thr(O*t*-Bu) as AA1 (a comparison is shown in Chart 1.1).

Chart 1.1: AA1 screening data with AA2 = Thr(OTrt) (purple) *or* Phe (blue)

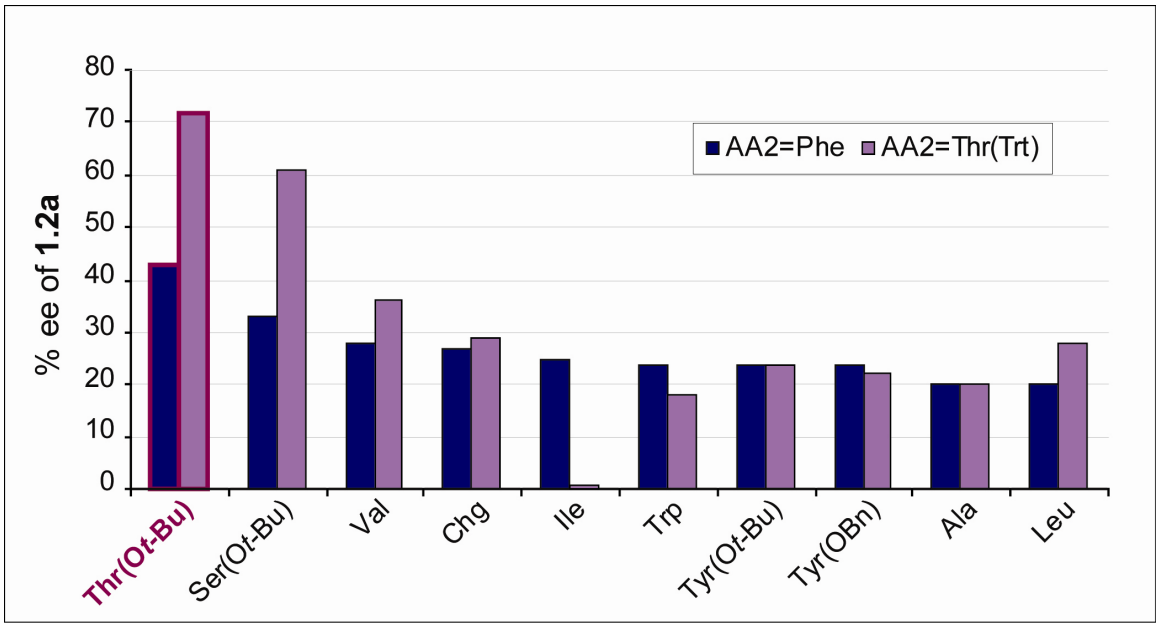

1.2.b.2 *Optimization of the C-terminus of chiral ligand 1.15*

We next turned our attention to the *C*-terminus of our chiral ligand (NH*n*-Bu, **1.15**). As shown in Chart 1.2, we found that an alkyl-substituted amide terminus was required (no selectivity was observed with aniline-derived *C*-termini of the type NH*aryl*), but that the size of this alkyl group (NH*alkyl*) was not important, as enantioselectivity was unaffected by changing the alkyl group to Me or *t*-Bu. However, employment of a disubstituted amine (R=R'=Me) resulted in a marked decrease in enantioselectivity (<10% ee).

Chart 1.2: Screen of amine group at the C-terminus

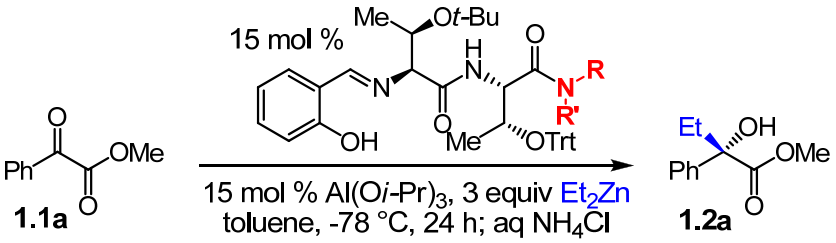

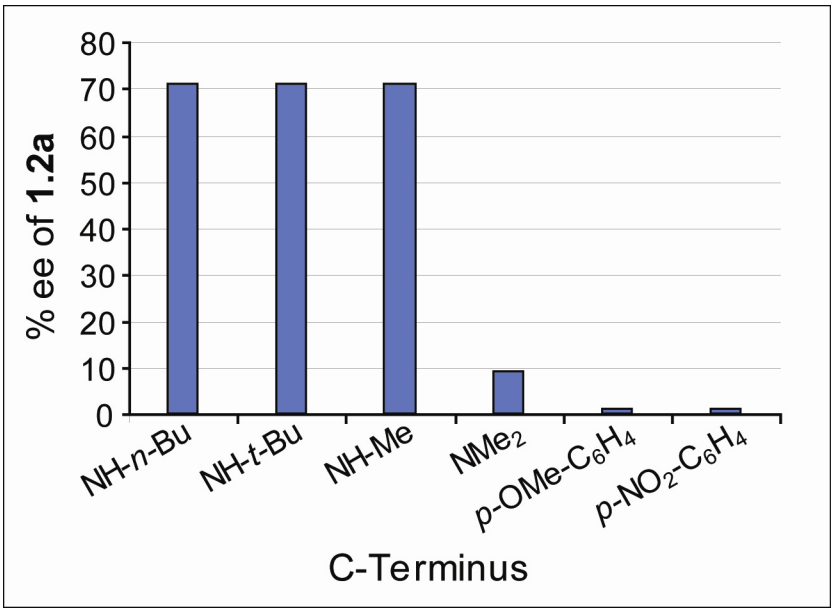

1.2.b.3 *Optimization of the N-terminus of chiral ligand 1.15*

Prior to screening the Schiff base (*N*-terminus) portion of the ligand, we tested electron-rich substrate **1.1b** bearing a *p*-OMe group under the optimized reaction conditions (15 mol % Al(O*i*-Pr)$_3$, 15 mol % **1.15**, 3 equiv Et_2Zn, toluene, -78 ºC), and found that Et_2Zn addition more slowly and with greater reproducibility than with phenyl substrate **1.1a** (45 min, 65-68% ee with **1.1b**; ~5 min, 58-72% ee with **1.1a**). We thus continued our screening with **1.1b**. As shown in Table 1.1, we tested 18 different salicyl-derived Schiff bases with varying electronic and steric properties. We found that when an OMe was installed *para*- to the hydroxyl group (**1.16**, Table 1.1), we could obtain the desired tertiary alcohol in full conversion and 82% ee (vs. 68% ee with **1.15**).

Table 1.1: Data from Schiff base screen

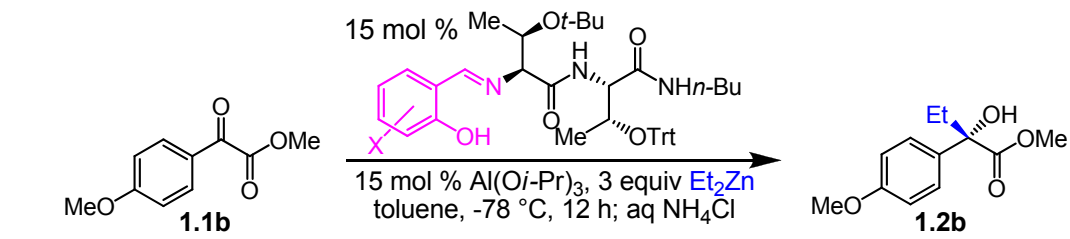

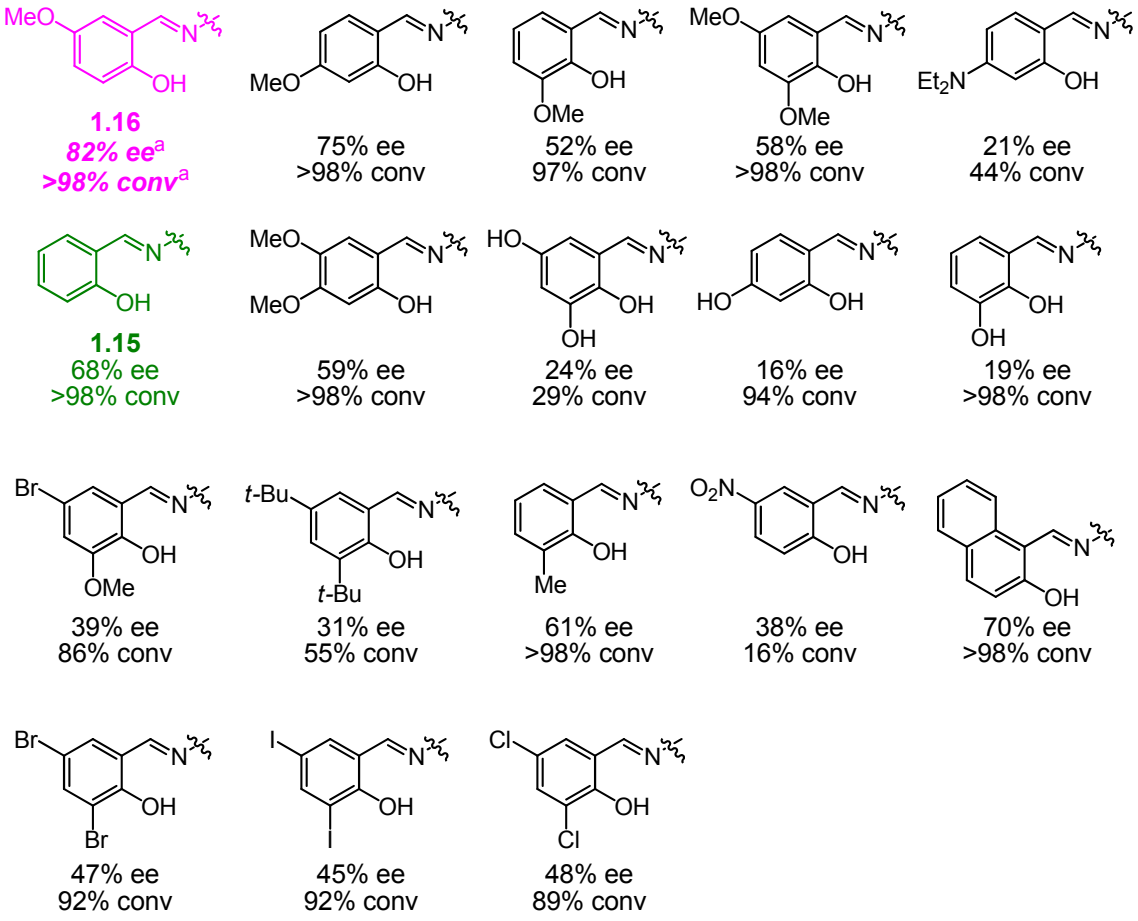

[a] Determined by chiral GLC analysis; see Experimentals section for details.

1.2.c Enhancement of enantioselectivity by an achiral additive

While we had significantly increased the selectivity of this alkylation reaction through our positional screening strategy, we were not satisfied with the observed level of enantioselectivity (≤82% ee). We decided to explore achiral additives, which have been

shown to have positive impacts on the selectivity and/or efficiency of a variety of catalytic enantioselective transformations.[20] As shown in Table 1.2, we tested several classes of achiral additives, including basic (entries 1-4), dehydrating (entries 5-6), protic (entries 7-9), and nucleophilic (entries 10-18) additives. Only this last class provided any enhancement in enantioselectivity. Basic additives had a minor but negative effect, and enantioselectivities ranged from 50-70% ee (vs. 82% ee without any additive). Protic and dehydrating additives, however, were extremely detrimental to the reaction outcome, and the product was obtained in <2% ee in all cases. Fortunately, we were able to observe an enhancement in selectivity in the case of nucleophilic additives, specifically with diethylphosphoramidate (**1.17**, Table 1.2, entry 12) which provided the desired tertiary alcohol **1.2b** in 89% ee.[21] Further optimization indicated that 50 mol % of the achiral additive was sufficient to access this observed increase in selectivity (Table 1.3).

(20) For an excellent review on the application of achiral additives to catalytic enantioselective transformations, see: "Towards Perfect Asymmetric Catalysis: Additives and Cocatalysts," Vogl, E. M.; Gröger, H.; Shibasaki, M. *Angew. Chem. Int. Ed.* **1999**, *38*, 1570-1577.

(21) This is truly a serendipitous result. Dr. John Traverse, who was a graduate student in Prof. Marc Snapper's group at the time, had ordered this chemical accidentally, and it had come in moments before I walked into his lab to ask for phosphine oxides to include in my screen. He handed me the bottle and told me to keep it, as he had no use for it.

Table 1.2: Achiral additive screen

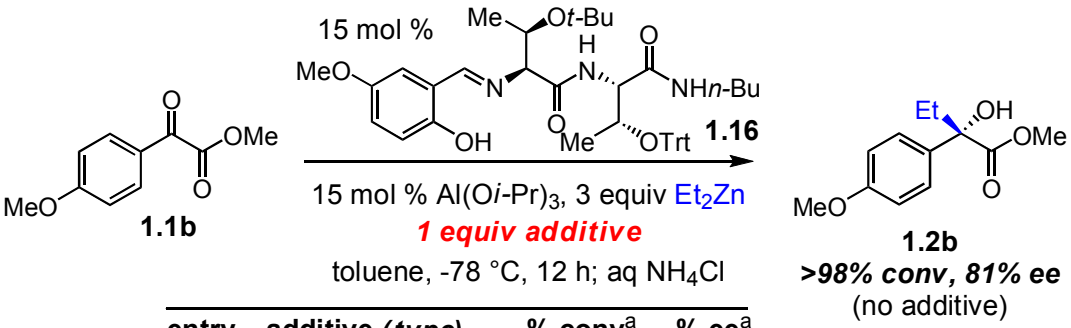

entry	additive *(type)*	% conv[a]	% ee[a]
	basic		
1	imidazole	69	59
2	TMEDA	>98	54
3	*i*-Pr_2NH	>98	50
4	1-methyl imidazole	>98	70
	dehydrating		
5	$MgSO_4$	62	<2
6	3 & 4 Å MS	>98	<2
	protic		
7	H_2O	>98	<2
8	*i*-PrOH	>98	<2
9	MeOH	>98	<2
	nucleophilic		
10	$O=PPh_3$	12	67
11	$O=P(n\text{-}Bu)_3$	70	85
12	***$H_2NP(O)(OEt)_2$***	***>98***	***89***
13	$Me_2NP(O)(OEt)_2$	>98	75
14	$H_2NP(O)(OPh)_2$	90	87
15	HMPA	84	40
16	NMO	80	82
17	TEA N-oxide dihydrate	>98	81
18	DMSO	<2	-

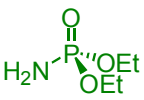

1.17

[a] Determined by chiral GLC analysis.

Table 1.3: Effect of additive amount in the Al-catalyzed enantioselective addition of Et_2Zn to α-ketoester **1.1b**

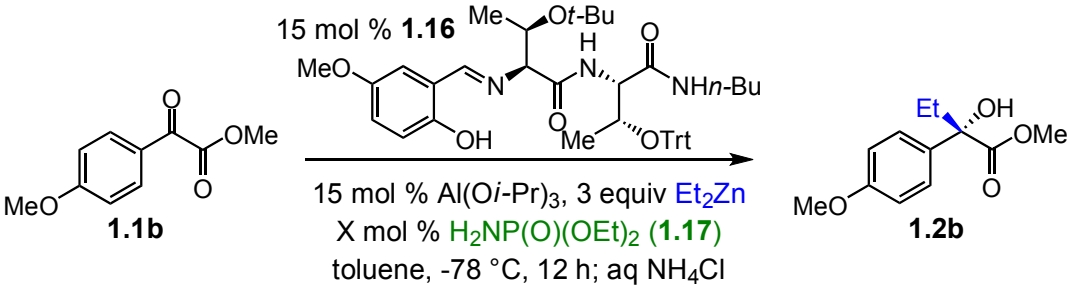

entry	equiv $H_2NP(O)(OEt)_2$	% conv[a]	% ee[a]
1	0	>98	81
2	5 mol %	>98	84
3	15 mol %	>98	87
4	***50 mol %***	***>98***	***89***
5	1 equiv	>98	89
6	1.5 equiv	>98	89
7	2 equiv	>98	88

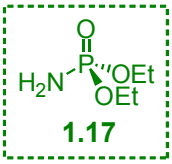

[a] determined by chiral GLC analysis

1.3 *Substrate scope for the Al-catalyzed enantioselective alkylation of α-ketoesters with Et_2Zn*

With a method in hand for enantioselective alkylation of electron-rich aromatic substrate **1.1b**, we set out to investigate the generality of our method with a variety of aromatic and aliphatic-based α-ketoester substrates (Table 1.4). Perhaps not surprisingly, the highest level of enantioselectivity was obtained with *p*-OMe-substituted substrate **1.1b**; the substrate we utilized at the end of our optimization studies (89% ee, entry 4). We were able to isolate **1.2a** in 98% yield and 84% ee (entry 1), and we found that the identity of the ester substituent did not have a significant effect on reaction outcome (entries 3-4). The alkylation product from electron-poor ketone **1.1f** was obtained in only 47% ee, independent of the presence of 50 mol % **1.17** (entry 6). This result indicated to us that there may be a high level of background reactivity associated with this substrate. Unfortunately, alkylations of aliphatic substrates **1.1k-l** with Et_2Zn were significantly less

selective, and the desired tertiary alcohols **1.2k-l** were obtained in 56% ee and 58% ee, respectively.

We observed low selectivity in the alkylation reaction of 2-furyl substituted substrate **1.1i** (43% ee, entry 9), however when the heteroatom was moved one position away from the prochiral ketone (3-furyl substrate **1.1j**, entry 10), we were able to obtain the product **1.2j** in 72% ee. We believe this is most likely due to competitive chelation of the α-oxygen of 2-furyl substrate **1.1i** (vs. the α-ketoester moiety) to the Lewis-acidic Al.[22] With *o*-OMe-substituted substrate **1.1e**, longer reaction times were required for the alkylation reaction to go to completion (48 h with **1.1e**, vs. 20 min-1 h for all other substrates). This may also be due to competitive chelation of the OMe, which could tie up the catalyst and slow the alkylation reaction.

(22) See Section 1.9 (page 43) for a proposed transition state.

Table 1.4: Substrate scope for the Al-catalyzed enantioselective alkylation of α-ketoesters with Et_2Zn

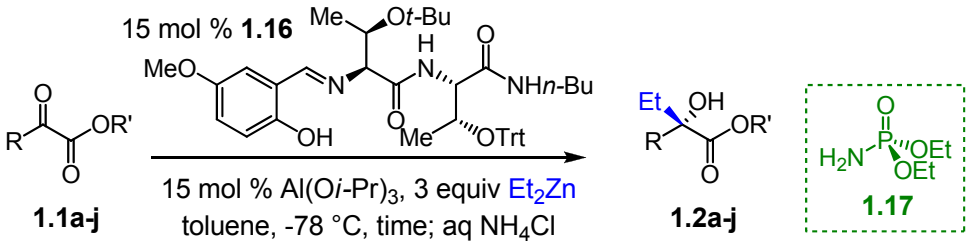

					without additive		***with 50 mol % 1.17***		
entry	**R**	**R'**		**time**	**yield (%)**[b]	***ee* (%)**[a]	**yield (%)**[b]	***ee* (%)**[a]	**config.**
1	Ph	Me	**1.1a**	20 min	95	75	98	84	(+)
2	*p*-$OMeC_6H_4$	Me	**1.1b**	45 min	96	83	98	89	(+)
3	Ph	*t*-Bu	**1.1c**	20 min	63	70	95	78	(+)
4	Ph	Bn	**1.1d**	20 min	95	80	75	86	(-)
5	*o*-$OMeC_6H_4$	Me	**1.1e**	48 h	87	<5	92	75	(-)
6	*p*-$CF_3C_6H_4$	Me	**1.1f**	20 min	82	47	92	47	nd
7	*p*-IC_6H_4	Me	**1.1g**	20 min	84	60	98	84	(+)
8	*p*-MeC_6H_4	Me	**1.1h**	20 min	63	70	53	79	(+)
9	2-fur	Me	**1.1i**	1 h	96	26	90	43	(+)
10	3-fur	Me	**1.1j**	20 min	88	44	90	72	(+)
11	Me	Me	**1.1k**	20 min	>98[c]	39	>98[c]	56	(+)
12	Cy	Me	**1.1l**	20 min	nd	50	82	58	(+)

[a] Determined by chiral GLC analysis; see Experimentals section for details. [b] Isolated yield, all reactions proceeded to >98% conv. nd = not determined. [c] Percent conversion (accurate yield was difficult to measure due to product volatility).

Each alkylation reaction was tested in both the presence and absence of diethylphosphoramidate **1.17** in order to highlight the general effect that this additive had on the reaction outcome. In all cases, there was an enhancement of selectivity in the presence of 50 mol % **1.17**, however this effect was the most remarkable in the case of *o*-OMe-substituted **1.1e**. *In the absence of the achiral additive, the product (**1.2e**) was obtained in 87% yield, with <5% ee. However, in the presence of 50 mol % **1.17**, the selectivity was increased to 75% ee (92% yield, entry 5).*

1.4 *Al-catalyzed enantioselective addition of Me_2Zn to α-ketoesters*

Our initial goal was to develop a *general* method for alkylations of α-ketoesters with dialkylzinc reagents, however thus far we have only described investigations with the highly reactive Et_2Zn. We next assessed the less reactive Me_2Zn in the Al-catalyzed enantioselective alkylation of α-ketoesters. Fortunately, we were able to obtain the desired methyl adducts in good yields and enantioselectivities, however the reaction required a large excess of Me_2Zn (10 equiv vs. 3 equiv Et_2Zn) and extended reaction times (24 h vs. 20 min with Et_2Zn). The beneficial effect on enantioselectivity that we observed in the presence of 50 mol % diethylphosphoramidate (**1.17**) in alkylations with Et_2Zn was more pronounced in reactions with this less reactive dialkylzinc reagent. In each of the examples shown in Table 1.5, there was a significant increase in selectivity in the presence of 50 mol % **1.17** compared to reactions without the additive. In addition, we often observed an *increase in reaction efficiency* (i.e. <98% conv was observed in the absence of 50 mol % **1.17** in most cases). In entry 3, for example, sterically encumbered substrate **1.1c** proceeded to only 43% conv (50% ee) in the absence of additive **1.17**, compared with 83% conv (85% ee) in the presence of additive.

Unlike alkylations with Et_2Zn, aliphatic-based substrate **1.1m** was a suitable substrate for alkylations with Me_2Zn, and methyl addition product **1.4m** was obtained in >98% conv and 92% ee. (vs. 93% conv and 70% ee in the absence of additive, entry 5). This stereogenic center (**1.4m**, R = Et) is a common motif found in natural products and drug-like molecules, but has never been efficiently synthesized in a catalytic enantioselective manner.[23]

---

(23) For the synthesis of hydrolyzed **1.4m** (R' = H) by resolution techniques, see: "Practical enantioselective synthesis of a COX-2 specific inhibitor," Tan, L.; Chen, C-y.; Chen, W.; Frey, L.; King, A. O.; Tillyer, R. D.; Xu, F.; Zhao, D.; Grabowski, E. J. J.; Reider, R. J.; O'Shea, R.; Dagneau, P.; Wang, X. *Tetrahedron*, **2002**, *58*, 7403-7410.

Table 1.5: Al-catalyzed enantioselective addition of Me_2Zn to α-ketoesters

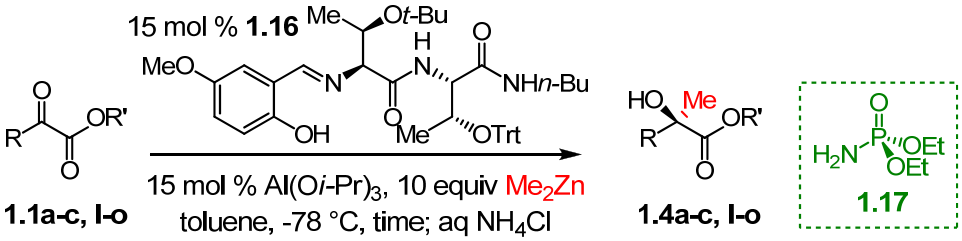

					without additive		*with 50 mol % 1.17*		
entry	**R**	**R'**		**time**	**conv (%)[a]; yield (%)[b]**	***ee* (%)[a]**	**conv (%)[a]; yield (%)[b]**	***ee* (%)[a]**	**config.**
1	Ph	Me	**1.1a**	24 h	92; nd	67	>98; 97	95	(-)
2[c]	*p*-OMeC$_6$H$_4$	Me	**1.1b**	48 h	66; 53	77	98; 71	84	(-)
3	Ph	*t*-Bu	**1.1c**	24 h	43; nd	50	83; 71	85	(-)
4	Cy	Me	**1.1l**	24 h	>98; 91	70	>98; 89	75	(-)
5[d]	Et	Me	**1.1m**	24 h	93; nd	70	>98; 44	92	(-)
6	PhHC=CH	Me	**1.1n**	24 h	>98; 97	30	>98; 91	56	(-)
7	PhC≡C	Me	**1.1o**	24 h	nd	nd	>98; nd	18	(+)

[a] Determined by chiral GLC analysis, see Experimentals section for details. nd = not determined.
[b] Isolated yields. [c] Reaction carried out at -60 °C. [d] Low yield due to product volatility.

α,β-Unsaturated substrates **1.1n-o** did not undergo efficient enantioselective alkylation under the described reaction conditions (56% ee and 18% ee, respectively, entries 6-7). We believe that a highly specific mode of substrate-catalyst coordination is required for high selectivity, and can be disrupted by changes in the steric environment surrounding the prochiral carbonyl carbon.

1.5 *Optimization of catalyst loading*

All of the above alkylation reactions have been carried out in the presence of 15 mol % chiral catalyst, 50 mol % diethylphosphoramidate **1.17**, and with large excesses of dialkylzinc reagents; fortunately, we were able to lower the loading of these reagents with only minimal decreases in reaction selectivity and efficiency. We subjected three substrates (**1.1a, d-e**, Table 1.6) to alkylation reactions with Et_2Zn with reduced reagent loadings (5 mol % Al(O*i*-Pr)$_3$, 5 mol % chiral ligand **1.16**, 1.5 equiv Et_2Zn, and 25 mol % phosphoramidate additive **1.17**). In fact, enantioselectivities were only moderately

reduced (76% ee (vs. 84% ee) with R = Ph, entry 1; 85% ee (vs. 89% ee) with R = *p*-OMe-C_6H_4, entry 2; 64% ee (vs. 84% ee) with R = *p*-I-C_6H_4, entry 3, Table 1.6).

Table 1.6: Enantioselective addition of Et_2Zn to α-ketoesters with 5 mol % catalyst loading

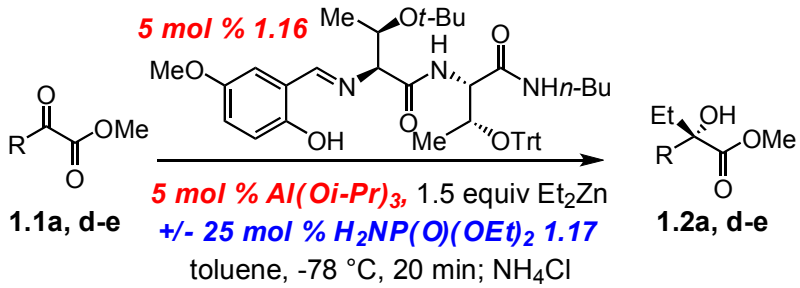

			without additive		*with 25 mol % **1.17***	
entry	**R**		**yield (%)[a]**	**ee (%)[a]**	**yield(%)[a]**	**ee (%)[a]**
1	Ph	**a**	95	71	93	76
2	*p*-OMe-C_6H_4	**d**	81[b]	73	97	85
3	*p*-I-C_6H_4	**e**	40[b]	61	98	64

[a] determined by chiral GLC analysis. [b] % conv

In reactions with Me_2Zn, we were able to lower the catalyst loading to 10 mol % Al(O*i*-Pr)$_3$ and 10 mol % chiral ligand **1.16** with minimal loss of selectivity and efficiency (94% conv, 89% ee with 10 mol % catalyst vs. >98% conv, 91% ee with 15 mol % catalyst; entries 1-2, Table 1.7). Further lowering of the catalyst loading below 10 mol % resulted in significant degradation of conversion and enantioselectivity (47-77 % conv, 83-86% ee, entries 3-4).

Table 1.7: The effect of catalyst loading on the Al-catalyzed alkylation of α-ketoesters with Me_2Zn

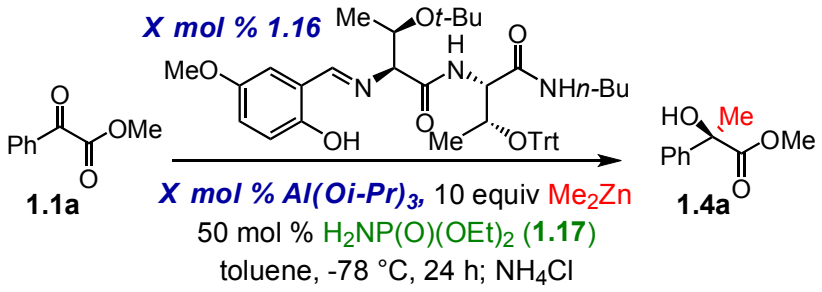

entry	catalyst loading	% conv[a]	% ee[a]
1	15 %	>98	91
2	10 %	94	89
3	7.5 %	77	86
4	5 %	47	83

[a] determined by chiral GLC analysis

1.6 *Limitations of this method: Alkylations with R_2Zn reagents other than Me_2Zn or Et_2Zn*

While we were able to develop an efficient method for alkylations of α-ketoesters with both Me_2Zn and Et_2Zn, we decided to test the scope of this method in terms of dialkylzinc reagents. Unfortunately, no selectivity was observed with either Ph_2Zn or *i*-Pr_2Zn (Scheme 1.5). Full conversion was observed after 20 minutes in each case, and we attribute the lack of selectivity to non-catalyzed background reactions with these highly reactive nucleophiles. Despite our attempts at optimization, we were unable to improve reactions with either nucleophile, and this lack of reagent generality remains a significant problem that needs to be addressed.[24]

(24) This same lack of reagent generality was observed in a related Al-peptide catalyzed addition of Et_2Zn and Me_2Zn to pyridyl-alkynylketones. See ref. 15a.

Scheme 1.5: Al-catalyzed additions of Ph_2Zn and *i*-Pr_2Zn to α-ketoesters

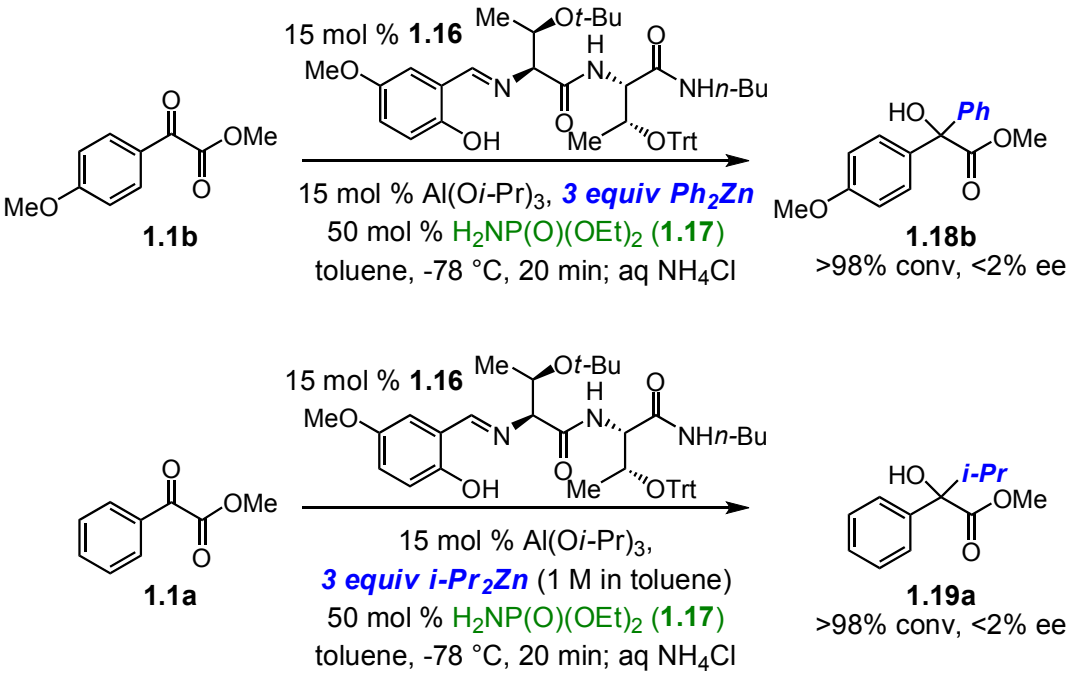

1.7 *Mechanistic investigations*

1.7.a The identity of each amino acid is important for reaction efficiency as well as selectivity

In order to probe the origin of enantioselectivity with chiral peptide-based ligand **1.16**, we synthesized modified ligand **1.20**, which contains D-Thr(O*t*-Bu) as AA1, and ligands **1.21-22**, which contain a Gly residue as either AA1 or AA2 (Table 1.8). With 15 mol % of diastereomer **1.20** and in the presence of 15 mol % Al(O*i*-Pr)$_3$ and 3 equiv Et_2Zn (in the absence of Lewis basic additive **1.17**), we found that both reactivity and enantioselectivity were significantly diminished (80% conv, -15% ee after 24 h; entry 2, Table 1.8). When we removed chirality at either position (**1.21** and **1.22**, AA1 or AA2 = Gly; entries 3-4), reactivity was further diminished (15-20 % conv), and selectivity again suffered significantly (-30-<10% ee). These findings indicate that each amino acid has an active role in determining selectivity and influencing reactivity in the transition state (see Figure 1.13, Section 1.9 (page 46)).

Table 1.8: AA1 and AA2 are equally important for both reactivity and selectivity

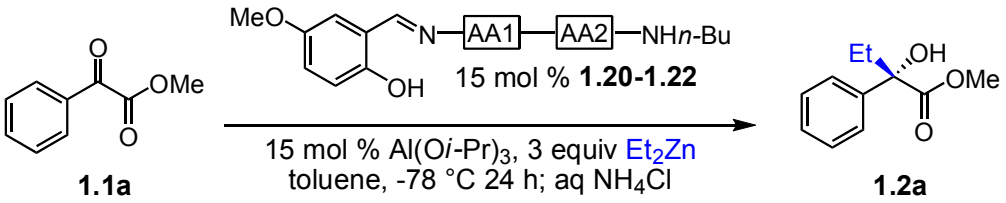

1.1a **1.2a**

entry	AA1	AA2		conv. (%)[a]	ee (%)[a]
1	L-Thr(*t*-Bu)	L-Thr(Trt)	**1.16**	>98	72
2	D-Thr(*t*-Bu)	L-Thr(Trt)	**1.20**	80	-15
3	Gly	L-Thr(Trt)	**1.21**	20	-30
4	L-Thr(*t*-Bu)	Gly	**1.22**	15	<10

[a] Determined by chiral GLC

1.7.b Identity of active Lewis acid (AlX_3)

We were interested in determining whether Al(O*i*-Pr)$_3$ was maintained as the active Lewis acid during the course of the alkylation reaction, or if it was alkylated *in situ* to generate $Et_xAl(O\textit{i}\text{-Pr})_{3-x}$. We generated these mixed Al species (x = 1-3),[25] and discovered that EtAl(O*i*-Pr)$_2$ was an equally effective Lewis acid (>98% conv, 72% ee with either EtAl(O*i*-Pr)$_2$ or Al(O*i*-Pr)$_3$; entries 1-2, Table 1.9). Increasing the number of alkyl substituents (vs. O*i*-Pr) on Al lead to a decrease in conversion as well as enantioselectivity (65% conv, 45% ee with Et_2Al(O*i*-Pr); entry 3). Triethylaluminum (entry 4) was a totally inactive Lewis acid, affording less than one catalytic turnover. These data suggest that the active Lewis acidic Al(III) species present under the described reaction conditions is likely either Al(O*i*-Pr)$_3$ or EtAl(O*i*-Pr)$_2$.

(25) AlX_3 compounds were prepared by mixing the appropriate amounts of Al(O*i*-Pr)$_3$ and $AlEt_3$ as described in: "Chemical Vapor Deposition of Al_2O_3 Films Using Highly Volatile Single Sources," Koh, W.; Ku, S.-J.; Kim, Y. *Thin Solid Films,* **1997**, *304*, 222-224.

Table 1.9: Activity of various Al(III) Lewis Acids

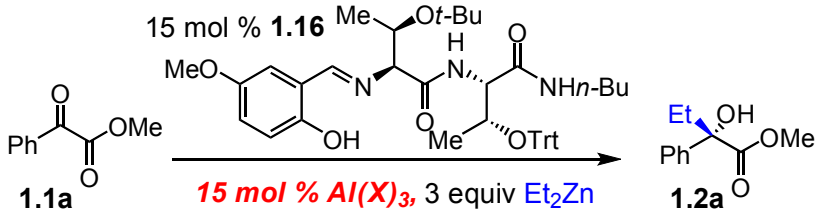

entry	Lewis Acid (AlX_3)	% conv[a]	% ee[a]
1	$Al(O\textit{i}\text{-}Pr)_3$	>98	72
2	$EtAl(O\textit{i}\text{-}Pr)_2$	>98	72
3	$Et_2AlO\textit{i}\text{-}Pr$	65[b]	45
4	Et_3Al	10	<2

[a] determined by chiral GLC analysis
[b] 7% reduced product

1.7.c The nature of the active nucleophile: Alkylzinc vs. alkylaluminum[26]

We next set out to determine whether $EtAl(O\textit{i}\text{-}Pr)_2$ is not only an effective Lewis acid, but an efficient alkylating agent. In the presence 1-2 equiv $EtAl(O\textit{i}\text{-}Pr)_2$ and one equiv ligand **1.16** (entries 1-2, Table 1.10), the alkylation product **1.2a** was observed in <10% conv and <2% ee. When a catalytic amount of ligand **1.16** was utilized, **1.2a** was observed in 31% conv and <2% ee (entry 3). The same result was observed in the absence of chiral ligand (35% conv, <2% ee, entry 4), which indicates that the observed reactivity was non-ligand-accelerated. These results suggested that $EtAl(O\textit{i}\text{-}Pr)_2$ was not an effective alkylating agent in the enantioselective Al-catalyzed addition of Et_2Zn to α-ketoesters. Thus, we concluded that the alkyl group is transferred from Zn, rather than Al.

(26) In $Ti(O\textit{i}\text{-}Pr)_4$ catalyzed alkylations with $(alkyl)_2Zn$ reagents, the active alkylating species is alkyl-$Ti(OR)_3$, where R = *i*-Pr or a chiral ligand. (a) "Ti-TADDOLate-Catalyzed, Highly Enantioselective Addition of Alkyl- and Aryl-titanium Derivatives to Aldehydes," Weber, B.; Seebach, D. *Tetrahedron* **1994**, *50*, 7473-7484. (b) "Titanium-Catalyzed Enantioselective Additions of Alkyl Groups to Aldehydes: Mechanistic Studies and New Concepts in Asymmetric Catalysis," Walsh, P. J. *Acc. Chem. Res*. **2003**, *36*, 739-749.

Table 1.10: Investigations of the active alkylating species: alkylaluminum vs. alkylzinc

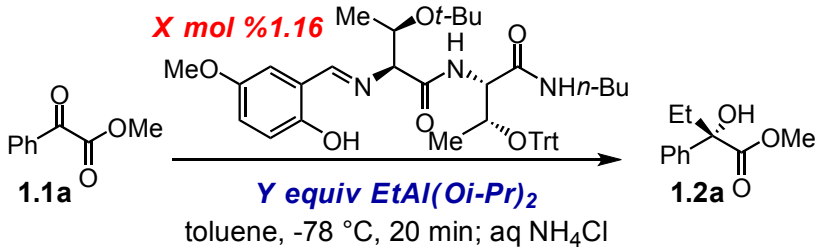

entry	mol % 1.16	equiv $EtAl(O\textit{i}\text{-}Pr)_2$	% conv[a]	% ee[a]
1	100	1	<10	<2
2	100	2	<10	<2
3	5	1	31	<2
4	-	1	35	<2

[a] Determined by chiral GLC analysis.

1.7.d Non-linear studies

We tested the Al-catalyzed alkylation of **1.1a** with Et_2Zn in the presence of non-enantiopure catalyst to determine whether there was nonlinearity associated with this catalytic enantioselective transformation (i.e. a 'nonlinear' relationship between % ee of product and % ee of catalyst). Nonlinearity in catalytic systems is commonly attributed to the formation of catalyst dimers or other higher order aggregates.[27] We specifically wanted to test the hypothesis that diethylphosphoramidate (**1.17**) may simply break up aggregates formed from combinations of ligand **1.16**, $Al(O\textit{i}\text{-}Pr)_3$ and R_2Zn. This would partly explain the observed increase in reactivity in the presence of diethylphosphoramidate **1.17**. As shown in Figure 1.6, there is a positive nonlinear effect observed in both the presence and the absence of **1.17**. Since the non-linearity is so similar in both cases, we concluded that the main function of **1.17** is not to break up these aggregates. It is important to note that the presence of a non-linear effect indicates the

(27) "Nonlinear Effects in Asymmetric Catalysis," Guillaneux, D.; Zhao, S.-H.; Samuel, O.; Rainford, D.; Kagan, H. B. *J. Am. Chem. Soc*. **1994**, *116*, 9430-0439.

possibility that the active catalyst is dimeric, however further mechanistic studies would be required in order to elucidate the structure of the active catalyst.[28]

Figure 1.6: Nonlinear studies in the presence (▲) and absence (●) of ligand **1.17**

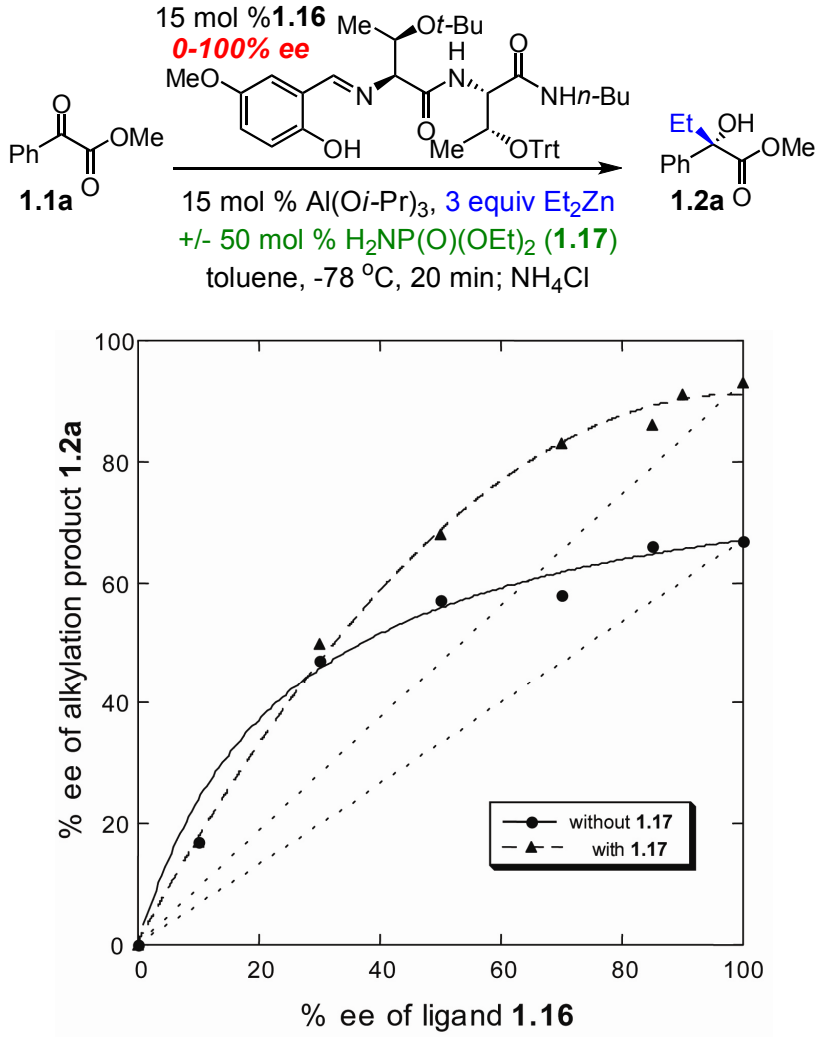

(28) A similar level of non-linearity was observed in the Sharpless asymmetric epoxidation. In this case, the active catalyst was explicitly shown to be dimeric. For relevant references, see: (a) "Mechanism of Asymmetric Epoxidation. 2. Catalyst Structure," Finn, M. G.; Sharpless, B. K. *J. Am. Chem. Soc*. **1991**, *113*, 113-126. (b) "Nonlinear Effects in Asymmetric Synthesis. Examples in Asymmetric Oxidations and Aldolization Reactions," Puchot, C.; Samuel, O. Cuñach, E.; Zhao, S.; Agami, C.; Kagan, H. B. *J. Am. Chem. Soc.* **1986**, *108*, 2353-2357.

1.7.e Absolute configuration of tertiary alcohols 1.2 and 1.4 derived from Al-catalyzed enantioselective addition of dialkylzinc reagents to α-ketoesters 1.1

We determined the absolute configuration of aromatic tertiary alcohols **1.2a** and **1.4a** and were surprised to find that the absolute configurations of these two alcohols were opposite.[29,30,31] This implied that the facial selectivity for nucleophilic attack was opposite for Et_2Zn compared to Me_2Zn for this substrate (**1.1a**). In order to confirm this observation, we converted the tertiary alcohols into the related diols (***(S)*-(-)-1.20a**[32] and **(*R*)-(-)-1.21a**[33]) and tertiary α-hydroxy acid (***(S)*-(+)-1.19a**)[34] and determined the absolute configuration of each of these compounds independently by comparison to known values (Figure 1.7). Evaluation of these data led us to affirm that, in the case of methylbenzoylformate (**1.1a**), Me_2Zn approaches from the *si* face to give ***(R)*-(-)-1.4a**, whereas Et_2Zn approaches from the *re* face to give ***(S)*-(+)-1.2a**.

---

(29) (a) $[\alpha]_D$ +24.7 (neat) reported for ***(S)*-(+)-1.2a**; $[\alpha]_D$ +18.3 (neat) reported for ***(S)*-(+)-1.4a**: "Optically Active Methyl- and Ethyl-Benzoins," McKenzie, A.; Ritchie, A. *Chem. Ber*. **1937**, *70B*, 23-36.
(30) $[\alpha]_D$ +7.35 (c 9.6, MeOH) reported for ***(S)*-(+)-1.2a**: "Asymmetric Syntheses Based on 1,3-Oxathianes. 2. Synthesis of Chiral Tertiary α-Hydroxy Aldehydes, α-Hydroxy Acids, Glycols [$R_1R_2C(OH)CH_2OH$], and Carbinols [$R_1R_2C(OH)Me$] in High Enantiomeric Purity," Lynch, J. E.; Eliel, E. L. *J. Am. Chem. Soc*. **1984**, *106*, 2943-2948.
(31) $[\alpha]_D$ -4.6 (c 1.17, MeOH) reported for ***(R)*-(-)-1.4a**: ref. 6. The authors confirmed their stereochemical assignment by comparison with the compound prepared by methanolysis of a known chiral cyanohydrin: "Switching Enantiofacial Selectivities Using One Chiral Source: Catalytic Enantioselective Synthesis of the Key Intermediate for (20S)-Camptothecin Family by (S)-Selective Cyanosilylation of Ketones," Yabu, K.; Masumoto, S.; Yamasaki, S.; Hamashima, Y.; Kanai, M.; Du, W.; Curran, D. P.; Shibasaki, M. *J. Am Chem. Soc.* **2001**, *123*, 9908-9909.
(32) $[\alpha]_D$ +7.3 (c 0.7, EtOH) reported for ***(R)*-(-)-1.20a**: "*N*-Boc 2-Acyloxazolidines: Useful Precursors to Enantiopure 1,2-Diols via Highly Diastereoselective Nucleophilic Additions," Agami, C.; Couty, F.; Lequesne, C. *Tetrahedron* **1995**, *51*, 4043-4056.
(33) $[\alpha]_D$ +8.9 (c 0.67, Et_2O) reported for ***(S)*-(+)-1.21a**: "The Mechanism of Halide Reductions with Lithium Aluminum Hydride II. Reduction of 2-Chloro-2-phenylpropionic Acid," Eliel, E. L.; Freeman, J. P. *J. Am. Chem. Soc*. **1952**, *74*, 923-928.
(34) $[\alpha]_D$ +33.7 reported for ***(S)*-(+)-1.19a**: "Absolute Configurations of 2-Phenyl-2-Butanol, 2-Hydroxy-2-Phenylbutyric Acid, and 3-Phenyl-1,3-Butanediol," Mitsui, S.; Imaizumi, S.; Senda, Y.; Konno, K. *Chem. Ind. (London, UK)* **1964**, *6*, 233-234.

Figure 1.7: Facial selectivity of Et_2Zn and Me_2Zn observed with **1.1a**

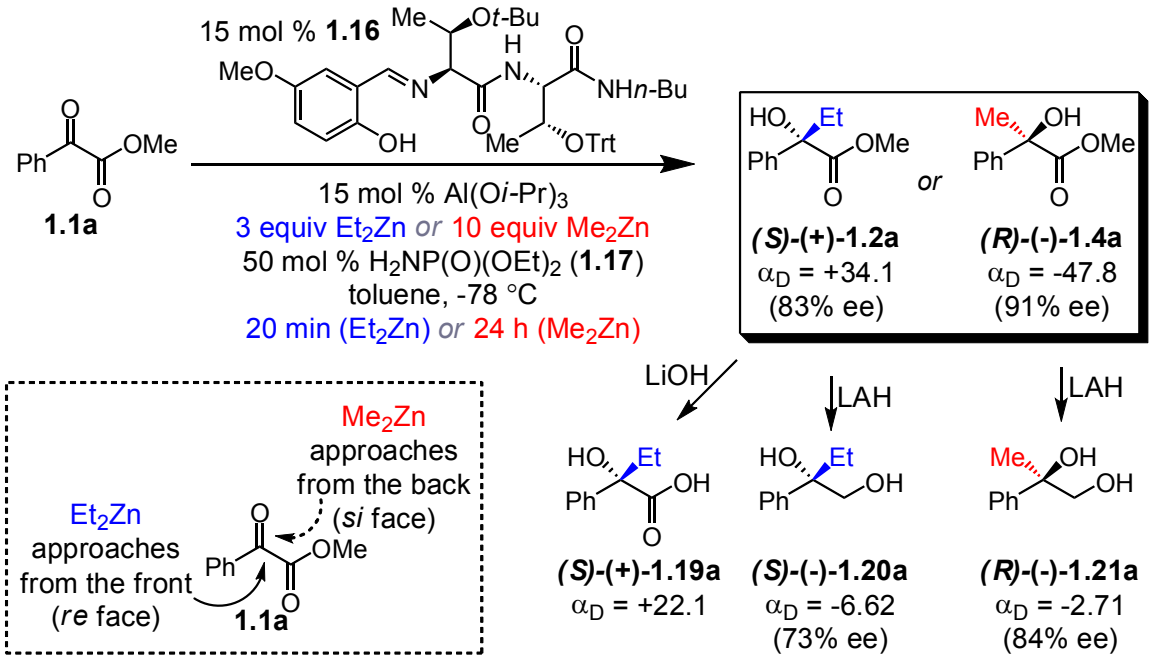

This appears to hold true for all aromatic substrates, although this has only been suggested by qualitative observations. For each nucleophile (Et_2Zn or Me_2Zn), the same enantiomer consistently elutes first by chiral GLC (Table 1.11 and Table 1.12, below). However, there are two cases within Et_2Zn addition where the sign for optical rotation is negative (entries 3 and 5, Table 1.11), suggesting the possibility that there may be variations within a substrate class.

Table 1.11: Optical rotation data for *ethyl*-substituted tertiary alcohols **1.2a-l**

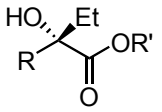

1.2a-l

entry	R	R'		α_D^{20}	c (g/dL)	First enantiomer eluted on GLC
1	Ph	Me	**1.2a**	+ 34.1	0.493	minor[a]
2	Ph	*t*-Bu	**1.2b**	+ 30.0	0.713	minor[b]
3	Ph	Bn	**1.2c**	- 3.10	1.13	minor[a]
4	*p*-$OMeC_6H_4$	Me	**1.2d**	+ 41.3	0.667	minor[a]
5	*o*-$OMeC_6H_4$	Me	**1.2e**	- 21.4	0.606	minor[a]
6	*p*-IC_6H_4	Me	**1.2g**	+ 22.9	0.220	minor[a]
7	*p*-MeC_6H_4	Me	**1.2h**	+ 33.1	0.553	minor[b]
8	2-fur	Me	**1.2i**	+ 24.5	0.513	minor[a]
9	3-fur	Me	**1.2j**	+ 15.9	0.540	minor[a]
10	Cy	Me	**1.2l**	+ 12.6	0.429	minor[a]

[a]β-dex [b]CD-BPM

Table 1.12: Optical rotation data for *methyl*-substituted tertiary alcohols **1.4a-c, l-o**

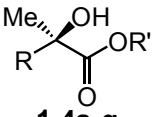

1.4a-g

entry	R	R'		α_D^{20}	c (g/dL)	First enantiomer eluted on GLC
1	Ph	Me	**1.4a**	- 47.8	0.780	major[a]
2	*p*-$OMeC_6H_4$	Me	**1.4b**	- 37.6	0.400	major[a]
3	Ph	*t*-Bu	**1.4c**	- 38.8	0.493	major[b]
4	Cy	Me	**1.4l**	- 15.0	0.453	major[a]
5	Et	Me	**1.4m**	- 6.78	0.853	major[b]
6	PhHC=CH	Me	**1.4n**	- 34.7	0.453	major[b]
7	PhC≡C	Me	**1.4o**	+ 17.2	0.693	major[c]

[a]β-dex [b]CDGTA [b]CD-BPM

In order to establish whether Et_2Zn and Me_2Zn always add from opposite faces, we tested aliphatic substrates **1.1m** (R = Et) and **1.1k** (R = Me) under the standard reaction conditions (Figure 1.8). We were surprised to find that the products of these alkylations were enantiomers, indicating that nucleophilic attack occurred from the same

face with either dialkylzinc reagent.[35] We determined the absolute configuration of **1.4m** (the product of Me_2Zn addition to **1.1m**) to be ***R*** through comparison with literature values, thus the product of Et_2Zn addition was ***S***.[36] In this case, both Et_2Zn and Me_2Zn approached from the back, which is in analogy to Me_2Zn addition to methylbenzoylformate (**1.1a**), and opposite to Et_2Zn addition to **1.1a**. The apparent anomaly within this series of alkylations is Et_2Zn addition to aryl-substituted **1.1a**, and therefore we based our transition state model (discussed in Section 1.9) on the absolute stereochemistry which was observed in the three other cases (i.e. approach from the *si* face).

Figure 1.8: Facial selectivity of Et_2Zn and Me_2Zn observed with aliphatic substrates **1.1m** and **1.1k**

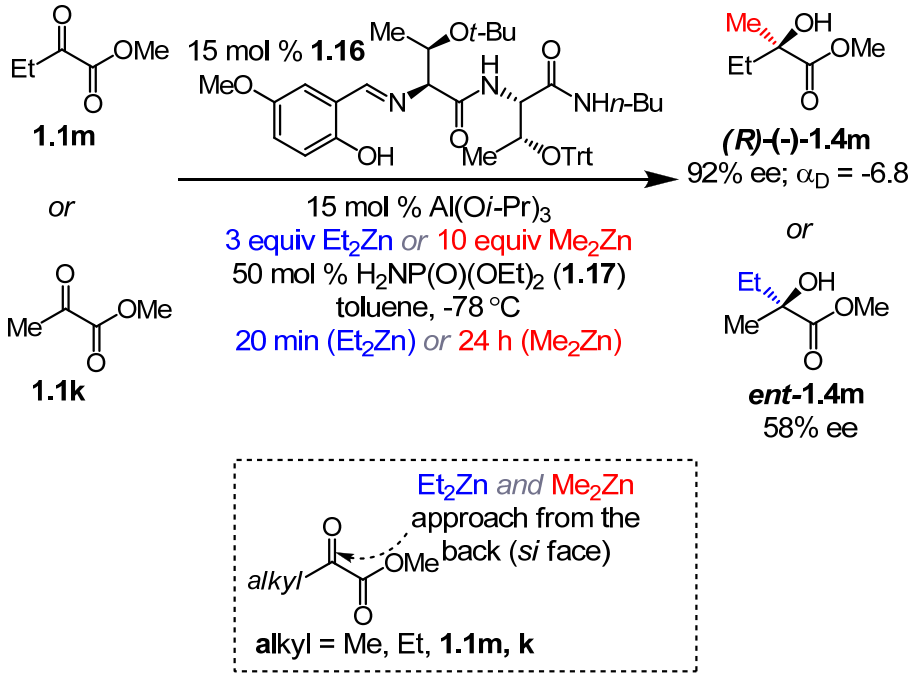

(35) The major enantiomer observed for the two alkylation products ***(R)*-(-)-1.4m** and *ent*-**1.4m** was opposite (determined by chiral GLC analysis) thus we determined these products to be enantiomers.
(36) $[\alpha]_D$ -2.5 (neat) reported for ***(R)*-(-)-1.4m**: "The Absolute Configuration of 2-Hydroxy-2-Methylbutyric Acid," Christensen, B. W.; Kjaer, A. *Acta. Chem. Scand*. **1962**, *16*, 2466-2467.

1.8 *Reactivity of dialkylzinc reagents, and Lewis base activation of Lewis acids*

1.8.a Structure and reactivity of dialkylzinc reagents

As mentioned in the introduction of this chapter, all of the methods described in the literature for additions of dialkylzinc reagents to α-ketoesters involved the use of Me_2Zn *or* Et_2Zn, but never both. This is most likely due to the large difference in reactivity between these two alkylzinc reagents. The reason for this reactivity difference has not been reported, but it can be rationalized by calculations which reveal that the C-Zn bond of Me_2Zn is stronger than in Et_2Zn.[37] As shown in

(37) "The length, strength and polarity of metal-carbon bonds: dialkylzinc compounds studied by density functional theory calculations, gas electron diffraction and photoelectron spectroscopy," Haaland, A.; Green, J. C.; McGrady, G. Sean, Downs, A. J.; Gullo, E.; Lyall, M. J.; Timberlake, J.; Tutukin, A. V.; Volden, H. V.; Østby, K.-A. *Dalton Trans*. **2003**, 4356-4366.

Table ***1.13***, there is a higher degree of charge separation between Zn and C in Me_2Zn (charge on Zn is +0.65 and charge on C is -0.99, leading to a difference of 1.64, entry 1), compared with Et_2Zn (charge on Zn is +0.52 and charge on C is -0.62, with a 1.14 difference in charge, entry 2). This charge separation correlates to increased ionic character of the C-Zn bond in Me_2Zn vs. Et_2Zn, as well as to the shorter bond length and greater bond strength of C-Zn in Me_2Zn vs. Et_2Zn (1.945 Å and 44.4 kcal/mol vs. 1.960 Å and 37.5 kcal/mol, respectively, entries 1-2).[37]

Table 1.13: Structural and electronic data of dialkylzinc reagents[a]

entry	R_2Zn	Length of C-Zn Bond (Å)	Strength of C-Zn Bond (kcal/mol)	C-Zn-C Angle (°)	Charge on Zn (e)	Charge on R (e)
1	Me_2Zn	1.945	44.4	180.0	+0.65	-0.99
2	Et_2Zn	1.960	37.5	179.9	+0.52	-0.62
3	*i*-Pr_2Zn	1.975	31.5	179.9	+0.42	-0.07
4	*t*-Bu_2Zn	1.988	27.7	180.0	+0.39	+0.09
5	*n*-Pr_2Zn	1.960	37.5	180.0	+0.52	-0.65
6	(neo-pentyl)$_2$Zn	1.963	37.5	179.4	+0.41	-0.70
7	$(Me_3SiCH_2)_2Zn$	1.948	46.6	179.9	+0.60	-1.13

[a] Determined by DFT calculations at the B3LYP/SDD level of theory and gas electron diffraction (GED)

Coordination of a Lewis basic ligand to a dialkylzinc reagent can drastically alter the length of the C-Zn bond (and thus its reactivity). X-ray crystallographic data of ten dialkylzinc-containing complexes are shown in Table 1.14. The Et_2Zn(18-crown-6) complex (entry 1) is essentially non-complexed Et_2Zn,[38] and was included as a comparison between the calculation data in

(38) This complex consists of Et_2Zn 'threaded' through an 18-crown-6. The Zn-O bond length is 2.867 Å, which is more consistent with an electrostatic interaction than an actual bonding interaction.

Table ***1.13*** (C-Zn bond distance = 1.960 Å) and the structural data in this table (C-Zn bond distance = 1.957 Å). In the complexed dialkylzinc species described in entries 2-10, the C-Zn bond lengths are significantly longer than their non-complexed counterparts (in Me_2Zn complexes, the C-Zn bond length ranges from 1.987 Å to 2.022 Å, vs. 1.945 Å for free Me_2Zn). This observed bond lengthening and concomitant increase in nucleophilicity of bound dialkylzinc reagents can be explained in terms of Lewis-base (donor) interactions with Lewis acids (acceptor) as described by Viktor Gutmann in 1978.[39]

Table 1.14: Structural data from X-ray crystal structures of some dialkylzinc complexes

entry	Complex	C-Zn (Å)	C-Zn-C angle (°)	N-Zn (Å)	N-Zn-N angle (°)	ref
1	Et_2Zn(18-crown-6)	1.957(5)	180	2.867[a,b]	na	40
2	$Me_2Zn[(CH_2NMe)_3]_2$	1.987(6)	145.1	2.410	105.6	41
3	Me_2Zn(*t*-Bu-dab)[c]	2.010(7)	137.3	2.010(7)	137.3	42
4	Me_2Zn[(-)-sparteine]	2.012[b]	128.2(4)	2.239[b]	80.4(2)	43
5	$Me_2Zn[Me_2N(CH_2)_2NMe_2]$	1.982[b]	135.8(3)	2.269(8)	79.8(3)	44
6	$(Me_3CCH_2)_2Zn[Me_2N(CH_2)_2NMe_2]$	2.000(5)	148.3(5)	2.411(4)	77.3(2)	44
7	$[Me_2Zn(C_5H_4N)(CH_2)_3(C_5H_4N)]_n$	2.000(5)	145.5(2)	2.241(3)	98.4(1)	45

(39) "The Donor-Acceptor Approach to Molecular Interactions," Gutmann, V. 1978, Plenum Press, New York.

(40) "X-ray Structures of Threaded Et_2Mg(18-crown-6) and Et_2Zn(18-crown-6)," Pajerski, A. D.; BergStresser, G. L.; Parvez, M.; Richey, H. G. Jr. *J. Am. Chem. Soc.* **1988**, *110*, 4844-4845.

(41) (a) "Triazine Adducts of Dimethylzinc and Dimethylcadmium: X-ray Crystal Structure of $Me_2Zn[(CH_2NMe)_3]_2$," Hursthouse, M. B.; Motevalli, M.; O'Brien, P.; Walsh, J. R. *Organometallics* **1991**, *10*, 3196-3200. (b) "X-ray Crystal Structure of a Triazene Adduct of Dimethylzinc: An Important Precursor for the Deposition of II/IV Materials," Hursthouse, M. B.; Motevalli, M.; O'Brien, P.; Walsh, J. R.; Jones, A. C. *J. Mater. Chem*. **1991**, *1*, 139-140.

(42) "Theoretical and Experimental Study of Diamagnetic and Paramagnetic Products from Thermal and Light-Induced Alkyl Transfer between Zinc or Magnesium Dialkyls and 1,4-Diaza-1,3-butadiene Substrates," Kaupp, M.; Stoll, H.; Preuss, H.; Kaim, W.; Stahl, T.; van Koten, G.; Wissing, E.; Smeets, W. J. J.; Spek, A. L. *J. Am. Chem. Soc*. **1991**, *113*, 5606-5618.

(43) "The Preparation, Reactivity, and Crystal Structure of a 1:1 Adduct of Dimethylzinc and (-)-Sparteine," Motevalli, M.; O'Brien, P.; Robinson, A. J.; Walsh, J. R.; Wyatt, P. B.; Jones, A. C. *J. Organomet. Chem*. **1993**, *461*, 5-7.

(44) "Structural Studies of Some Group 12 Metal Alkyl Adducts: the X-ray Crystal Structures of $Me_2Zn[Me_2N(CH_2)_2NMe_2]$, $Me_2Cd[Me_2N(CH_2)_2NMe_2]$, $(Me_3CCH_2)_2Zn[Me_2N(CH_2)_2NMe_2]$ and $(Me_3CCH_2)_2$ $Cd[Me_2N(CH_2)_2NMe_2]$," O'Brien, P.; Hursthouse, M. B.; Motevalli, M.; Walsh, J. R.; Jones, A. C. *J. Organomet. Chem.* **1993**, *449*, 1-8.

8	$(CF_3)_2Zn(C_5H_5N)_2$	2.062(9)[b]	121.7(1)	2.078(7)[b]	99.40(9)	46
9	$(Me_2Zn)_2$[N_4-aza crown]	2.022(6)[b]	125.5(2)	2.282(3)	87.19(1)	47
10	$(Me_2Zn)_2$[N_6-aza crown]	2.000(3)	138.10(13)	2.294(2)[b]	80.35(7)	47

[a]O-Zn bond length. [b]Average value. [c]dab = 1,4-Diaza-1,3-butadiene.

1.8.b Lewis base activation of Lewis acids: Gutmann's rules for bond-length variation[39]

While we generally consider the binding of a Lewis basic donor to a Lewis acidic acceptor as a net transfer of charge from the donor atom to the acceptor atom, Viktor Gutmann has established that this explanation may be an oversimplification. In 1978, Gutmann put together a set of four empirical rules which described variations in bond length and charge density within donor-acceptor complexes. His first rule states that in a donor-acceptor interaction, "the smaller the intermolecular distance between the donor and acceptor atoms, the greater the induced lengthening of the adjacent intramolecular bonds both in the donor and the acceptor molecules" (Figure 1.9).[39]

Figure 1.9: Induced bond-lengthening in intermolecular donor-acceptor complexes

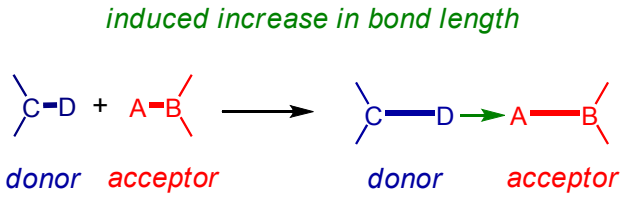

This rule is supported by the bond distances observed for BF_3 (Lewis acid) and NH_3 (Lewis base), compared to their adducts (Table 1.15).[39] Both the N-H and B-F bond distances are increased when NH_3 and BF_3 are complexed.

---

(45) "Nitrogen Lewis Base Adducts of Group 12 Alkyls: Molecular Structure of Poly[1,3-bis(4-pyridyl)propane]dimethylzinc, $[Me_2Zn(C_5H_4N)CH_2CH_2CH_2(C_5H_4N)]_n$," Pickett, N. L.; Lightfoot, P.; Cole-Hamilton, D. J. *Adv. Mater. Opt. Electron*. **1997**, *7*, 23-28.
(46) "Kristall- und Molekulstruktur von Bis(pyridine)bis(trifluoromethyl)zink," Behm, J.; Lotz, S. D.; Herrmann, W. A. *Z. Anorg. Allg. Chem*. **1993**, *619*, 849.
(47) "Dimethylzinc Adducts with Macrocyclic Amines," Coward, K. M.; Jones, A. C.; Steiner, A.; Bickley, J. F.; Smith, L. M.; Pemble, M. E. *J. Chem. Soc., Dalton Trans*. **2000**, 3480-3482.

Table 1.15: Bond distances in BF_3, NH_3, and their adduct

Compound	N-H distance (Å)	B-F distance (Å)	N-B distance (Å)
BF_3	-	1.30	-
NH_3	1.015	-	-
$H_3N{\rightarrow}BF_3$	a	1.38	1.60

[a]N-H bond distance in ammonium = 1.031 Å

The second bond-length variation rule states that "changes in bond lengths are induced throughout the molecule as the charge-density rearrangement takes place."[39] As shown in Figure 1.10, in the complexation of $SbCl_5$ with tetrachloroethylene carbonate, bond lengths increase when the charge transfer is from a more electropositive atom to a more electronegative atom (i.e. C→O), and vice verse (i.e. Cl→C).[39]

Figure 1.10: Changes in bond lengths of tetrachloroethylene carbonate and $SbCl_5$

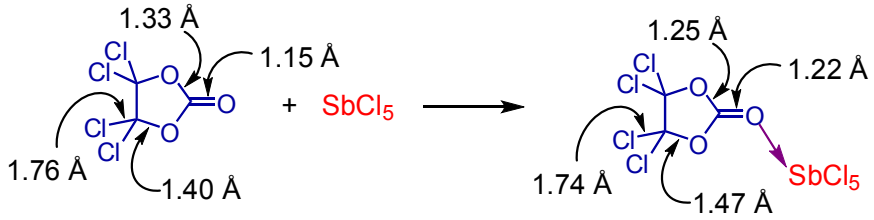

The third bond-length variation rule applies to adducts which also undergo a geometrical change and states that "as the coordination number increases, so do the lengths of the bonds originating from the coordination center."[39] This trend is observed in each adduct listed in Table 1.16.

Table 1.16: Bond length variations in coordination complexes[39]

Acceptor	M-X (Å)	Complex ion	M-X (Å)
$CdCl_2$	2.235	$CdCl_6^{4-}$	2.53
SiF_4	1.54	SiF_6^{2-}	1.71
$TiCl_4$	2.18-2.21	$TiCl_6^{2-}$	2.35
$ZrCl_4$	2.33	$ZrCl_6^{2-}$	2.45
GeF_4	1.67	GeF_6^{2-}	1.77
SnI_4	2.64	SnI_6^{2-}	2.85
PF_5	1.54-1.57	PF_6^-	1.73
I_2	2.53	I_3^-	2.83

Gutmann's fourth rule states that, "although a donor-acceptor interaction will result in a net transfer of electron density from the donor species to the acceptor species, it will, in the case of polyatomic species, actually lead to a net increase or 'pileup' of electron density at the donor atom of the donor species and to a net *decrease* or 'spillover' of electron density at the acceptor atom of the acceptor species."[48] Examples of this occurrence are shown in Figure 1.11.[49]

Figure 1.11: Lewis base donation into dihalide compounds.

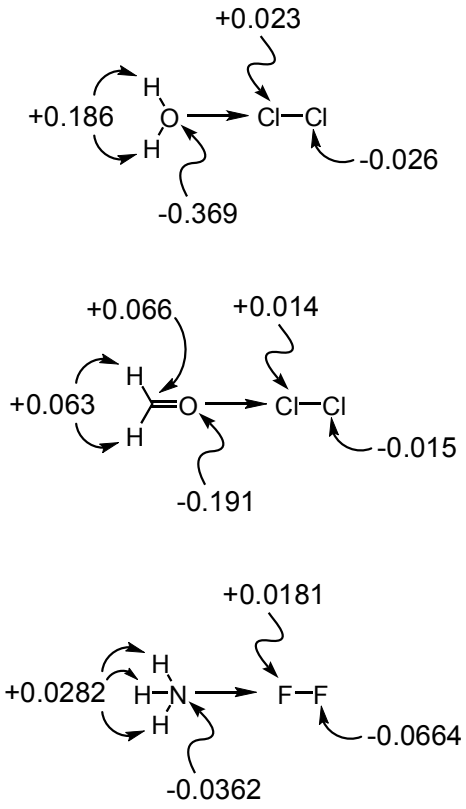

(48) "The Lewis Acid-Base Concepts: An Overview," Jensen, W. B. 1980, John Wiley & Sons, Inc., United States.
(49) Supported by self-consistent field (SCF, also referred to as HF, or Hartree-Fock) calculations.

1.8.c Lewis base activation of dialkylzinc complexes

In the context of nucleophilic additions, this 'pileup' of negative charge adjacent to the acceptor is called Lewis base *activation* of the nucleophile, as the increased negative charge on the adjacent group corresponds to an increase in nucleophilicity.[50]

Relevant to this work (Al-catalyzed enantioselective alkylations of α-ketoesters with dialkylzinc reagents) is a theoretical study on the structure and electronic properties of Me_2Zn complexes with a variety of bidentate ligands.[51] Data from these studies are shown in Table 1.17. As described above, coordination of bidentate ligands containing N and O results in lengthening of the C-Zn bond (as in Gutmann's first and third rule) and *an increase in the positive charge on Zn* ('spillover'), while *the charge on C becomes more negative* ('pileup' as in Gutmann's fourth rule).[52] In addition, the heteroatoms of the ligand (X and Y) become more negative, indicating that the charge is being distributed among all of the ligands on the Zn center (as in Gutmann's second rule).

Table 1.17: Structural and electronic data for Me_2Zn and complexes[51, a]

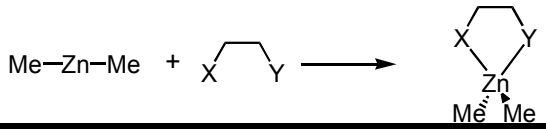

	ligand on Me_2Zn	C-Zn (Å)	Charge on Zn (e)	Charge on C (e)	Charge on X (e)	Charge on Y (e)	C-Zn-C angle (°)
1	None (Me_2Zn)	1.957	+1.247	-1.265	na	na	180.0
2	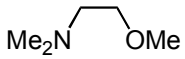	1.994	+1.337	-1.283	-0.605	-0.618	155.9
3	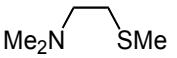	1.993	+1.316	-1.282	-0.603	+0.177	155.6
4	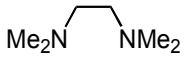	2.009	+1.364	-1.294	-0.642	-0.642	147.2

(50) Denmark has explored this concept for reactions involving Si-based nucleophiles. (a) "Lewis Base Catalysis in Organic Synthesis," Denmark, S. E.; Beutner, G. L. *Angew. Chem. Int. Ed*. **2008**, *47*, 1560-1638. (b) "Lewis Base Activation of Lewis Acids: Catalytic, Enantioselective Addition of Silylketene Acetals to Aldehydes," Denmark, S. E.; Beutner, G. L.; Wynn, T.; Eastgate, M. D. *J. Am. Chem. Soc*. **2005**, *127*, 3774-3789.

(51) "Theoretical Study on the Structure and Electronic Properties of Mono- and Bimetallic Methylzinc Complexes Containing Bidentate Ligands," Weston, J. *Organometallics* **2001**, *20*, 713-720.

(52) There is a strong Zn-S hyperconjugative interaction in ligands where X or Y = S.

5		1.977	+1.311	-1.275	-0.615	-1.006	164.1
6		1.976	+1.238	-1.270	+0.131	+0.131	165.6

[a]Calculated at the B3LYP/6-311+G(d,p) level of theory.

1.8.d Lewis base activation of dialkylzinc reagents by 1.17

In the context of our enantioselective alkylation reaction, we propose that diethylphosphoramidate additive **1.17** coordinates to the metal center of R_2Zn, resulting in an increase in the Lewis acidity of the zinc as well as an increase in electron density at the alkyl groups (Figure 1.12). The increased Lewis acidity of the Zn center may result in a stronger chelation with a Lewis basic portion of the chiral peptide ligand, leading to a more organized transition state which could result in the observed increase in enantioselectivity. The increased electron density on the alkyl groups, and the concomitant increase in nucleophilicity of these ligands, may result in the higher level of reactivity observed in the presence of phosphoramidate additive **1.17**.

Figure 1.12: Lewis base activation of dialkylzinc by diethylphosphoramidate

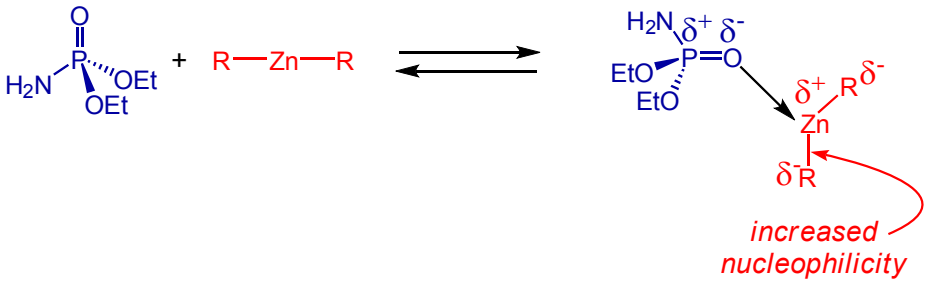

1.9 *Proposed transition state for the Al-catalyzed enantioselective addition of dialkylzinc reagents to α-ketoesters*

Drawing from observations described above, we propose the transition state structure illustrated in Figure 1.13. Based on studies with furyl substrates **1.1i-j** (Table 1.4), as well as the tendency of aluminum to exist as an octahedral complex,[53] we propose

(53) "The Structures of Some Aluminum Alkoxides," Shiner, V. J. Jr.; Whittaker, D.; Fernandez, V. P. *J. Am. Chem. Soc.* **1963**, *85*, 2318-2322.

that the α-ketoester substrate binds to Al in a two-point manner, chelating with the carbonyl moieties of the ester and ketone. Given the importance of the identity of AA2 on selectivity as well as reactivity, we propose that the amide of AA2 coordinates to Et_2Zn and delivers the nucleophile to the *si* face of the α-ketoester.[54] Association of Lewis basic additive **1.17** with the transition metal center of the alkylzinc reagent (**I→II**)[54] may lead to a beneficial redistribution of electron density ('pileup' as described above), enhancing the nucleophilicity of the alkylzinc reagent. The consequent 'spillover,' which gives rise to a more Lewis acidic Zn center, may result in a stronger Zn chelation with the Lewis basic amide, potentially producing a more organized transition state. Such electronic alteration would facilitate and promote directed delivery of the alkylzinc reagent by the AA2 moiety (vs. nondirected addition, which may lead to attack on the alternative face of the Al-bound carbonyl).

(54) **I** and **II** are proposed based on previous mechanistic studies of a related system. See: "Mechanism of Enantioselective Ti-Catalyzed Strecker Reaction. Peptide-Based Metal Complexes as Bifunctional Catalysts," Josephsohn, N. S.; Kuntz, K. W.; Snapper, M. L.; Hoveyda, A. H. *J. Am. Chem. Soc*. **2001**, *123*, 11594-11599.

Figure 1.13: Proposed transition state for Al-catalyzed enantioselective addition of dialkylzinc reagents to α-ketoesters

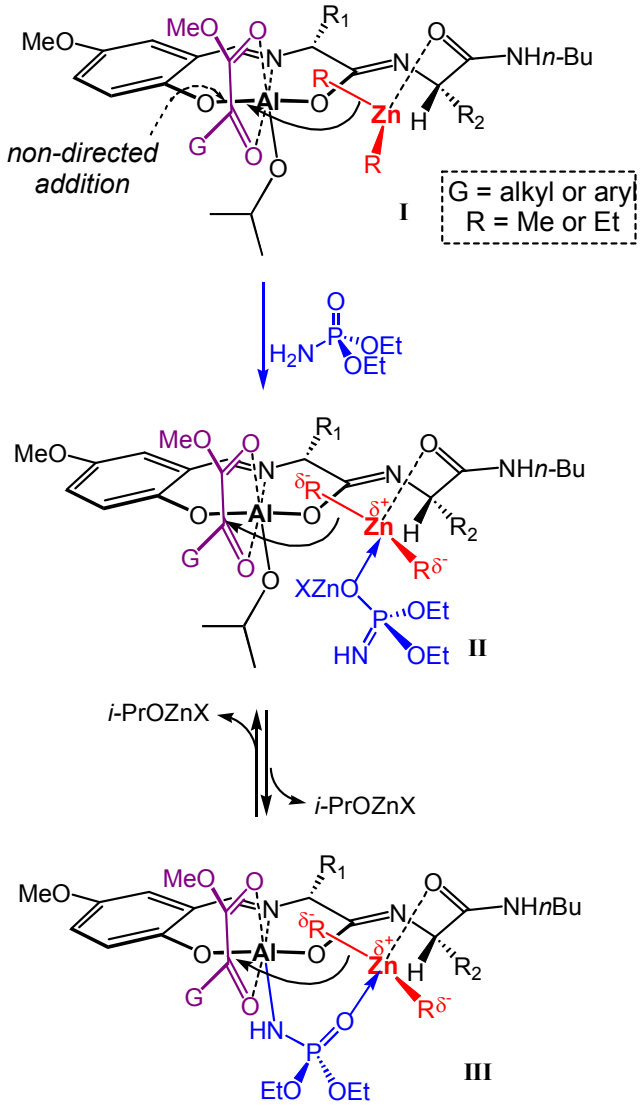

An alternative possibility, which would give rise to an even more organized transition state structure, is that diethylphosphoramidate **1.17** forms a bridging complex with Al, with extrusion of *i*-PrOH (**III**, Figure 1.13).

1.10 *Conclusions*

Enantioselective alkylation reactions with α-ketoesters have been described in the literature, however, *no general methods existed for addition of a variety of dialkylzinc*

reagents to this class of activated ketones. The work described herein is the most general report to date, as efficient and selective reactions with both Et_2Zn and Me_2Zn are included. While the vast difference in reactivity and selectivity observed among seemingly similar dialkylzinc reagents is not entirely clear, it can be partially explained by analysis of their electronic properties. We were able to quickly identify a selective amino acid-based chiral ligand for Al-catalyzed addition of Et_2Zn to α-ketoesters **1.1** through positional screening methods. In addition, we identified achiral Lewis basic additive diethylphosphoramidate (**1.17**), which has allowed us to apply this method to the far less reactive Me_2Zn**.** The addition of 50 mol % **1.17** to the reaction mixture resulted in an *increase in enantioselectivity* in all cases, and a *noticeable increase in reactivity* in almost all cases. In the absence of this Lewis basic additive, reactions with Et_2Zn are moderately efficient (ee's ranging from 44-83%) and reactions with Me_2Zn are substantially less practical (ee's ranging from 30-77%, with moderate yields). Ultimately, we aspire to discover a method for the addition of all dialkyl- and diarylzinc reagents to α-ketoesters (or similarly activated ketones). Our efforts toward this challenge have been unsuccessful thus far with systems similar to that presented herein, and will require the development of a new type of catalytic system.

1.11 *Experimentals*

General. Infrared (IR) spectra were recorded on a Perkin Elmer 781 spectrophotometer, ν_{max} in cm^{-1}. Bands were characterized as broad (br), strong (s), medium (m) or weak (w). ^1H NMR spectra were recorded on a Varian Unity INOVA 400 (400 MHz) spectrometer. Chemical shifts were reported in ppm from tetramethylsilane with the solvent resonance resulting from incomplete deuteration as the internal standard ($CDCl_3$: δ 7.26). Data were reported as follows: chemical shift, integration, multiplicity (s = singlet, d = doublet, t = triplet, q = quartet, br = broad, m = multiplet), coupling constants, and assignment. ^{13}C NMR spectra were recorded on a Varian Unity INOVA 400 (100 MHz) with complete proton decoupling. Chemical shifts were reported in ppm from tetramethylsilane with the solvent resonance as the internal standard ($CDCl_3$: δ 77.16). Enantiomeric ratios were

determined by chiral GLC analysis; (Alltech Associates Chiraldex GTA (CDGTA) column (30 m x 0.25 mm), Supelco Betadex (β-dex) 120 column (30 m x 0.25 mm), Supelco Alpha Dex (α-dex) 120 column (30m x 0.25 mm), or Alltech Associates Chiraldex B-PM (CDBPM) column (30m x 0.25 mm)) in comparison with authentic racemic materials. Elemental analyses were performed by Robertson Microlit Laboratories (Madison, New Jersey). High-resolution mass spectrometry was performed on a Micromass LCT ESI-MS (positive mode)) at the Mass Spectrometry Facility (Boston College). or at the University of Illinois Mass Spectrometry Laboratories (Urbana, Illinois). Optical rotation values were recorded on a Rudolph Research Analytical Autopol IV polarimeter.

Unless otherwise stated, all reactions were conducted in oven- (135 °C) and flame-dried glassware under an inert atmosphere of nitrogen. Solvents were purified under a positive pressure of dry argon by a modified Innovative Technologies purification system – toluene was purified through Cu and alumina columns. Diethylzinc was purchased from Aldrich and dimethylzinc was purchased from Strem and both were used without purification. Aluminum *iso*-propoxide was purchased from Strem and distilled (under vacuum, air-cooled condenser) immediately prior to use.[55] Diethylphosphoramidate (**1.17**) was purchased from Aldrich or synthesized using a known procedure[56] and distilled (under vacuum, air-cooled condenser) immediately prior to use. Unless otherwise stated, substrates were purchased from commercial sources or synthesized from commercially available starting materials using known methods[57] and purified immediately prior to use. EDC•HCl, HOBt•H_2O, piperidine, butylamine, Fmoc-protected

(55) Al(O*i*-Pr)$_3$ is a white powder prior to distillation and is insoluble in toluene. It exists as a clear liquid after distillation and is highly soluble. For details, see reference 53.

(56) "N,N-Dihalophosphoramides. Synthesis of Diethyl N,N-Dichlorophosphoroamidate (DCPA) and Some of its Structural Analogues," Zwierzac, A.; Koziara, A. *Tetrahedron*, **1970**, *26*, 3521-3525.

(57) (a) "(Cyanomethylene)phosphoranes as Novel Carbonyl 1,1-Dipole Synthons: An Efficient Synthesis of α-Keto Acids, Esters, and Amides," Wasserman, H. H.; Ho, W. B. *J. Org. Chem.* **1994**, *59*, 4364-4366. (b) "A General and Straightforward Approach to α,ω-Ketoesters," Babudri, F.; Fiandanese, V.; Marchese, G.; Punzi, A. *Tetrahedron* **1996**, *52*, 13513-13520. (c) "A Selective Method for the Preparation of Aliphatic Methyl Esters in the Presence of Aromatic Carboxylic Acids," Rodriguez, A.; Nomen, M.; Spur, B. W. *Tetrahedron Lett*, **1998**, *39*, 8563-8566. (d) "A Mild, Rapid, and Convenient Esterification of α-Keto Acids," Domagala, J. M. *Tetrahedron Lett*. **1980**, *21*, 4997-5000.

amino acids and 2-hydroxy-5-methoxybenzaldehyde were purchased from commercial sources and used without further purification.

Representative experimental procedure for Al-catalyzed addition of dialkylzinc reagents to α-ketoesters: An oven-dried 13x100 mm test tube was charged with Al(O*i*-Pr)$_3$ (1.5 mg, 7.5 μmol, in 250 μL toluene) and **1.16** (5.3 mg, 7.5 μmol, in 250 μL toluene) under an atmosphere of N_2 in a glove box. This solution was allowed to stir for 5 min. *t*-Butylbenzoylformate (**1.1c,** 10.3 mg, 0.0500 mmol) followed by diethyl phosphoramidate (**1.17,** 3.8 mg, 0.025 mmol) were added to this solution. The tube was sealed with a septum, electrical tape and Teflon tape and removed from the glove box. The resulting light yellow solution was allowed to cool to –78 °C, and Me_2Zn (CAUTION, PYROPHORIC! USE EXTREME CAUTION!, 35 μL, 0.50 mmol) was added through a syringe with stirring. The mixture was kept at –78 °C for 20 min before addition of a saturated solution of aqueous NH_4Cl (1 mL). The aqueous layer was washed with EtOAc (3 x 2 mL). Combined organic layers were passed through a short plug of silica and concentrated under reduced pressure to yield a pale yellow oil, which was purified by silica gel chromatography (20:1 hexanes/EtOAc) to afford **1.2c** as a clear liquid (10.6 mg, 0.048 mmol, 95% yield).

Analytical Data for Products of Al-Catalyzed Alkylations of a-Ketoesters with Et_2Zn:

1.2a: IR (neat): 3509 (s), 2961 (m), 1727 (s), 1451 (m), 1250 (s), 1115 (m). ^{1}H NMR (400 MHz, $CDCl_3$): δ 7.59 (2H, d, *J* = 8.4 Hz, Ar-**H**), 7.34 (2H, t, *J* = 8.4 Hz, Ar-**H**), 7.28 (1H, d, *J* = 6.9 Hz, Ar-**H**), 3.80 (1H, s, O**H**), 3.76 (3H, s, OC**H**$_3$), 2.23 (1H, dq, *J* = 14.3, 7.3 Hz, C**H**$_2$CH$_3$), 2.04 (1H, dq, *J* = 14.6, 7.3 Hz, C**H**$_2$CH$_3$), 0.92 (3H, dd, *J* = 7.3, 7.3 Hz, CH$_2$C**H**$_3$). ^{13}C NMR (100 MHz, $CDCl_3$): δ176.0, 142.0, 128.4 127.9, 125.8, 79.0, 53.4, 32.9, 8.3. HRMS Calcd for $C_{11}H_{14}O_3$ (M + Na): 217.0841; Found: 217.0838. $[\alpha]^{20}_D$ +34.1 (*c* = 0.493, $CHCl_3$) for an 84% ee sample. The optical purity of the compound was determined by chiral GLC analysis (β-dex, 140 °C, 15 psi.): t_R of **1.2a**

13.6 min (minor) and 14.0 min (major). The absolute configuration was assigned based on comparison with reported values. [29, 30]

rac-**1.2a**	**1.2a**
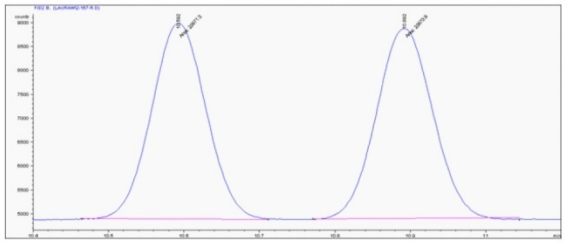	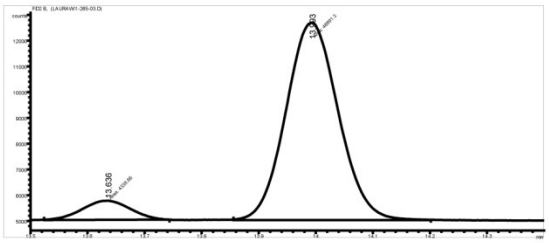

#	Time	Area	Height	Width	Area%	Symmetry
1	13.778	222239	32501.5	0.114	49.785	1.15
2	14.123	227796.6	32782.8	0.1091	50.215	0.911

#	Time	Area	Height	Width	Area%	Symmetry
1	13.636	4339.7	743.3	0.0973	8.153	1.12
2	13.993	48891.3	7665.8	0.1063	91.847	0.958

1.2b: IR (neat): 3509 (s), 2955 (s), 2835 (m), 1753 (s), 1608 (m). ^{1}H NMR (400 MHz, $CDCl_3$): δ 7.49 (2H, d, *J* = 8.4 Hz, Ar-**H**), 6.88 (2H, d, *J* = 8.8 Hz, Ar-**H**), 3.81 (3H, s, OC**H**$_3$), 3.78 (3H, s, OC**H**$_3$), 3.69 (1H, s, O**H**), 2.20 (1H, dq, *J* = 7.3, 7.0 Hz, C**H**$_2$CH$_3$), 2.01 (1H, dq, *J* = 7.3, 7.0 Hz, C**H**$_2$CH$_3$), 0.91 (3H, dd, *J* = 7.3, 7.3 Hz, CH$_2$C**H**$_3$). ^{13}C NMR (100 MHz, $CDCl_3$): δ 176.2, 159.0, 134.0, 126.8, 114.0, 78.8, 57.4, 53.2, 33.0, 8.8. HRMS Calcd for $C_{12}H_{16}O_4$ (M + Na): 247.0946; Found: 247.0942. $[\alpha]_D^{20}$ +41.268 (*c* = 0.667, $CHCl_3$) for an 89% ee sample. The optical purity of the compound was determined by chiral GLC analysis (CD-BPM, 140 ^{o}C, 10 psi.): t_R of **1.2b** 58 min (minor) and 60 min (major).

rac-**1.2b**	**1.2b**
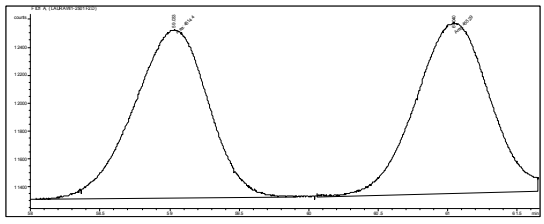	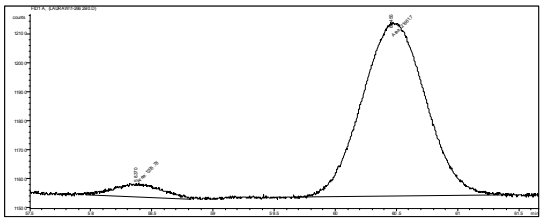

#	Time	Area	Height	Width	Area%	Symmetry
1	59.033	45144	1207.3	0.6232	49.788	1.171
2	61.04	45529	1226	0.6189	50.212	1.017

#	Time	Area	Height	Width	Area%	Symmetry
1	58.37	1205.8	47.1	0.427	5.273	0.836
2	60.455	21661.7	598.1	0.6036	94.727	0.844

1.2c: IR (neat): 3502 (s), 2980 (m), 2930 (m), 1715 (s), 1369 (m). ^{1}H NMR (400 MHz, $CDCl_3$): δ 7.58 (2H, d, *J* = 7.0 Hz, Ar-**H**), 7.32 (2H, t, *J* = 7.0 Hz, Ar-**H**), 7.24 (1H, d, *J* = 7.2 Hz, Ar-**H**), 3.81 (1H, s, O**H**), 2.17 (1H, dq, *J* = 14.7, 7.3 Hz, C**H**$_2$CH$_3$), 1.95 (1H, dq, *J* = 14.7, 7.3 Hz, C**H**$_2$CH$_3$), 1.43 (9H, s, OC(C**H**$_3$)$_3$), 0.92 (3H, dd, *J* = 7.3, 7.3 Hz, CH$_2$C**H**$_3$). ^{13}C NMR (100 MHz, $CDCl_3$): δ 174.7, 142.6, 128.2, 125.8, 127.6, 83.3, 78.7, 32.9 28.0, 8.2. HRMS Calcd for $C_{14}H_{20}O_3$: 236.1412; Found: 236.1414. $[\alpha]^{20}_D$ +30.0 (*c* = 0.713, $CHCl_3$) for a 66% ee sample. The optical purity of the compound was determined by chiral GLC analysis (β-dex, 120 °C, 15 psi.): t_R of **1.2c** 55 min (minor) and 56 min (major).

***rac*-1.2c**						**1.2c**					
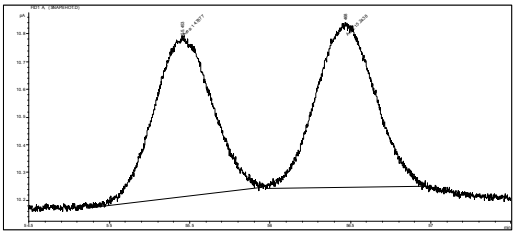						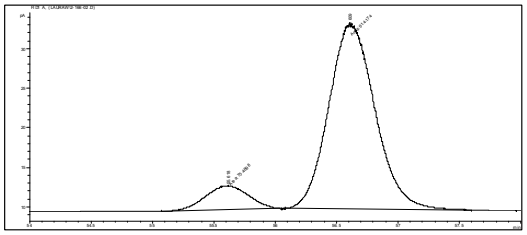					
#	Time	Area	Height	Width	Area%	Symmetry	#	Time	Area	Height	Width	Area%	Symmetry
1	55.453	14.8	5.8E-1	0.4236	49.241	0.942	1	55.618	75.5	3.1	0.4106	10.946	1.156
2	56.468	15.2	6E-1	0.4247	50.759	0.964	2	56.609	614.2	23.6	0.4335	89.054	0.829

1.2d: IR (neat): 3509 (m, br), 3062 (m), 3024 (m), 2961 (m), 2936 (m), 2878 (m), 1727 (s), 1495 (m), 1457 (m), 1231 (s), 1149 (s). ^{1}H NMR (400 MHz, CDCl3): δ 7.57 (2H, d, *J* = 8.1 Hz, Ar-H), 7.28 (8H, m, Ar-H), 5.23 (1H, d, *J* = 12.5 Hz, OCH2Ph), 5.13 (1H, d, *J* = 12.5 Hz, OCH2Ph), 3.72 (1H, s, OH), 2.23 (1H, dq, *J* = 14.7, 7.3 Hz, CH2CH3), 2.04 (1H, dq, *J* = 14.7, 7.3 Hz, CH2CH3), 0.88 (3H, dd, *J* = 7.3, 7.3 Hz, CH2CH3). ^{13}C NMR (100 MHz, CDCl3): δ. 175.4, 141.8, 135.3, 128.8, 128.7, 128.4, 128.3, 127.9, 125.8, 79.0, 68.2, 32.8, 8.2. Anal. Calcd for C17H18O3: 75.54% C, 6.71% H; Found: 75.50% C, 6.94% H. [α]20D -3.10 (c = 1.13, CHCl3) for an 82% ee sample. The optical purity of the compound was determined by chiral GLC analysis (β-dex, 140 °C, 20 psi.): t_R of **1.2d** 195 min (minor) and 199 min (major).

rac-**1.2d**	**1.2d**
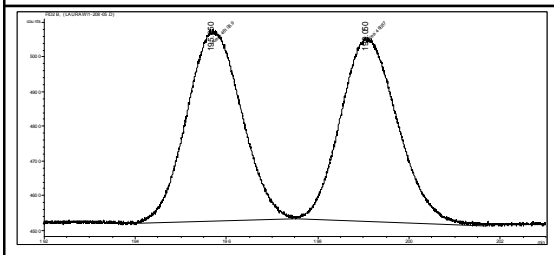	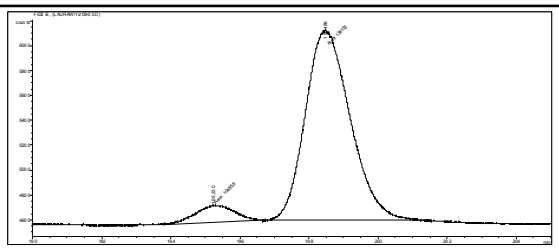

#	Time	Area	Height	Width	Area%	Symmetry
1	195.65	46106.9	554.5	1.3859	50.011	0.778
2	199.05	46087	528.3	1.454	49.989	0.774

#	Time	Area	Height	Width	Area%	Symmetry
1	195.23	10485.8	137.1	1.2752	7.055	0.854
2	198.48	138152.2	1535.2	1.4998	92.945	0.812

1.2e: IR (neat): 3503 (s, br), 2936 (m), 1741 (s), 1602 (w), 1489 (m), 1464 (m), 1438 (m), 1249 (s). ^{1}H NMR (400 MHz, $CDCl_3$): δ 7.46 (1H, d, *J* = 7.7 Hz,), 7.30 (1H, dd, *J* = 8.1, 7.7 Hz,), 6.99 (1 H, dd, *J* = 7.7, 7.7 Hz), 6.89 (1H, d, *J* = 8.1 Hz), 4.04 (1H, s, O**H**), 3.81 (3H, s, OC**H**$_3$), 3.70 (3H, s, OC**H**$_3$), 2.22 (2H, m, C**H**$_2$CH$_3$), 0.99 (3H, dd, *J* = 7.3, 7.3 Hz, CH$_2$C**H**$_3$). ^{13}C NMR (100 MHz, $CDCl_3$): δ 175.9, 157.2, 131.0, 129.5, 126.8, 121.0, 111.5, 76.9, 55.7, 52.7, 29.7, 8.1. HRMS Calcd for $C_{12}H_{16}O_4$: 224.1049; Found: 224.1054. $[\alpha]^{20}_D$ -21.4 (*c* = 0.606, $CHCl_3$) for a 75% ee sample. The optical purity of the compound was determined by chiral GLC analysis (β-dex, 120 ^oC, 15 psi.): t_R of **1.2e** 206 min (minor) and 209 min (major).

rac-**1.2e**	**1.2e**
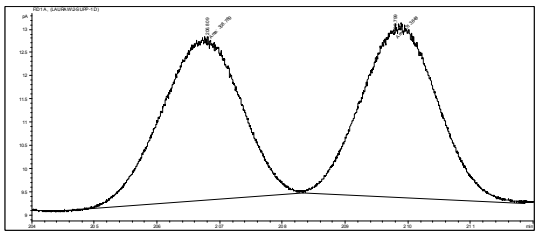	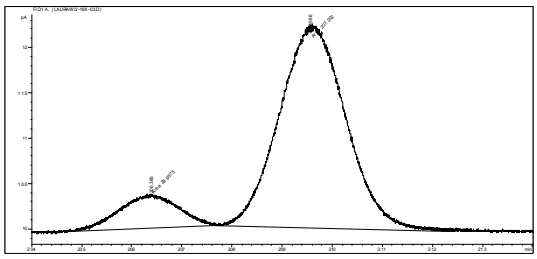

#	Time	Area	Height	Width	Area%	Symmetry
1	206.809	308.8	3.5	1.4692	49.610	1.331
2	209.799	313.6	3.7	1.4001	50.390	0.804

#	Time	Area	Height	Width	Area%	Symmetry
1	206.385	30	3.7E-1	1.3388	12.632	1.174
2	209.566	207.2	2.2	1.5417	87.368	0.865

1.2g: IR (neat): 3509 (s), 2967 (m), 1728 (s), 1482 (m). ^{1}H NMR (400 MHz, $CDCl_3$): δ 7.67 (2H, d, *J* = 8.8 Hz, Ar-**H**), 7.34 (2H, d, *J* = 8.4 Hz, Ar-**H**), 3.77 (3H, s, OC**H**$_3$), 3.70

(1H, s, O**H**), 2.15 (1H, dq, *J* = 14.3, 7.3 Hz, C**H**$_2$CH$_3$), 1.98 (1H, dq, *J* = 14.3, 7.3 Hz, C**H**$_2$CH$_3$), 0.90 (3H, dd, *J* = 7.3, 7.3 Hz, CH$_2$C**H**$_3$). ^{13}C NMR (100 MHz, $CDCl_3$): δ175.6, 141.6, 137.5, 128.0, 93.8, 78.7, 53.6, 32.9, 8.15. HRMS Calcd for $C_{11}H_{13}IO_3$ (M + Na): 342.9807; Found: 342.9814. $[\alpha]_D^{20}$ +22.9 (*c* = 0.220, $CHCl_3$) for an 82% ee sample. The optical purity of the compound was determined by chiral GLC analysis (β-dex, 140 °C, 20 psi.): t_R of **1.2g** 134 min (minor) and 142 min (major).

rac-**1.2g**							**1.2g**						
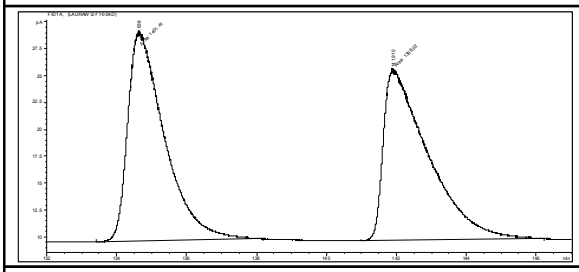							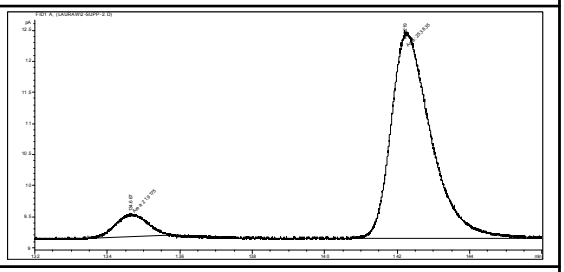						
#	Time	Area	Height	Width	Area%	Symmetry	#	Time	Area	Height	Width	Area%	Symmetry
1	134.638	1401.4	19.5	1.197	50.096	0.434	1	134.667	21.9	3.6E-1	1.0028	7.954	0.944
2	141.91	1396	15.9	1.4592	49.904	0.277	2	142.219	253.6	3.3	1.269	92.046	0.531

1.2h: IR (neat): 3521 (m, br), 2955 (m), 2930 (m), 1728 (s), 1243 (s). ^{1}H NMR (400 MHz, $CDCl_3$): δ 0.90 (3H, dd, *J* = 7.3 Hz, CH$_2$C**H**$_3$), 2.00 (1H, dq, *J* = 7.3, 14.7 Hz, C**H**$_2$CH$_3$), 2.32 (1H, dq, *J* = 7.3, 14.7 Hz, C**H**$_2$CH$_3$), 2.32 (3H, s, Ar-C**H**$_3$), 3.67 (1H, s, O**H**), 3.76 (3H, s, OC**H**$_3$), 7.14 (2H, d, *J* = 8.1 Hz, Ar-**H**), 7.45 (2H, d, *J* = 8.4 Hz, Ar-**H**). ^{13}C NMR (100 MHz, $CDCl_3$): δ 176.17, 139.02, 137.58, 129.13, 125.67, 78.88, 53.36, 32.77, 21.20, 8.25. HRMS Calcd for $C_{12}H_{16}O_3$: 208.11; Found: 208.1097. $[\alpha]^{20}_D$ +33.1 (c = 0.553, $CHCl_3$) for a 75% ee sample. The optical purity of the compound was determined by chiral GLC analysis (CDBPM, 140°C, 20 psi.) t_R of **1.2h** 17.2 min (minor) and 17.7 min (major).

1.2i: IR (neat): 3458 (s), 1741 (m), 1652 (m), 1256 (m), 1149 (m). ^{1}H NMR (400 MHz, $CDCl_3$): δ 0.92 (3H, dd, *J* = 7.3 Hz, CH$_2$C**H**$_3$), 2.13 (1H, ddq, *J* = 7.3, 14.6 Hz, C**H**$_2$CH$_3$), 3.74 (1H, s, O**H**), 3.79 (3H, s, OC**H**$_3$), 6.33 (2H, s, Ar-**H**), 7.39 (1H, s, Ar-**H**). ^{13}C NMR

(100 MHz, $CDCl_3$): δ 174.33, 163.60, 142.62, 110.49, 107.00, 75.66, 53.59, 29.98, 7.79. Elemental analysis: Calcd for $C_9H_{12}O_4$: C = 58.69%, H = 6.57%; Found: C = 58.82%, H = 6.21%. $[\alpha]^{20}_D$ +24.5 (c = 0.513, $CHCl_3$) for a 33% ee sample. The optical purity of the compound was determined by chiral GLC analysis (β-dex, 80°C, 15 psi.) t_R of **1.2i** 155 min (minor) and 162 min (major).

1.2j: IR (neat): 3515 (m, br), 2955 (m), 2936 (m), 1740 (s), 1444 (m). ^{1}H NMR (400 MHz, $CDCl_3$): δ 7.43 (1H, s, Ar-**H**), 7.34 (1H, s, Ar-**H**), 6.40 (1H, s, Ar-**H**), 3.80 (3H, s, O**CH**$_3$), 3.59 (1H, s, O**H**), 2.03 (1H, dq, *J* = 14.3, 7.3 Hz, C**H**$_2$CH$_3$), 1.93 (1H, dq, *J* = 14.3, 7.3 Hz, C**H**$_2$CH$_3$), 0.89 (3H, dd, *J* = 7.3, 7.3 Hz, CH$_2$C**H**$_3$). ^{13}C NMR (100 MHz, $CDCl_3$): δ175.8, 143.3, 139.9, 128.2, 109.2, 75.4, 53.4, 33.2, 7.9. HRMS Calcd for $C_9H_{12}O_4$: 184.0736 Found: 184.0738. $[\alpha]^{20}_D$ +15.9 (*c* = 0.540, $CHCl_3$) for an 63% ee sample. The optical purity of the compound was determined by chiral GLC analysis (β-dex, 140 °C, 15 psi.) t_R of **1.2j** 10.6 min (minor) and 10.9 min (major).

***rac*-1.2j**

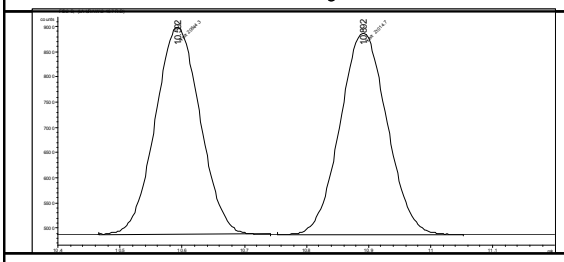

#	Time	Area	Height	Width	Area%	Symmetry
1	10.592	20644.3	4102.5	0.0839	49.555	0.96
2	10.892	21014.7	3999.5	0.0876	50.445	0.974

1.2j

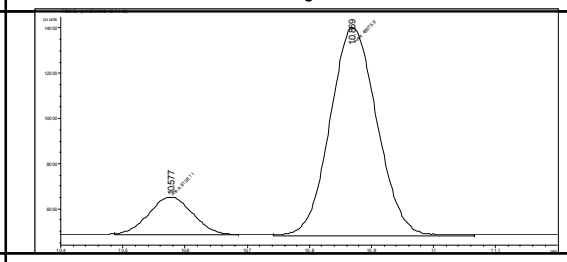

#	Time	Area	Height	Width	Area%	Symmetry
1	10.577	8108.1	1655.5	0.0816	85.721	0.984
2	10.869	48675.9	9241.9	0.0878	14.279	0.871

Analytical Data for Products of Al-Catalyzed Alkylations of a-Ketoesters with Et_2Zn:

1.4m (*ent*-1.2k): IR (neat): 3358 (m, br), 2917 (m), 2848 (m), 1772 (m) 1740 (m), 1652 (s), 1652 (s) , 1489 (s) , 1275 (s). ^{1}H NMR (400 MHz, $CDCl_3$): δ 3.77 (3H, s, O**CH**$_3$), 3.11 (1H, s, O**H**), 1.76 (1H, dq, *J* = 14.7, 7.3 Hz, C**H**$_2$CH$_3$), 1.67 (1H, dq, *J* = 14.7, 7.3 Hz, C**H**$_2$CH$_3$), 1.39 (3H, s, C**H**$_3$), 0.86 (3H, dd, *J* = 7.3, 7.3 Hz, CH$_2$C**H**$_3$). ^{13}C NMR (100 MHz, $CDCl_3$): δ147.3, 75.1, 52.8, 38.5, 33.2, 25.7. HRMS Calcd for $C_6H_{12}O_3$ (M +

Na): 155.0684; Found: 155.0685. $[\alpha]^{20}_{D}$ -6.78 (*c* = 0.853, $CHCl_3$) for an 80% ee sample of **8i**. The optical purity of the compound was determined by chiral GLC analysis (CDGTA, 60 ^{o}C, 15 psi.) t_R of **1.4m** 17 min (minor) and 18 min (major). The absolute configuration was assigned based on comparison with a reported value. [36]

***rac*-1.2k, 1.4m**

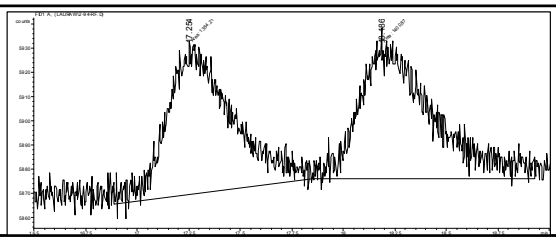

#	Time	Area	Height	Width	Area%	Symmetry
1	17.254	1354.2	64.7	0.3487	49.152	0.554
2	18.186	1400.9	63.5	0.3676	50.848	0.457

1.2k

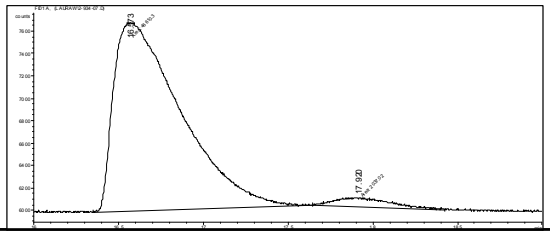

#	Time	Area	Height	Width	Area%	Symmetry
1	16.573	46610.3	1684.8	0.4611	95.813	0.337
2	17.92	2037	89.2	0.3806	4.187	0.705

1.4m

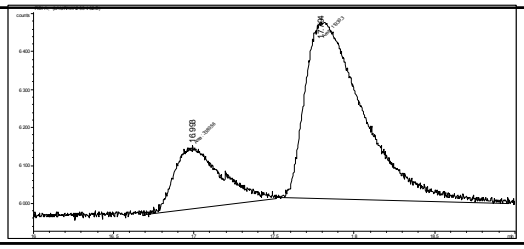

#	Time	Area	Height	Width	Area%	Symmetry
1	16.993	3389.6	167.8	0.3367	22.112	0.625
2	17.794	11939.3	466.1	0.4269	77.888	0.377

1.4a: IR (neat): 3503 (s), 2987 (m), 2955 (m), 1734 (s), 1445 (m). ^{1}H NMR (400 MHz, $CDCl_3$): δ 7.53 (2H, d, *J* = 7.6 Hz,), 7.35 (1H, t, *J* = 7.6 Hz), 7.30 (2H, d, *J* = 7.2 Hz), 3.77 (3H, s, OC**H**$_3$), 3.70 (1H, s, O**H**), 1.77 (3H, s, C**H**$_3$). ^{13}C NMR (100 MHz, $CDCl_3$): δ176.3, 142.9, 128.6, 128.1, 125.4, 76.0, 53.5, 26.9. HRMS Calcd for $C_{10}H_{12}O_3$ (M + Na): 203.0684; Found: 203.0675. $[\alpha]^{20}_{D}$ -47.8 (*c* = 0.780, $CHCl_3$) for a 91% ee sample. The optical purity of the compound was determined by chiral GLC analysis (β-dex, 135

°C, 15 psi.) t_R of **1.4a** 72 min (major) and 77 min (minor). The absolute configuration was assigned based on comparison with reported values.[58]

rac-**1.4a**						**1.4a**					
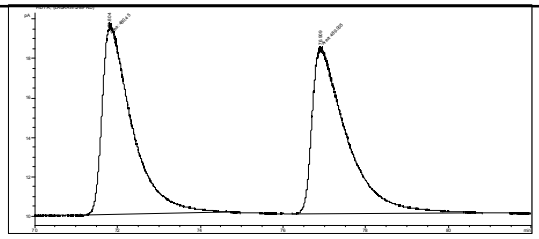						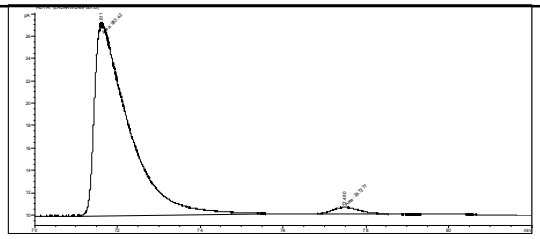					
#	Time	Area	Height	Width	Area%	Symmetry	#	Time	Area	Height	Width	Area%	Symmetry
1	71.804	480.4	9.8	0.8199	49.559	0.305	1	71.611	983.4	17.3	0.9472	97.354	0.244
2	76.909	489	8.5	0.9609	50.441	0.314	2	77.48	26.7	6.2E-1	0.7233	2.646	0.689

1.4b: IR (neat): 3490 (m, br), 2949 (m), 2835 (m), 1734 (s) 1513 (s), 1249 (s). ^{1}H NMR (400 MHz, $CDCl_3$): δ 7.44 (2H, d, *J* = 8.8 Hz, Ar-**H**), 6.85 (2H, d, *J* = 8.8 Hz, Ar-**H**), 3.78 (3H, s, OC**H**$_3$), 3.75 (3H, s, OC**H**$_3$), 3.73 (1H, s, O**H**), 1.75 (3H, s, C**H**$_3$). ^{13}C NMR (100 MHz, $CDCl_3$): δ 176.5, 159.4, 135.1, 126.7, 113.9, 75.6, 55.5, 53.4, 26.9. HRMS Calcd for $C_{11}H_{14}O_4$ (M + Na): 233.0790; Found: 233.0789. $[\alpha]^{20}_D$ -37.6 (*c* = 0.400, $CHCl_3$) for an 83% ee sample. The optical purity of the compound was determined by chiral GLC analysis (β-dex, 140 ºC, 15 psi.) t_R of **1.4b** 66 min (major) and 69 min (minor).

rac-**1.4b**						**1.4b**					
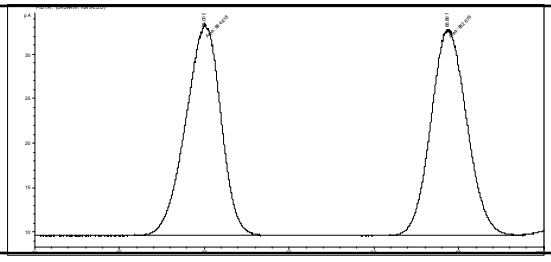						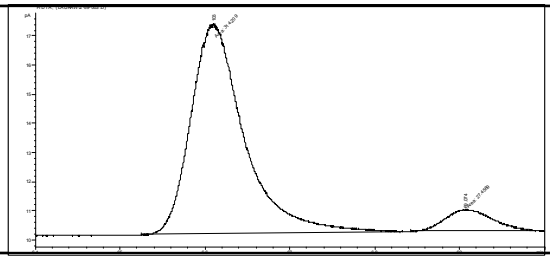					
#	Time	Area	Height	Width	Area%	Symmetry	#	Time	Area	Height	Width	Area%	Symmetry
1	66	684.6	23.7	0.4813	50.071	1.106	1	66.103	314.2	7.2	0.7268	91.964	0.712
2	68.867	682.7	23.2	0.4898	49.929	0.86	2	69.074	27.5	7.3E-1	0.6268	8.036	0.758

(58) (a) "A Virtually Completely Asymmetric Synthesis," Eliel, E. L, Koskimies, J. K., Lohri, B., *J. Am. Chem. Soc.* **1978**, *100*, 1614-1616. (b) "Synthesis, Chiroptical Properties and Absolute Configuration of α-Phenylglycidic Acid," Whitman, C. P.; Craig, J. C.; Kenyon, G. L. *Tetrahedron* **1985**, *41*, 1183-1192.

1.4c: IR (neat): 3503 (s), 2987 (m), 2935 (m), 1728 (s), 1376 (m), 1256 (m), 1149 (s). ^{1}H NMR (400 MHz, $CDCl_3$): δ 7.56 (2H, d, *J* = 7.3 Hz, Ar-**H**), 7.34 (2H, t, *J* = 7.7 Hz, Ar-**H**), 7.28 (1H, d, *J* = 7.0 Hz, Ar-**H**), 3.87 (1H, s, O**H**), 1.74 (3H, s, C$\mathbf{H}_3$), 1.44 (9H, s, O(C$\mathbf{H}_3$)$_3$). ^{13}C NMR (100 MHz, $CDCl_3$): δ175.1, 143.5 128.3, 127.7, 125.4, 83.2, 75.8, 28.0, 26.9. HRMS Calcd for $C_{13}H_{18}O_3$ (M + Na): 245.1154; Found: 245.1153. $[\alpha]^{20}_D$ -38.8 (*c* = 0.493, $CHCl_3$) for an 83% ee sample. The optical purity of the compound was determined by chiral GLC analysis (CDGTA, 100 ^{o}C, 15 psi.) t_R of **1.4c** 45 min (major) and 48 min (minor).

***rac*-1.4c**	**1.4c**
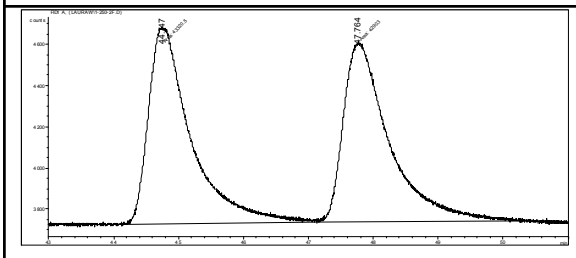	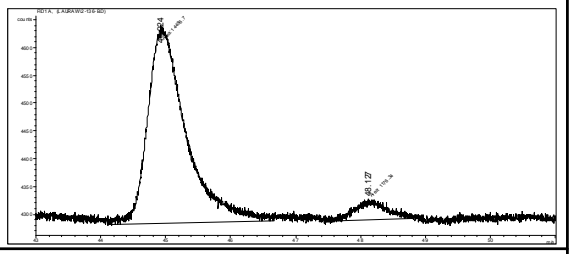

#	Time	Area	Height	Width	Area%	Symmetry
1	44.747	43320.5	952.1	0.7583	50.242	0.457
2	47.764	42903	874.7	0.8175	49.758	0.453

#	Time	Area	Height	Width	Area%	Symmetry
1	44.924	14486.7	358.1	0.6743	92.490	0.512
2	48.127	1176.3	39.2	0.5005	7.510	0.81

1.4l: IR (neat): 3527 (m, br), 2930 (m), 2855 (m), 1728 (s) 1451 (m), 1262 (m). ^{1}H NMR (400 MHz, $CDCl_3$): δ 1.16 (m, 6H), 1.34 (s, 3H, C$\mathbf{H}_3$), 1.68 (m, 5H), 3.01 (1H, s, O**H**), 3.76 (3H, s, OC$\mathbf{H}_3$). ^{13}C NMR (100 MHz, $CDCl_3$): δ 178.15, 77.40, 52.80, 45.82, 27.59, 26.51 (2 C), 26.38, 25.93, 23.36. HRMS Calcd for $C_{10}H_{18}O_3$ (M + Na): 209.1154; Found: 209.1158. $[\alpha]^{20}_D$ -15.0 (c = 0.453, $CHCl_3$) for an 64% ee sample. The optical purity of the compound was determined by chiral GLC analysis (β-dex, 120^{o}C, 15 psi.) t_R of **1.4l** 26 min (major) and 27 min (minor).

rac-**1.4l**	**1.4l**
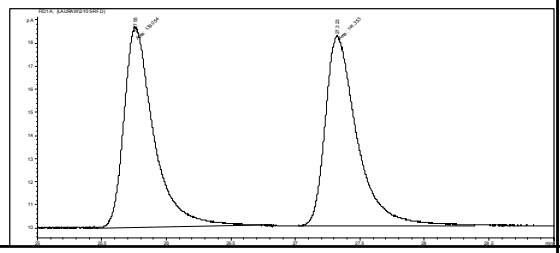	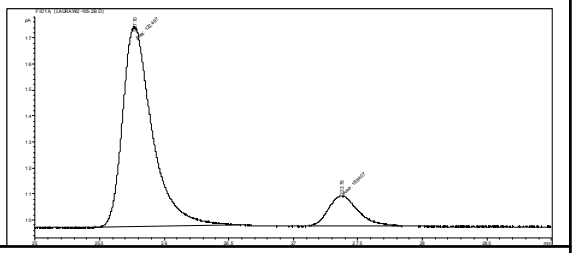

#	Time	Area	Height	Width	Area%	Symmetry
1	25.755	139.1	8.7	0.2674	49.590	0.55
2	27.323	141.4	8.3	0.2849	50.410	0.572

#	Time	Area	Height	Width	Area%	Symmetry
1	25.77	122.5	7.7	0.2659	86.792	0.638
2	27.375	18.6	1.2	0.2648	13.208	0.765

1.4n: IR (neat): 3502 (m, br), 2917 (m), 2848 (m), 1734 (s), 1249 (m). ^{1}H NMR (400 MHz, $CDCl_3$): δ 7.37 (2H, d, *J* = 7.3 Hz, Ar-**H**), 7.30 (2H, t, *J* = 7.3 Hz, Ar-**H**), 7.23 (1H, d, *J* = 7.3 Hz, Ar-**H**), 6.78 (1H, d, *J* = 15.8 Hz, C**H**), 6.32 (1H, d, *J* = 15.8 Hz, C**H**), 3.81 (3H, s, OC$\mathbf{H}_3$), 3.40 (1H, s, O**H**), 1.58 (3H, s, C$\mathbf{H}_3$). ^{13}C NMR (100 MHz, $CDCl_3$): δ176.3, 136.5, 130.9, 129.7, 128.8, 128.1, 126.9, 75.1, 53.4, 26.8. HRMS Calcd for $C_{12}H_{14}O_3$ (M + Na): 229.0841; Found: 229.0843. $[\alpha]^{20}_D$ -34.7 (*c* = 0.453, $CHCl_3$) for a 62% ee sample. The optical purity of the compound was determined by chiral GLC analysis (CDGTA, 140 ^{o}C, 15 psi.) t_R of **1.4n** 24 min (major) and 25 min (minor).

rac-**1.4n**	**1.4n**
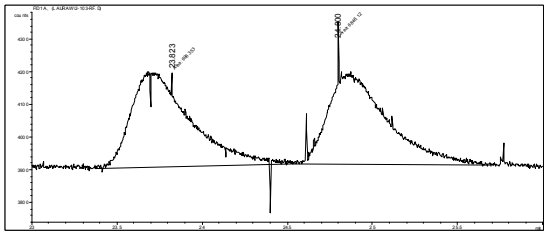	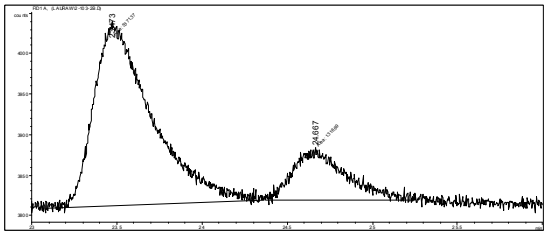

#	Time	Area	Height	Width	Area%	Symmetry
1	23.823	6963.5	292.3	0.397	50.425	1.551
2	24.8	6846.1	450	0.2535	49.575	0.263

#	Time	Area	Height	Width	Area%	Symmetry
1	23.473	5371.4	228.6	0.3915	80.313	0.467
2	24.667	1316.7	64.7	0.3392	19.687	0.703

1.4o: [59] IR (neat): 3483 (m, br), 3005 (m), 2961 (m), 1740 (s) 1489 (m), 1444 (m), 1256 (s) , 1123 (s). ^{1}H NMR (400 MHz, $CDCl_3$): δ 1.77 (s, 3H, C**H**$_3$), 3.50 (1H, s, O**H**), 3.88 (3H, s, OC**H**$_3$), 7.30 (m, 3H), 7.43 (d, 2H, *J*=7.7 Hz). ^{13}C NMR (100 MHz, $CDCl_3$): δ 173.44, 132.06, 128.97, 128.45, 122.12, 88.43, 84.25, 68.53, 53.96, 27.50. $[\alpha]^{20}_{D}$ +17.2 (c = 0.693, $CHCl_3$) for an 24% ee sample. The optical purity of the compound was determined by chiral GLC analysis (CDBPM, 140°C, 15 psi.) t_R of **1.4o** 31.0 min (minor) and 32.2 min (major).

(59) For substrate synthesis, see: "Novel Synthesis of 2-Oxo-3-butynoates by Copper-Catalyzed Cross-Coupling Reaction of Terminal Alkynes and Monooxalyl Chloride," Guo, M., Li, D., Zhang, Z. *J. Org. Chem*. **2003**, *68*, 10172-10174.

Synthesis of Chiral Phosphine 1.16:

Fmoc-L-Thr(Trt)-OH (2.0 g, 3.4 mmol) was dissolved in 40 mL of CH_2Cl_2, and HOBt•H_2O (0.53 g, 3.4 mmol), EDC•HCl (0.66 g, 3.4 mmol) and butylamine (0.68 mL, 6.9 mmol) were added successively at 22 °C. The resulting solution was allowed to stir at 22 °C for four hours at which time TLC analysis showed absence of starting material (12:1 CH_2Cl_2/ MeOH; R_f starting material = 0.7, R_f product = 0.8). 40 mL of a 10 wt. % aqueous solution of citric acid was added and the two layers were separated. The organic layer was washed twice each with 40 mL of 10 wt. % aqueous citric acid and 40 mL of saturated aqueous $NaHCO_3$, followed by 40 mL of saturated NaCl. The organic layer was then dried over $MgSO_4$ and filtered. Piperidine (1.7 ml, 17 mmol) was added to the solution of Fmoc-L-Thr(Trt)-NHBu in CH_2Cl_2 at 22 °C and was allowed to stir for two hours. At this time, the mixture was concentrated and purified by silica gel chromatography (4:1 hexanes:EtOAc to 100% EtOAc to 4:1 EtOAc:MeOH) to give a yellow oil (1.2 g, 85% yield for 2 steps). The product was identified by ^{1}H NMR before proceeding to the next amide coupling reaction.

Fmoc-L-Thr(*t*-Bu)-OH (1.15 g, 2.89 mmol) was dissolved in 20 mL CH_2Cl_2 and HOBt•H_2O (0.44 g, 2.9 mmol), EDC•HCl (0.55 g, 2.9 mmol) and a solution of L-Thr(Trt)-NHBu (1.2 g, 2.9 mmol) in 20 mL CH_2Cl_2 were successively added at 22 °C. The resulting solution was stirred at 22 °C for 4 h before quenching, extracting, and deprotecting as above. The reaction was concentrated and the resulting solid purified by silica gel chromatography (4:1 hexanes:EtOAc to 100% EtOAc to 4:1 EtOAc:MeOH) to give a yellow oil (1.2 g, 73% yield for 2 steps). This amine was identified by ^{1}H NMR before the final coupling.

Magnesium sulfate (0.51 g, 4.2 mmol) was added to a solution of 2-hydroxy-5-methoxybenzaldehyde (0.26 ml, 2.1 mmol) and H_2N-L-Thr(*t*-Bu)-L-Thr(Trt)-NHBu (1.2 g, 2.1 mmol) in 20 mL CH_2Cl_2 at 22 °C. The resulting suspension was stirred for 12 h. The magnesium sulfate was filtered off and the product was concentrated under reduced pressure. The crude product was purified by silica gel chromatography (4:1 pentane:Et_2O

to 100% Et_2O) to give a yellow oil. Ligand was recrystallized (ether/pentane) to give a yellow powder (0.92 g, 1.3 mmol, 62% yield).

1.16: M.p. 75-78 ^oC. IR (solid film): 3333 (m, br), 3055 (m), 2967 (s), 2930 (s), 2873 (m), 2244 (m), 1665 (s), 1589 (m), 1495 (s), 1451 (m), 1338 (m), 1275 (m), 1193 (m), 1162 (m), 1086 (m), 910 (m), 734 (m), 702 (m). ^1H NMR (400 MHz, $CDCl_3$): δ 12.24 (1H, s, ArO**H**), 8.22 (1H, s, Ar-C**H**=N), 7.32 (6H, d, *J* = 7.5 Hz, Ar**H**), 7.30 (9H, m, Ar**H**), 7.20 (1H, d, *J* = 6.2 Hz, N**H**), 6.92 (2H, m, Ar**H**), 6.76 (1H, d, *J* = 2.6 Hz, Ar**H**), 6.63 (1H, t, *J* = 5.1 Hz, N**H**Bu), 4.32 (1H, dt, *J* = 10.3, 6.2 Hz, C**H**(Me)(OTrt)), 3.99 (1H, dt, *J* = 11.7, 5.9 Hz, C**H**(Me)(O*t*-Bu)), 3.83 (1H, dd, *J* = 5.9, 3.7 Hz, NC**H**CO (Thr(OTrt)), 3.77 (3H, s, OC$\mathbf{H}_3$), 3.63 (1H, d, *J* = 5.5 Hz, NC**H**CO (Thr(O*t*-Bu)), 3.33 (1H, dq, *J* = 13.2, 7.0 Hz, NHC$\mathbf{H}_2$), 3.17 (1H, dq, *J* = 13.2, 7.0 Hz, NHC$\mathbf{H}_2$), 1.47 (2H, m, $CH_2C\mathbf{H}_2CH_2CH_3$), 1.31 (2H, m, $CH_2CH_2C\mathbf{H}_2CH_3$), 1.16 (3H, d, *J* = 6.2 Hz, C$\mathbf{H}_3$ (Thr(O*t*-Bu)), 1.07 (9H, s, C(C$\mathbf{H}_3$)$_3$), 0.95 (3H, d, *J* = 6.2 Hz, C$\mathbf{H}_3$ (Thr(OTrt)), 0.89 (3H, m, $CH_2CH_2CH_2C\mathbf{H}_3$). ^{13}C NMR (100 MHz, $CDCl_3$): δ169.2, 168.9, 167.6, 155.4, 152.3, 144.3, 129.0, 128.3, 127.7, 120.2, 118.4, 118.3, 115.4, 88.4, 79.3, 74.7, 69.6, 69.1, 56.1, 39.6, 31.7, 28.8, 20.4, 20.2, 17.0, 14.0. Anal. Calcd for $C_{43}H_{53}N_3O_6$: C, 72.96; H, 7.55; N, 5.94; Found: C, 72.68; H, 7.79; N, 5.85. $[\alpha]^{20}_D$ -6.8 (*c* = 0.980, $CHCl_3$).

1.20: ^1H NMR (400 MHz, $CDCl_3$) of $C_{43}H_{53}N_3O_6$: δ 12.23 (1H, s), 8.15 (1H, s), 7.48 (6H, d, *J* = 7.0 Hz), 7.27 (10H, m), 6.91 (2H, m), 6.74 (1H, d, *J* = 2.9 Hz), 6.45 (1H, t, *J* = 5.5 Hz), 4.23 (1H, dt, *J* = 10.62, 6.2 Hz), 3.97 (1H, dt, *J* = 11.7, 5.9 Hz), 3.75 (3H, s), 3.62 (1H, d, *J* = 5.9 Hz), 3.62 (1H, d, *J* = 5.9 Hz), 3.28 (1H, dq, *J* = 12.8, 7.0 Hz), 3.22 (1H, dq, *J* = 12.8, 7.0 Hz), 1.45 (2H, m), 1.31 (2H, m), 1.13 (3H, d, *J* = 6.2 Hz), 1.09 (9H, s), 0.93 (3H, d, *J* = 6.6 Hz), 0.89 (3H, t, *J* = 6.96 Hz).

1.21: ^1H NMR (400 MHz, $CDCl_3$) of $C_{37}H_{41}N_3O_5$: δ 11.83 (1H, s), 8.25 (1H, s), 7.48 (6H, d, *J* = 8.2 Hz), 7.28 (9H, m), 7.06 (1H, d, *J* = 5.9 Hz), 6.92 (2H, m), 6.72 (1H, d, *J*

= 2.9 Hz), 6.60 (1H, t, *J* = 5.5 Hz), 4.29 (1H, dq, *J* = 6.2, 1.8 Hz), 4.20 (2H, s), 3.75 (1H, m), 3.75 (3H, s), 3.30 (1H, dq, *J* = 13.2, 7.0 Hz), 3.21 (1H, dq, *J* = 13.2, 7.0 Hz), 1.46 (2H, m), 1.32 (2H, m), 0.92 (3H, d, *J* = 6.2 Hz), 0.88 (3H, t, *J* = 7.0 Hz).

1.22: ^{1}H NMR (400 MHz, $CDCl_3$) of $C_{22}H_{35}N_3O_5$: δ 12.25 (1H, s), 8.26 (1H, s), 7.09 (1H, t, *J* = 5.1 Hz), 6.92 (2H, m), 6.78 (1H, d, *J* = 2.9 Hz), 6.14 (1H, t, *J* = 5.5 Hz), 4.05 (1H, m), 3.96 (1H, d, *J* = 5.9 Hz), 3.88 (1H, d, *J* = 5.5 Hz), 3.78 (1H, d, *J* = 4.8 Hz), 3.76 (3H, s), 3.22 (2H, dq, *J* = 7.3, 2.2 Hz), 1.44 (2H, m), 1.29 (2H, m), 1.22 (3H, d, *J* = 6.2 Hz), 1.16 (9H, s), 0.88 (3H, t, *J* = 7.3 Hz).

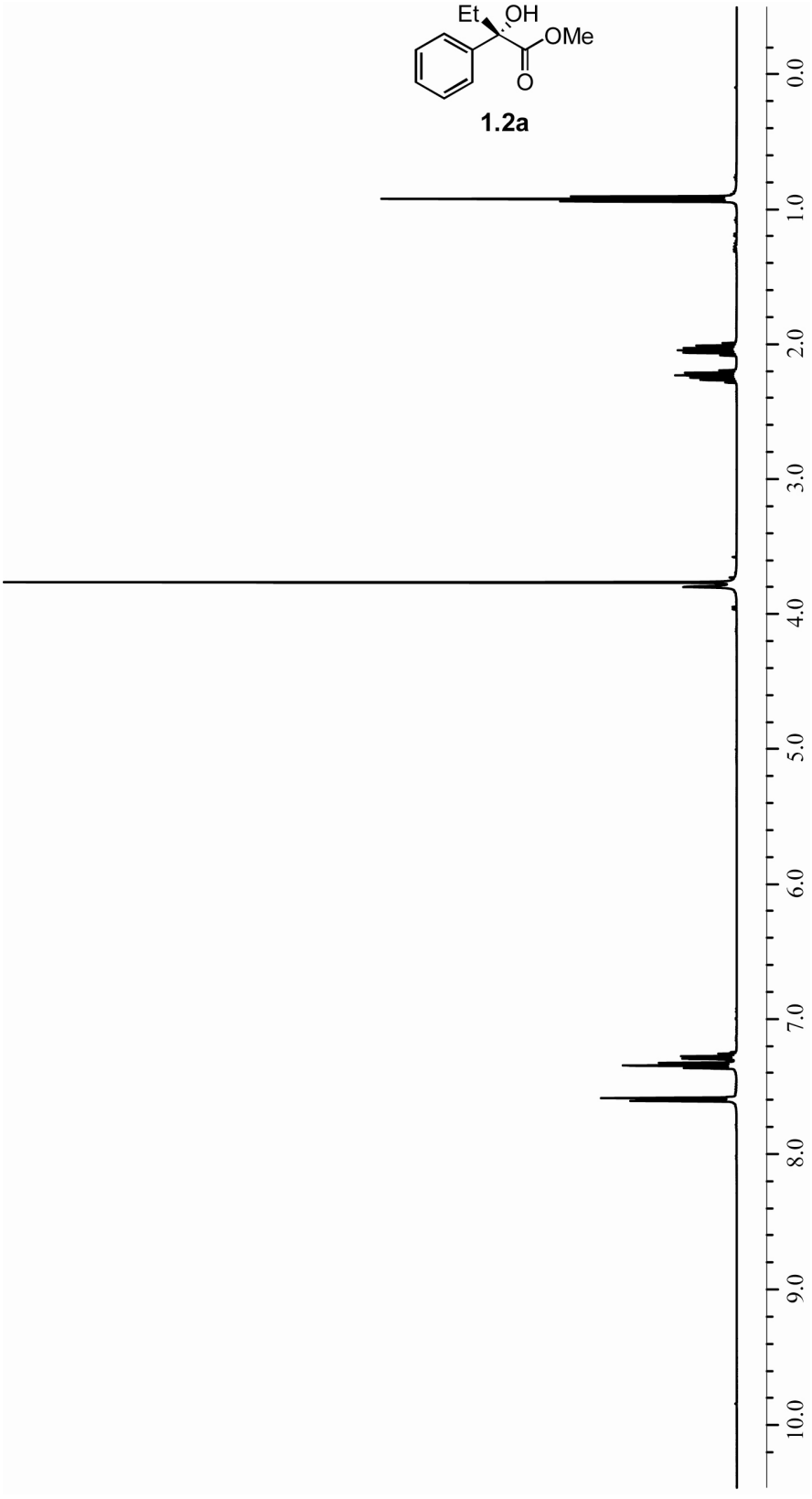
Et
OH
OMe
O
1.2a
0.0
1.0
2.0
3.0
4.0
5.0
6.0
7.0
8.0
9.0
10.0

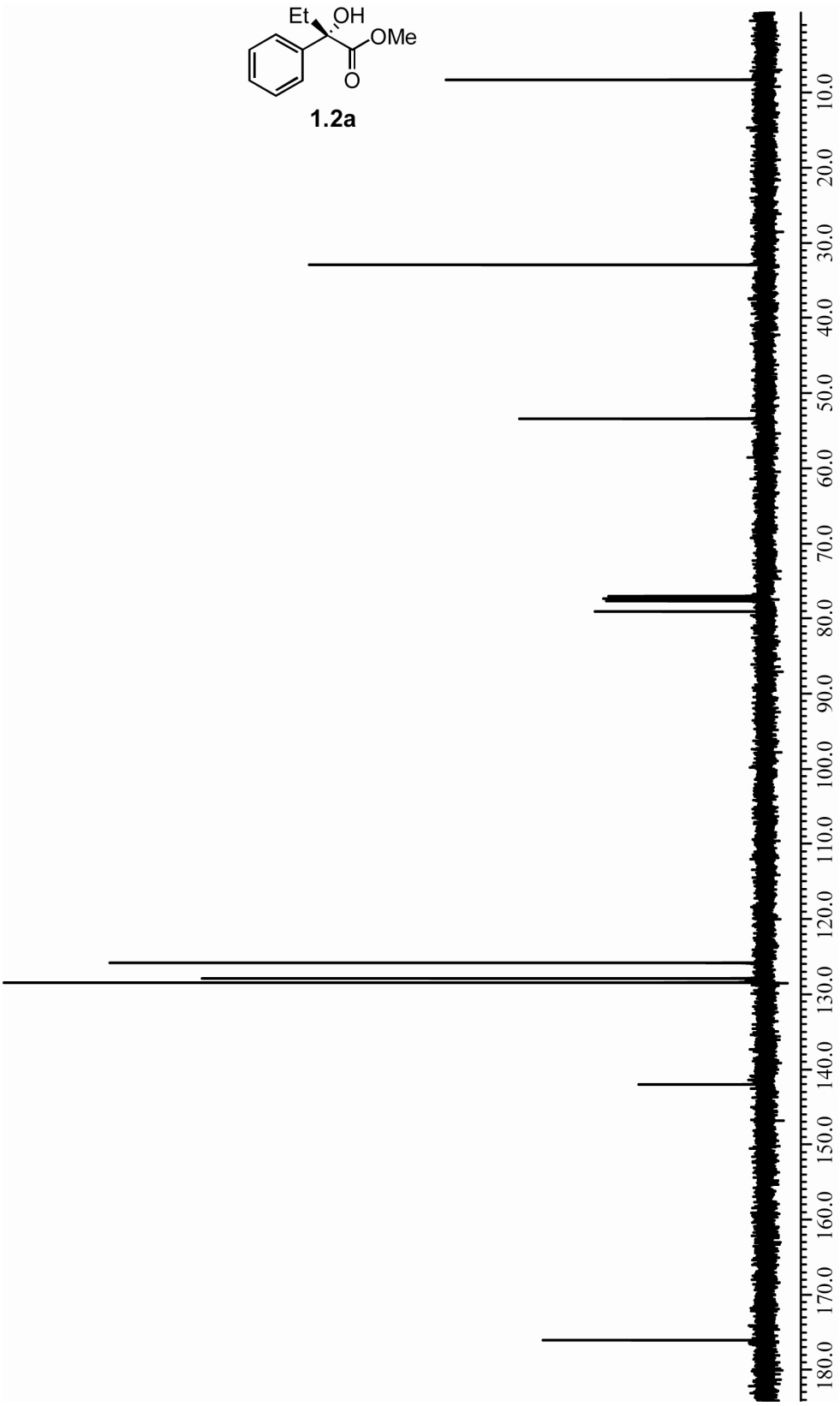
Et
OH
OMe
O
1.2a
10.0
20.0
30.0
40.0
50.0
60.0
70.0
80.0
90.0
100.0
110.0
120.0
130.0
140.0
150.0
160.0
170.0
180.0

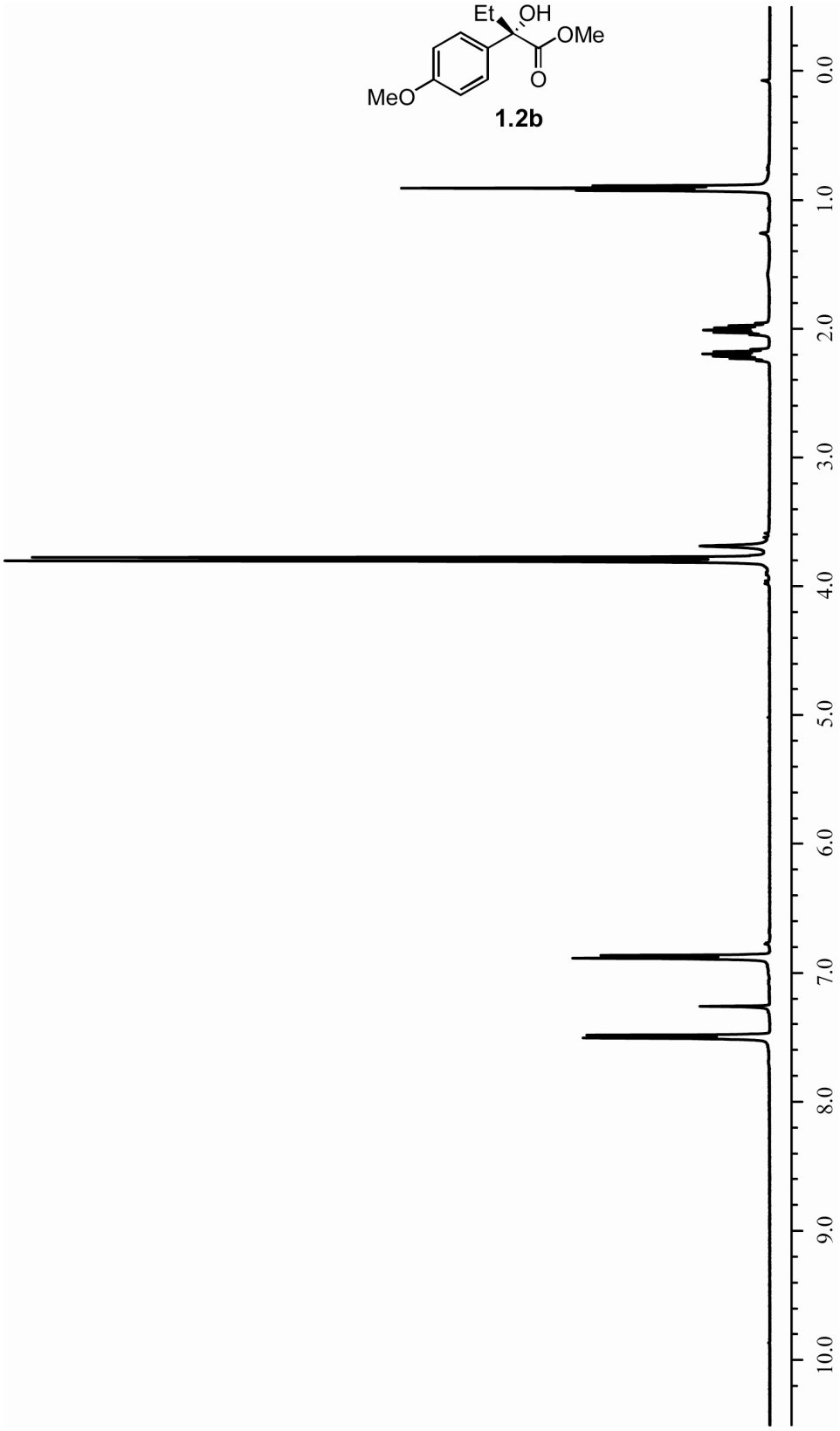
Et
OH
OMe
O
MeO
1.2b
0.0
1.0
2.0
3.0
4.0
5.0
6.0
7.0
8.0
9.0
10.0

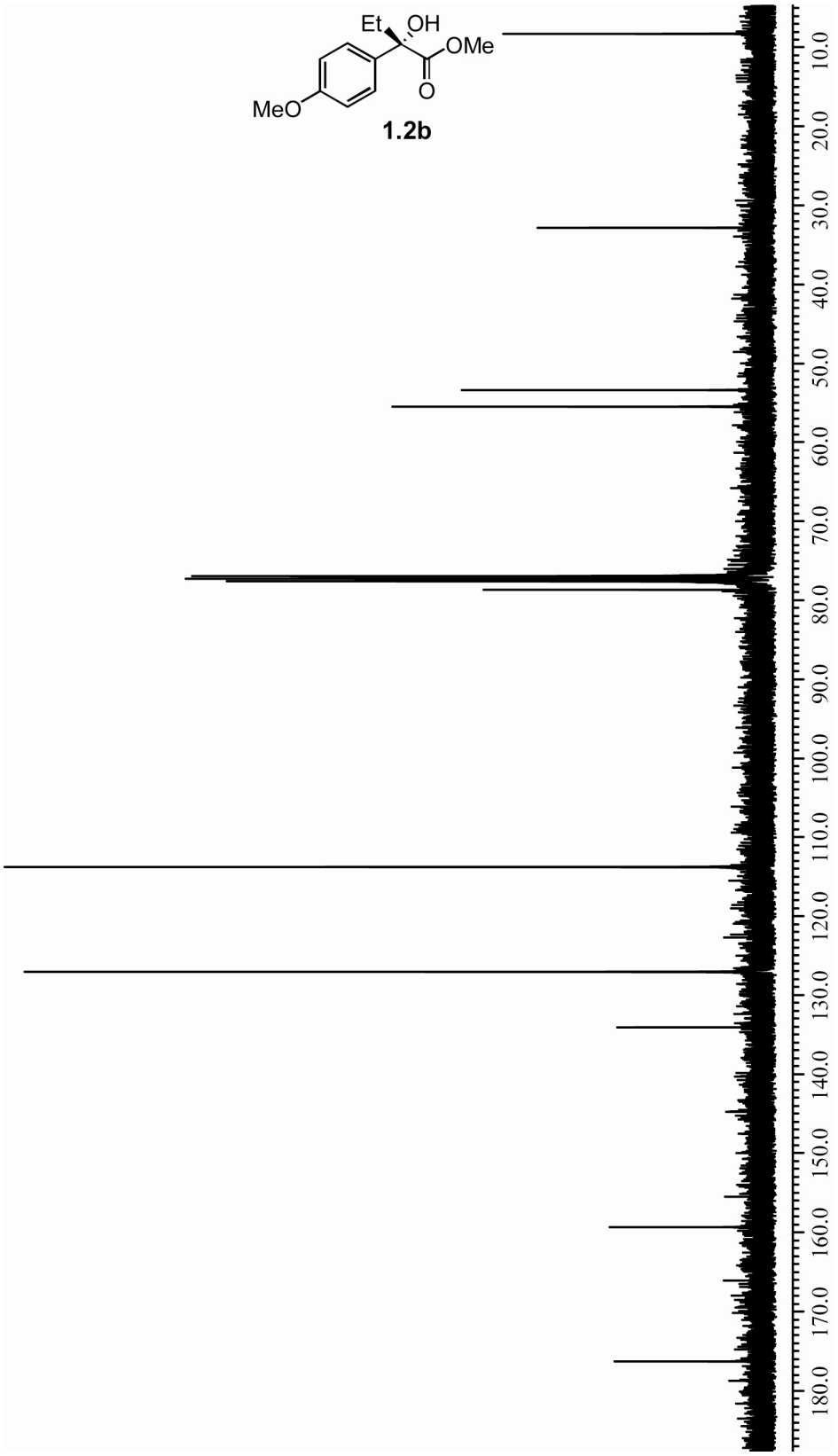
Et
OH
OMe
O
MeO
1.2b
10.0
20.0
30.0
40.0
50.0
60.0
70.0
80.0
90.0
100.0
110.0
120.0
130.0
140.0
150.0
160.0
170.0
180.0

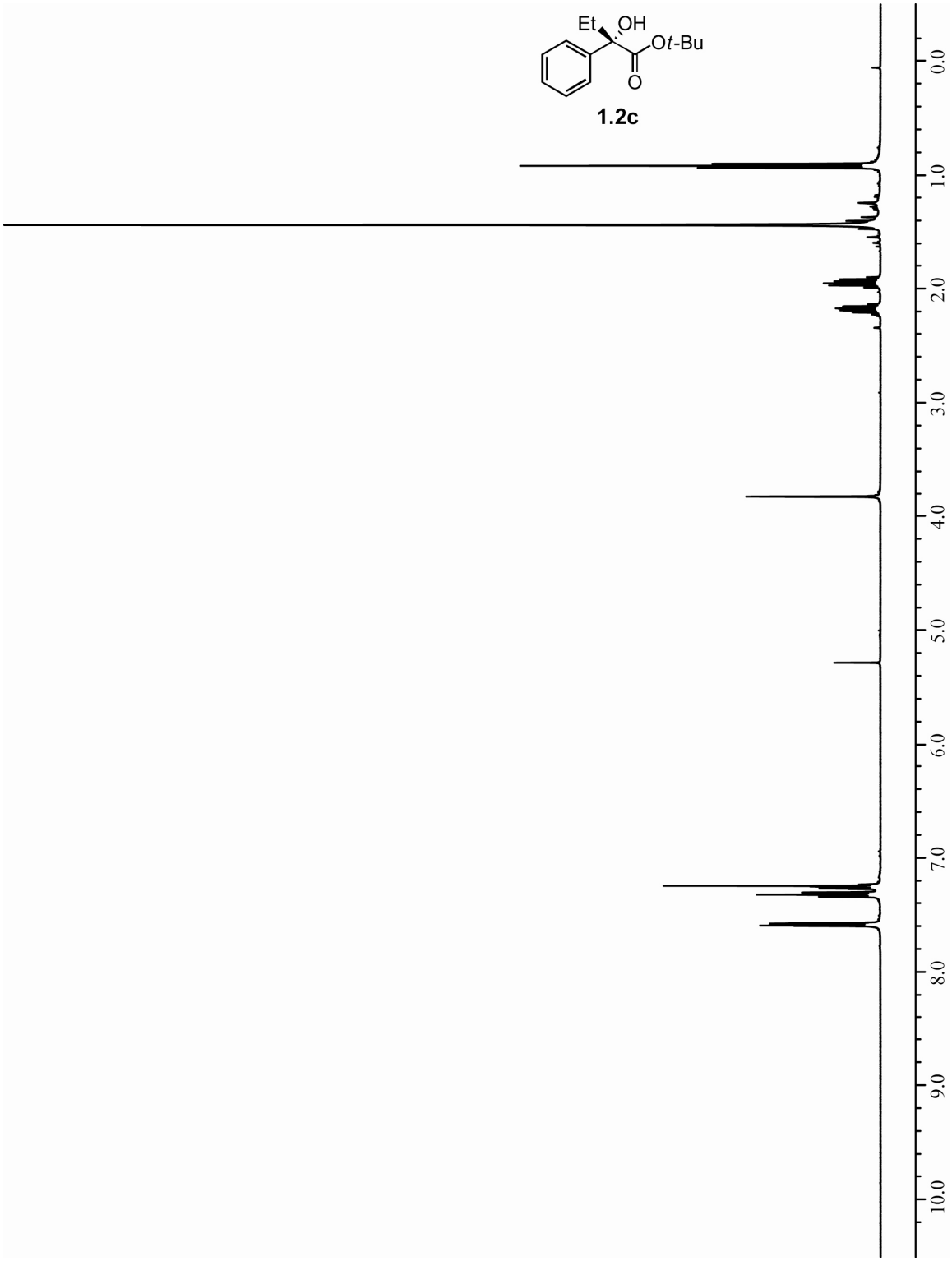
Et
OH
Ot-Bu
O
1.2c
0.0
1.0
2.0
3.0
4.0
5.0
6.0
7.0
8.0
9.0
10.0

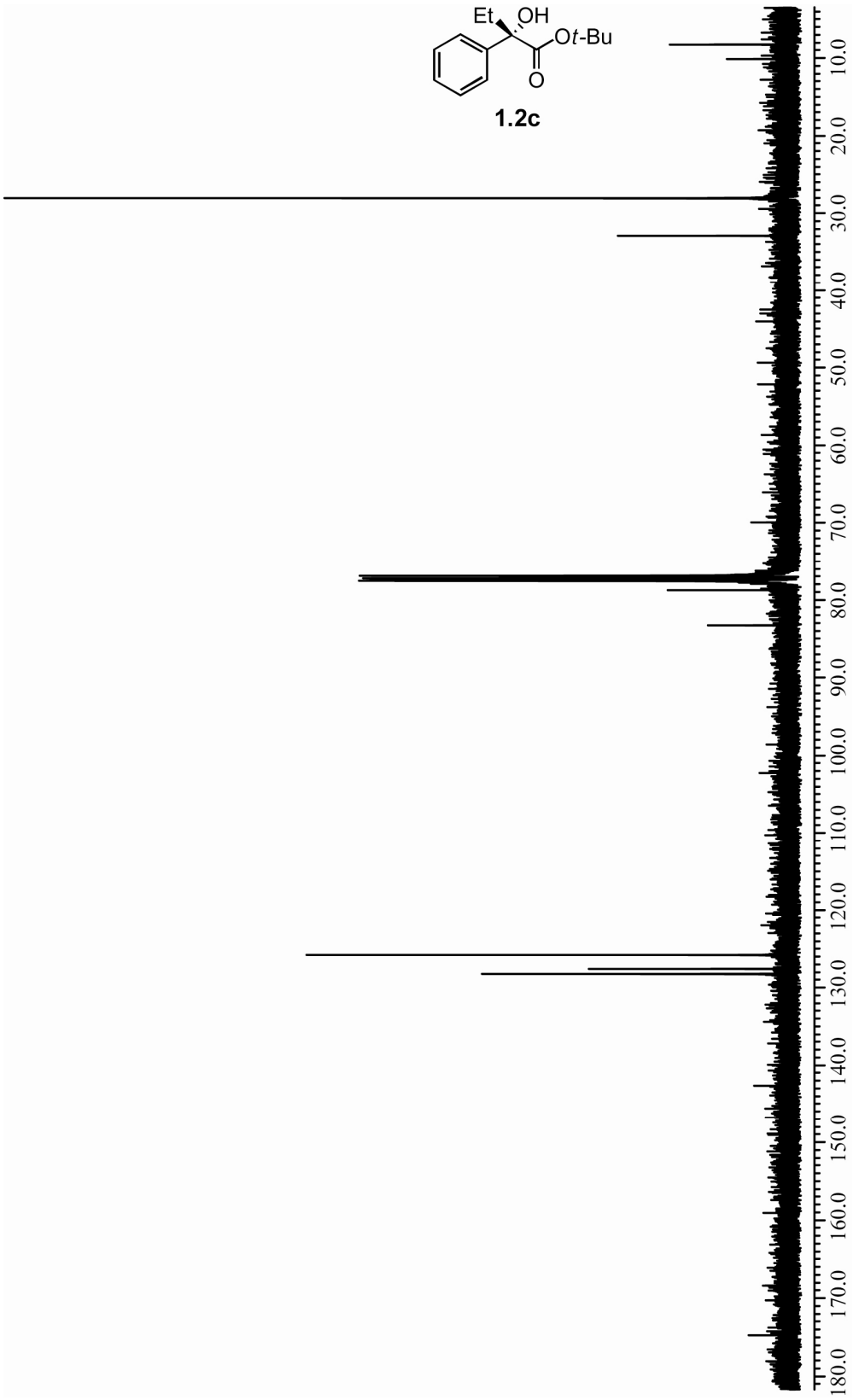
Et
OH
Ot-Bu
O
1.2c
10.0
20.0
30.0
40.0
50.0
60.0
70.0
80.0
90.0
100.0
110.0
120.0
130.0
140.0
150.0
160.0
170.0
180.0

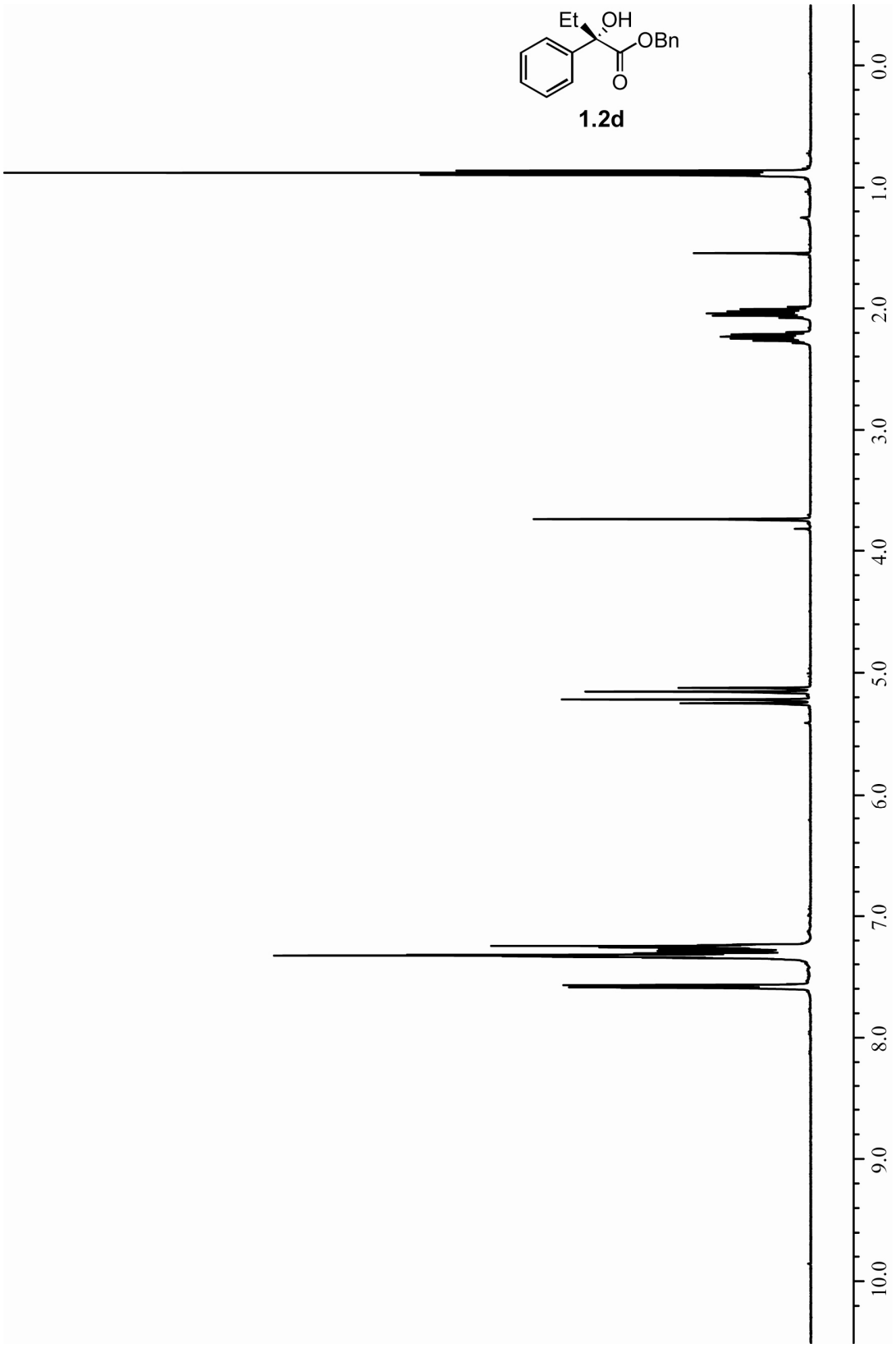
Et
OH
OBn
O
1.2d
0.0
1.0
2.0
3.0
4.0
5.0
6.0
7.0
8.0
9.0
10.0

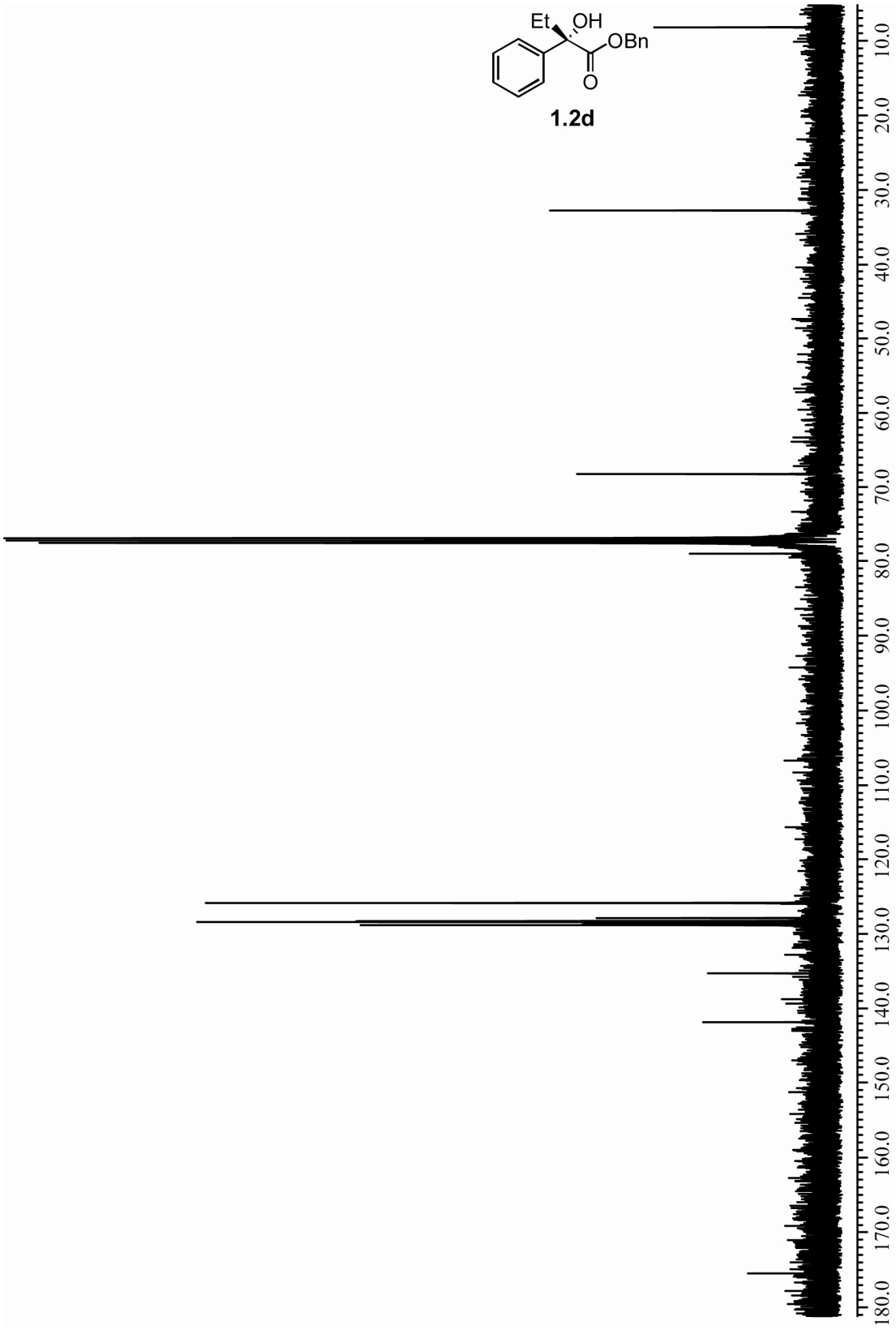
Et
OH
OBn
O
1.2d
10.0
20.0
30.0
40.0
50.0
60.0
70.0
80.0
90.0
100.0
110.0
120.0
130.0
140.0
150.0
160.0
170.0
180.0

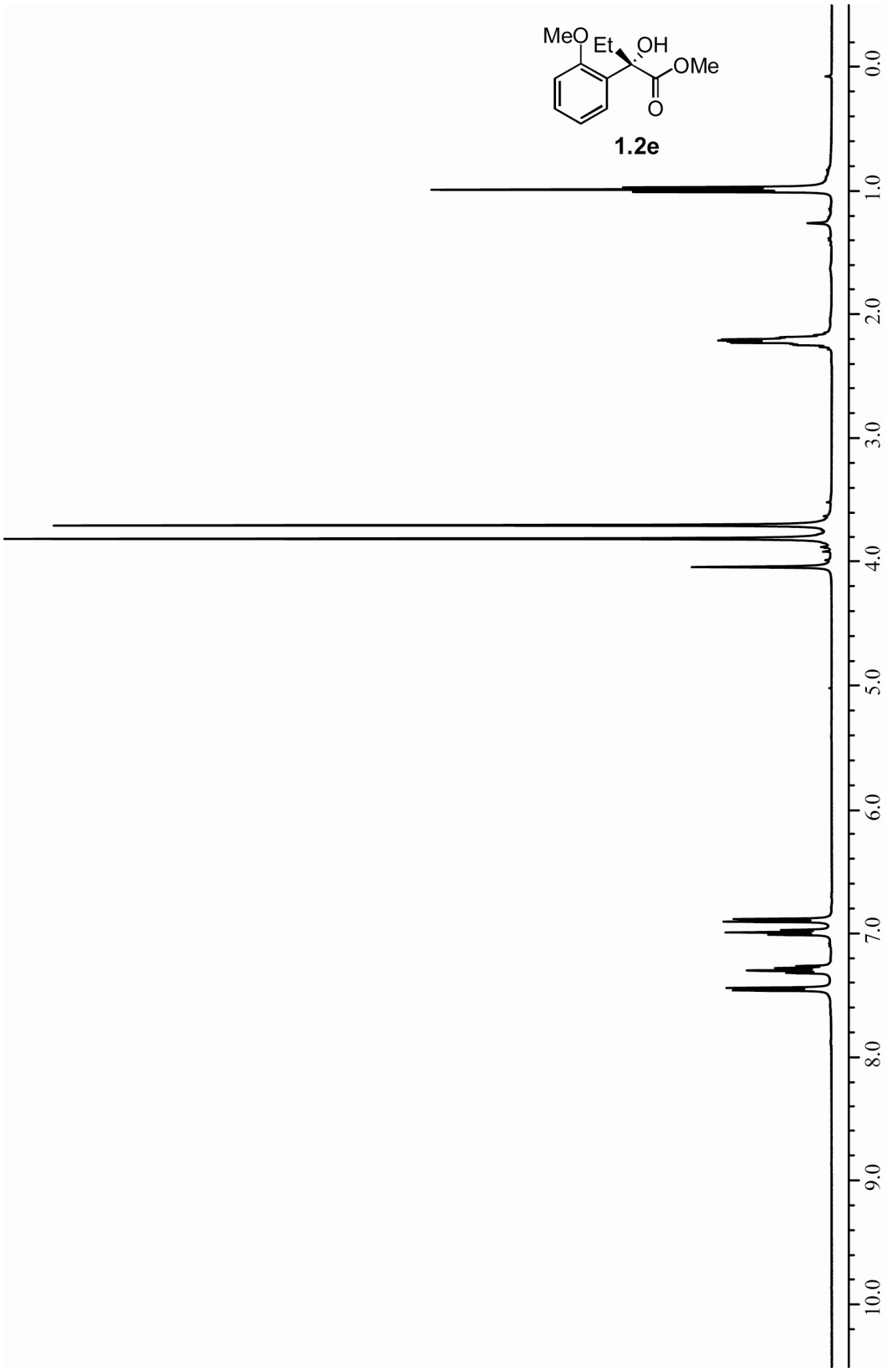
MeO
Et
OH
OMe
O
1.2e
0.0
1.0
2.0
3.0
4.0
5.0
6.0
7.0
8.0
9.0
10.0

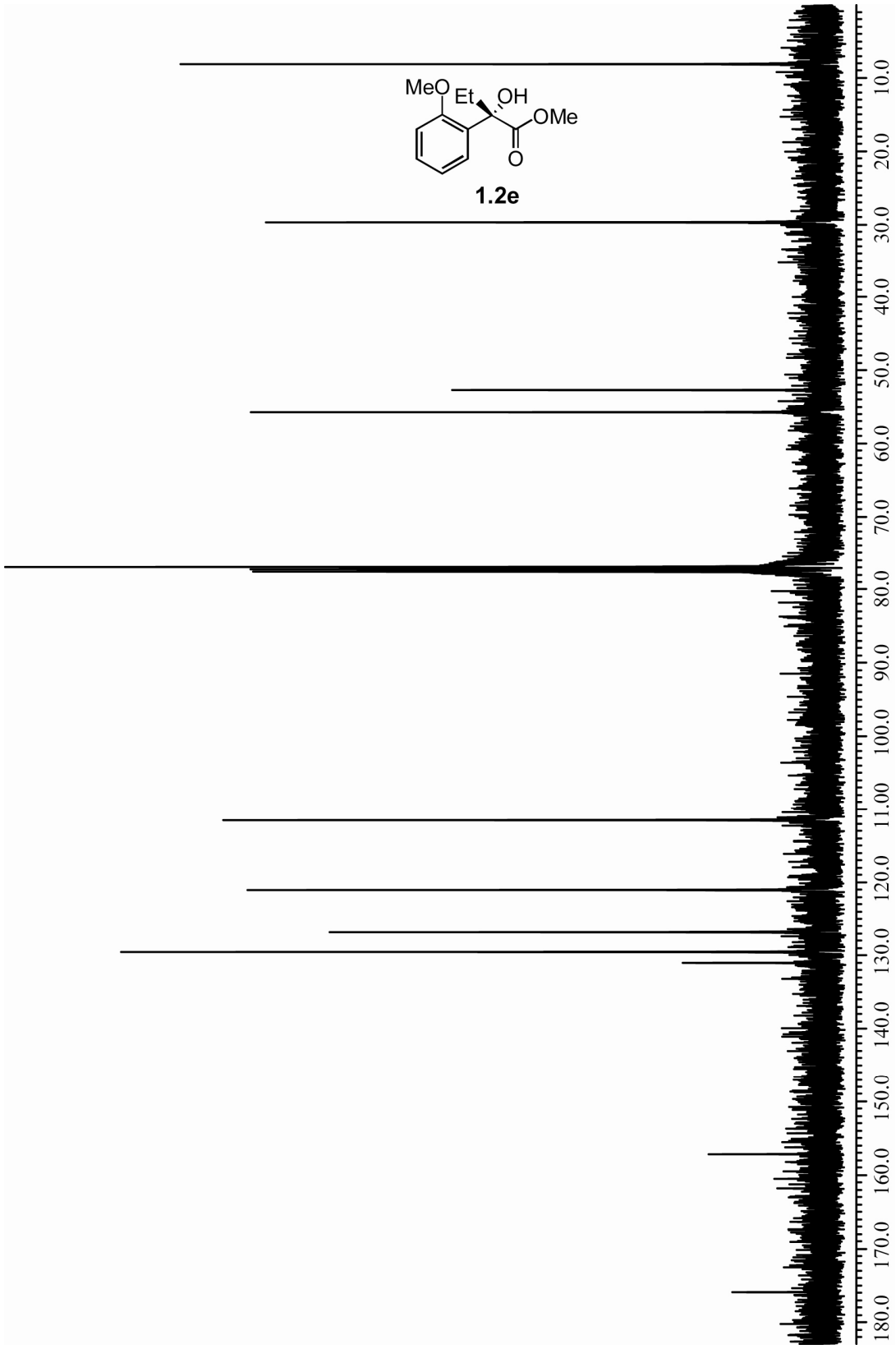
MeO
Et
OH
OMe
O
1.2e
10.0
20.0
30.0
40.0
50.0
60.0
70.0
80.0
90.0
100.0
11.00
120.0
130.0
140.0
150.0
160.0
170.0
180.0

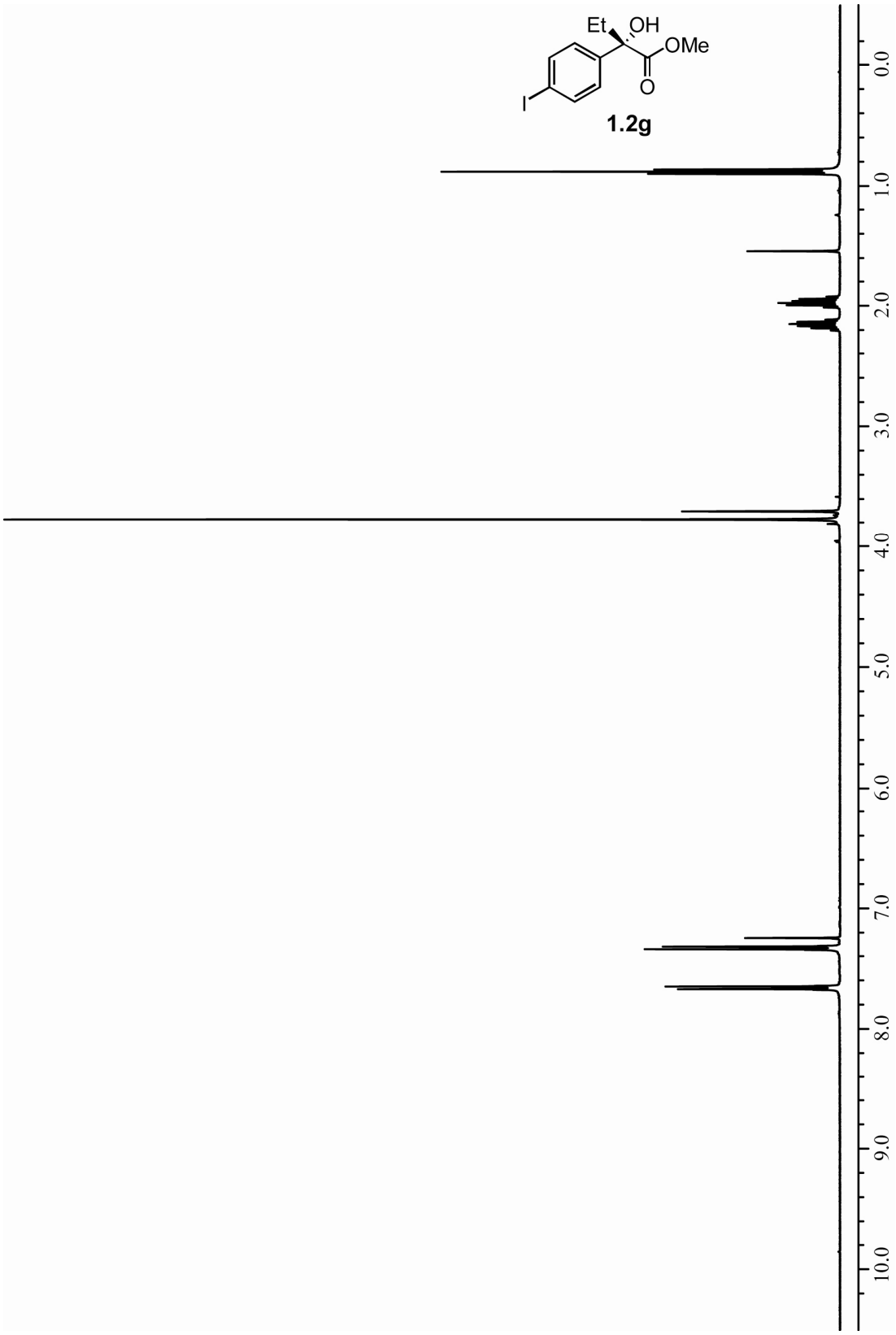
Et
OH
OMe
O
I
1.2g
0.0
1.0
2.0
3.0
4.0
5.0
6.0
7.0
8.0
9.0
10.0

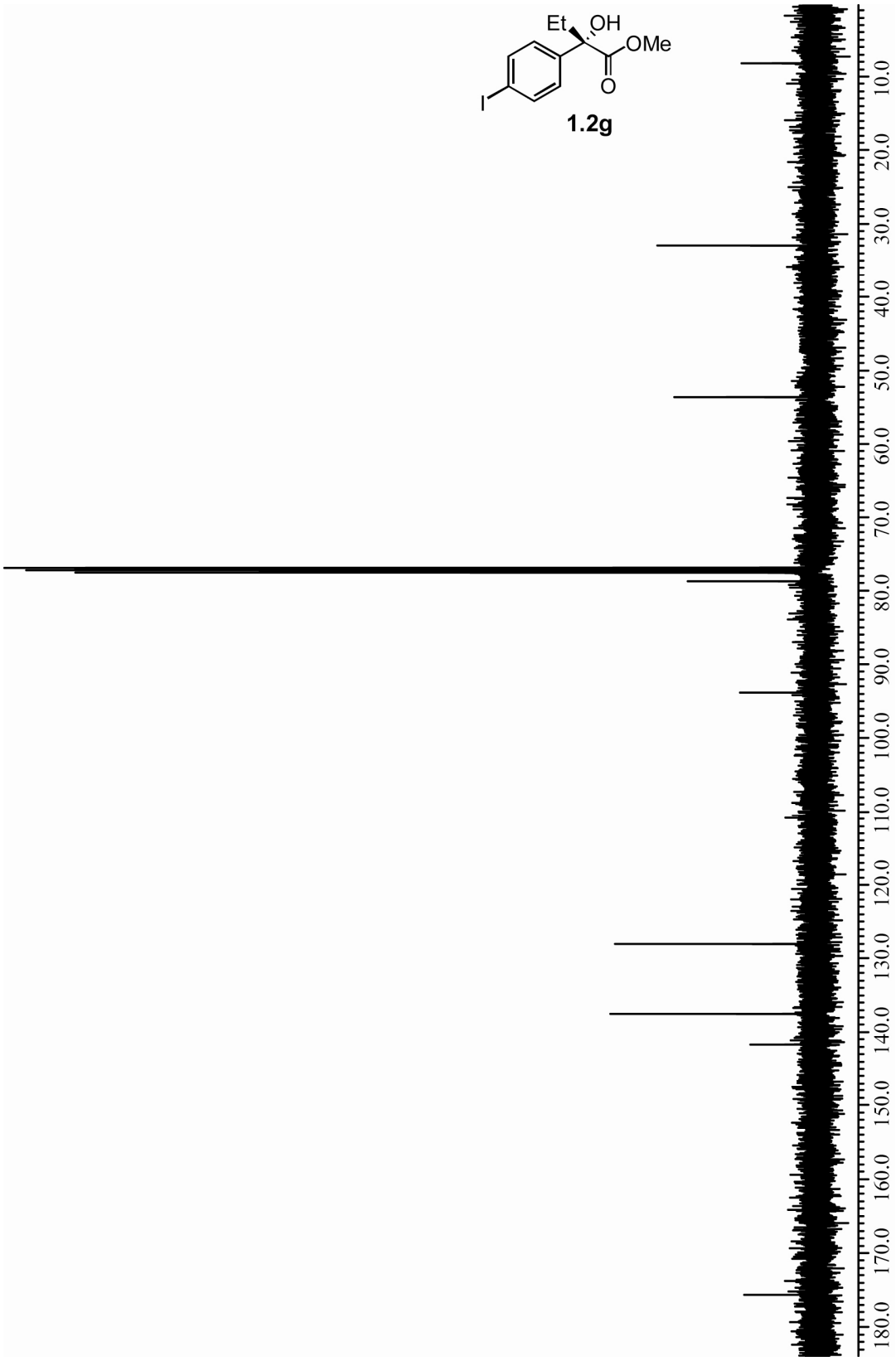
Et
OH
OMe
O
I
1.2g
180.0
170.0
160.0
150.0
140.0
130.0
120.0
110.0
100.0
90.0
80.0
70.0
60.0
50.0
40.0
30.0
20.0
10.0

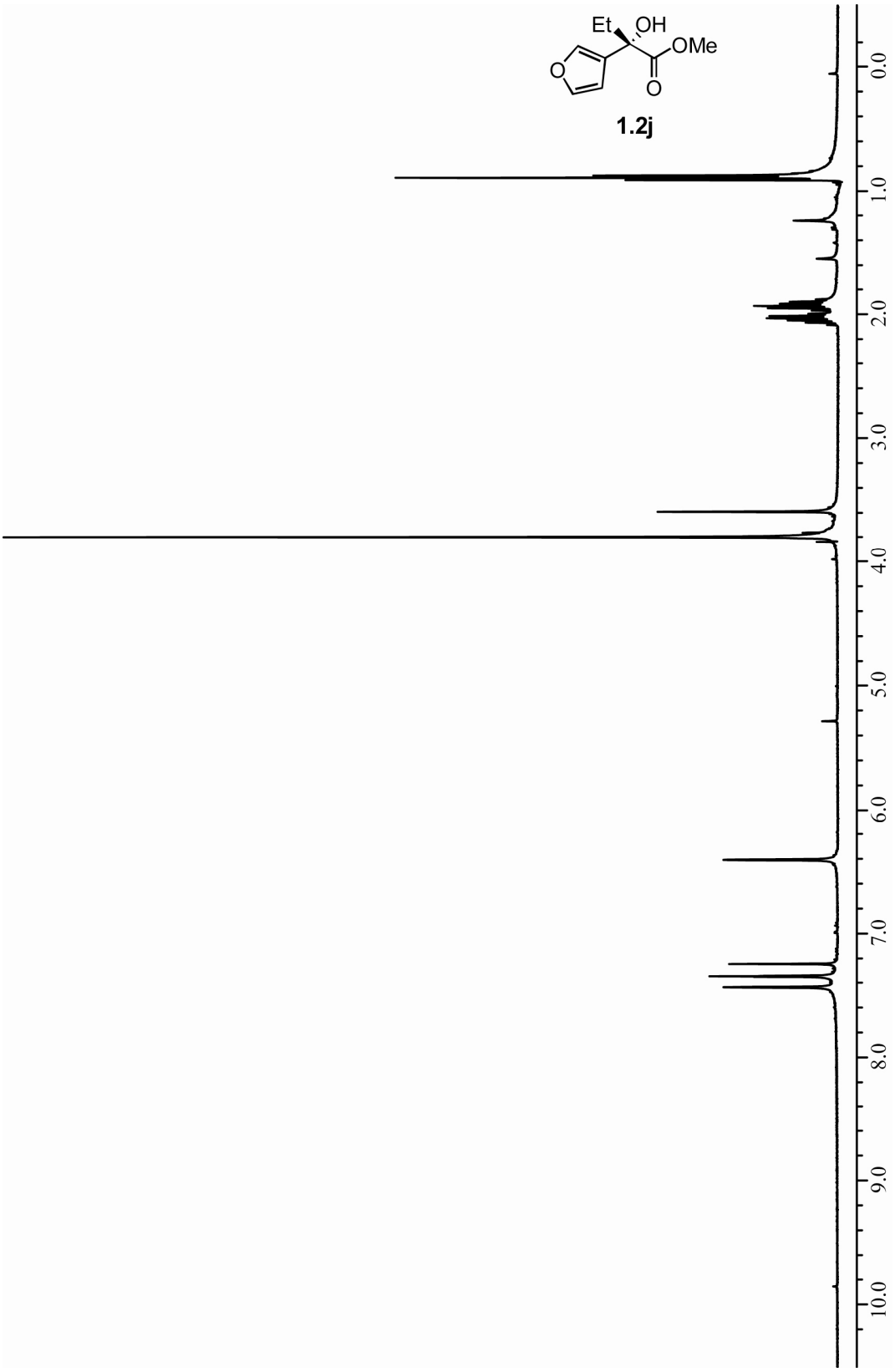
Et
OH
OMe
O
O
1.2j
0.0
1.0
2.0
3.0
4.0
5.0
6.0
7.0
8.0
9.0
10.0

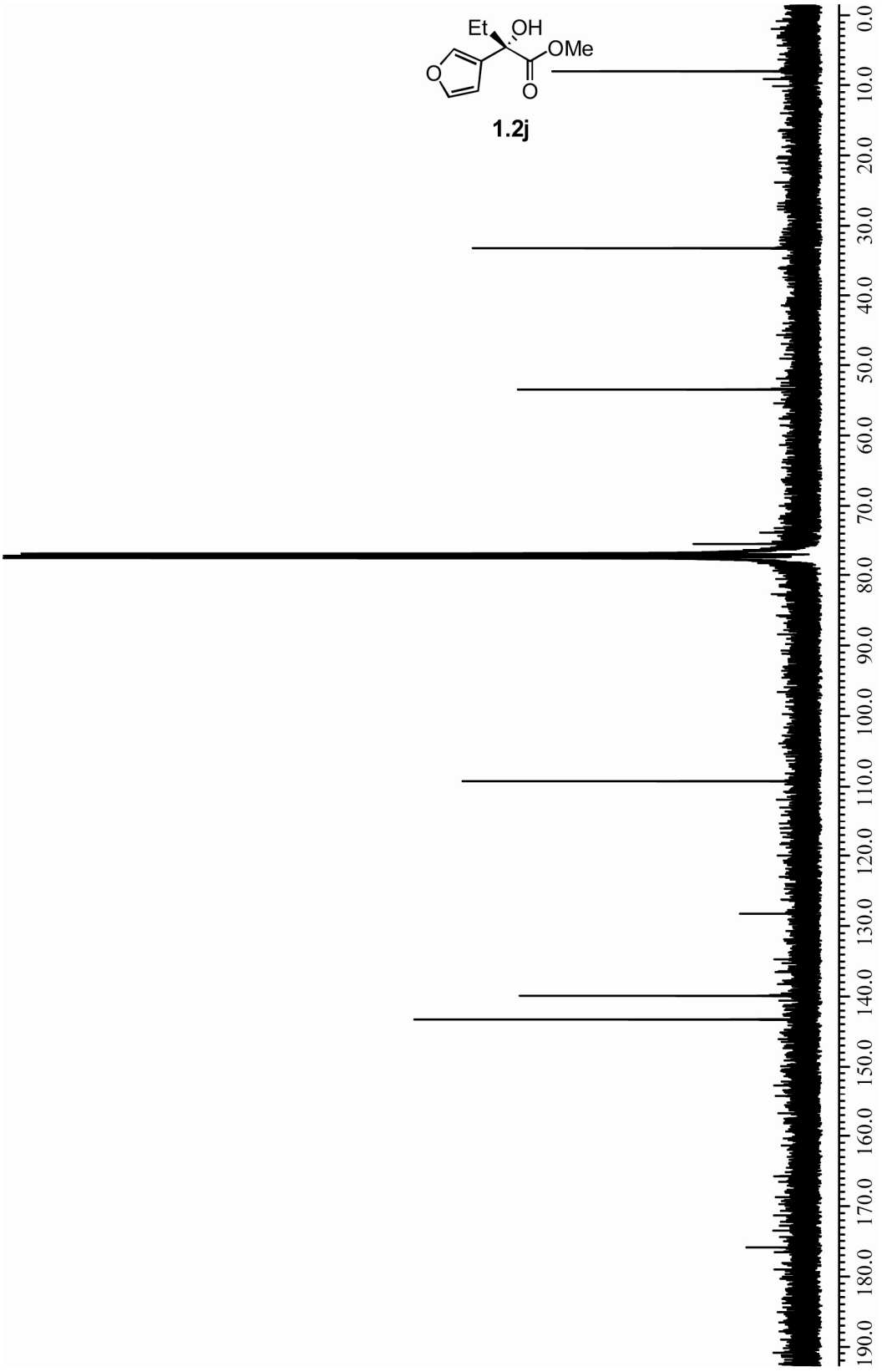
Et
OH
OMe
O
O
1.2j
0.0
10.0
20.0
30.0
40.0
50.0
60.0
70.0
80.0
90.0
100.0
110.0
120.0
130.0
140.0
150.0
160.0
170.0
180.0
190.0

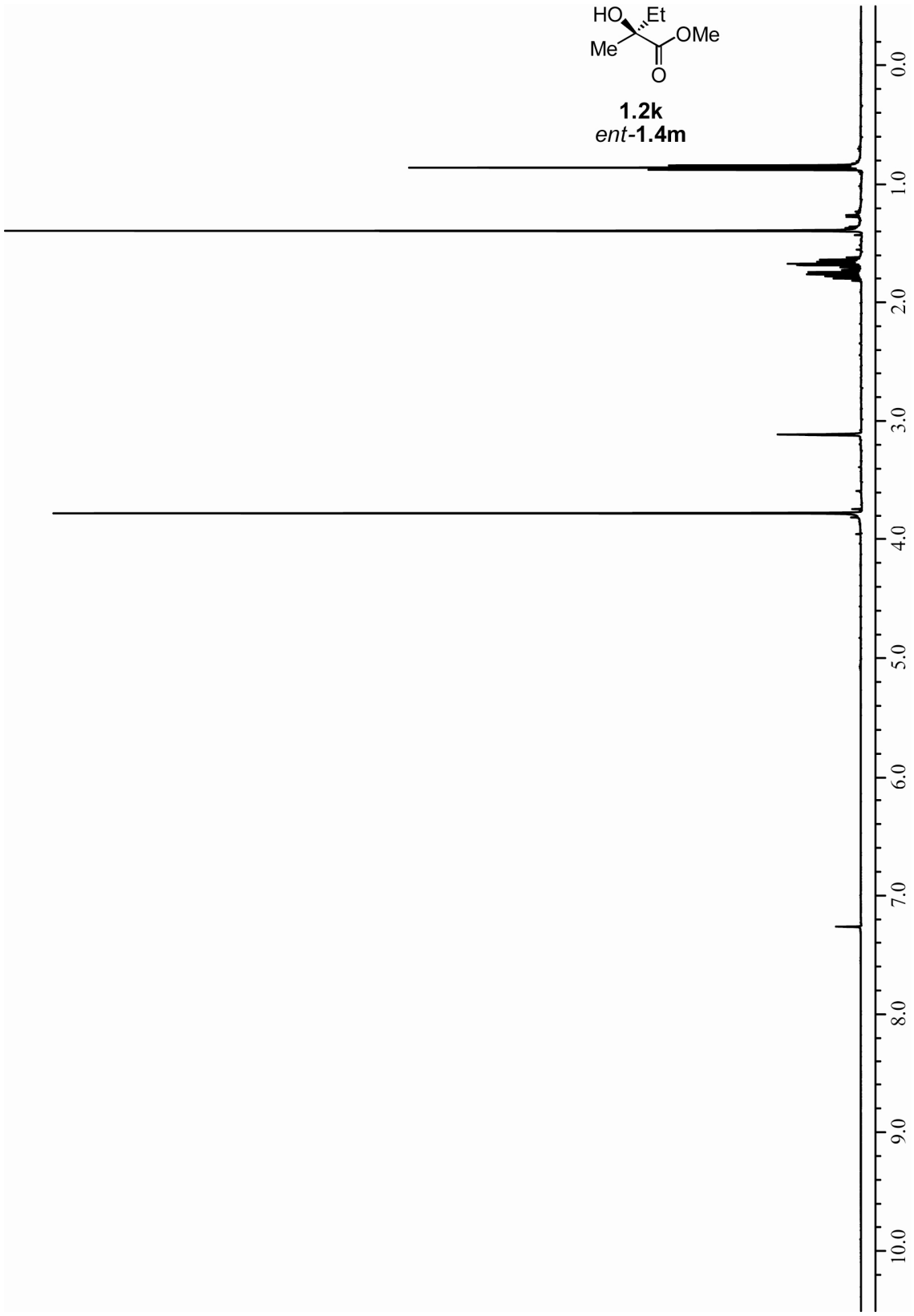
HO
Et
Me
OMe
O
1.2k
ent-1.4m
0.0
1.0
2.0
3.0
4.0
5.0
6.0
7.0
8.0
9.0
10.0

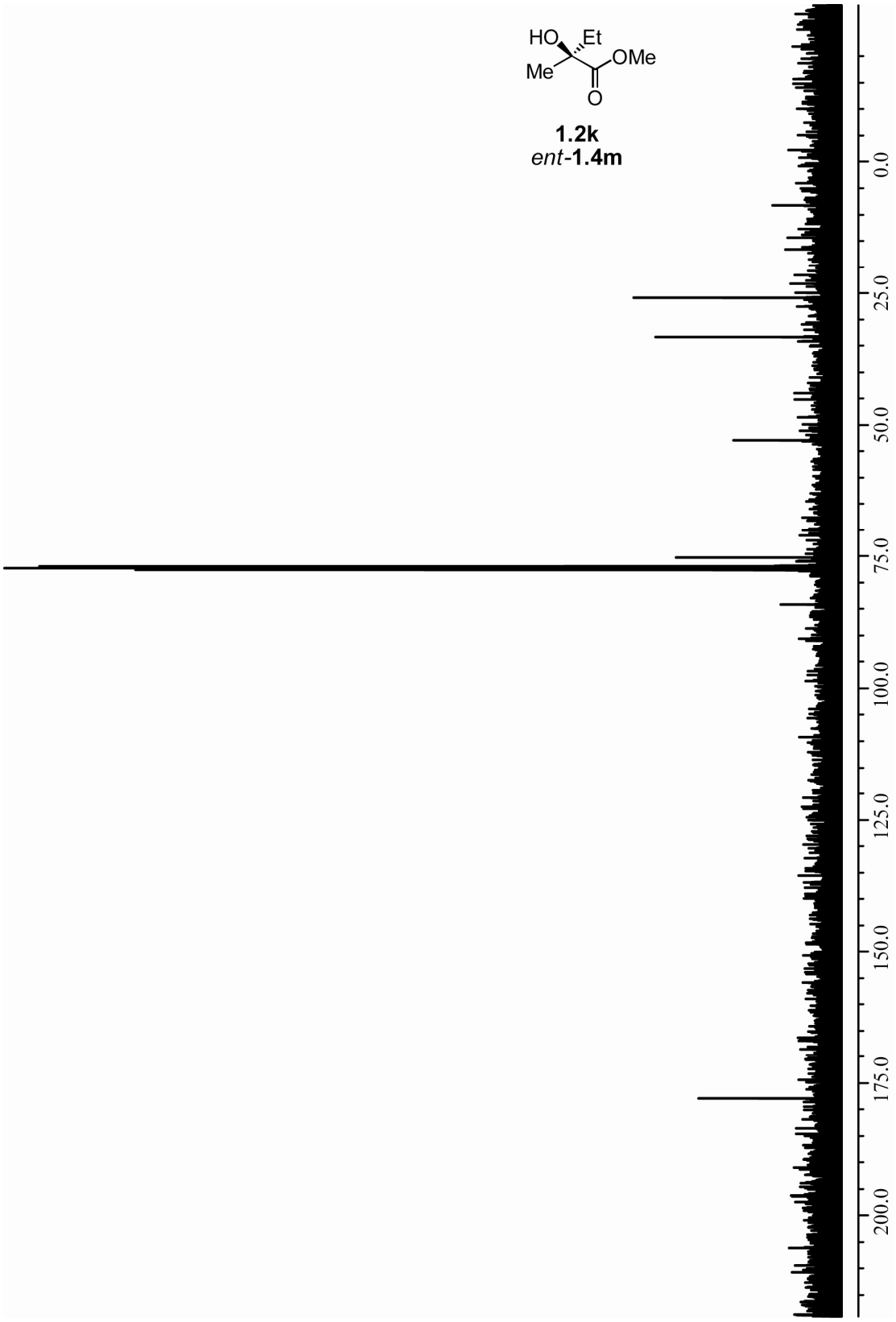
HO
Et
Me
OMe
O
1.2k
ent-1.4m
0.0
25.0
50.0
75.0
100.0
125.0
150.0
175.0
200.0

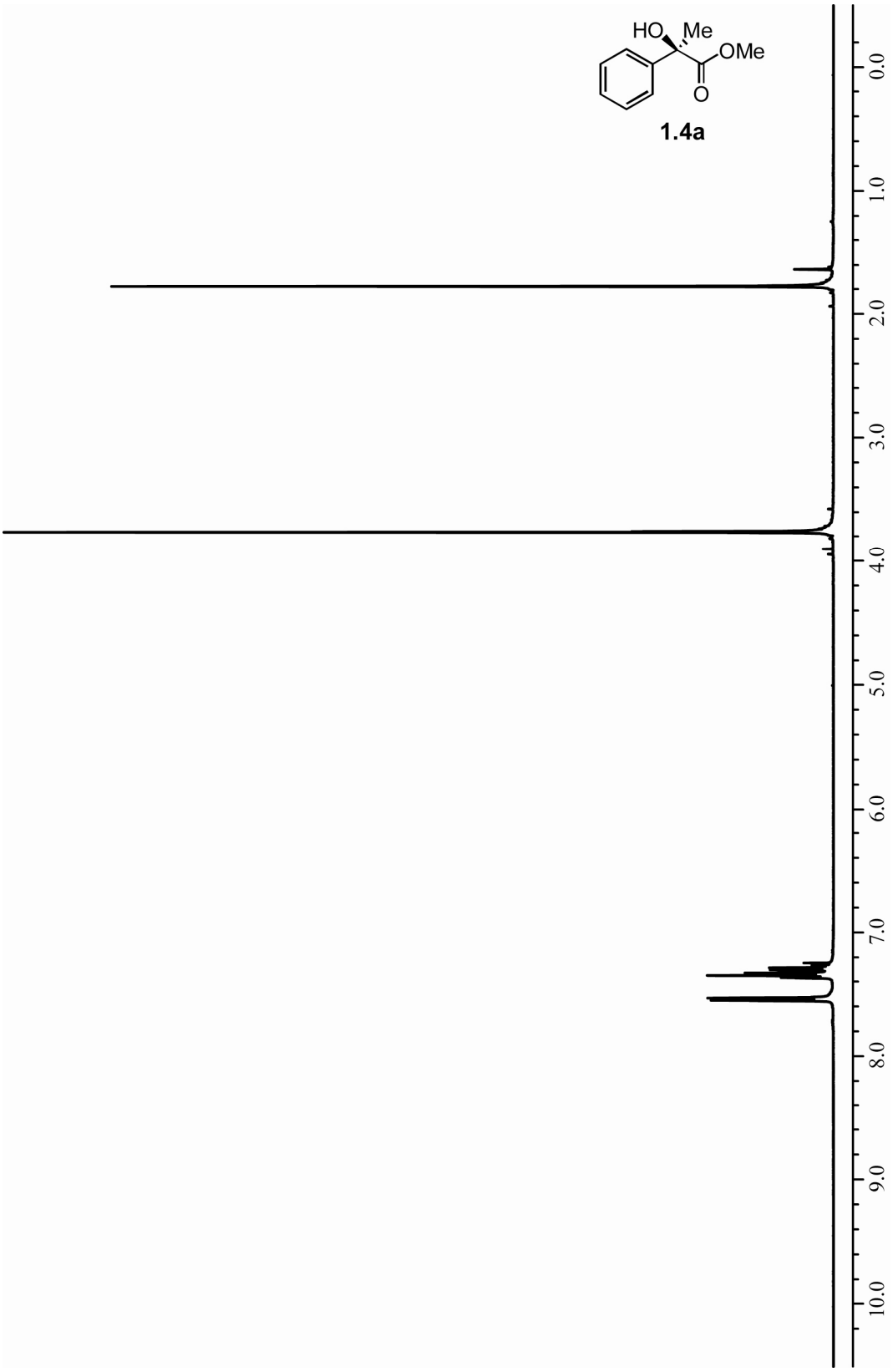
HO
Me
OMe
O
1.4a
0.0
1.0
2.0
3.0
4.0
5.0
6.0
7.0
8.0
9.0
10.0

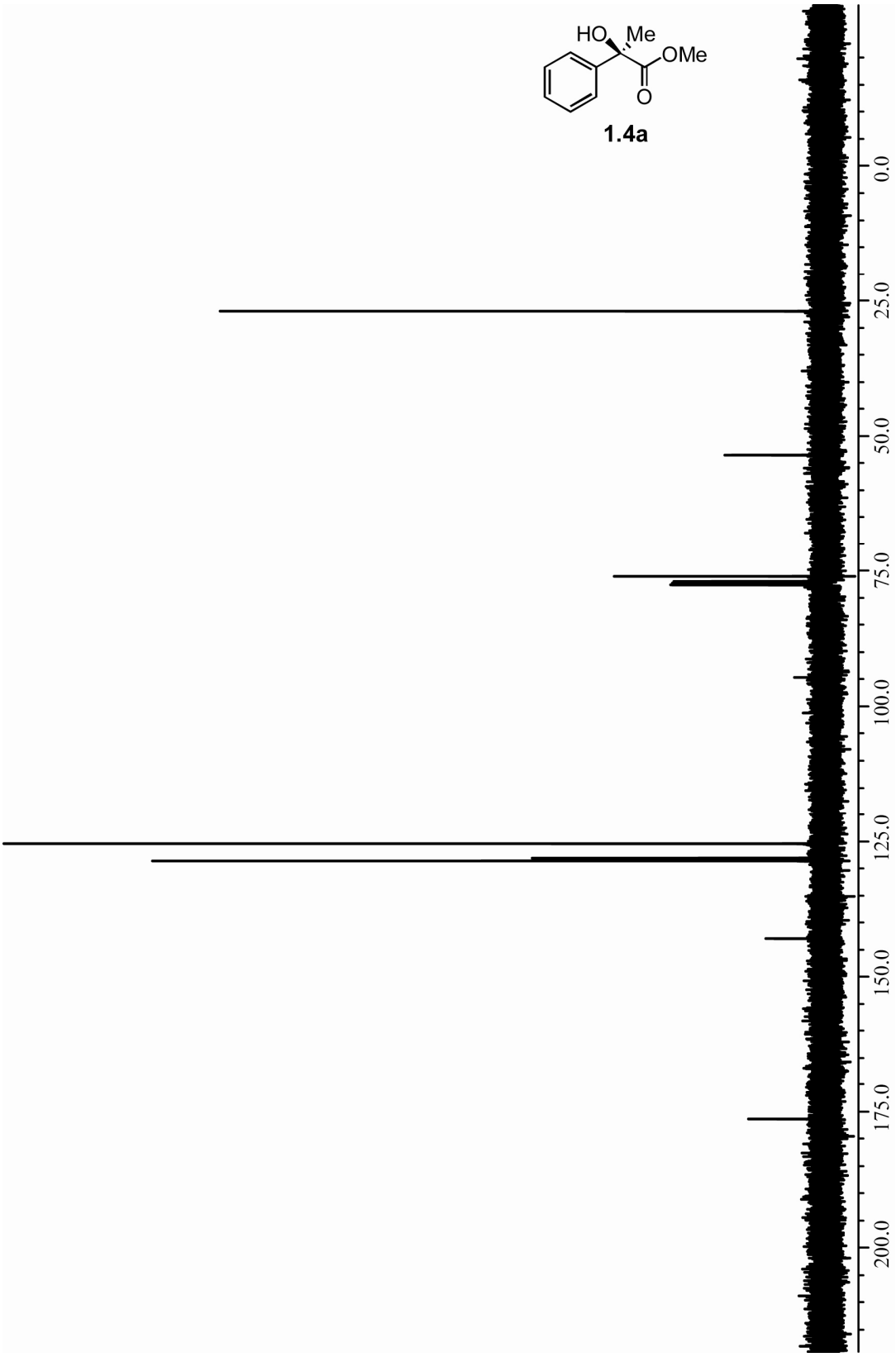
HO
Me
OMe
O
1.4a
0.0
25.0
50.0
75.0
100.0
125.0
150.0
175.0
200.0

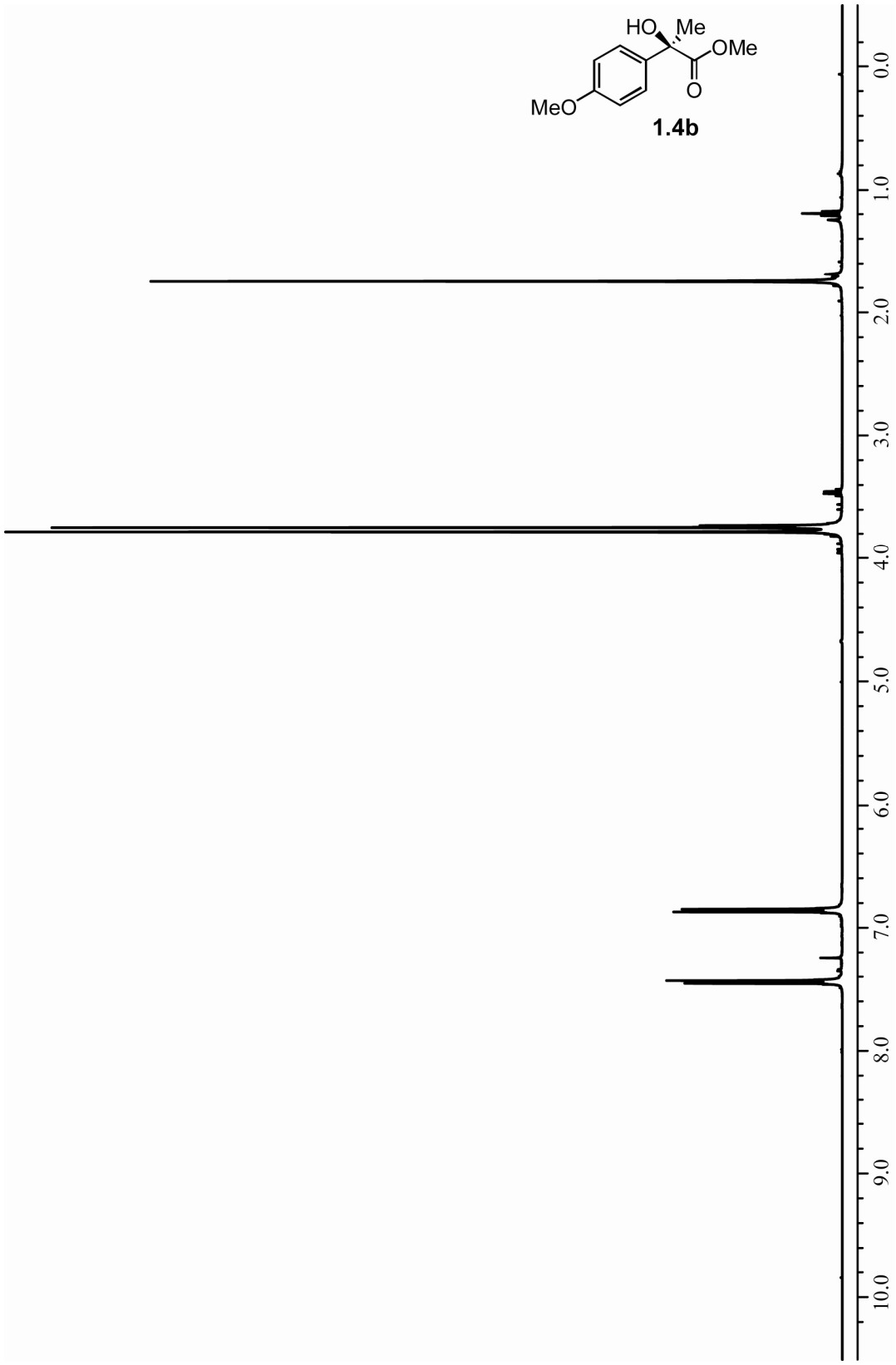
HO
Me
OMe
O
MeO
1.4b
0.0
1.0
2.0
3.0
4.0
5.0
6.0
7.0
8.0
9.0
10.0

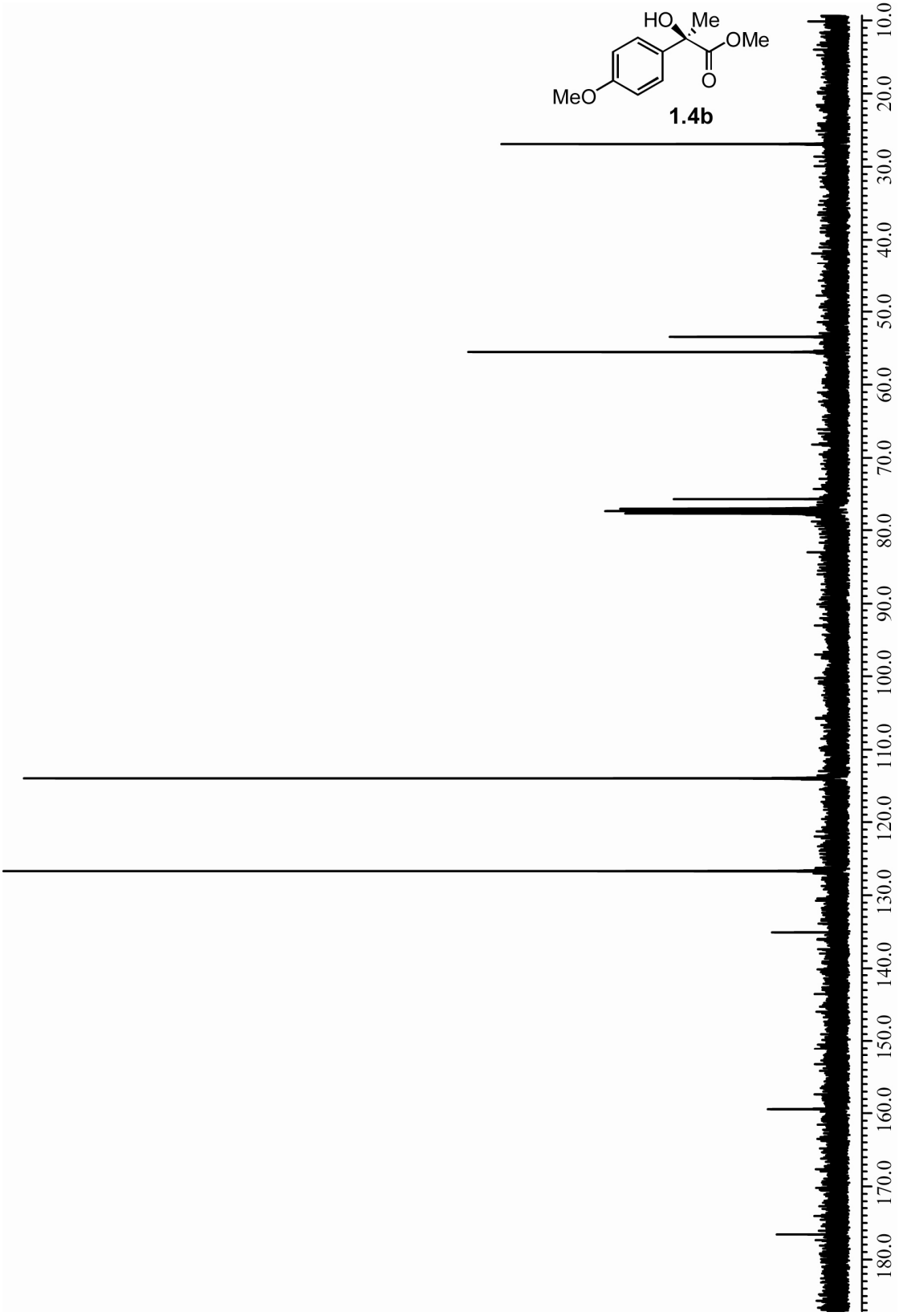
HO
Me
OMe
O
MeO
1.4b
10.0
20.0
30.0
40.0
50.0
60.0
70.0
80.0
90.0
100.0
110.0
120.0
130.0
140.0
150.0
160.0
170.0
180.0

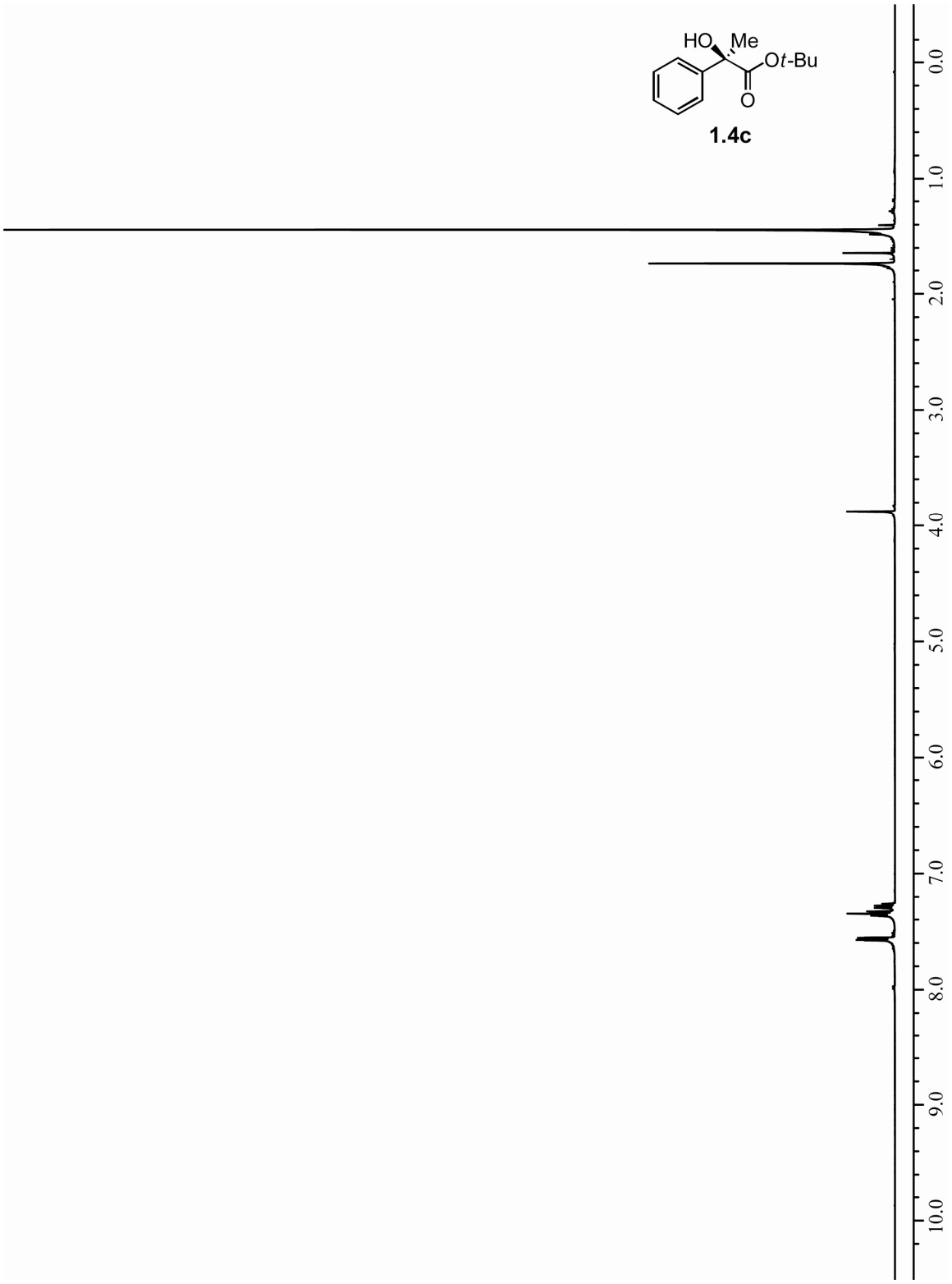
HO
Me
Ot-Bu
O
1.4c
0.0
1.0
2.0
3.0
4.0
5.0
6.0
7.0
8.0
9.0
10.0

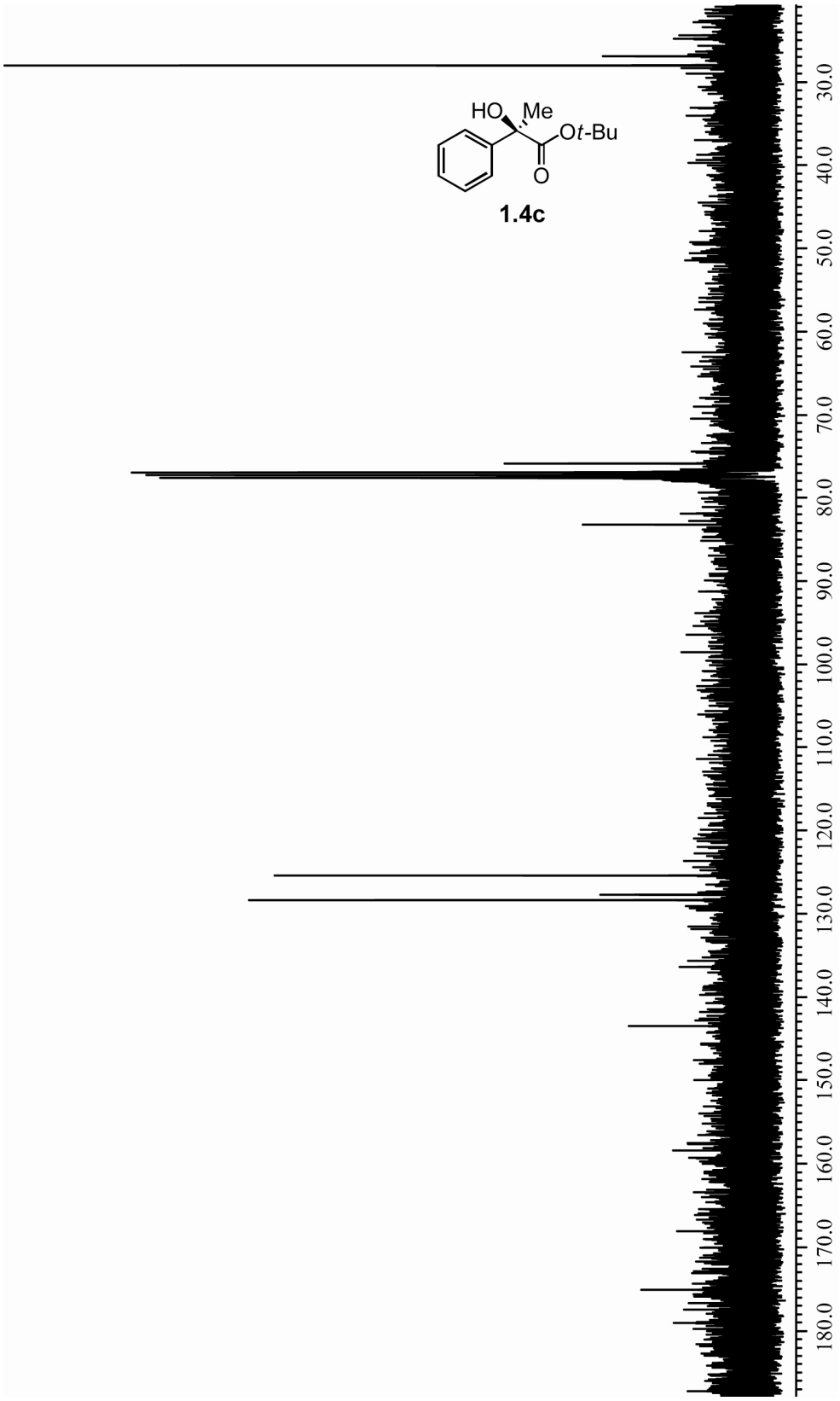
HO
Me
Ot-Bu
O
1.4c
30.0
40.0
50.0
60.0
70.0
80.0
90.0
100.0
110.0
120.0
130.0
140.0
150.0
160.0
170.0
180.0

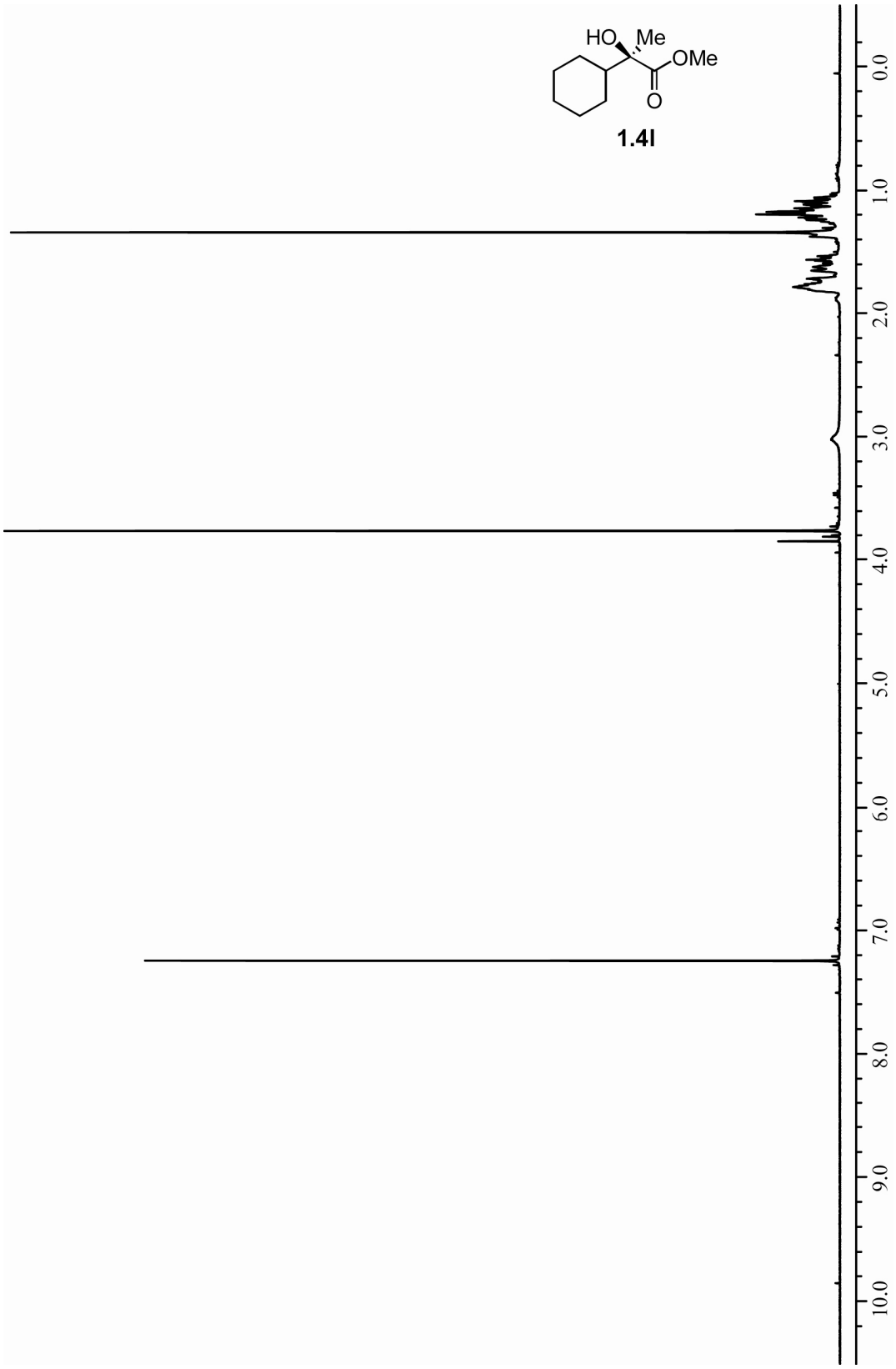
HO
Me
OMe
O
1.4l
0.0
1.0
2.0
3.0
4.0
5.0
6.0
7.0
8.0
9.0
10.0


HO
Me
OMe
O
1.4l
10.0
20.0
30.0
40.0
50.0
60.0
70.0
80.0
90.0
100.0
110.0
120.0
130.0
140.0
150.0
160.0
170.0
180.0

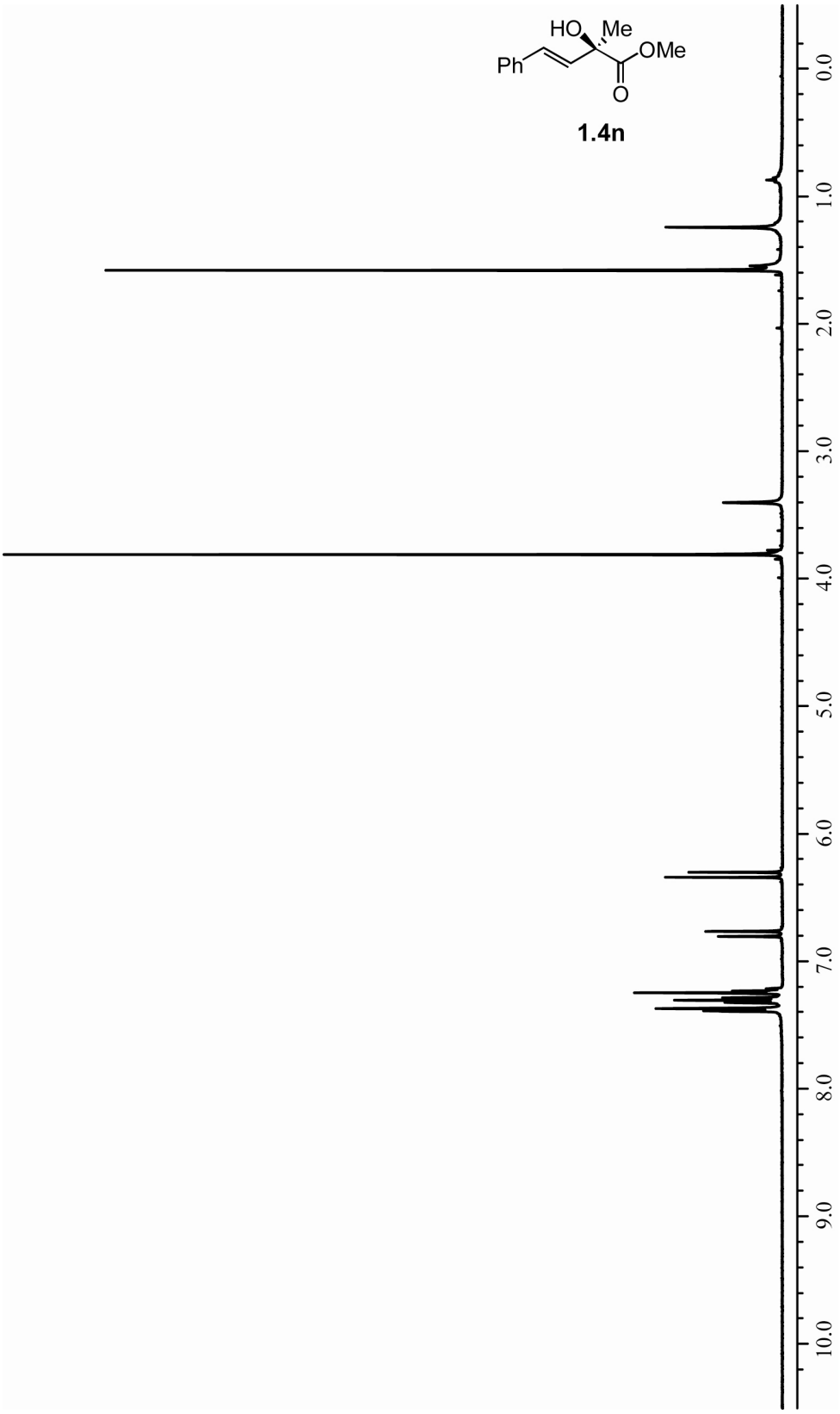
HO
Me
OMe
Ph
O
1.4n
0.0
1.0
2.0
3.0
4.0
5.0
6.0
7.0
8.0
9.0
10.0

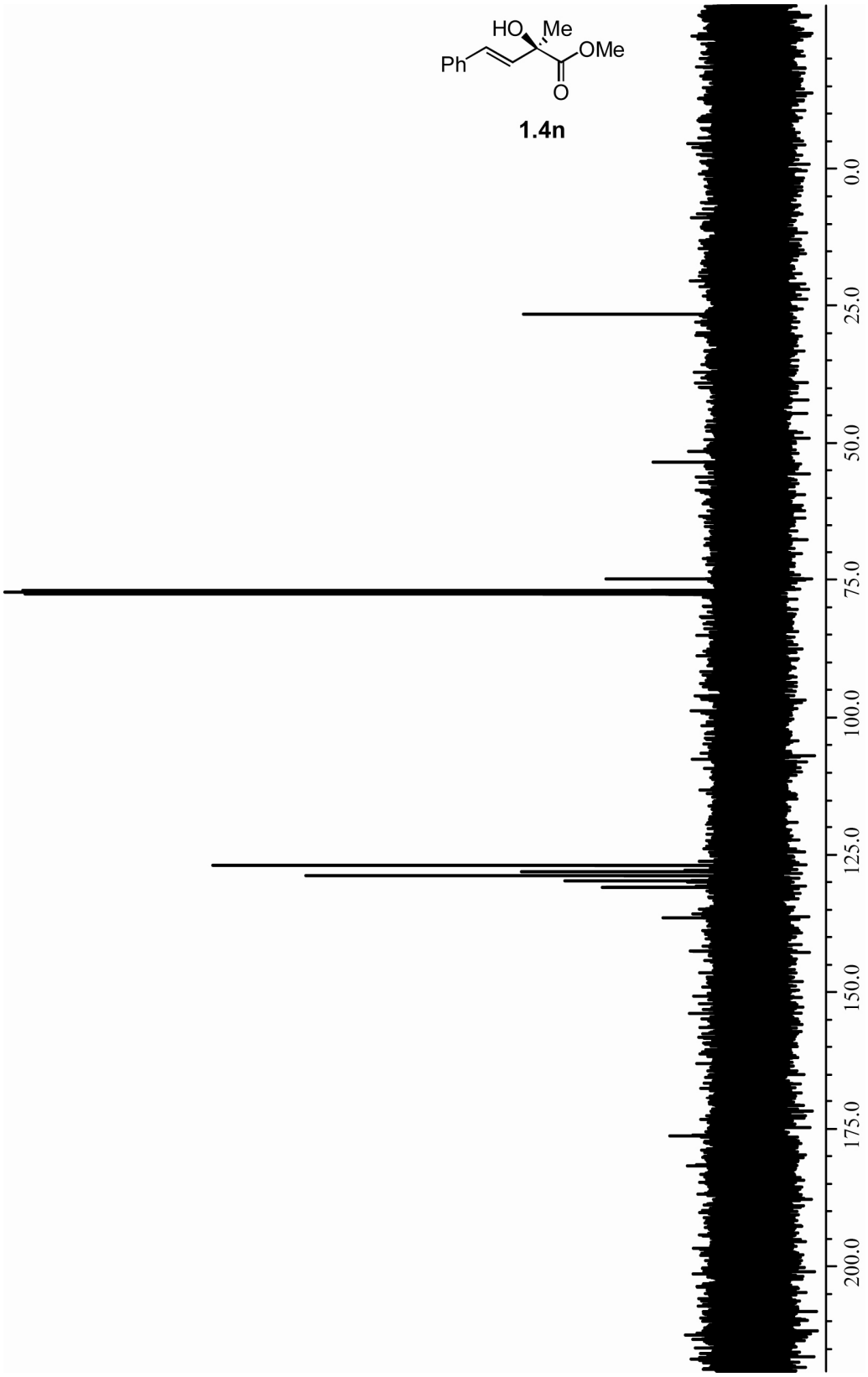
HO
Me
Ph
OMe
O
1.4n
0.0
25.0
50.0
75.0
100.0
125.0
150.0
175.0
200.0

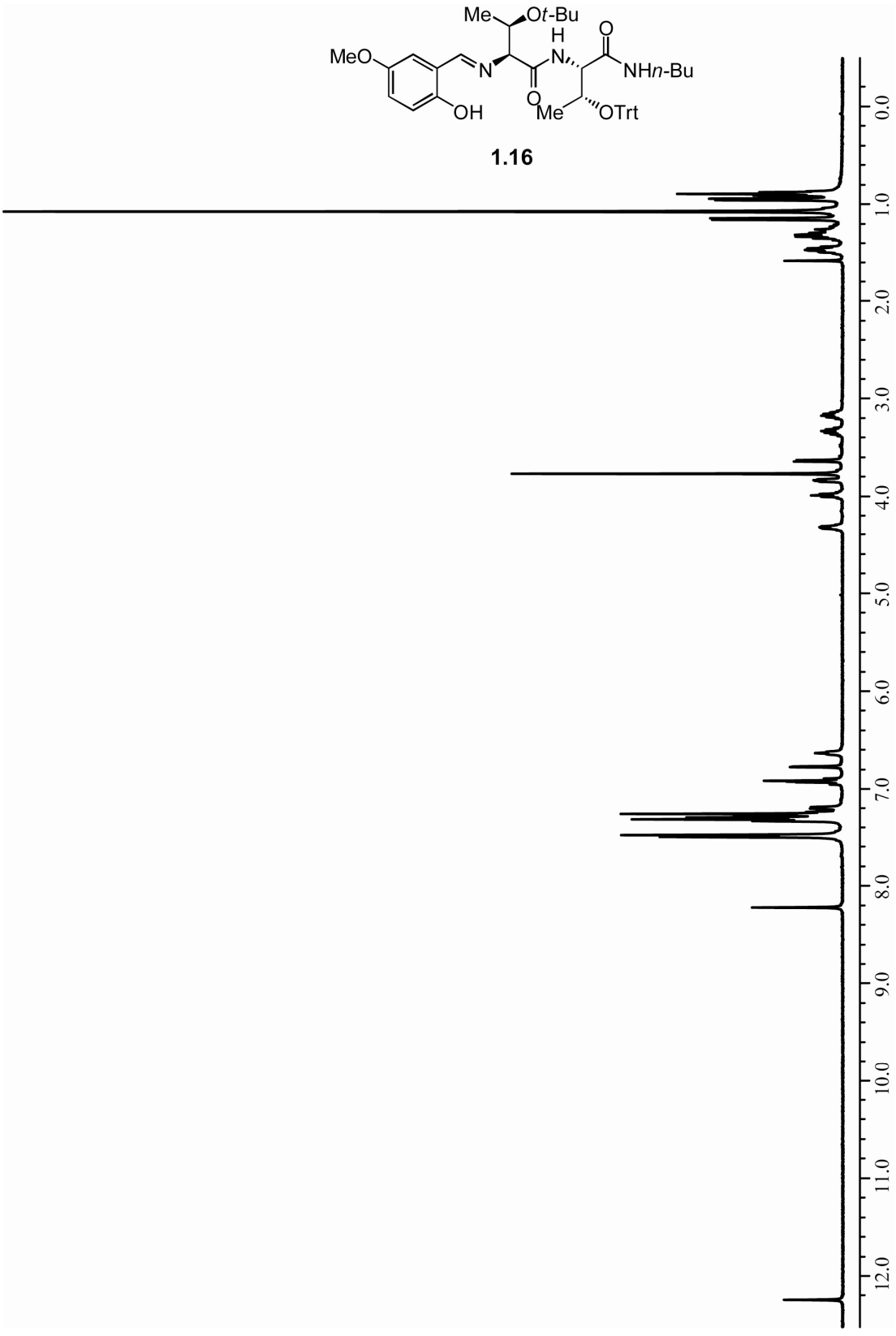
Me
Ot-Bu
H
N
O
MeO
N
NHn-Bu
O
OH
Me
OTrt
1.16
0.0
1.0
2.0
3.0
4.0
5.0
6.0
7.0
8.0
9.0
10.0
11.0
12.0

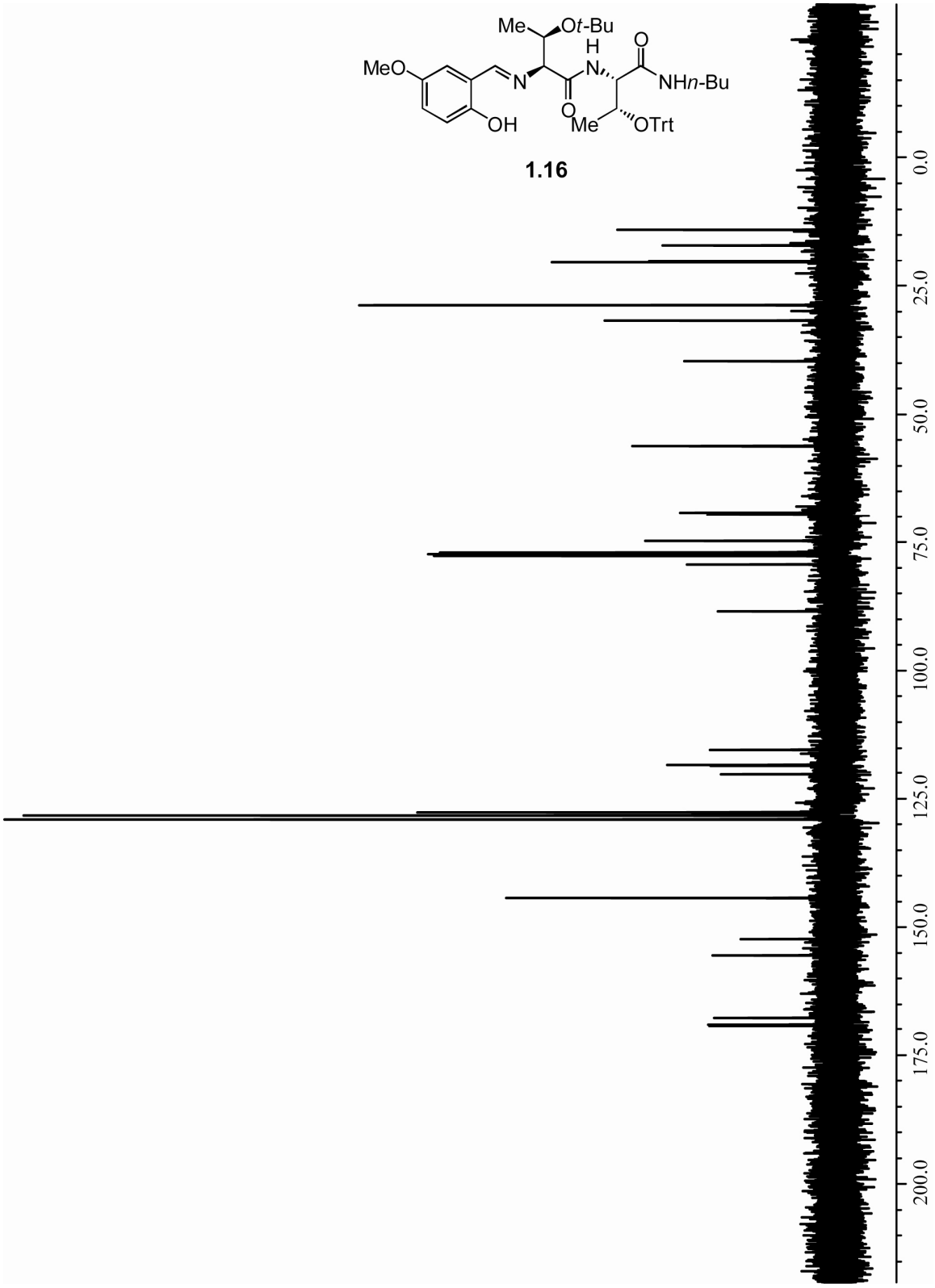
Me
Ot-Bu
H
O
MeO
N
N
NHn-Bu
O
OH
Me
OTrt
0.0
25.0
50.0
75.0
100.0
125.0
150.0
175.0
200.0

1.16

Chapter 2. **Ag-Catalyzed Enantioselective Vinylogous Mannich-Type Reactions with of α-Ketoimine Esters with Siloxyfuran**

2.1 *Introduction*

According to a 1999 review in Pure and Applied Chemistry,[60] "greater than 75% of drugs and drug candidates incorporate amine functionality." A significant number of methods have been developed to synthesize chiral amines in a catalytic enantioselective fashion, however a vast majority of these methods are only effective for the synthesis of secondary carbinamines (see Figure 2.1). Current methods for the enantioselective synthesis of chiral amines include the addition of carbon nucleophiles to imines[61] (i.e. alkylation with alkyl metals,[62] Strecker reactions,[63] Mannich-type reactions,[64] and allylations[65]); however, many of the methods currently available for the synthesis of chiral amines involve the addition of a hydride[66] (i.e. hydrosilylation, hydrogenation, reductive amination), thus rendering the formation of quaternary *N*-substituted carbon

---

(60) "Stereoselective reactions with imines," Dai, L.-X.; Lin, T.-R.; Hou, X.-L.; Zhou, Y.-G. *Pure Appl. Chem.* **1999**, *71*, 1033-1040.
(61) For reviews see: (a) "Catalytic Enantioselective Addition to Imines," Kobayashi, S.; Ishitani, H. *Chem. Rev.* **1999**, *99*, 1069-1094. (b) "Recent Advances in Catalytic Asymmetric Addition to Imines and Related C=N Systems," Vilaivan, T.; Bhanthumnavin, W.; Sritana-Anant, Y. *Curr. Org. Chem*. **2005**, *9*, 1315-1392. (c) "Recent Developments in Asymmetric Catalytic Addition to C=N Bonds," Friestad, G. K.; Mathies, A. K. *Tetrahedron* **2007**, *63*, 2541-2569.
(62) For a review see: "Ligand-Mediated Addition of Organometallic Reagents to Azomethine Functions," Denmark, S. E.; Nicaise, O., J.-C. *Chem. Commun*. **1996**, 999-1004.
(63) For a review see: "Catalytic Enantioselective Strecker Reactions and Analogous Syntheses," Gröger, H. *Chem. Rev*. **2003**, *103*, 2795-2827.
(64) For reviews see: (a) "Modern Variants of the Mannich Reaction," Arend, M.; Westermann, B.; Risch, N. *Angew. Chem. Int. Ed*. **1998**, *37*, 1044-1070. (b) "Vinylogous Mannich Reactions: Selectivity and Synthetic Utility," Bur, S. K.; Martin, S. F. *Tetrahedron* **2001**, *57*, 3221-3242. (c) "The Direct Catalytic Asymmetric Mannich Reaction," Córdova, A. *Acc. Chem. Res*. **2004**, *37*, 102-112. (d) Marques, M. M. B. *Angew. Chem. Int. Ed*. **2006**, *45*, 348-352. (c) "Catalytic Enantioselective Cross-Mannich Reaction of Aldehydes," Marques, M. M. B. *Angew. Chem. Int. Ed*. **2006**, *45*, 348-352.
(65) "Catalytic Enantioselective Allylation of Ketoimines," Wada, R.; Shibuguchi, T.; Makino, S.; Oisaki, K.; Kanai, M.; Shibasaki, M. *J. Am. Chem. Soc.* **2006**, *128*, 7687-7691.
(66) For reviews see: (a) "Asymmetric Reductions of Carbon Nitrogen Double Bonds. A Review," Zhu, Q.-C.; Hutchins, R. O.; Hutchins, M. K. *Org. Prep. Proced. Int.* **1994**, *26*, 193-236. (b) "Recent Advances in Asymmetric Reduction of Imines and Imine Derivatives," Brunel, J. M. *Recent Res. Dev. Org. Chem.* **2003**, *7*, 155-190.

centers impossible. As synthetic organic chemists, it is important that we discover effective ways to synthesize biologically important molecules, and we must also push ourselves to discover solutions to the most difficult problems in organic synthesis. With both of these goals in mind, we focused our attention on catalytic enantioselective Mannich reactions with ketoimines.

Figure 2.1: The asymmetric Mannich reaction in the generation of β-amino acid derivatives

R = H: secondary carbinamine
R = alkyl: tertiary carbinamine

While the Mannich reaction has long been recognized as an efficient method for the generation of β-amino carbonyls (Figure 2.1),[67] its utility in the synthesis of quaternary α-amino acids has not been well established. The synthesis of quaternary α-amino acids is a challenging problem, and one that has received a significant amount of attention,[68] however there are limited methods to synthesize these stereocenters in a catalytic enantioselective manner,[69] and industrial syntheses of these stereocenters principally rely on diastereoselective methodologies or resolution techniques.[70]

---

(67) For reviews, see: (a) "Recent Advances in the Stereoselective Synthesis of β-Amino Acids," Liu, M.; Sibi, M. P. *Tetrahedron* **2002**, *58*, 7991-8035. (b) "Recent Developments in the Catalytic Asymmetric Synthesis of α- and β-Amino Acids," Ma, J.-A. *Angew. Chem. Int. Ed*. **2003**, *42*, 4290-4299.

(68) For a reviews on the stereoselective synthesis of quaternary α-amino acids see: (a) "Stereoselective Synthesis of Quaternary α-Amino Acids. Part 1: Acyclic Compounds," Cativiela, C.; Díaz-de-Villegas, M. D. *Tetrahedron: Asymmetry*, **1998**, *9*, 3517-3599. (b) "Stereoselective Synthesis of Quaternary α-Amino Acids. Part 2: Cyclic Compounds," Cativiela, C.; Díaz-de-Villegas, M. D. *Tetrahedron: Asymmetry*, **2000**, *11*, 645-732. (c) "Towards Control of χ-Space: Conformationally Constrained Analogues of Phe, Tyr, Trp, and His," Gibson, S. E.; Guillo, N.; Tozer, J. J. *Tetrahedron* **1999**, *55*, 585-615. (d) "Cyclic Amino Acid Derivatives," Park, K.-H.; Kurth, M. J. *Tetrahedron* **2002**, *58*, 8629-8659. (e) "Enantio- and Diastereoselective Construction of α,α-Disubstituted α-Amino Acids for the Synthesis of Biologically Active Compounds," Ohfune, Y.; Shinada, T. *Eur. J. Org. Chem*. **2005**, 5127-5143. (f) "Recent Progress on the Stereoselective Synthesis of Acyclic Quaternary α-Amino Acids," Cativiela, C.; Díaz-de-Villegas, M. D. *Tetrahedron: Asymmetry* **2007**, *18*, 569-623.

(69) "Catalytic Asymmetric Synthesis of α-Amino Acids," Najera, C.; Sansano, J. M. *Chem. Rev*. **2007**, *107*, 4584-4671.

(70) "Asymmetric Synthesis of Active Pharmaceutical Ingredients," Farina, V.; Reeves, J. T.; Senanayake, C. H.; Song, J. J. *Chem. Rev*. **2006**, *106*, 2734-2793.

Quaternary α-amino acids and their derivatives are motifs found in a number of naturally-occurring and biologically important compounds (Figure 2.2).[71]

Figure 2.2: The asymmetric Mannich reaction in the generation of quaternary α-amino acid derivatives, and some biologically important molecules which contain a chiral N-substituted quaternary carbon center

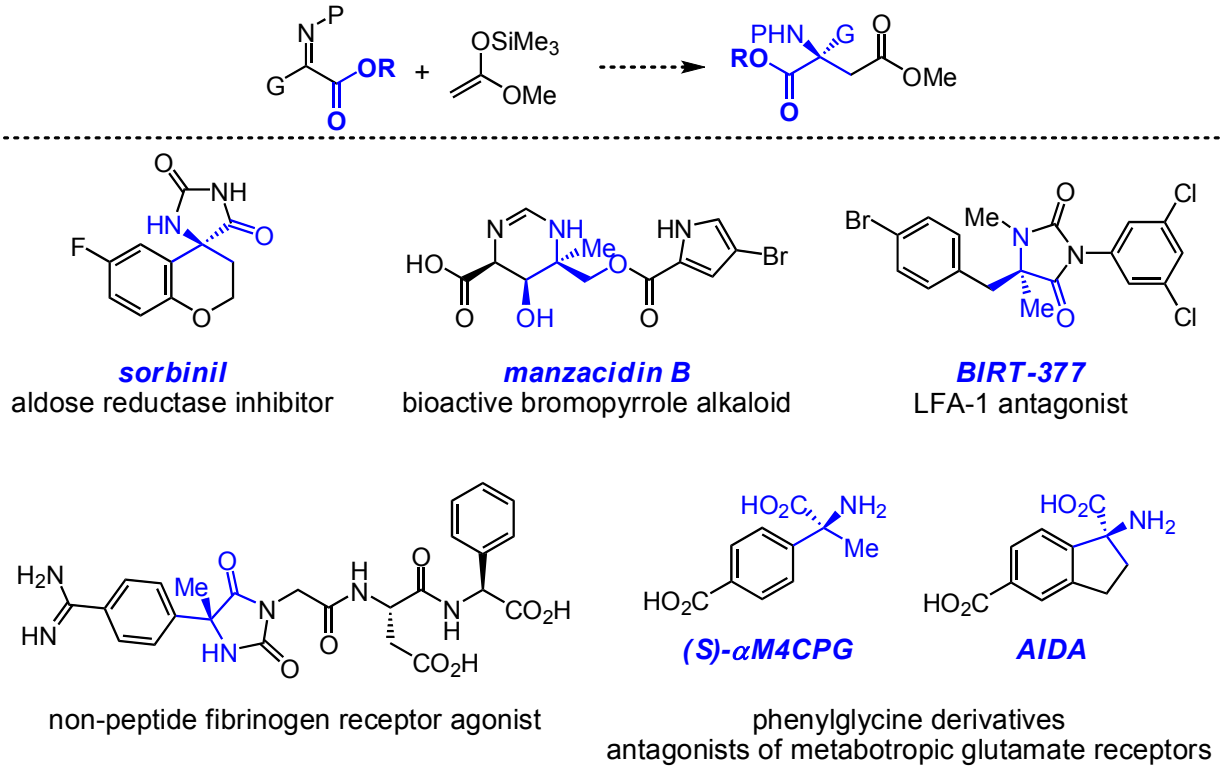

2.2 *Background*

2.2.a Ketoimines as substrates: some general considerations[72]

Several methods have been developed within these laboratories for catalytic, enantioselective nucleophilic additions to aldimines to generate non-racemic tertiary

(71) "Total Synthesis of Natural *tert*-Alkylamino Hydroxy Carboxylic Acids," Kang, S. H.; Kang, S. Y.; Lee, H.-S.; Buglass, A. J. *Chem. Rev.* **2005**, *105*, 4537-4558.
(72) For a review on catalytic enantioselective additions to ketones and ketoimines, see: "Asymmetric Catalysis for the Construction of Quaternary Carbon Centres: Nucleophilic Addition on Ketones and Ketoimines," Riant, O.; Hannedouche, J. *Org. Biomol. Chem.* **2007**, *5*, 873-888.

carbinamines. These methods include alkylation with dialkylzinc reagents,[73] aza-Diels-Alder reactions,[74] Mannich-type reactions,[75] and Strecker reactions.[76] It is only recently that we have shifted our attention towards reactions with ketoimines.[15b] There are several considerations to bear in mind when comparing ketoimines with aldimines. First, ketoimines are significantly less reactive than aldimines towards nucleophilic attack. Imines in general are inherently non-electrophilic due to the lack of polarity of the C=N double bond. In fact, the C=N double bond is more similar to an olefin, than to a carbonyl, both in bond strength and bond length (Figure 2.3).

Figure 2.3: The bond strength and length of some C=X bonds

C=X:			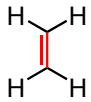
bond strength:	***178 kcal/mol***	***143 kcal/mol***	***149 kcal/mol***
bond length:	***1.21Å***	***1.28 Å***	***1.32 Å***

(73) (a) "Enantioselective Synthesis of Arylamines Through Zr-Catalyzed Addition of Dialkylzincs to Imines. Reaction Development by Screening of Parallel Libraries," Porter, J. R.; Traverse, J. F.; Hoveyda, A. H.; Snapper, M. L. *J. Am. Chem. Soc*. **2001,** *123*, 984-985. (b) "Three-Component Catalytic Asymmetric Synthesis of Aliphatic Amines," Porter, J. R.; Traverse, J. F.; Hoveyda, A. H.; Snapper, M. L. *J. Am. Chem. Soc*. **2001,** *123*, 10409-10410. (c) "Enantioselective Synthesis of Propargylamines through Zr-Catalyzed Addition of Mixed Alkynylzinc Reagents to Arylimines," Traverse, J. F.; Hoveyda, A. H.; Snapper, M. L. *Org. Lett*. **2003**, *5*, 3273-3275. (d) "Three-Component Enantioselective Synthesis of Propargylamines through Zr-Catalyzed Additions of Alkyl Zinc Reagents to Alkynylimines," Akullian, L. C.; Snapper, M. L.; Hoveyda, A. H. *Angew. Chem. Int. Ed*. **2003**, *42*, 4244-4247. (e) "Asymmetric Synthesis of Acyclic Amines Through Zr- and Hf-Catalyzed Enantioselective Alkylzinc Reagents to Imines," Akullian, L. C.; Porter, J. R.; Traverse, J. F.; Snapper, M. L.; Hoveyda, A. H. *Adv. Synth. Catal*. **2005**, *347*, 417-425.

(74) "Efficient and Practical Ag-Catalyzed Cycloadditions between Arylimines and the Danishefsky Diene," Josephsohn, N. S.; Snapper, M. L.; Hoveyda, A. H. *J. Am. Chem. Soc.* **2003**, 125, 4018-4019.

(75) (a) "Ag-Catalyzed Asymmetric Mannich Reactions of Enol Ethers with Aryl, Alkyl, Alkenyl, and Alkynyl Imines," Josephsohn, N. S.; Snapper, M. L.; Hoveyda, A. H. *J. Am. Chem. Soc.* **2004**, 126, 3734-3735. (b) "Practical and Highly Enantioselective Synthesis of β-Alkynyl-β-amino Esters through Ag-Catalyzed Asymmetric Mannich Reactions of Silylketene Acetals and Alkynyl Imines," Josephsohn, N. S.; Carswell, E. L.; Snapper, M. L.; Hoveyda, A. H. *Org. Lett.,* **2005**, *7*, 2711-2713. (c) "A Highly Efficient and Practical Method for Catalytic Asymmetric Vinylogous Mannich (AVM) Reactions," Carswell, E. L.; Snapper, M. L.; Hoveyda, A. H. *Angew. Chem. Int. Ed*. **2006**, *45*, 7230-7233.

(76) (a) **"**Ti-Catalyzed Enantioselective Addition of Cyanide to Imines. A Practical Synthesis of Optically Pure α-Amino Acids," Krueger, C. A.; Kuntz, K. W.; Dzierba, C. D.; Wirschun, W. G.; Gleason, J. D.; Snapper, M. L.; Hoveyda, A. H. *J. Am. Chem. Soc*. **1999**, *121*, 4284-4285. (b) "Ti-Catalyzed Regio- and Enantioselective Synthesis of Unsaturated α-Amino Nitriles, Amides, and Acids. Catalyst Identification through Screening of Parallel Libraries," Porter, J. R.; Wirschun, W. G.; Kuntz, K. W.; Snapper, M. L.; Hoveyda, A. H. *J. Am. Chem. Soc.* **2000**, *122*, 2657-2658. (c) "Mechanism of Enantioselective Ti-Catalyzed Strecker Reaction: Peptide-Based Metal Complexes as Bifunctional Catalysts," Josephsohn, N. S.; Kuntz, K. W.; Snapper, M. L.; Hoveyda, A. H. *J. Am. Chem. Soc.* **2001,** *123*, 11594-11599.

In the case of ketoimines, the imine is even less electrophilic due to both steric and electronic factors (Figure 2.4). The steric environment surrounding the prochiral carbon is more crowded, hindering nucleophilic attack. Additionally, the prochiral carbon of a ketoimine has two alkyl substituents attached to it, in comparison to one alkyl substituent and one proton in the case of aldimines. This additional alkyl group is generally more electron-donating than a proton, further decreasing the electrophilicity at the prochiral carbon.

Figure 2.4: Ketoimines are less reactive than aldimines to nucleophilic attack

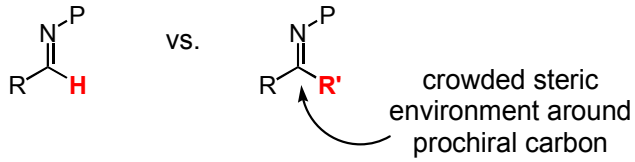

alkyl groups are more electron-donating than a hydrogen
causing a ***decrease in electrophilicity*** at the prochiral carbon

Additionally, tautomerization can be a problem in aliphatic substrates which have an α-proton (Figure 2.5), and results in a nucleophilic enamine (rather than an electrophilic imine).

Figure 2.5: Imines bearing an α-proton are susceptible to enamine formation

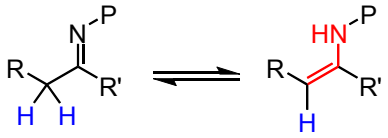

One final consideration which applies to ketoimines, but not aldimines, is *E:Z* selectivity in the ketoimine substrate synthesis (Figure 2.6). When R' ≠ H, there is less stereodifferentiation between R and R', and the energy difference between the *E* and *Z* imine isomers is minimized.

Figure 2.6: Ketoimines cannot always be synthesized in good *E:Z* selectivity

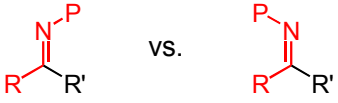

2.2.b Literature precedence for catalytic, enantioselective Mannich-type reactions with ketoimines

To date, there are three reports in the literature on catalytic, enantioselective Mannich-type reactions with ketoimines. The first two examples, from the Jørgensen group, utilized a specific α-ketoimine ester substrate, which was engineered to address the issues with ketoimine substrates that were described above (**2.1**, Figure 2.7).[77] The prochiral C=N bond in ketoimine **2.1** was activated by both the electron-withdrawing ester group at the α-position, as well as the electron-withdrawing carbamate protecting group. These highly electron-withdrawing groups would not be well tolerated in an aliphatic ketoimine; however, the substrate does not have α-protons capable of tautomerization. Finally, the carbamate protecting group was anchored to the aryl ring thus ensuring that the ketoimine was synthesized as a single (*E*) stereoisomer.

Figure 2.7: α-Ketoimine ester substrate utilized by the Jørgensen group

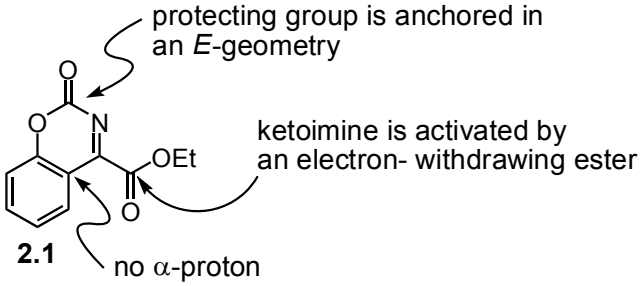

In the first report by the Jørgensen group, ketoimine substrate **2.1** underwent Zn-pybox-catalyzed enantioselective Mannich-type reactions with silylketene acetals in high selectivities and with good yields (Scheme 2.1). In reactions with mono-substituted silylketene acetals, diastereoselectivities ranged from 5:1 to 8:1, however, the diastereomeric products were inseparable. The Mannich product **2.4a** could be deprotected to form lactone **2.5** in good yield (79%).

---

(77) (a) "The First Catalytic Highly Enantioselective Alkylation of Ketoimines – A novel Approach to Optically Active Quaternary α-Amino Acids," Saaby, S.; Nakama, K.; Lie, M. A.; Hazell, R. G.; Jørgensen, K. A. *Chem. Eur. J.* **2003**, *9*, 6145-6154. (b) "Direct Organocatalytic Enantioselective Mannich Reactions of Ketoimines: An Approach to Optically Active Quaternary α-Amino Acid Derivatives," Zhuang, W.; Saaby, S. Jørgensen, K. A. *Angew. Chem,. Int. Ed.* **2004**, *43*, 4476-4478.

Scheme 2.1: Zn-pybox-catalyzed enantioselective Mannich-type reactions with α-ketoimine ester **2.1**

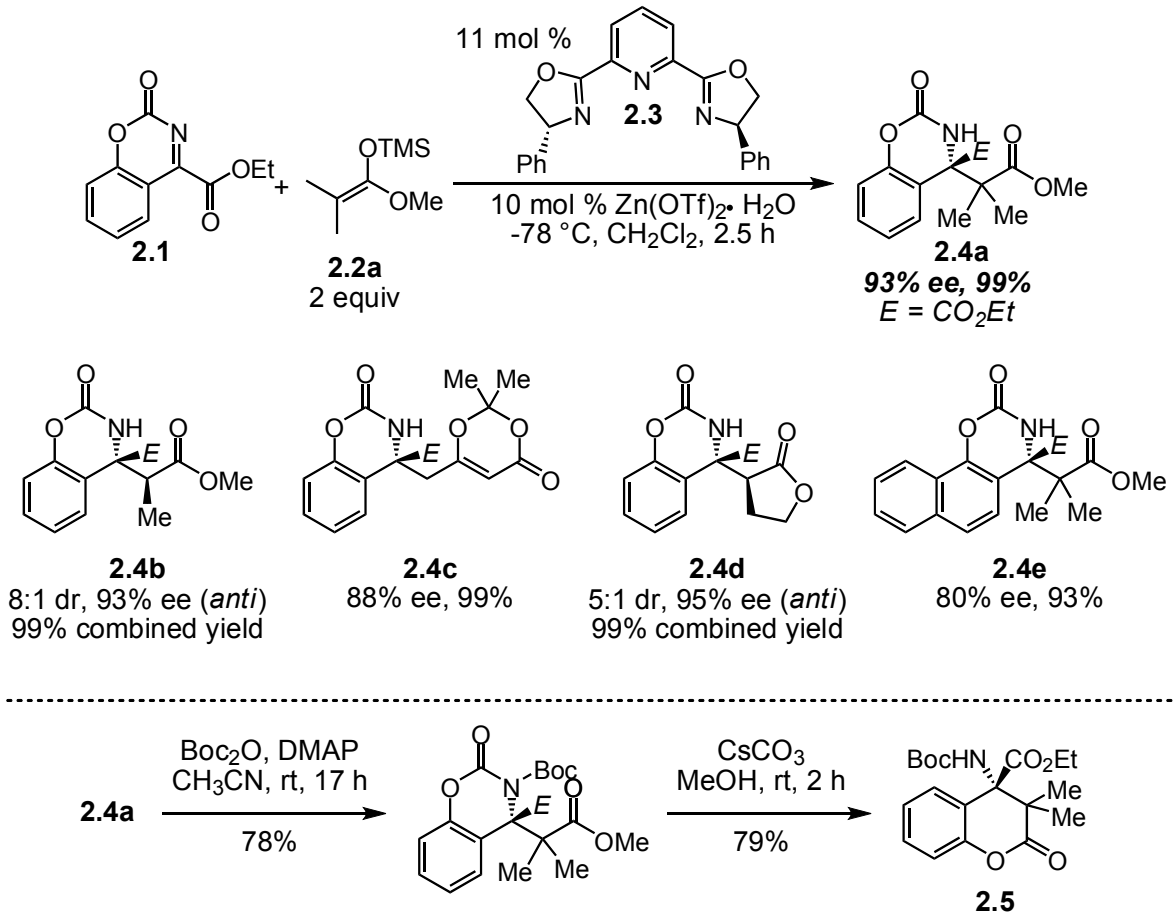

The second report from the Jørgensen group demonstrated the utility of ketoimine substrate **2.1** in the direct Mannich-type reaction with aldehydes (Scheme 2.2). The resulting β-amino aldehydes (i.e. **2.8a**, Scheme 2.2) were obtained in high enantioselectivities and yields (83-98% ee, 72-99% yield). Diastereoselectivities ranged from 4:1->20:1, and as with the previous example, mixtures of diastereomers could not be separated. Notably, when ketoimine **2.9**, in which the protecting group is not anchored, was subjected to the optimal reaction conditions, there was <2% conversion to the Mannich adduct.

Scheme 2.2: Direct enantioselective Mannich-type reactions with α-ketoimine ester **2.1**

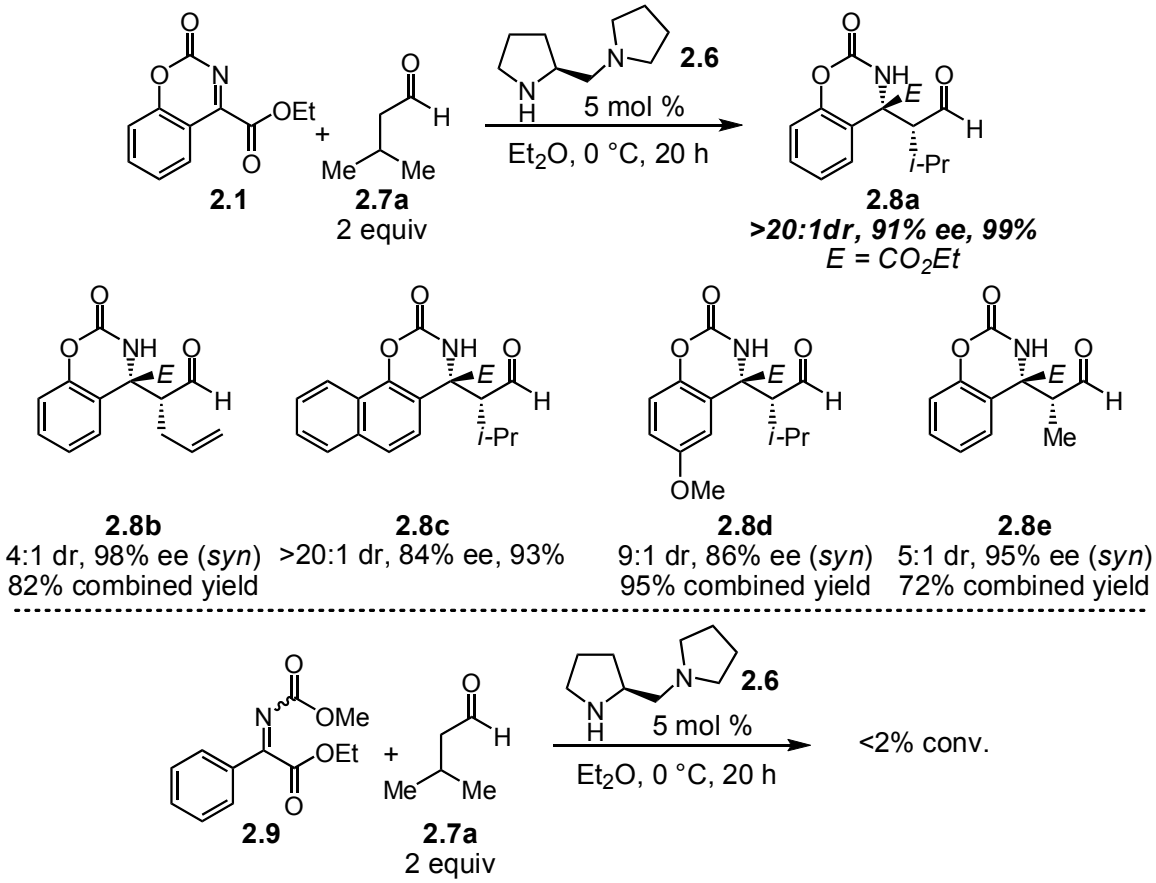

Most recently, Kanai and Shibasaki reported a Mannich-type reaction of silylketene acetals and *N*-phosphinoyl ketoimines derived from 'simple' ketones (i.e. acetophenone-derived ketoimines such as **2.10a**, Scheme 2.3).[78] In the presence of 10 mol % CuOAc, 10 mol % (*R*)-DTBM-SEGPHOS (**2.13**), and one equiv $(EtO)_2Si(OAc)_2$, aryl ketoimines underwemt efficient Mannich-type reaction with silylketene acetals to afford the β,β-disubstituted amino acid derivatives in good yields and enantioselectivities (61-87% yield, 91-97% ee, Scheme 2.3).

(78) "Catalytic Enantioselective Mannich-type Reactions of Ketoimines," Suto, Y.; Kanai, M.; Shibasaki, M. *J. Am. Chem. Soc.* **2007**, *129*, 500-501.

Scheme 2.3: Catalytic enantioselective Mannich-type reactions with aryl *N*-phosphinoyl ketoimines **2.10**

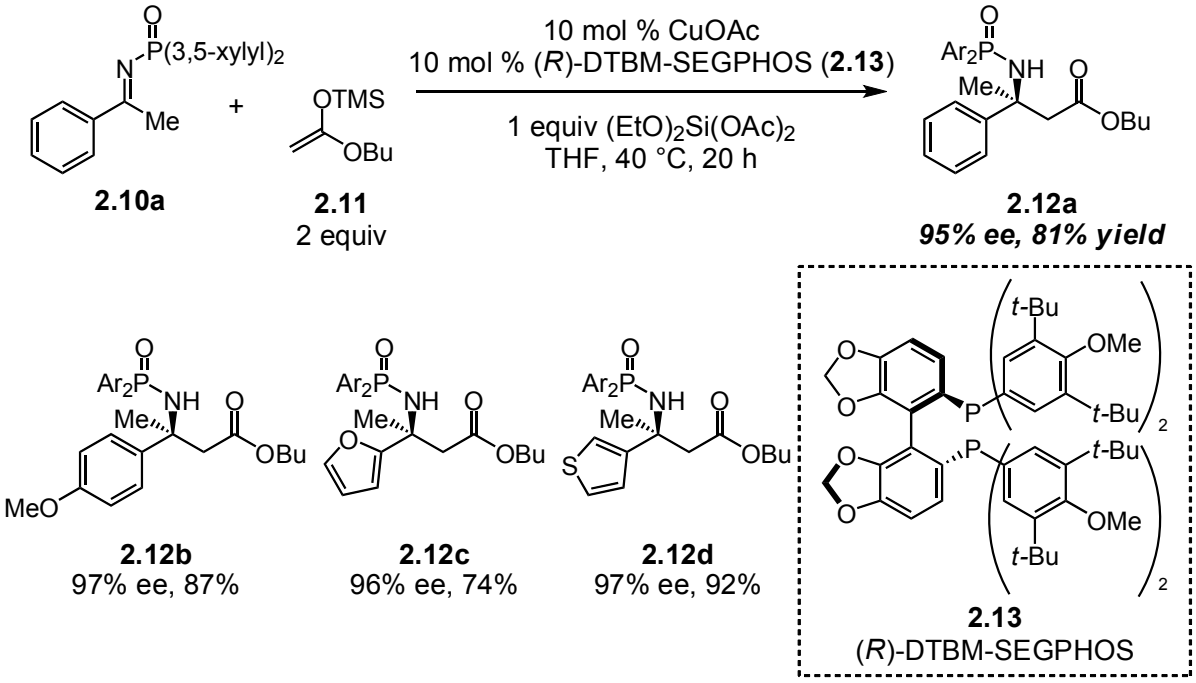

This report followed studies on the CuF-Taniphos-catalyzed enantioselective aldol reaction of ketones with silylketene acetals.[79] The authors proposed that a chiral Cu-enolate was generated *in situ* and served as the active nucleophile. The proposed turnover-limiting step was regeneration of the catalyst from the Cu-aldolate; this slow step was facilitated by addition of a stoichiometric amount of $(EtO)_3SiF$ and a catalytic amount of $PhBF_3K$. This combination of additives generated a small amount of a highly electrophilic silicon species [$(EtO)_{4-n}SiF_n$, $n \geq 2$], which can trap the Cu-aldolate as a $(EtO)_3Si$-aldolate, regenerating the catalyst.

Under the reaction conditions described in Scheme 2.3, alkyl-derived ketoimines (i.e. **2.14a**, Scheme 2.4) underwent Mannich-type reactions with good enantioselectivity, however the products were isolated in low yields (87% ee, 27% yield for **2.15a**, data not shown). This was attributed to tautomerization of the ketoimine substrates and side

(79) "Catalytic Enantioselective Aldol Reactions to Ketones," Oisake, K.; Zhao, D.; Kanai, M.; Shibasaki, M. *J. Am. Chem. Soc*. **2006**, *128*, 7164-7165.

reactions with the corresponding enamines. The yields of these reactions were improved by modifying the reaction conditions (10 mol % CuOAc, 10 mol % DuPHOS-derived ligand **2.16a**, four equiv **2.10**, and 1.2 equiv $(EtO)_3SiF$), however the enantioselectivity suffered under these new reaction conditions (81% ee, 99% yield for **2.15a**, Scheme 2.4).

Scheme 2.4: Catalytic enantioselective Mannich-type reactions with alkyl *N*-phosphinoyl ketoimines **2.14**

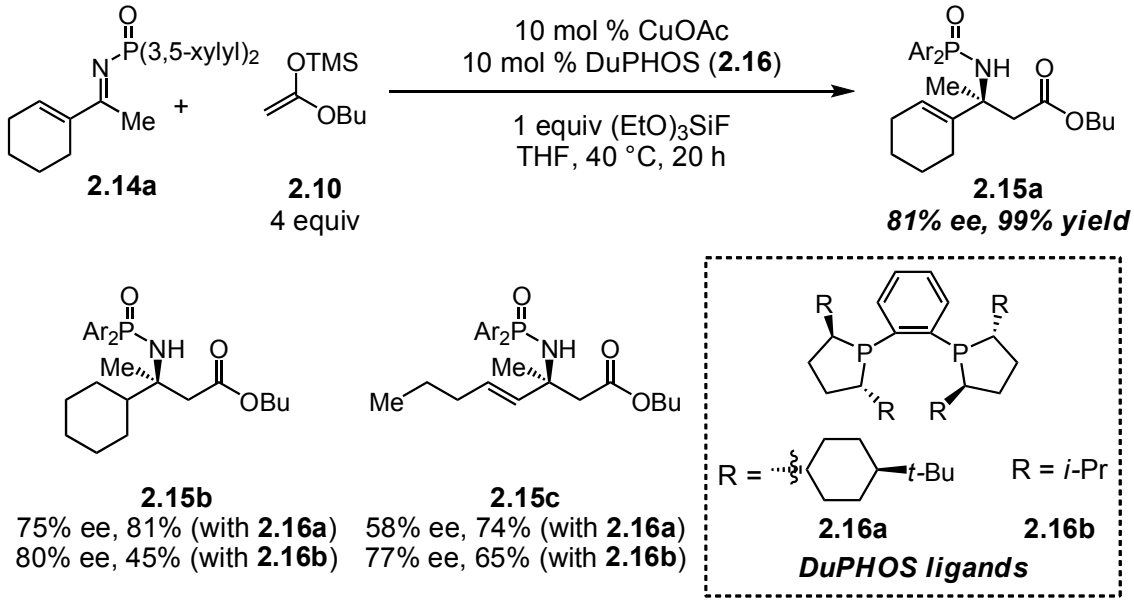

2.3 *Ag-catalyzed asymmetric Mannich-type reactions with α-ketoimine esters*

The problem of developing efficient catalytic, enantioselective Mannich-type reactions with ketoimines is far from being solved. While the methods described above were state of the art for this transformation, they were limited in terms of substrate and nucleophile generality. We set out to develop a new method for this catalytic transformation, utilizing chiral amino acid-based ligands previously developed within these laboratories for Ag-catalyzed enantioselective Mannich-type reactions with aldimines.[75] Representative examples of these Ag-catalyzed reactions are shown in Figure 2.8. A wide range of nucleophiles were utilized in these Ag-catalyzed processes, including silyl enol ethers (**2.20**), Danishefsky's diene (**2.21**), silylketene acetals (**2.23**)

and siloxyfurans (**2.25**). The range of substrates which undergo efficient enantioselective Mannich-type reactions with the aforementioned nucleophiles was equally varied, and included aromatic (**2.22a-b**, **2.26b**), heteroaromatic (**2.26a**) aliphatic (**2.18c**), alkenyl (**2.18b**), and alkynyl-aldimines (**2.17a**, **2.24a-b**). A unifying feature of these aldimine substrates is an *o*-anisidyl *N*-protecting group. The authors proposed that this protecting group acted not only to stabilize the aldimine substrate, thus allowing for the utility of aliphatic-based substrates, but also to provide a bidentate chelation site for Ag. Chiral phosphine ligand **2.19a** provided an additional bidentate chelation site, thus allowing AgOAc to exist in a tetrahedral conformation in the proposed transition state. We therefore included this versatile *o*-anisidyl *N*-protecting group as well as chiral amino acid-based phosphine ligand **2.19a** in our initial investigations into the development of Ag-catalyzed enantioselective Mannich-type reactions with ketoimines.

Figure 2.8: Representative enantioselective Mannich-type reactions with *o*-anisidine-protected aldimines (i.e. **2.17a**) catalyzed by AgOAc and chiral phosphine ligand **2.19a**

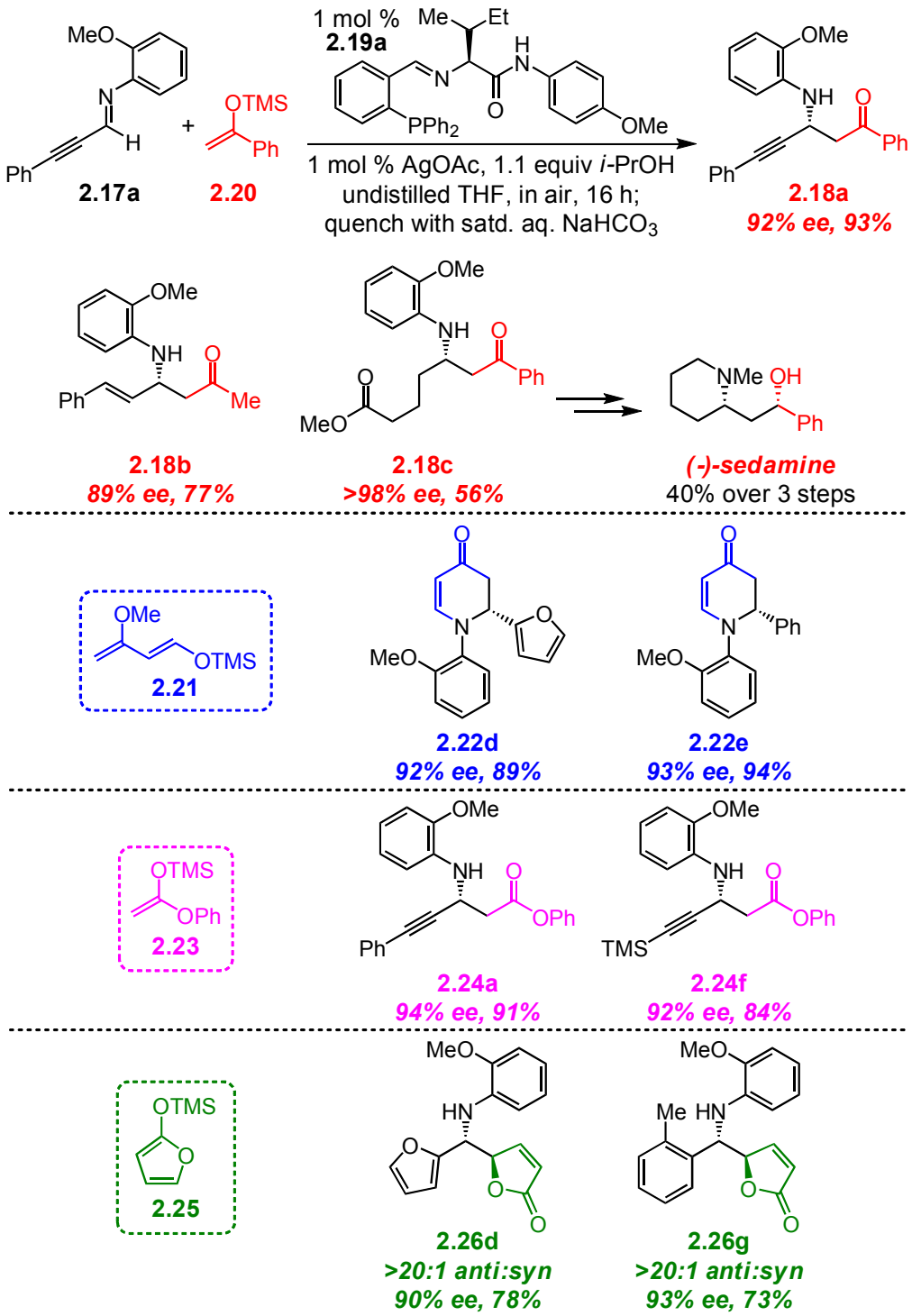

2.3.a Initial studies with acetophenone-derived silyl enol ether 2.20

In the presence of 10 mol % mono-amino acid-based ligand **2.19a** and 10 mol % AgOAc, α-ketoimine ester **2.27a** underwent Mannich-type reaction with acetophenone-derived silyl enol ether **2.20** to afford the desired Mannich-adduct **2.31a** in 21% conv, and 23% ee (entry 1, Table 2.1). Interestingly, when we re-positioned the *o*-chelating OMe group to the *p*-position (i.e. **2.28**), selectivity and conversion were unaffected (entries 1 and 3, Table 2.1). With Tle-derived mono-amino acid-based ligand **2.20a**, conversion and selectivity were significantly enhanced for both of these substrates (Table 1, entries 2 and 4).

Table 2.1: Initial studies with silyl enol ether **2.20** and methyl benzoylformate-derived α-ketoimine esters **2.27a-2.28**

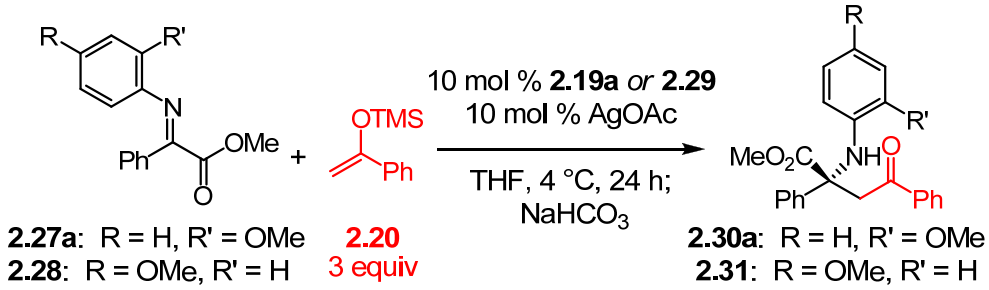

2.27a: R = H, R' = OMe
2.28: R = OMe, R' = H

2.20
3 equiv

2.30a: R = H, R' = OMe
2.31: R = OMe, R' = H

entry	Substrate	Ligand	% conv[a]	% ee[b]
1	**2.27a**	**2.19a**	21	23
2	**2.27a**	**2.29**	72	40
3	**2.28**	**2.19a**	23	23
4	**2.28**	**2.29**	75	40

[a]Determined by analysis of 400 MHz ^{1}H NMR spectra of the unpurified reaction mixtures. [b]Determined by chiral HPLC analysis; see Experimentals section for details.

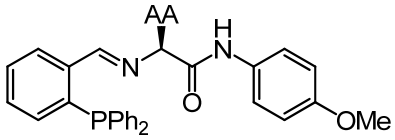

2.19a: AA = Ile
2.29: AA = Tle

Analogs of **2.19a** that contained variations at the C-terminus (**2.19b-f**, Table 2.2) were tested under the above conditions. A slight increase in enantioselectivity was observed with *p*-$Me_2NC_6H_4$ as the terminus (**2.19b**, 20% conv, 50% ee, entry 2), however a significantly more selective and reactive ligand was not identified from this screen.

Table 2.2: Mono-amino acid-based phosphine ligands **2.19a-f** in Ag-catalyzed Mannich-type reactions of silyl enol ether **2.20** with α-ketoimine ester **2.27a**

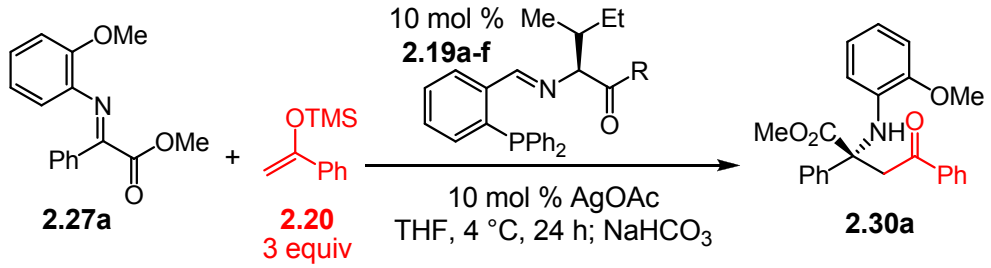

entry	ligand	R	% conv[a]	% ee[b]
1	**2.19a**	*p*-OMe-C_6H_4NH	21	23
2	**2.19b**	*p*-NMe_2-C_6H_4NH	20	50
3	**2.19c**	*p*-CF_3-C_6H_4NH	25	24
4	**2.19d**	2,6-Me-C_6H_3NH	<2	-
5	**2.19e**	OMe	<2	-
6	**2.19f**	NH*n*-Bu	<2	-

[a]Determined by analysis of 400 MHz ^{1}H NMR spectra of the unpurified reaction mixtures. [b]Determined by chiral HPLC analysis; see Experimentals section for details.

The ligand structure examined thus far was derived from a single amino acid. Therefore, minimal structural diversity was available through ligand modifications. Accordingly, we began to look at ligands derived from dipeptides. These results are summarized in Table 2.3. When AA2 was the naturally-occurring L-amino acid (and AA1 = Val or Tle), there was <5% ee (entries 1 and 6). Additionally, when AA2 was achiral (AA2 = Gly, AA1 = Val or Tle), the same lack of selectivity was observed (entries 2 and 5). However, when AA2 was the non-natural D-amino acid, up to 34% ee was observed (entries 3 and 4). *The sense of selectivity was opposite that observed with the mono-amino acid.* Also, it is important to note that the amide substitution at the C-terminus (N-dialkyl vs. NH-alkyl) did not affect the reaction outcome (entries 4 and 7).

Table 2.3: Dipeptide-based phosphine ligands in Ag-catalyzed Mannich-type reactions of silyl enol ether **2.20** and ketoimine **2.27a**

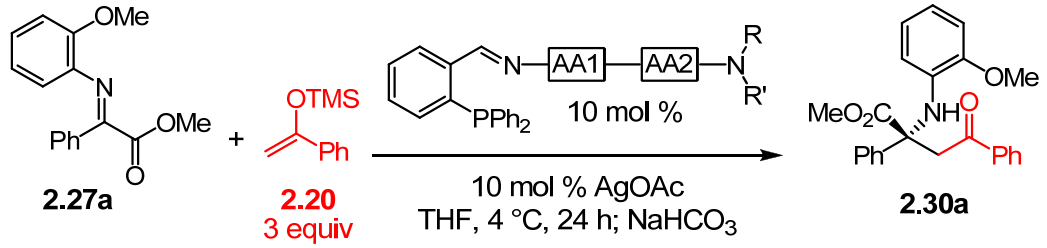

entry	AA1	AA2	R	R'	% conv[a]	% ee[b]
1	Val	Phe	*n*-Bu	H	40	<5
2	Val	Gly	*n*-Bu	H	23	<5
3	Val	D-Phe	*n*-Bu	H	30	-13
4	Tle	D-Tyr(OBn)	*n*-Bu	H	50	-34
5	Tle	Gly	*n*-Bu	H	50	<5
6	Gly	Tyr(OBn)	*n*-Bu	H	12	<5
7	Tle	D-Tyr(OBn)	Et	Et	50	-30
8	Tle	Gly	Et	Et	60	<5

[a]Determined by analysis of 400 MHz ^{1}H NMR spectra of the unpurified reaction mixtures. [b]Determined by chiral HPLC analysis; see Experimentals section for details.

In addition to testing alternative ligand structures, we prepared alternate substrates and nucleophiles and tested them in Ag-catalyzed Mannich-type reactions promoted by ligands **2.19a** and **2.29.** Ketoimine **2.32**, bearing a *p*-methoxybenzyl protecting group, was unreactive towards Ag-catalyzed Mannich-type reaction with silyl enol ether **2.20**. We also prepared the silylketene acetal **2.23**, derived from phenyl acetate for the synthesis of β-amino acids, but we found this nucleophile to be unreactive under the reaction conditions (Scheme 2.5).

Scheme 2.5: Unreactive substrates and nucleophiles in Ag-catalyzed Mannich-type reactions with α-ketoimine esters

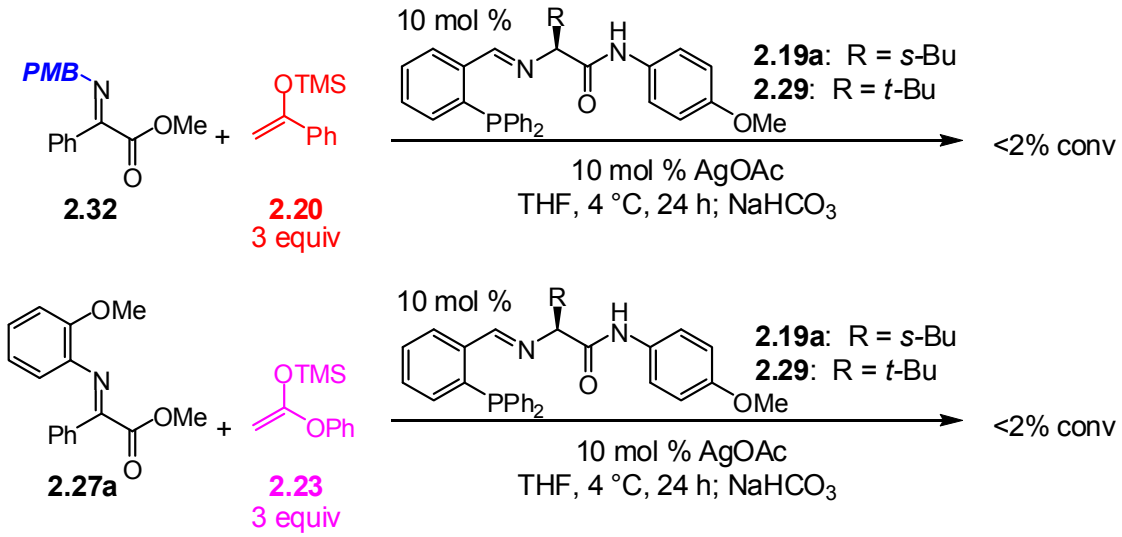

We next turned our focus to methyl pyruvate-derived α-ketoimine ester **2.33a**, which we hoped would be more reactive based on steric considerations. In fact, at -15 °C, **2.33a** underwent efficient Mannich reaction with silyl enol ether **2.20**, however the selectivity was minimal (Scheme 2.6). This reaction was repeated in the presence of protic additives,[80] however no change was observed. Additionally, cooling the reaction to -78 °C resulted in only a slight increase to 42% ee.

Scheme 2.6: Ag-catalyzed enantioselective Mannich-type reaction of acetophenone-derived silyl enol ether **2.20** and methyl pyruvate-derived α-ketoimine ester **2.33a**

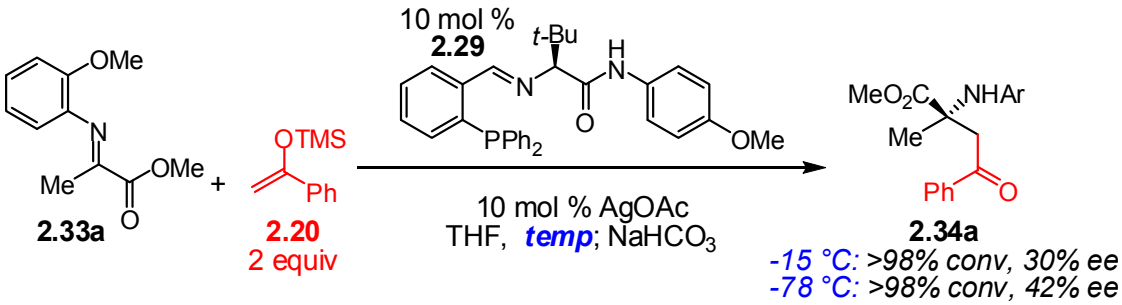

(80) Protic additives were found to be important for selectivity in reactions with siloxyfurans at low temperatures. See Table 2.8, page 114.

2.3.b Ag-catalyzed enantioselective *vinylogous* Mannich-type reactions of siloxyfuran 2.25 with α-ketoimine esters: initial studies

As our attempts to optimize the enantioselectivity in the Ag-catalyzed Mannich-type reaction of acetophenone-derived silyl enol ether **2.20** with α-ketoimine esters were met with minimal success, we decided to turn our focus to a more reactive class of nucleophiles.[81] Concurrent with these studies, a Ag-catalyzed enantioselective Mannich-type reactions of siloxyfurans (i.e. **2.25,** Figure 2.8, Scheme 2.7) with aldimines was being developed by Dr. Emma Carswell, a post-doctoral fellow in our laboratory.[75c] In the presence of one mol % chiral phosphine ligand **2.19a,** one mol % AgOAc, and 1.1 equiv *i*-PrOH, aldimine **2.17e** underwent efficient Mannich-type reaction with siloxyfuran **2.25** *at -78 ºC* to afford the desired Mannich adduct *anti*-**2.26a**[82] as a single diastereomer[83] and in 82% yield, 96% ee.

Scheme 2.7: Ag-catalyzed enantioselective vinylogous Mannich-type reactions with aldimine **2.17e**

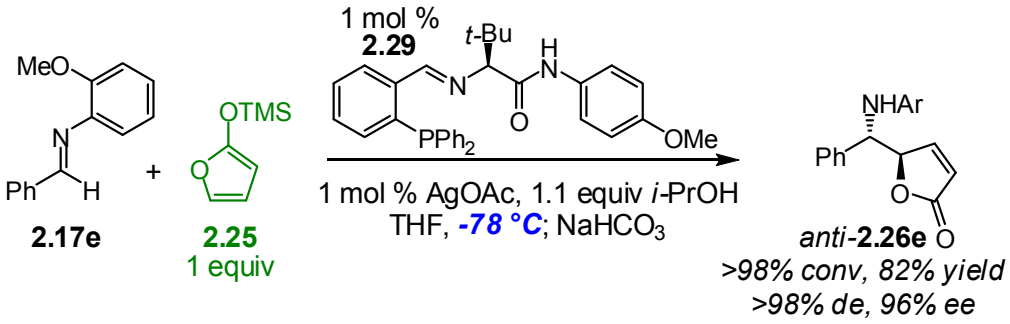

Vinylogous nucleophiles add preferentially at the γ-position (unless that position is sterically hindered, in which case chemoselectivity can be challenging).[84] Denmark and co-workers provide an excellent description of the reactivity and chemoselectivity of vinylogous systems in their review on catalytic, enantioselective, vinylogous aldol

(81) "Determination of the Nucleophilicities of Silyl and Alkyl Enol Ethers," Burfeindt, J.; Patz, M.; Muller, M.; Mayr, H. *J. Am. Chem. Soc.* **1998**, *120*, 3629-3634.
(82) "*Syn*" and "*anti*" refer to the relative stereochemistry observed between the N and O substituents.
(83) Absolute and relative configuration were determined by X-ray crystallography.
(84) "Catalytic Enantioselective, Vinylogous Aldol Reactions," Denmark, S. E.; Heemstra, J. R. Jr.; Beutner, G. L. *Angew. Chem. Int. Ed.* **2005**, 44, 2-18.

reactions.[84] In this review, they cite calculations of the HOMO and partial charges (which are generally cited when explaining reactivity) as well as frontier-orbital density calculations, which are calculated for electrophilic or nucleophilic attack.[85] As shown in Figure 2.9, both the HOMO coefficient (O.C.) and the electrophilic susceptibility (E.S.) were calculated for a Li-dienolate as well as the analogous vinylogous silylketene acetal. In the case of the Li-dienolate, the highest HOMO coefficient and electrophilic susceptibility were located at the C2 position (the α-position). In contrast, the highest HOMO coefficient and electrophilic susceptibility for the silylketene acetal were located at the C4 position (the γ-position).

Figure 2.9: Properties of vinylogous nucleophiles[84]

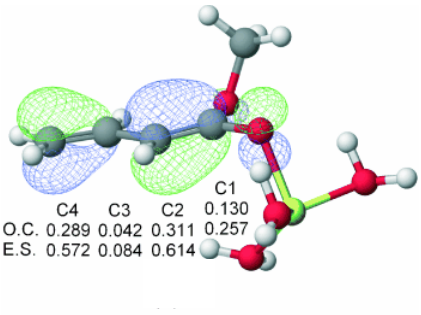

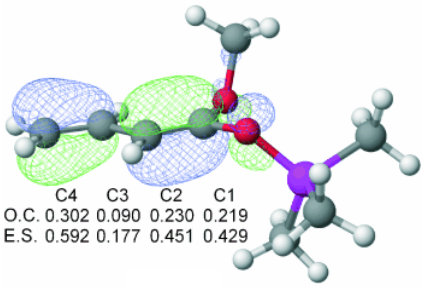

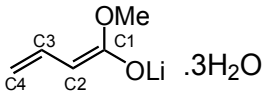

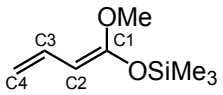

Higher O.C.[a] and E.S.[b] at C2 than at C4

Higher O.C.[a] and E.S.[b] at C4 than at C2

[a]O.C. = HOMO Orbital Coefficients; [b]E.S. = Electrophilic Susceptibility

Perhaps the most intriguing aspect of the method developed by Dr. Carswell, in terms of its application to these studies, was the high reactivity observed with siloxyfuran **2.25** (reactions with **2.25** were run at -78 ºC, while reactions with acetophenone-derived silyl enol ether **2.20** were run at -10 ºC). We decided to test this highly reactive nucleophile (**2.25**) in Ag-catalyzed vinylogous Mannich-type reactions with ketoimines.

(85) The authors state that frontier-orbital density calculations are computationally more accurate than partial charge or HOMO coefficient calculations. See ref. 84.

In fact, when ketoimine **2.27a** was treated with 10 mol % ligand **2.29,** 11 mol % AgOAc, one equiv *i*-PrOH, and two equiv siloxyfuran **2.25**, we observed significant levels of conversion to Mannich adduct *syn*-**2.35a**[82,83] even at -30 °C (76% conv.). However, enantioselectivity still suffered (up to 30% ee, Table 2.4).

Table 2.4: Ag-catalyzed Mannich-type reactions of methyl-benzoylformate derived ketoimine **2.27a** and siloxyfuran **2.25**

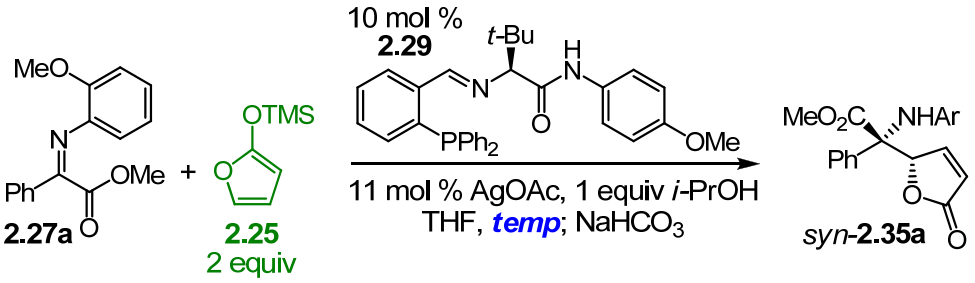

entry	temp	% conv[a]	dr (*syn:anti*)[a]	% ee[b]
1	rt	96	>20:1	15
2	4 °C	>98	>20:1	19
3	-15 °C	76	>20:1	24
4	-30 °C	60	>20:1	30
5	-78 °C	1	>20:1	-

[a]Determined by analysis of 400 MHz ^{1}H NMR spectra of the unpurified reaction mixtures. [b]Determined by chiral HPLC analysis; see Experimentals section for details.

Encouraged by the increased reactivity at lower temperature, we tested a variety of mono-amino acid-derived phosphine ligands in the context of this reaction, Chart 2.1.[86] While we did observe increased enantioselectivity in some cases, low conversion remained a challenge (<60% conv in all cases).

(86) We also screened approximately 40 dipeptide ligands which were synthesized on solid support, however we were not able to reproduce the data that we obtained from that screen when we synthesized the ligands in the solution phase.

Chart 2.1: Mono-amino acid ligand screen in the Ag-catalyzed Mannich-type reaction of siloxyfuran **2.25** with α-ketoimine ester **2.27a**

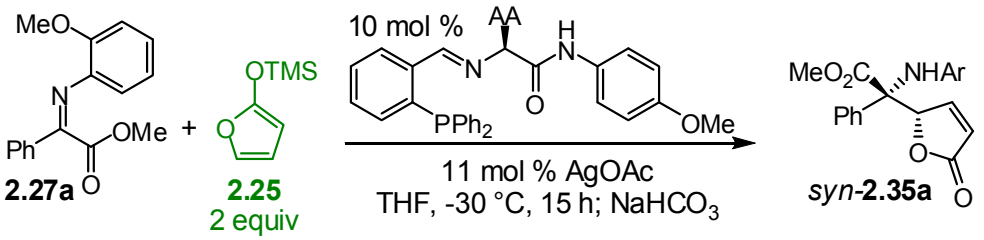

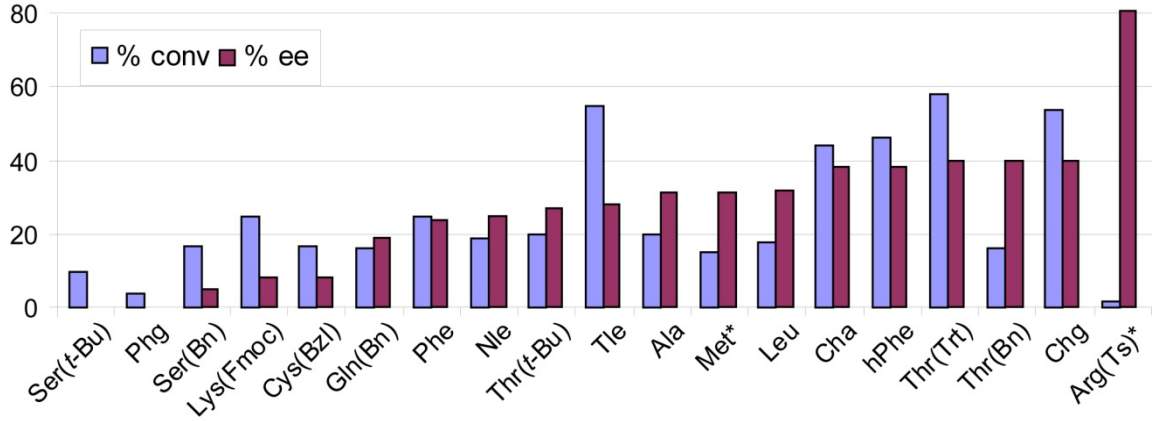

*The major enantiomer was *ent-syn*-**2.35a**.

The optimal ligands from this screen were tested in the presence of one equiv *i*-PrOH, and again there was some improvement in certain cases (AA = Chg, entry 4, Table 2.5), however we continued to observe moderate conversion as well as enantioselectivity (Table 2.5).

Table 2.5: Effect of *i*-PrOH on the Ag-catalyzed Mannich-type reaction of siloxyfuran **2.25** with **2.27a**

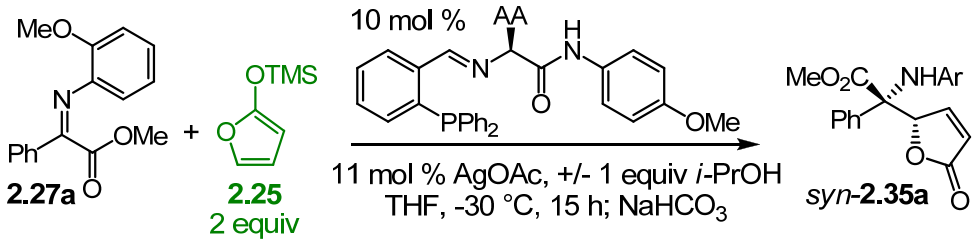

entry	AA	*no i-PrOH* % conv[a]	% ee[b]	*1 equiv i-PrOH* % conv[a]	% ee[b]
1	Tle	55	28	60	30
2	Thr(Trt)	58	40	60	40
3	hPhe	46	38	78	-18
4	Chg	54	40	79	50
5	Cha	44	38	33	-10

[a]Determined by analysis of 400 MHz ^{1}H NMR spectra of the unpurified reaction mixtures. [b]Determined by chiral HPLC analysis; see Experimentals section for details.

2.3.c Ag-catalyzed enantioselective vinylogous Mannich-type reactions with *aliphatic-based* α-ketoimine esters.

2.3.c.1 *Initial studies*

We decided to test the more reactive methyl pyruvate-derived ketoimine (**2.33a**, Scheme 2.6) in the Ag-catalyzed enantioselective Mannich reaction with siloxyfuran **2.25**. This proved to be a much more selective reaction, and we were able to obtain the desired Mannich adduct *syn*-**2.36a**[82,83] as a single diastereomer in full conversion and up to 72% ee at -30 °C with mono-amino acid-derived phosphine ligands, however this result was not very reproducible, and selectivities ranged from 40-72% ee (Scheme 2.8).

Scheme 2.8: Initial studies with the Ag-catalyzed enantioselective vinylogous Mannich-type reaction with ketoimine **2.33a** and phosphine ligands

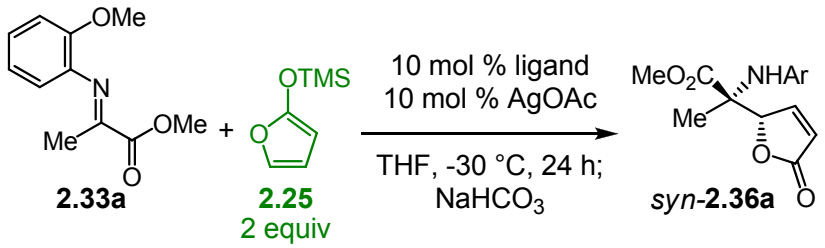

entry	R	AA	R'	% conv[c]	dr (*syn:anti*)[c]	% ee *syn*-**2.36a**[d]
1[a]	H	Tle	OMe	>98	20:1	72
2	OMe	Tle	OMe	>98	15:1	66
3	H	Tle	NMe_2	>98	20:1	72
4[b]	H	*s*-Bu	OMe	>98	6:1	72
5	H	Thr(O*t*-Bu)	OMe	>98	20:1	30

[a]**2.29**. [b]**2.19a**. [c]Determined by analysis of 400 MHz ^{1}H NMR spectra of the unpurified reaction mixtures. [d]Determined by chiral HPLC analysis; see Experimentals section for details.

We synthesized pyruvate-derived substrates **2.33b-c,** which contain sterically encumbered ester substituents in the hopes that the increased stereodifferentiation between the methyl group and the ester group would result in greater levels of enantioselectivity (Table 2.6). Unfortunately, this was not the case, and increased steric bulk on the ester substituent led to a decrease in enantioselectivity (61% ee with R = Et, entry 1; 52% ee with R = Bn, entry 2, Table 2.6).

Table 2.6: Effect of the ester substituent of pyruvate-derived α-ketoimine esters **2.33a-c** on enantioselectivity in the Ag-catalyzed enantioselective Mannich-type reaction

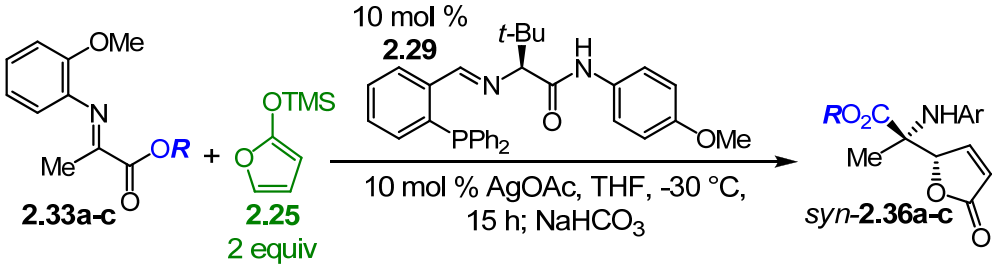

entry		R	% conv[a]	dr[a] (*syn:anti*)	% ee[b] *syn*-**2.36**
1	**2.33a**	Me	>98	>20:1	72
2	**2.33b**	Et	>98	>20:1	61
3	**2.33c**	Bn	>98	>20:1	52

[a]Determined by analysis of 400 MHz ^{1}H NMR spectra of the unpurified reaction mixtures. [b]Determined by chiral HPLC analysis; see Experimentals section for details.

We proposed that higher levels of selectivity may be obtained by lowering the reaction temperature. Interestingly, we found the reverse to be true (lower enantioselectivity at lower temperature), despite the fact that high conversion was maintained (>98% conv, 40% ee at -78 °C, entry 4, Table 2.7).

Table 2.7: The effect of temperature on the Ag-catalyzed vinylogous Mannich-type reaction of siloxyfuran **2.25** with methyl pyruvate-derived substrate **2.33a**.

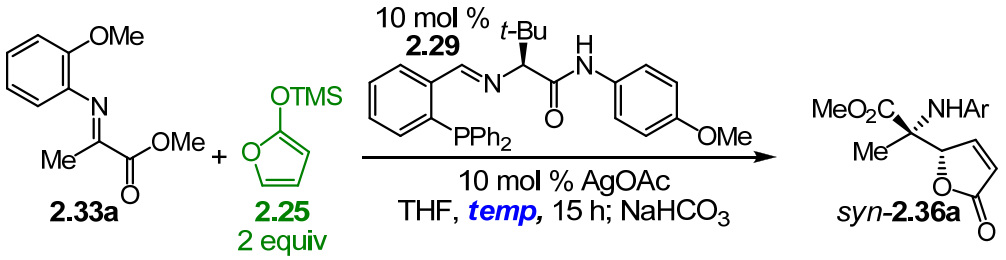

entry	temp	time	% conv[a]	dr (*syn:anti*)[a]	% ee *syn*-**2.36a**[b]
1	-15 °C	15 h	97	9:1	59
2	-30 °C	46 h	>98	>20:1	72
3	-60 °C	46 h	>98	>20:1	56
4	-78 °C	46 h	>98	>20:1	40

[a]Determined by analysis of 400 MHz ^{1}H NMR spectra of the unpurified reaction mixtures. [b]Determined by chiral HPLC analysis; see Experimentals section for details.

Upon further investigation of the above reaction at -78 ºC (entry 4, Table 2.7), we were surprised to discover that the reaction was complete after only 5 min (entry 1, Table 2.8)! However, low enantioselectivity was observed (>98% conv, 26% ee after 5 min). Interestingly, the enantioselectivity increased as time progressed, and in the presence of MeOH, this increase was significant (64% ee with one equiv MeOH, 36% ee in the absence of MeOH after 3 h; entry 4, Table 2.8). We were able to attribute the high levels of reactivity after only 5 min to a background reaction that occurs in the presence of AgOAc upon quench with satd. $NaHCO_3$.[87] We did not observe any additional increase in selectivity between 15 and 72 h; therefore we concluded that the catalyzed reaction was complete after 15 h.

As previously stated, the addition of one equiv *i*-PrOH did not have an effect on the outcome in Mannich reactions with aromatic α-ketoimine ester **2.27a**, and

(87) In the presence of 10 mol % AgOAc (no chiral ligand), **2.33a** undergoes a highly *syn*-selective Mannich-type reaction at -30 ºC to afford Mannich-adduct *syn*-**2.36a** in >20:1 dr (*syn:anti*, 21% conv after 10 min, and >20:1 dr, 60% conv after 24 h. No reaction Z observed (<2% conv) in the absence of AgOAc.

accordingly, it did not have an effect on the Ag-catalyzed enantioselective vinylogous Mannich reaction with methyl-pyruvate derived α-ketoimine ester **2.33a** *at temperatures* ≥ *-30 °C*. However, we have just seen that at -78 °C, the addition of one equiv MeOH lead to a significant increase in selectivity (entry 4, Table 2.8). In order to explain this apparent discrepancy, we propose that the role of the protic additive in the catalytic cycle is to release the catalyst by protonating an intermediate Ag-N bond. This protonation event is likely not the rate-determining step at -30 °C, as no change in the reaction outcome was observed in the presence of a protic additive at this temperature, however it may be involved in the kinetics of this transformation at low temperatures. The proposed mechanism of this reaction will be discussed in detail in Section 2.4 (page 143).

Table 2.8: Reaction time of the Ag-catalyzed enantioselective vinylogous Mannich-type reaction of ketoimine **2.33** with siloxyfuran **2.25**

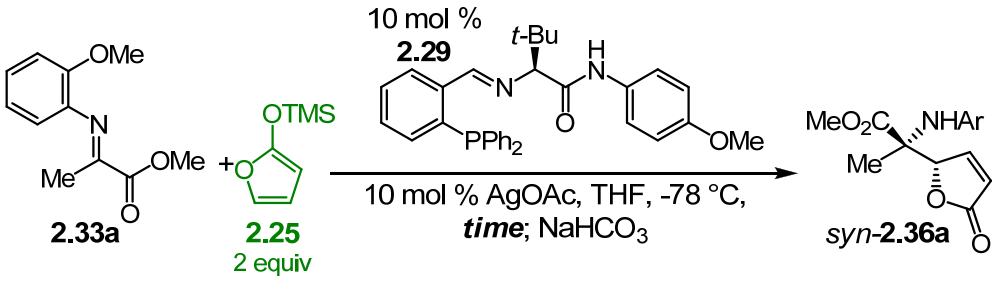

		no MeOH			*1 equiv MeOH*		
entry	**time**	**% conv[a]**	**% yield[b]**	**% ee[c]**	**% conv[a]**	**% yield[b]**	**% ee[c]**
1	5 min	>98	55	26	>98	56	28
2	30 min	>98	60	30	>98	59	36
3	1 h	>98	58	34	>98	65	62
4	3 h	>98	52	36	>98	67	64

[a]Determined by analysis of 400 MHz ^{1}H NMR spectra of the unpurified reaction mixtures. [b]Determined by chiral HPLC analysis; see Experimentals section for details.

Upon further optimization, we discovered that *i*-PrOH was more effective than MeOH in increasing the reaction selectivity (80% ee with *i*-PrOH vs. 70% ee with MeOH, entries 2-3, Table 2.9).

Table 2.9: Protic additive screen for the Ag-catalyzed enantioselective Mannich-type reaction with **2.33a**

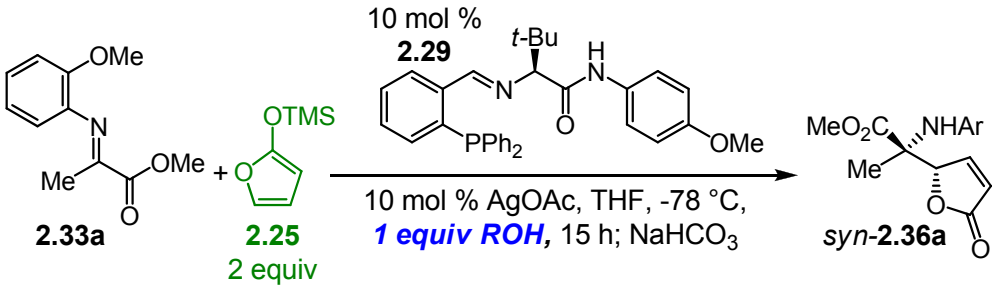

entry	ROH	% conv[a]	% yield[b]	dr (*syn:anti*)[a]	% ee *syn*-**2.36a**[c]
1	H_2O	>98	55	>20:1	72
2	MeOH	>98	56	>20:1	70
3	*i*-PrOH	>98	52	>20:1	80
4	*t*-BuOH	>98	57	>20:1	46
5	PhOH	>98	45	>20:1	60

[a]Determined by analysis of 400 MHz ^{1}H NMR spectra of the unpurified reaction mixtures. [b]Isolated yield of purified *syn*-**2.36a**. [c]Determined by chiral HPLC analysis; see Experimentals section for details.

We tested other electron-rich aniline protecting groups (i.e. **2.33d-e**, Scheme 2.9), with the idea that alteration of the electronic nature of this chelation site may affect substrate binding with Ag.[88] Unfortunately, we did not observe an increase in enantioselectivity with either of these modified protecting groups.

(88) In Ag-catalyzed enantioselective Mannich-type reactions of aliphatic aldimines, a sulfur-containing chelation group is optimal (vs. oxygen-containing; i.e. **2.33e** vs. **2.33a**). H. Mandai *et al*; manuscript in preparation.

Scheme 2.9: Alternative aniline protecting groups in the Ag-catalyzed enantioselective Mannich-type reaction with methyl pyruvate-derived ketoimines.

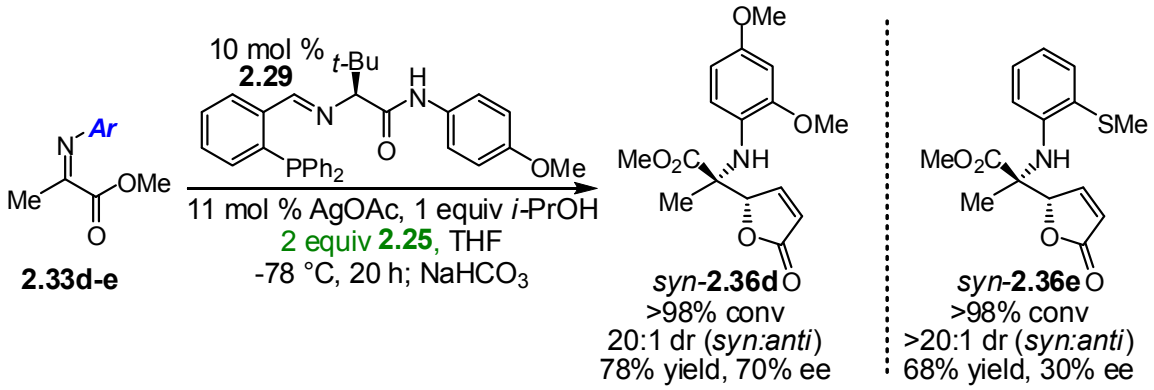

Furthermore, we determined that this Ag-catalyzed process was equally effective at five mol % catalyst loading. A slight excess of AgOAc (5.5 mol % AgOAc vs. 5.0 mol % chiral phosphine ligand **2.20a**) was required.[89]

2.3.c.2 *Ligand optimization*

We tested a variety of different ligand structural motifs, such as dipeptide-based phosphine ligands derived from both possible diastereomers of D- and L- amino acids (entries 1-4, Table 2.10) as well as two mono-amino acid-derived phosphine ligands (other than those shown in Scheme 2.8, entries 5-6, Table 2.10), however we did not observe an increase in enantioselectivity.

(89) After screening a variety of ratios of phosphine ligand **2.29** to AgOAc, we determined that a slight excess of AgOAc is required for a selective and highly reproducible AVM reaction. We found this observation to be true for aromatic substrates **2.45** as well (future sections, data not shown).

Table 2.10: Mono amino acid and dipeptide-based chiral phosphine ligands in the Ag-catalyzed enantioselective Mannich-type reaction with methyl pyruvate-derived ketoimine **2.33a**

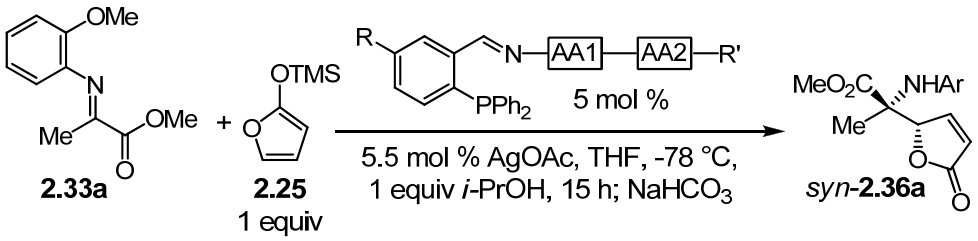

entry	R	AA1	AA2	R'	% conv[a]	dr[a] (*syn:anti*)	% yield[b] *syn*-**2.36a**	% ee[c] *syn*-**2.36a**
1	H	Tle	D-Tyr(OBn)	NH*n*-Bu	>98	>20:1	63	32
2	H	Tle	D-Tyr(OBn)	$N(Et)_2$	>98	>20:1	70	45
3	OMe	Tle	D-Tyr(OBn)	$N(Et)_2$	>98	>20:1	59	28
4	H	Val	L-Phe	NH*n*-Bu	>98	>20:1	<2% conv	--
5	H	Thr(O*t*-Bu)	--	NH-*p*-$OMeC_6H_4$	>98	>20:1	51	48
6	H	Thr(OTrt)	--	NH-*p*-$OMeC_6H_4$	>98	>20:1	41	46

[a]Determined by analysis of 400 MHz ^{1}H NMR spectra of the unpurified reaction mixtures. [b]Isolated yield of purified *syn*-**2.36a.** [c]Determined by chiral HPLC analysis; see Experimentals section for details.

We then returned to Tle-derived mono amino acid-based ligands, and we varied the electronic and steric nature of both the Schiff base portion of the ligand, as well as the aryl amide (Table 2.11). From these screens, we determined that more electron rich Tle-derived mono amino acid ligand **2.37** was optimal for this transformation, affording Mannich adduct *syn*-**2.36a** in 20:1 dr (*syn:anti*), 67% yield, and 86% ee (entry 1, Table 2.11).

Table 2.11: *Electron-rich* phosphine ligands afford *increased* enantioselectivity in Ag-catalyzed vinylogous Mannich-type reactions with **2.33a**

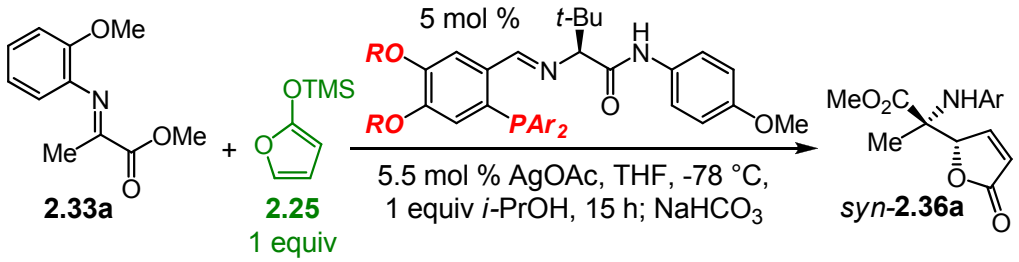

entry	R	Ar	% conv[b]	dr[b] (*syn:anti*)	% yield[c] *syn*-**2.36a**	% ee[d] *syn*-**2.36a**
1[a]	OMe	Ph	>98	>20:1	67	86
2	OMe	*p*-Tol	>98	>20:1	69	85
3	OMe	*p*-$OMeC_6H_4$	>98	>20:1	70	83
4	OCH_2-	Ph	>98	>20:1	67	86
5	OCH_2-	*p*-Tol	>98	>20:1	71	80
6	OCH_2-	*p*-$OMeC_6H_4$	>98	>20:1	64	80

[a]**2.37**. [b]Determined by analysis of 400 MHz ^{1}H NMR spectra of the unpurified reaction mixtures. [c]Isolated yield of purified *syn*-**2.36a.** [d]Determined by chiral HPLC analysis; see Experimentals section for details.

As expected, ligands bearing an electron-withdrawing CF_3 group provided Mannich-adduct *syn*-**2.36a** in lower selectivity (Table 2.12).

Table 2.12: *Electron-poor* phosphine ligands afford *decreased* enantioselectivity in Ag-catalyzed vinylogous Mannich-type reactions with **2.33a**

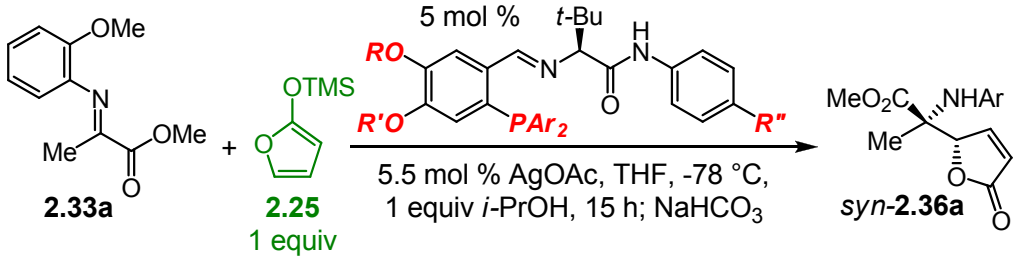

entry	R	R'	Ar	R"	% conv[b]	dr[b] (*syn:anti*)	% yield[c] *syn*-**2.36a**	% ee[d] *syn*-**2.36a**
1	H	H	Ph	CF_3	>98	>20:1	64	59
2	OMe	OMe	Ph	CF_3	>98	>20:1	55	43
3	O-CH_2-O		*p*-Tol	CF_3	>98	>20:1	50	20
4	CF_3	H	Ph	OMe	>98	>20:1	73	72
5	H	H	*o*-Tol	OMe	>98	>20:1	nd	60

[a]Determined by analysis of 400 MHz ^{1}H NMR spectra of the unpurified reaction mixtures. [b]Isolated yield of purified *syn*-**2.36a.** [c]Determined by chiral HPLC analysis; see Experimentals section for details. nd = not determined.

2.3.c.3 *Nucleophile scope*

We next tested substituted siloxyfurans **2.38-39** under the optimal reaction conditions shown in Table 2.11 (with chiral phosphine **2.37**), and we were delighted to find that Me-substituted siloxyfuran **2.38** behaved comparably to its unsubstituted counterpart, and *syn*-**2.40a** was obtained in >98% conv, >20:1 dr, 81% yield, 73% ee, (Scheme 2.10). However, with OMe-substituted siloxyfuran **2.39**, the corresponding Mannich-adduct *syn*-**2.41a** was obtained in >98% conv, 20:1 dr, 64% yield, but with only 4% ee.

Scheme 2.10: Substituted siloxyfurans **2.38-39** in the Ag-catalyzed Mannich-type reaction with **2.33a**

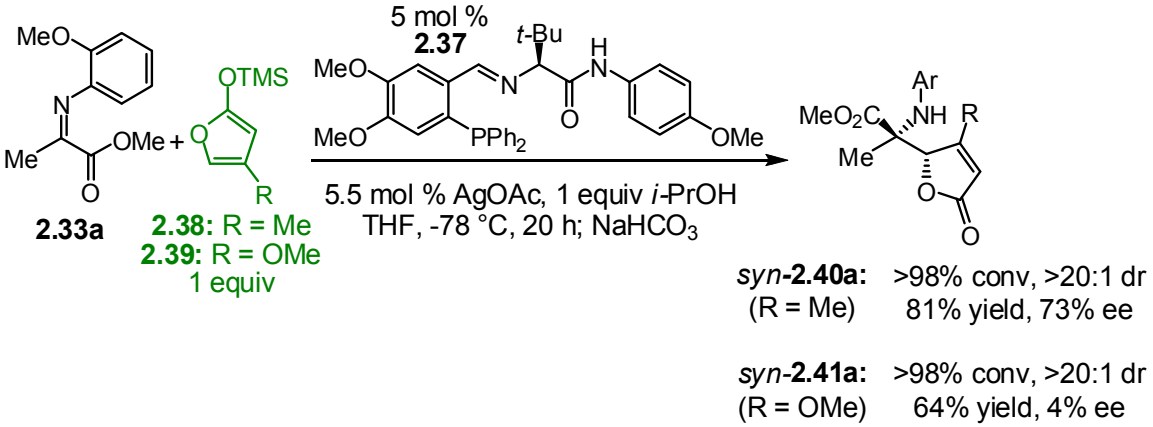

We were able to obtain *syn*-**2.41a** (R = OMe) in up to 60% ee through screening of mono-amino acid-based ligands and protic additives (Chart 2.2, Table 2.13). We were intrigued by the fact that an Ala-derived ligand (R = Me, Chart 1.2) provided *syn*-**2.54a** with the highest enantioselectivity. In our experience, it is rare that removing steric bulk from the chiral ligand results in increased levels of selectivity. We attribute this anomaly to the possibility that the Ag/ligand-catalyzed vinylogous Mannich-type reaction may not proceed to full conversion until it is quenched with aq. $NaHCO_3$[90] (see Table 2.8), thus much of the observed high reactivity is actually non-catalyzed 'background' reactivity. A less sterically-congested ligand may result in increased rate of the desired catalytic process, which would, in turn, decrease the level of non-catalyzed addition.

(90) On a purely qualitative level, reactions with OMe-substituted siloxyfuran **2.39** appear to be slower than reactions with Me-substituted siloxyfuran **2.38** or with unsubstituted **2.25.** Further studies are required to determine the actual rate difference.

Chart 2.2: Ligand screen for Ag-catalyzed Mannich-type reaction with OMe-substituted siloxyfuran **2.39**

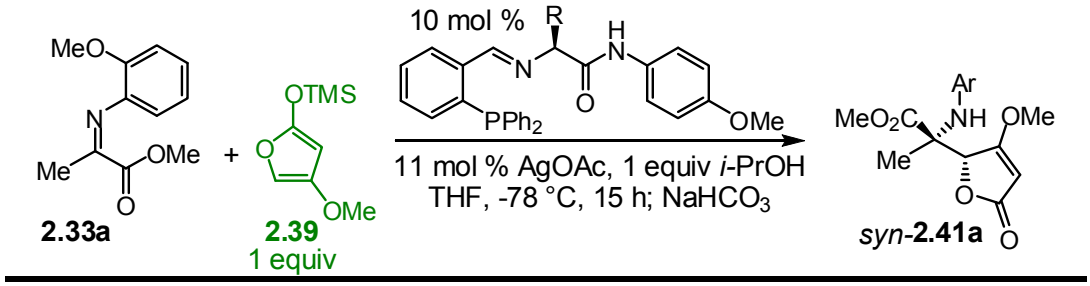

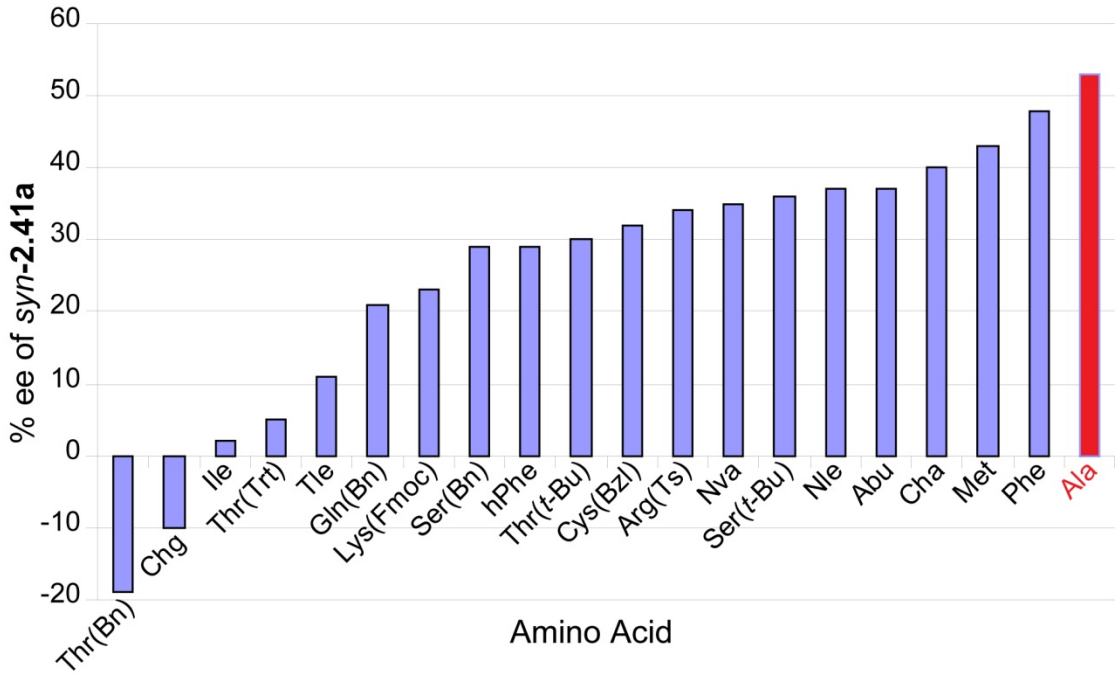

Table 2.13: Protic additives in the Ag-catalyzed enantioselective vinylogous Mannich-type reaction of OMe-substituted siloxyfuran **2.39** with Ala-derived chiral phosphine ligand

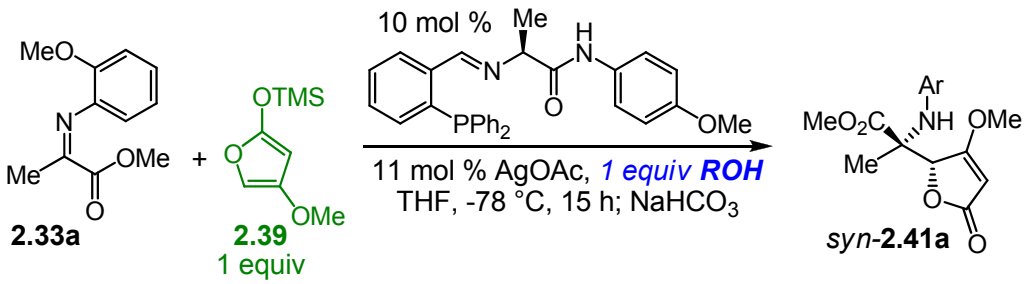

entry	ROH	% conv[a]	dr[a] (*syn:anti*)	% ee[b] *syn*-**2.41a**
1	none	>98	>20:1	50
2	H_2O	>98	>20:1	56
3	MeOH	>98	>20:1	59
4	*i*-PrOH	>98	>20:1	53
5	*t*-BuOH	>98	>20:1	48
6	PhOH	>98	>20:1	59
7	AcOH	>98	>20:1	60

[a]Determined by analysis of 400 MHz ^{1}H NMR spectra of the unpurified reaction mixtures. [b]Determined by chiral HPLC analysis.

2.3.c.4 *Substrate scope*

We examined aliphatic ketoimines **2.33f-h** under the optimal conditions, however a selective or efficient Mannich reaction was not observed with any of these substrates (Scheme 2.11).

Scheme 2.11: Aliphatic substrates in the Ag-catalyzed vinylogous Mannich-type reaction

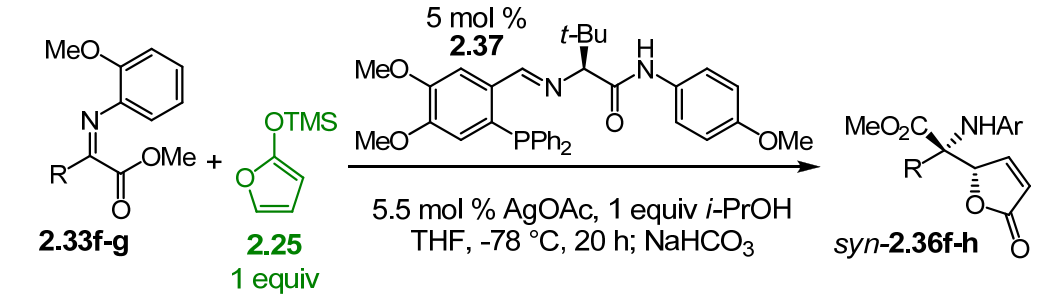

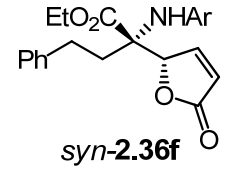

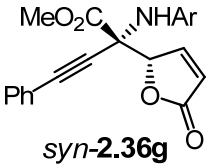

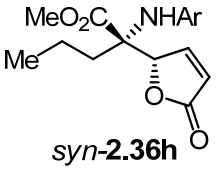

[a]Determined by analysis of 400 MHz ^{1}H NMR spectra of the unpurified reaction mixtures.
[b]Determined by chiral HPLC analysis.

At this point it was clear that a new catalytic system would be required for enantioselective vinylogous Mannich-type reactions with aliphatic-based substrates other than **2.33a**. The pursuit of this new type of catalytic system was set aside such that we could re-focus our attention on Ag-catalyzed vinylogous Mannich-type reactions with aromatic-based α-ketoimine esters such as **2.27a**.

2.3.d Optimization of the Ag-catalyzed enantioselective vinylogous Mannich-type reaction with phenyl-substituted α-ketoimine ester 2.27

Our key stumbling block with aromatic-based ketoimine substrates was the low reactivity associated with this substrate class. We presumed that we would be able to successfully utilize this class of substrates in a highly selective AVM reaction if the reaction temperature could be lowered. Consequently, we set forth to identify a more electrophilic substrate that would react at lower temperatures. Our first attempt involved installation of an electron-withdrawing CF_3 group on both the aryl substituent as well as on the ester substituent (i.e. **2.27b-c**, Scheme 2.12). While modification of the ester

substituent had little effect (25% conv, 35% ee at -30 °C with **2.27b**), CF_3-substitution of the aromatic group produced a much more reactive substrate (*syn*-**2.35c** was obtained in 44% yield, 47% ee at -78 °C, Scheme 2.12). Unfortunately, there was no increase in enantioselectivity.

Scheme 2.12: Electron poor substrates for Ag-catalyzed enantioselective Mannich reactions with siloxyfuran **2.25**.

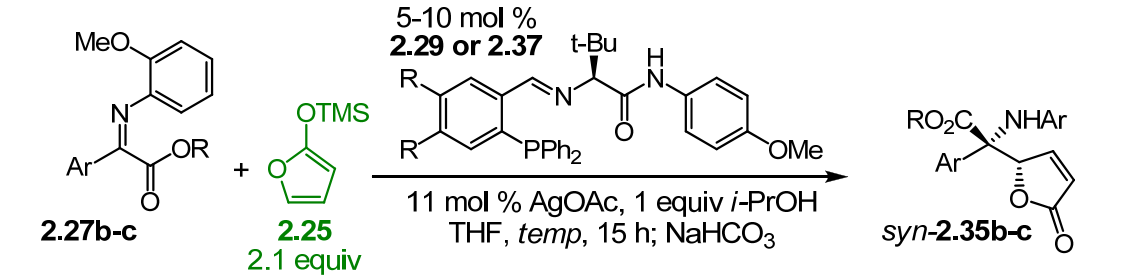

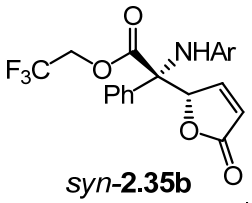

syn-**2.35b**
20% conv,[a] 35% ee[b]
(-30 °C, with 10 mol % **2.29**)

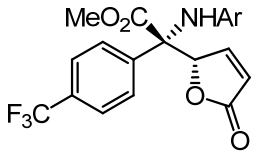

syn-**2.35c**
64% conv,[a] 39% ee[b]
(-30 °C, with 5 mol % **2.37**

44% yield,[c] *47 % ee*[b]
*(**-78 °C**, with 5 mol % **2.37**)*

[a]Determined by analysis of 400 MHz ^{1}H NMR spectra of the unpurified reaction mixtures. [b]Determined by chiral HPLC analysis. [c]Isolated yield of purified *syn*-**2.35c.**

Next, we investigated electronic modifications to the *N*-aryl protecting group. Installation of a CF_3 group *meta*- to the imine nitrogen (i.e. **2.42**, Table 2.14) significantly enhanced the reactivity of the ketoimine substrate. At -50 °C, we observed 94% conv, however a mixture of *syn*- and *anti*- diastereomers was formed.[91] Surprisingly, with this electron-deficient *N*-protecting group, the major diastereomer formed at temperatures ≤30 ºC was *anti*-**2.43**. In all of our previous studies, the *syn*- diastereomer was favored. We were pleased to discover that at -50 °C, we obtained a 3:1 mixture of *anti:syn*-**2.43**, and

(91) Relative stereochemistry was assigned based on analogy to known products (*syn*-**2.35a**, *anti*-**2.45a**).

anti-**2.43** was obtained in 76% ee, while *syn*-**2.43** was obtained in 62% ee.[92] Unfortunately, further cooling of the reaction mixture led to significant decreases in both efficiency and selectivity (25% conv after 70 h, 3:1 *anti:syn*-**2.43**, 15% ee for *anti*-**2.43**, 26% ee for *syn*-**2.43**).

Table 2.14: Electron-deficient *N*-aryl protecting group enhances reactivity in the Ag-catalyzed vinylogous Mannich-type reaction

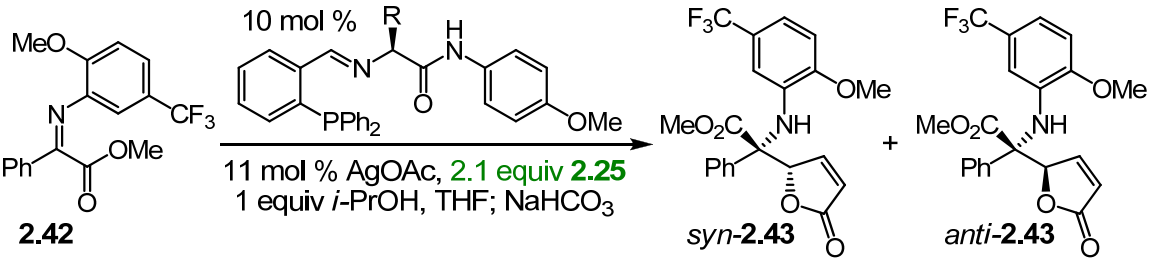

entry	R	temp (°C)	time	% conv[c]	dr[c] (*anti:syn*)	%ee[d] (*anti*-**2.43**)	%ee[d] (*syn*-**2.43**)
1	*t*-Bu[a]	-30	18 h	>98	1:5.5	nd	46
2	Cy[b]	-50	70 h	94	3:1	76	62
3	Cy[b]	-78	70 h	25	3:1	15	26

[a]**2.29**. [b]**2.44**. [c]Determined by analysis of 400 MHz ^{1}H NMR spectra of the unpurified reaction mixtures. [d]Determined by chiral HPLC analysi.

We then examined another electron-poor aryl *N*-protecting group, with an electron-withdrawing NO_2 group *para*- to the imine nitrogen (**2.45a**, Table 2.15). This proved to be the magic protecting group, as the formation of *anti*-**2.46a** was favored even more so than in the above CF_3-substituted case (13:1 dr, entry 6, Table 2.15). Fortunately, the two diastereomers were easily separable, and *anti*-**2.46a** was isolated in 72% yield and 92% ee when the reaction was carried out at -78 ºC. We tested this substrate with a variety of mono-amino acid derived phosphine ligands, and at varying temperatures, and found that Chg- and Tle-derived ligands provided *anti*-**2.46a** with the

(92) Tle- and Chg-derived ligands (**2.29**, **2.44**) were used interchangeably during these studies. We found that there was no significant difference between them in terms of selectivity or yield of the derived Mannich-adducts.

highest selecetivity,[92] and that -78 °C was the optimal temperature. Interestingly, the formation of *syn*-**2.46a** was favored at higher temperatures, whereas at lower temperatures, *anti*-**2.46a** was favored (entries 1 and 3; 4 and 6, Table 2.15).

Table 2.15: Effect of *p*-NO_2 substituent on *N*-aryl protecting group

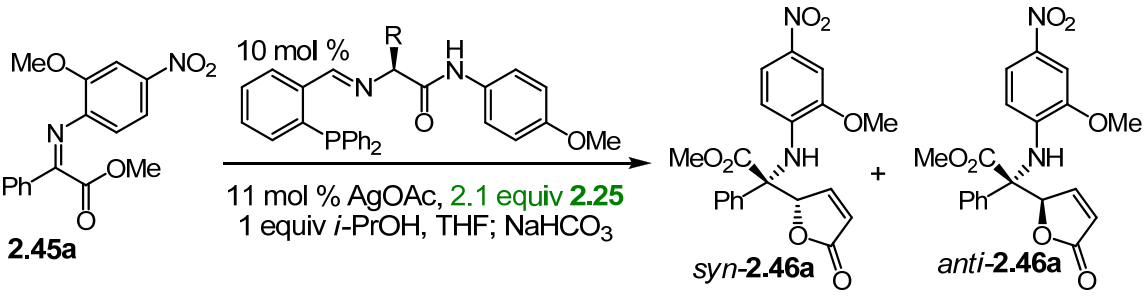

entry	AA	temp (°C)	time	% conv[d]	dr[d] (*anti:syn*)	%ee[e] (*anti*-**2.46a**)	%ee[e] (*syn*-**2.46a**)
1	Tle[a]	-30	15 h	>98	1:2	nd	52
2		-50	48 h	>98	1:1	74	59
3		-78	24 h	>98	10:1	91	69
4	Chg[b]	-30	15 h	>98	1:1	nd	73
5		-50	48 h	>98	4:1	84	62
6[f]		-78	24 h	>98	13:1	92	73
7	Thr(Trt)	-30	15 h	>98	1:13	nd	43
8		-50	48 h	>98	1:3	26	54
9	Thr(*t*-Bu)	-30	15 h	>98	1:3	nd	52
10	hPhe	-30	15 h	>98	1:3	nd	46
11	Ile[c]	-78	24 h	>98	7:1	88	69
12	Val	-78	24 h	>98	8:1	87	66

[a]**2.29**. [b]**2.44**. [c]**2.19a**. [d]Determined by analysis of 400 MHz ^{1}H NMR spectra of the unpurified reaction mixtures. [e]Determined by chiral HPLC analysis; see Experimentals section for details. [f]*Anti*-**2.46a** was isolated in 72% yield.

This reversal in diastereoselectivity with temperature was puzzling, and in fact, the diastereoselectivity also reversed as a function of *reaction time* (Table 2.16). We set up several reactions side by side and quenched them at varying times, and at -78 ºC, we

observed a significant amount of reaction after only 24 min (71% conv.). We had observed a similar trend with our methyl pyruvate-derived ketoimine **2.33a** (Table 2.8). We were, however, surprised to see that the generation of *syn*-**2.46a** was favored after short reaction times (entries 1 and 2), while *anti*-**2.46a** was formed preferentially after extended reaction time (entries 3-5). We attributed the *syn*-selectivity observed at high temperatures (Table 2.15) and after short reaction time (Table 2.16) to a highly *syn*-selective background reaction which occurs in the presence of AgOAc.

Table 2.16: Dependence of diastereoselectivity on reaction time

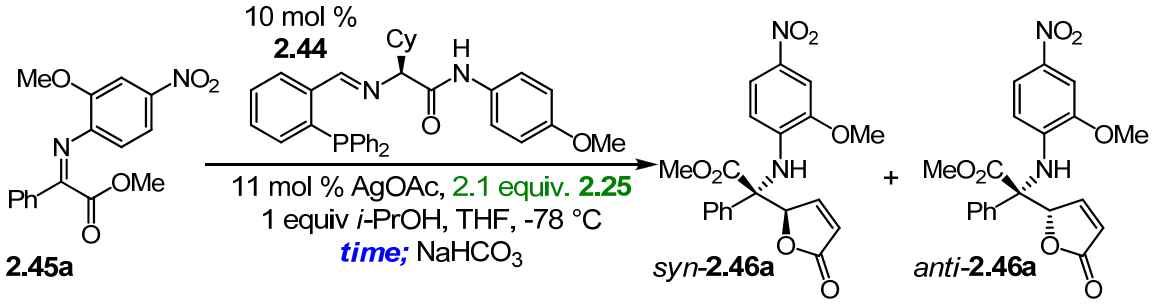

entry	time	% conv[a]	dr[a] (*anti*:*syn*)	% ee[b] *anti*	% ee[b] *syn*
1	25 min	71	1:4	22	24
2	1 h	73	1:1	74	26
3	3.5 h	96	5:1	90	40
4	6 h	>98	10:1	90	60
5	24 h	>98	13:1	92	74

[a]Determined by analysis of 400 MHz ^{1}H NMR spectra of the unpurified reaction mixtures. [b]Determined by chiral HPLC analysis; see Experimentals section for details.

As shown in Eq. 1, there was <2% conv in the absence of both AgOAc and chiral phosphine ligand. Yet, in the presence of 10 mol % AgOAc, without chiral phosphine, there was a significant amount of reaction (10% conv, 1:6 *anti:syn*-**2.46a** after 5 min; 34-76% conv, 1:7-2:1 *anti:syn*-**2.46a** after 15 h; Eq. 2). This variability in of conversion and diastereoselectivity indicated that the reaction was not effectively quenched at -78 °C, and that further reaction with siloxyfuran **2.25** was occurring at higher temperatures. We tested the hypothesis that vinylogous Mannich addition occurs through an acid-

catalyzed pathway caused by the release of a small amount of AcOH from AgOAc and *i*-PrOH, however there was <2% conv after 15 h in the presence of 10 mol % AcOH (Eq. 3).

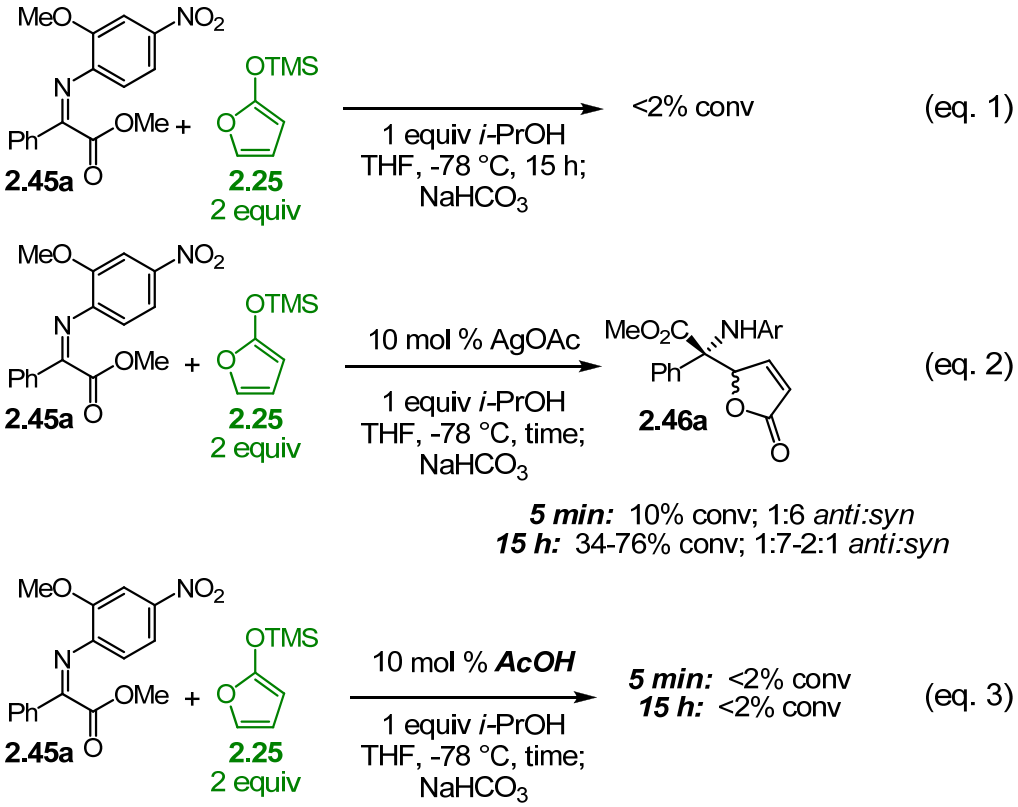

Aside from the highly *syn*-selective background reaction shown in Eq. 2, we were concerned with the low isolated yield of *anti*-**2.46a**: for a product formed in 13:1 dr, the theoretical yield is 92%, however we were only able to isolate the anti-product in 72% yield. We proposed that a side reaction involving siloxyfuran **2.25** occurs upon quench with $NaHCO_3$ and may account for the low yield. We were able to identify byproduct **2.47** as the product of Michael addition of an equivalent of unreacted siloxyfuran **2.25** to the α,β-unsaturated lactone of Mannich-adduct **2.46a** (Scheme 2.13).[93] Studies are underway to determine whether this Michael reaction is diastereoselective (either in the sense that it favors one diastereomer of Mannich-adduct **2.46a** over the other, or in the stereoselectivity of the newly formed contiguous stereogenic centers).

(93) The identity of **2.47** was supported by mass spectrometry.

Scheme 2.13: Mukaiyama Michael reaction of excess siloxyfuran **2.25** with Mannich adduct **2.46a**

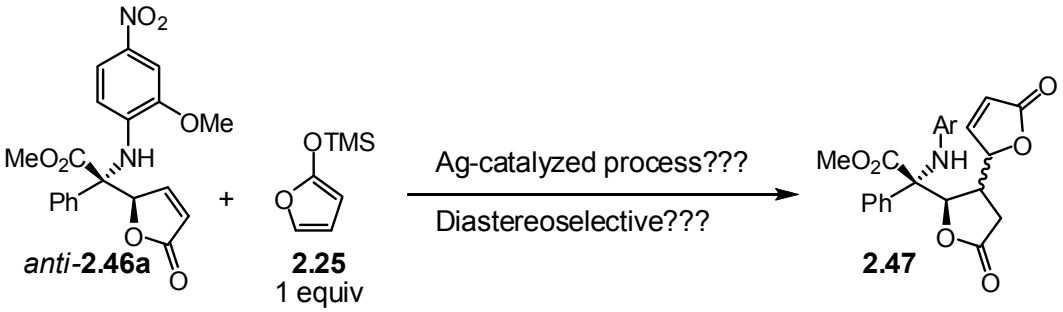

In an attempt to minimize this undesired side reaction, the AVM reaction was conducted with 1.05 equiv siloxyfuran (rather than the standard 2.1 equiv). This modification resulted in a highly inefficient reaction, which lead us to conclude that 2.1 equiv siloxyfuran **2.25** were required to obtain full conversion under the catalytic conditions (Scheme 2.14).

Scheme 2.14: AVM reaction with one equiv siloxyfuran **2.25**

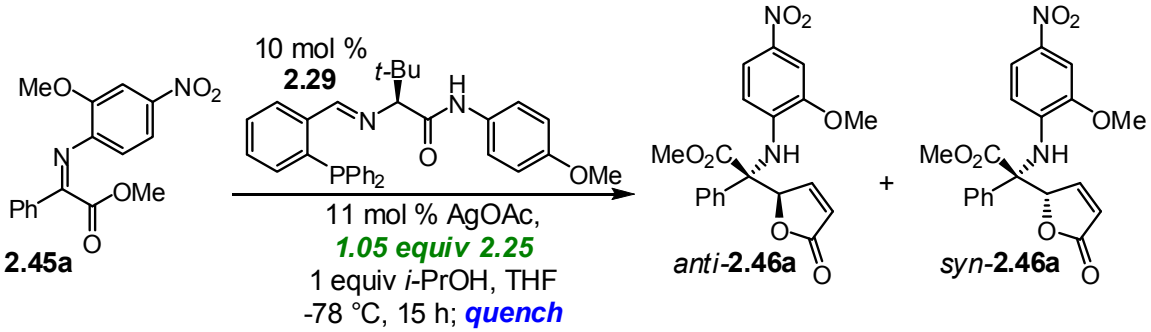

NaHCO$_3$[a] Quench: 95% conv, 2:1 *anti:syn*, 88% yield (comb.), 84% ee (*anti*), 44% ee (*syn*)
AcOH[b] Quench: 68% conv, 2:1 *anti:syn*, 65% yield (comb.), 80% ee (*anti*), 54% ee (*syn*)

[a]A saturated aqueous solution of $NaHCO_3$ was added at -78 °C. The reaction mixture was allowed to warm to 25 °C. [b]AcOH (0.5 equiv) in MeOH was added at -78 °C. The reaction mixture was kept at -78 °C for an additional 3 h before being allowed to warm to 25 °C.

To overcome this adventitious Michael reaction, as well as other possible side reactions that may occur upon quench, we sought to establish an alternative quench

procedure that would effectively destroy the remaining siloxyfuran at -78 °C.[94] We screened several quench procedures, and found the most reliable procedure to be the dropwise addition of two equiv AcOH in a solution of MeOH to the reaction mixture, followed by keeping the reaction mixture at -78 °C for an additional three hours. When we employed this quench procedure, we were delighted to find that we could now obtain **2.46a** in >98% conv and 20:1 dr (*anti*-**2.46a**:*syn*-**2.46a)**, and we could isolate *anti*-**2.46a** in 88% yield and 92% ee (entry 1, Table 2.17). Employment of this quench procedure at elevated temperatures, resulted in prompt deterioration of diastereoselectivity, and formation of *syn*-**2.46a** was favored even at -50 °C, thus demonstrating the importance of an effective quench at -78 °C.

Table 2.17: Effect of temperature in AVM reactions with **2.45a**

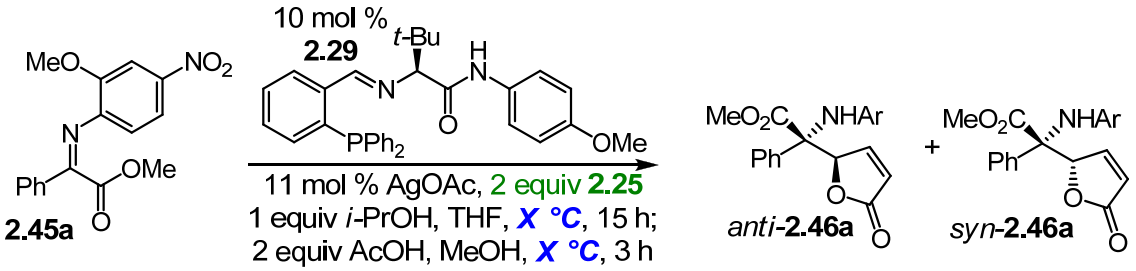

entry	Temp (°C)	% conv[a]	dr[a] (*anti*:*syn*)	% ee[b] *anti*-**2.46a**	%ee[b] *syn*-**2.46a**
1[c]	-78	>98	20:1	92	10
2	-50	>98	1:2	70	70
3	-30	>98	1:6	16	62
4	-15	>98	1:9	26	59
5	4	>98	1:12	6	54
6	rt	>98	1:9	-4	43

[a]Determined by analysis of 400 MHz ^{1}H NMR spectra of the unpurified reaction mixtures. [b]Determined by chiral HPLC analysis; see Experimentals section for details. [c]*Anti*-**2.46a** was obtained in 88% yield.

(94) Saturated aqueous $NaHCO_3$ promptly freezes when added to a reaction mixture at -78 °C, thus the desired protodesilylation of remaining **2.25** cannot occur until the reaction mixture has warmed sufficiently to thaw the aqueous solution.

Discovery of the importance of an effective quench on the reaction outcome of AVM reactions with **2.45a**, led us to examine the effect of our optimized quench on reactions with ketoimine substrate **2.27a** that lacks a nitro group. In fact, there was no difference in reaction outcome when this reaction was quenched with AcOH vs. $NaHCO_3$ (Scheme 2.15).

Scheme 2.15: Importance of quench on AVM reactions with non-NO_2 substituted ketoimine **2.27a**

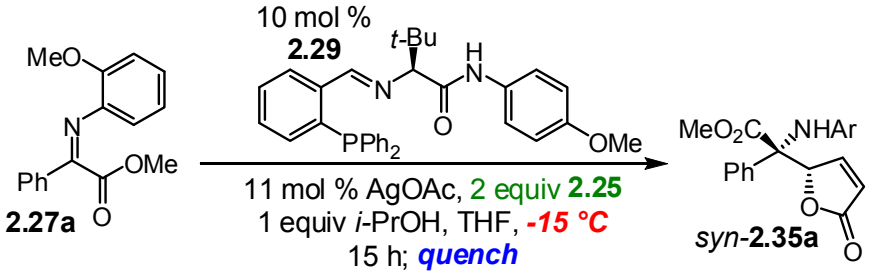

$NaHCO_3$ quench: 64% conv, >98% *syn*, 60% yield, 26% ee
AcOH quench: 76% conv, >98% *syn*, 67% yield, 28% ee

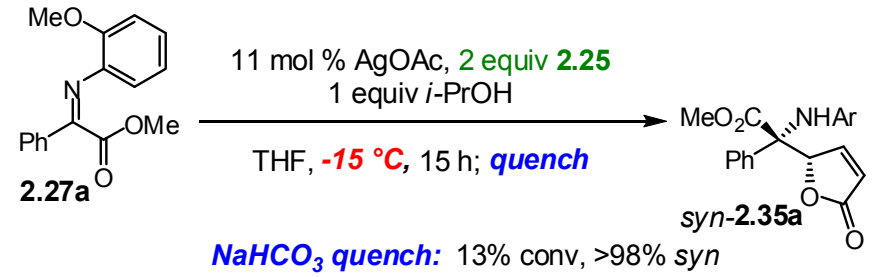

$NaHCO_3$ quench: 13% conv, >98% *syn*
AcOH quench: 12% conv, >98% *syn*

2.3.e Substrate scope of Ag-catalyzed AVM reactions of siloxyfuran 2.25 with ketoimines

As shown in Table 2.18, *diastereoselectivity was enhanced in every case with the AcOH quench vs. the $NaHCO_3$ quench*. In some cases, this change was quite drastic. For example, in the case of *p*-I substituted substrate **2.45f**, we obtained the product as a 6:1 mixture of diastereomers with the $NaHCO_3$ quench, however with the AcOH workup we were able to obtain *anti*-**2.46f** as a single diastereomer (entry 6).

Table 2.18: Ag-catalyzed AVM reactions of aromatic and heteroaromatic-substituted α-ketoimine esters **2.45a-k**

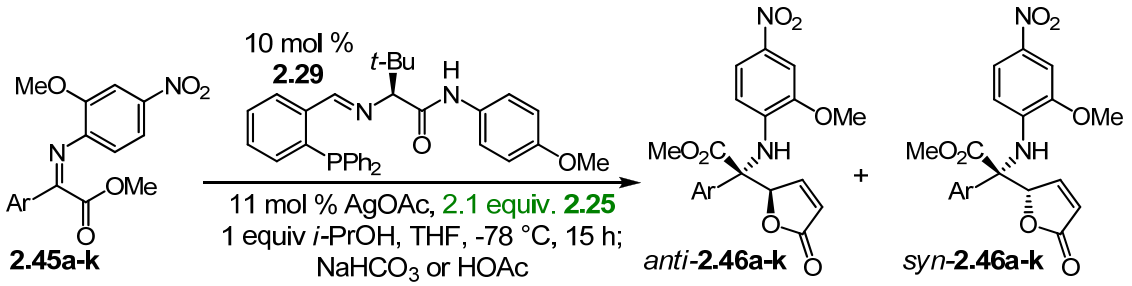

			NaHCO$_3$ workup			*HOAc workup*		
entry	Ar		**dr**[a] (*anti*:*syn*)	**yield (%)**[b] *anti*-**2.46**	**ee (%)**[c] *anti*-**2.46**	**dr**[a] (*anti*:*syn*)	**yield (%)**[b] *anti*-**2.46**	**ee (%)**[c] *anti*-**2.46**
1	C_6H_5	**2.45a**	93:7	72	91	95:5	88	92
2	*m*-$OMeC_6H_4$	**2.45b**	80:20	76	86	95:5	95	93
3	*m*-ClC_6H_4	**2.45c**	75:25	51	81	92:8	72	87
4	*p*-ClC_6H_4	**2.45d**	95:5	-	-	>98:<2	78	95
5	*p*-BrC_6H_4	**2.45e**	88:12	78	92	96:4	80	92
6	*p*-I-C_6H_4	**2.45f**	86:14	62	90	>98:<2	81	93
7	*p*-*t*-BuC_6H_4	**2.45g**	75:25	68	86	95:5	77	90
8	*p*-$CF_3C_6H_4$	**2.45h**	89:11	67	91	97:3	87	94
9	2-naphthyl	**2.45i**	93:7	68	90	>98:<2	81	91
10	2-furyl	**2.45j**	50:50	39	81	66:34	60	80
11	3-thiophene	**2.45k**	67:33	-	-	97:3	70	92

[a]Determined by analysis of 400 MHz ^{1}H NMR spectra of the unpurified reaction mixtures. [b]Yields of purified *syn*-**2.36.** [c]Determined by chiral HPLC analysis; see Experimentals section for details.

2.3.e.1 *Ag-catalyzed AVM reactions with Val-derived ligand 2.48*

Although Tle-derived ligand **2.29** was optimal for Ag-catalyzed AVM reactions with ketoimines, ligand **2.48**, synthesized from valine (which is much less expensive than Tle),[95] also promoted a highly efficient reaction (>98% conv, 20:1 *anti:syn*, 86% ee, 84% yield for *anti*-**2.46a**; >98% conv, 1.5:1 *anti:syn*, 54% yield, 81% ee for *anti*-**2.46j**, Scheme 2.16). Val-derived ligand **2.48** is a cost-effective alternative that provides AVM-adducts with slightly diminished, but useful levels of enantioselectivity.

(95) Aldrich catalogue (2007-2008): $515 for 25 g (L)-Tle vs. $20.10 for 25 g (or $284 for 1 kg) (L)-Val.

Scheme 2.16: AVM reactions with Val-derived phosphine ligand **2.48**

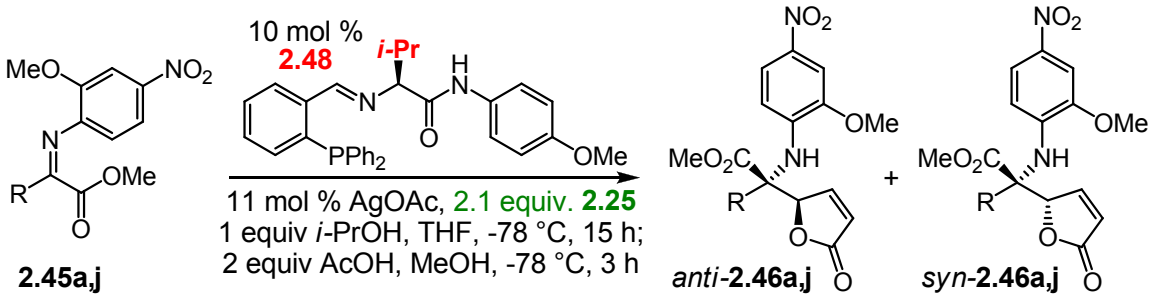

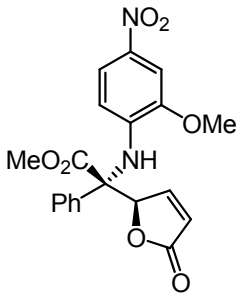

***anti*-2.46**
>98% conv, 20:1 *anti:syn*
84% yield, 86% ee

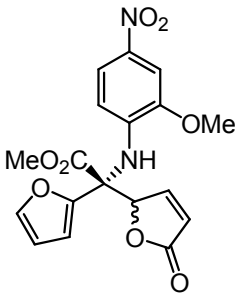

2.46j
>98% conv, 1.5:1 *anti:syn*
anti-**2.46j**: 54% yield, 81% ee
syn-**2.46j**: 37% yield, 45% ee

2.3.e.2 *Deprotection of Mannich-adduct anti-2.46a*

The *O*-aryl protecting group of Mannich-adducts derived from aldimines could be easily oxidatively removed by treatment with $PhI(OAc)_2$. We anticipated difficulties with this deprotection protocol due to the steric congestion surrounding the stereogenic protected amine, as well as the presence of an electron-withdrawing NO_2 group on the aryl protecting group, which lends the amine less electron rich (i.e. less nucleophilic, thus less likely to attack $PhI(OAc)_2$). Indeed, treatment of *anti*-**2.46a** with four equiv $PhI(OAc)_2$ under a variety of conditions resulted in >98% conv to a mixture of unidentified products (<2% conv to the desired free amine) (Eq. 4). Treatment of *anti*-**2.46a** with DDQ resulted in <2% conv (only *anti*-**2.46a** was observed by ^1H NMR in the crude reaction mixture) (Eq. 5). We were able to obtain the desired free amine, *anti*-**2.49a**, cleanly and without the need for chromatography, by treatment with CAN.

However after extensive optimization, the highest yield that we were able to obtain was 45% (optimized conditions are shown in Eq. 6).

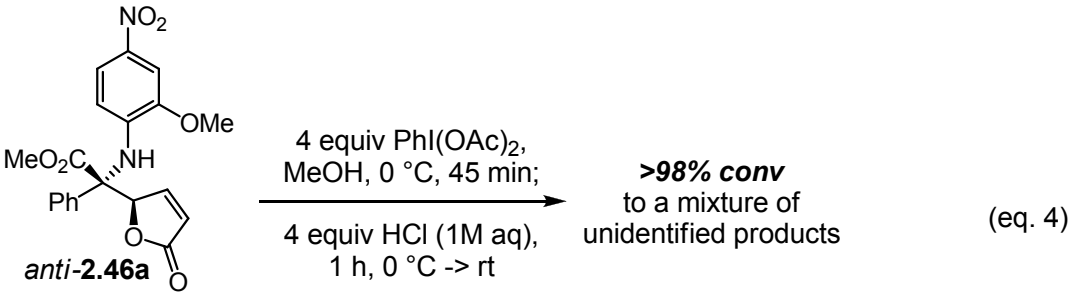

(eq. 4)

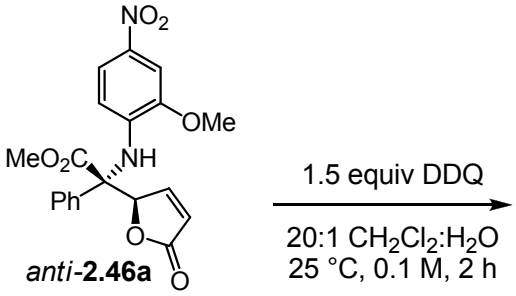

(eq. 5)

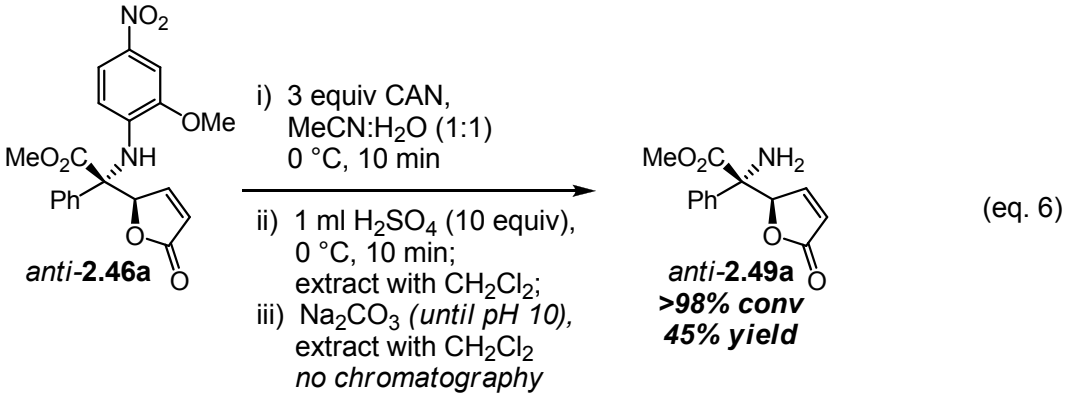

(eq. 6)

We proposed that the reduced form of *anti*-**2.46a** (i.e. *anti*-**2.53a**, Eq. 10) would be more amenable to oxidative removal, due to the electron-rich nature of the N-aryl group, as well as the easily-accessible free amine. Treatment of *anti*-**2.46a** with Fe^0 and a proton source (HCl and EtOH or MeOH) resulted in decomposition (Eqs. 7-8). Hydrogenation of *anti*-**2.46a** resulted in a mixture of saturated lactones *anti*-**2.50a** and

anti-**2.51a** in a 1:1 mixture after 12 hours, however only NO_2-containing *anti*-**2.51a** could be isolated in good yield (98% conv, 10% over-reduction, after 4 h, 79% yield; Eq. 9).

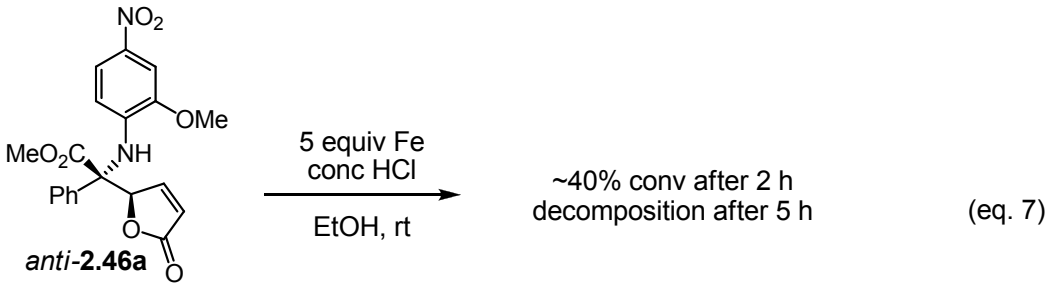

(eq. 7)

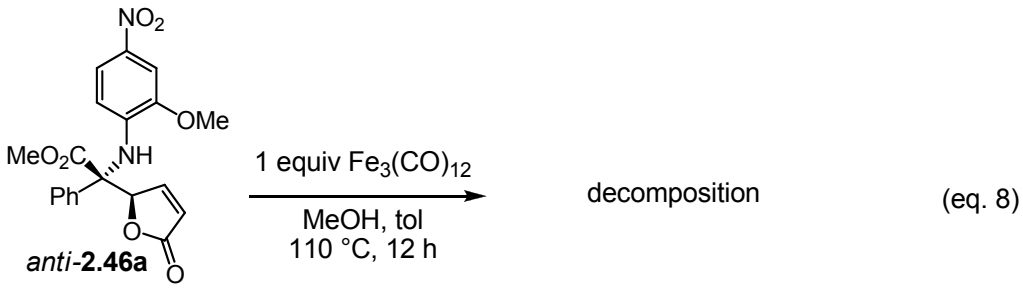

(eq. 8)

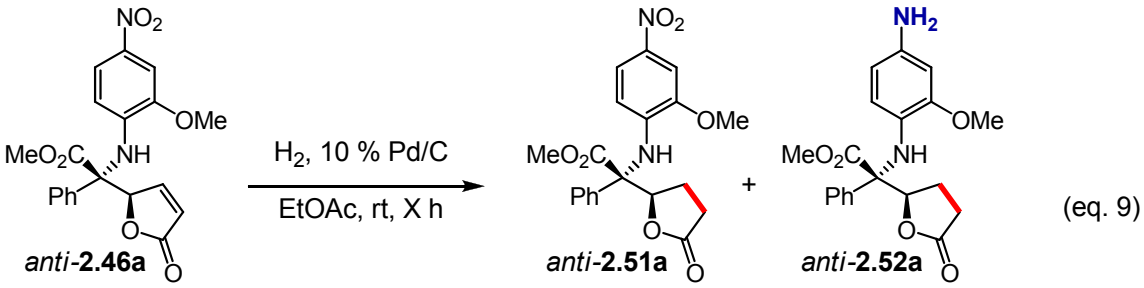

(eq. 9)

12 h: >98% conv, 1:1 mixture of *anti*-**2.51a** and *anti*-**2.52a**
4 h: >98% conv, 90:10 mixture of *anti*-**2.51a** and *anti*-**2.52a**; 79% yield of *anti*-**2.51a**

We tested whether saturated lactone *anti*-**2.51a** was more stable to oxidative conditions that *anti*-**2.46**. Under the same optimized conditions shown in Eq. 6 (3 equiv CAN), we could obtain the desired free amine in 37% yield, which implied that less harsh oxidative conditions were required (Eq. 10).

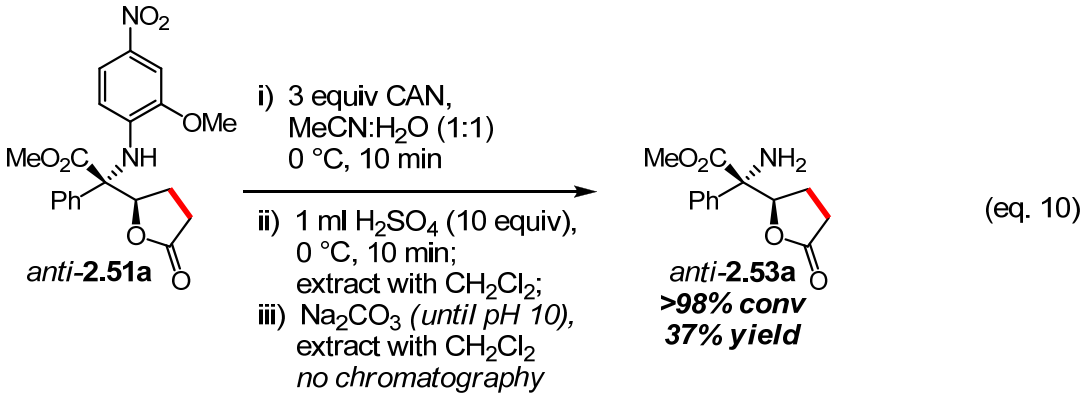

(eq. 10)

Finally, we were able to obtain the desired aniline product (*anti*-**2.54a**) in 77% yield upon treatment of *anti*-**2.46a** with $SnCl_2$ in EtOH/EtOAc (Eq. 11). Importantly, oxidative removal of this aniline-derived *N*-protecting group by treatment with $PhI(OAc)_2$ proceeded cleanly and we could obtain the desired free amine (*anti*-**2.49a**) in 85% yield (Eq. 12). This two-step deprotection protocol could be performed without purification of *anti*-**2.54a** and in 81% overall yield from *anti*-**2.46a** (Eq. 13).

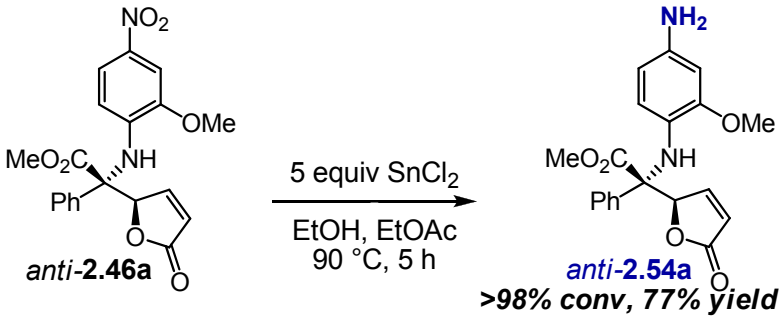

(eq. 11)

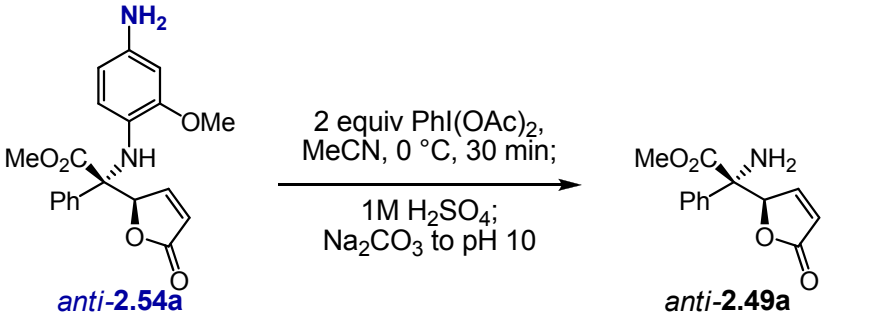

(eq. 12)

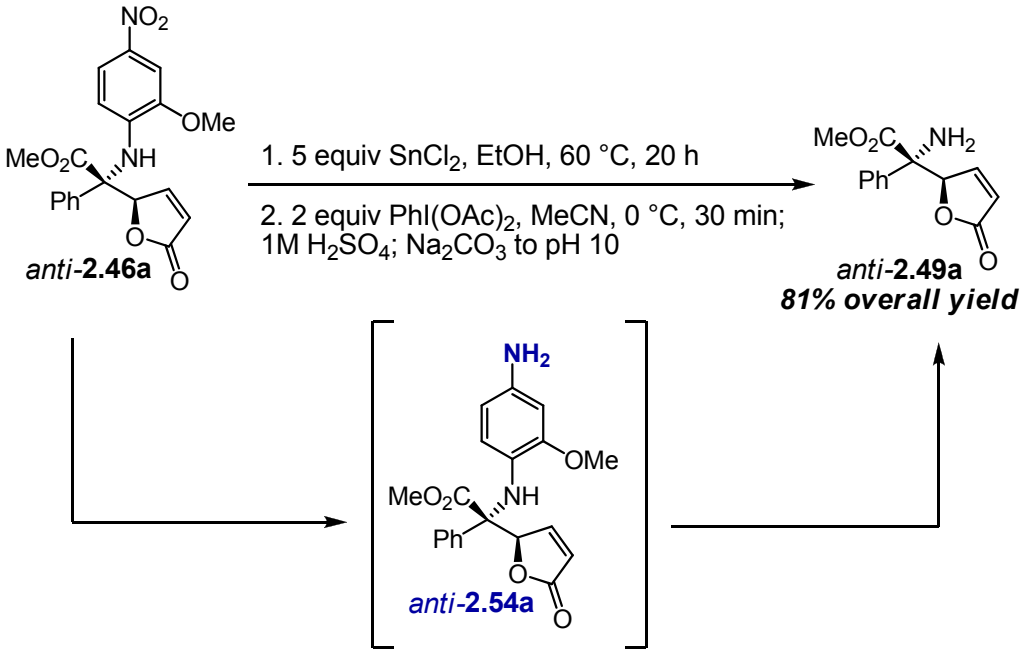

(eq. 13)

2.3.f Substrates and nucleophiles that are inefficient for Ag-catalyzed AVM reactions

We have developed an effective method for AVM of aromatic substrates, however this method is not general for all aryl-substituted ketoimines. Ag-catalyzed AVM reactions with highly sterically encumbered substrates (Table 2.19) and nucleophiles (**2.38**, Figure 2.10) lead to the formation of the corresponding *syn*-products (*syn*-**2.55a,e**), almost exclusively. While the products were obtained in good yields, selectivities were <40% ee. We propose that these substrates and nucleophiles with steric bulk in close proximity to either of the prochiral centers had difficulty binding in the manner required for high selectivity, due to steric congestion.

Table 2.19: Aryl substrates which are ineffective in AVM reactions

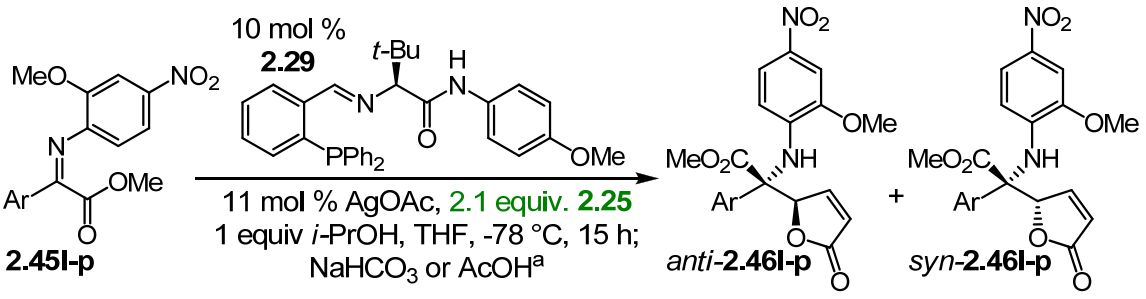

entry	Ar		% conv[b]	dr[b] (*anti:syn*)	% ee[c] (*anti*-**2.46**)	% yield[d] (*syn*-**2.46**)	% ee[c] (*syn*-**2.46**)
1	*p*-OMe-C_6H_4	**2.45l**	89	1:4	7	nd	40
2	*o*-Br-C_6H_4	**2.45m**	>98	<1:20	na	87	32
3	*o*-Cl-C_6H_4	**2.45n**	>98	<1:20	na	nd	30
4	*o*-Me-C_6H_4	**2.45o**	>98	<1:20	na	89	39
5	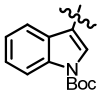	**2.45p**	<98	<1:20	na	80	40

[a]Results with $NaHCO_3$ quench were identical to results with AcOH quench. [b]Determined by analysis of 400 MHz ^1H NMR spectra of the unpurified reaction mixtures. [c]Determined by chiral HPLC analysis. [d]Yields of the purified *syn*-**2.46**.

Figure 2.10: AVM reaction with Me-substituted siloxyfuran **2.38**

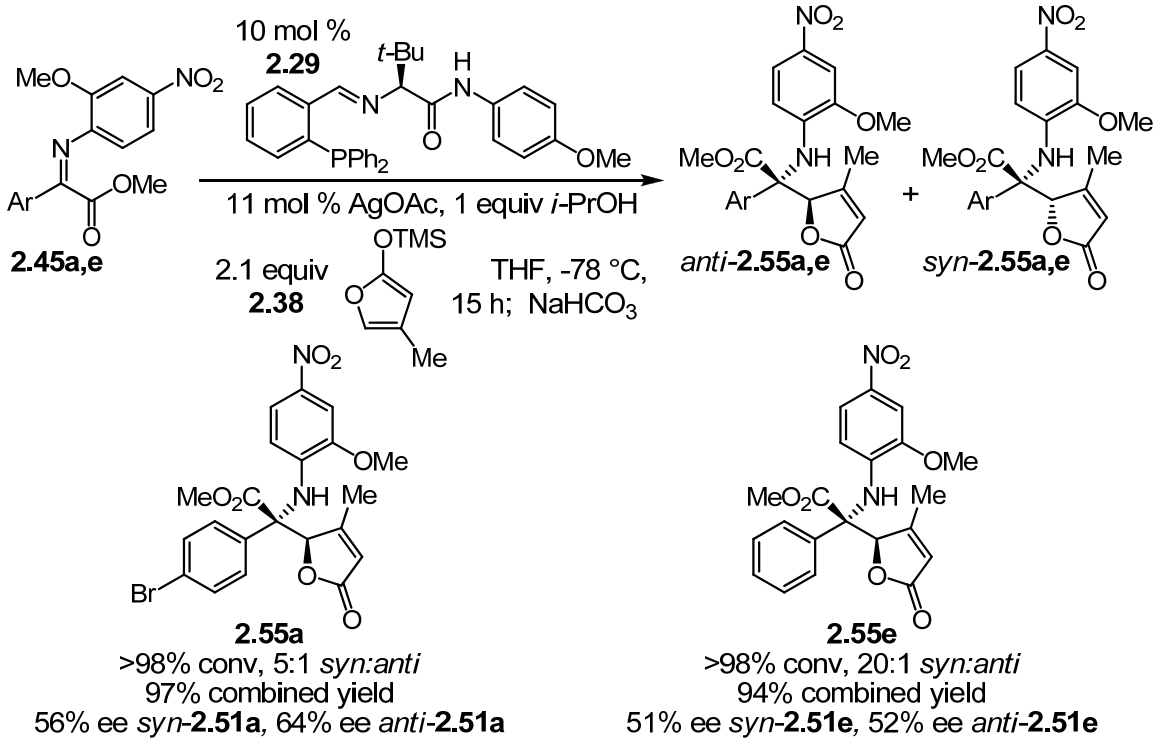

When OMe-substituted siloxyfuran (**2.39** Table 2.20) was subjected to standard AVM reaction conditions, the *syn*-diastereomer was favored exclusively at temperatures ranging from 25 °C to -50 °C, however with minimal enantioselectivity (<15% ee in all cases). At -78 °C, the *anti*-diastereomer was observed as the minor diastereomer (5:1 dr, favoring *syn*-**2.56a**), moreover *syn*-**2.56a** was obtained in <2% ee. The reason for this entire lack of enantioselectivity was unclear to us. We did find it intriguing that the only temperature at which we were able to observe formation of *anti*-**2.56a** was at -78 °C. This result was consistent with observations from reactions with unsubstituted siloxyfuran **2.25**: temperature drastically affected diastereoselectivity, and the only temperature where the *anti*-diastereomer was almost exclusively favored was -78 °C. We believe that these observations have implications concerning the nature of the catalyst at different temperatures. This topic will be discussed in greater detail in Section 2.4.b .

Table 2.20: AVM reaction with OMe-substituted siloxyfuran **2.39**

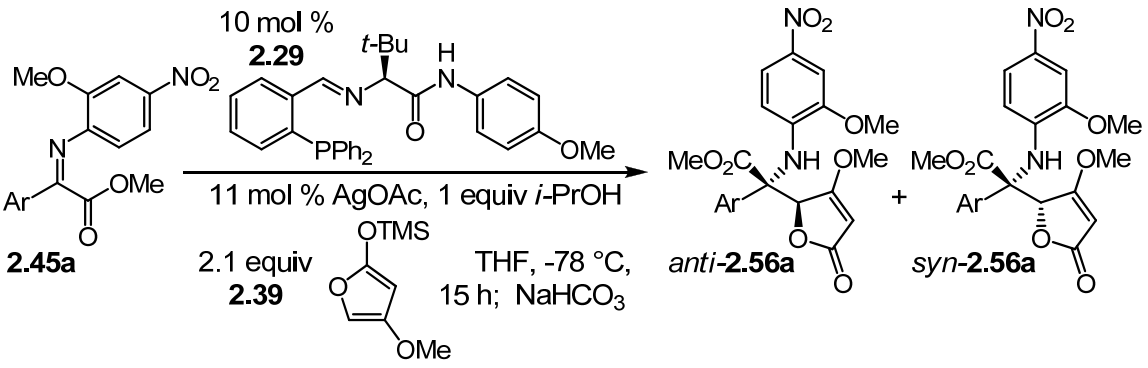

entry	temp (°C)	% conv[a]	dr[a] (*anti*:*syn*)	% ee[b] *syn*-**2.56a**
1	rt	>98	<1:20	8
2	0	>98	<1:20	5
3	-30	>98	<1:20	14
4	-50	>98	<1:20	8
5	-78	81	1:5	<2

[a]Determined by analysis of 400 MHz ^{1}H NMR spectra of the unpurified reaction mixtures. [b]Determined by chiral HPLC analysis.

2.4 *Synthesis, characterization, and utilization of highly active and air-stable Ag-phosphine complexes for the AVM of aromatic ketoimines*

2.4.a Synthesis of Ag-ligand complexes, and their utility in AVM reactions with aromatic ketoimines

We were able to synthesize, isolate, and characterize two discrete and highly stable Ag-phosphine complexes (Scheme 2.17). ^{1}H NMR (400 MHz) analysis of these two complexes indicated that they differed only in the ratio of ligand **2.29**:AgOAc (i.e. the powder was a 3:2 mixture of **2.29**:AgOAc, while crystalline **2.57** was a 2:1 mixture of **2.29**:AgOAc),[96] however we found their reactivity to be substantially different.

(96) Ratios were determined by 400 MHz ^{1}H NMR analysis.

Scheme 2.17: Synthesis of two distinct Ag-ligand complexes

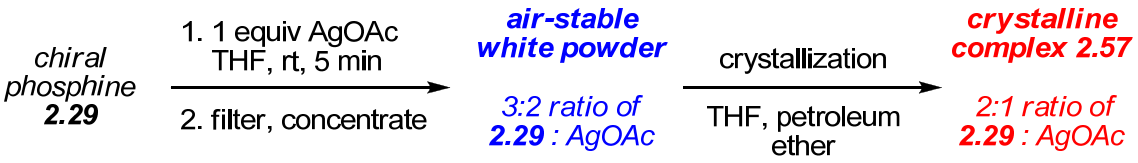

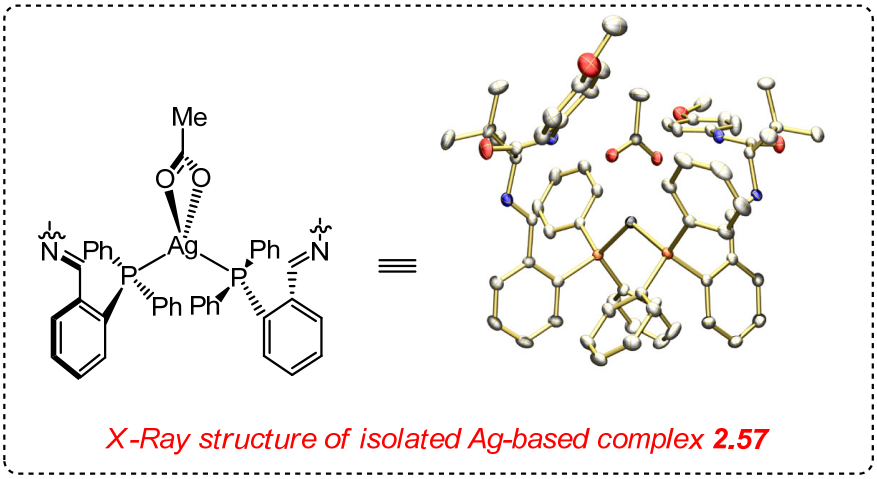

X-Ray structure of isolated Ag-based complex ***2.57***

2.4.a.1 *Synthesis and utility of an air stable white powder that serves as an effective AVM catalyst*

The powder form of this complex was prepared by mixing a solution of phosphine ligand **2.29** with AgOAc and filtering the resulting suspension through celite. After concentration, we obtained a white powder which was a 3:2 mixture of chiral phosphine **2.29** to AgOAc. This complex was stored *under air* and with the exclusion of light for *one year*, and its activity was tested in the AVM reaction of aryl ketoimines (Figure 2.11). We were pleased to find that, in comparison to reactions in which the catalyst was generated *in situ* (with 10 mol % phosphine ligand **2.29** and 11 mol % AgOAc), this highly stable powder was equally efficient in affecting highly enantio- and diastereoselective AVM reactions with both electron-rich and electron-poor aromatic ketoimines (**2.45b** and **2.45h**, Figure 2.11).

Figure 2.11: Isolated Ag-phosphine complex in AVM of aromatic ketoimines **2.45a,b,h**

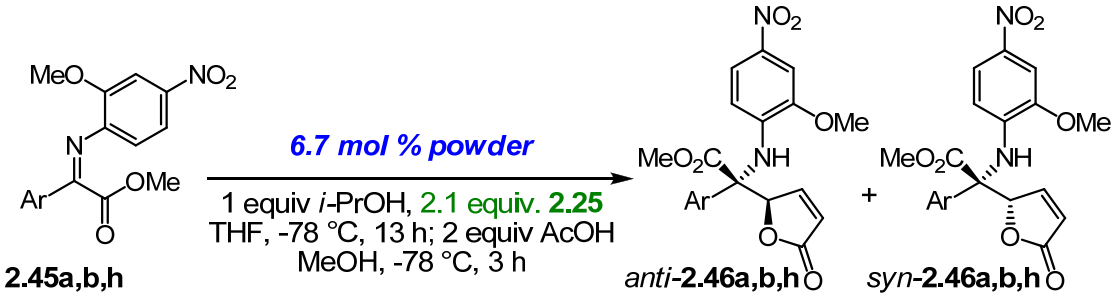

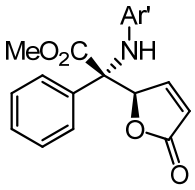

*anti-**2.46a***
***18:1 dr** (anti:syn)[a]*
90% ee,[b] 89% yield[c]
compare to:[d]
20:1 dr (anti:syn)[a]
91% ee,[b] 88% yield[c]

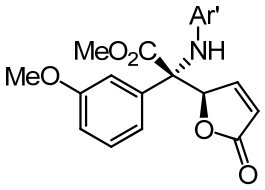

*anti-**2.46b***
***18:1 dr** (anti:syn)[a]*
90% ee,[b] 82% yield[c]
compare to:[d]
18:1 dr (anti:syn)[a]
93% ee,[b] 95% yield[c]

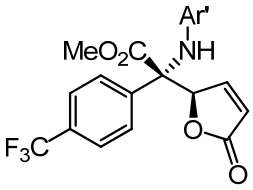

*anti-**2.46h***
***20:1 dr** (anti:syn)[a]*
94% ee,[b] 89% yield[c]
compare to:[d]
20:1 dr(anti:syn)[a]
94% ee,[b] 87% yield[c]

[a]Determined by analysis of 400 MHz ^{1}H NMR spectra of the unpurified reaction mixtures. [b]Determined by chiral HPLC analysis; see Experimentals section for details. [c]Yields of the purified *anti*-**2.46**; all conv >98%. [d]With catalyst generated *in situ* from 10 mol % chiral ligand **2.29** and 11 mol % AgOAc.

We observed a highly efficient and selective reaction with 6.7 mol % of this powder, which corresponds to 10 mol % chiral ligand **2.29** and 6.7 mol % AgOAc. However, lower catalyst loading in Ag-catalyzed AVM reactions with *in situ*-generated catalyst results in a marked decrease in the observed enantio- and diastereoselectivity (Table 2.21).

Table 2.21: Effect of catalyst loading on the Ag-catalyzed AVM reaction with ketoimine **2.45a**

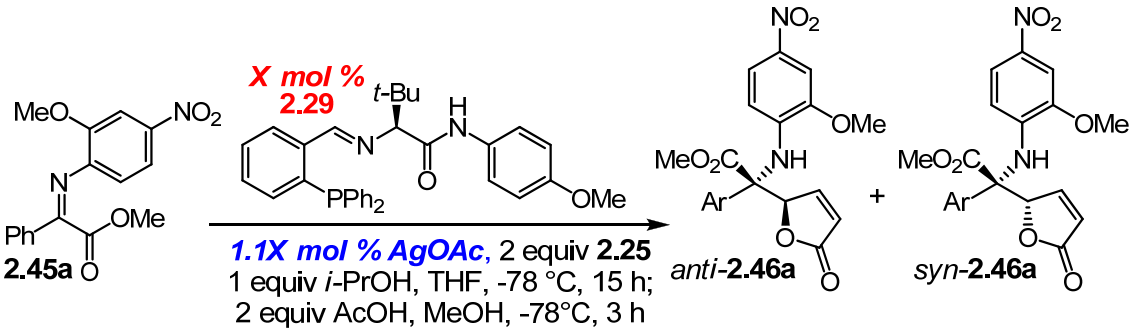

entry	mol % 2.29	mol % AgOAc	% conv[a]	dr (*anti*:*syn*)[a]	% ee[b] *anti*-**2.46a**	% ee[b] *syn*-**2.46a**
1	10	11	>98	20:1	92	60
2	5	5.5	76	4:1	78	66
3	3	3.3	29	1:10	16	52

[a]Determined by analysis of 400 MHz ^{1}H NMR spectra of the unpurified reaction mixtures. [b]Determined by chiral HPLC analysis; see Experimentals section for details.

We have shown previously that a slight excess of AgOAc is required for reproducibly high selectivity.[89] In fact, when we tested this AVM reaction with a 2:3 ratio of AgOAc and chiral phosphine **2.29** generated *in situ* from 6.6 mol % AgOAc and 10 mol % ligand **2.29**, the reaction was much less efficient (<25% conv, with *syn*-**2.45a** as the major diastereomer). In order to explain this apparent discrepancy, we propose that the complexation of AgOAc and chiral phosphine **2.29** may be a slow process, and when the active catalyst complex is generated *in situ*, excess AgOAc is required to drive this complexation towards completion. Therefore, in reactions with the pre-formed white powder, complexation may be complete thus an excess of AgOAc would not be required.

2.4.a.2 *Synthesis and utility of crystalline complex 2.57*

We obtained crystalline AgOAc:**2.29** complex **2.57** through crystallization of a solution of the white powder in THF/Et_2O with petroleum ether. The X-ray structure of **2.57** did not indicate a 2:3 AgOAc:**2.29** complex as was observed for the powder, but a

bisphosphine complex on AgOAc (1:2 AgOAc:**2.29** complex, supported by ^{1}H NMR analysis). As mentioned above, the ^{1}H NMR spectra of the white powder and **2.57** were identical, except for the ratio of the acetate peak relative to **2.29**. Therefore, when we tested **2.57** in the catalytic AVM reaction with **2.45a**, we were surprised to find that this crystalline complex was not an efficient catalyst for AVM reactions with ketoimines. As shown in Table 2.22, in the presence of 5 mol % **2.57**,[97] we observed only 30% conversion after 13 h, and *syn*-**2.46a** was formed exclusively. When we increased catalyst loading to 10 mol %, we again saw low conversion (48 %), however we observed *anti*-**2.46a** in the reaction mixture (1:2 *anti:syn*-**2.46a**).

Table 2.22: Crystalline AgOAc-**2.29** complex **2.57** is not an effective catalyst for AVM reactions with **2.45a**

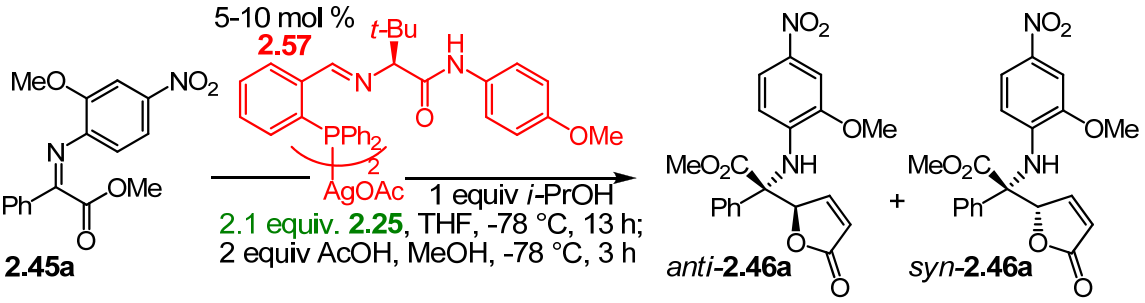

entry	catalyst loading	% conv[a]	dr[a] (*anti:syn*)	%ee[b] *anti*-**2.46a**	%ee[b] *syn*-**2.46a**
1	5 mol %	30%	<2:>98	na	56%
2	10 mol %	48%	33:67	48%	66%

[a]Determined by analysis of 400 MHz ^{1}H NMR spectra of the unpurified reaction mixtures. [b]Determined by chiral HPLC analysis; see Experimentals section for details.

2.4.a.3 *AgOAc-Phosphine complexes exist as a mixture*

We were intrigued by the difference in reactivity observed between these two AgOAc-**2.29** complexes**.** In fact, complex formation appears to be a dynamic process. As shown in Eqs. 5-7, we found that we could achieve desired levels of reactivity and

(97) 5 mol % **2.57** corresponds to 5 mol % AgOAc and 10 mol % **2.29**.

selectivity by simply adding excess AgOAc[98] to reactions with each isolated AgOAc-ligand complex. A control reaction is shown in Eq. 5.[99] As discussed above, *anti*-**2.46a** was obtained with good diastereoselectivity (96:4 *anti:syn*) and enantioselectivity (91% ee for *anti*-**2.46a**). In Eq. 6, 6.7 mol % of the isolated powder was used along with an additional 4.3 mol % AgOAc, and virtually identical results were obtained. Most importantly, catalytic activity was completely restored with crystalline complex **2.57** upon addition of excess AgOAc (>98% conv, 95:5 dr (*anti:syn*), 91% ee (*anti*-**2.46a**), and 68% ee (*syn*-**2.46a**), Eq. 7).

(98) The appropriate amount of AgOAc was added in order to achieve the AgOAc:**2.29** ratio in the control reaction shown in eq. 1 (10 mol % **2.29** and 11 mol % AgOAc).
(99) The reactions shown in Eqs. 14-16 were performed simultaneously.

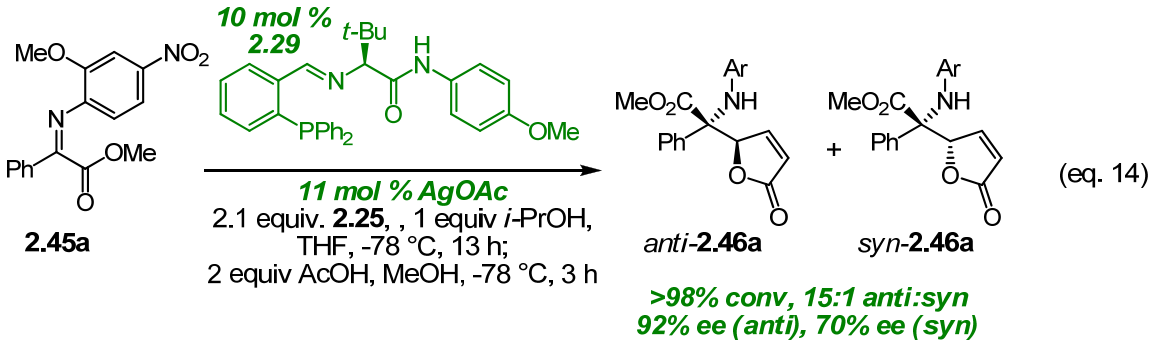

(eq. 14)

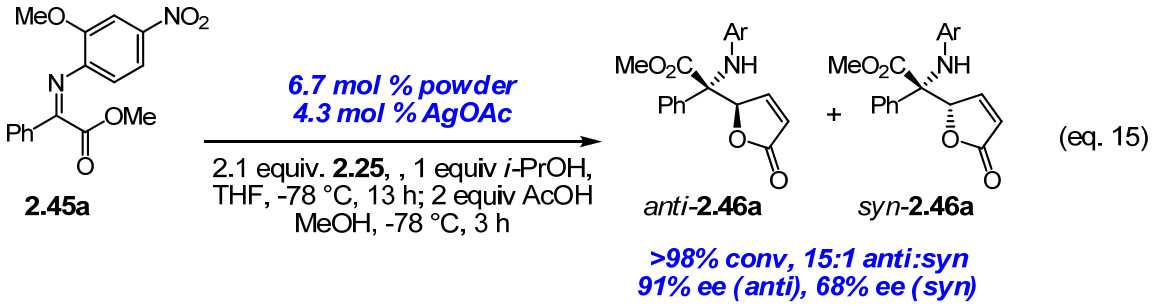

(eq. 15)

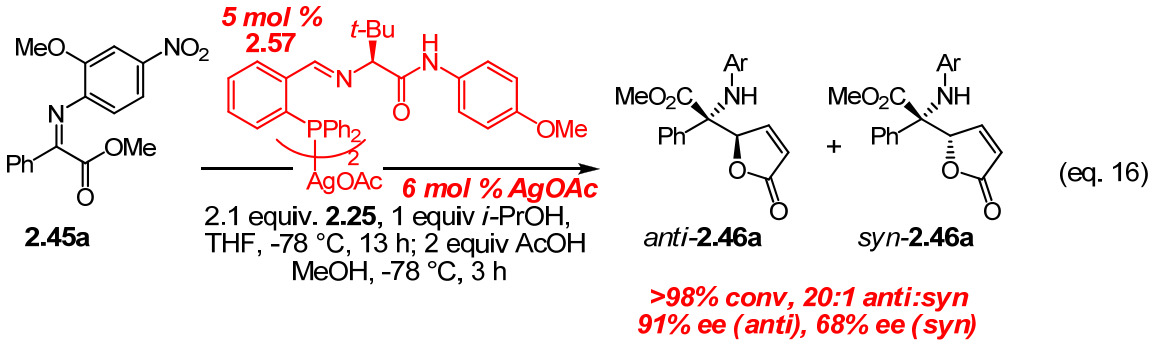

(eq. 16)

2.4.b Effect of temperature on the ^{1}H NMR spectra of the isolated Ag-ligand complexes

We have demonstrated that multiple catalytically active AgOAc-**2.29** complexes are accessible. Because of the variable efficiencies and selectivities observed with these complexes, we became interested in the identity of these distinct complexes.[100] ^{1}H NMR analysis (400 MHz, d_8-THF) at room temperature indicated that these two complexes

(100) Studies to elucidate the structure of AgOAc-**2.29** complexes **2.57**-**2.58** were performed in collaboration with Ms. Erika Vieira.

were identical.[101] As the solutions were cooled from 25 to -78 ºC, there was a marked change in the chemical shifts of the amide NH, imine, and aromatic protons. These peaks began to resolve, indicating the presence of two distinct species in each sample. In fact, the two complexes consisted of different ratios of the same two species. In the powder, the integration of H_a from each complex showed a 1:1 ratio (downfield component : upfield component, Figure 2.12), while in the crystalline complex, this ratio was 5:1.

(101) The only difference between these complexes as determined by ^{1}H NMR analysis at room temperature was the integration of the OAc peak.

Figure 2.12: Variable-temperature 400 MHz ^{1}H NMR studies indicated that Ag-phosphine complexes were mixtures of two distinct species

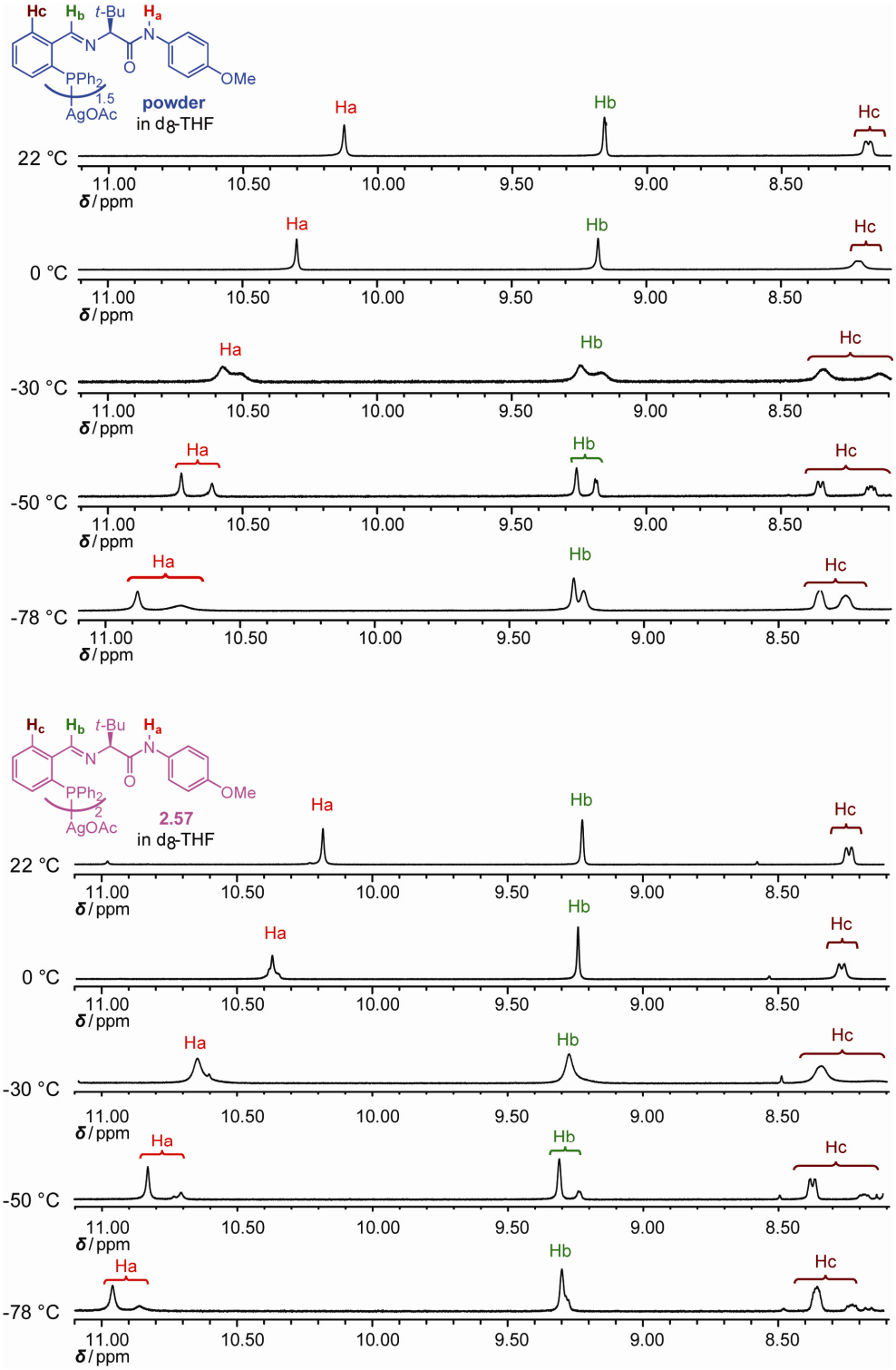

We compared the ^{1}H NMR spectra of these complexes with catalyst generated *in situ* (Figure 2.13). As previously observed, complexes that were catalytically active (powder, catalyst generated *in situ*, and crystalline **2.57** which had been treated with excess AgOAc) contained more of the upfield component, while crystalline **2.57** contained more of the downfield component.

Figure 2.13: 400 MHz ^{1}H NMR spectra of AgOAc-**2.29** complexes in d_8-THF at -78 ºC

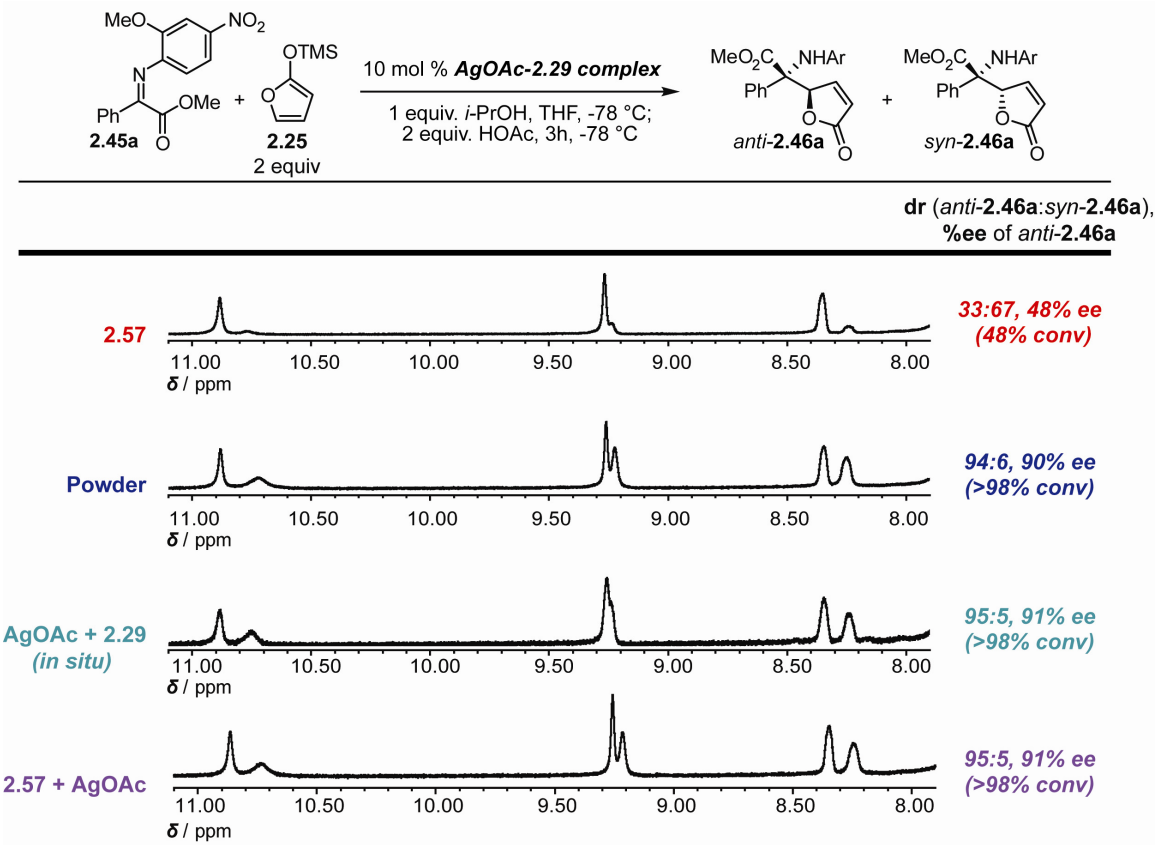

2.4.c Elucidation of the components of Ag-ligand complexes powder and 2.57 by ^{31}P NMR analysis

We were able to elucidate the structures of these two catalyst components through analysis of the 162 MHz ^{31}P NMR spectra of these AgOAc-**2.29** complexes. At 25 ºC, the ^{31}P NMR spectra of both complexes showed a broad singlet (Figure 2.14). At -78 ºC, this broad singlet resolved into two sets of peaks, which resembled a quartet but were actually two doublets.

Figure 2.14: 162 MHz ^{31}P NMR spectra of AgOAc-**2.29** complexes at 25 ºC and -78 ºC

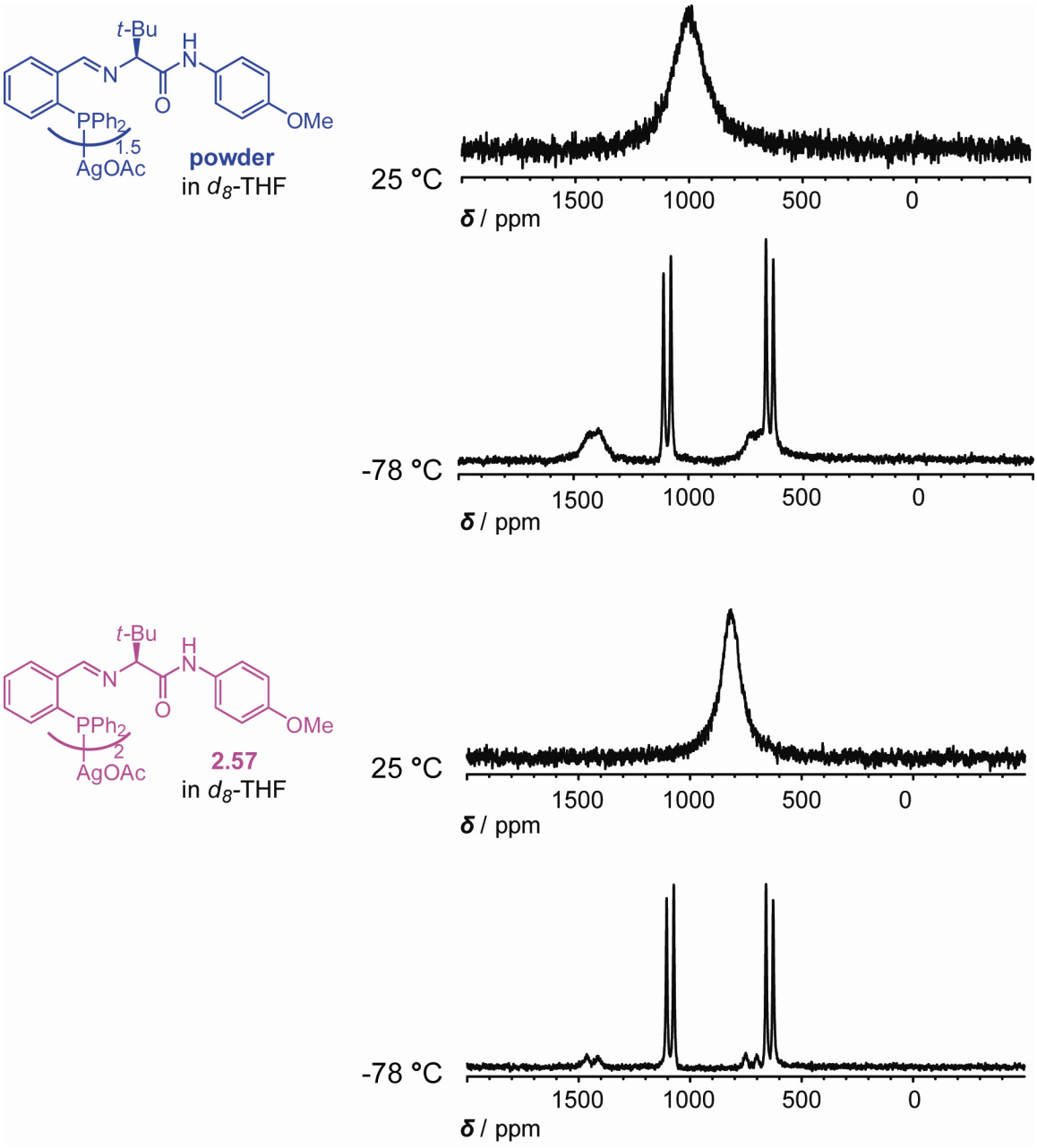

This appearance of a quartet was caused by coupling of ^{31}P with ^{107}Ag and ^{109}Ag, which exist in nearly equal abundance in nature.[102] The Ag-P coupling constants are

(102) Isotope abundance of ^{109}Ag = 51.839%; isotope abundance of ^{107}Ag = 48.161%. "Isotopic Compositions of the Elements 1997," Rosman, K. J. R.; Taylor, P. D. P. *Pure and Applied Chemistry*, **1998**, *70*, 217-239.

indicative of the number of phosphorus atoms bound to Ag (AgP_2 vs. AgP).[103] When we compared the *J*-values from our Ag-ligand complexes to literature values (shown in Table 2.23), *the identities of the two Ag complexes became readily apparent.*

Table 2.23: Literature values for some Ag-P coupling constants

Complex	AgP_x	$J^{109}Ag\text{-}^{31}P$	$J^{107}Ag\text{-}^{31}P$
(*t*-Bu)$_3$PAgOAc	AgP	735	635
(dppf)AgOAc	AgP_2	498	433

As shown in Figure 2.15, the more upfield component, which was more prevalent in the highly *anti*-selective catalyst, had coupling constants indicative of a 1:1 complex of AgOAc and phosphine ligand **2.29** (i.e. **2.58**), while the major component, which was the *syn*-selective catalyst, had coupling constants indicative of a 1:2 complex of AgOAc and **2.29** (i.e. crystalline **2.57**).[104] When the integrations were adjusted for the number of chiral ligands contained within each complex, we found that, in the highly *anti*-selective catalyst, the ratio of **2.58:2.57** = 2:1, while in the *syn*-selective catalyst, the ratio of **2.58:2.57** = 1:10.

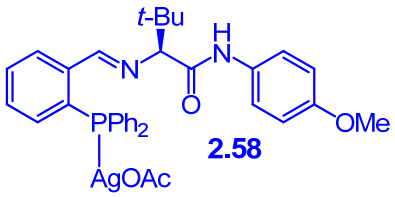

2.58

(103) (a) "Tri-*tert*-Butylphosphine Complexes of Silver(I). Preparation, Characterization, and Spectral Studies," Goel, R. G.; Pilon, P. *Inorganic Chemistry* **1978**, *17*, 2876-2879. (b) "Mechanism of Silver(I)-Catalyzed Mukaiyama Aldol Reaction: Active Species in Solution in AgPF6-(S)-BINAP Versus AgOAc-(S)-BINAP Systems," Ohkouchi, M.; Masui, D.; Yamaguchi, M.; Yamagishi, T. *Journal of Molecular Catalysis A: Chemical* **2001**, *170*, 1-15.

(104) When a solution of AgOAc, chiral ligand **2.29**, and ketoimine substrate **2.45a** were subjected to HRMS analysis, we were able to observe 1:1 and 1:2 complexes of AgOAc and **2.29**, as well as a 1:1:1 complex of AgOAc, **2.29**, and substrate **2.45a**.

Figure 2.15: Ag-P coupling constants calculated for Ag-**2.29** complexes at -78 ºC

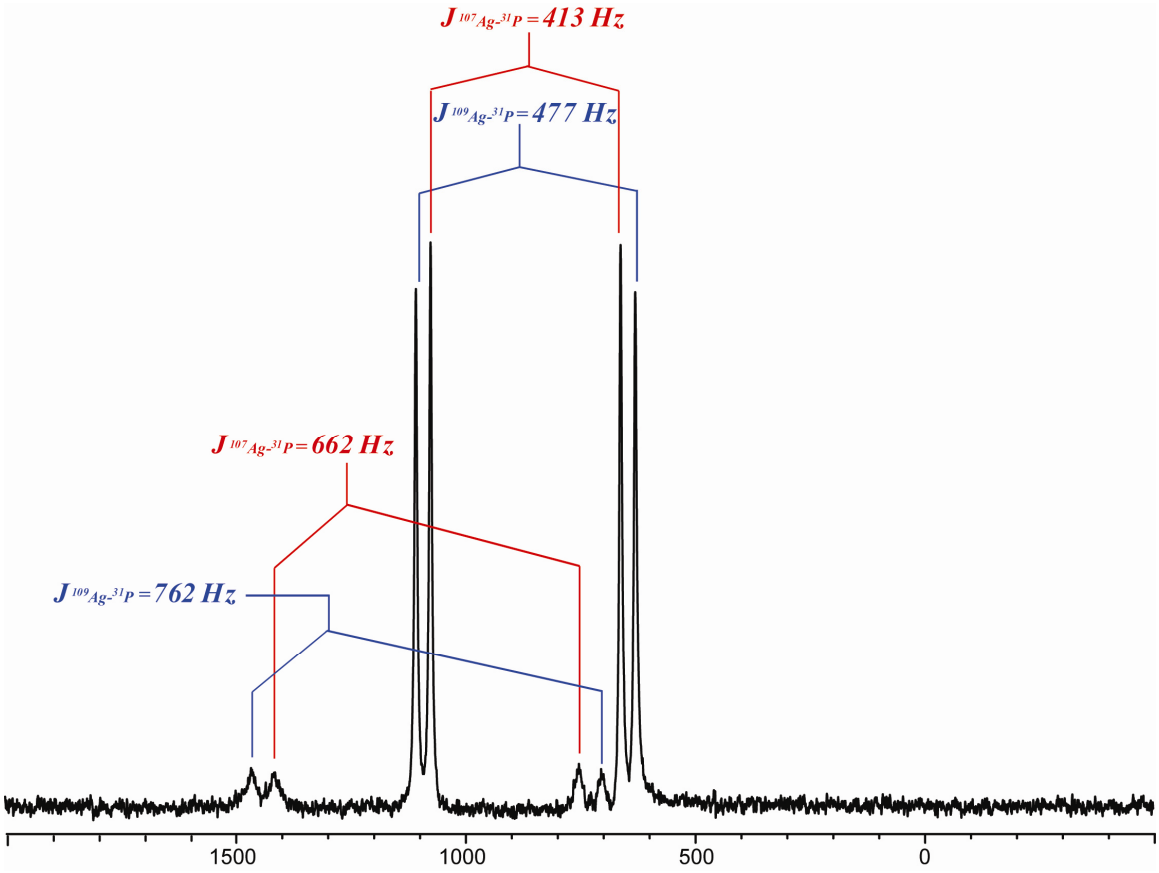

2.4.d Working transition state model

The highly *anti*-selective catalyst is likely 1:1 complex **2.58**. This finding supports previous models which we have proposed for Ag-catalyzed Mannich-type reactions with aldimines (Figure 2.16).[75] In the transition state, we propose that Ag is bound in the pocket formed by the phosphine and imine portions of **2.29**, and that substrate **2.45a** binds to Ag in a two-point manner between the imine nitrogen and the OMe (the NO_2 group was omitted for clarity). Lewis basic activation of siloxyfuran **2.25** (to give **II**) followed by Mannich addition results in the formation of a full N-Ag bond (**III**). We propose that *i*-PrOH may act to turn over the catalyst by desilylating the chiral ligand and protonating the N-Ag bond to release both the AVM product (*anti*-**2.46a**) and

regenerate the chiral catalyst. This working model accounts both for the vital role of *i*-PrOH on reaction efficiency and selectivity, as well as for the absolute sense of enantioinduction.[105]

Figure 2.16: Working transition state model of AVM

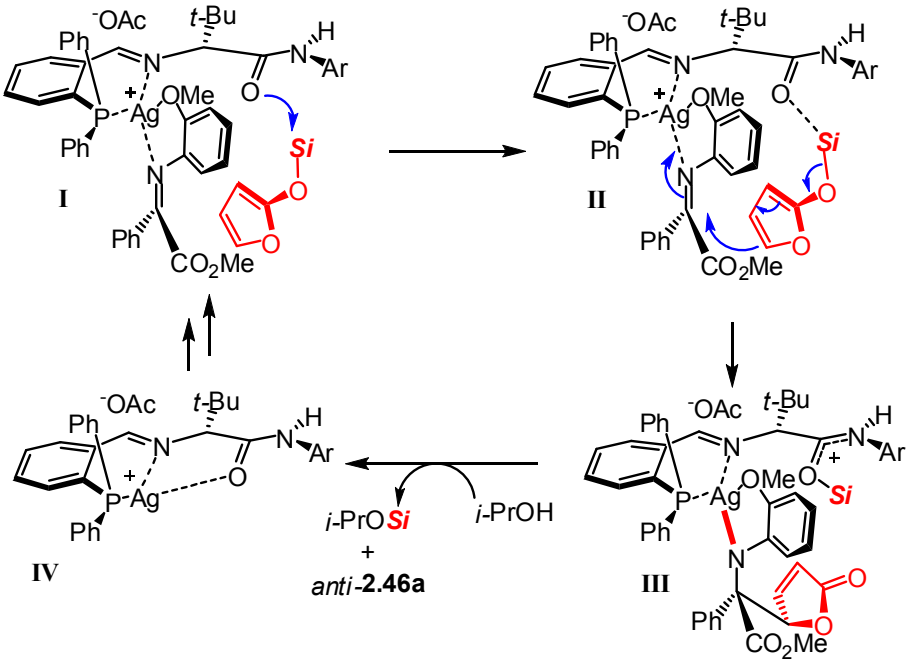

2.5 *Conclusions.*

We developed the first method for Ag-catalyzed AVM reactions of siloxyfuran **2.25** with ketoimines. This method is highly effective for methyl-pyruvate derived α-ketoimine ester **2.33a**, as well as for a variety of aryl-substituted α-ketoimine esters bearing an electron-withdrawing *N*-aryl protecting group (**2.45**). In addition, we have determined the structure of a highly enantio- and diastereoselective Ag-ligand complex which can be stored in air for extended periods of time without losing catalytic activity.

(105) Confirmed through X-ray crystallography of the reduced aniline form of *anti*-**2.46e** (i.e. *anti*-**2.49e**).

2.6 *Experimentals.*

General. Infrared (IR) spectra were recorded on a Perkin Elmer 781 spectrophotometer, ν_{max} in cm^{-1}. Bands were characterized as broad (br), strong (s), medium (m) or weak (w). ^1H NMR spectra were recorded on a Varian Unity INOVA 400 (400 MHz) spectrometer. Chemical shifts were reported in ppm from tetramethylsilane with the solvent resonance resulting from incomplete deuteration as the internal standard ($CDCl_3$: δ 7.26). Data were reported as follows: chemical shift, integration, multiplicity (s = singlet, d = doublet, t = triplet, q = quartet, br = broad, m = multiplet), and coupling constants. ^{13}C NMR spectra were recorded on a Varian Unity INOVA 400 (100 MHz) with complete proton decoupling. Chemical shifts were reported in ppm from tetramethylsilane with the solvent resonance as the internal standard ($CDCl_3$: δ 77.16 ppm). ^{31}P NMR spectra were recorded on a Varian Unity INOVA 400 (162 MHz) with complete proton decoupling. Chemical shifts were reported in ppm (H_3PO_4: δ 0.00 ppm). Enantiomeric ratios were determined by analytical liquid chromatography (HPLC) Shimazu chromatograph (Chiral Technologies Chiralpak AS (4.6 x 250 mm), Chiral Technologies Chiralcel OD (4.6 x 250 mm) or Chiral Technologies Chiralpak AD (4.6 x 250 mm)) in comparison with authentic racemic materials. High-resolution mass spectrometry was performed on a Micromass LCT ESI-MS (positive mode)) at the Mass Spectrometry Facility (Boston College). Optical rotation values were recorded on a Rudolph Research Analytical Autopol IV polarimeter. Unless otherwise stated, all reactions were conducted under an inert atmosphere of nitrogen. Tetrahydrofuran was purified by distillation from sodium benzophenone ketal immediately prior to use. All work-up and purification procedures were carried out with reagent solvents in air. All solvents were purchased from Doe and Ingalls. 2-(Trimethylsilyloxy)furan and AgOAc were purchased from Aldrich and used as received. α–Ketoesters were purchased from commercial sources or synthesized from commercially available starting materials through known methods.[106] The corresponding

(106) (a) **"**(Cyanomethylene)phosphoranes as Novel Carbonyl 1,1-Dipole Synthons: An Efficient Synthesis of **α**-Keto Acids, Esters, and Amides," Wasserman, H. H.; Ho, W.B. *J. Org. Chem*. **1994**, 59, 4364-4366. (b) "A General and Straightforward Approach to α,ω-Ketoesters," Babudri, F.; Fiandanese, V.; Marchese,

ketoimines were synthesized using known methods.[107] EDC•HCl, HOBt•H_2O, trifluroacetic acid, *p*-anisidine, Boc-protected amino acids and 2-(diphenylphosphino)benzaldehyde were purchased from commercial sources and used without further purification. Phosphino amino-acid based ligand **2.29** was prepared as previously reported.[75c]

Analytical Data for α-Ketoimine Substrates:

2.33a: IR (neat): 3001 (w), 2951 (w), 2837 (w), 1722 (s), 1656 (m), 1591 (m), 1506 (m), 1489 (s), 1454 (m), 1436 (m), 1367 (w), 1314 (m), 1275 (m), 1244 (s), 1224 (m), 1193 (m), 1138 (s), 1113 (s), 944 (m), 853 (m), 812 (m), 77 (m), 744 (s) cm^{-1}. ^1H NMR (400 MHz, $CDCl_3$), major isomer: δ 7.05 (1H, ddd, *J* = 7.6, 7.6, 1.6 Hz), 6.90-6.85 (2H, m), 6.89 (1H, dd, *J* = 7.6, 1.6 Hz), 3.85 (3H, s), 3.72 (3H, s), 1.98 (3H, s). ^{13}C NMR (100 MHz, $CDCl_3$): δ 165.2, 162.1, 148.3, 138.1, 126.0, 120.9, 120.2, 111.6, 55.7, 53.2, 17.6. HRMS Calcd for $C_{11}H_{14}NO_3$ (M + H): 208.09737; Found: 208.09785.

2.45a: 10:1 mixture of *E*/*Z* isomers. mp = 106–107 °C. IR (neat): 3101 (w), 3008 (w), 2945 (w), 2911 (w), 2865 (w, br), 2835 (w), 1729 (s), 1623 (s), 1585 (s), 1514 (s), 1484 (m), 1451 (m), 1409 (m), 1350 (s), 1336 (m), 1303 (s), 1260 (s), 1231 (s), 1181 (m), 1096 (m), 1020 (m), 1007 (m), 797 (m), 687 (m) cm^{-1}. ^1H NMR (400 MHz, $CDCl_3$, major isomer): δ 7.90 (2H, d, *J* = 7.3 Hz), 7.85 (1H, dd, *J* = 8.8, 2.2 Hz), 7.77 (1H, d, *J* = 2.2 Hz), 7.55 (1 H, t, *J* = 7.3 Hz), 7.48 (2H, t, *J* = 7.3 Hz), 6.89 (1H, d, *J* = 8.4 Hz), 3.89 (3H, s), 3.66 (3H, s). ^{13}C NMR (100 MHz, $CDCl_3$): δ 164.1, 161.8, 150.1, 145.9, 145.6,

---

G.; Punzi, A. *Tetrahedron* **1996**, *52*, 13513–13520. (c) "A Selective Method for the Preparation of Aliphatic Methyl Esters in the Presence of Aromatic Carboxylic Acids," Rodriguez, A.; Nomen, M.; Spur, B. W. *Tetrahedron Lett*, **1998**, *39*, 8563–8566. (d) "A Mild, Rapid, and Convenient Esterification of α-Keto acids," Domagala, J. M. *Tetrahedron Lett*. **1980**, *21*, 4997–5000.

(107) (a) **"**Efficient Synthesis of 1-Azadienes Derived from **α**-Aminoesters. Regioselective Preparation of **α**-Dehydroamino Acids, Vinylglycines, and **α**-Amino Acids,**"** Palacios, F.; Vicario, J.; Aparicio, D. *J. Org. Chem*. **2006**, 71, 7690-7696. (b) **"**Tandem N-Alkylation-C-Allylation Reaction of **α**-Imino Esters with Organoaluminums and Allyltributyltin,**"** Niwa, Y.; Shimizu, M. *J. Am. Chem. Soc*. **2003**, *125*, 3720–3721.

133.3, 132.8, 129.1, 128.8, 119.5, 117.0, 106.7, 56.5, 52.4. HRMS Calcd for $C_{16}H_{15}N_2O_5$ (M + H): 315.09810; Found: 315.09849.

2.45b: 5:1 mixture of *E*/*Z* isomers. mp = 104–105 °C. IR (neat): 3084 (w, br), 3008 (w, br), 2957 (w, br), 2839 (w, br), 1742 (s), 1641 (m), 1585 (m), 1523 (s), 1354 (s), 1320 (m), 1253 (s), 1096 (m), 1028 (m), 796 (m), 670 (m) cm^{-1}. ^1H NMR (400 MHz, $CDCl_3$, major isomer): δ 7.86 (1H, dd, *J* = 8.4, 2.0 Hz), 7.77 (1H, d, *J* = 2.0 Hz), 7.51 (1H, s), 7.38 (2 H, d, *J* = 4.8 Hz), 7.13-7.08 (1H, m), 6.90 (1H, d, *J* = 8.4 Hz), 3.91 (3H, s), 3.87 (3H, s), 3.66 (3H, s). ^{13}C NMR (100 MHz, $CDCl_3$): δ 164.0, 161.7, 160.2, 150.1, 145.9, 145.6, 134.6, 130.0, 121.7, 119.5, 119.3, 117.0, 112.8, 106.7, 56.5, 55.7, 52.4. HRMS Calcd for $C_{17}H_{17}N_2O_6$ (M + H): 345.10866; Found: 345.10892.

2.45c: 13:1 mixture of *E*/*Z* isomers. mp = 106–108 °C. IR (neat): 3111 (w, br), 3015 (w), 2955 (w), 2843 (w), 1725 (s), 1615 (s), 1579 (s), 1507 (s), 1487 (m), 1450 (m), 1412 (m), 1342 (s), 1318 (s), 1276 (m), 1250 (s), 1223 (s), 1175 (s), 1091 (m), 1024 (s), 938 (m), 866 (m), 830 (m), 794 (m), 714 (m), 682 (m), 665 (m) cm^{-1}. ^1H NMR (400 MHz, $CDCl_3$, major isomer): δ 7.94 (1H, s), 7.87 (1H, dd, *J* = 8.4, 2.2 Hz), 7.78 (1H, d, *J* = 2.2 Hz), 7.74 (1 H, d, *J* = 7.7 Hz), 7.53 (1H, d, *J* = 8.4 Hz), 7.42 (1H, t, *J* = 8.4 Hz), 6.89 (1H, d, *J* = 8.4 Hz), 3.91 (3H, s), 3.67 (3H, s). ^{13}C NMR (100 MHz, $CDCl_3$): δ 163.5, 160.4, 150.0, 145.8, 145.4, 135.3, 135.1, 132.7, 130.3, 128.6, 127.1, 119.4, 117.0, 106.7, 56.5, 52.6. HRMS Calcd for $C_{16}H_{14}ClN_2O_5$ (M + H): 349.05912; Found: 349.05871.

2.45d: IR (neat): 3354 (w), 3091 (w), 3009 (w), 2957 (w), 2835 (w, br), 1734 (s), 1629 (s), 1581 (s), 1507 (s), 1493 (m), 1461 (m), 1405 (m), 1339 (s), 1310 (m), 1253 (m), 1224 (s), 1176 (m), 1090 (s), 1029 (m), 1008 (m), 858 (m), 842 (m), 796 (m), 766 (m), 744 (m), 727 (m), 671 (m) cm^{-1}. ^1H NMR (400 MHz, $CDCl_3$, major isomer): δ 7.85-7.77 (4H, m), 7.44 (2H, d, *J* = 8.4 Hz), 6.88 (1 H, d, *J* = 8.4 Hz), 3.89 (3H, s), 3.66 (3H, s). ^{13}C

NMR (100 MHz, $CDCl_3$): δ 163.6, 160.6, 149.9, 145.7, 145.6, 132.32, 132.26, 130.2, 127.7, 119.4, 117.0, 106.7, 56.5, 52.5. HRMS Calcd for $C_{16}H_{14}ClN_2O_5$ (M + H): 349.05912; Found: 349.05911. mp=132-134.

2.45e: 10:1 mixture of *E*/*Z* isomers. mp = 154–155 °C. IR (neat): 3352 (w), 3088 (w), 3007 (w), 2971 (w), 2834 (w), 2657 (w, br), 1732 (s), 1626 (s), 1581 (s), 1566 (m), 1505 (s), 1489 (m), 1462 (m), 1400 (m), 1309 (s), 1253 (m), 1224 (s), 1176 (m), 1123 (m), 1091 (m), 1069 (m), 1028 (m), 1005 (m), 859 (m), 687 (m) cm^{-1}. ^1H NMR (400 MHz, $CDCl_3$, major isomer): δ 7.86 (1H, dd, *J* = 8.4, 2.2 Hz), 7.78-7.76 (3H, m), 7.63 (2H, d, *J* = 8.8 Hz), 6.88 (1H, d, *J* = 8.4 Hz), 3.90 (3H, s), 3.66 (3H, s). ^{13}C NMR (100 MHz, $CDCl_3$): δ 163.6, 160.5, 150.0, 145.7, 145.6, 139.1, 131.9, 130.2, 129.3, 119.4, 117.0, 106.7, 56.5, 52.6. HRMS Calcd for $C_{16}H_{14}BrN_2O_5$ (M + H): 393.00861; Found: 393.00875.

2.45f: 10:1 mixture of *E*/*Z* isomers. mp = 166–169 °C. IR (neat): 3070 (w), 3004 (w), 2959 (w), 2915 (w), 2833 (w, br), 2655 (w), 1730 (s), 1624 (m), 1579 (m), 1504 (s), 1487 (m), 1462 (m), 1395 (m), 1309 (s), 1251 (m), 1223 (s), 1175 (s), 1123 (m), 1092 (m), 1056 (m), 1026 (m), 1001 (s), 859 (m), 841 (m), 829 (m), 794 (m), 743 (m), 721 (m) cm^{-1}. ^1H NMR (400 MHz, $CDCl_3$, major isomer): δ 7.88-7.84 (3H, m), 7.78 (1H, d, *J* = 2.2 Hz), 7.62 (2H, d, *J* = 8.4 Hz), 6.88 (1 H, d, *J* = 8.4 Hz), 3.90 (3H, s), 3.66 (3H, s). ^{13}C NMR (100 MHz, $CDCl_3$): δ 163.6, 160.9, 150.0, 145.7, 145.6, 138.3, 132.9, 130.2, 119.4, 117.0, 106.8, 100.2, 56.5, 52.5. HRMS Calcd for $C_{16}H_{14}IN_2O_5$ (M + H): 440.99474; Found: 440.99559.

2.45g: 10:1 mixture of *E*/*Z* isomers. mp = 148–151 °C. IR (neat): 3101 (w), 3006 (w, br), 2866 (w), 2835 (w), 1730 (s), 1601 (m), 1578 (m), 1561 (m), 1488 (s), 1410 (m), 1312 (s), 1231 (m), 1191(m), 1173 (m), 1128 (m), 1091 (m), 1022 (m), 1005 (m), 873

(m), 843 (m), 793 (m), 736 (m), 536 (m) cm^{-1}. ^1H NMR (400 MHz, $CDCl_3$, major isomer): δ 7.87-7.77 (4H, m), 7.51 (2H, d, *J* = 8.1 Hz), 6.88 (1H, d, *J* = 8.4 Hz), 3.90 (3H, s), 3.66 (3H, s), 1.35 (9H, s). ^{13}C NMR (100 MHz, $CDCl_3$): δ 164.2, 161.6, 156.6, 150.2, 146.2, 145.4, 130.6, 128.7, 126.1, 119.5, 117.0, 106.7, 56.5, 52.3, 35.3, 31.3. HRMS Calcd for $C_{20}H_{23}N_2O_5$ (M + H): 371.16070; Found: 371.16194.

2.45h: 11:1 mixture of *E*/*Z* isomers. mp = 128–130 °C. IR (neat): 3118(w), 3012 (w), 2958 (w), 2839 (w), 2653 (w, br), 2514 (w), 1742 (s), 1641 (s), 1582 (s), 1523 (s), 1489 (m), 1464 (m), 1417 (m), 1328 (s), 1316 (m), 1256 (s), 1223 (s), 1181 (m), 1131 (m), 1067 (m), 1028 (m), 1007 (m), 910 (m), 873 (m), 856 (m), 801 (m), 742 (m) cm^{-1}. ^1H NMR (400 MHz, $CDCl_3$, major isomer): δ 8.02 (2H, d, *J* = 8.4 Hz), 7.86 (1H, dd, *J* = 8.4, 2.0 Hz), 7.78 (1H, d, *J* = 2.0 Hz), 7.73 (2H, d, *J* = 8.4 Hz), 6.90 (1H, d, *J* = 8.4 Hz), 3.90 (3H, s), 3.69 (3H, s). ^{13}C NMR (100 MHz, $CDCl_3$): δ 163.3, 160.4, 149.8, 145.9, 145.3, 136.6, 133.5 (q, *J* = 32.6 Hz), 129.2, 125.9 (q, *J* = 3.8 Hz), 123.9 (q, *J* = 217 Hz), 119.4, 117.0, 106.8, 56.5, 52.6. HRMS Calcd for $C_{17}H_{14}F_3N_2O_5$ (M + H): 383.08548; Found: 383.08515.

2.45i: 20:1 mixture of *E*/*Z* isomers. mp = 128–129 °C. IR (neat): 3109 (w), 3063 (w), 3017 (w), 2953 (w), 2854 (w, br), 2839 (w), 1742 (s), 1619 (s), 1582 (s), 1518 (s), 1493 (m), 1468 (m), 1412 (m), 1350 (s), 1312 (m), 1257 (s), 1223 (m), 1168 (m), 1126 (m), 1096 (m), 1033 (m), 1016 (m), 868 (m), 797 (m), 733 (m) cm^{-1}. ^1H NMR (400 MHz, $CDCl_3$, major isomer): δ 8.25 (1H, s), 8.12 (1H, dd, *J* = 8.6, 1.4 Hz), 7.94-7.87 (4H, m), 7.80 (1H, d, *J* = 2.0 Hz), 7.61-7.53 (2H, m), 6.95 (1H, d, *J* = 8.4 Hz), 3.91 (3H, s), 3.72 (3H, s). ^{13}C NMR (100 MHz, $CDCl_3$): δ 164.2, 161.8, 150.2, 146.1, 145.6, 135.5, 132.9, 130.8, 129.5, 129.1, 128.7, 128.1, 127.2, 124.1, 119.5, 117.0, 106.8, 56.5, 52.5. HRMS Calcd for $C_{20}H_{17}N_2O_5$ (M + H): 365.11375; Found: 365.11481.

2.45j: 2.5:1 mixture of *E*/*Z* isomers. mp = 98–100 °C. IR (neat): 3147 (w), 3118 (w), 2953 (w), 2835 (w), 1742 (s), 1628 (m), 1518 (s), 1472 (s), 1354 (s), 1337 (s), 1257 (s), 1239 (m), 1096 (m), 1045 (s), 1016 (m), 1155 (m), 805 (m), 762 (m) cm^{-1}. ^{1}H NMR (400 MHz, $CDCl_3$, mixture of isomers): δ 7.84-7.81 (1 + [0.4]H, m), [7.72 (0.4H, s)], 7.71 (1H, m), 7.65 (1H, s), [7.28 (0.4H, s)], 7.12 (1H, d, *J* = 3.2 Hz), [7.03 (0.4H, d, *J* = 2.2 Hz)], 6.92 (1H, d, *J* = 8.8 Hz), [6.86 (0.4H, d, *J* = 8.4 Hz)], 6.56 (1H, t, *J* = 1.6 Hz), [6.41 (0.4H, s)], [3.97 (1.2H, s)], 3.84 (3H, s), [3.75 (1.2H, s)], 3.65 (3H, s). ^{13}C NMR (100 MHz, $CDCl_3$, mixture of isomers): δ [163.7], 161.8, 150.2, 149.5, 149.2, [148.6], [147.9], 147.5, [146.8], [146.5], [145.9], 145.4, 145.3, [145.1], [120.6], 120.3, 119.3, [118.8], [117.2], 117.1, 112.9, [112.5], 106.6, [106.6], 56.4, [56.4], [53.7], 52.7. HRMS Calcd for $C_{14}H_{13}N_2O_6$ (M + H): 305.07736; Found: 305.07696.

2.45k: 8:1 mixture of *E*/*Z* isomers. mp = 153–154 °C. IR (neat): 3085 (w), 2960 (w), 2916 (w), 2848 (w), 1734 (s), 1617 (s), 1581 (m), 1511 (s), 1486 (m), 1465 (m), 1406 (m), 1345 (s), 1288 (m), 1226 (s), 1170 (s), 1125 (m), 1091 (m), 1023 (s), 860 (m), 803 (m), 731 (m), 687 (m) cm^{-1}. ^{1}H NMR (400 MHz, $CDCl_3$, major isomer): δ 7.96 (1H, s), 7.86 (1H, dd, *J* = 8.4, 2.2 Hz), 7.77 (1H, d, *J* = 2.2 Hz), 7.69 (1H, d, *J* = 4.8 Hz), 7.42-7.38 (1H, m), 6.90 (1H, d, *J* = 8.8 Hz), 3.89 (3H, s), 3.65 (3H, s). ^{13}C NMR (100 MHz, $CDCl_3$): δ 163.5, 156.0, 149.7, 145.9, 145.4, 137.3, 131.8, 127.1, 127.0, 119.8, 117.1, 106.7, 56.4, 52.5. HRMS Calcd for $C_{14}H_{13}N_2O_5S$ (M + H): 321.05452; Found: 321.05540.

Representative experimental procedure for gram-scale Ag-catalyzed addition of vinylogous silyl enol ether 2.25 to an α-ketoimine ester: A flame-dried 100 mL round bottom flask was charged with AgOAc (117 mg, 0.700 mmol), **2.29** (320 mg, 0.636 mmol), and **2.45a** (2.00 g, 6.36 mmol). The flask was sealed with a septum and purged with a N_2 atmosphere. Freshly distilled THF was added (64 mL) through a syringe, followed by *i*-PrOH (487 μL, 0.636 mmol), and the resulting homogenous yellow

solution was allowed to cool to –78 ºC (dry ice/acetone) with stirring. 2-Trimethylsiloxyfuran (**2.25**) (2.53 mL, 13.4 mmol) was added, and the resulting solution was kept at –78 ºC for 15 h before addition of HOAc (765 μL, 13.4 mmol) in MeOH (10 mL). The resulting solution was allowed to stir at –78 ºC for an additional three hours, after which it was allowed to warm to 22 ºC. A saturated aqueous solution of $NaHCO_3$ was added, after which the aqueous layer was washed with EtOAc (3 x 100 mL), dried over $MgSO_4$, and the volatiles were removed *in vacuo*. The unpurified residue (typically yellow oil) was a 20:1 mixture of *anti*-**2.46a:***syn*-**2.46a** by ^{1}H NMR analysis, which can be separated by silica gel chromatography (3:1 petroleum ether:EtOAc) to furnish pure *anti*-**2.46a** as a yellow solid (2.24 g, 5.62 mmol, 88% yield, 92% ee of *anti*-**2.46a**), which was recrystallized from MeOH to afford *anti*-**2.46a** (yellow crystals) in >98% ee (1.53 g, 3.84 mmol, 68% yield, >98% ee).

Analytical Data for Products of Ag-catalyzed AVM Reactions with α-Ketoimine Esters:

syn-**2.36a:** IR (neat): 3396 (w, br), 3006 (w), 2949 (w), 2829 (w), 1761 (m), 1759 (s), 1757 (m), 1595 (m), 1520 (m), 1464 (m), 1250 (m), 1224 (m), 1162 (m), 1092 (m), 1048 (m), 1029 (m), 746 (m) cm^{-1}. ^{1}H NMR (400 MHz, $CDCl_3$): δ 7.50 (1H, dd, *J* = 5.6, 1.6 Hz), 6.76-7.72 (3H, m), 6.52-6.48 (1H, m), 6.03 (1 H, dd, *J* = 6.0, 2.0 Hz), 5.56 (1H, dd, *J* = 1.8, 1.8 Hz), 4.66 (1H, br s), 3.81 (3H, s), 3.76 (3H, s), 1.59 (3H, s). ^{13}C NMR (100 MHz, $CDCl_3$): δ 173.2, 172.7, 153.7, 148.4, 134.5, 122.8, 120.9, 119.8, 14.3, 10.3, 85.5, 62.9, 55.8, 53.1, 21.4. HRMS Calcd for $C_{15}H_{17}NO_5$: 291.11067; Found: 291.11070. $[\alpha]^{26}_D$ = 135.73 (*c* = 1.0, $CHCl_3$) for an 87% ee sample. The optical purity of the compound is determined by chiral HPLC analysis (OD, 80:20 hexanes:*i*-PrOH, 1 ml/min, 254 nm): t_R of *syn*-**2.36a** 17 min (minor) and 18 min (major).

rac-syn-**2.36a**

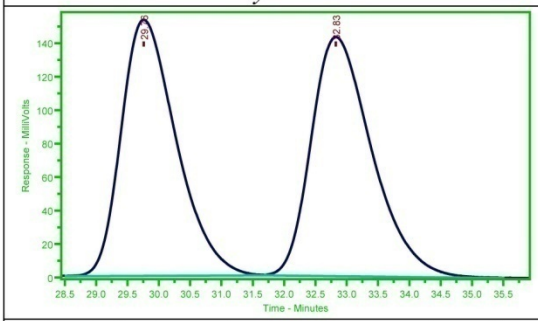

Peak #	Ret. Time	Area	Area %
1	29.76	9370419	49.250
2	32.83	9655780	50.750

syn-**2.36a**

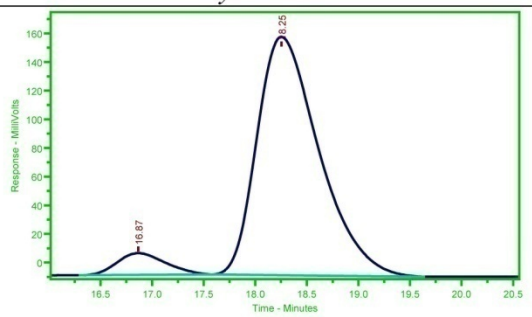

Peak #	Ret. Time	Area	Area %
1	16.87	498065	6.677
2	18.25	6960887	93.323

Recrystallized *syn*-**2.36a**

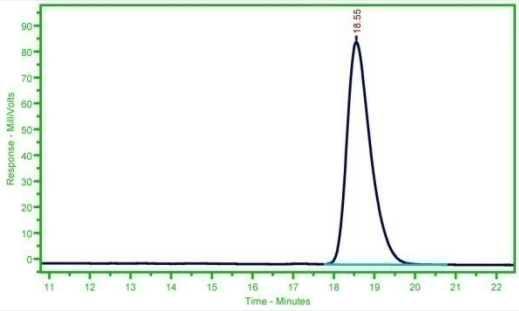

Peak #	Ret. Time	Area	Area %
1	18.55	3476269.0	100.000

***syn*-2.40:** IR (neat): 3367 (w, br), 3105 (w), 2952 (w), 2839 (w), 2141 (w), 1761 (m), 1756 (s), 1738 (s), 1721 (s), 1641 (m), 1600 (m), 1516 (m), 1488 (m), 1459 (m), 1263 (s), 1223 (s), 1181 (m), 1162 (m), 1153 (m), 1108 (m), 1047 (m), 1025 (m), 905 (m), 745 (m) cm^{-1}. ^1H NMR (400 MHz, $CDCl_3$): δ 6.78 (3H, t, *J* = 4.5 Hz), 5.88-5.87 (1H, m), 5.45 (1 H, s), 4.72 (1H, br s), 3.81 (3H, s), 3.74 (3H, s), 2.11 (3H, s), 1.48 (3H, s). ^{13}C NMR (100 MHz, $CDCl_3$): δ173.0, 167.0, 153.7, 149.0, 134.1, 121.1, 120.0, 119.8, 115.8, 110.3, 86.2, 63.0, 55.9, 53.1, 18.7, 16.0. HRMS Calcd for $C_{16}H_{20}NO_5$ [M + H]: 306.13415; Found: 306.13391. $[\alpha]^{24}_D$ = +16.464 (*c* = 1.00, CHCl3) for a 72% ee sample. The optical purity of the compound is determined by chiral HPLC analysis (OD, 95:5 hexanes:*i*-PrOH, 1 ml/min, 254 nm): t_R of **18:** 28 min (major) and 40 min (minor).

rac-syn-2.40a				*syn*-2.40a			
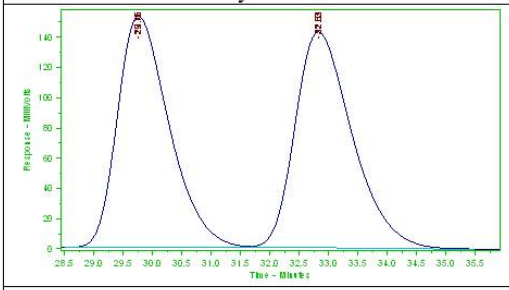				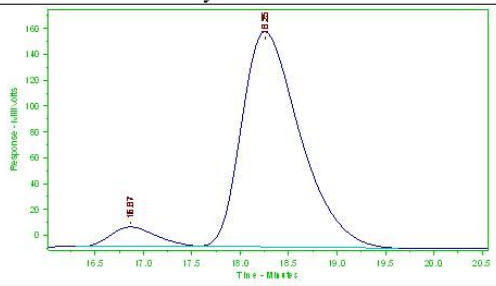			
Peak #	**Ret. Time**	**Area**	**Area %**	**Peak #**	**Ret. Time**	**Area**	**Area %**
1	27.70	2949347	50.887	1	27.23	7470072	86.245
2	40.28	2846474	49.113	2	40.25	1191339	13.755

anti-**2.46a:** IR (neat): 3396 (w, br), 1791 (m), 1766 (s), 1595 (m), 1532 (m), 1501 (m), 1338 (m), 1293 (s), 1256 (m), 1231 (m), 1092 (m), 734 (m) cm^{-1}. ^{1}H NMR (400 MHz, $CDCl_3$): δ 7.62 (1H, d, *J* = 2.4 Hz), 7.52 (1H, ddd, *J* = 6.8, 2.4, 0.4 Hz), 7.50 (1H, dd, *J* = 5.8, 1.6 Hz), 7.46-7.39 (5 H, m), 6.21 (1H, br s), 6.11 (1H, dd, *J* = 2.0, 1.6 Hz), 6.04 (1H, dd, *J* = 5.6, 2.0 Hz), 5.84 (1H, d, *J* = 8.8 Hz), 3.98 (3H, s), 3.80 (3H, s). ^{13}C NMR (100 MHz, $CDCl_3$): δ 171.6, 170.6, 152.4, 146.4, 140.6, 138.7, 133.5, 129.7, 129.6, 127.0, 124.0, 118.1, 111.4, 105.1, 84.7, 68.6, 56.4, 54.1. HRMS Calcd for $C_{20}H_{18}N_2O_7$ [M + H]: 399.11923; Found: 399.11946. $[\alpha]^{26}_D$ = +165.45 (*c* = 1.00, $CHCl_3$) for a 92% ee sample. The enantiomeric purity of this compound was determined by chiral HPLC analysis (OD, 80:20 hexanes:*i*-PrOH, 1 mL/min, 254 nm): t_R of *anti*-**2.46a**: 16 min (major) and 24 min (minor); t_R of *syn*-**2.46a**: 19 min and 21 min.

rac-anti-**2.46a**

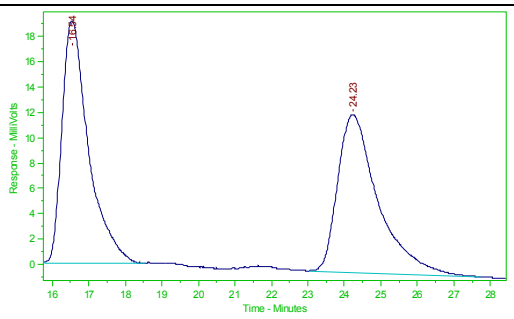

Peak #	Ret. Time	Area	Area %
1	16.54	967379	50.226
2	24.23	958669	49.774

anti-**2.46a**

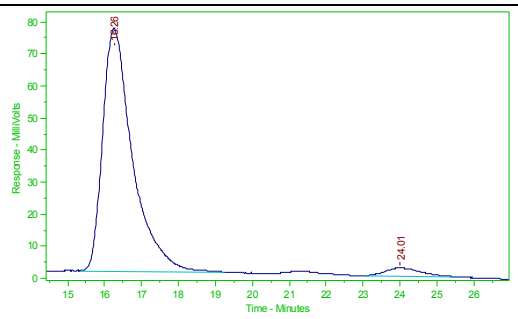

Peak #	Ret. Time	Area	Area %
1	16.26	4274050	96.33
2	24.01	162829	3.67

Recrystallized *anti*-**2.46a**

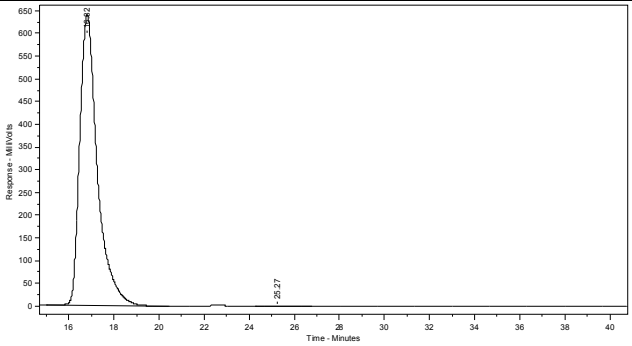

Peak #	Ret. Time	Area	Area %
1	16.82	35044100	99.858
2	25.27	49883	0.142

syn-**2.46a:** IR (neat): 3390 (w, br), 3100 (w, br), 2961 (w, br), 1791 (m), 1766 (s), 1596 (m), 1527 (m), 1501 (m), 1338 (m), 1294 (s), 1262 (m), 1161 (m), 1098 (m), 733 (m) cm^{-1}. ^{1}H NMR (400 MHz, $CDCl_3$): δ 7.61 (1H, d, *J* = 2.4 Hz), 7.53-7.50 (2H, m), 7.49 (1H, dd, *J* = 9.2, 2.4 Hz), 7.41-7.39 (3H, m), 7.30 (1H, dd, *J* = 6.0, 1.6 Hz), 6.26 (1H, br s), 6.17 (1H, dd, *J* = 6.0, 2.0 Hz), 6.05 (1H, d, *J* = 9.2 Hz), 5.93 (1H, dd, *J* = 1.8, 1.8 Hz), 3.89 (3H, s), 3.77 (3H, s). ^{13}C NMR (100 MHz, $CDCl_3$): δ 171.5, 170.2, 152.4, 146.4, 140.5, 138.8, 134.0, 129.54, 129.49, 127.6, 123.9, 118.3, 112.6, 104.9, 85.9, 69.2, 56.4, 54.0. HRMS Calcd for $C_{20}H_{18}N_2O_7Na$: [M + Na] 421.1012; Found: 421.1009. $[\alpha]^{26}_D$ = +34.99 (*c* = 1.00, $CHCl_3$) for a 75% ee sample. The enantiomeric purity of the compound was determined by chiral HPLC analysis (OD, 80:20 hexanes:*i*-PrOH, 1

mL/min, 254 nm): t_R of *syn*-**2.46a**: 19 min and 21 min; t_R of *anti*-**2.46a**: 16 min (major) and 24 min (minor).

rac-syn-**2.46a**

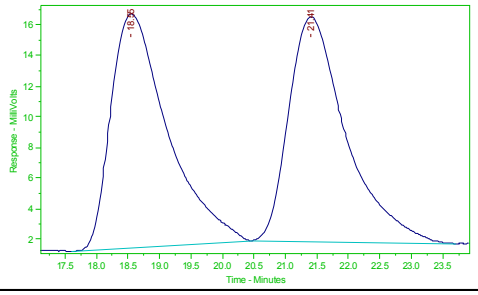

Peak #	Ret. Time	Area	Area %
1	18.55	960705	50.794
2	21.41	930684	49.206

syn-**2.46a**

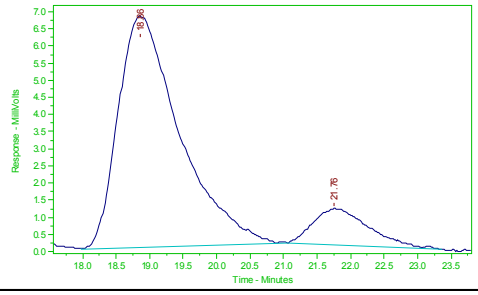

Peak #	Ret. Time	Area	Area %
1	18.86	432036	87.415
2	21.76	62198	12.585

rac-syn-**2.46a** and *rac-anti*-**2.46a**

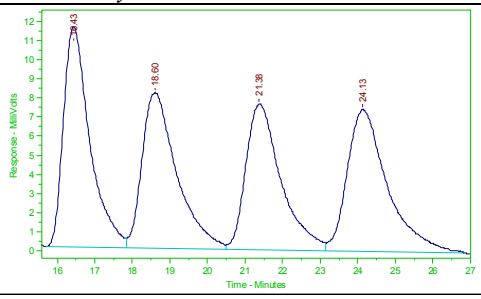

Peak #	Ret. Time	Area	Area %
1	16.43	565621	26.445
2	18.6	525228	24.557
3	21.38	498033	23.285
4	24.13	549947	25.713

***anti*-2.46b:** IR (neat): 3389 (w, br), 3096 (w, br), 2954 (w, br), 2835 (w, br), 1795 (m), 1758 (s), 1596 (s), 1521 (s), 1503 (m), 1334 (m), 1303 (s), 1260 (m), 1228 (m), 1153 (w), 1098 (m), 1029 (w), 736 (w), 662 (w) cm^{-1}. ^1H NMR (400 MHz, $CDCl_3$): δ 7.61 (1H, d, J = 2.2 Hz), 7.53 (1H, dd, J = 8.8, 2.4 Hz), 7.50 (1H, dd, J = 5.7, 1.7 Hz), 7.34 (1H, t, J = 7.9 Hz), 7.02 (1H, ddd, J = 7.7, 1.1, 0.7 Hz), 6.98 (1H, t, J = 2.2 Hz), 6.93 (1H, ddd, J = 8.3, 2.5, 0.7 Hz), 6.19 (1H, br s), 6.10 (1H, t, J = 1.8 Hz), 6.03 (1H, dd, J = 5.9, 2.2 Hz), 5.86 (1H, d, J = 8.8 Hz), 3.98 (3H, s), 3.80 (3H, s), 3.77 (3H, s). ^{13}C NMR (100 MHz, $CDCl_3$): δ 171.6, 170.5, 160.5, 152.4, 146.4, 140.7, 138.7, 135.2, 130.8, 123.9, 119.0, 118.1, 114.3, 113.5, 111.4, 105.1, 84.7, 68.5, 56.5, 55.6, 54.1. HRMS Calcd for $C_{21}H_{21}N_2O_8$ [M + H]: 429.1297; Found: 429.1302. $[\alpha]^{23}_D$ = +75.26 (c = 1.00, $CHCl_3$) for

a 93% ee sample. The enantiomeric purity of the compound was determined by chiral HPLC analysis (OD, 80:20 hexanes:*i*-PrOH, 1 mL/min, 254 nm): t_R of *anti*-**2.46b**: 19 min (major) and 30 min (minor); t_R of *syn*-**2.46b:** 22 min (major) and 28 min (minor).

rac-anti-**2.46b**

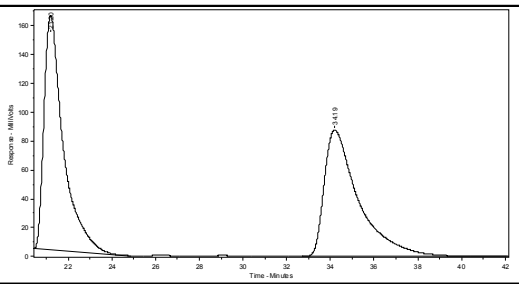

Peak #	Ret. Time	Area	Area %
1	21.2	9968915	50.844
2	34.19	9638127	49.156

anti-**2.46b**

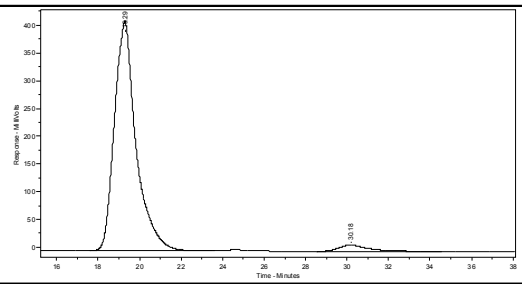

Peak #	Ret. Time	Area	Area %
1	19.29	29958420	96.254
2	30.18	1165924	3.746

rac-syn-**2.46b**

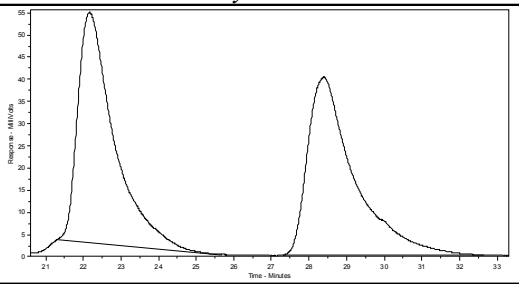

Peak #	Ret. Time	Area	Area %
1	22.17	3506655	50.345
2	28.39	3458649	49.655

rac-anti-**2.46b**

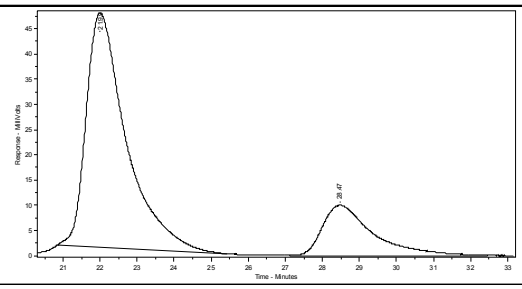

Peak #	Ret. Time	Area	Area %
1	21.99	3503242	78.338
2	28.47	968738	21.662

anti-**2.46c:** IR (neat): 3383 (w, br), 3100 (w, br), 3018 (w, br), 2955 (w, br), 2943 (w, br), 2848 (w, br), 1784 (s), 1759 (s), 1590 (s), 1527 (s), 1507 (m), 1338 (m), 1239 (s), 1256 (m), 1231 (m), 1092 (m), 1029 (w) cm^{-1}. ^1H NMR (400 MHz, $CDCl_3$): δ 7.65 (1H, d, J = 2.6 Hz), 7.56 (1H, dd, J = 9.2, 2.6 Hz), 7.52-7.50 (1H, m), 7.46 (1H, dd, J = 5.9, 1.5 Hz), 7.41-7.33 (3H, m), 6.18 (1H, br s), 6.10 (1H, dd, J = 5.7, 1.8 Hz), 6.01 (1H, t, J = 1.8 Hz), 5.85 (1H, d, J = 9.2 Hz), 4.00 (3H, s), 3.80 (3H, s). ^{13}C NMR (100 MHz, $CDCl_3$): δ 171.3, 170.0, 152.0, 146.5, 140.1, 139.0, 135.70, 135.67, 130.8, 129.9, 127.5, 125.5, 124.3, 118.0, 111.4, 105.2, 84.4, 68.3, 56.5, 54.3. HRMS Calcd for $C_{20}H_{17}N_2O_7ClNa$ [M + Na]: 455.0609; Found: 455.0622. $[\alpha]^{25}_D$ = +106.65 (c = 1.00, $CHCl_3$) for an 88% ee sample. The enantiomeric purity of the compound was determined

by chiral HPLC analysis (OD, 90:10 hexanes:*i*-PrOH, 1 mL/min, 254 nm): t_R of *anti*-**2.46c**: 42 min (major) and 80 min (minor); t_R of *syn*-**2.46c**: 46 min (major) and 66 min (minor).

rac-anti-**2.46c**

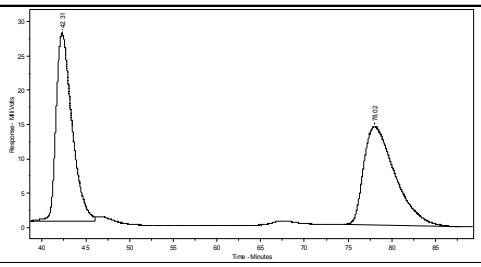

Peak #	Ret. Time	Area	Area %
1	42.31	3496745	49.405
2	78.02	3581021	50.595

anti-**2.46c**

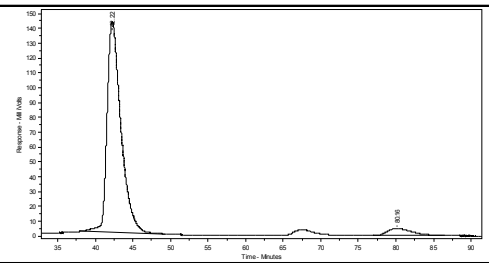

Peak #	Ret. Time	Area	Area %
1	42.22	18325730	94.174
2	80.16	1133718	5.826

rac-syn-**2.46c** and *rac-anti*-**2.46c**

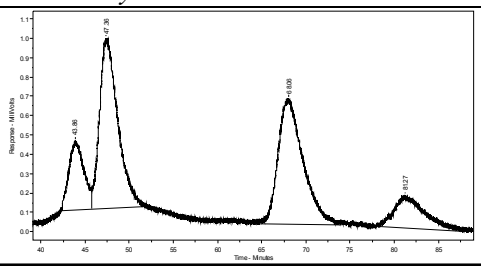

Peak #	Ret. Time	Area	Area %
1	43.86	42012	12.522
2	47.36	126276	37.636
3	68.06	127110	37.884
4	81.27	40123	11.958

syn-**2.46c**

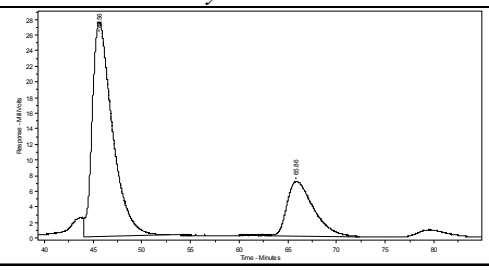

Peak #	Ret. Time	Area	Area %
1	45.56	3955760	75.204
2	65.86	1304255	24.796

anti-**2.46d:** IR (neat): 3381(w, br), 3094 (w, br), 2953 (w, br), 2846 (w, br), 1787 (m), 1754 (m), 1592 (m), 1523 (m), 1493 (m), 1324 (m), 1292 (s), 1228 (m), 1093 (m), 1026 (m), 816 (m), 796 (m), 744 (m) cm^{-1}. ^1H NMR (400 MHz, $CDCl_3$): δ 7.63 (1H, d, J = 2.6 Hz), 7.56-7.53 (1H, dd, J = 8.8, 2.6 Hz), 7.47-7.45 (1H, dd, J = 5.9, 1.5 Hz), 7.43-7.36 (4 H, m), 6.18 (1H, br s), 6.09-6.07 (1H, dd, J = 5.9, 1.8 Hz), 6.01 (1H, t, J = 1.8 Hz), 5.86 (1H, d, J = 8.8 Hz), 3.99 (3H, s), 3.79 (3H, s). ^{13}C NMR (100 MHz, $CDCl_3$): δ. 171.6, 170.4, 152.3, 146.7, 140.3, 139.2, 136.0, 132.2, 130.0, 129.0, 124.5, 118.3, 111.7, 105.4, 84.6, 68.5, 56.7, 54.4. HRMS Calcd for $C_{20}H_{18}N_2O_7Cl$ (M + H): 433.08025; Found: 433.07983. $[\alpha]^{25}_D$ = 67.6 (c = 1.0, $CHCl_3$) for a 96% ee sample. The optical purity of the compound was determined by chiral HPLC analysis (OD, 80:20

hexanes:*i*-PrOH, 1 ml/min, 254 nm): t_R of *anti*-**2.46d**: 18 min (major) and 41 min (minor).

rac-anti-**2.46d**	*anti*-**2.46d**
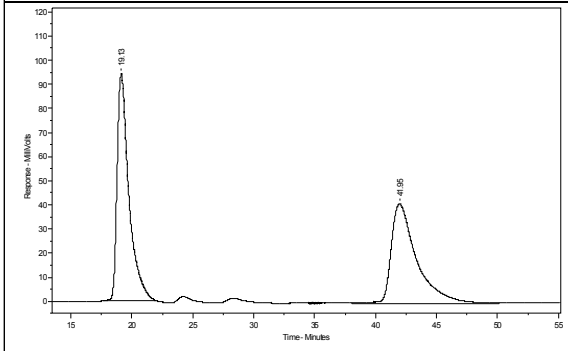	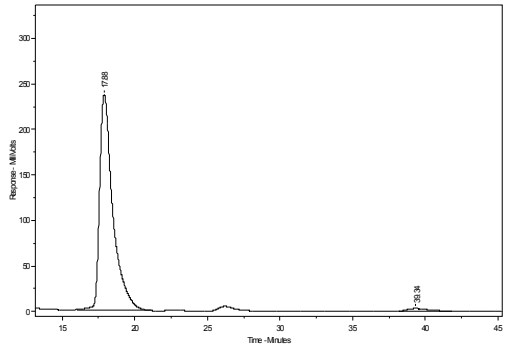

Peak #	Ret. Time	Area	Area %
1	19.1	2641062	50.596
2	41.9	2578827	49.404

Peak #	Ret. Time	Area	Area %
1	17.88	15232200	97.901
2	39.34	326651	2.099

anti-**2.46e:** IR (neat): 3386 (w, br), 3094 (w, br), 3019 (w, br), 2926 (w, br), 2846 (w, br), 1791 (m), 1753 (m), 1591 (m), 1523 (m), 1505 (m), 1338 (m), 1288 (s), 1232 (m), 1095 (m), 741 (m) cm^{-1}. ^1H NMR (400 MHz, $CDCl_3$): δ 7.63 (1H, d, *J* = 2.6 Hz), 7.56-7.52 (3H, m), 7.46 (1H, dd, *J* = 5.9, 1.5 Hz), 7.35 (2 H, ddd, *J* = 9.2, 2.3, 2.3 Hz), 6.17 (1H, br s), 6.08 (1H, dd, *J* = 5.8, 1.8 Hz), 6.00 (1H, t, *J* = 1.8 Hz), 5.86 (1H, d, *J* = 9.2 Hz), 3.99 (3H, s), 3.79 (3H, s). ^{13}C NMR (100 MHz, $CDCl_3$): δ 171.3, 170.1, 152.1, 146.5, 140.1, 139.0, 132.8, 132.5, 129.0, 124.3, 124.0, 118.1, 111.5, 105.2, 84.3, 68.3, 56.5, 54.2. HRMS Calcd for $C_{20}H_{17}N_2O_7BrNa$ [M + Na]: 499.0117; Found: 499.0121. $[\alpha]^{26}_D$ = +67.8 (*c* = 1.00, $CHCl_3$) for a 94% ee sample. The enantiomeric purity of the compound was determined by chiral HPLC analysis (OD, 80:20 hexanes:*i*-PrOH, 1 mL/min, 254 nm): t_R of *anti*-**2.46e**: 21 min (major) and 57 min (minor).

rac-anti-**2.46e**
(***OD***, 80:20 hexanes:*i*-PrOH, 1 ml/min, 254 nm)

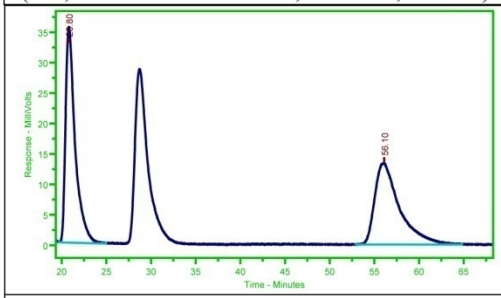

Peak #	Ret. Time	Area	Area %
1	20.8	2641062	50.596
2	56.1	2578827	49.404

peak at 28 min is Rac-syn-

anti-**2.46e**
(***OD***, 80:20 hexanes:*i*-PrOH, 1 ml/min, 254 nm)

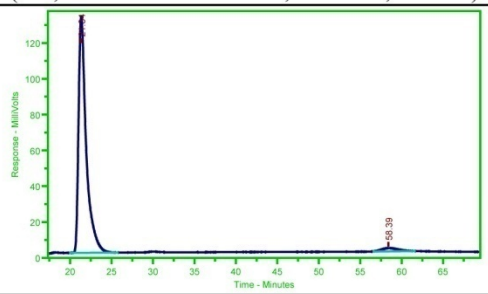

Peak #	Ret. Time	Area	Area %
1	21.34	8461288	96.822
2	58.39	277741	3.178

rac-syn-**2.46e**
(***AD***, 90:10 hexanes:*i*-PrOH, 1 ml/min, 254 nm)

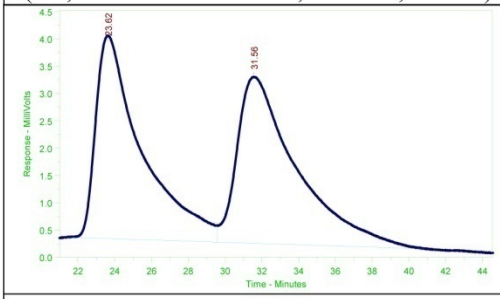

Peak #	Ret. Time	Area	Area %
1	23.62	645454	48.541
2	31.56	684247	51.459

syn-**2.46e**
(***OD***, 80:20 hexanes:*i*-PrOH, 1 ml/min, 254 nm)

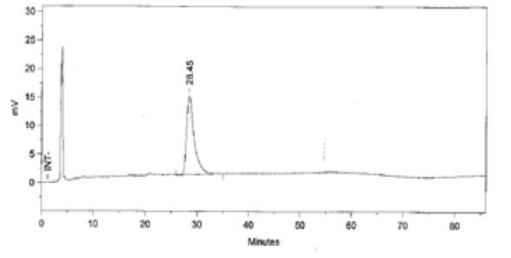

***anti*-2.46f:** IR (neat): 3387 (w, br), 1789 (m), 1758 (s), 1593 (m), 1526 (m), 1295 (s), 1231 (m), 1096 (m), 1028 (m), 746 (m) cm^{-1}. ^1H NMR (400 MHz, $CDCl_3$): δ 7.73 (2H, ddd, *J* = 8.8, 2.2, 2.2 Hz), 7.63 (1H, d, *J* = 2.6 Hz), 7.55 (1H, dd, *J* = 8.8, 2.6 Hz), 7.45 (1H, dd, *J* = 5.8, 1.5 Hz), 7.21 (2H, ddd, *J* = 8.4, 2.2, 2.2 Hz), 6.16 (1H, br s), 6.08 (1H, dd, *J* = 5.9, 2.2 Hz), 6.00 (1H, dd, *J* = 1.8, 1.8 Hz), 5.86 (1H, d, *J* = 8.8 Hz), 3.98 (3H, s), 3.78 (3H, s). ^{13}C NMR (100 MHz, $CDCl_3$): δ 171.3, 170.1, 152.1, 146.5, 140.1, 138.9, 138.7, 133.2, 129.1, 124.3, 118.1, 111.5, 105.2, 95.8, 84.3, 68.4, 56.5, 54.2. HRMS Calcd for $C_{20}H_{18}N_2O_7I$ [M + H]: 525.01587; Found: 525.01710. $[\alpha]^{24}_D$ = +69.9 (*c* = 1.00, $CHCl_3$) for a 94% ee sample. The enantiomeric purity of the compound was determined by chiral HPLC analysis (OD, 80:20 hexanes:*i*-PrOH, 1 mL/min, 254 nm): t_R of *anti*-**2.46f**: 26 min (major) and 89 min (minor); t_R of *syn*-**2.46f**: 33 min and 39 min.

rac-anti-**2.46f**

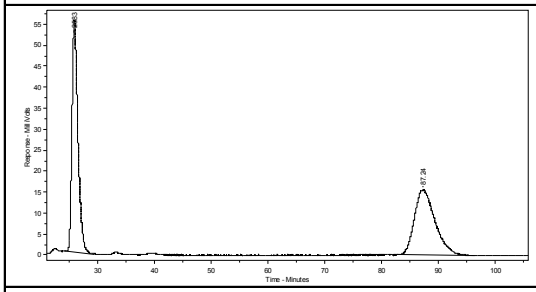

Peak #	Ret. Time	Area	Area %
1	25.83	4071878	50.713
2	87.24	3957386	49.287

anti-**2.46f**

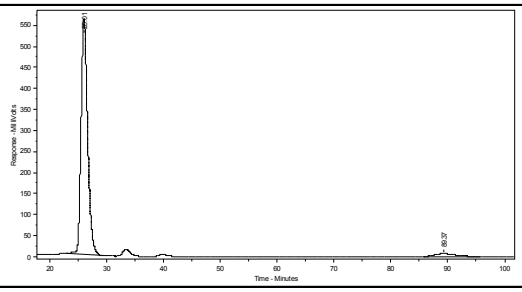

Peak #	Ret. Time	Area	Area %
1	26.01	45087000	96.968
2	89.37	1409877	3.032

rac-syn-**2.46f**

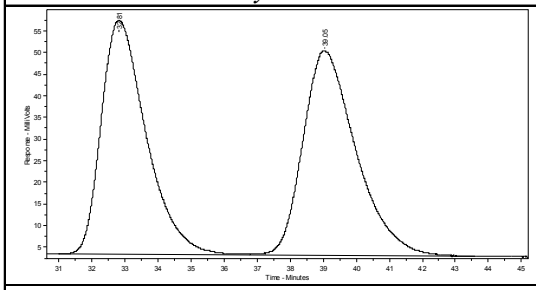

Peak #	Ret. Time	Area	Area %
1	32.81	5117000	49.346
2	39.05	5252693	50.654

syn-**2.46f**

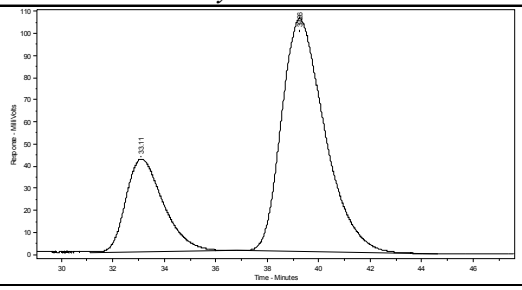

Peak #	Ret. Time	Area	Area %
1	33.11	4254926	25.684
2	39.26	12311430	74.316

anti-**2.46g:** IR (neat): 3387 (w, br), 3099 (w, br), 3019 (w, br), 2961 (w, br), 2870 (w, br), 1788 (m), 1755 (m), 1592 (m), 1526 (m), 1504 (m), 1321 (m), 1292 (s), 1229 (m), 1093 (m), 1026 (m), 817 (m), 797 (m), 744 (s) cm^{-1}. ^1H NMR (400 MHz, $CDCl_3$): δ 7.61 (1H, d, J = 2.2 Hz), 7.54 (1H, dd, J = 8.8, 2.2 Hz), 7.48 (1H, dd, J = 5.9, 1.8 Hz), 7.43-7.33 (4 H, m), 6.15 (1H, br s), 6.11 (1H, t, J = 1.8 Hz), 6.03 (1H, dd, J = 5.9, 2.2 Hz), 5.86 (1H, d, J = 9.2 Hz), 3.97 (3H, s), 3.79 (3H, s), 1.31 (9H, s). ^{13}C NMR (100 MHz, $CDCl_3$): δ 171.7, 170.8, 152.8, 152.5, 146.4, 140.8, 138.6, 130.4, 126.62, 126.58, 124.0, 118.1, 111.4, 105.1, 84.9, 68.4, 56.5, 54.0, 34.9, 31.4. HRMS Calcd for $C_{24}H_{27}N_2O_7$ [M + H]: 455.18183; Found: 455.18032. $[\alpha]^{23}_D$ = +90.6 (c = 0.500, $CHCl_3$) for a 90% ee sample. The enantiomeric purity of the compound was determined by chiral HPLC analysis (OD, 80:20 hexanes:*i*-PrOH, 1 mL/min, 254 nm): t_R of *anti*-**2.46g**: 12 min (major) and 26 min (minor); t_R of *syn*-**2.46g**: 15 min and 17 min.

rac-anti-**2.46g** and *rac-syn*-**2.46g**	*anti*-**2.46g**
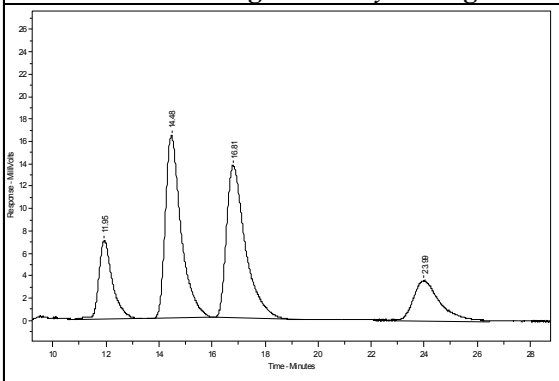	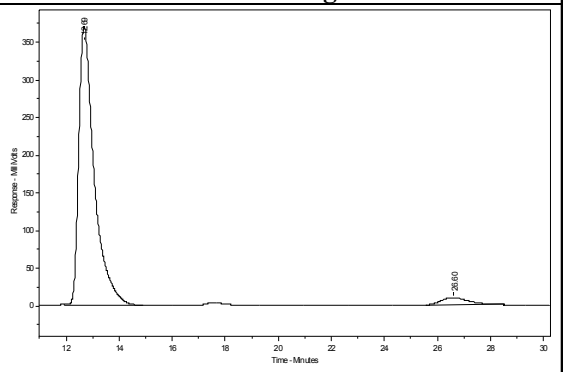

Peak #	Ret. Time	Area	Area %
1	11.95	253446	13.634
2	14.48	674813	36.301
3	16.81	679463	36.551
4	23.99	251214	13.514

Peak #	Ret. Time	Area	Area %
1	12.69	14923210	94.871
2	26.60	806859	5.129

anti-**2.46h:** IR (neat): 3389 (w, br), 3106 (w, br), 2986 (w, br), 2873 (w, br), 1791 (m), 1759 (m), 1589 (m), 1527 (m), 1508 (m), 1325 (s), 1294 (s), 1256 (m), 1237 (m), 1167 (m), 1130 (m), 1099 (m) cm^{-1}. ^1H NMR (400 MHz, $CDCl_3$): δ 7.67-7.63 (5H, m), 7.53 (1H, dd, J = 8.8, 2.4 Hz), 7.46 (1H, dd, J = 5.8, 1.8 Hz), 6.24 (1H, br s), 6.10 (1H, dd, J = 6.0, 2.0 Hz), 6.03 (1H, t, J = 1.8 Hz), 5.82 (1H, d, J = 9.2 Hz), 4.00 (3H, s), 3.80 (3H, s). ^{13}C NMR (100 MHz, $CDCl_3$): δ 171.2, 169.9, 151.9, 146.5, 139.9, 139.1, 137.6, 131.8 (q, J = 33.0 Hz), 128.0, 126.5 (q, J = 3.8 Hz), 125.4 (q, J = 202 Hz), 124.4, 118.1, 111.3, 105.3, 84.2, 68.5, 56.5, 54.3. HRMS Calcd for $C_{21}H_{17}N_2O_7F_3Na$ [M + Na]: 489.0886; Found: 489.0882. $[\alpha]^{25}_D$ = +43.5 (c = 0.630, $CHCl_3$) for a 91% ee sample. The enantiomeric purity of the compound was determined by chiral HPLC analysis (OD, 80:20 hexanes:*i*-PrOH, 1 mL/min, 254 nm): t_R of *anti*-**2.46h**: 15 min (major) and 30 min (minor).

rac-anti-**2.46h**				*anti*-**2.46h**			
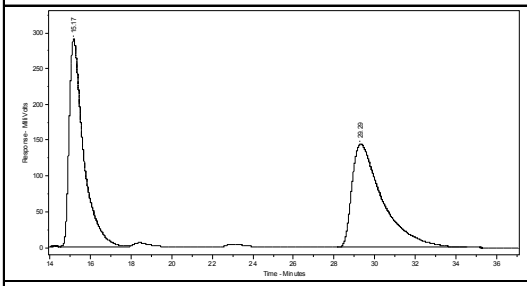				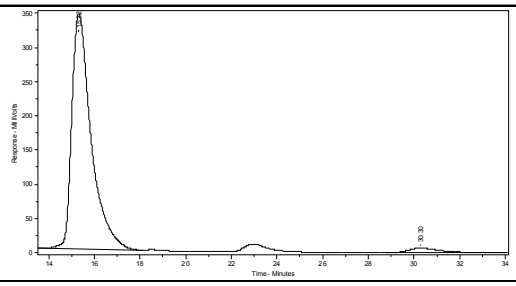			
Peak #	**Ret. Time**	**Area**	**Area %**	**Peak #**	**Ret. Time**	**Area**	**Area %**
1	15.17	14290790	48.836	1	15.32	20258000	96.862
2	29.29	14971950	51.164	2	30.3	656256	3.138

anti-**2.46i:** IR (neat): 3382 (w, br), 3102 (w, br), 2953 (w, br), 1788 (m), 1759 (s), 1587 (s), 1527 (m), 1331 (m), 1301 (s), 1230 (m), 1093 (m) cm^{-1}. ^1H NMR (400 MHz, $CDCl_3$): δ 8.04 (1H, d, *J* = 2.2 Hz), 7.89-7.85 (2H, m), 7.85 (1H, d, *J* = 8.4 Hz), 7.62 (1 H, d, *J* = 2.6 Hz), 7.58-7.54 (3H, m), 7.44 (2H, ddd, *J* = 10.4, 6.0, 2.0 Hz), 6.33 (1H, br s), 6.24 (1H, dd, *J* = 1.8, 1.8 Hz), 6.05 (1H, dd, *J* = 5.6, 2.0 Hz), 5.85 (1H, d, *J* = 8.8 Hz), 4.01 (3H, s), 3.80 (3H, s). ^{13}C NMR (100 MHz, $CDCl_3$): δ 171.6, 170.6, 152.3, 146.5, 140.7, 138.7, 133.5, 133.4, 131.2, 129.7, 128.7, 128.0, 127.7, 127.3, 126.7, 124.1, 124.0, 118.1, 111.5, 105.1, 84.9, 68.8, 56.5, 54.2. HRMS Calcd for $C_{24}H_{20}N_2O_7Na$ [M + Na]: 471.1168; Found: 471.1164. $[\alpha]^{26}_D$ = +114.7 (*c* = 1.00, $CHCl_3$) for a 90% ee sample. The optical purity of the compound was determined by chiral HPLC analysis (OD, 80:20 hexanes:*i*-PrOH, 1 mL/min, 254 nm): t_R of *anti*-**2.46i**: 39 min (major) and 183 min (minor); t_R of *syn*-**2.46i**: 52 min and 64 min.

rac-anti-**2.46i** and *rac-syn*-**2.46i**			
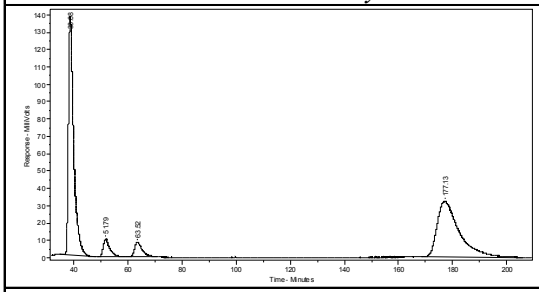			
Peak #	**Ret. Time**	**Area**	**Area %**
1	38.68	18403890	45.821
2	51.79	1812002	4.511
3	63.52	1719289	4.281
4	177.13	18229490	45.387

anti-**2.46i**			
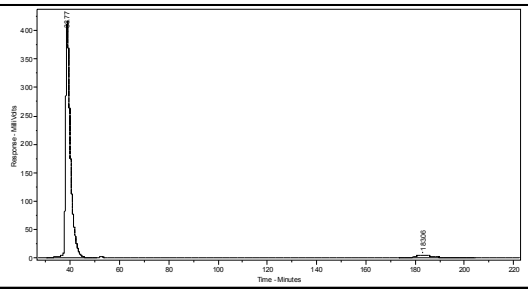			
Peak #	**Ret. Time**	**Area**	**Area %**
1	38.77	56347020	95.269
2	183.06	2798026	4.731

anti-**2.46j:** IR (neat): 3392 (w, br), 3101 (w), 2949 (w), 1793 (m), 1759 (m), 1594 (s), 1527 (m), 1502 (m), 1337 (m), 1294 (s), 1257 (m), 1159 (m), 1105 (m), 1025 (m), 910 (m), 881 (m), 797 (m), 750 (m) cm^{-1}. ^1H NMR (400 MHz, $CDCl_3$): δ 7.63-7.60 (2H, m), 7.58 (1H, dd, J = 6.0, 1.6 Hz), 7.45 (1H, dd, J = 2.0, 0.80 Hz), 6.58 (1H, dd, J = 3.2, 0.40 Hz), 6.46 (1H, dd, J = 3.2, 2.0 Hz), 6.13 (1H, br s), 6.11 (1H, dd, J = 5.6, 2.0 Hz), 5.96 (1H, dd, J = 1.8, 1.8 Hz), 5.89 (1H, d, J = 9.6 Hz), 3.96 (3H, s), 3.85 (3H, s). ^{13}C NMR (100 MHz, $CDCl_3$): δ 171.5, 168.8, 152.2, 146.8, 146.5, 143.7, 140.6, 139.0, 124.0, 118.4, 111.6, 111.0, 109.8, 105.1, 84.2, 65.1, 56.5, 54.4. HRMS Calcd for $C_{18}H_{16}N_2O_8Na$ [M + Na]: 411.0804; Found: 411.0797. $[\alpha]^{24}_D$ = +139.98 (c = 0.230, $CHCl_3$) for an 86% ee sample. The enantiomeric purity of the compound was determined by chiral HPLC analysis (OD, 80:20 hexanes:*i*-PrOH, 1 mL/min, 254 nm): t_R of *anti*-**2.46j**: 17 min (major) and 23 min (minor).

rac-anti-**2.46j**				*anti*-**2.46j**			
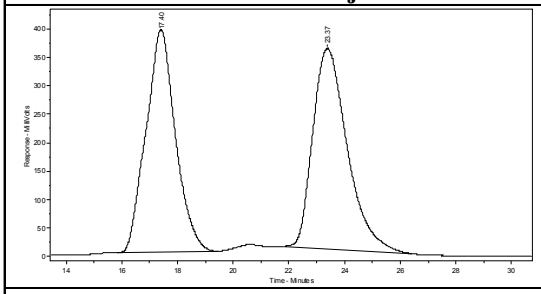				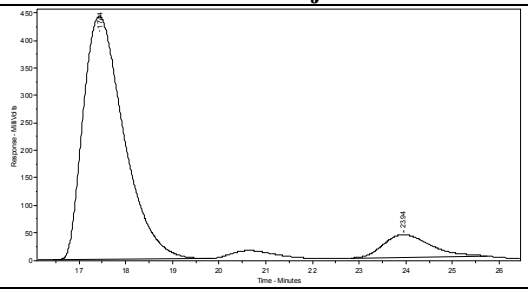			
Peak #	**Ret. Time**	**Area**	**Area %**	**Peak #**	**Ret. Time**	**Area**	**Area %**
1	17.4	28905790	48.901	1	17.44	26744090	90.121
2	23.37	30205150	51.099	2	23.94	2931802	9.879

syn-**2.46j:** IR (neat): 3375 (w, br), 3105 (w), 2957 (w), 2919 (w), 2847 (w), 1792 (m), 1755 (m), 1595 (m), 1531 (m), 1509 (m), 1337 (m), 1299 (s), 1265 (m), 1236 (m), 1159 (m), 1101 (m), 1025 (m), 906 (m), 797 (m), 733 (m) cm^{-1}. ^1H NMR (400 MHz, $CDCl_3$): δ 7.63-7.61 (2H, m), 7.45 (1H, dd, *J* = 6.0, 1.4 Hz), 7.42 (1H, dd, *J* = 2.0, 0.80 Hz), 6.70 (1H, dd, *J* = 3.6, 0.80 Hz), 6.45 (1H, dd, *J* = 3.4, 1.6 Hz), 6.27 (1H, br s), 6.24 (1H, d, *J* = 9.2 Hz), 6.19 (1H, dd, *J* = 5.8, 2.2 Hz), 5.87 (1H, dd, *J* = 1.4, 1.4 Hz), 3.98 (3H, s), 3.78 (3H, s). ^{13}C NMR (100 MHz, $CDCl_3$): δ 171.3, 168.4, 152.2, 147.1, 146.6, 143.8, 140.7, 139.3, 123.8, 118.6, 112.0, 111.4, 110.7, 105.1, 84.1, 65.9, 56.4, 54.2. HRMS Calcd for $C_{18}H_{16}N_2O_8Na$ [M + Na]: 411.0804; Found: 411.0793. $[\alpha]^{24}_D$ = +3.49 (*c* = 0.230, $CHCl_3$) for a 58% ee sample. The enantiomeric purity of the compound was determined by chiral HPLC analysis (OD, 80:20 hexanes:*i*-PrOH, 1 mL/min, 254 nm): t_R of *syn*-**2.46j**: 20 min and 25 min.

rac-syn-**2.46j**				*syn*-**2.46j**			
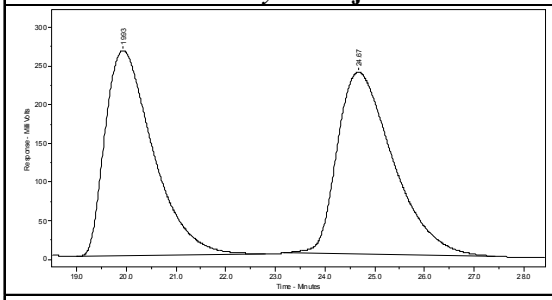				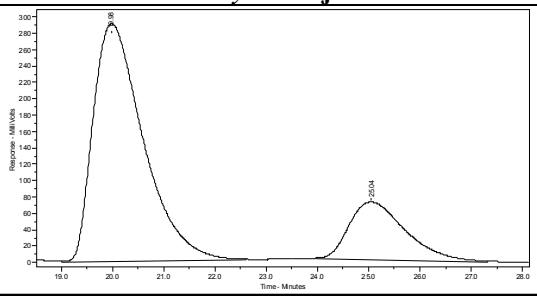			
Peak #	**Ret. Time**	**Area**	**Area %**	**Peak #**	**Ret. Time**	**Area**	**Area %**
1	19.93	17917710	49.454	1	19.98	19664200	78.665
2	24.67	18313550	50.546	2	25.04	5333194	21.335

anti-**2.46k:** IR (neat): 3384(w, br), 3104 (w, br), 2926 (w), 2852 (w), 1789 (m), 1732 (s), 1592 (s), 1525 (m), 1505 (m), 1323 (m), 1292 (s), 1229 (s), 1155 (m), 1095 (m), 1043 (m), 1026 (m), 890 (m), 798 (m), 745 (m) cm^{-1}. ^1H NMR (400 MHz, $CDCl_3$, major isomer): δ 7.63 (1H, d, *J* = 2.2 Hz), 7.58 (1H, m), 7.54 (1H, dd, *J* = 2.9, 1.5 Hz), 7.44 (1 H, dd, *J* = 5.9, 1.5 Hz), 7.35 (1H, dd, *J* = 5.1, 2.9 Hz), 7.04 (1H, dd, *J* = 5.1, 1.5 Hz), 6.13 (1H, dd, *J* = 5.8, 2.2 Hz), 6.03 (1H, s), 5.95 (1H, d, *J* = 8.8 Hz), 5.88 (1H, t, *J* = 2.2 Hz), 3.97 (3H, s), 3.80 (3H, s). ^{13}C NMR (100 MHz, $CDCl_3$): δ 171.4, 170.2, 152.2, 146.3, 140.6, 138.9, 134.6, 127.4, 126.8, 124.8, 124.0, 118.1, 111.0, 105.1, 85.0, 66.4, 56.4, 54.0. HRMS Calcd for $C_{18}H_{17}N_2O_7S$ [M + H]: 405.07565; Found: 405.07530. $[\alpha]^{23}_D$ = +107.9 (*c* = 1.00, $CHCl_3$) for a 92% ee sample. The enantiomeric purity of the compound was determined by chiral HPLC analysis (OD, 80:20 hexanes:*i*-PrOH, 1 mL/min, 254 nm): t_R of *anti*-**2.46k**: 18 min (major) and 29 min (minor).

rac-anti-**2.46k** and *rac-syn*-**2.46k**	*anti*-**2.46k**
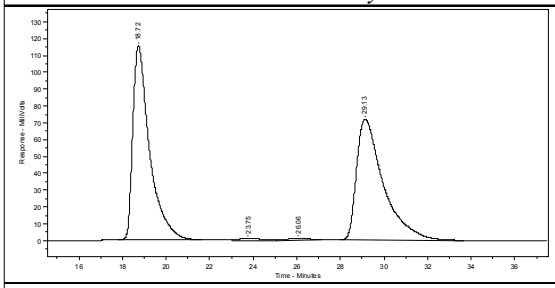	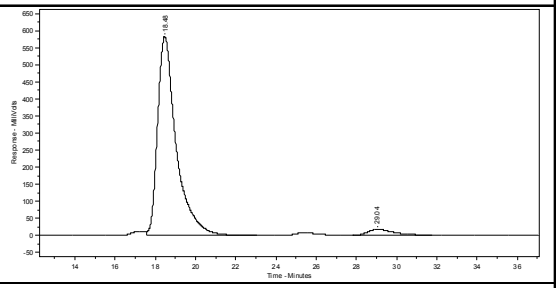

Peak #	Ret. Time	Area	Area %
1	18.72	6209680	49.379
2	23.75	99198	0.789
3	26.06	94179	0.749
4	29.13	6172575	49.084

Peak #	Ret. Time	Area	Area %
1	18.48	37587020	96.053
2	29.04	1544582	3.947

anti-**2.51a:** IR (neat): 3445 (w), 3388 (m), 3096 (w), 3067 (w), 2953 (m), 1793 (s), 1746 (s), 1599 (m), 1535 (s), 1506 (s), 1480 (m), 1332 (s), 1291 (s), 1261 (m), 1151 (m), 1101 (m), 1029 (m) cm^{-1}. ^1H NMR (400 MHz, $CDCl_3$): δ 7.65 (1H, d, *J* = 2.2 Hz), 7.52 (1H, dd, *J* = 8.8, 2.6 Hz), 7.49-7.46 (2H, m), 7.41-7.38 (3H, m), 6.13 (1H, br s), 5.97 (1H, d, *J* = 9.2 Hz), 5.40 (1H, t, *J* = 7.2 Hz), 4.00 (3H, s), 3.76 (3H, s), 2.44-2.05 (4H, m). ^{13}C NMR (100 MHz, $CDCl_3$): δ 176.0, 171.1, 146.5, 141.0, 138.7, 137.6, 133.3, 129.4, 127.6, 118.1, 111.8, 105.0, 82.4, 68.8, 56.4, 53.7, 28.0, 23.8. HRMS Calcd for $C_{20}H_{21}N_2O_7$ [M + H]: 401.13488; Found: 401.13493. $[\alpha]^{25}_D$ = -114.72 (*c* = 1.00, $CHCl_3$) for a >98% ee sample

anti-**2.53a:** IR (neat): 3396 (w), 3320 (w), 2953 (w), 2923 (w), 1780 (s), 1729 (s), 1607 (w), 1447 (w), 1332 (w), 1244 (s), 1181 (s), 1151 (s), 1033 (m), 699 (m) cm^{-1}. ^1H NMR (400 MHz, $CDCl_3$): δ 7.57-7.56 (2H, m), 7.40-7.32 (3H, m), 5.37 (1H, t, *J* = 7.7 Hz), 3.77 (3H, s), 2.56-2.39 (2H, m), 2.19-2.09 (1H, m), 1.99 (2H, br s), 1.73-1.65 (1H, m). ^{13}C NMR (100 MHz, $CDCl_3$): δ 177.2, 174.4, 137.1, 129.1, 128.8, 125.7, 83.3, 65.5, 53.3, 29.9, 22.0. HRMS Calcd for $C_{13}H_{16}NO_4$ [M + H]: 250.10793; Found: 250.10873. $[\alpha]^{25}_D$ = +13.26 (*c* = 1.00, $CHCl_3$) for a 77% ee sample

Experimental procedure for $SnCl_2$-mediated reduction of anti-2.46a followed by $PhI(OAc)_2$-mediated deprotection: A 50 mL round bottom flask was charged with catalytic AVM product *anti*-**2.46a** (200 mg, 0.502 mmol), $SnCl_2$ (476 mg, 2.51 mmol), and ethanol (10.0 mL). The round bottom flask was fitted with a reflux condensor, and the mixture was allowed to warm to 65 °C with stirring. The resulting homogeneous solution was kept at 65 °C for 15 h before careful addition of a saturated solution of $NaHCO_3$. The aqueous layer was washed with EtOAc (3 x 50 mL). The organic layers were combined, dried over $MgSO_4$, and the volatiles were removed *in vacuo*. The residue was redissolved in EtOAc and the solution was passed through a plug of SiO_2 (EtOAc). The volatiles were again removed *in vacuo*, and the resulting brown oil residue was analyzed by ^{1}H NMR spectroscopy. The residue was dissolved in MeCN (5.00 mL). The resulting homogeneous solution was allowed to cool to 0 °C with stirring. $PhI(OAc)_2$ (322 mg, 1.00 mmol) was added as a solid, and the homogeneous mixture was kept at 0 °C for 30 min before addition of 1M H_2SO_4 (10.0 equiv, 5.00 mL). The aqueous layer was washed with dichloromethane (3 x 5 mL). The organic layers were combined and set aside. The aqueous layer was basified (pH = 10) by dropwise addition of a saturated solution of Na_2CO_3, and was subsequently washed with dichloromethane (6 x 5 mL). The organic layers were combined, dried over $MgSO_4$, and the volatiles were removed *in vacuo*. The dark brown oil was purified by silica gel chromatography (2:1 petroleum ether:EtOAc) to deliver *anti*-**2.49a** as an off-white oil (100 mg, 0.404 mmol, 81% yield over two steps). IR (neat): 3384 (w), 3321 (w), 2953 (w), 2924 (w), 1784 (m), 1759 (s),, 1734 (m), 1601 (m), 1489 (m), 145 (s), 1434 (m), 1244 (m), 1144 (m), 1096 (m), 1050 (m), 1024 (m), 890 (m), 834 (m), 704 (m) cm^{-1}. ^{1}H NMR (400 MHz, $CDCl_3$): δ 7.61-7.59 (2H, m), 7.44-7.36 (3H, m), 6.97 (1H, dd, J = 5.8, 1.4 Hz), 6.14 (1H, dd, J = 6.0, 2.0 Hz), 5.89 (1H, dd, J = 2.0, 1.6 Hz), 3.82 (3H, s), 1.89 (2H, br s). ^{13}C NMR (100 MHz, $CDCl_3$): δ 173.2, 172.8, 153.4, 137.1, 129.3, 129.2, 125.7, 123.5 86.7, 65.2, 53.6. HRMS Calcd for $C_{13}H_{14}NO_4$ [M + H]: 248.09228; Found: 248.09293. $[\alpha]^{26}_D$ = +94.45 (*c* = 0.733, $CDCl_3$) for a >98% ee sample.

Experimental procedure for $SnCl_2$-mediated reduction of anti-2.46a: A 100 mL round bottom flask was charged with *anti*-**2.46a** (398 mg, 1.00 mmol), $SnCl_2$ (1.14 g, 6.00 mmol), and ethanol (20.0 mL). The round bottom flask was fitted with a reflux condensor, and the mixture was allowed to warm to 65 °C with stirring. The resulting homogeneous solution was kept at 65 ^oC for 15 h before careful addition of a saturated solution of $NaHCO_3$. The aqueous layer was washed with EtOAc (3 x 100 mL). The organic layers were combined, dried over $MgSO_4$, and the volatiles were removed *in vacuo*. The dark brown oil residue was purified by silica gel chromatography (1:1 petroleum ether:EtOAc) to afford *anti*-**2.54a** as an off-white solid (285 mg, 0.771 mmol, 77% yield).

anti-**2.54a:** IR (neat): 3445 (w), 3356 (w), 2951 (w), 1785 (w), 1735 (s), 1616 (m), 1592 (m), 1512 (s), 1458 (m), 1429 (m), 1283 (m), 1238 (s), 1199 (s), 1166 (m), 1095 (m), 1061 (m), 1031 (m), 1004 (m), 948 (m), 906 (m), 836 (m), 826 (m), 795 (m), 725 (s), 696 (s), 612 (m) cm^{-1}. ^1H NMR (400 MHz, $CDCl_3$): δ 7.50 (2H, dd, *J* = 8.0, 1.5 Hz), 7.46 (1H, dd, *J* = 5.8, 1.5 Hz), 7.36-7.29 (3H, m), 6.19 (1H, d, *J* = 2.2 Hz), 5.98 (1H, d, *J* = 4.8 Hz), 5.96 (1H, d, *J* = 1.8 Hz), 5.90 (1H, dd, *J* = 8.4, 2.6 Hz), 5.83 (1H, dd, *J* = 5.9, 2.2 Hz), 5.10 (1H, br s), 3.76 (3H, s), 3.69 (3H, s), 3.37 (2H, br s). ^{13}C NMR (100 MHz, $CDCl_3$): δ. 172.6, 172.2, 154.1, 150.1, 140.2, 136.5, 128.9, 128.8, 127.6, 126.2, 122.3, 117.4, 106.8, 99.8, 84.5, 69.9, 55.8, 53.4. HRMS Calcd for $C_{20}H_{21}N_2O_5$ [M + H]: 369.14505; Found: 369.14474. $[\alpha]^{25}_D$ = +76.25 (*c* = 1.00, $CHCl_3$) for a >98% ee sample.

anti-**2.54d:** IR (neat): 3444 (w, br), 3363 (w, br), 3098 (w, br), 3010 (w, br), 2850 (w, br), 2846 (w, br), 1763 (m), 1737 (m), 1515 (m), 1523 (m), 1463 (m), 1250 (s), 1201 (m), 1090 (m), 1026 (m), 947(m), 892(m), 821 (m) cm^{-1}. ^1H NMR (400 MHz, $CDCl_3$): δ 7.54-7.50 (2H, m), 7.45 (1H, dd, *J* = 5.9, 1.8 Hz), 7.35-7.32 (2 H, m), 6.23 (1H, d, *J* = 2.2 Hz), 6.01-5.94 (3H, m), 5.90 (1H, t, *J* = 1.8 Hz), 5.10 (1H, br s), 3.82 (3H, s), 3.72 (3H, s), 3.38 (2H, br s). ^{13}C NMR (100 MHz, $CDCl_3$): δ 172.2, 171.5, 153.6, 150.0, 140.1,

135.0, 134.6, 129.3, 128.9, 125.6, 122.7, 117.5, 106.8, 99.6, 84.2, 69.3, 55.7, 53.4. HRMS Calcd for $C_{20}H_{20}N_2O_5Cl$ [M + H]: 403.10607; Found: 403.10422. $[\alpha]^{23}_D$ = +41.8 (c = 0.500, $CHCl_3$) for a >98% ee sample. The enantiomeric purity of the compound was determined by chiral HPLC analysis (OJ, 70:30 hexanes:*i*-PrOH, 1 mL/min, 254 nm): t_R of *anti*-**2.53d**: 40.0 min (major) and 79.9 min (minor).

rac-anti-**2.54d**				*anti*-**2.54d**			
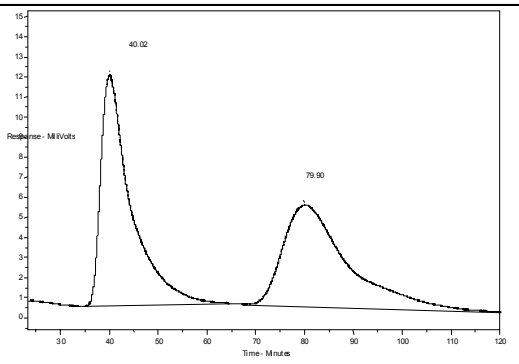				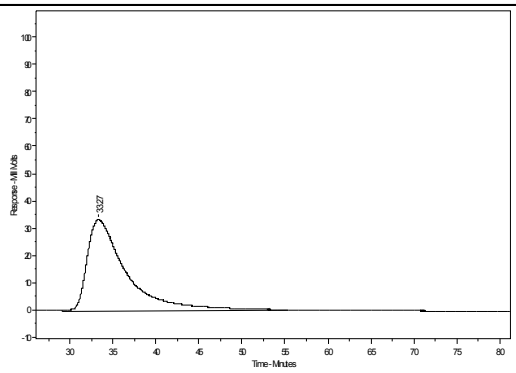			
Peak #	**Ret. Time**	**Area**	**Area %**	**Peak #**	**Ret. Time**	**Area**	**Area %**
1	40.02	4940318	51.877	1	40.06	12910630	100.000
2	79.90	4582752	48.123				

Experimental procedure for PhI(OAc)$_2$ mediated deprotection of *anti*-***2.53a:*** A 13x100 mm test tube was charged with *anti*-**2.54a** (36.8 mg, 0.100 mmol) and acetonitrile (1.00 mL). The resulting homogeneous solution was allowed to cool to 0 °C with stirring. $PhI(OAc)_2$ (64.4 mg, 0.200 mmol) was added as a solid, and the resulting homogeneous solution was kept at 0 °C for 30 min before addition of 1M H_2SO_4 (10.0 equiv, 1.00 mL). The aqueous layer was washed with dichloromethane (3 x 2 mL). The organic layers were combined and set aside. The aqueous layer was basified (pH = 10) by dropwise addition of a saturated solution of Na_2CO_3, and was subsequently washed with dichloromethane (6 x 2 mL). The organic layers were combined, dried over $MgSO_4$, and the volatiles were removed *in vacuo*. The resulting brown oil residue was purified by silica gel chromatography (2:1 petroleum ether:EtOAc) to furnish *anti*-**2.49a** as an off-white oil (21.0 mg, 0.0849 mmol, 85% yield).

Experimental procedure for synthesis of Ag-based complex 2.57: A 50 mL round bottom flask was charged with **2.29** (203 mg, 0.400 mmol), AgOAc (66.8 mg, 0.400 mmol), and THF (5.0 mL). The mixture was allowed to stir at 25 °C for 5 min, and was then filtered through a pad of Celite® into a vial. Petroleum ether was added dropwise to the resulting homogeneous solution until the solution became slightly cloudy. At this point, THF was added dropwise until the solution was again clear, and the vial was sealed and stored in the dark for 12 hours. The resulting colorless crystals were isolated through filtration (193 mg, 0.325 mmol, 81% yield). mp = 128–132 °C. IR (neat): 3249 (w), 3057 (w), 2954 (m), 2865 (w), 1687 (m), 1627 (w), 1545 (m), 1508 (s), 1479 (m), 1460 (m), 1436 (m), 1409 (m), 1292 (m), 1236 (s), 1160 (s), 1097 (m), 1068 (m), 1031 (m), 826 (s), 798 (m), 756 (s) 690 (s), 505 (s) cm^{-1}. ^{1}H NMR (400 MHz, $CDCl_3$): δ 10.03 (1H, br s), 9.12 (1H, br s), 8.20 (1H, d, *J* = 6.0 Hz), 7.59-7.47 (5H, m), 7.42-7.20 (7H, m), 7.14 (2H, t, *J* = 7.6 Hz), 6.89 (1H, t, *J* = 7.6 Hz), 6.79 (2H, ddd, *J* = 9.2, 3.2, 2.2 Hz), 3.79 (1H, br s), 3.69 (3H, s), 2.08 (1.5H, s, *AgOAc*), 0.73 (9H, s). ^{13}C NMR (100 MHz, $CDCl_3$): δ 187.7, 178.0, 167.9, 160.3, 160.2, 155.7, 138.8, 138.7, 135.0, 134.8, 134.3, 134.1, 133.3, 132.8, 132.5, 132.2, 131.0, 130.7, 130.5, 130.4, 130.3, 129.6, 129.3, 129.2, 129.16, 129.1, 120.7, 113.4, 82.5, 54.7, 34.9, 26.3. $[\alpha]^{23}_{D} = -54.26$ (*c* = 1.00, $CHCl_3$).

Experimental procedure for synthesis of powder form of Ag-2.29 complex: A 50 mL round bottom flask was charged with **2.29** (200 mg, 0.393 mmol), AgOAc (65.6 mg, 0.393 mmol), and THF (5.0 mL). The mixture was allowed to stir at 25 °C for 5 min, and was subsequently filtered through a pad of Celite®. Volatiles were removed *in vacuo* to give a white powder (258.5 mg, 0.277 mmol, 71% yield). mp = 148-153 °C. IR (neat): 3119 (w), 2951 (w), 2833 (w), 1648 (w), 1545 (m), 1509 (s), 1478 (m), 1462 (m), 1435 (m), 1400 (m), 1362 (m), 1234 (s), 1163 (m), 1095 (m), 1032 (m), 828 (m), 744 (m), 693 (s), 658 (s), 484 (s) cm^{-1}. ^{1}H NMR (400 MHz, $CDCl_3$): δ 10.14 (1H, br s), 9.17 (1H, br s), 8.18 (1H, d, *J* = 6.4 Hz), 7.57-7.55 (3H, m), 7.50 (2H, dd, *J* = 7.4, 3.6 Hz), 7,41-7.27 (7H, m), 7.19 (2H, t, *J* = 6.6 Hz), 6.86 (1H, t, *J* = 8.2 Hz), 6.72 (2H, d, *J* = 8.8 Hz), 3.93 (1H, br s), 3.69 (3H, s), 2.03 (2H, s, *AgOAc*), 0.72 (9H, s). ^{13}C NMR (100 MHz, $CDCl_3$):

δ 178.0, 168.0, 160.3, 160.1, 155.7, 138.7, 138.67, 135.1, 134.9, 134.4, 134.2, 133.3, 132.9, 132.4, 132.45, 132.2, 131.8, 130.9, 130.8, 130.6, 130.5, 129.8, 129.4, 129.3, 129.15, 120.8, 113.4, 82.3, 54.7, 34.9, 26.4, 23.0. $[\alpha]^{23}_{D} = -69.25$ (*c* =1.00, $CHCl_3$).

Characterization data for phosphine 2.37: IR (neat): 3262 (w, br), 3052 (w), 2952 (w, br), 2838 (w, br), 1736 (m), 1675 (s), 1592 (m), 1557 (s), 1510 (m), 1462 (m), 1435 (m), 1338 (m), 1264 (s), 1242 (s), 1169 (m), 1058 (m), 828 (m), 784 (m), 745 (m), 697 (m) cm^{-1}. ^1H NMR (400 MHz, $CDCl_3$): δ 9.25 (1H, s br), 8.39 (1H, d, *J* = 2.8 Hz), 7.62-7.58 (2H, m), 7.38-7.18 (11H, m), 6.87-6.83 (2H, m), 6.36 (1H, d, *J* = 4.4 Hz), 3.98 (3H, s), 3.78 (3H, s), 3.52 (1H, d, *J* = 1.6 Hz), 3.47 (3H, s). ^{13}C NMR (100 MHz, $CDCl_3$): δ 169.5, 161.22, 161.17, 156.2, 150.5, 149.3, 140.1, 138.5, 138.4, 137.1, 137.0, 134.6, 134.4, 133.1, 133.0, 132.2, 132.1, 131.2, 129.2, 129.1, 128.83, 128.76, 128.65, 128.61, 128.5, 121.6, 117.4, 114.3, 114.2, 114.1, 85.5, 56.2, 55.6, 55.5, 35.5, 27.1. HRMS Calcd for $C_{34}H_{38}N_2O_4P$ [M + H]: 569.25692; Found: 569.25454. $[\alpha]^{23}_{D} = +70.1$ (*c* = 1.00, $CHCl_3$) for a >98% ee sample.

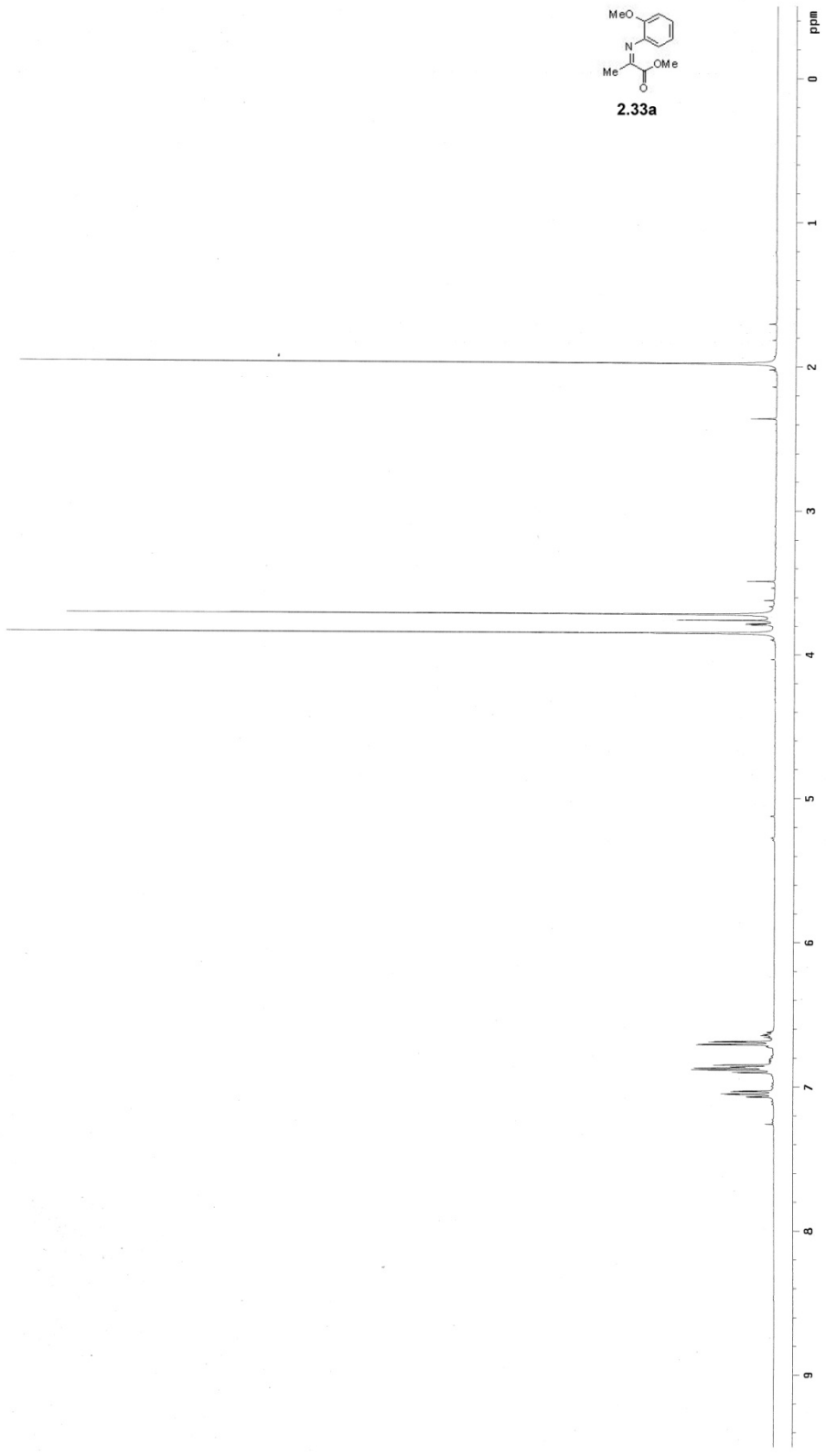
MeO
N
Me
OMe
O
2.33a
ppm
0
1
2
3
4
5
6
7
8
9

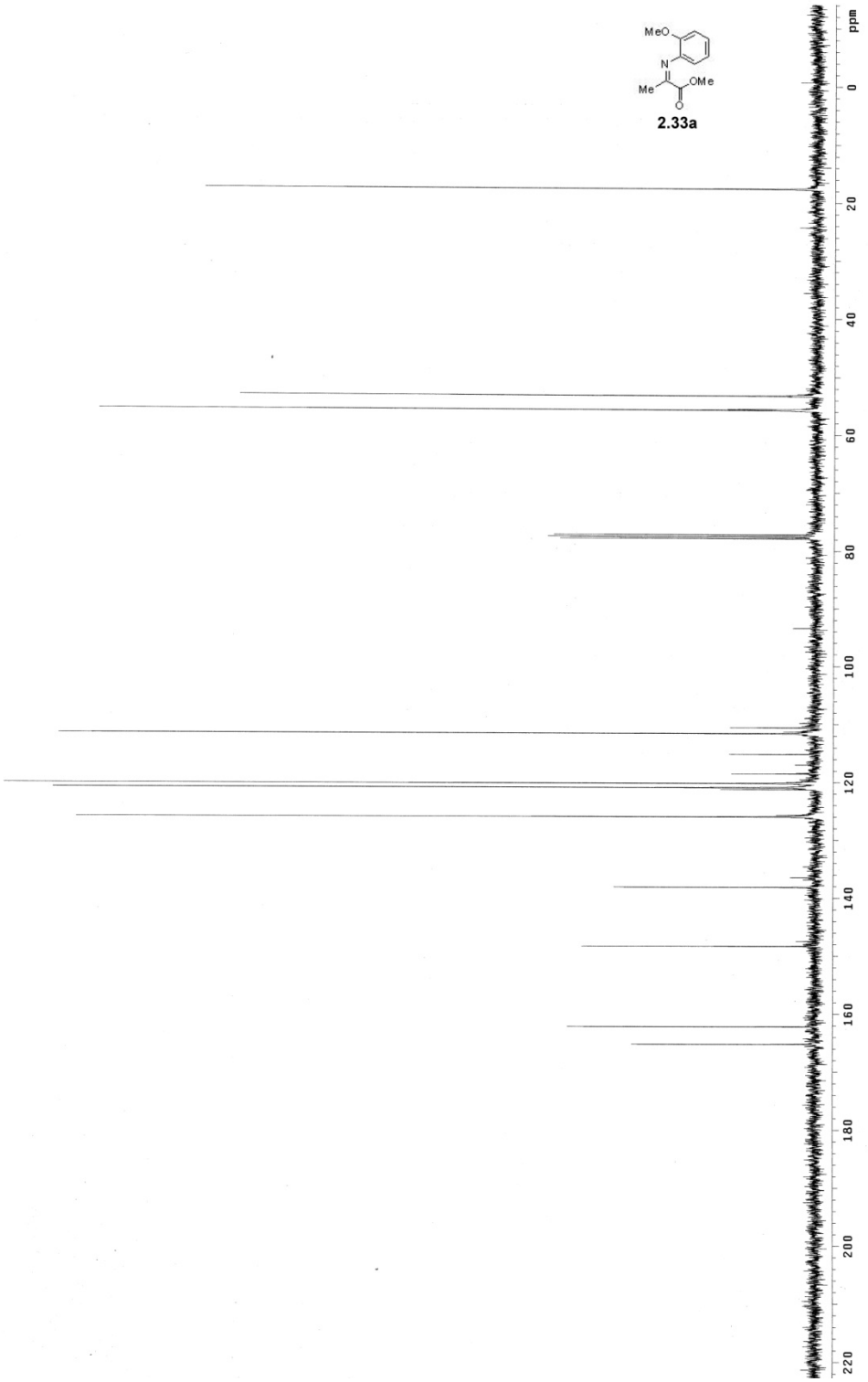
MeO
N
Me
OMe
O
2.33a
ppm
0
20
40
60
80
100
120
140
160
180
200
220


MeO
HN
MeO2C
Me
O
O
syn-2.36a
ppm
0
1
2
3
4
5
6
7
8
9

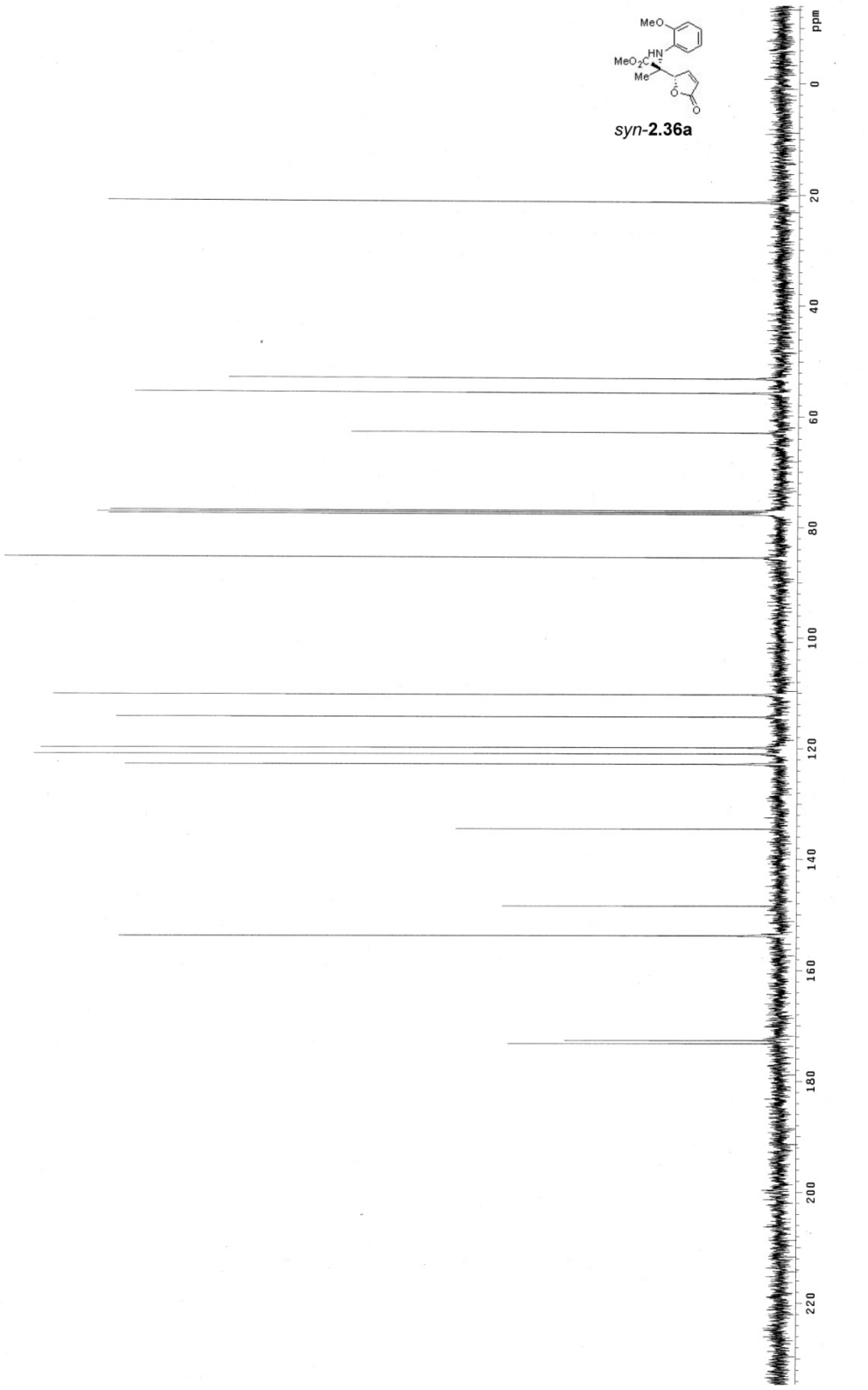
MeO
HN
MeO2C
Me
O
O
syn-2.36a
ppm
0
20
40
60
80
100
120
140
160
180
200
220


MeO
HN
MeO2C
Me
Me
O
O
syn-2.40a
ppm
0
1
2
3
4
5
6
7
8
9

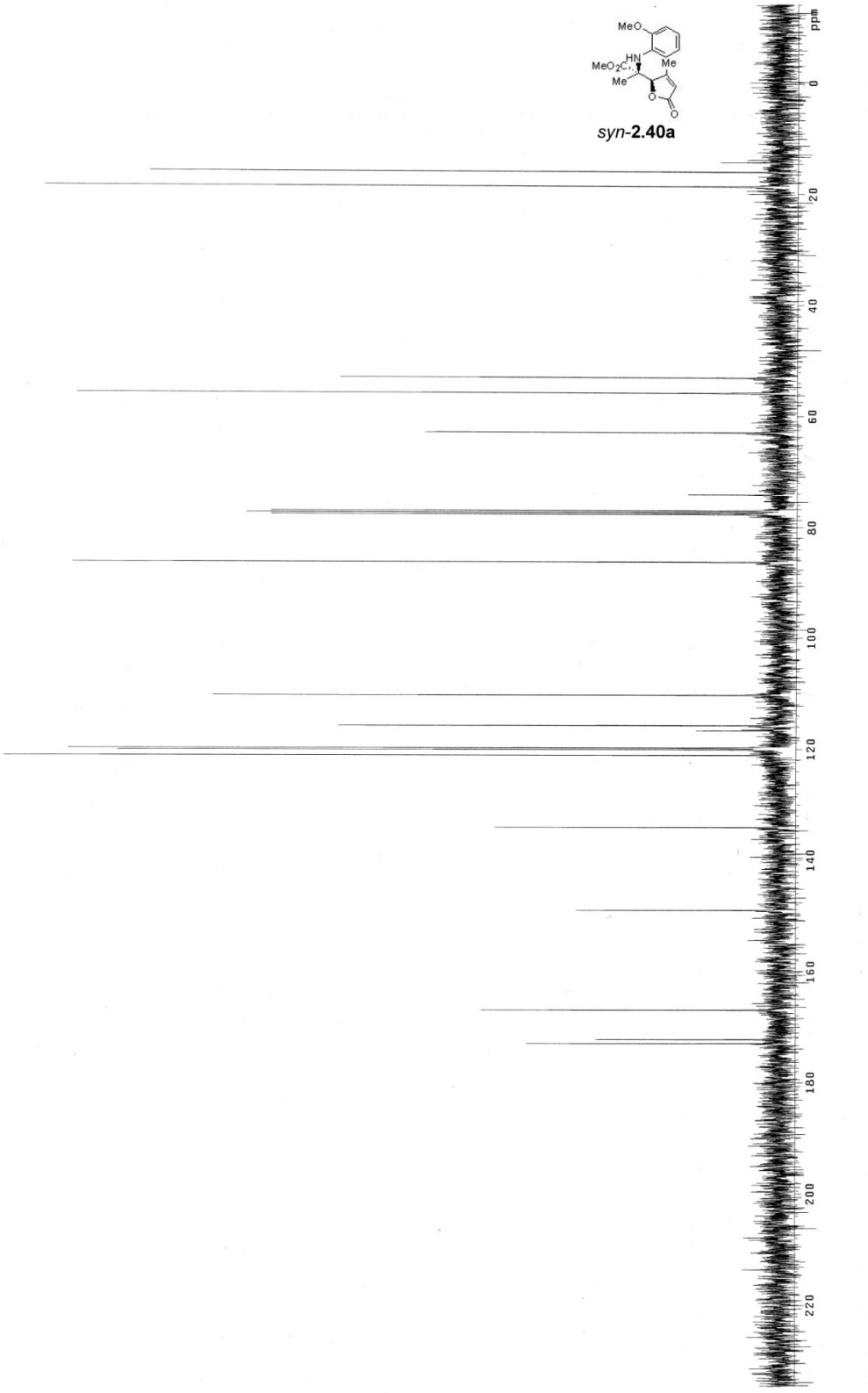
MeO
HN
Me
MeO2C
Me
O
O
syn-2.40a
ppm
0
20
40
60
80
100
120
140
160
180
200
220

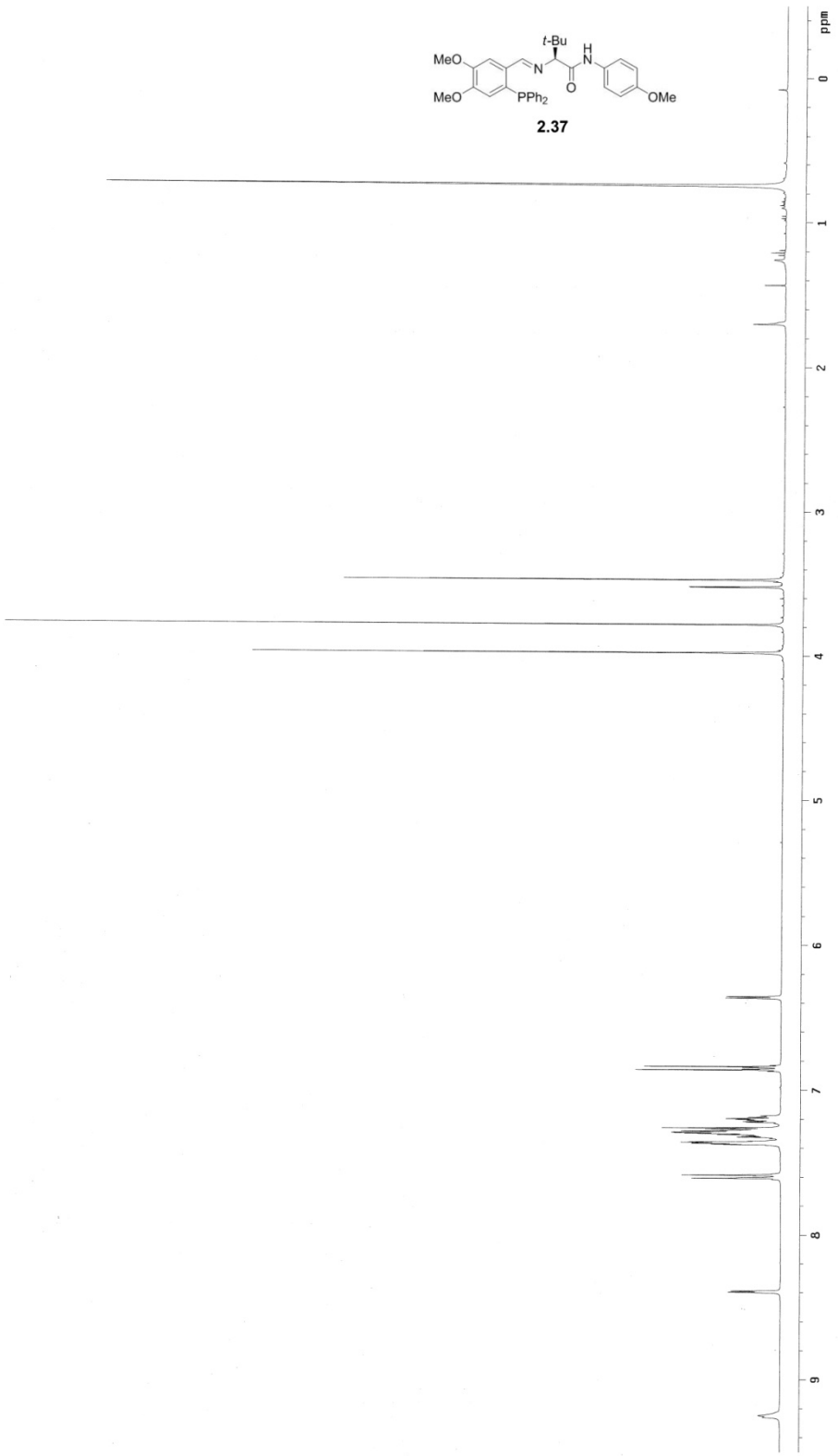
t-Bu
MeO
MeO
PPh2
OMe
2.37
ppm

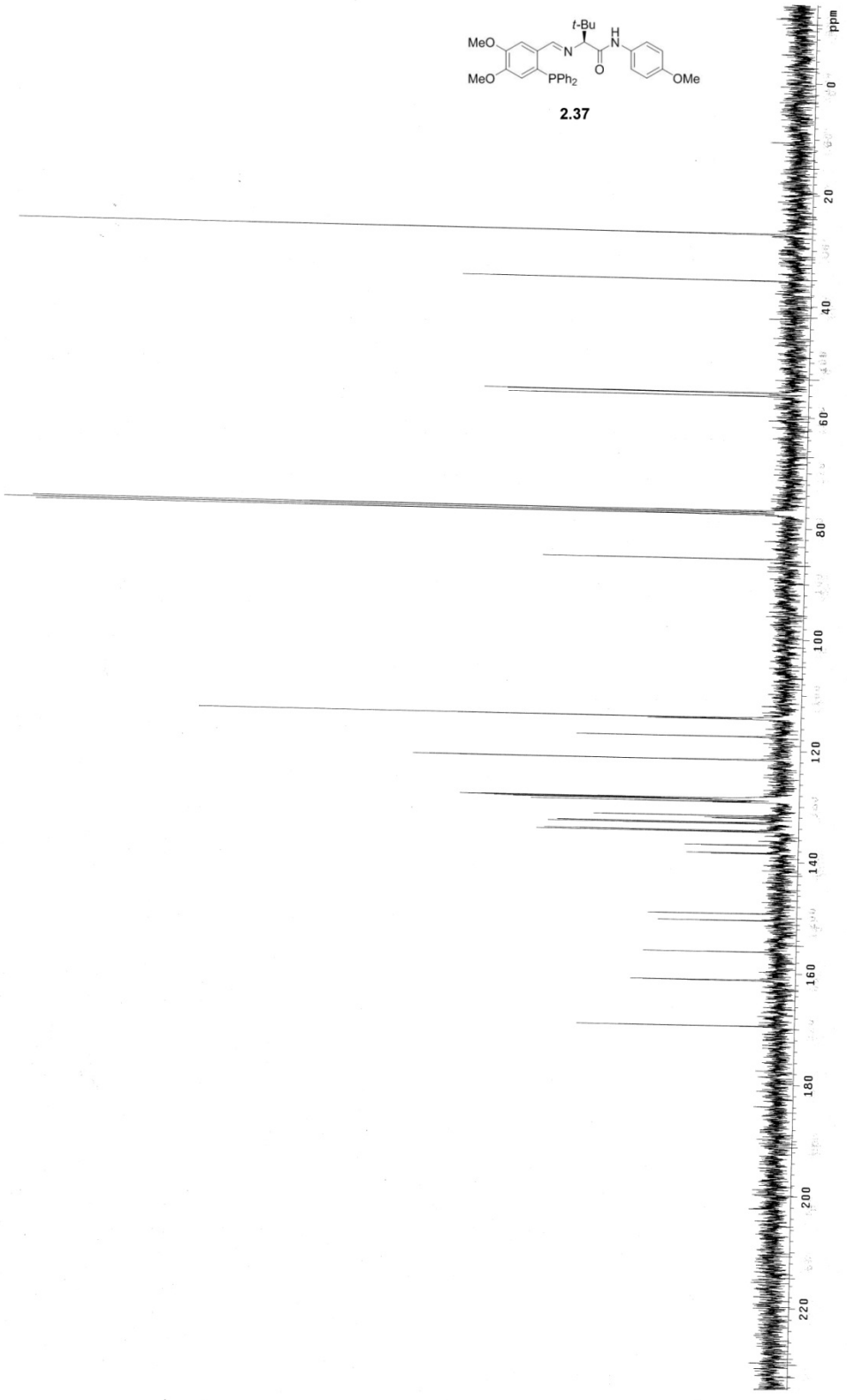
t-Bu
MeO
MeO
N
H
N
O
PPh2
OMe
2.37
ppm
0
20
40
60
80
100
120
140
160
180
200
220

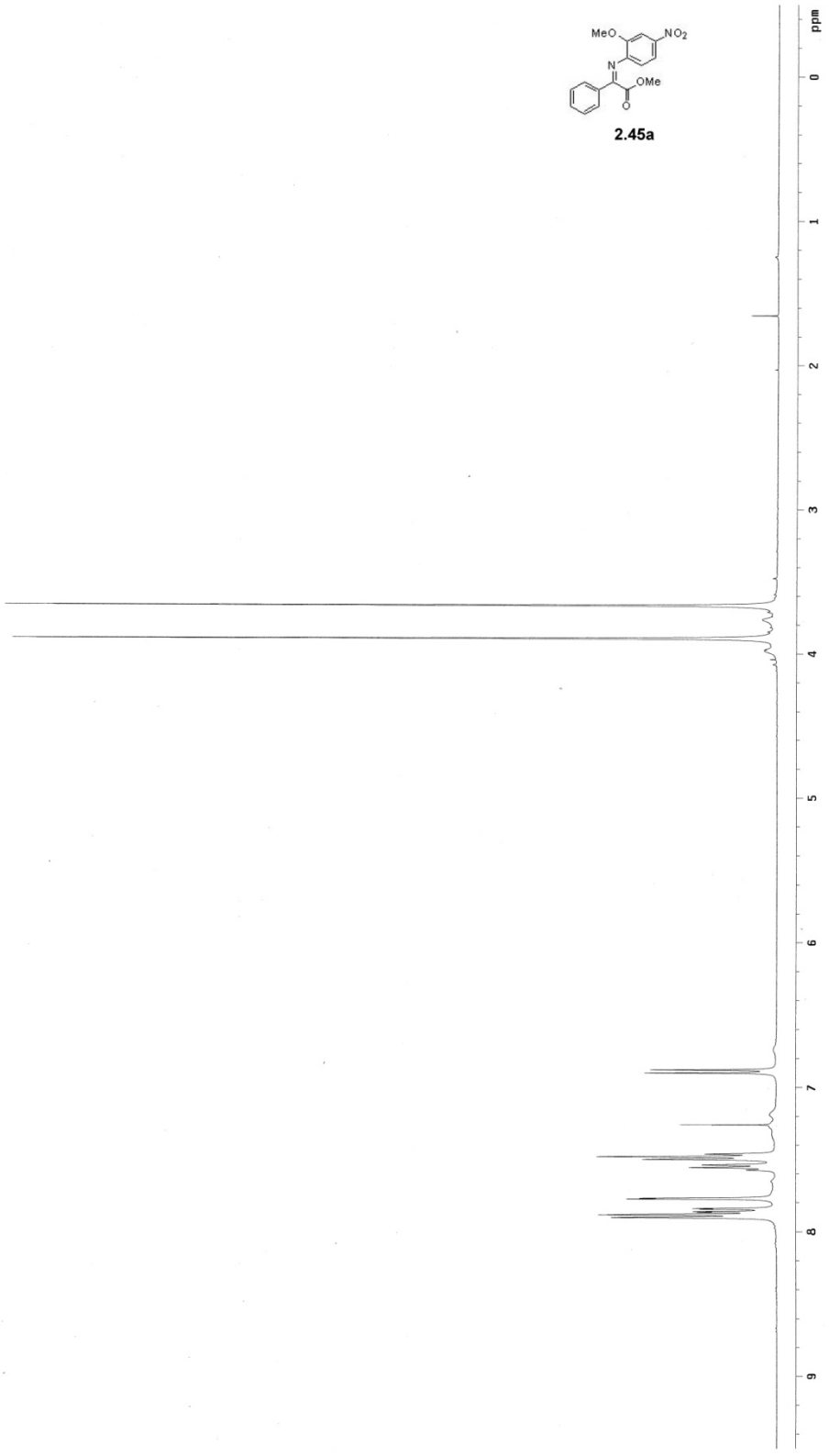
MeO
NO2
N
OMe
O
2.45a
ppm
0
1
2
3
4
5
6
7
8
9

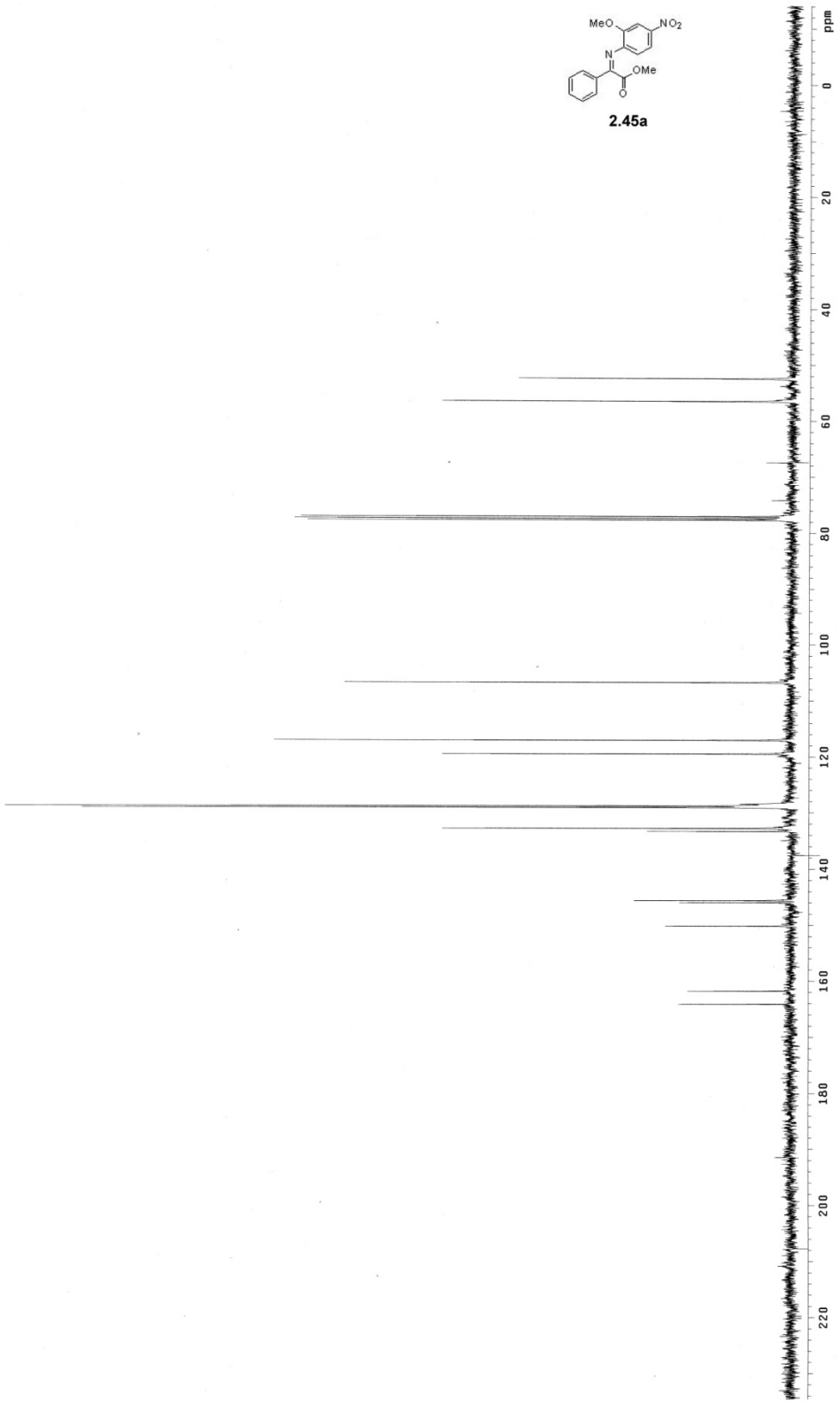
MeO
NO2
N
OMe
O
2.45a
ppm
0
20
40
60
80
100
120
140
160
180
200
220

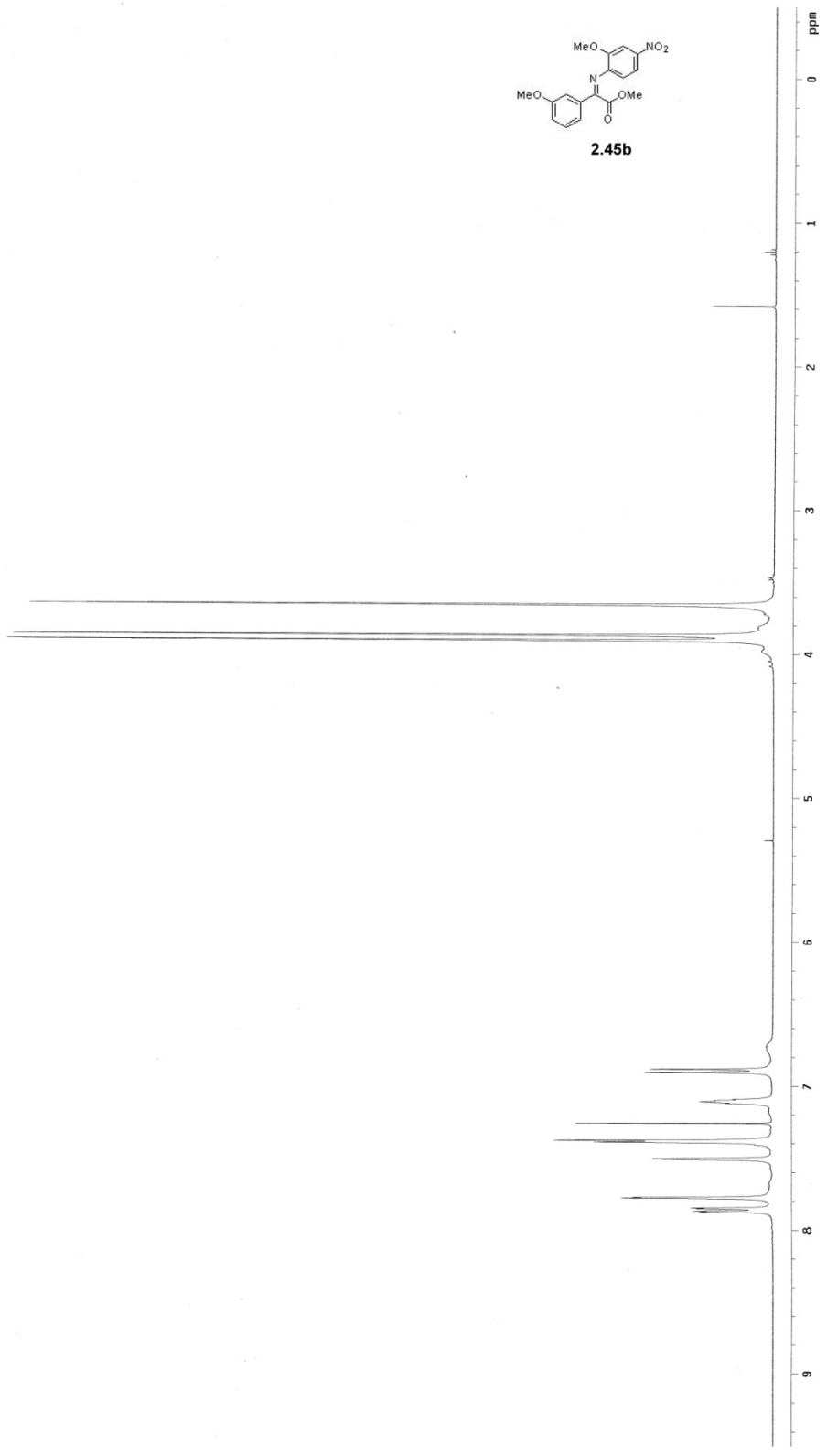
MeO
NO2
N
MeO
OMe
O
2.45b
ppm
0
1
2
3
4
5
6
7
8
9

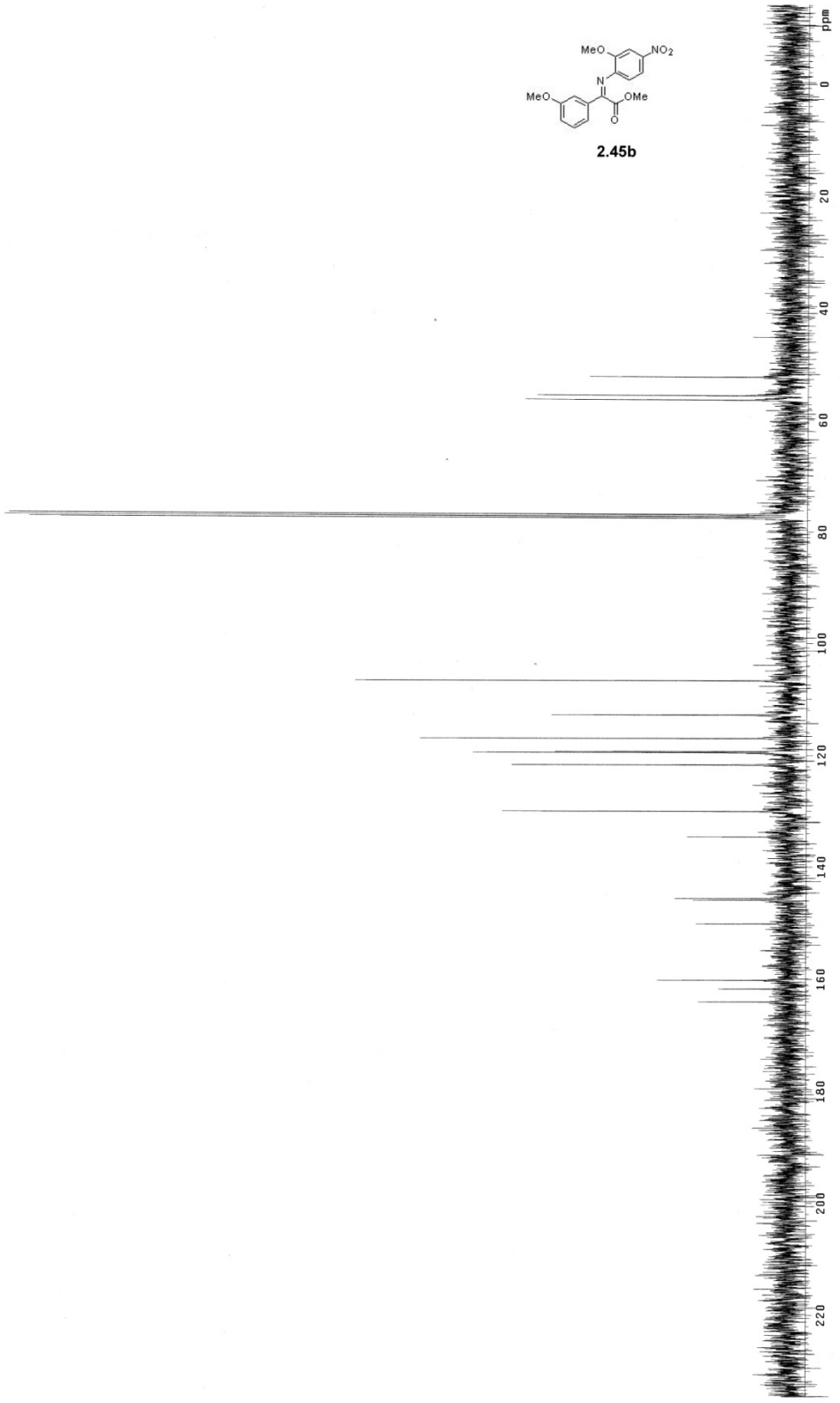
MeO
NO2
N
MeO
OMe
O
2.45b
ppm
0
20
40
60
80
100
120
140
160
180
200
220

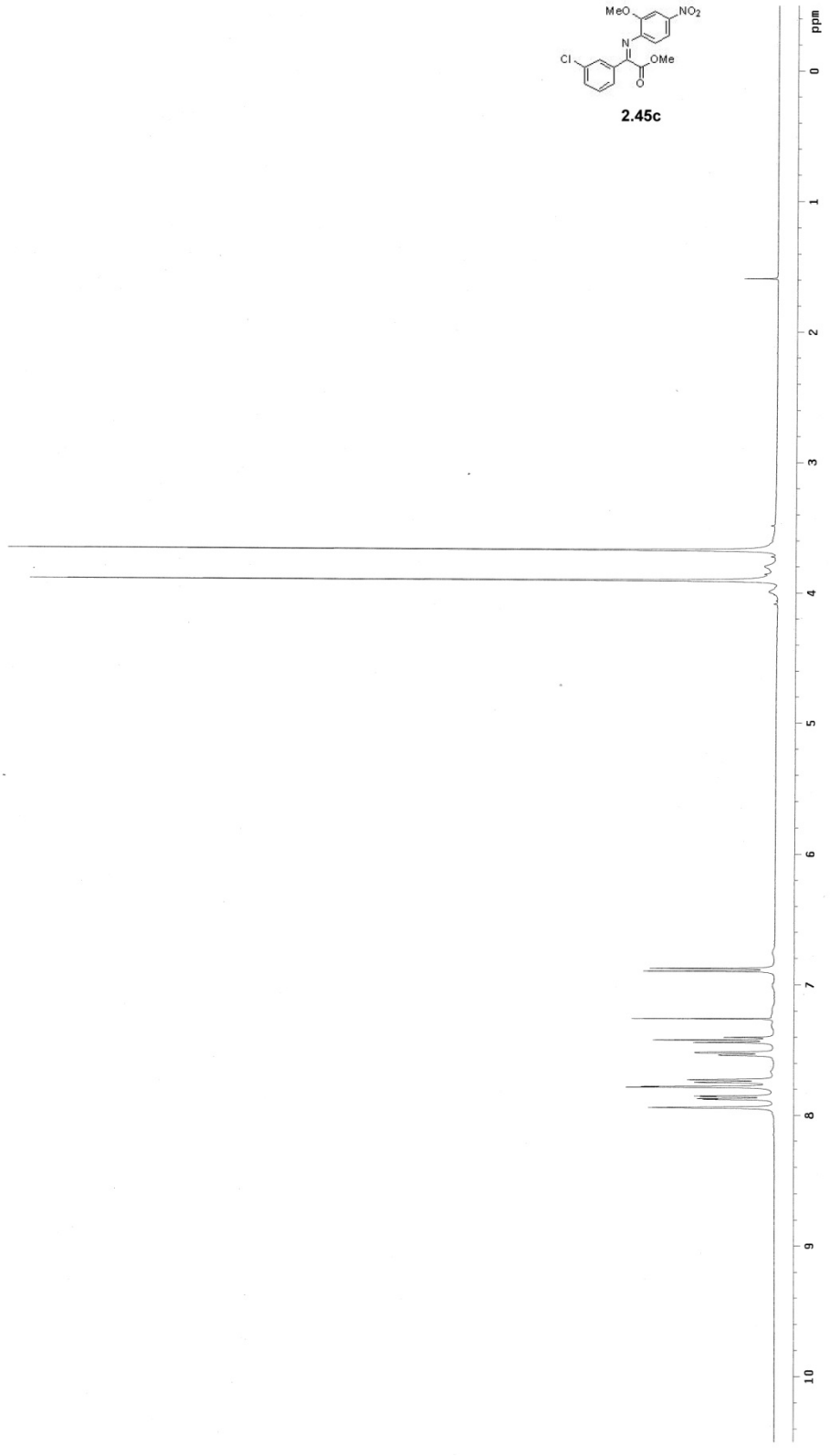
MeO
NO2
N
Cl
OMe
O
2.45c
ppm
0
1
2
3
4
5
6
7
8
9
10

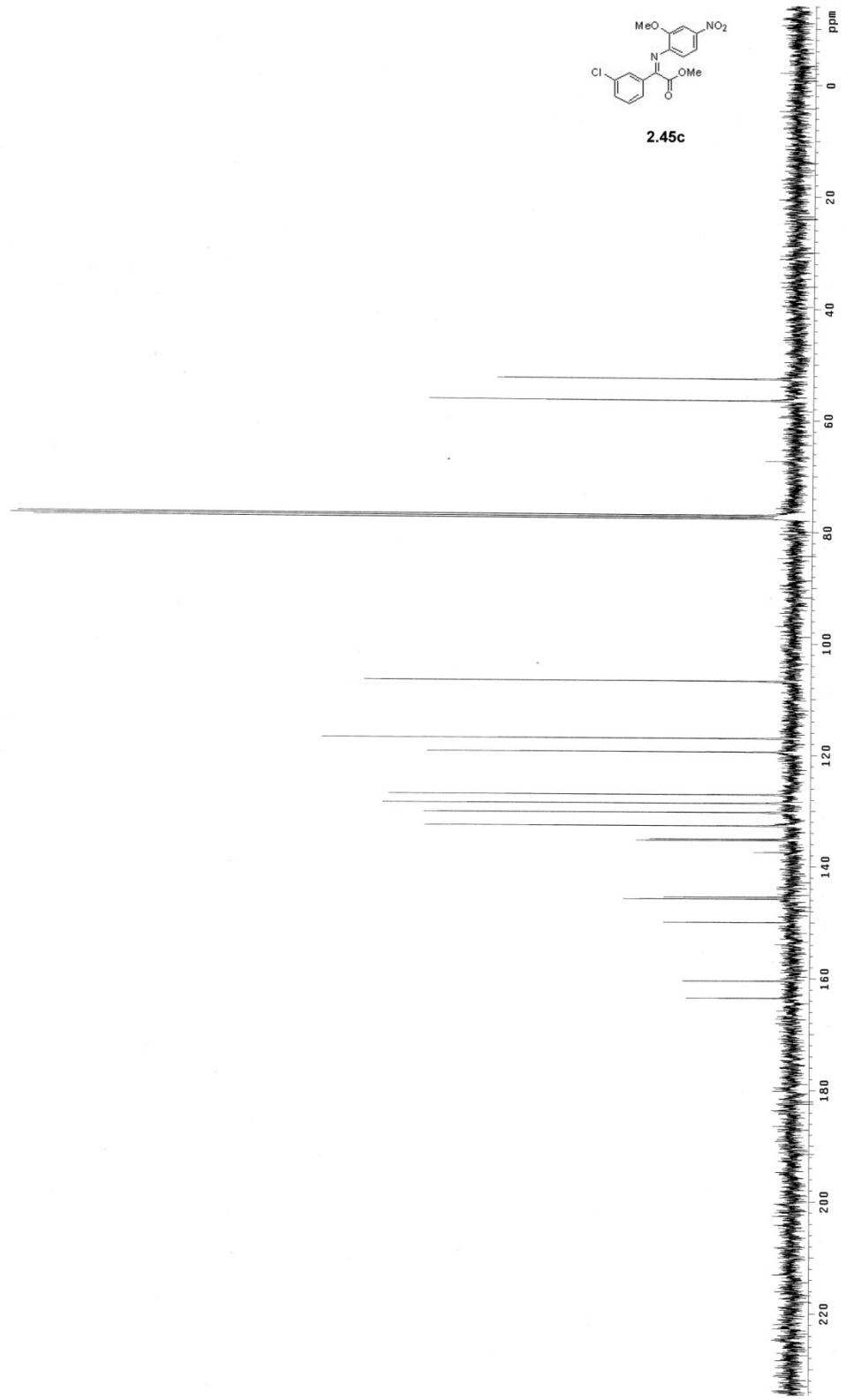
MeO
NO2
N
Cl
OMe
O
2.45c
ppm
0
20
40
60
80
100
120
140
160
180
200
220


MeO
NO2
N
OMe
O
Cl
2.45d
ppm
0
1
2
3
4
5
6
7
8
9
10

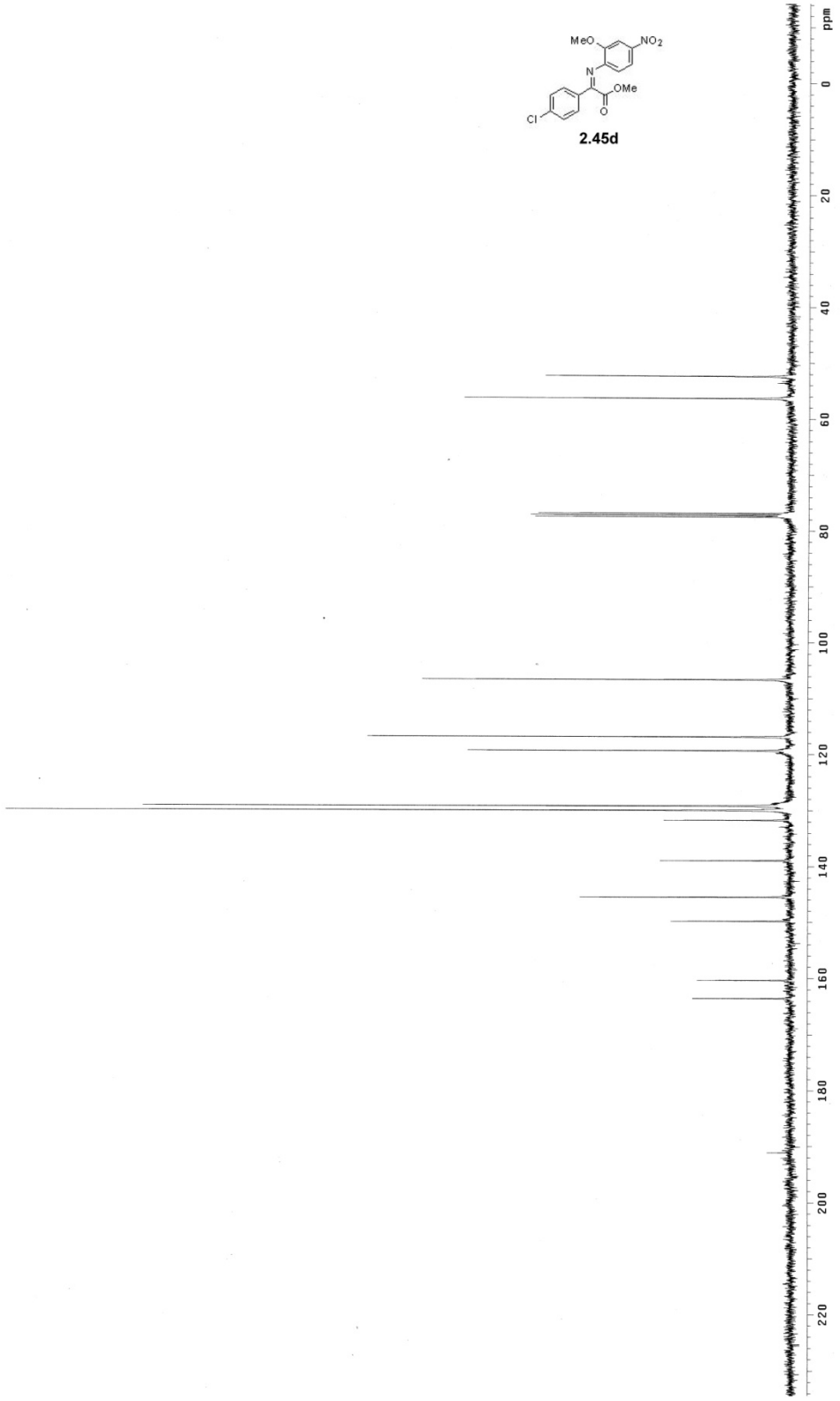
MeO
NO2
N
OMe
O
Cl
2.45d
ppm
0
20
40
60
80
100
120
140
160
180
200
220

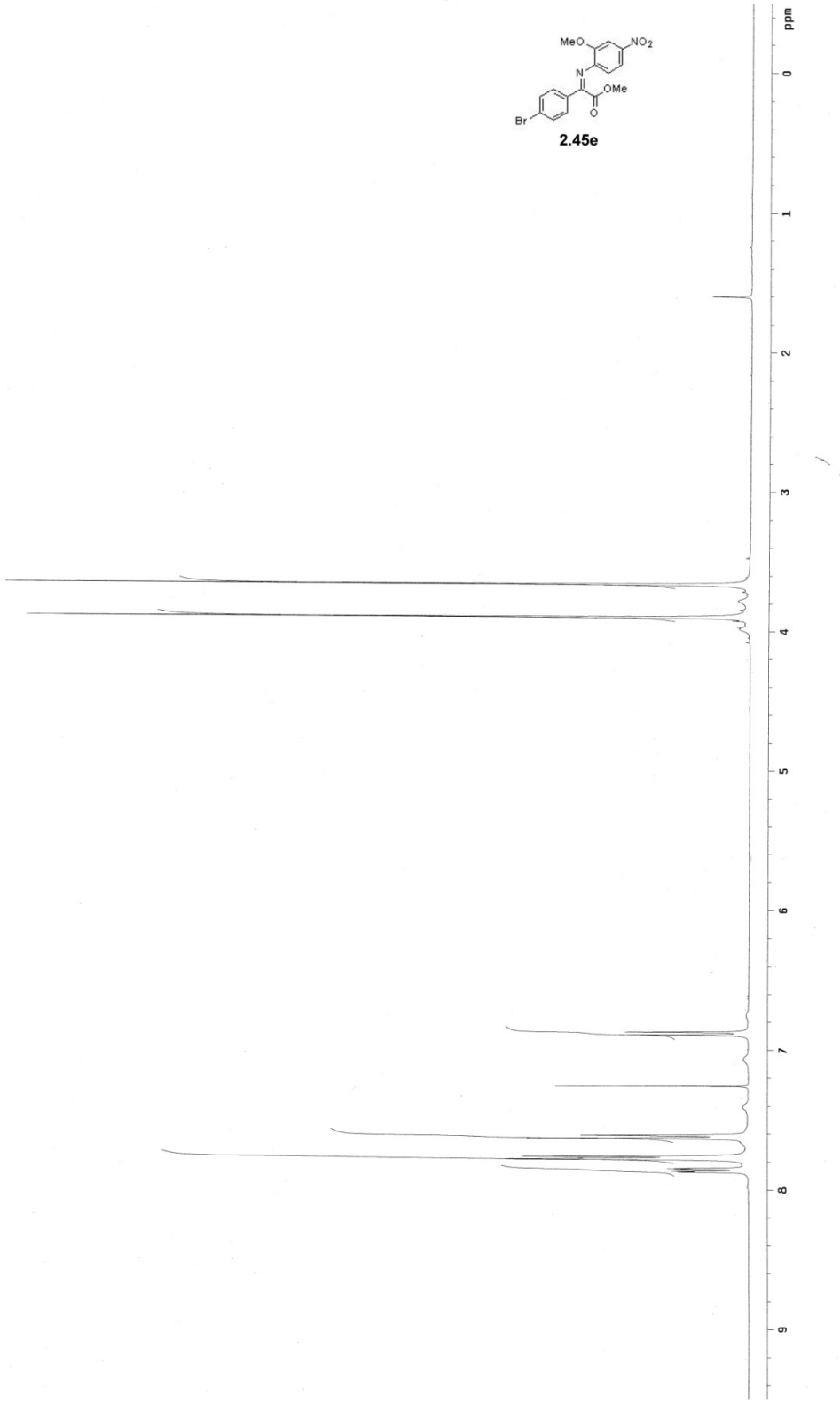
MeO
NO2
N
OMe
O
Br
2.45e
ppm
0
1
2
3
4
5
6
7
8
9

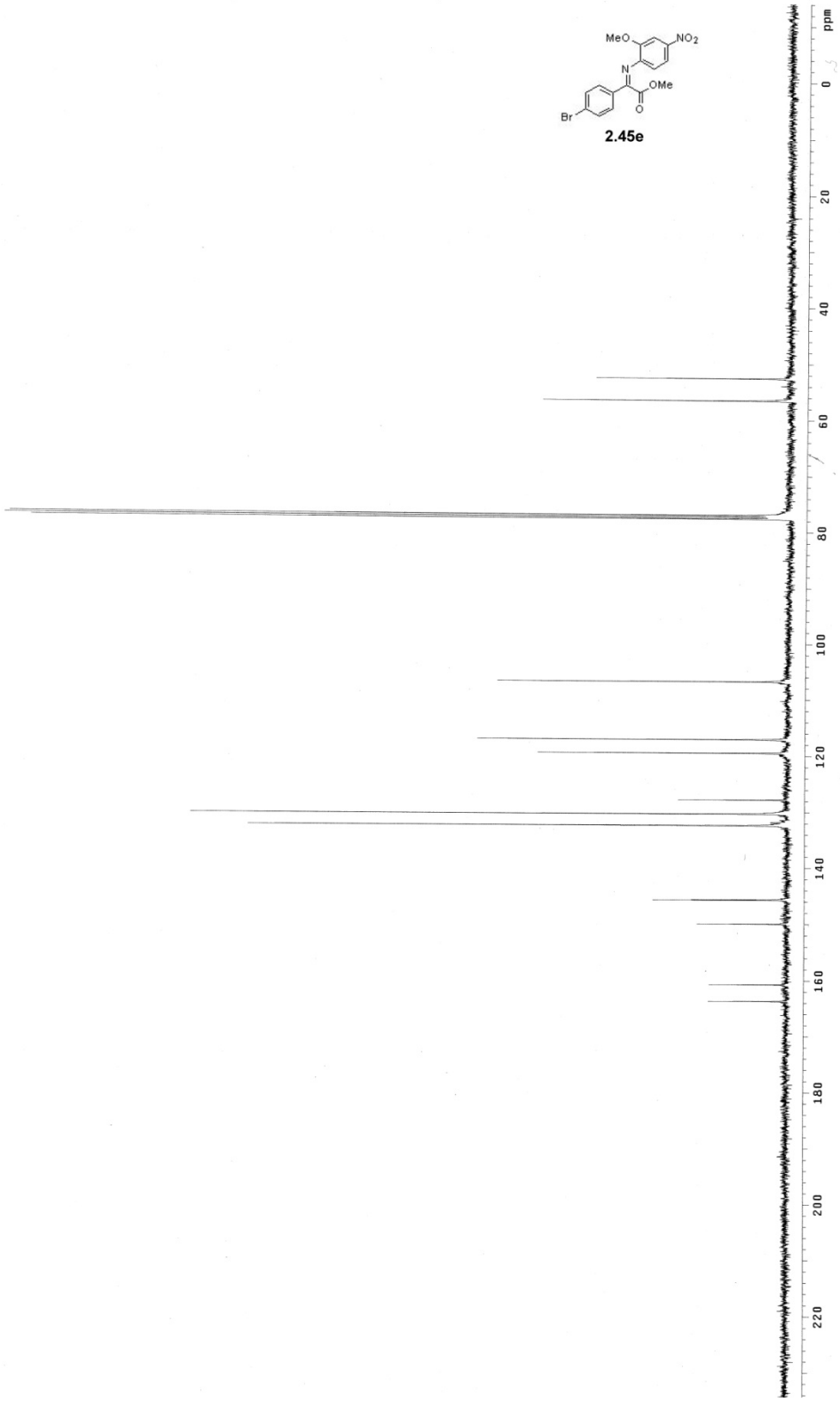
MeO
NO2
N
OMe
O
Br
2.45e
ppm
0
20
40
60
80
100
120
140
160
180
200
220

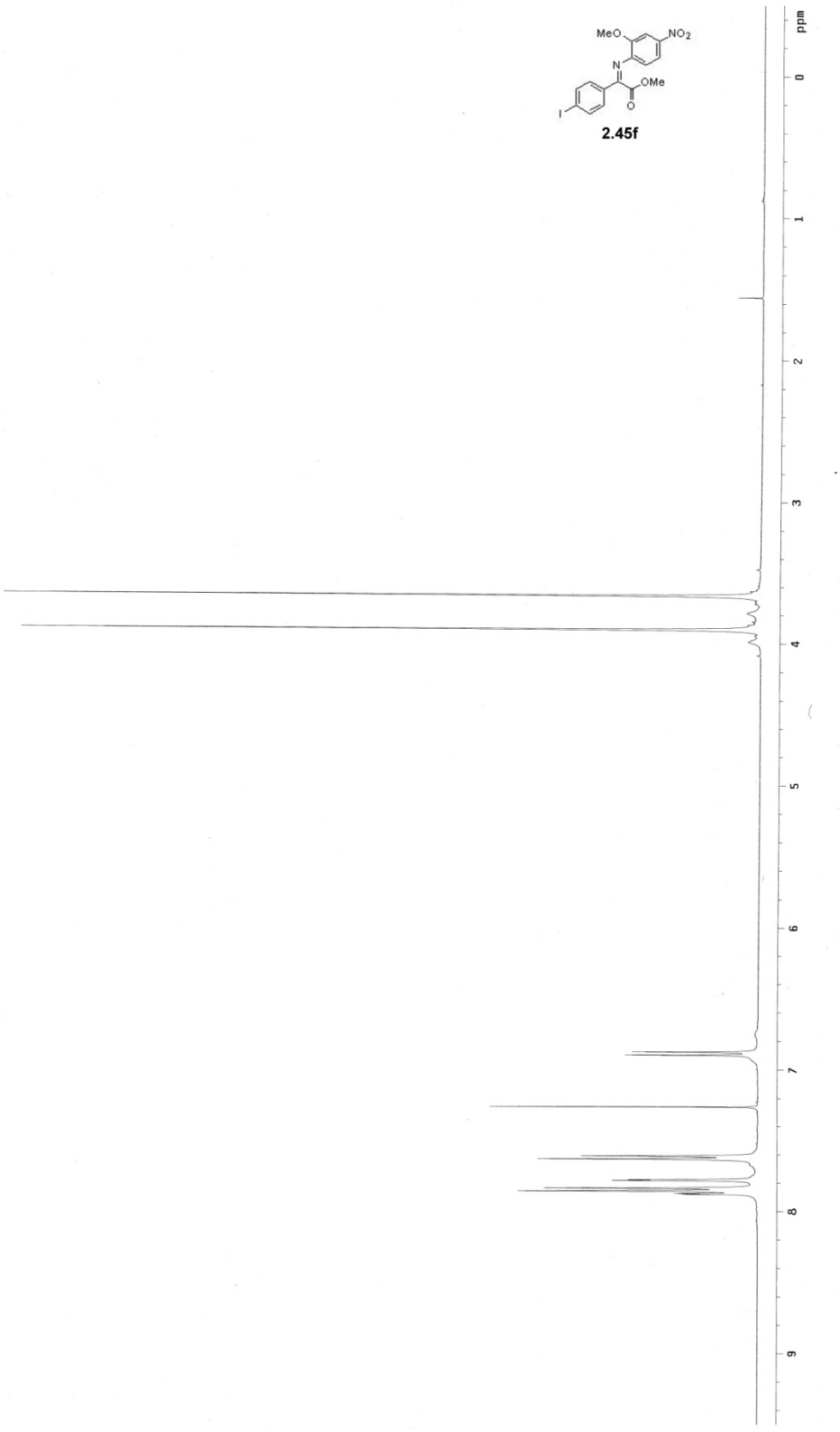
MeO
NO2
N
OMe
O
I
2.45f
ppm
0
1
2
3
4
5
6
7
8
9

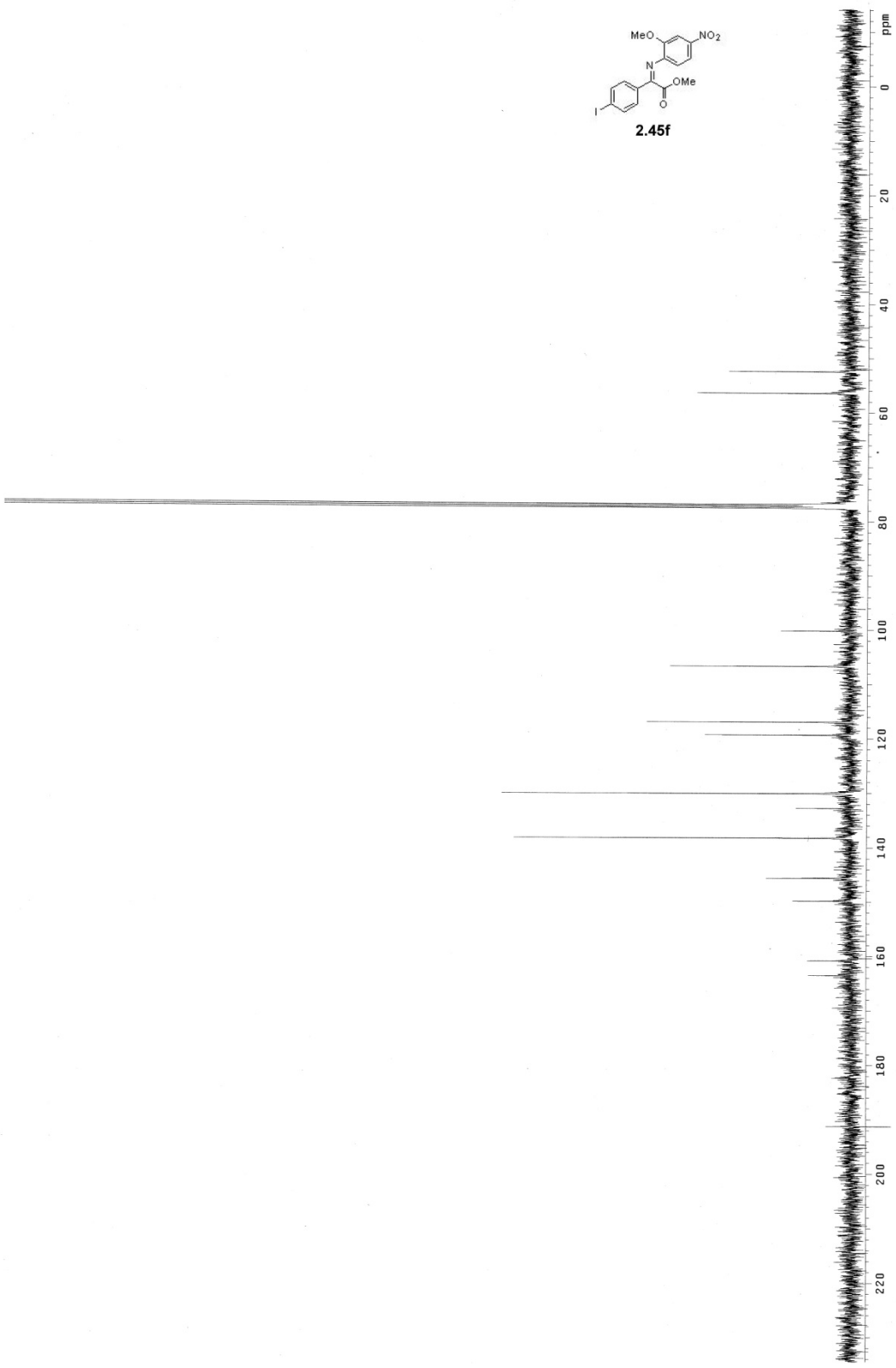
MeO
NO2
N
OMe
O
I
2.45f
ppm
0
20
40
60
80
100
120
140
160
180
200
220

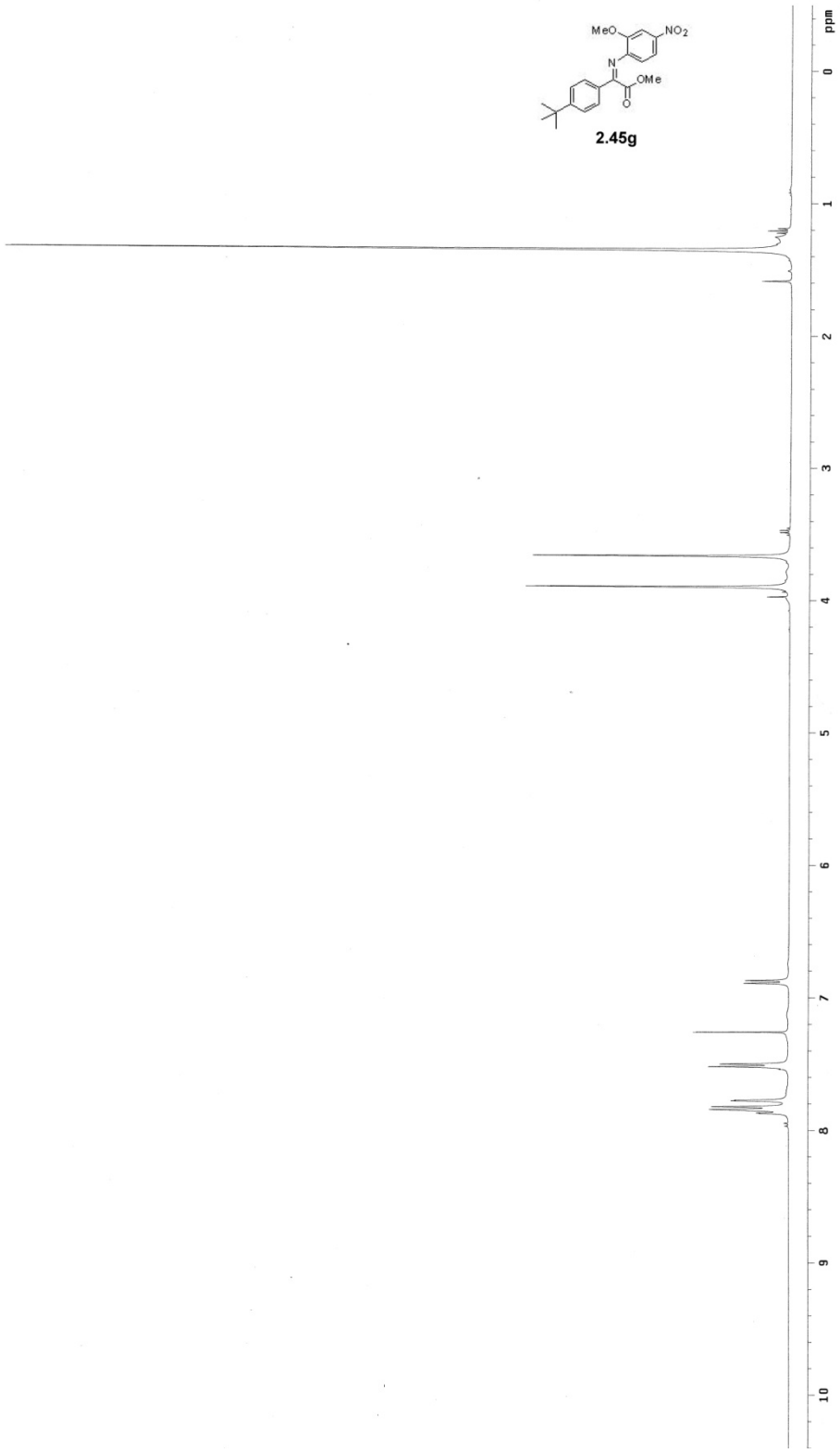
MeO
NO2
N
OMe
O
2.45g
ppm
0
1
2
3
4
5
6
7
8
9
10

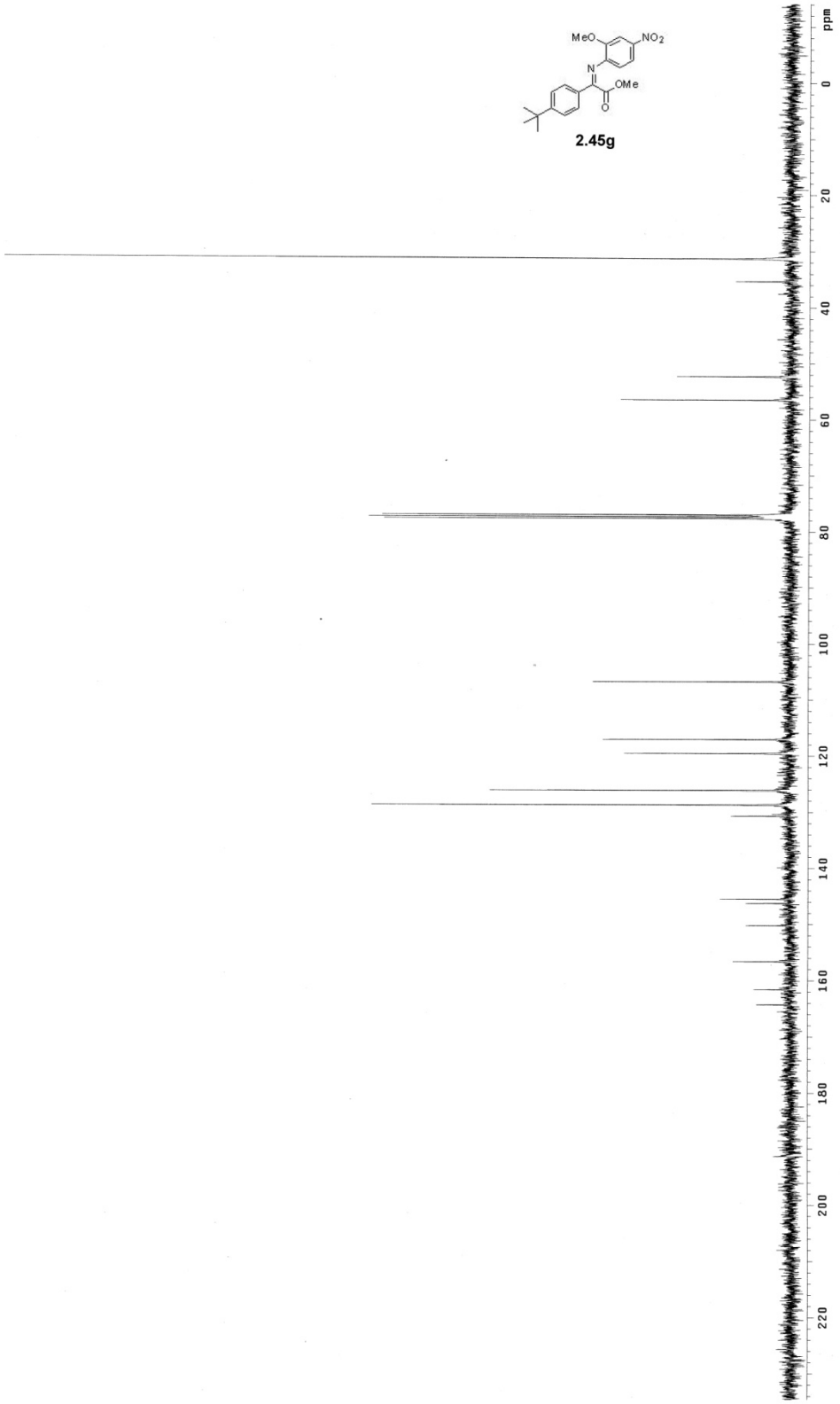
MeO
NO2
N
OMe
O
2.45g
ppm
0
20
40
60
80
100
120
140
160
180
200
220

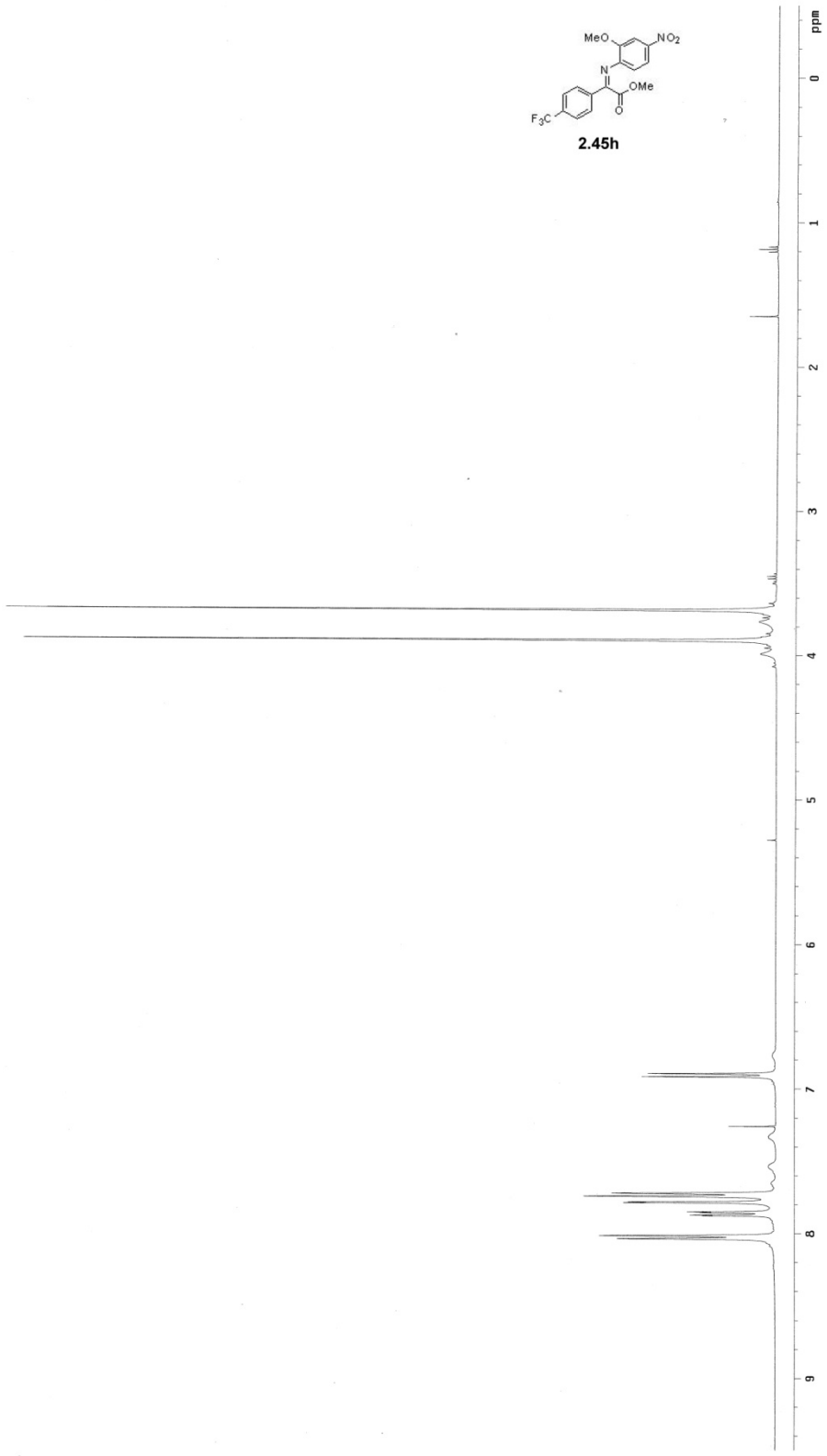
MeO
NO2
N
OMe
O
F3C
2.45h
ppm
0
1
2
3
4
5
6
7
8
9

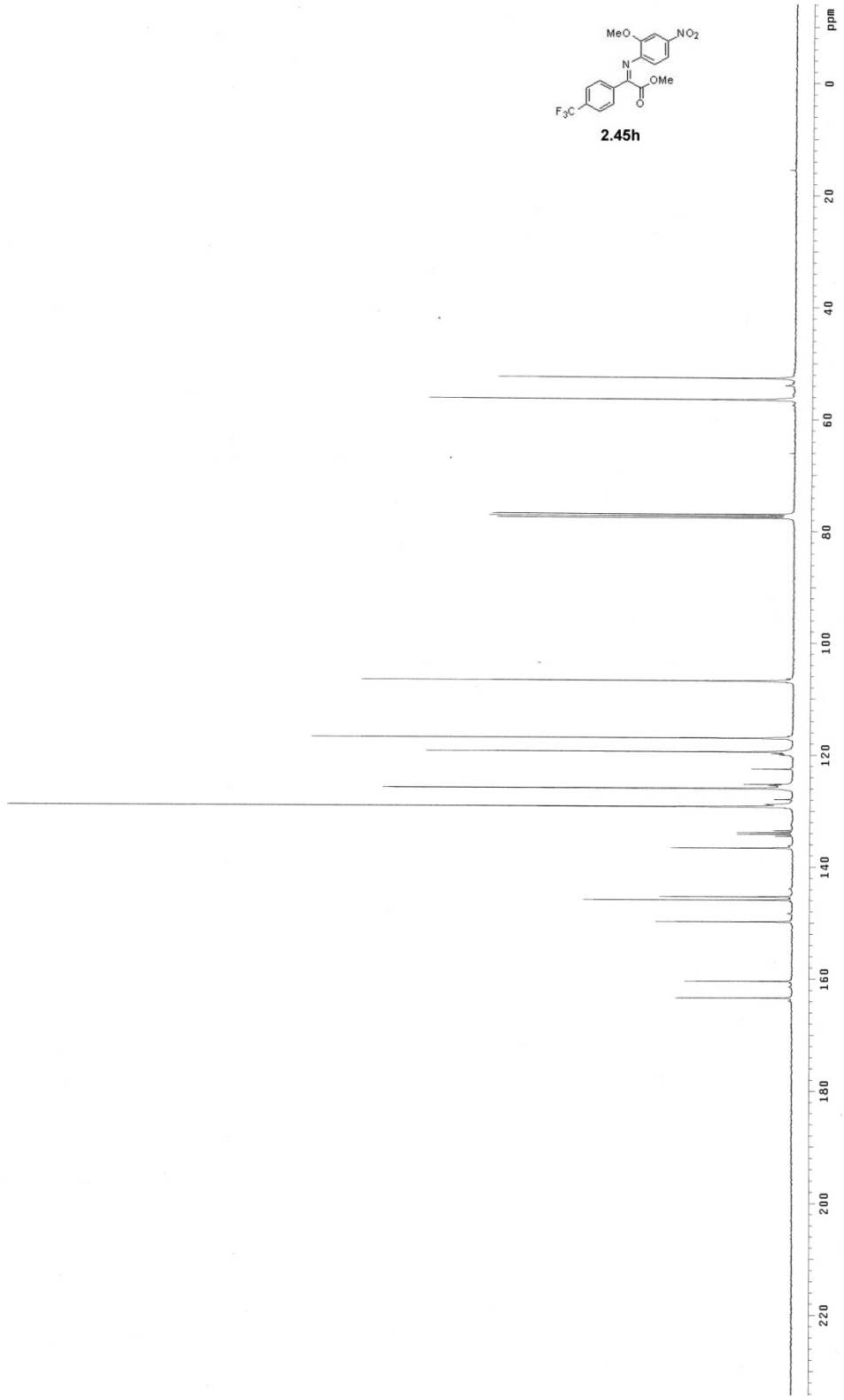
MeO
NO2
N
OMe
O
F3C
2.45h
ppm
0
20
40
60
80
100
120
140
160
180
200
220

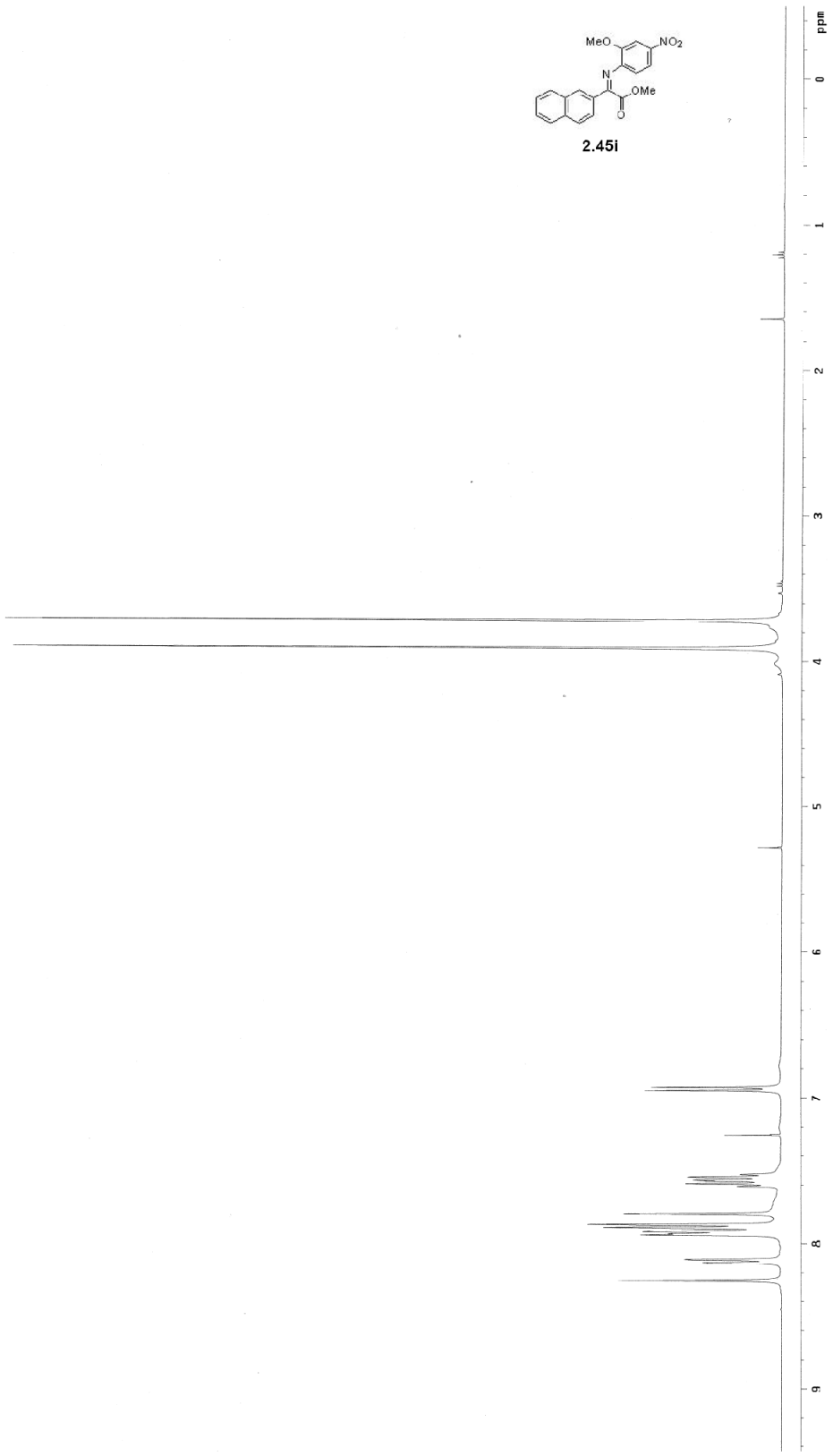
MeO
NO2
N
OMe
O
2.45i
ppm
0
1
2
3
4
5
6
7
8
9

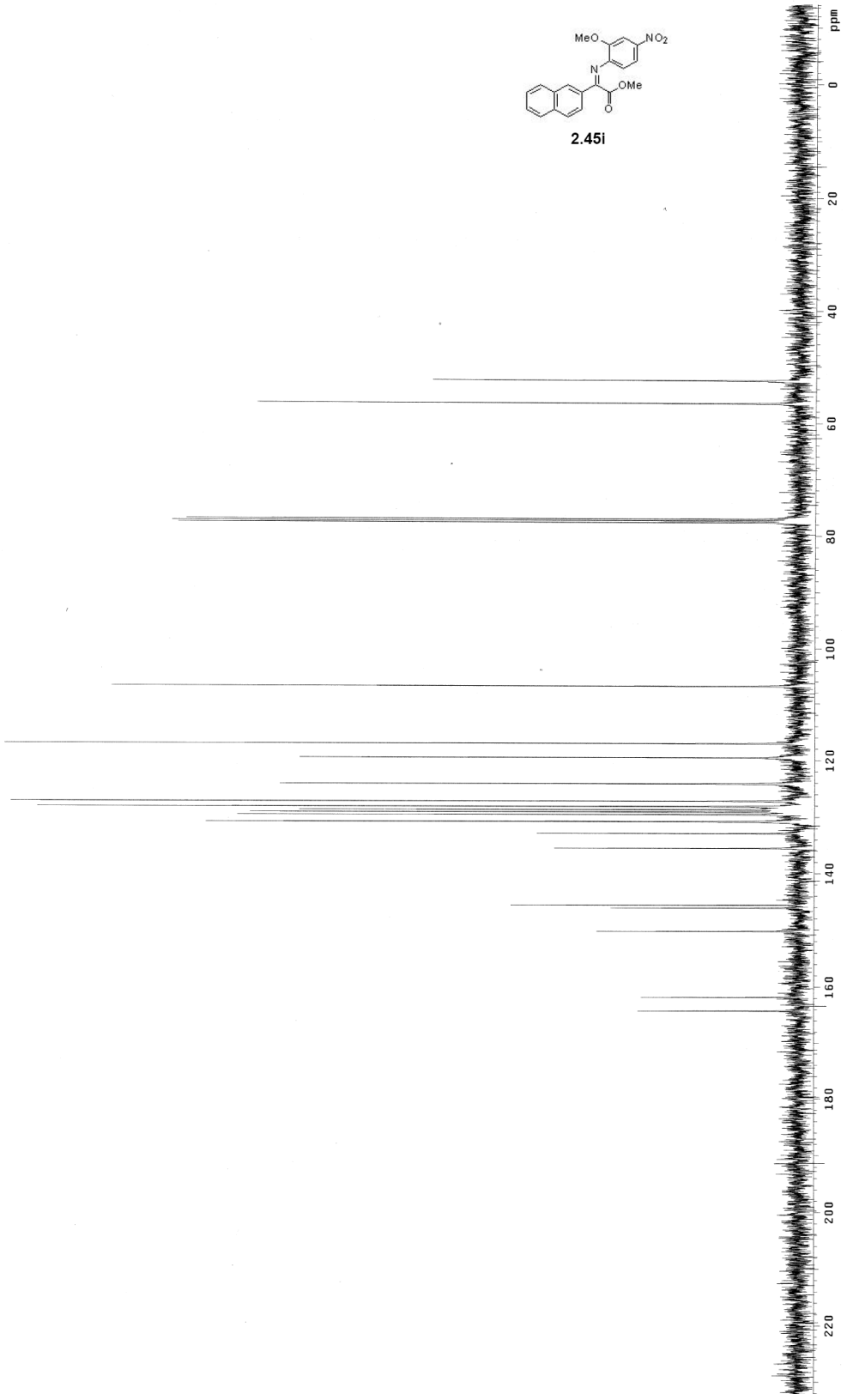
MeO
NO2
N
OMe
O
2.45i
ppm
0
20
40
60
80
100
120
140
160
180
200
220

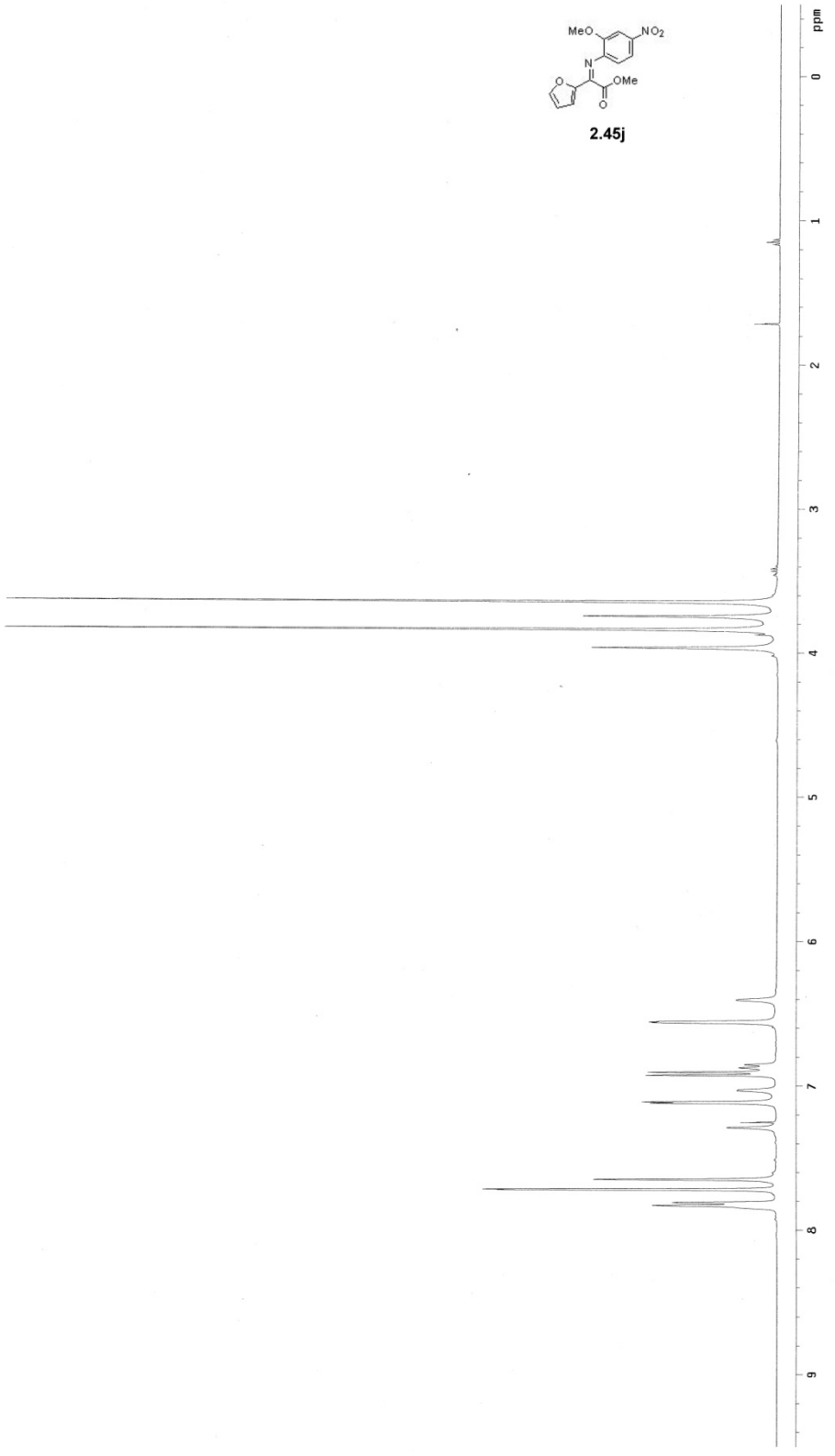
MeO
NO2
N
OMe
O
O
2.45j
ppm
0
1
2
3
4
5
6
7
8
9

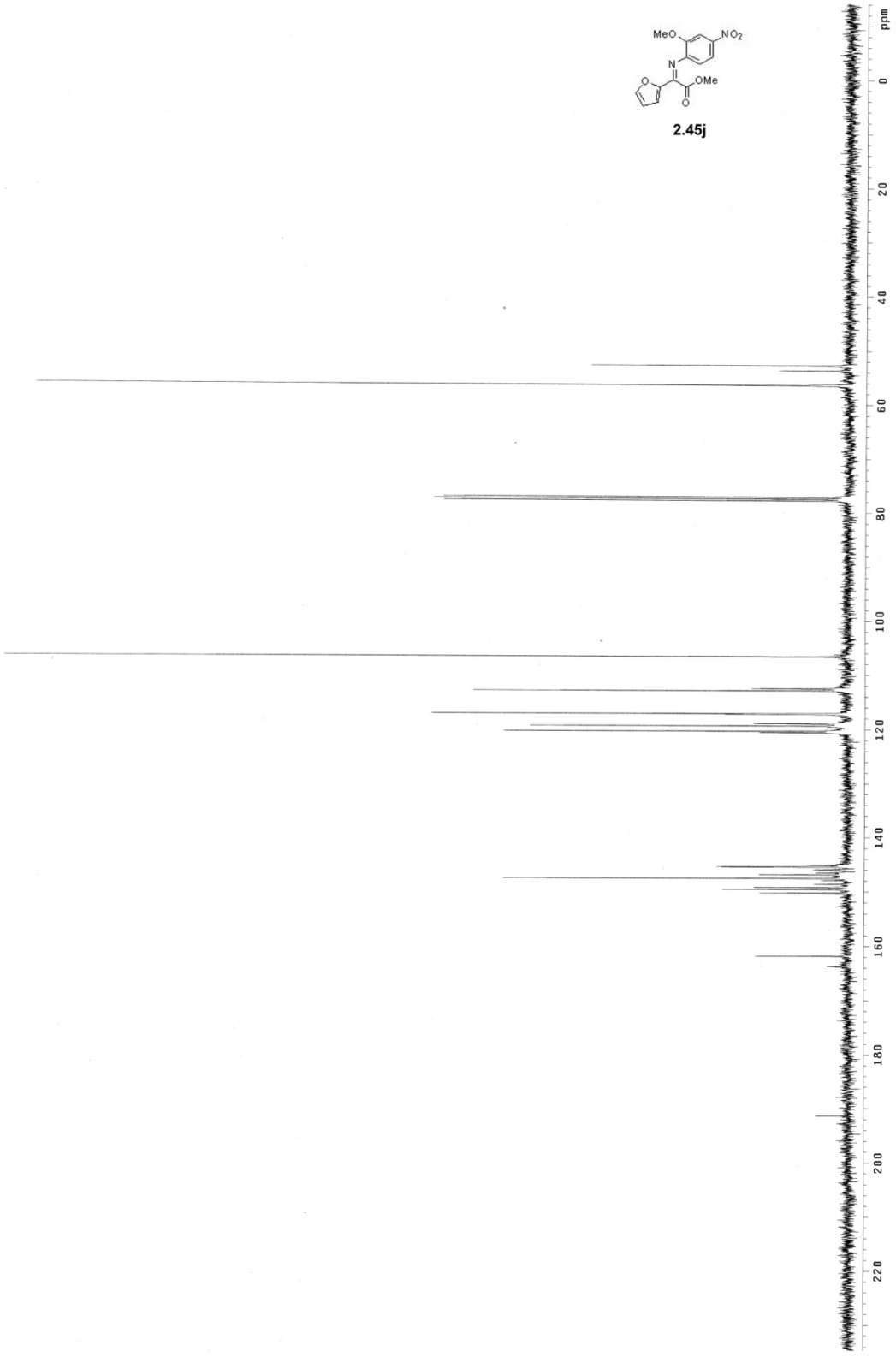
MeO
NO2
N
OMe
O
2.45j
ppm
0
20
40
60
80
100
120
140
160
180
200
220

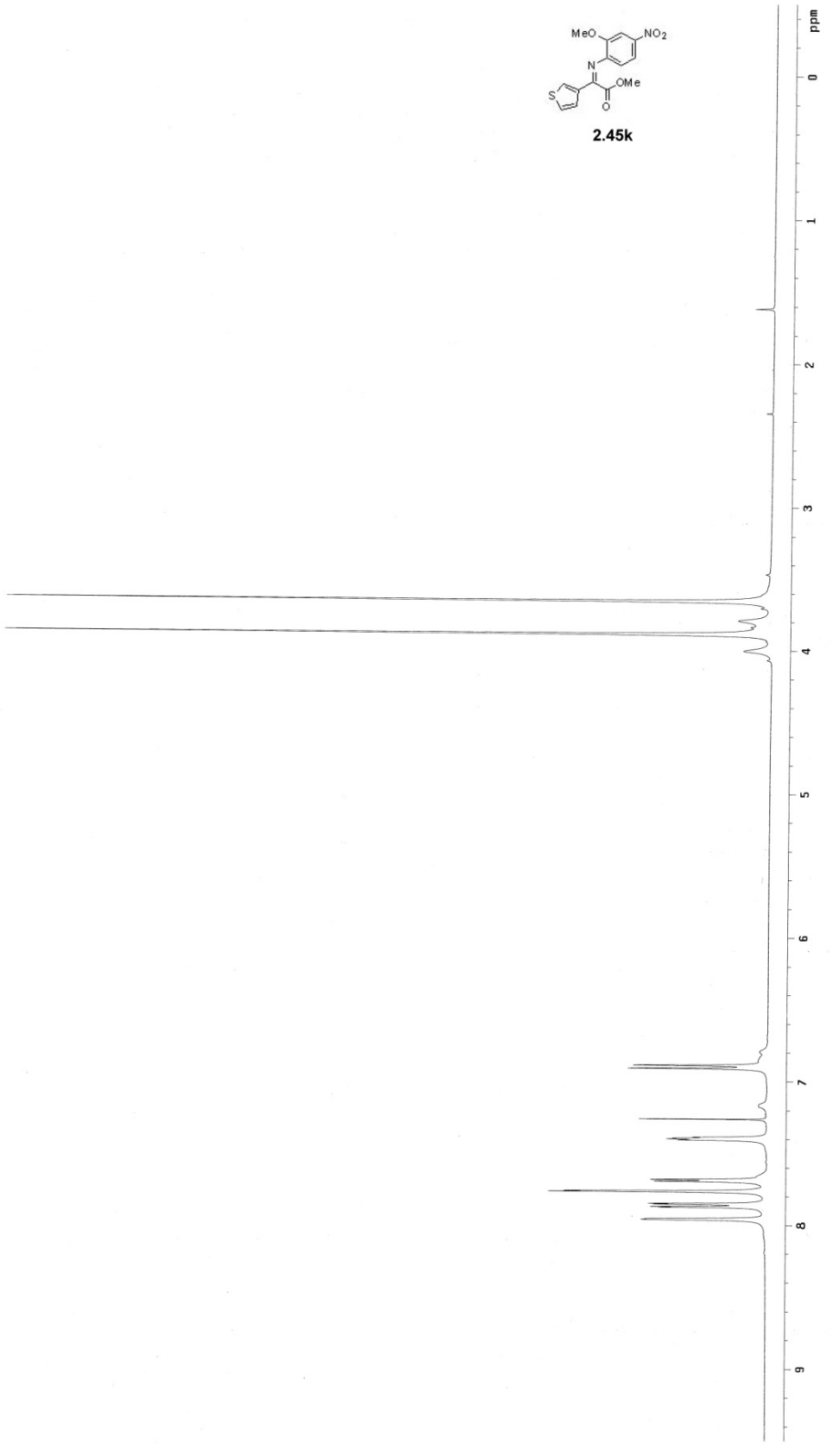
MeO
NO2
N
OMe
S
O
2.45k
ppm
0
1
2
3
4
5
6
7
8
9

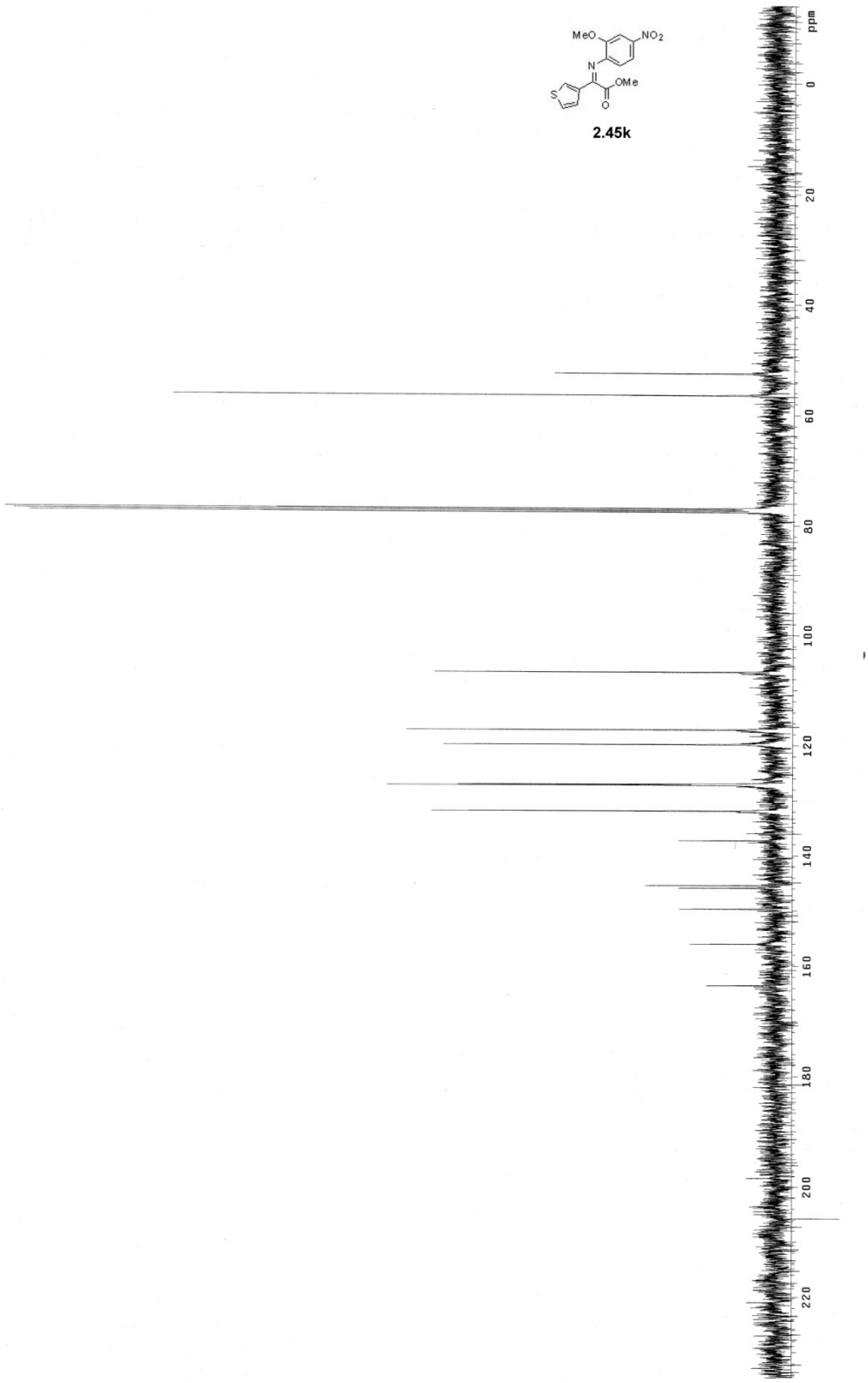
MeO
NO2
N
OMe
O
S
2.45k
ppm
0
20
40
60
80
100
120
140
160
180
200
220

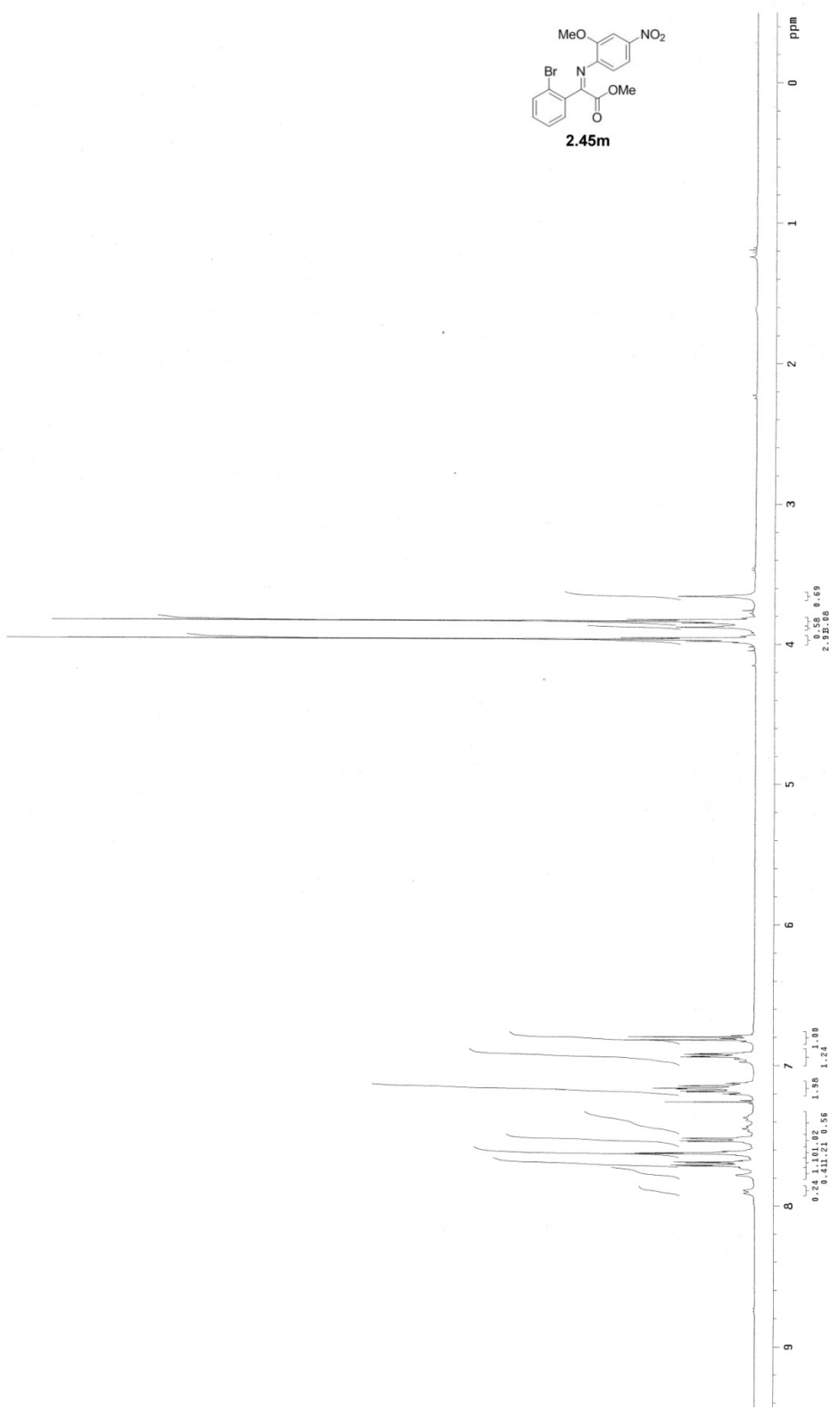
MeO
NO2
Br
N
OMe
O
2.45m
ppm
0
1
2
3
4
5
6
7
8
9

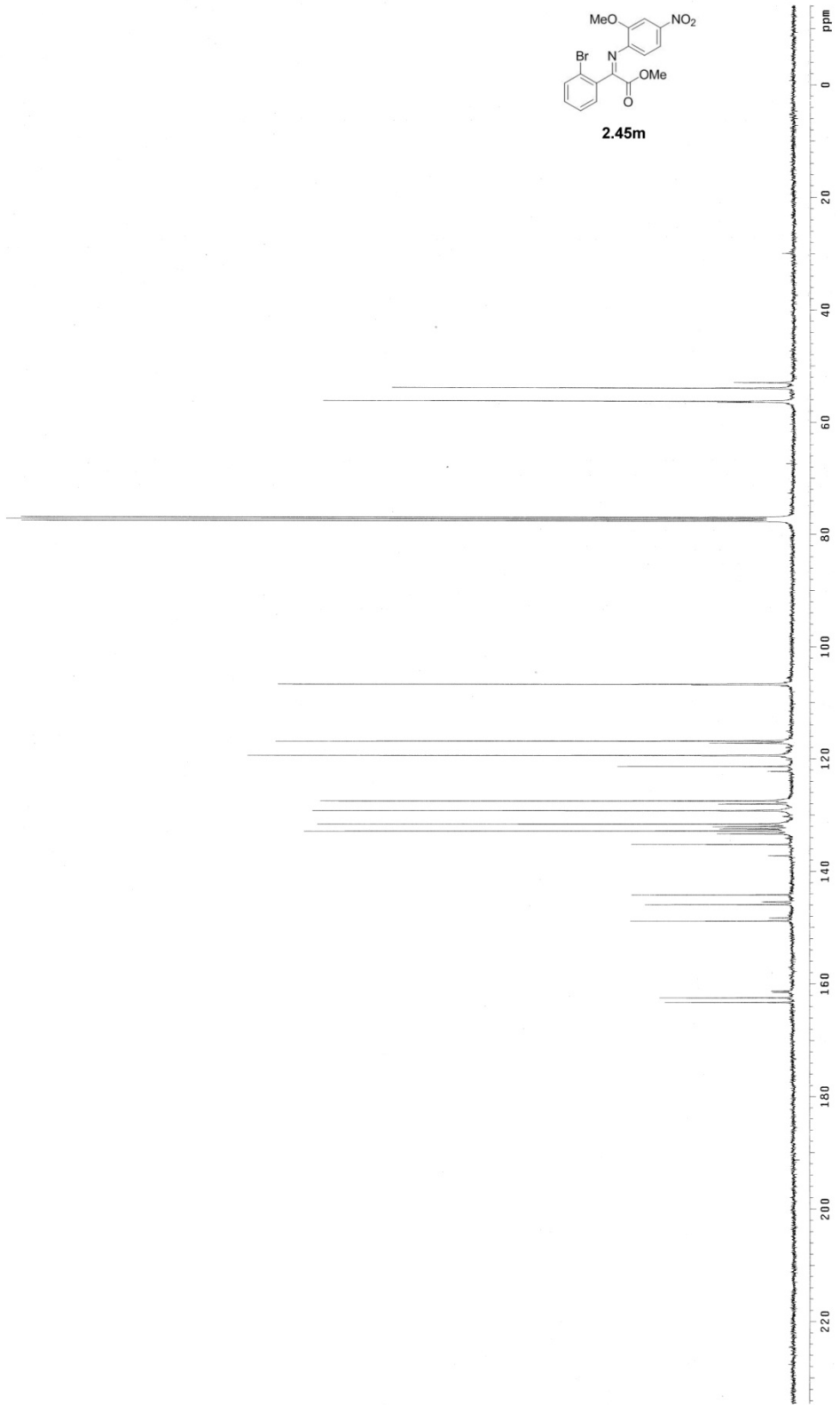
MeO
NO2
Br
N
OMe
O
2.45m
ppm
0
20
40
60
80
100
120
140
160
180
200
220

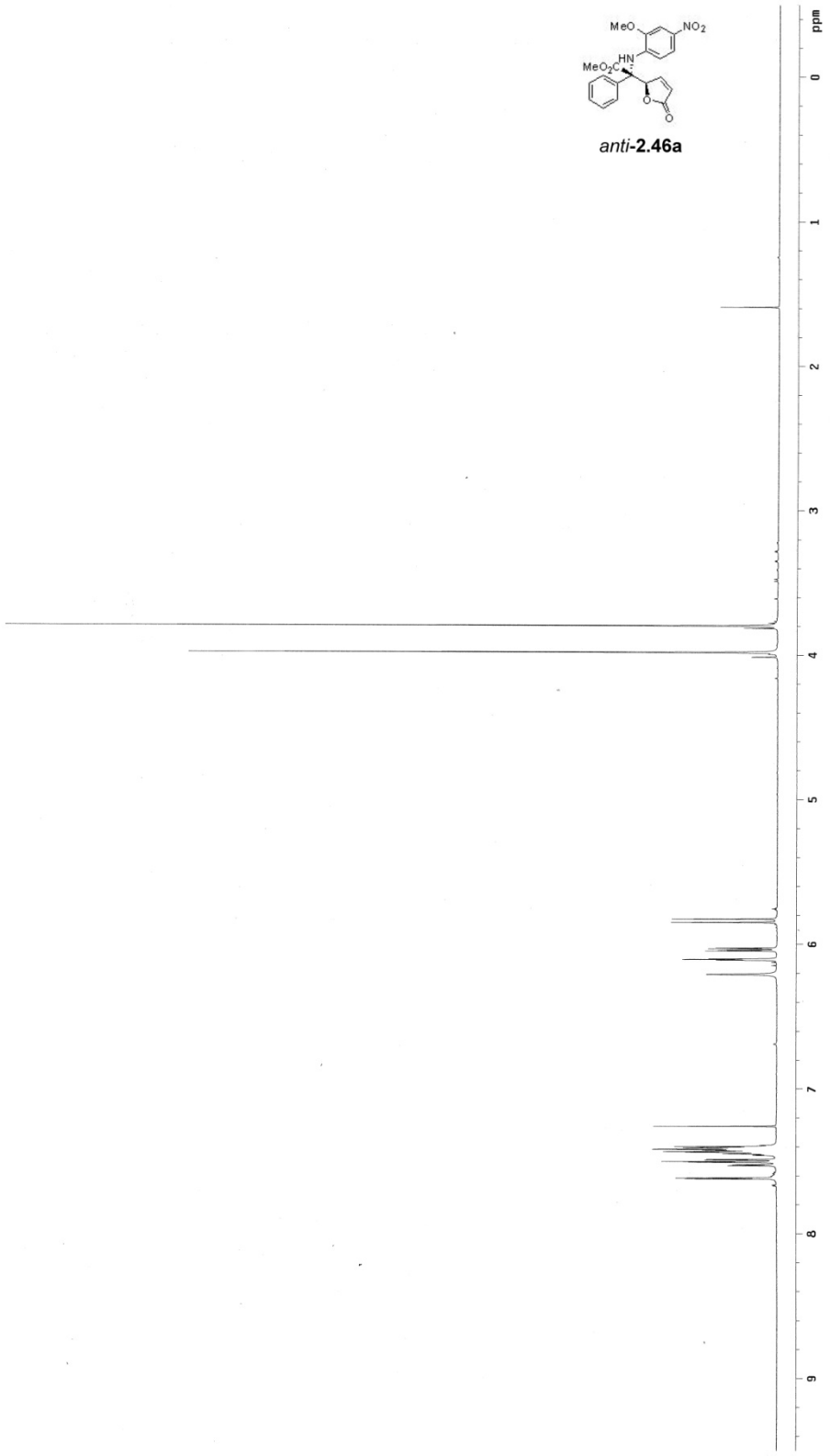
MeO
NO2
HN
MeO2C
O
O
anti-2.46a
ppm
0
1
2
3
4
5
6
7
8
9

anti-**2.46a**

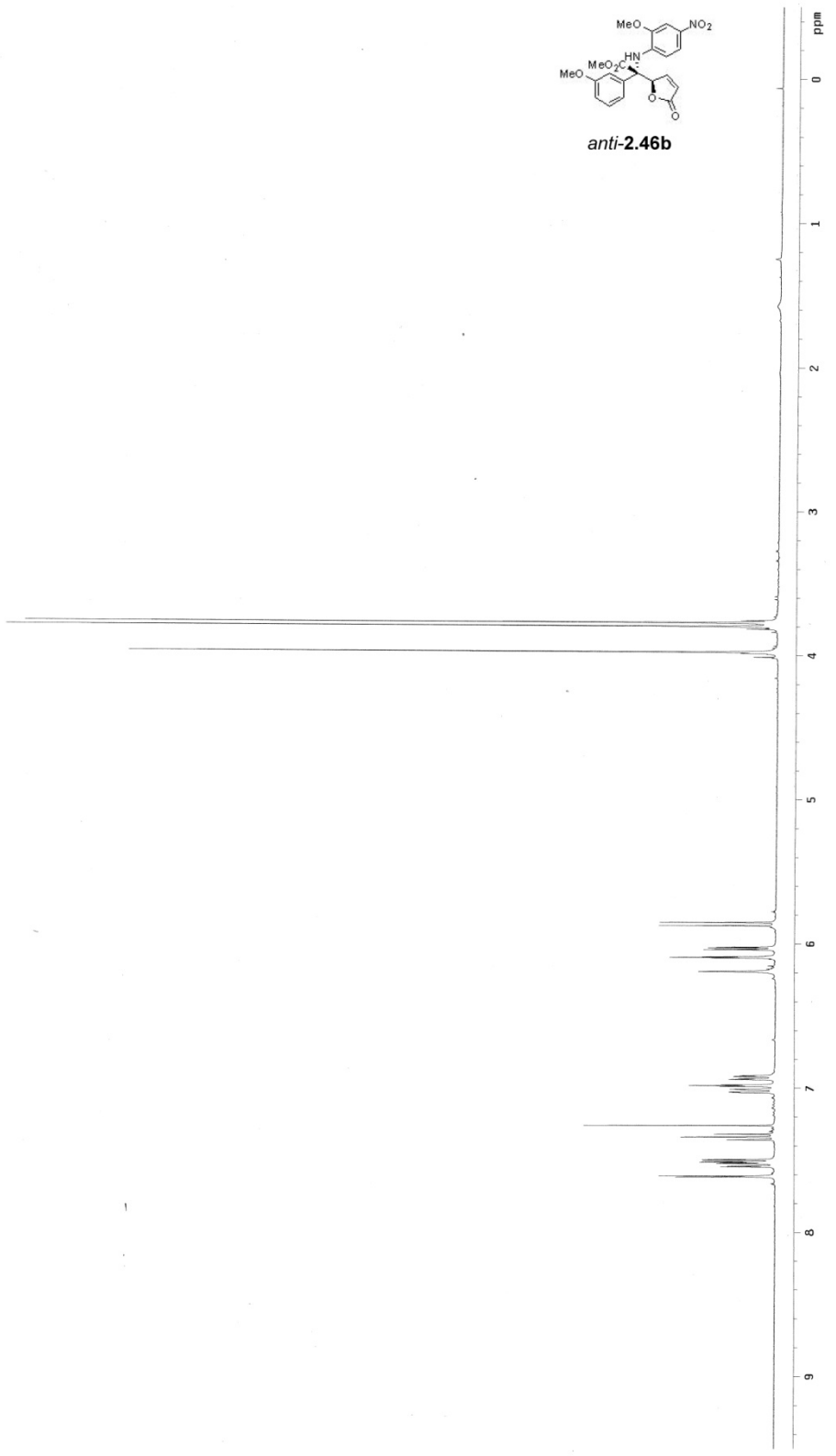

anti-**2.46b**

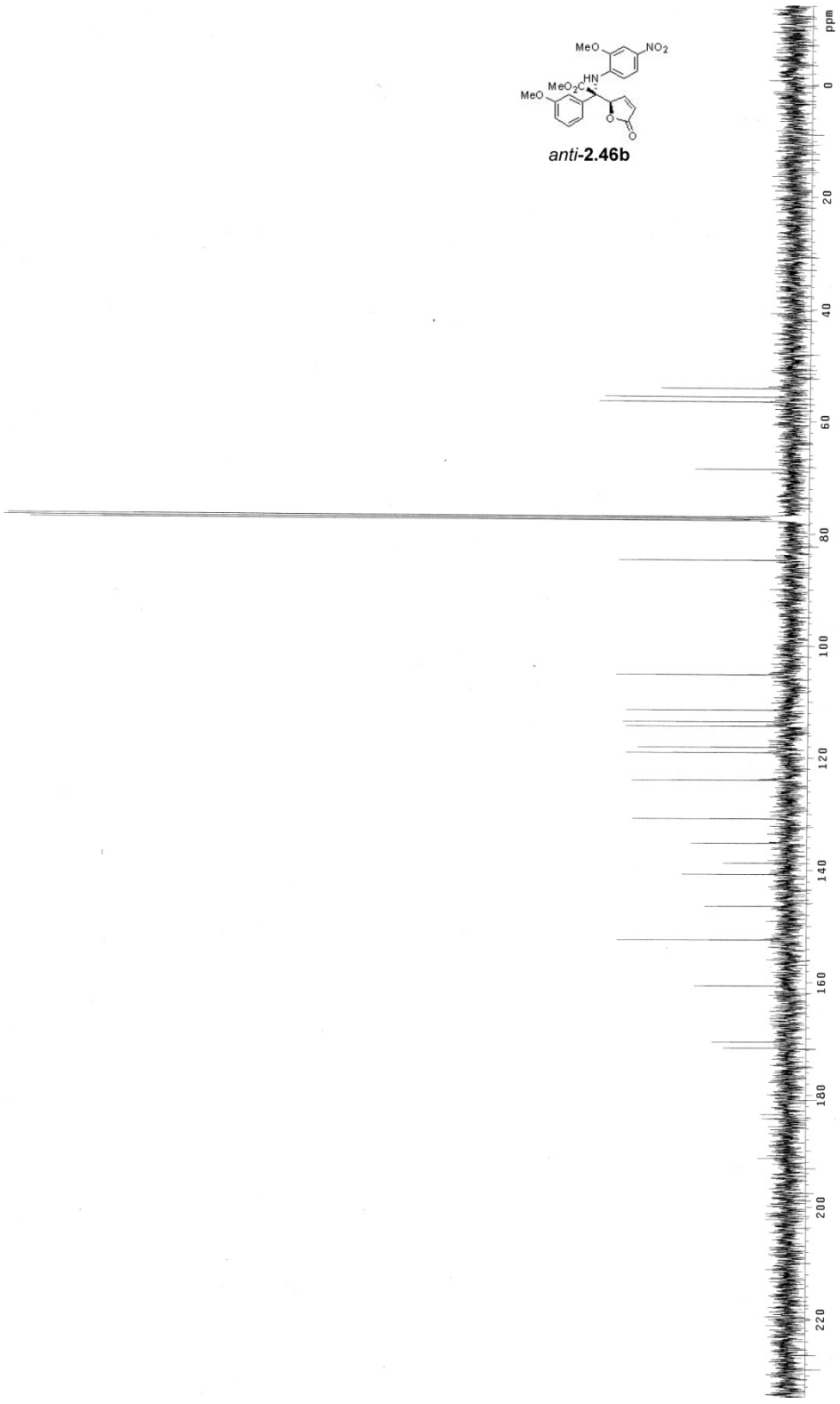
MeO
NO2
HN
MeO2C
MeO
O
O
ppm
0
20
40
60
80
100
120
140
160
180
200
220

anti-**2.46b**

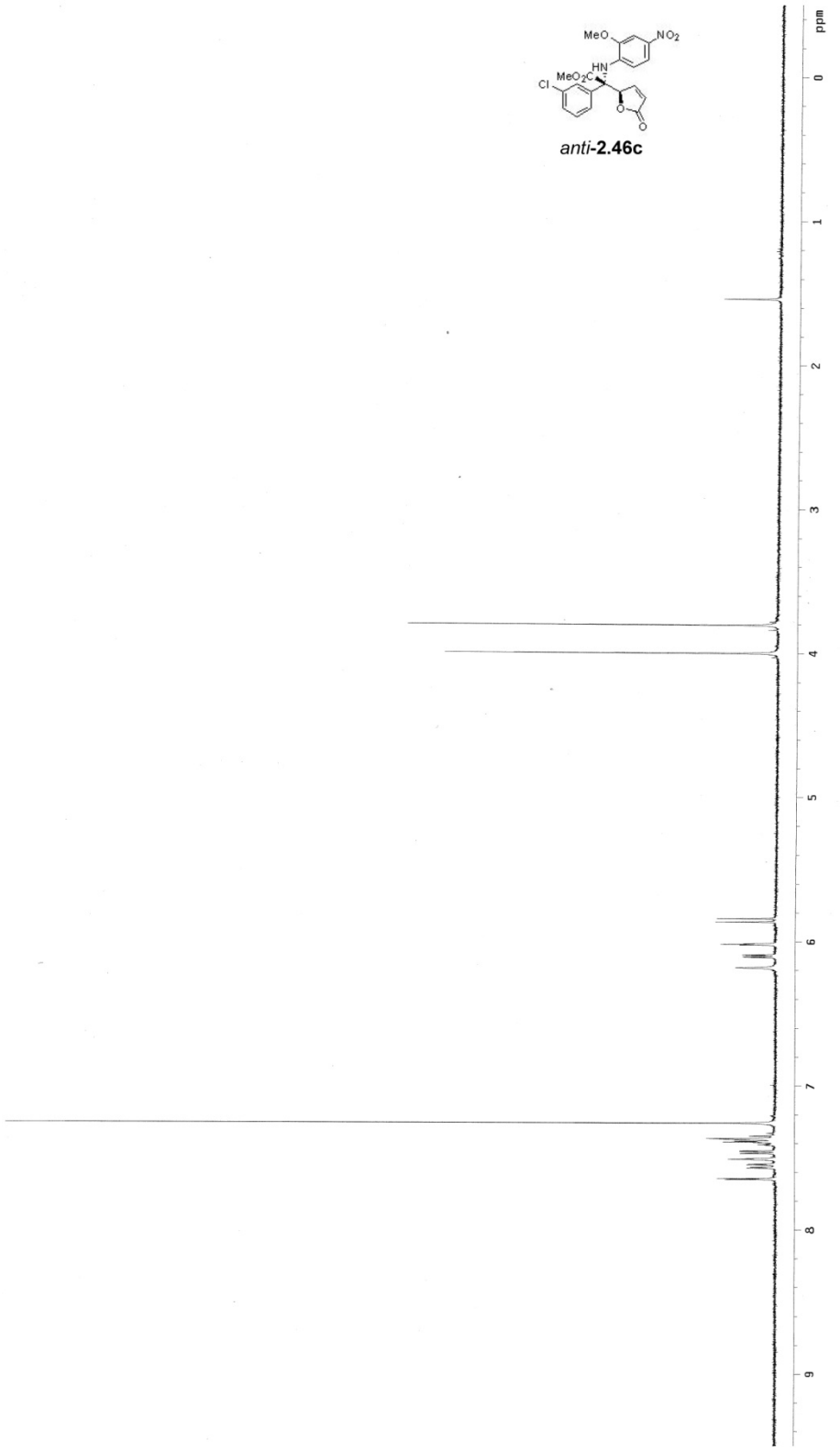
MeO
NO2
HN
MeO2C
Cl
O
O
anti-2.46c
ppm
0
1
2
3
4
5
6
7
8
9

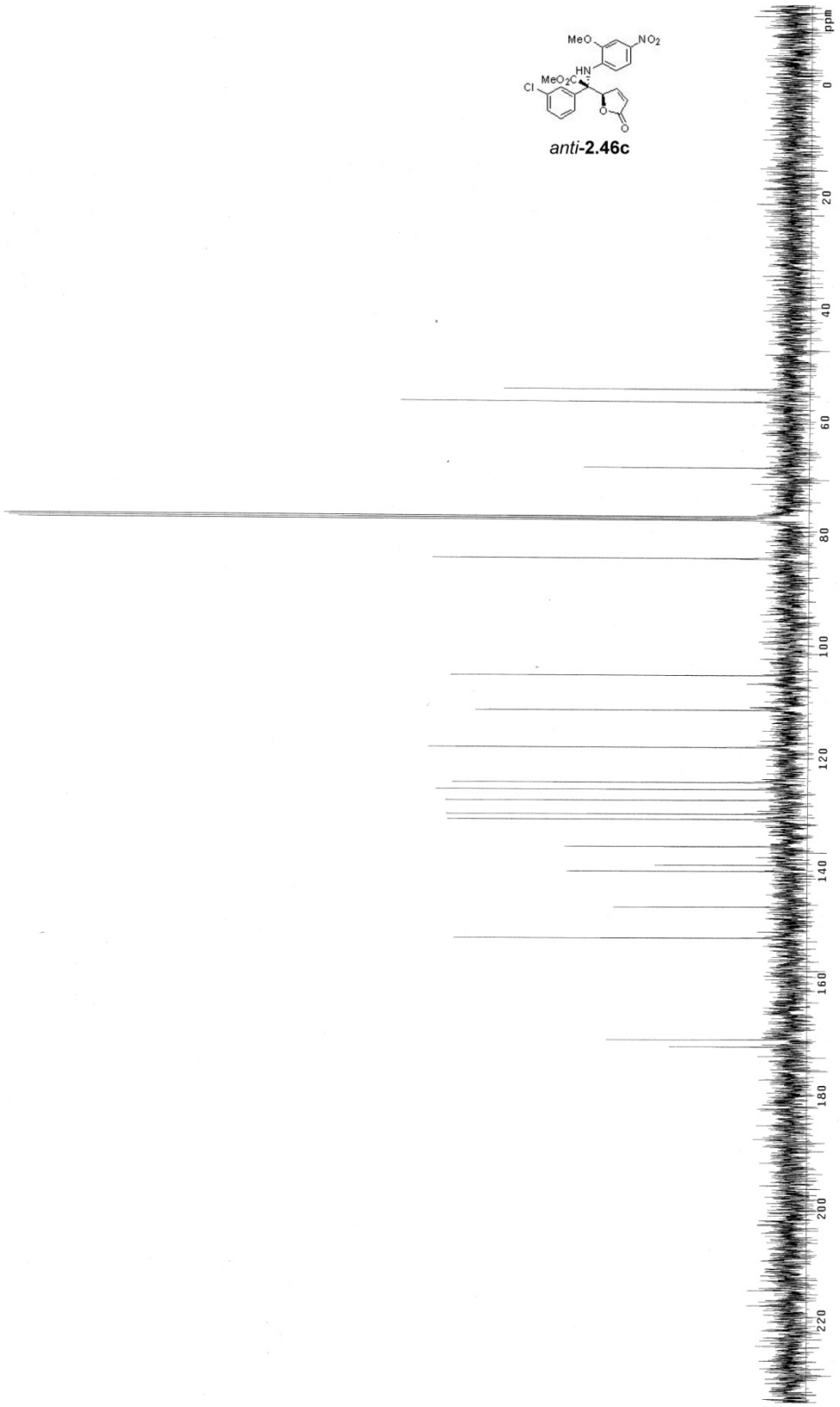
MeO
NO2
HN
MeO2C
Cl
O
O
anti-2.46c
ppm
0
20
40
60
80
100
120
140
160
180
200
220


MeO
NO2
HN
MeO2C
Cl
O
O
anti-2.46d
ppm
0
1
2
3
4
5
6
7
8
9

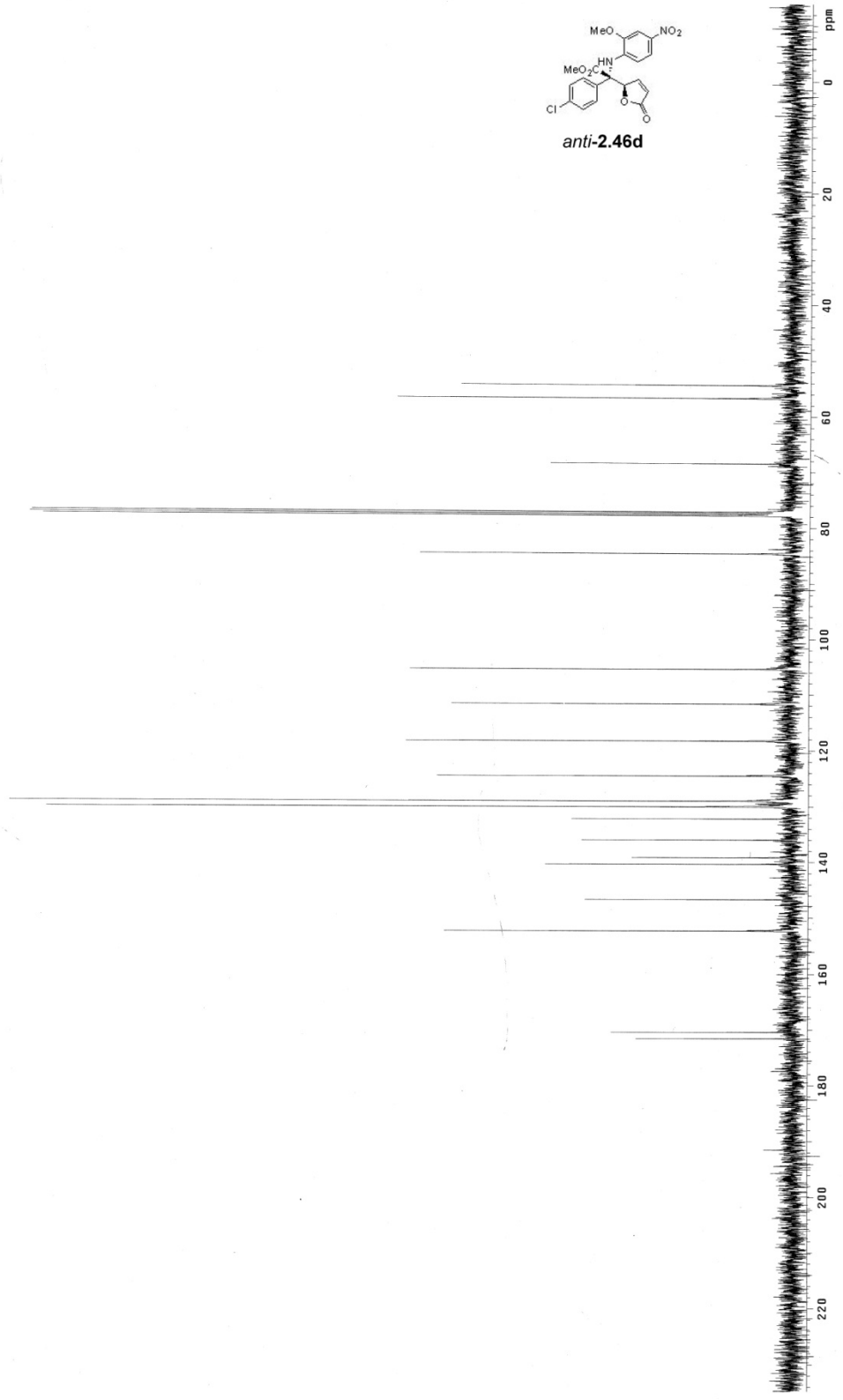
MeO
NO2
HN
MeO2C
Cl
O
O
anti-2.46d
ppm
0
20
40
60
80
100
120
140
160
180
200
220

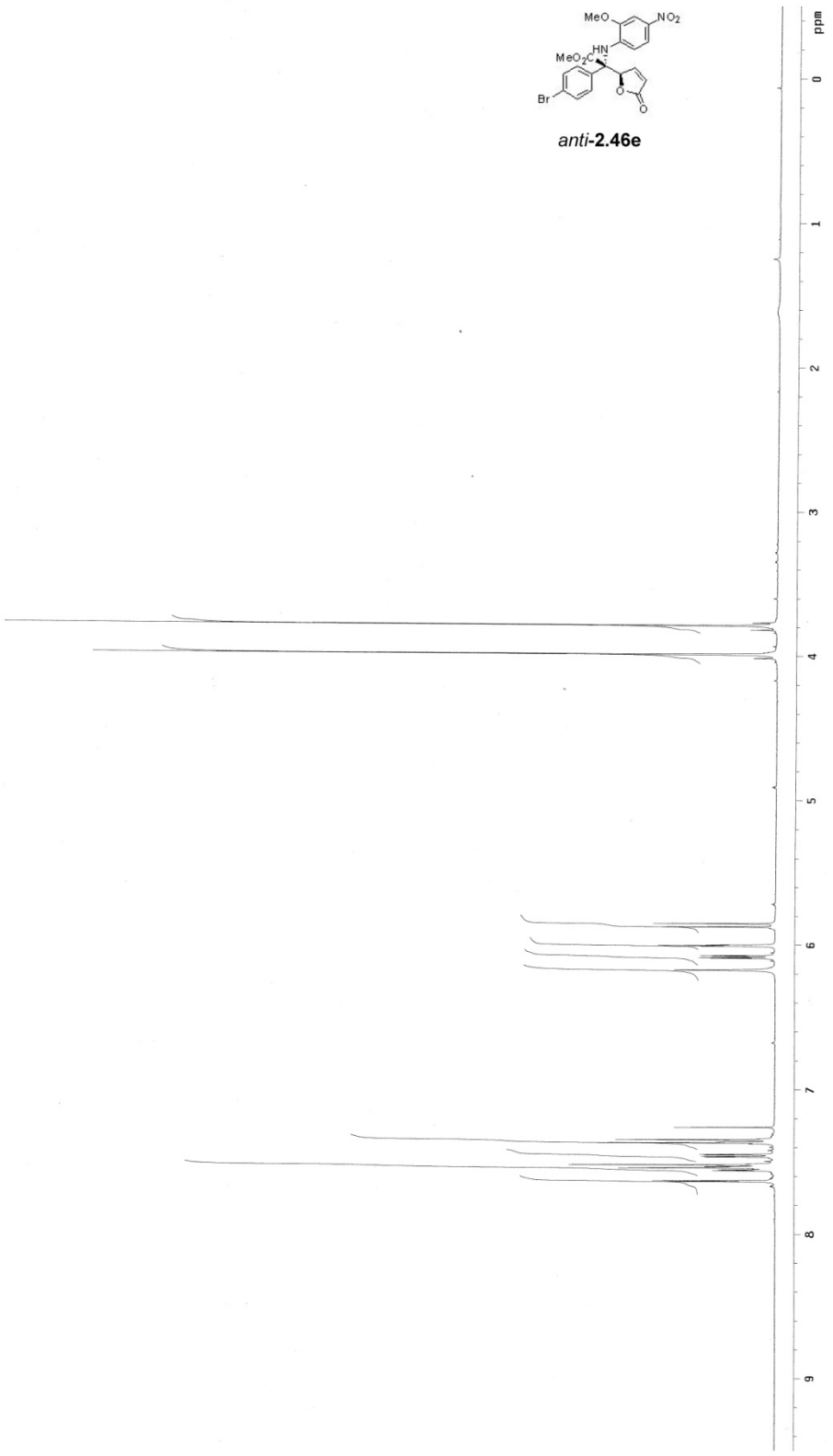

anti-**2.46e**


MeO
NO2
HN
MeO2C
Br
O
O
ppm
0
20
40
60
80
100
120
140
160
180
200
220

anti-**2.46e**

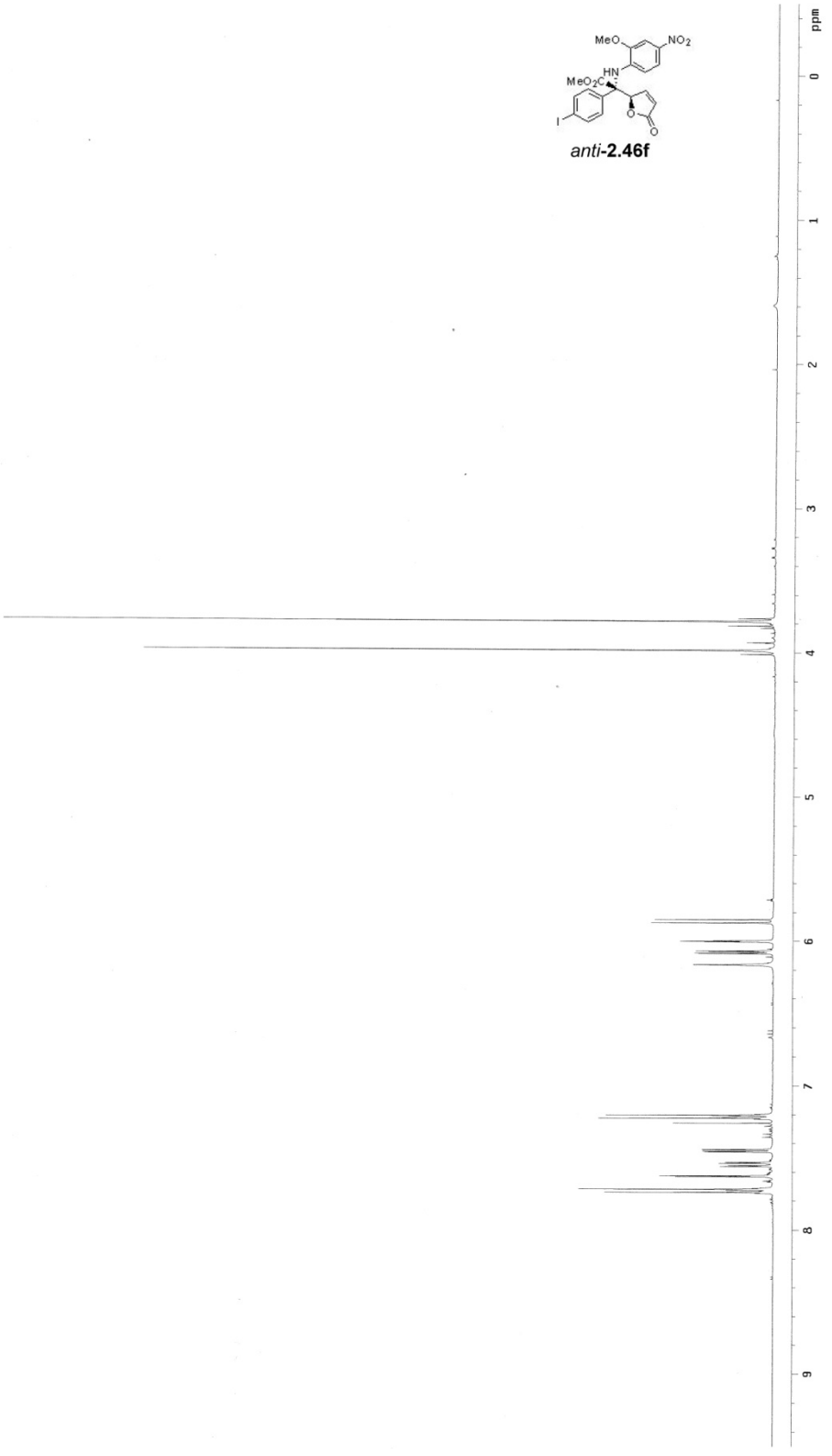
MeO
NO2
HN
MeO2C
I
O
O
anti-2.46f
ppm
0
1
2
3
4
5
6
7
8
9

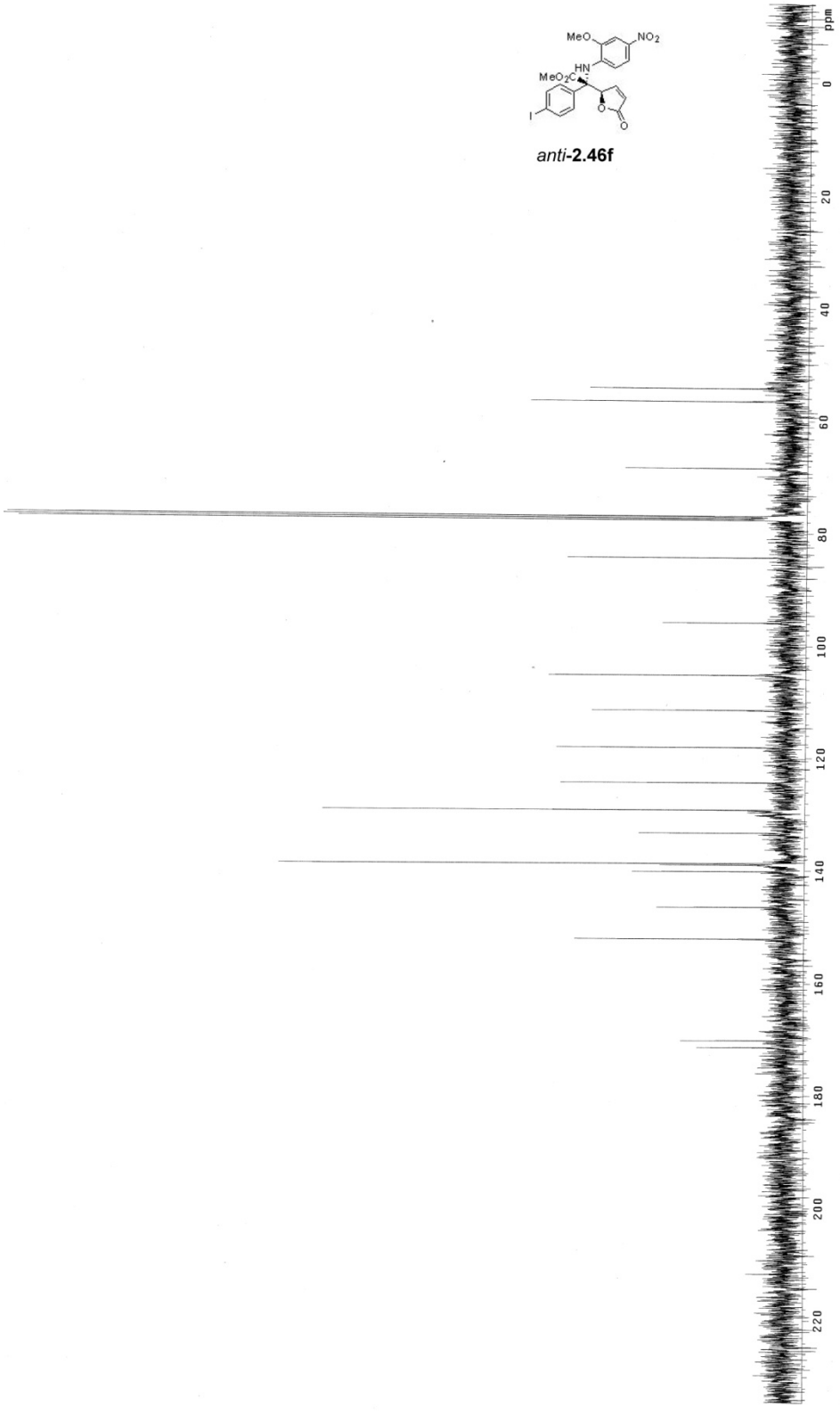

anti-**2.46f**

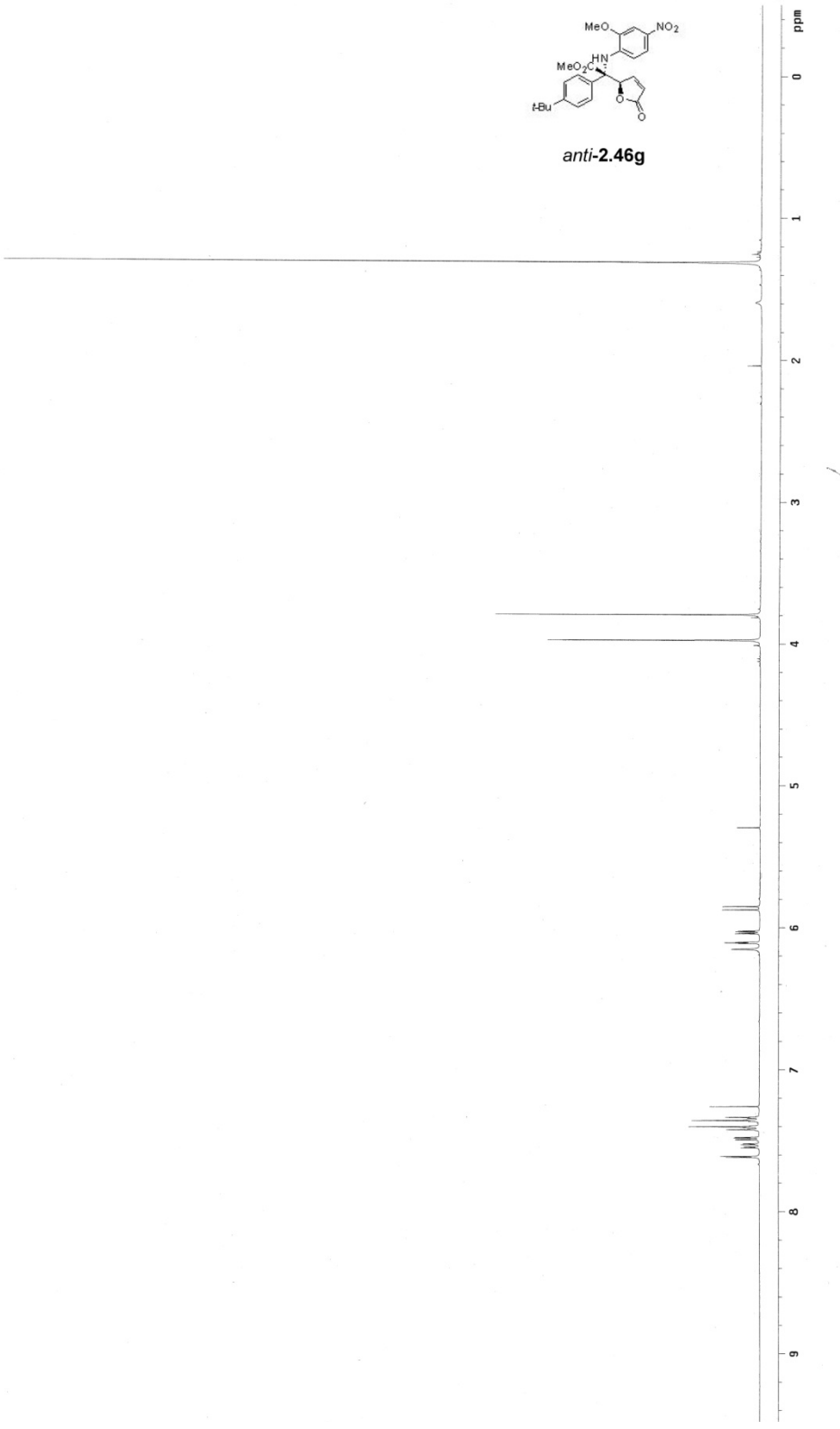

anti-**2.46g**


MeO
NO2
HN
MeO2C
t-Bu
O
O
anti-2.46g
ppm
0
20
40
60
80
100
120
140
160
180
200
220

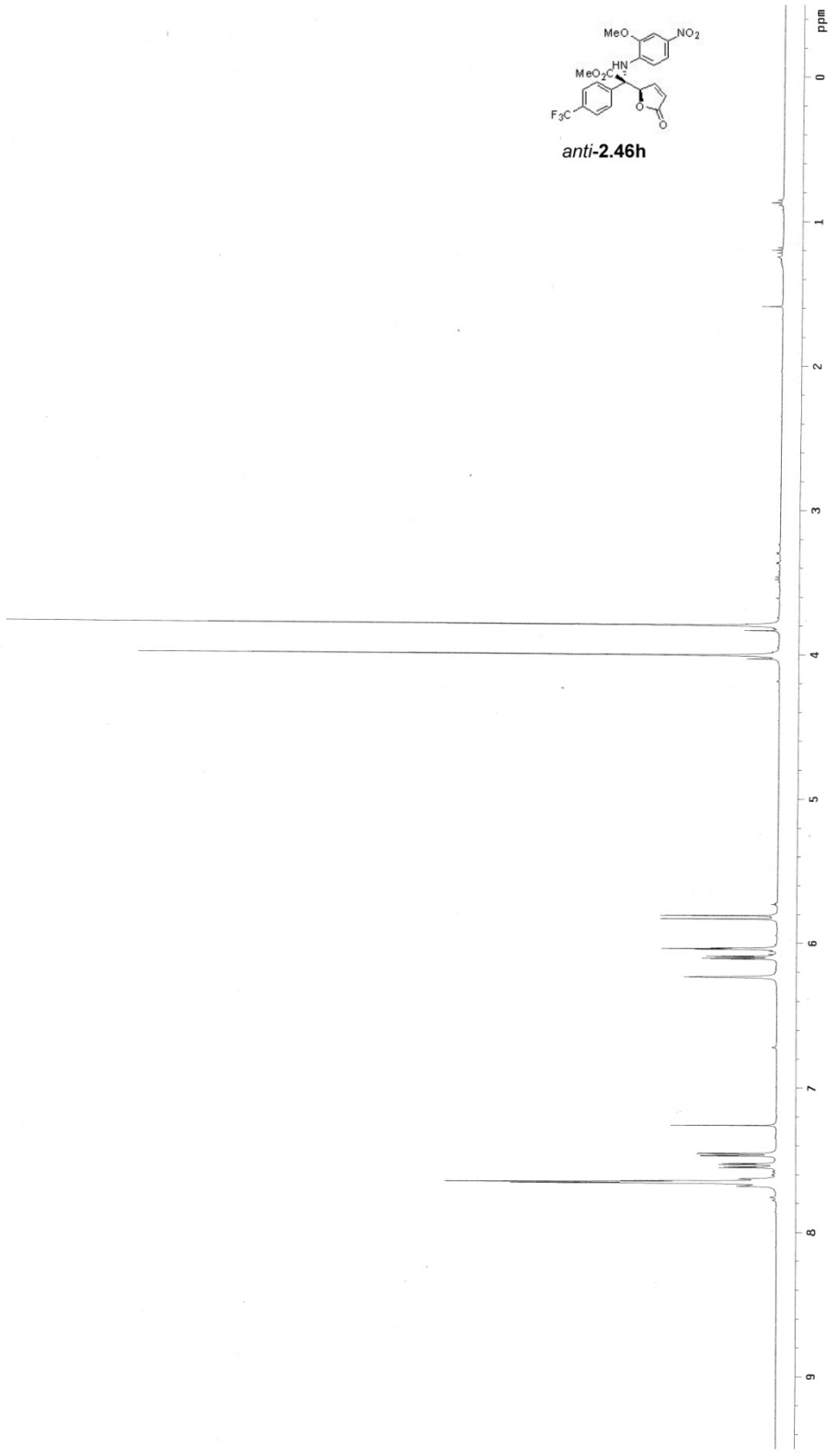
MeO
NO2
HN
MeO2C
F3C
O
O
anti-2.46h
ppm
0
1
2
3
4
5
6
7
8
9

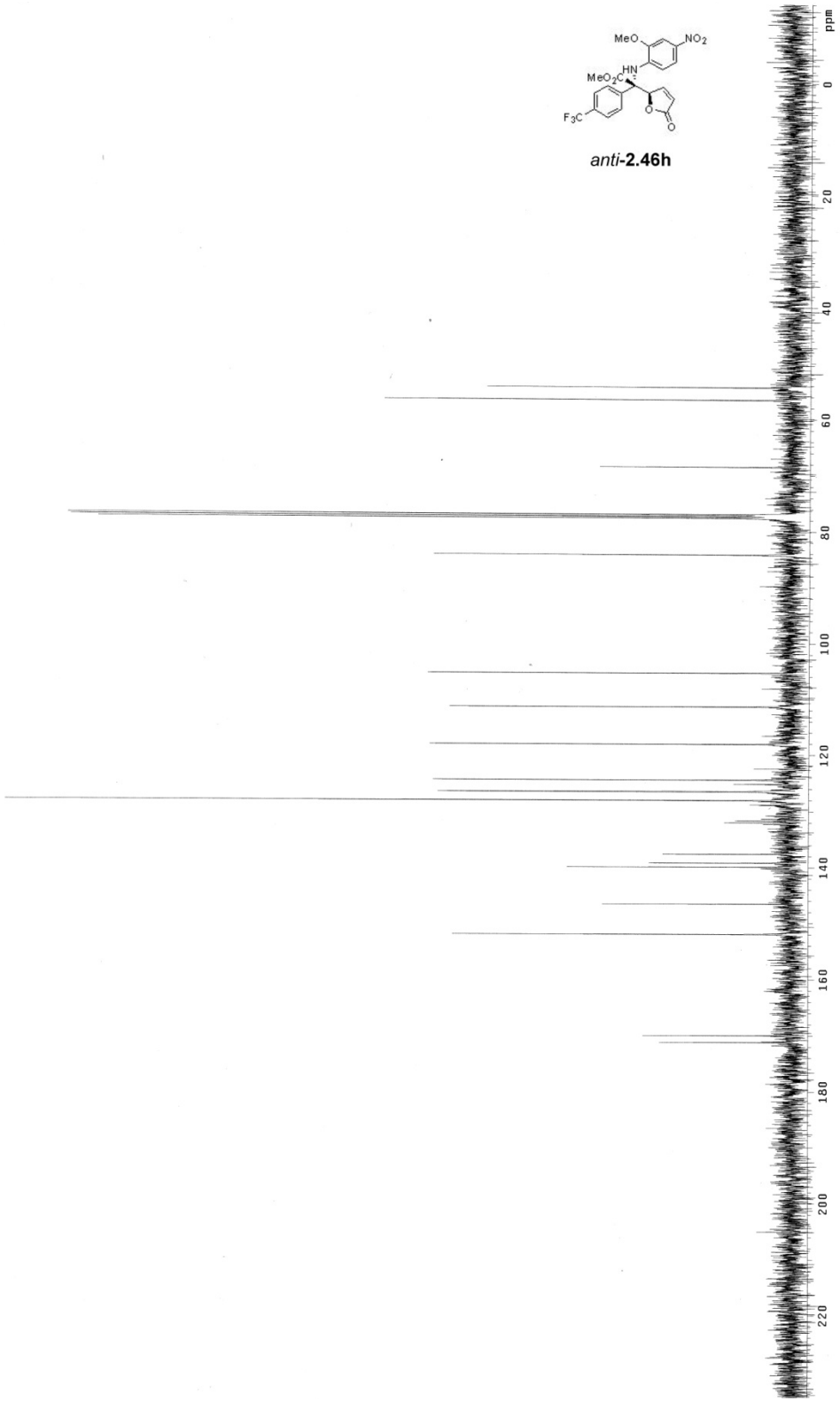
MeO
NO2
HN
MeO2C
F3C
O
O
anti-2.46h
ppm
0
20
40
60
80
100
120
140
160
180
200
220

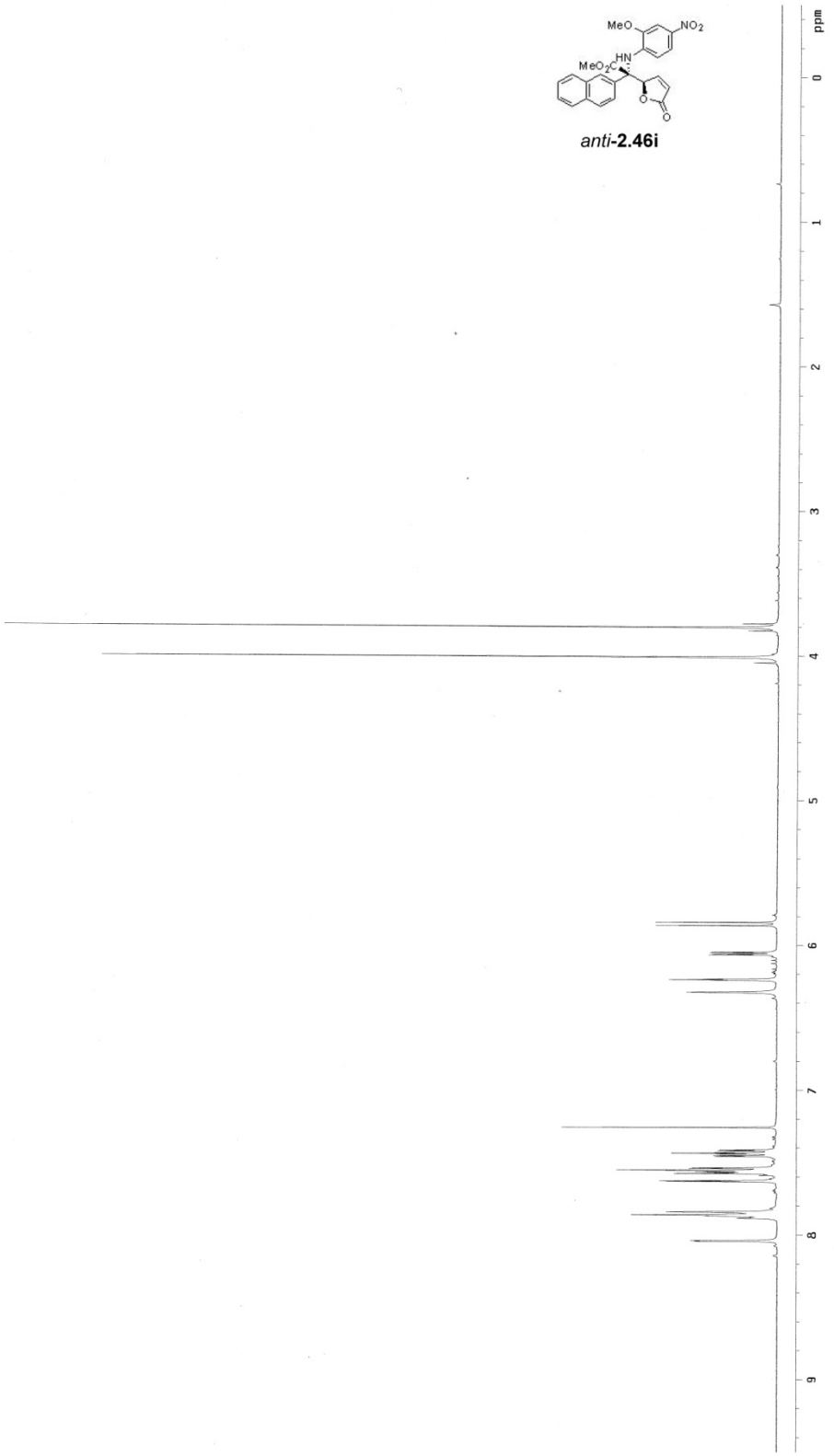

anti-**2.46i**

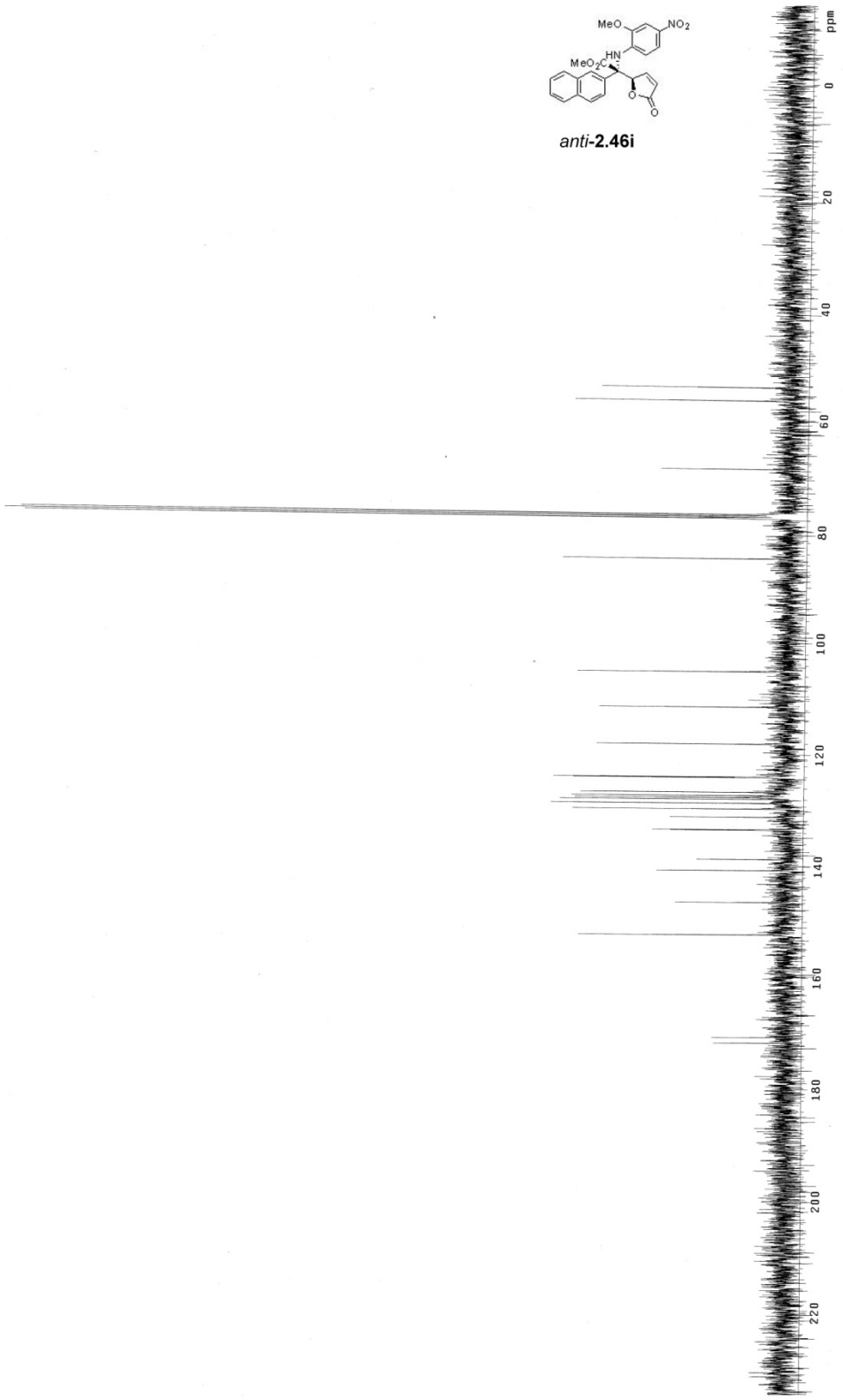

anti-**2.46i**


MeO
NO2
HN
MeO2C
O
O
O
O
anti-2.46j
ppm
0
1
2
3
4
5
6
7
8
9

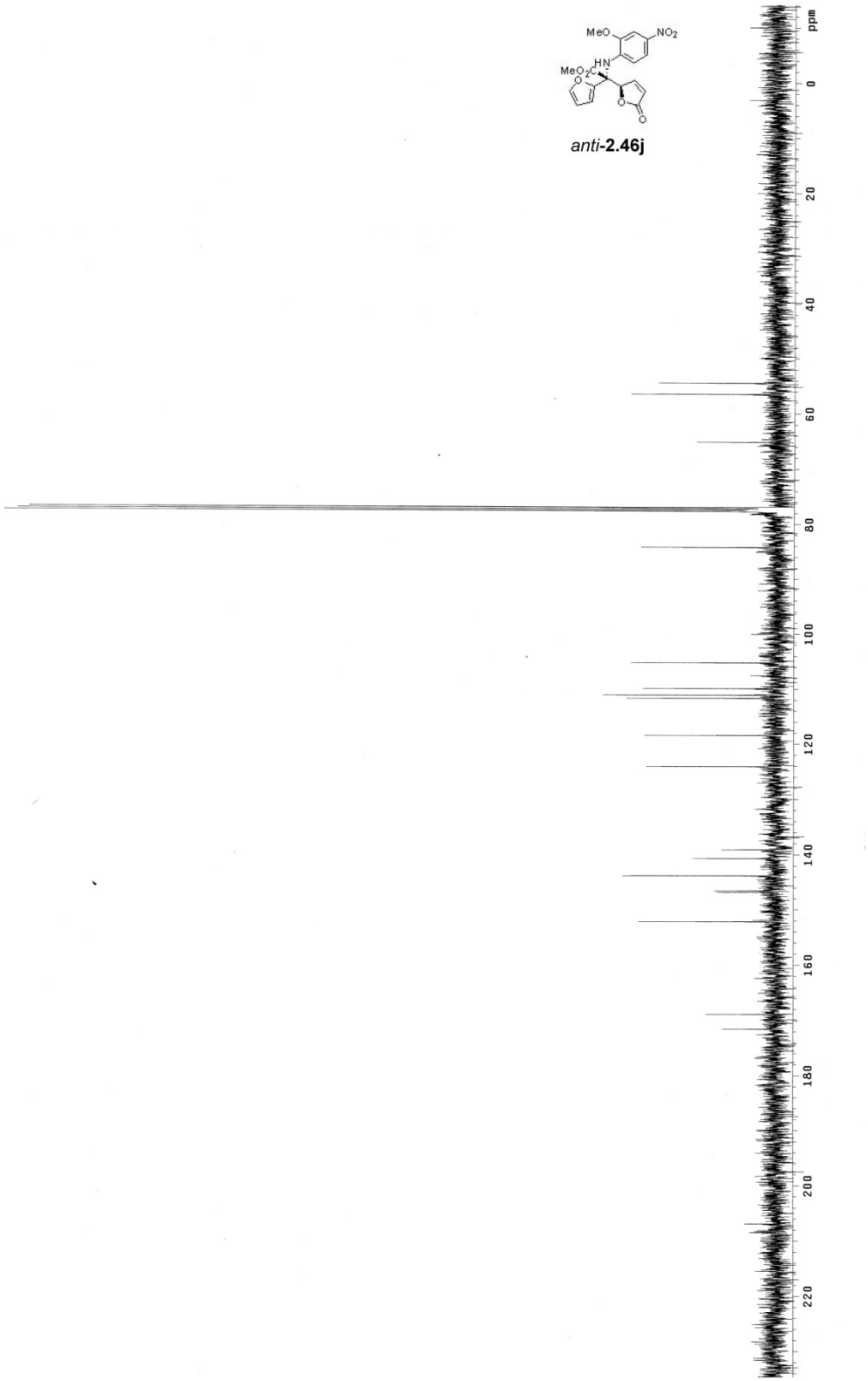

anti-**2.46j**

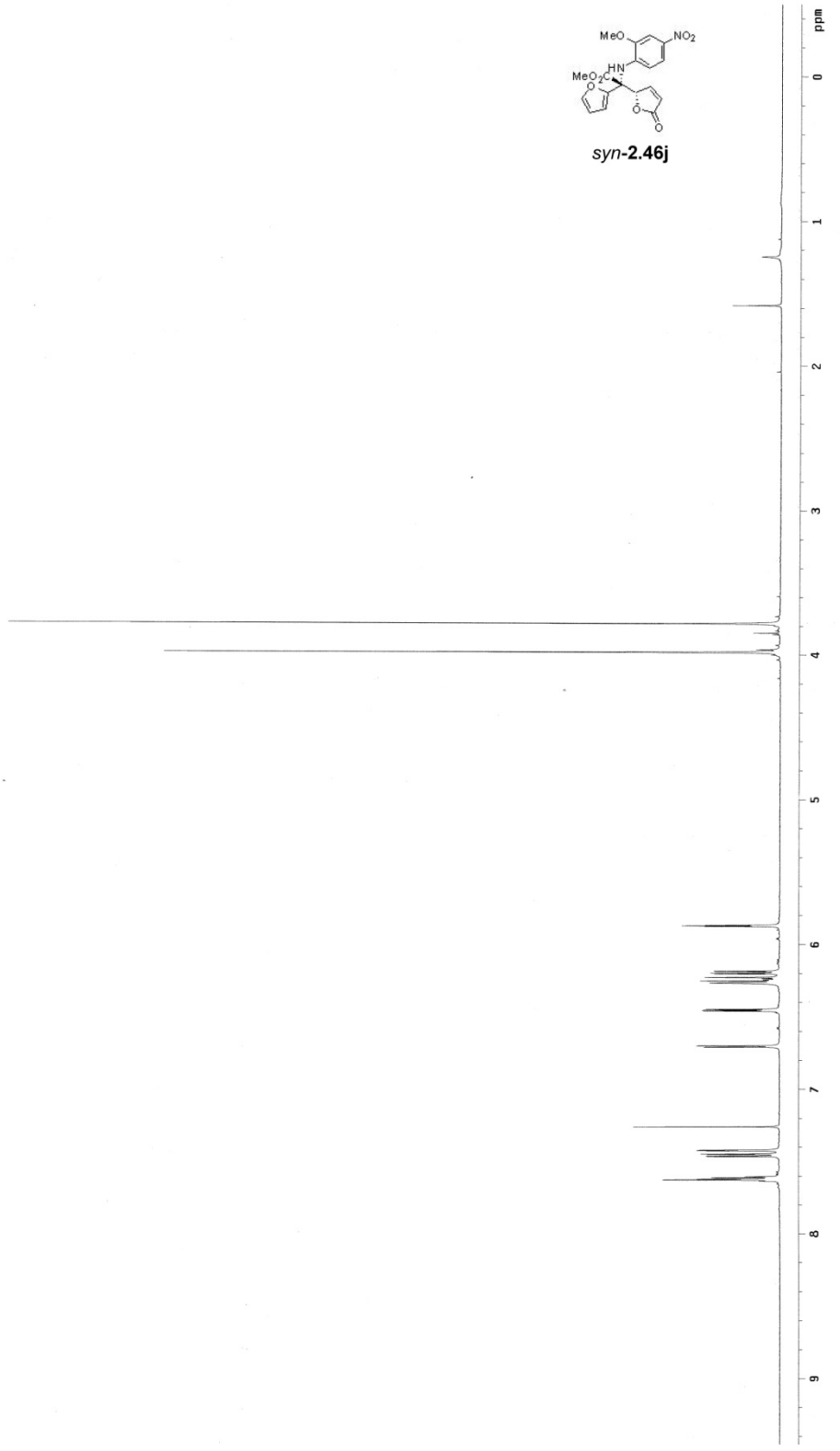

syn-**2.46j**

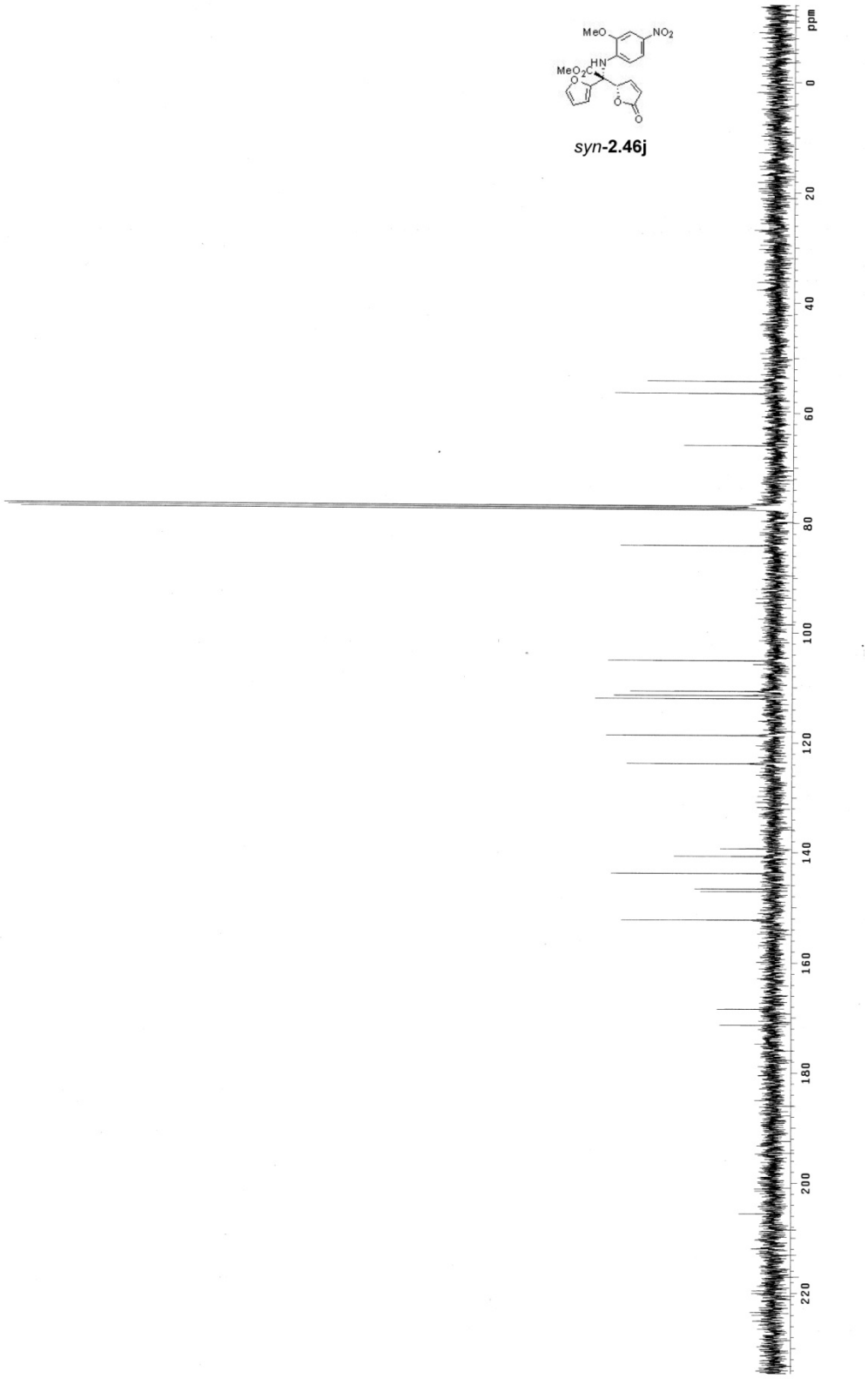

syn-**2.46j**


MeO
NO2
HN
MeO2C
S
O
O
anti-2.46k
ppm
0
1
2
3
4
5
6
7
8
9

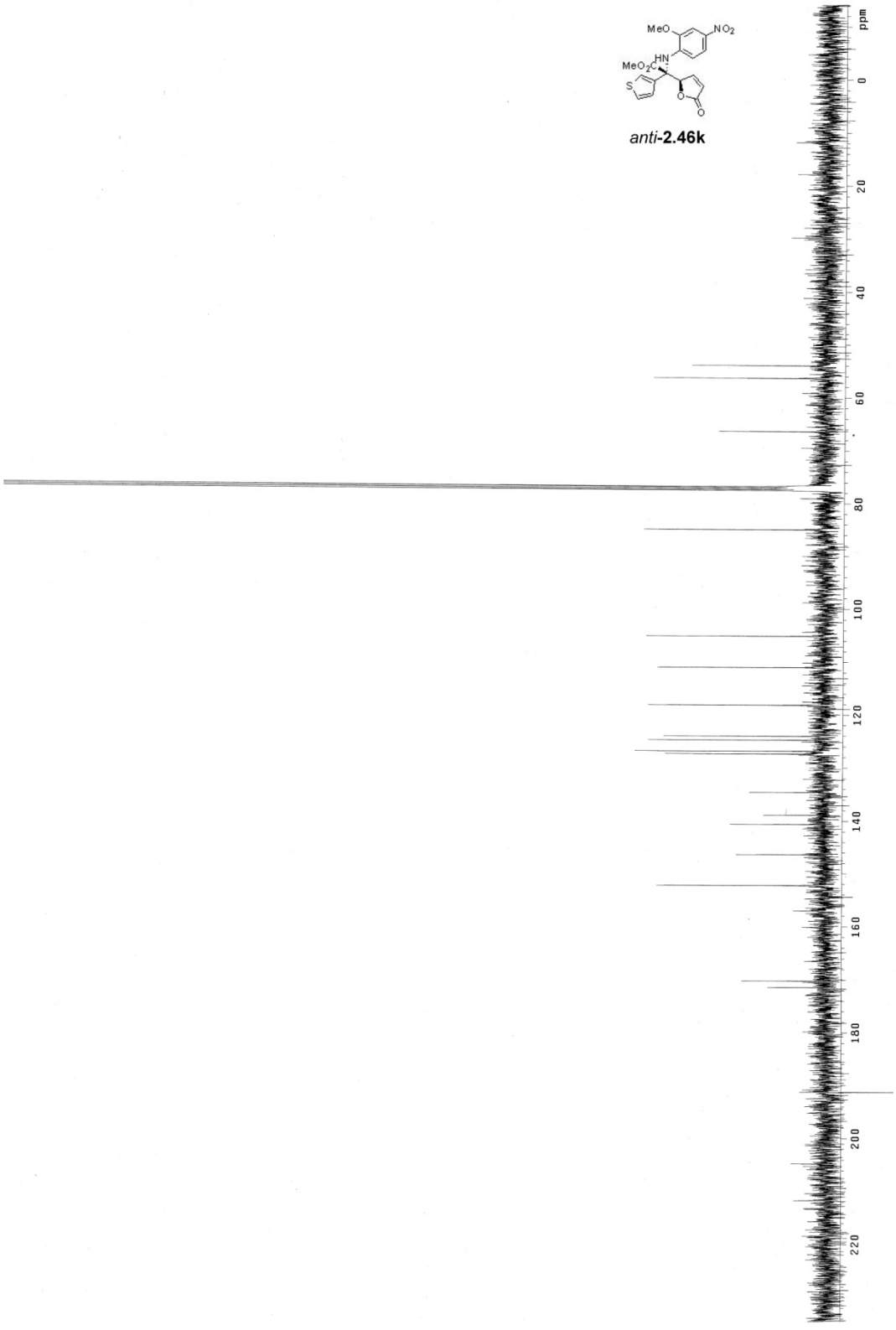
MeO
NO2
HN
MeO2C
S
O
O
anti-2.46k
ppm
0
20
40
60
80
100
120
140
160
180
200
220

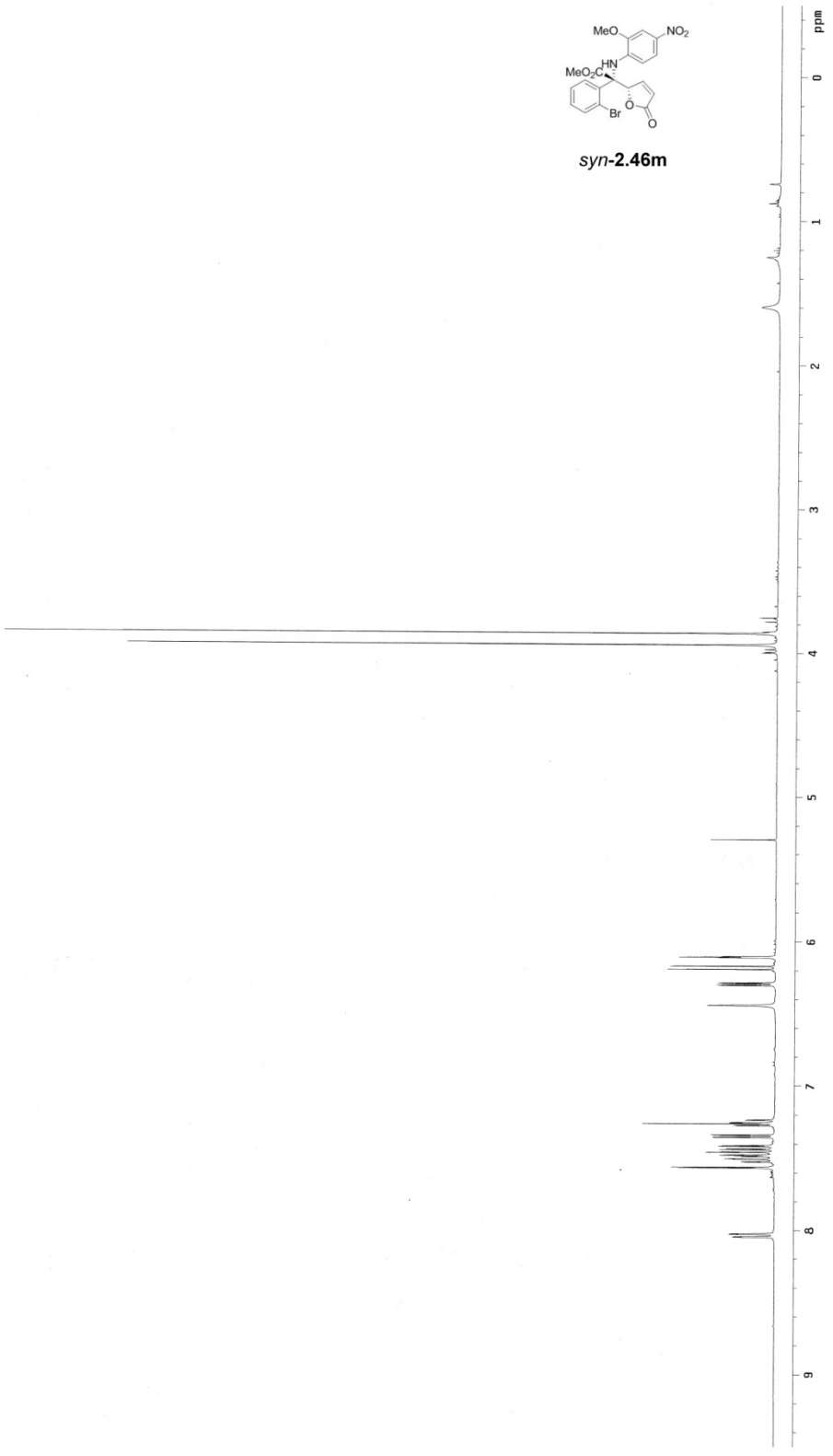

syn-**2.46m**

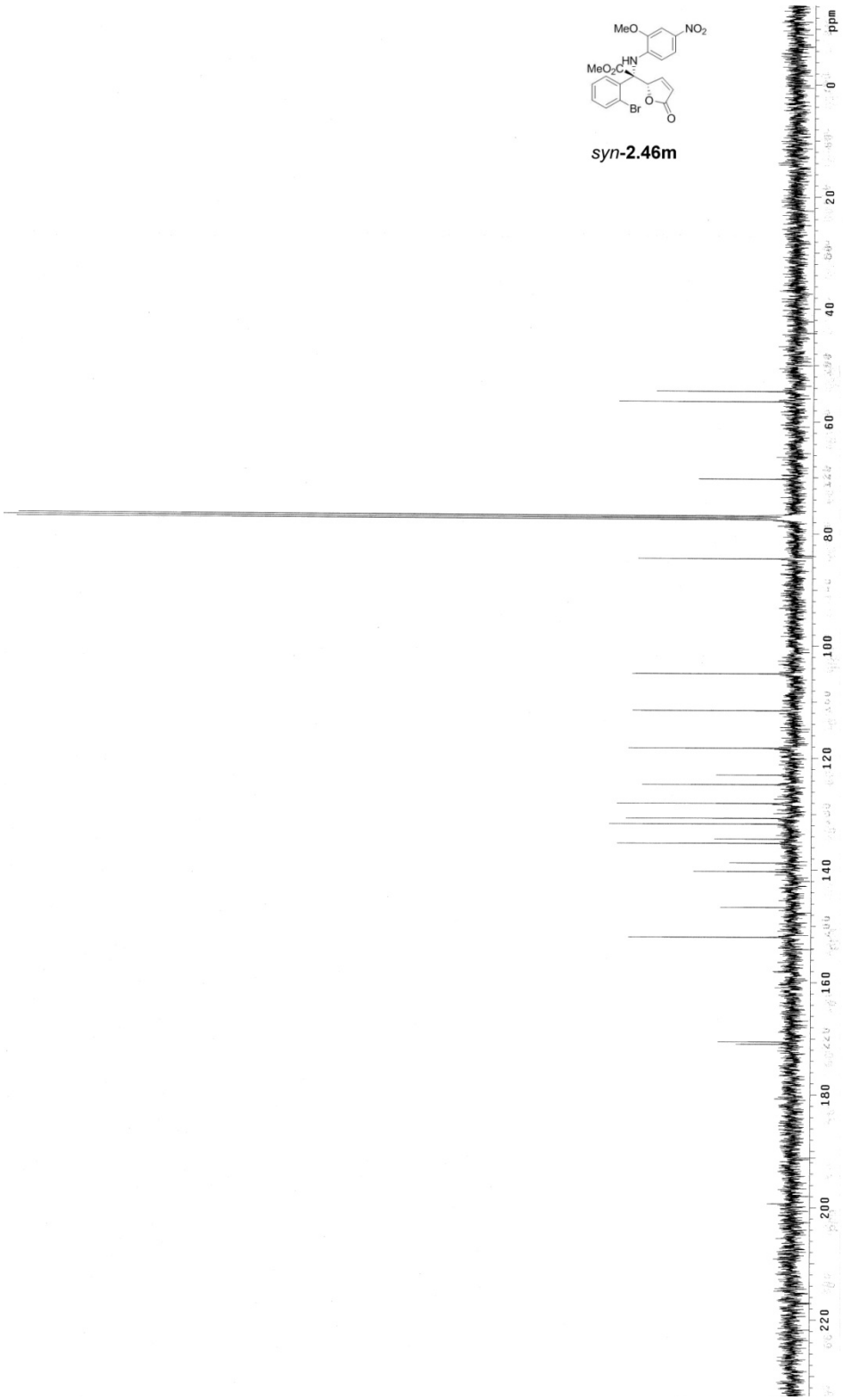
MeO
NO2
HN
MeO2C
Br
O
O
ppm
0
20
40
60
80
100
120
140
160
180
200
220

syn-**2.46m**

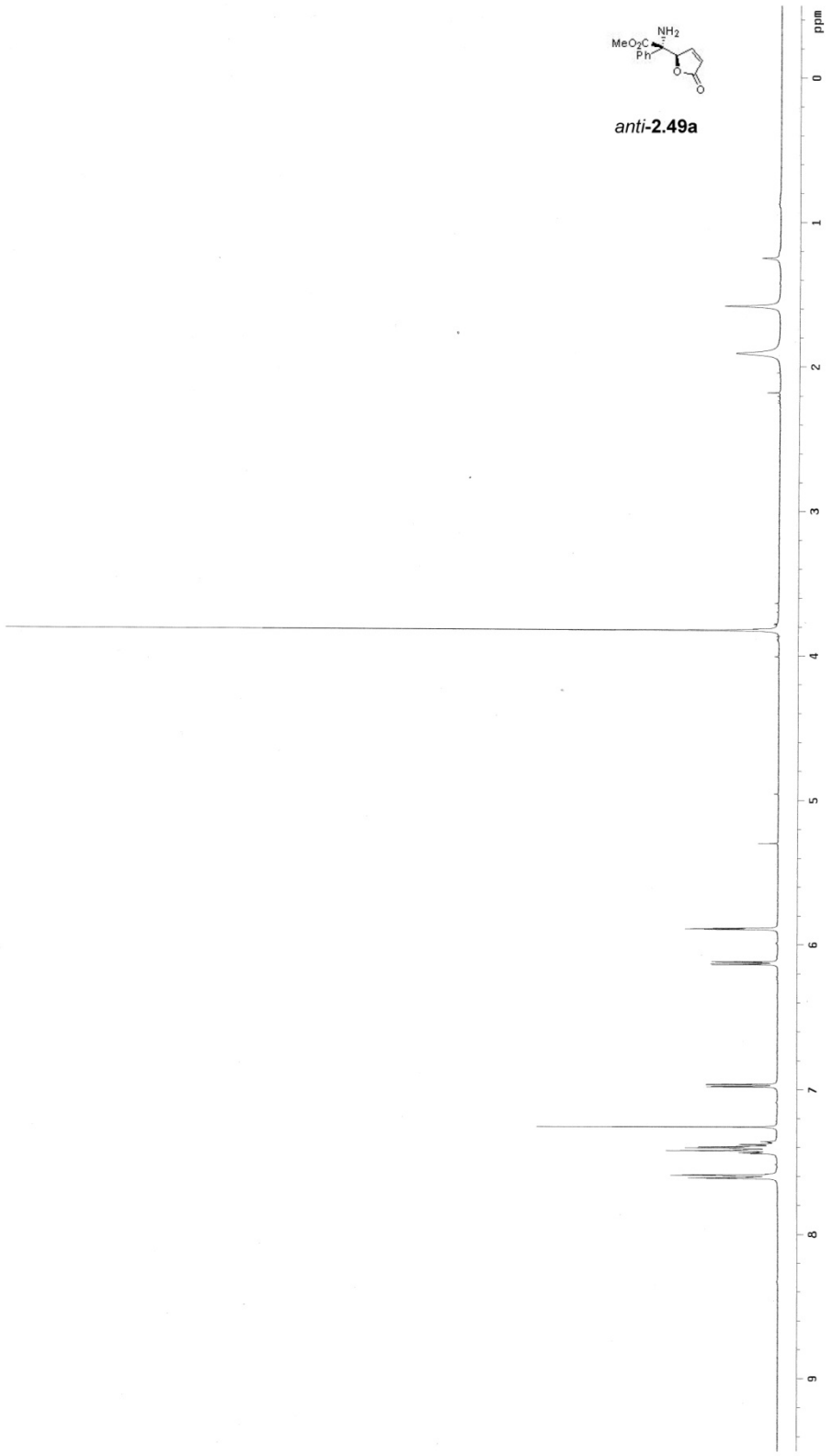
NH2
MeO2C
Ph
O
O
anti-2.49a
ppm
0
1
2
3
4
5
6
7
8
9

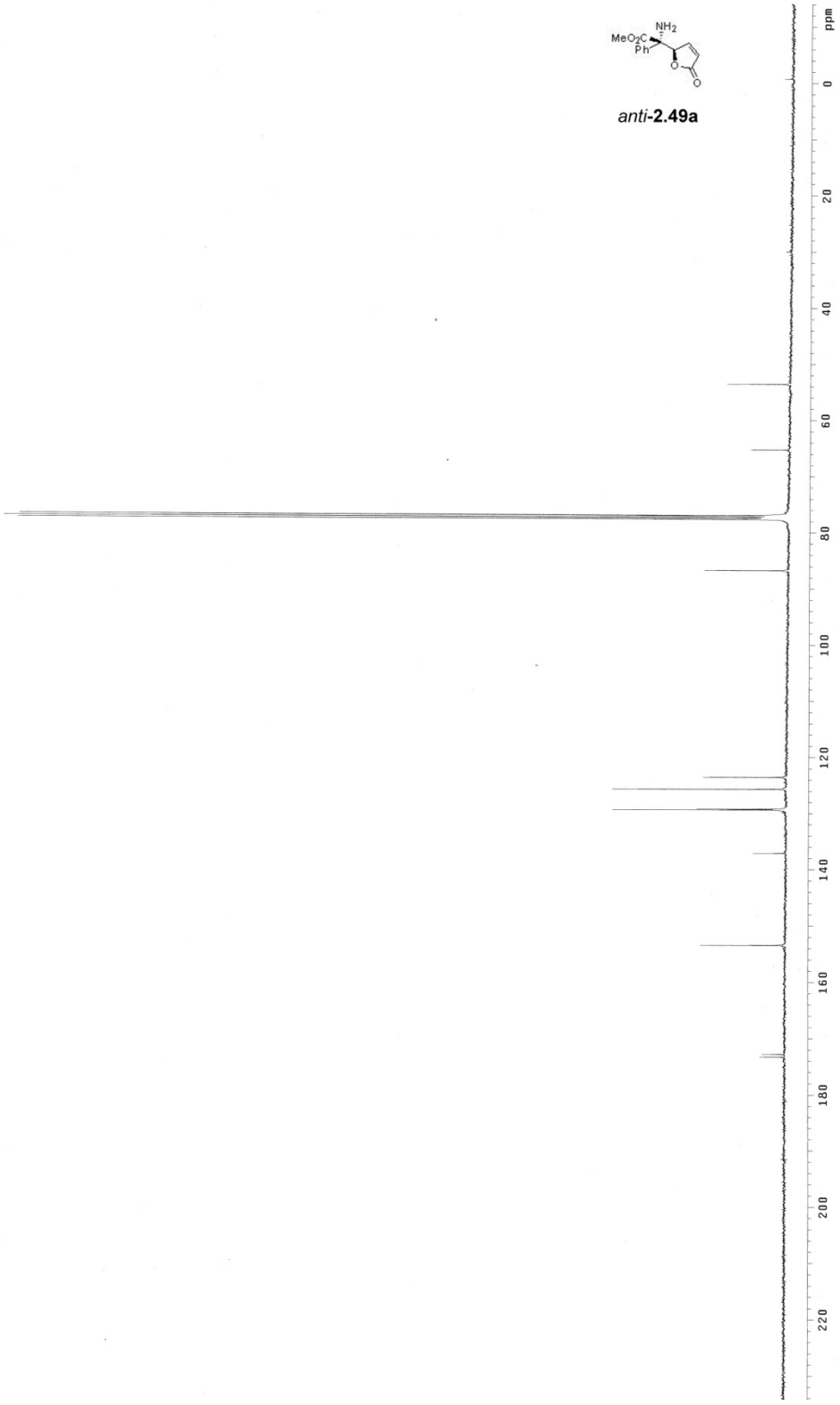
NH2
MeO2C
Ph
O
O
anti-2.49a
ppm
0
20
40
60
80
100
120
140
160
180
200
220


MeO
NO2
HN
MeO2C
Ph
O
O
anti-2.51a
ppm
0
1
2
3
4
5
6
7
8
9

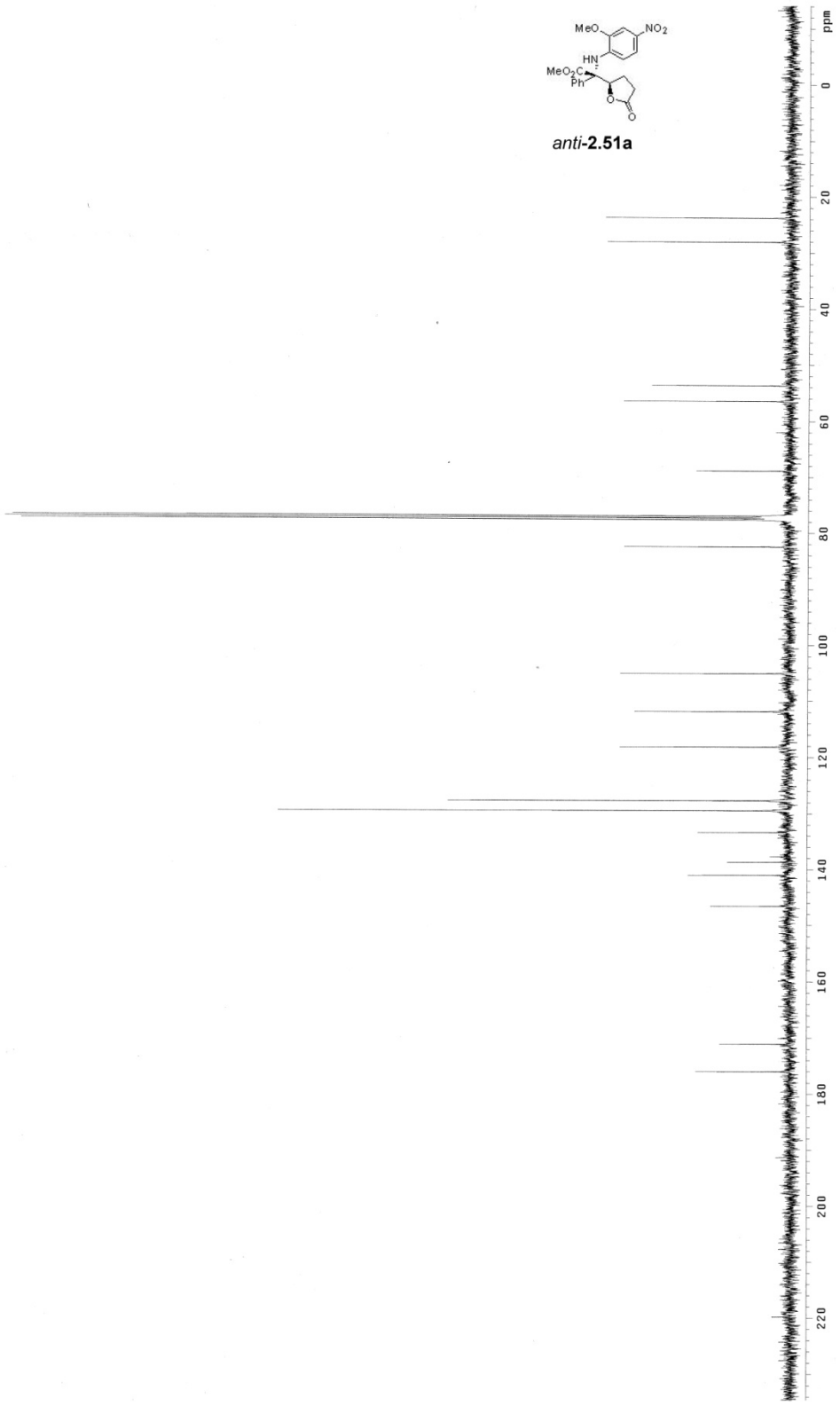
MeO
NO2
HN
MeO2C
Ph
O
O
anti-2.51a
ppm
0
20
40
60
80
100
120
140
160
180
200
220

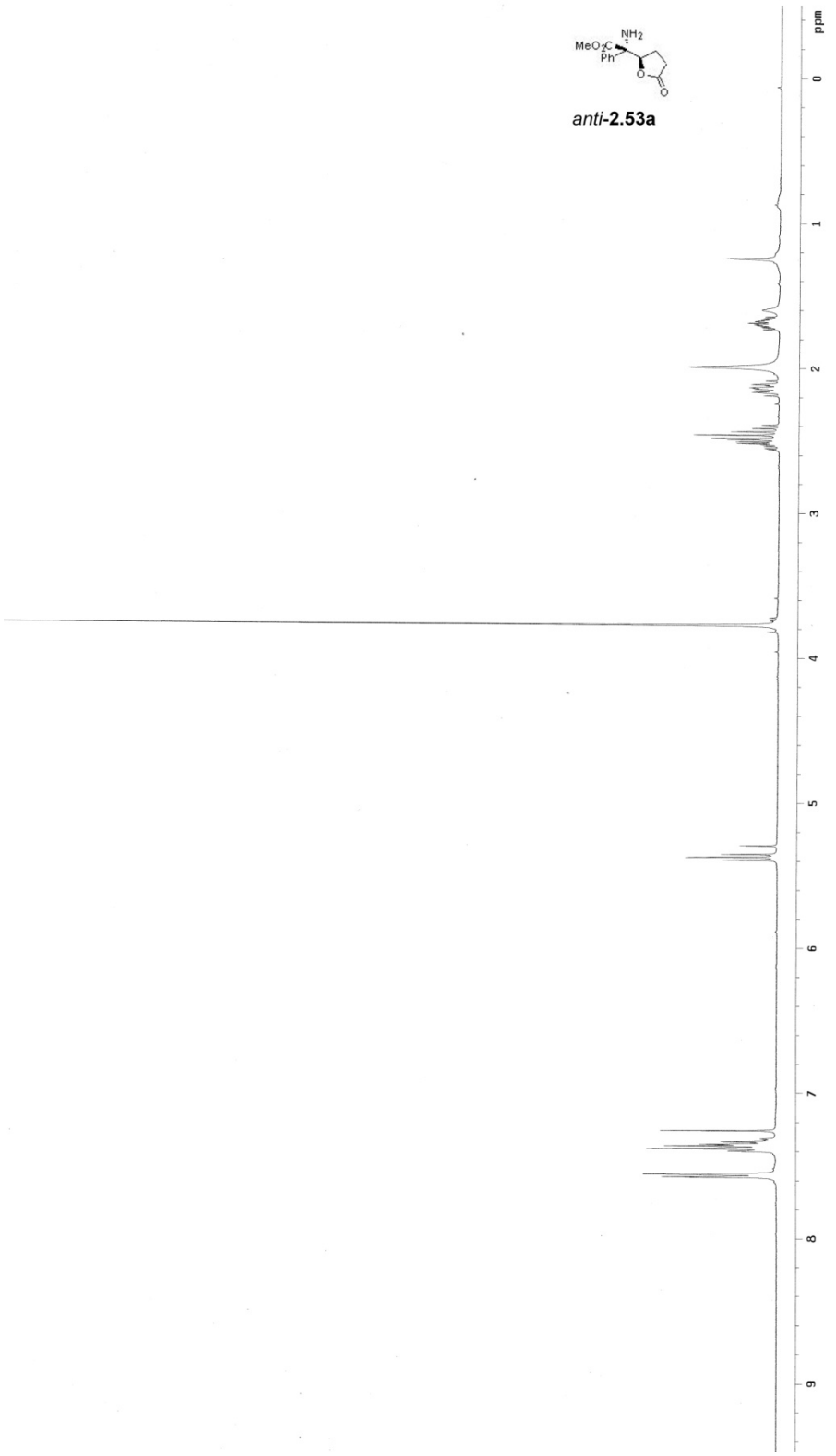
NH2
MeO2C
Ph
O
O
anti-2.53a
ppm
0
1
2
3
4
5
6
7
8
9

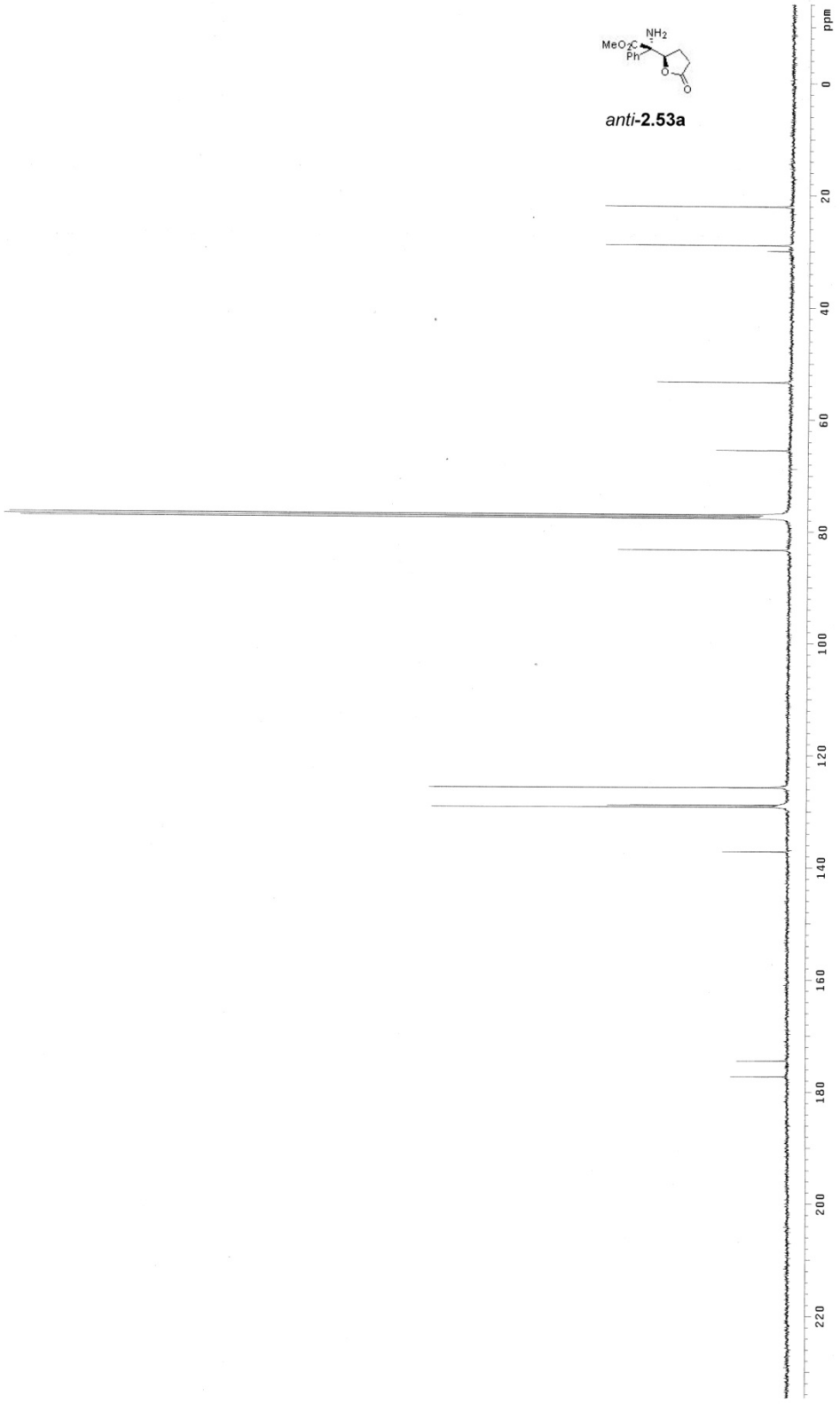
NH2
MeO2C
Ph
O
O
anti-2.53a
ppm
0
20
40
60
80
100
120
140
160
180
200
220

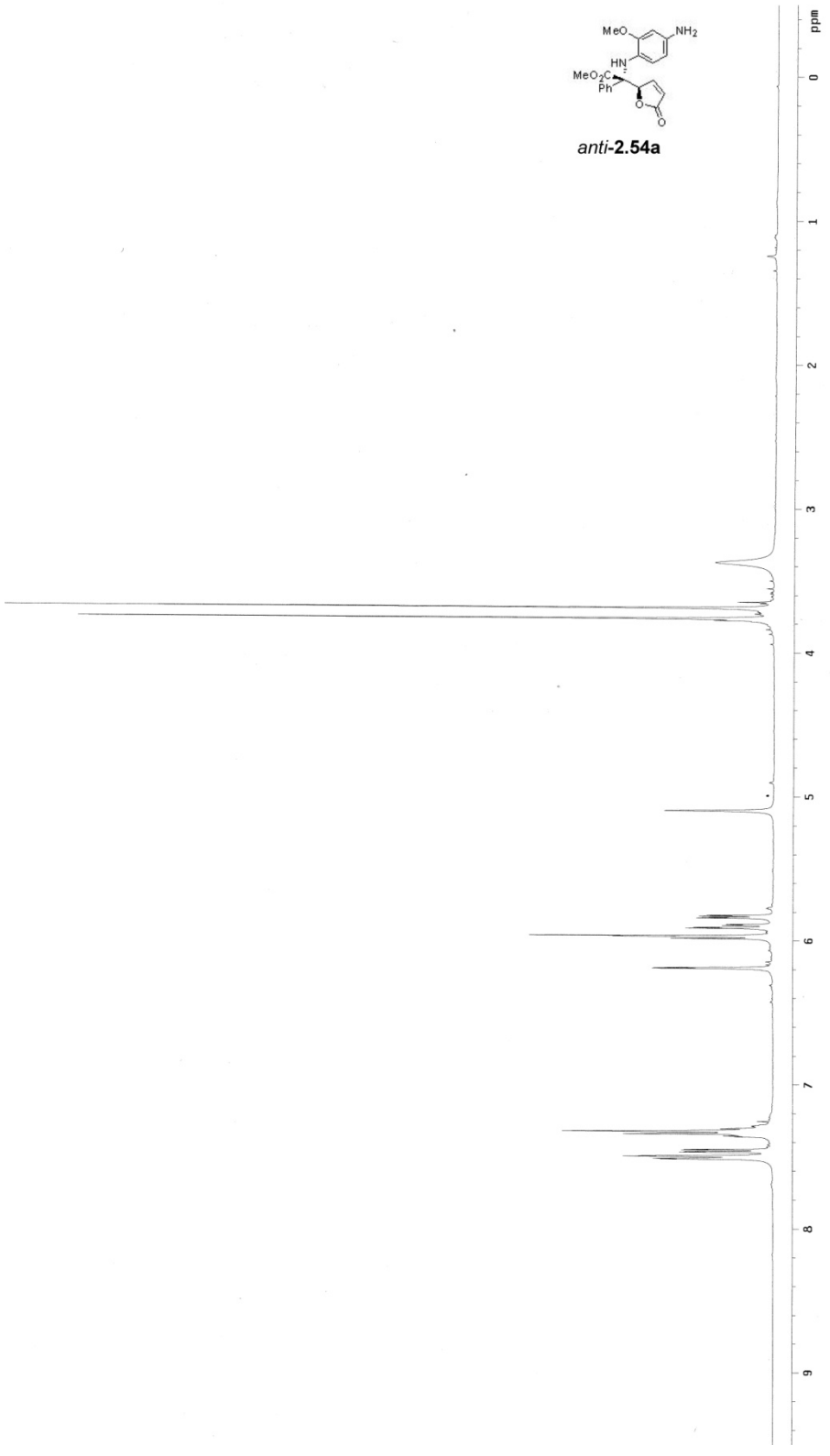

anti-**2.54a**

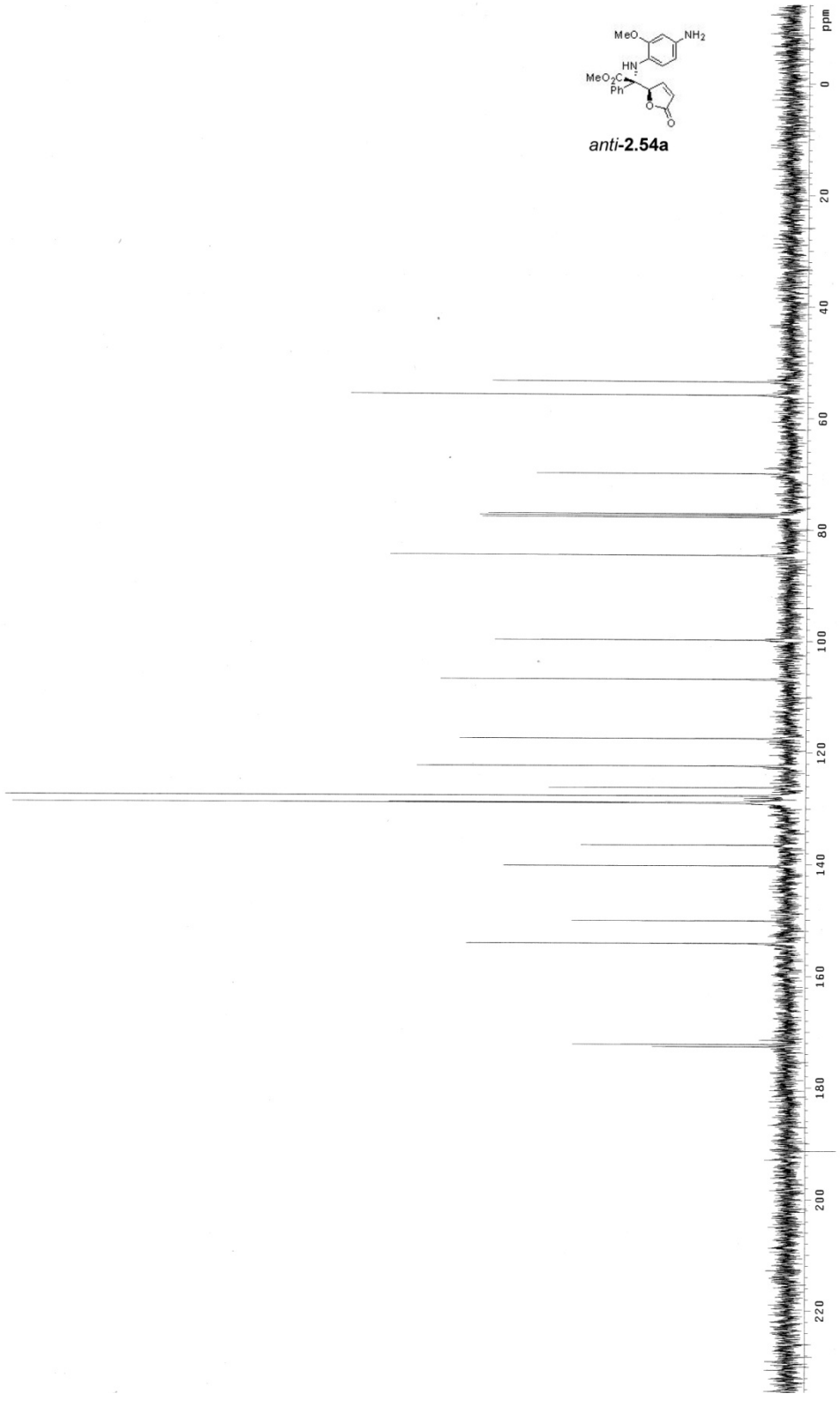
MeO
NH2
HN
MeO2C
Ph
O
O
anti-2.54a
ppm
0
20
40
60
80
100
120
140
160
180
200
220

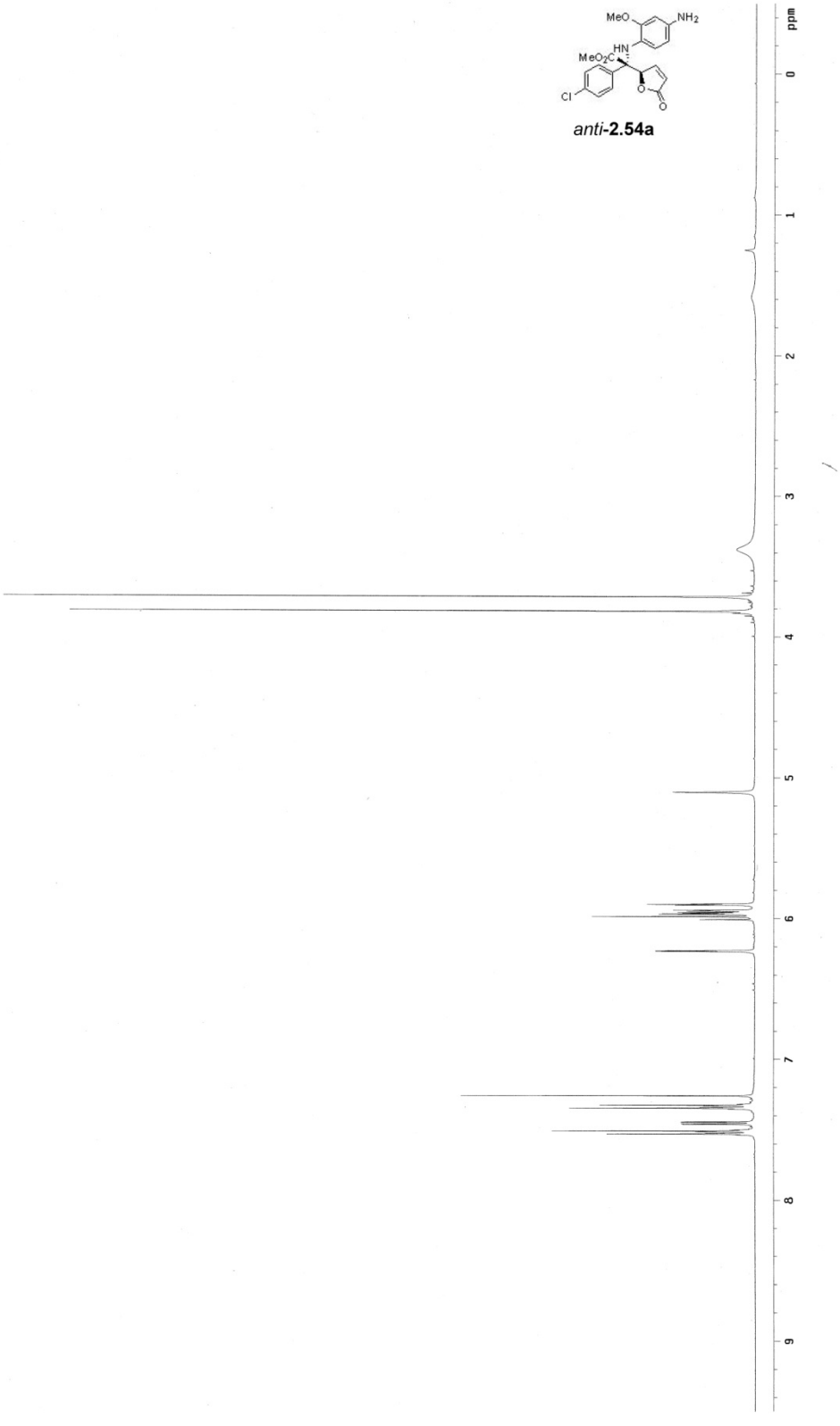
MeO
NH2
HN
MeO2C
Cl
O
O
anti-2.54a
ppm
0
1
2
3
4
5
6
7
8
9

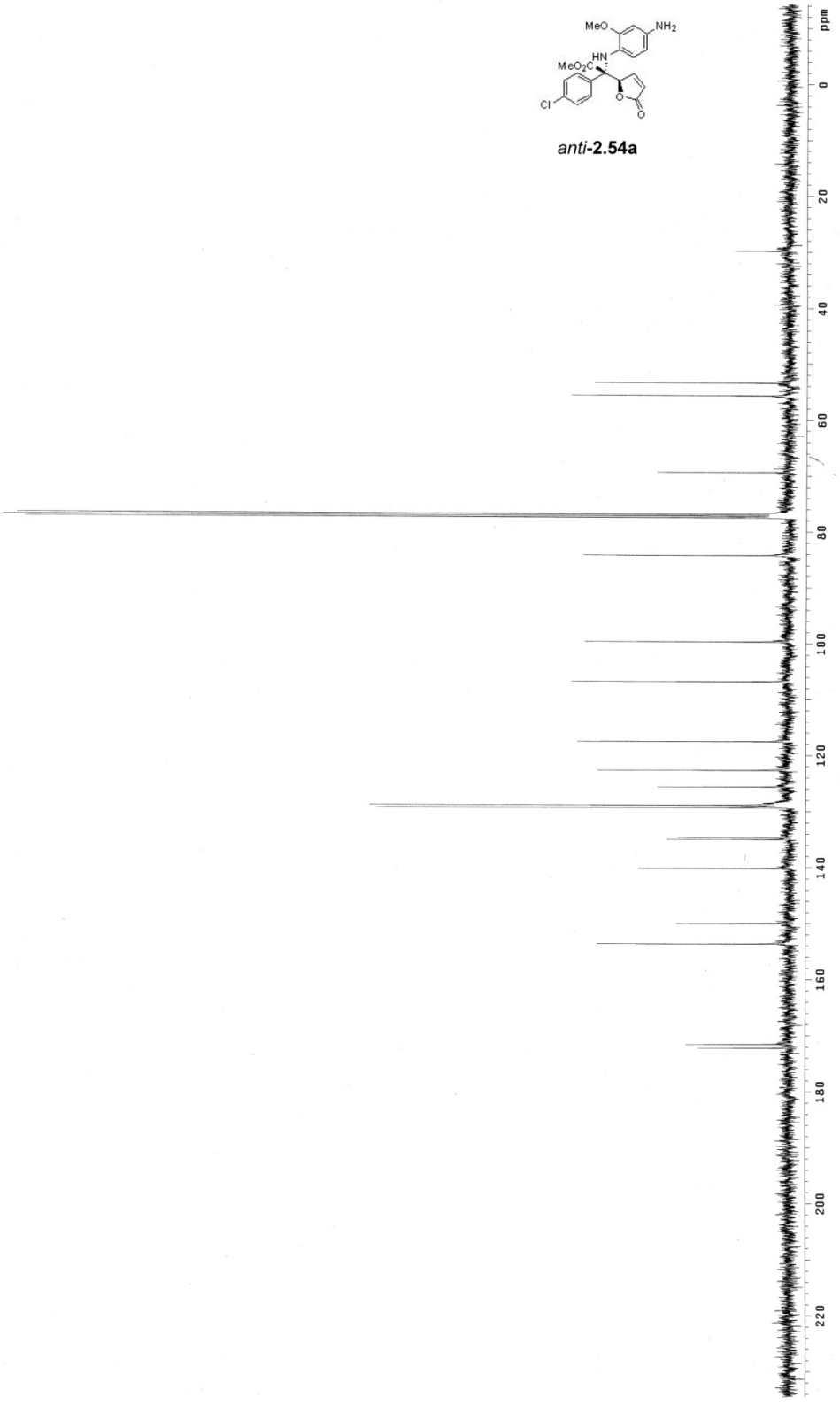
MeO
NH2
HN
MeO2C
Cl
O
O
anti-2.54a
ppm
0
20
40
60
80
100
120
140
160
180
200
220

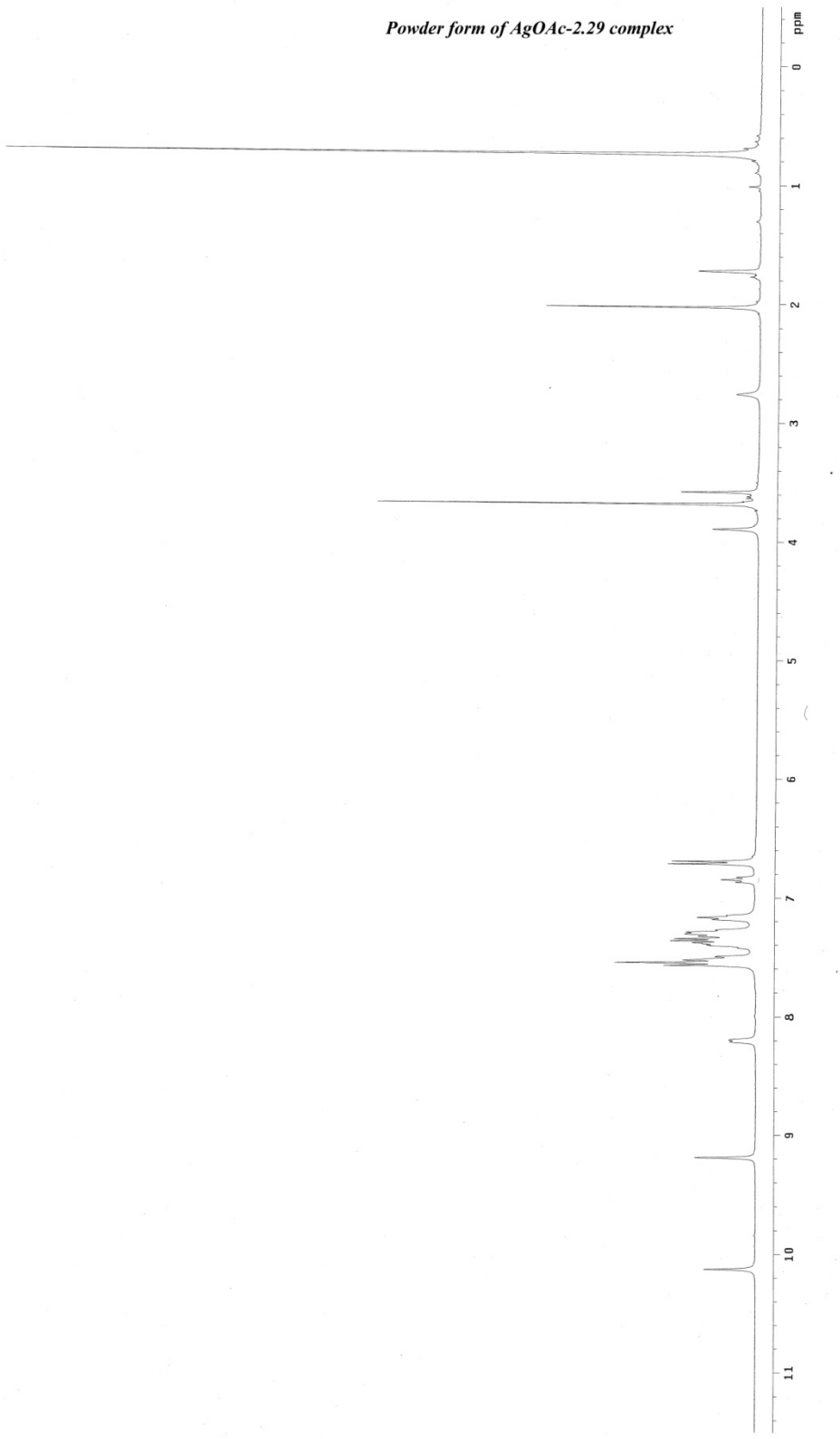
Powder form of AgOAc-2.29 complex
ppm
0
1
2
3
4
5
6
7
8
9
10
11

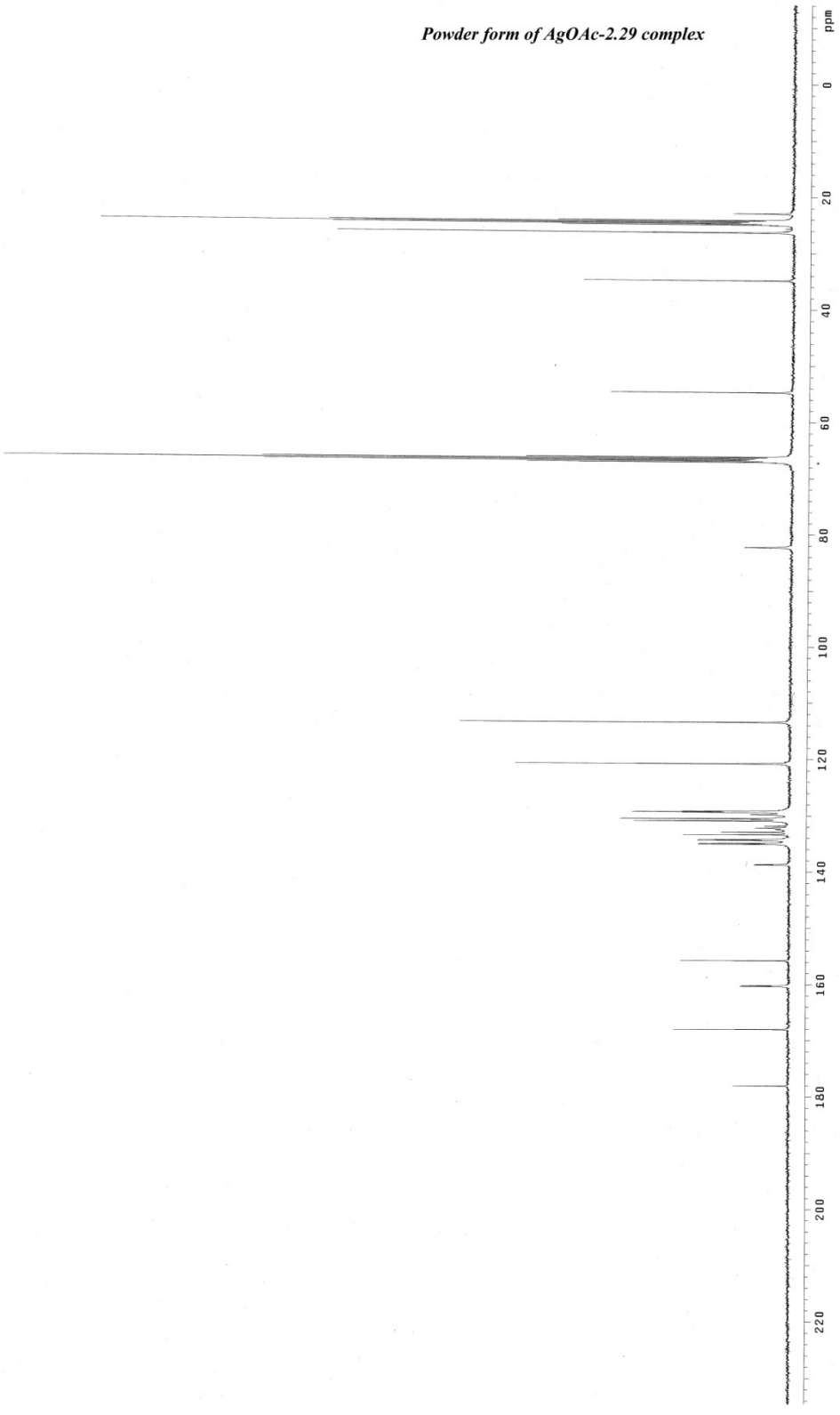
Powder form of AgOAc-2.29 complex
ppm
0
20
40
60
80
100
120
140
160
180
200
220

400 MHz ^{1}H NMR spectra of powder form of AgOAc-**2.29** complex in d_8-THF at various temperatures

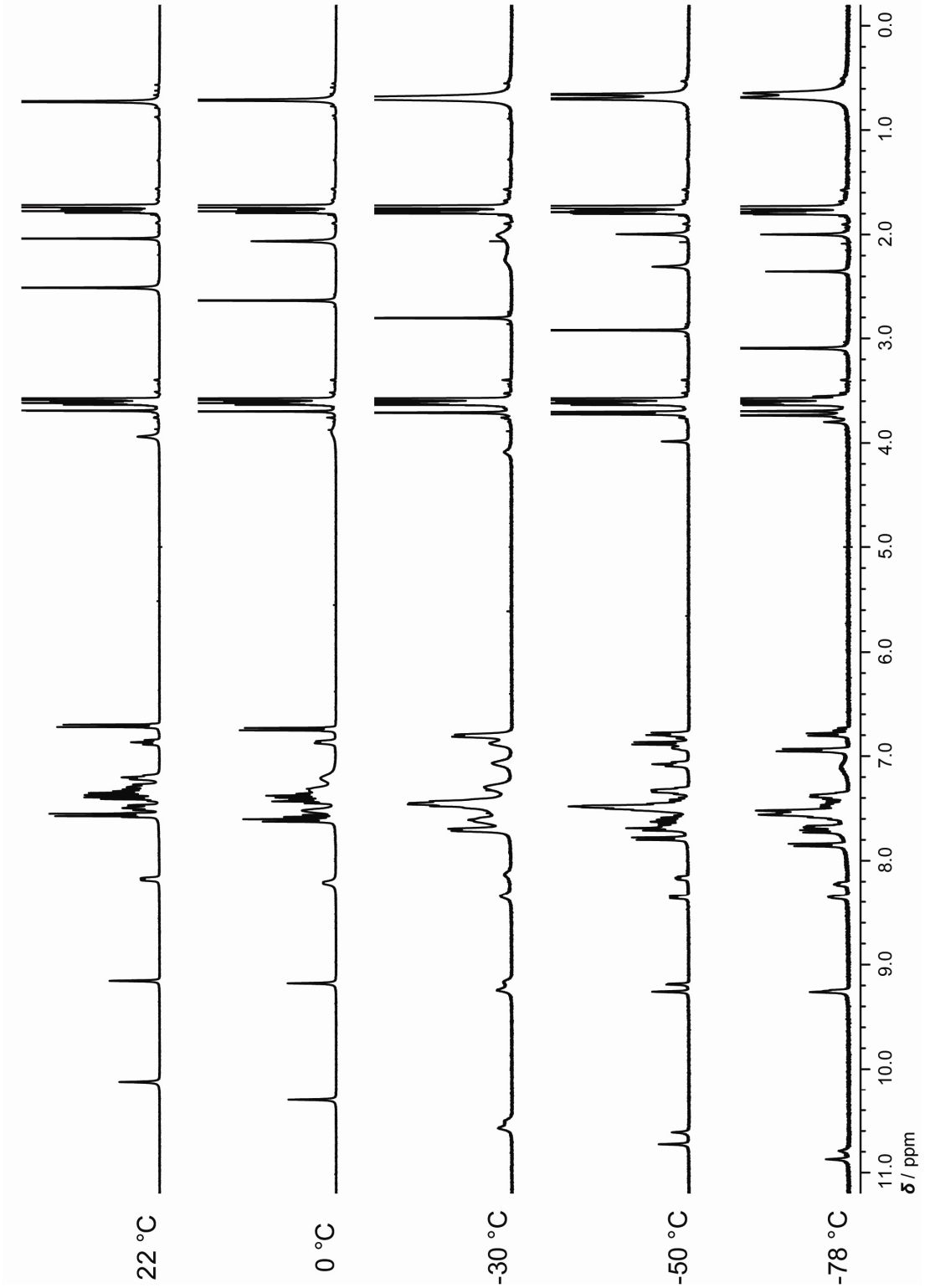

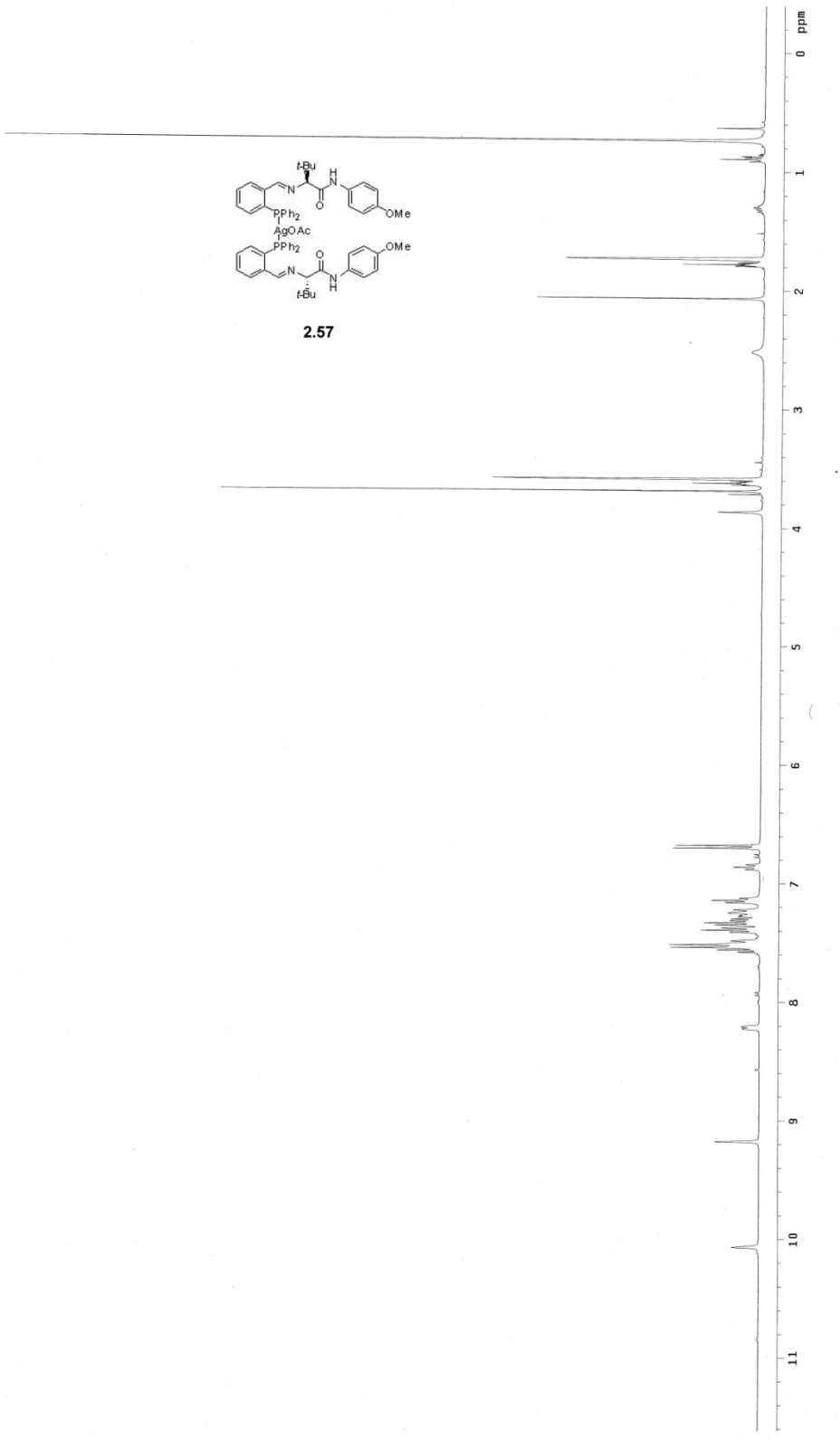
t-Bu
PPh2
AgOAc
OMe
2.57
ppm

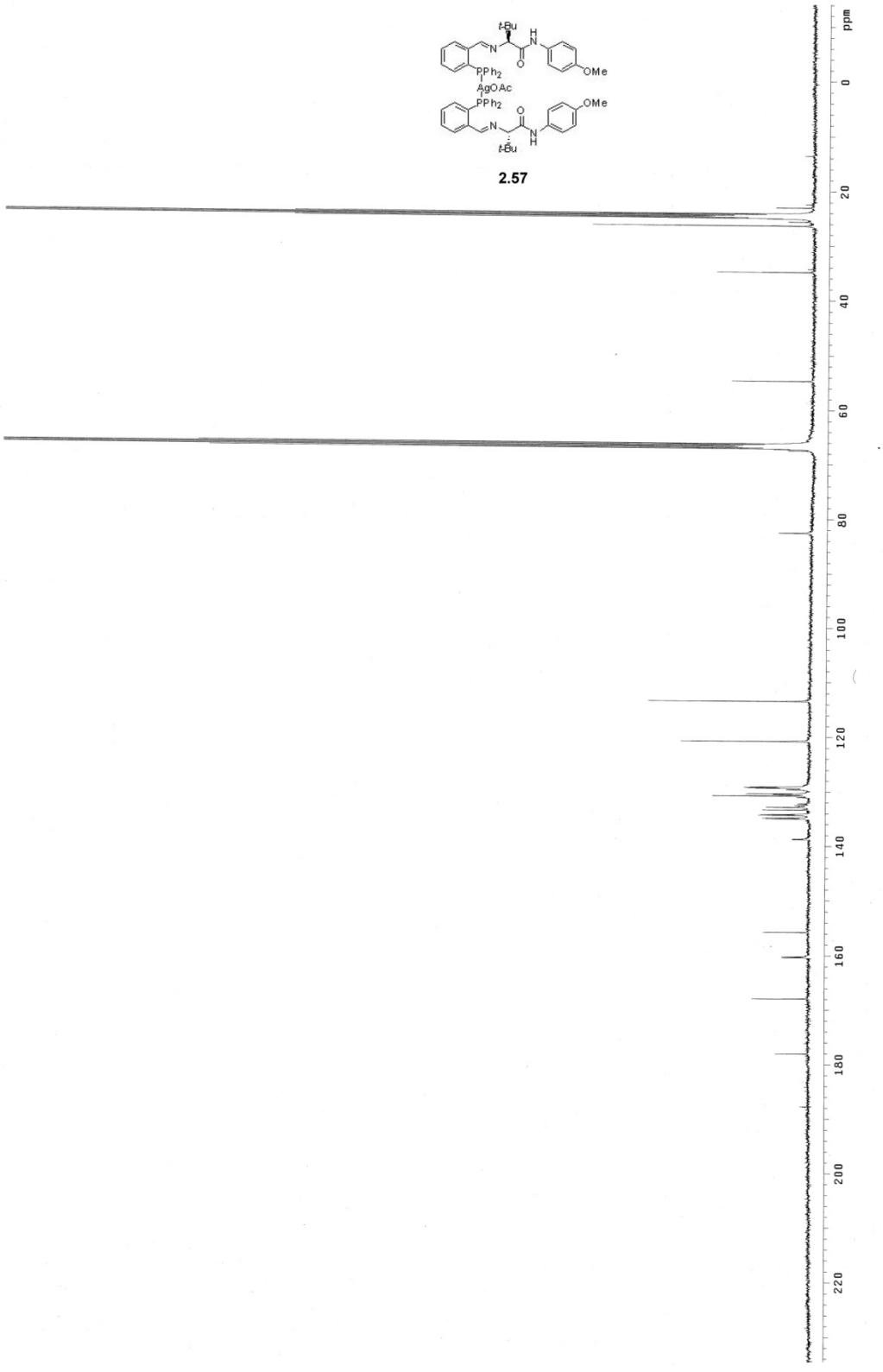
t-Bu
N
H
N
O
PPh2
OMe
AgOAc
PPh2
OMe
N
O
H
N
t-Bu
2.57
ppm
0
20
40
60
80
100
120
140
160
180
200
220

400 MHz ^{1}H NMR spectra of **2.57** in d_8-THF at various temperatures

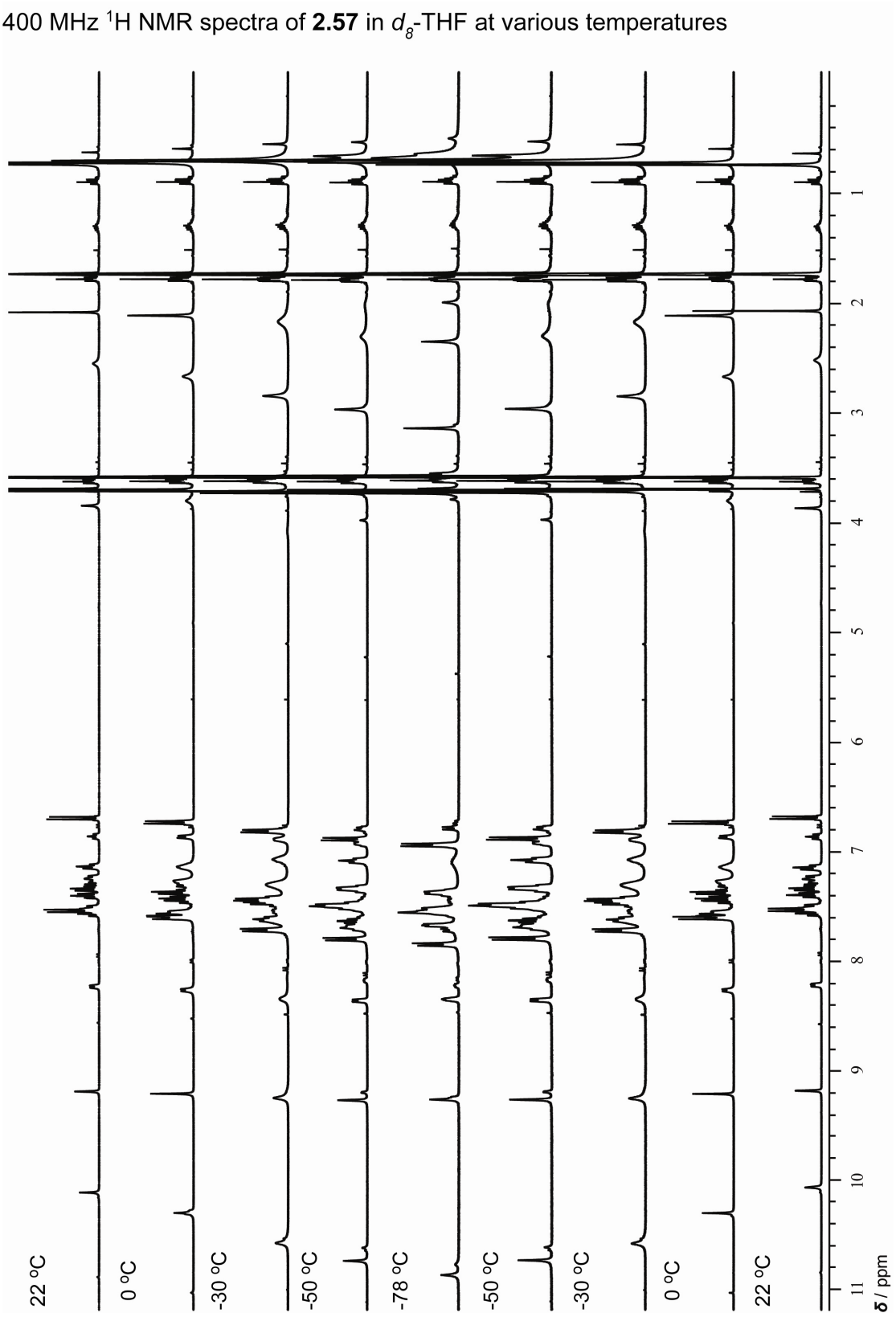

X-ray crystal structure of *syn*-2.36a:

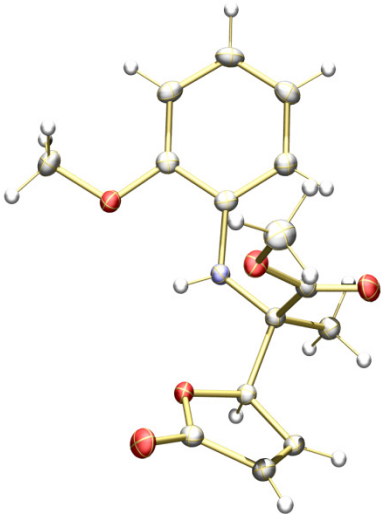

Table 1. Crystal data and structure refinement for ***syn*-2.36a**

Identification code	d08002
Empirical formula	C_{15} H_{17} N O_5
Formula weight	291.30
Temperature	100(2) K
Wavelength	1.54178 Å
Crystal system	Orthorhombic
Space group	P2(1)2(1)2(1)
Unit cell dimensions	a = 6.4323(2) Åα= 90°.
	b = 9.5882(2) Åβ= 90°.
	c = 23.5349(6) Åγ = 90°.
Volume	1451.50(7) $Å^3$
Z	4

Density (calculated)	1.333 Mg/m^3
Absorption coefficient	0.841 mm^{-1}
F(000)	616
Crystal size	0.45 x 0.15 x 0.15 mm^3
Theta range for data collection	3.76 to 67.56°.
Index ranges	-7<=h<=7, -11<=k<=10, -27<=l<=28
Reflections collected	19525
Independent reflections	2610 [R(int) = 0.0193]
Completeness to theta = 67.56°	99.9 %
Absorption correction	Semi-empirical from equivalents
Max. and min. transmission	0.8842 and 0.7033
Refinement method	Full-matrix least-squares on F^2
Data / restraints / parameters	2610 / 1 / 196
Goodness-of-fit on F^2	1.049
Final R indices [I>2sigma(I)]	R1 = 0.0241, wR2 = 0.0628
R indices (all data)	R1 = 0.0242, wR2 = 0.0629
Absolute structure parameter	0.05(12)
Largest diff. peak and hole	0.169 and -0.161 $e.Å^{-3}$

Table 2. Atomic coordinates (x 10^4) and equivalent isotropic displacement parameters ($Å^2$x 10^3). U(eq) is defined as one third of the trace of the orthogonalized U^{ij} tensor.

	x	y	z	U(eq)
O(3)	4092(1)	-1303(1)	7898(1)	18(1)
O(1)	2313(1)	2902(1)	8285(1)	20(1)
O(5)	4054(1)	-901(1)	9116(1)	21(1)
O(4)	7338(1)	-1421(1)	9365(1)	24(1)
N(1)	5459(2)	1152(1)	8400(1)	17(1)
O(2)	1862(1)	-3095(1)	7901(1)	26(1)
C(12)	3621(2)	-2681(1)	7951(1)	19(1)
C(7)	5166(2)	2147(1)	8830(1)	18(1)
C(8)	6711(2)	-100(1)	8497(1)	16(1)
C(13)	6112(2)	-874(1)	9050(1)	17(1)
C(1)	382(2)	3648(1)	8255(1)	23(1)
C(9)	6288(2)	-1105(1)	7992(1)	17(1)
C(10)	7104(2)	-2554(1)	8083(1)	19(1)
C(15)	9056(2)	195(1)	8480(1)	21(1)
C(6)	6396(2)	2269(1)	9315(1)	21(1)
C(11)	5545(2)	-3451(1)	8066(1)	20(1)
C(5)	6074(2)	3336(1)	9707(1)	24(1)
C(2)	3515(2)	3111(1)	8761(1)	18(1)
C(4)	4491(2)	4286(1)	9626(1)	25(1)
C(3)	3201(2)	4167(1)	9153(1)	22(1)
C(14)	3306(2)	-1668(1)	9606(1)	29(1)

Table 3. Bond lengths [Å] and angles [°].

O(3)-C(12)	1.3613(15)
O(3)-C(9)	1.4421(14)
O(1)-C(2)	1.3761(14)
O(1)-C(1)	1.4347(15)
O(5)-C(13)	1.3327(15)
O(5)-C(14)	1.4496(15)
O(4)-C(13)	1.2025(15)
N(1)-C(7)	1.4029(15)
N(1)-C(8)	1.4634(15)
N(1)-H(1)	0.870(13)
O(2)-C(12)	1.2053(15)
C(12)-C(11)	1.4664(17)
C(7)-C(6)	1.3939(17)
C(7)-C(2)	1.4172(17)
C(8)-C(15)	1.5356(16)
C(8)-C(13)	1.5479(15)
C(8)-C(9)	1.5535(15)
C(1)-H(1A)	0.9800
C(1)-H(1B)	0.9800
C(1)-H(1C)	0.9800
C(9)-C(10)	1.5007(16)

C(9)-H(9)	1.0000
C(10)-C(11)	1.3212(18)
C(10)-H(10)	0.9500
C(15)-H(15A)	0.9800
C(15)-H(15B)	0.9800
C(15)-H(15C)	0.9800
C(6)-C(5)	1.3941(17)
C(6)-H(6)	0.9500
C(11)-H(11)	0.9500
C(5)-C(4)	1.3791(19)
C(5)-H(5)	0.9500
C(2)-C(3)	1.3842(17)
C(4)-C(3)	1.3946(19)
C(4)-H(4)	0.9500
C(3)-H(3)	0.9500
C(14)-H(14A)	0.9800
C(14)-H(14B)	0.9800
C(14)-H(14C)	0.9800

C(12)-O(3)-C(9)	109.37(9)
C(2)-O(1)-C(1)	116.94(9)
C(13)-O(5)-C(14)	115.63(10)
C(7)-N(1)-C(8)	121.29(9)

C(7)-N(1)-H(1)	110.5(10)
C(8)-N(1)-H(1)	114.7(10)
O(2)-C(12)-O(3)	121.34(11)
O(2)-C(12)-C(11)	130.13(12)
O(3)-C(12)-C(11)	108.53(10)
C(6)-C(7)-N(1)	124.84(11)
C(6)-C(7)-C(2)	117.67(10)
N(1)-C(7)-C(2)	117.48(10)
N(1)-C(8)-C(15)	112.54(10)
N(1)-C(8)-C(13)	112.80(9)
C(15)-C(8)-C(13)	110.77(10)
N(1)-C(8)-C(9)	107.08(9)
C(15)-C(8)-C(9)	105.44(9)
C(13)-C(8)-C(9)	107.60(9)
O(4)-C(13)-O(5)	124.80(11)
O(4)-C(13)-C(8)	124.38(11)
O(5)-C(13)-C(8)	110.77(10)
O(1)-C(1)-H(1A)	109.5
O(1)-C(1)-H(1B)	109.5
H(1A)-C(1)-H(1B)	109.5
O(1)-C(1)-H(1C)	109.5
H(1A)-C(1)-H(1C)	109.5
H(1B)-C(1)-H(1C)	109.5

O(3)-C(9)-C(10)	104.03(9)
O(3)-C(9)-C(8)	111.72(9)
C(10)-C(9)-C(8)	113.84(9)
O(3)-C(9)-H(9)	109.0
C(10)-C(9)-H(9)	109.0
C(8)-C(9)-H(9)	109.0
C(11)-C(10)-C(9)	109.46(11)
C(11)-C(10)-H(10)	125.3
C(9)-C(10)-H(10)	125.3
C(8)-C(15)-H(15A)	109.5
C(8)-C(15)-H(15B)	109.5
H(15A)-C(15)-H(15B)	109.5
C(8)-C(15)-H(15C)	109.5
H(15A)-C(15)-H(15C)	109.5
H(15B)-C(15)-H(15C)	109.5
C(7)-C(6)-C(5)	121.35(12)
C(7)-C(6)-H(6)	119.3
C(5)-C(6)-H(6)	119.3
C(10)-C(11)-C(12)	108.55(11)
C(10)-C(11)-H(11)	125.7
C(12)-C(11)-H(11)	125.7
C(4)-C(5)-C(6)	120.16(12)
C(4)-C(5)-H(5)	119.9

C(6)-C(5)-H(5)	119.9
O(1)-C(2)-C(3)	124.55(11)
O(1)-C(2)-C(7)	114.80(10)
C(3)-C(2)-C(7)	120.66(11)
C(5)-C(4)-C(3)	119.73(11)
C(5)-C(4)-H(4)	120.1
C(3)-C(4)-H(4)	120.1
C(2)-C(3)-C(4)	120.38(11)
C(2)-C(3)-H(3)	119.8
C(4)-C(3)-H(3)	119.8
O(5)-C(14)-H(14A)	109.5
O(5)-C(14)-H(14B)	109.5
H(14A)-C(14)-H(14B)	109.5
O(5)-C(14)-H(14C)	109.5
H(14A)-C(14)-H(14C)	109.5
H(14B)-C(14)-H(14C)	109.5

Symmetry transformations used to generate equivalent atoms:

Table 4. Anisotropic displacement parameters ($Å^2 x\ 10^3$). The anisotropic displacement factor exponent takes the form: $-2\pi^2[\ h^2 a^{*2} U^{11} + ... + 2\ h\ k\ a^*\ b^*\ U^{12}\ ]$

U^{11}	U^{22}	U^{33}	U^{23}	U^{13}	U^{12}

O(3)	16(1)	18(1)	19(1)	-1(1)	-2(1)	2(1)
O(1)	20(1)	20(1)	21(1)	0(1)	0(1)	3(1)
O(5)	22(1)	22(1)	20(1)	6(1)	4(1)	0(1)
O(4)	29(1)	21(1)	21(1)	2(1)	-5(1)	2(1)
N(1)	19(1)	16(1)	17(1)	0(1)	-1(1)	0(1)
O(2)	17(1)	27(1)	33(1)	-2(1)	0(1)	-3(1)
C(12)	20(1)	19(1)	17(1)	-2(1)	2(1)	0(1)
C(7)	21(1)	13(1)	18(1)	2(1)	5(1)	-2(1)
C(8)	18(1)	14(1)	17(1)	0(1)	1(1)	0(1)
C(13)	22(1)	13(1)	16(1)	-3(1)	-1(1)	0(1)
C(1)	21(1)	20(1)	30(1)	3(1)	2(1)	3(1)
C(9)	15(1)	18(1)	17(1)	-1(1)	2(1)	-1(1)
C(10)	17(1)	20(1)	19(1)	-3(1)	1(1)	3(1)
C(15)	19(1)	20(1)	24(1)	-2(1)	1(1)	-2(1)
C(6)	24(1)	17(1)	21(1)	2(1)	2(1)	0(1)
C(11)	21(1)	18(1)	21(1)	-2(1)	0(1)	2(1)
C(5)	31(1)	21(1)	19(1)	0(1)	0(1)	-5(1)
C(2)	20(1)	17(1)	18(1)	3(1)	4(1)	-3(1)
C(4)	35(1)	18(1)	21(1)	-4(1)	6(1)	-2(1)
C(3)	26(1)	16(1)	24(1)	2(1)	7(1)	2(1)
C(14)	35(1)	27(1)	24(1)	7(1)	9(1)	0(1)

Table 5. Hydrogen coordinates (x 10^4) and isotropic displacement parameters ($Å^2$x 10^3).

	x	y	z	U(eq)
H(1)	4300(20)	1010(15)	8216(6)	20
H(1A)	661	4648	8217	35
H(1B)	-419	3480	8603	35
H(1C)	-416	3324	7926	35
H(9)	6928	-709	7640	20
H(10)	8520	-2790	8144	22
H(15A)	9426	830	8790	31
H(15B)	9418	626	8115	31
H(15C)	9822	-682	8523	31
H(6)	7475	1611	9379	25
H(11)	5653	-4431	8119	24
H(5)	6948	3410	10032	28
H(4)	4281	5018	9892	30
H(3)	2100	4813	9099	27
H(14A)	3770	-1203	9955	43
H(14B)	3857	-2620	9596	43
H(14C)	1783	-1699	9599	43

Table 6. Torsion angles [°].

C(9)-O(3)-C(12)-O(2)	178.67(11)
C(9)-O(3)-C(12)-C(11)	-1.85(12)
C(8)-N(1)-C(7)-C(6)	17.83(17)
C(8)-N(1)-C(7)-C(2)	-163.14(10)
C(7)-N(1)-C(8)-C(15)	-77.21(13)
C(7)-N(1)-C(8)-C(13)	49.13(14)
C(7)-N(1)-C(8)-C(9)	167.31(10)
C(14)-O(5)-C(13)-O(4)	-0.54(17)
C(14)-O(5)-C(13)-C(8)	176.79(9)
N(1)-C(8)-C(13)-O(4)	-141.54(11)
C(15)-C(8)-C(13)-O(4)	-14.19(16)
C(9)-C(8)-C(13)-O(4)	100.58(13)
N(1)-C(8)-C(13)-O(5)	41.11(13)
C(15)-C(8)-C(13)-O(5)	168.46(9)
C(9)-C(8)-C(13)-O(5)	-76.77(11)
C(12)-O(3)-C(9)-C(10)	2.47(11)
C(12)-O(3)-C(9)-C(8)	-120.75(10)
N(1)-C(8)-C(9)-O(3)	-50.61(12)
C(15)-C(8)-C(9)-O(3)	-170.82(9)
C(13)-C(8)-C(9)-O(3)	70.91(12)
N(1)-C(8)-C(9)-C(10)	-168.07(9)

C(15)-C(8)-C(9)-C(10)	71.71(12)
C(13)-C(8)-C(9)-C(10)	-46.56(12)
O(3)-C(9)-C(10)-C(11)	-2.26(12)
C(8)-C(9)-C(10)-C(11)	119.57(11)
N(1)-C(7)-C(6)-C(5)	176.36(11)
C(2)-C(7)-C(6)-C(5)	-2.54(17)
C(9)-C(10)-C(11)-C(12)	1.21(13)
O(2)-C(12)-C(11)-C(10)	179.79(13)
O(3)-C(12)-C(11)-C(10)	0.37(13)
C(7)-C(6)-C(5)-C(4)	1.18(19)
C(1)-O(1)-C(2)-C(3)	-12.97(16)
C(1)-O(1)-C(2)-C(7)	167.18(10)
C(6)-C(7)-C(2)-O(1)	-177.66(10)
N(1)-C(7)-C(2)-O(1)	3.24(15)
C(6)-C(7)-C(2)-C(3)	2.49(17)
N(1)-C(7)-C(2)-C(3)	-176.61(10)
C(6)-C(5)-C(4)-C(3)	0.58(19)
O(1)-C(2)-C(3)-C(4)	179.33(11)
C(7)-C(2)-C(3)-C(4)	-0.83(18)
C(5)-C(4)-C(3)-C(2)	-0.74(18)

Symmetry transformations used to generate equivalent atoms:

Table 7. Hydrogen bonds [Å and °].

D-H...A	d(D-H)	d(H...A)	d(D...A)	<(DHA)
N(1)-H(1)...O(3)	0.870(13)	2.344(15)	2.7764(13)	110.9(11)

Symmetry transformations used to generate equivalent atoms:

X-ray crystal structure of α-ketoimine ester 2.45a:

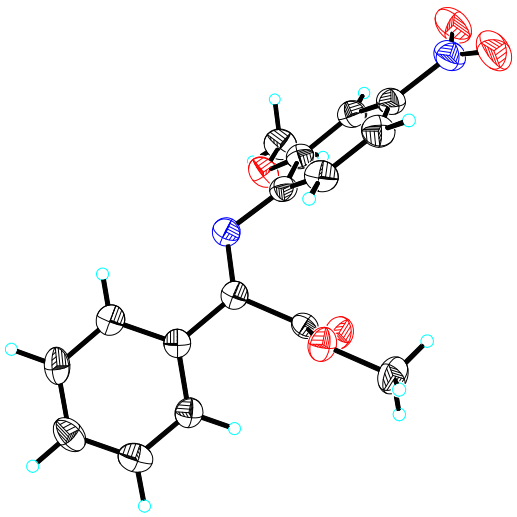

Table 1. Crystal data and structure refinement for **2.45a**

Identification code	lcw07

Empirical formula	C_{16} H_{14} N_2 O_5
Formula weight	314.29
Temperature	193(2) K
Wavelength	0.71073 Å
Crystal system	Trilinic
Space group	P -1
Unit cell dimensions	a = 8.595(2) Åα= 71.928(5)°.
	b = 9.799(3) Åβ= 85.027(5)°.
	c = 10.014(3) Åγ = 68.533(5)°.
Volume	745.9(3) $Å^3$
Z	2
Density (calculated)	1.399 Mg/m^3
Absorption coefficient	0.106 mm^{-1}
F(000)	328
Crystal size	0.16 x 0.12 x 0.09 mm^3
Theta range for data collection	2.14 to 28.38°.
Index ranges	-11<=h<=8, -13<=k<=13, -13<=l<=13
Reflections collected	5715
Independent reflections	3706 [R(int) = 0.0241]
Completeness to theta = 28.38°	99.1 %
Absorption correction	Semi-empirical from equivalents
Max. and min. transmission	0.9905 and 0.9833
Refinement method	Full-matrix least-squares on F^2

Data / restraints / parameters	3706 / 0 / 264
Goodness-of-fit on F^2	1.016
Final R indices [I>2sigma(I)]	R1 = 0.0510, wR2 = 0.1048
R indices (all data)	R1 = 0.0898, wR2 = 0.1220
Extinction coefficient	noref
Largest diff. peak and hole	0.193 and -0.225 e.$Å^{-3}$

Table 2. Atomic coordinates (x 10^4) and equivalent isotropic displacement parameters ($Å^2$x 10^3). U(eq) is defined as one third of the trace of the orthogonalized U^{ij} tensor

	x	y	z	U(eq)
O(1)	1737(2)	5641(1)	4945(1)	35(1)
O(2)	3939(2)	5382(1)	3545(1)	39(1)
O(3)	-1708(2)	10323(2)	-1104(2)	60(1)
O(4)	-202(2)	9249(2)	-2610(2)	56(1)
O(5)	3282(2)	3972(1)	370(1)	38(1)
N(1)	1872(2)	3621(2)	2895(1)	31(1)
N(2)	-696(2)	9209(2)	-1416(2)	43(1)
C(1)	2546(2)	3578(2)	4003(2)	27(1)
C(2)	3142(2)	2171(2)	5203(2)	27(1)
C(3)	2748(2)	894(2)	5276(2)	33(1)
C(4)	3346(3)	-426(2)	6390(2)	40(1)

C(5)	4352(3)	-503(2)	7431(2)	42(1)
C(6)	4747(2)	754(2)	7368(2)	39(1)
C(7)	4143(2)	2086(2)	6265(2)	32(1)
C(8)	2839(2)	4967(2)	4119(2)	27(1)
C(9)	1886(3)	7004(2)	5123(3)	44(1)
C(10)	1243(2)	5045(2)	1828(2)	29(1)
C(11)	-111(2)	6247(2)	2049(2)	36(1)
C(12)	-756(2)	7621(2)	998(2)	38(1)
C(13)	-44(2)	7752(2)	-288(2)	34(1)
C(14)	1296(2)	6565(2)	-565(2)	34(1)
C(15)	1945(2)	5204(2)	494(2)	30(1)
C(16)	4072(3)	4118(3)	-960(2)	43(1)

Table 3. Bond lengths [Å] and angles [°]

O(1)-C(8)	1.3276(19)
O(1)-C(9)	1.452(2)
O(2)-C(8)	1.196(2)
O(3)-N(2)	1.231(2)
O(4)-N(2)	1.227(2)
O(5)-C(15)	1.359(2)
O(5)-C(16)	1.432(2)
N(1)-C(1)	1.278(2)
N(1)-C(10)	1.415(2)
N(2)-C(13)	1.467(2)
C(1)-C(2)	1.473(2)
C(1)-C(8)	1.512(2)
C(2)-C(7)	1.390(2)
C(2)-C(3)	1.391(2)
C(3)-C(4)	1.378(3)
C(3)-H(3)	0.918(19)
C(4)-C(5)	1.378(3)
C(4)-H(4)	0.954(19)
C(5)-C(6)	1.375(3)
C(5)-H(5)	0.96(2)
C(6)-C(7)	1.379(3)
C(6)-H(6)	0.98(2)

C(7)-H(7)	0.956(18)
C(9)-H(9A)	0.98(2)
C(9)-H(9B)	0.996(19)
C(9)-H(9C)	0.95(2)
C(10)-C(11)	1.380(2)
C(10)-C(15)	1.405(2)
C(11)-C(12)	1.380(3)
C(11)-H(11)	0.956(19)
C(12)-C(13)	1.366(3)
C(12)-H(12)	0.949(19)
C(13)-C(14)	1.386(2)
C(14)-C(15)	1.376(2)
C(14)-H(14)	0.941(18)
C(16)-H(16A)	0.98(2)
C(16)-H(16B)	1.01(2)
C(16)-H(16C)	0.99(2)
C(8)-O(1)-C(9)	116.16(15)
C(15)-O(5)-C(16)	117.08(15)
C(1)-N(1)-C(10)	118.58(14)
O(4)-N(2)-O(3)	123.85(17)
O(4)-N(2)-C(13)	118.39(17)
O(3)-N(2)-C(13)	117.76(17)
N(1)-C(1)-C(2)	122.37(15)

N(1)-C(1)-C(8)	121.16(15)
C(2)-C(1)-C(8)	116.42(15)
C(7)-C(2)-C(3)	118.90(17)
C(7)-C(2)-C(1)	120.37(15)
C(3)-C(2)-C(1)	120.71(16)
C(4)-C(3)-C(2)	120.00(19)
C(4)-C(3)-H(3)	121.0(12)
C(2)-C(3)-H(3)	118.9(12)
C(5)-C(4)-C(3)	120.65(19)
C(5)-C(4)-H(4)	119.9(11)
C(3)-C(4)-H(4)	119.4(12)
C(6)-C(5)-C(4)	119.73(19)
C(6)-C(5)-H(5)	119.4(13)
C(4)-C(5)-H(5)	120.8(13)
C(5)-C(6)-C(7)	120.2(2)
C(5)-C(6)-H(6)	120.3(12)
C(7)-C(6)-H(6)	119.5(12)
C(6)-C(7)-C(2)	120.50(18)
C(6)-C(7)-H(7)	120.3(11)
C(2)-C(7)-H(7)	119.2(11)
O(2)-C(8)-O(1)	125.09(16)
O(2)-C(8)-C(1)	123.67(15)
O(1)-C(8)-C(1)	111.23(14)

O(1)-C(9)-H(9A)	112.3(12)
O(1)-C(9)-H(9B)	105.1(11)
H(9A)-C(9)-H(9B)	113.6(16)
O(1)-C(9)-H(9C)	109.5(13)
H(9A)-C(9)-H(9C)	105.0(18)
H(9B)-C(9)-H(9C)	111.4(16)
C(11)-C(10)-C(15)	119.41(16)
C(11)-C(10)-N(1)	121.18(15)
C(15)-C(10)-N(1)	119.30(15)
C(10)-C(11)-C(12)	121.28(17)
C(10)-C(11)-H(11)	119.8(11)
C(12)-C(11)-H(11)	119.0(11)
C(13)-C(12)-C(11)	118.17(18)
C(13)-C(12)-H(12)	118.8(12)
C(11)-C(12)-H(12)	123.0(12)
C(12)-C(13)-C(14)	122.52(17)
C(12)-C(13)-N(2)	119.09(17)
C(14)-C(13)-N(2)	118.38(16)
C(15)-C(14)-C(13)	118.94(17)
C(15)-C(14)-H(14)	123.8(10)
C(13)-C(14)-H(14)	117.2(10)
O(5)-C(15)-C(14)	124.72(15)
O(5)-C(15)-C(10)	115.59(15)

C(14)-C(15)-C(10)	119.66(16)
O(5)-C(16)-H(16A)	106.0(12)
O(5)-C(16)-H(16B)	109.2(11)
H(16A)-C(16)-H(16B)	109.2(16)
O(5)-C(16)-H(16C)	110.3(12)
H(16A)-C(16)-H(16C)	108.9(16)
H(16B)-C(16)-H(16C)	113.1(17)

Symmetry transformations used to generate equivalent atoms:

Table 4. Anisotropic displacement parameters ($Å^2 x\ 10^3$). The anisotropic displacement factor exponent takes the form: $-2\pi^2[\ h^2\ a^{*2}U^{11} + ...\ + 2\ h\ k\ a^*\ b^*\ U^{12}\ ]$

	U^{11}	U^{22}	U^{33}	U^{23}	U^{13}	U^{12}
O(1)	37(1)	32(1)	38(1)	-17(1)	10(1)	-13(1)
O(2)	42(1)	43(1)	38(1)	-13(1)	11(1)	-24(1)
O(3)	51(1)	39(1)	70(1)	-7(1)	-8(1)	0(1)
O(4)	62(1)	54(1)	38(1)	6(1)	-1(1)	-20(1)
O(5)	41(1)	37(1)	29(1)	-11(1)	9(1)	-8(1)
N(1)	34(1)	34(1)	26(1)	-10(1)	6(1)	-15(1)
N(2)	36(1)	40(1)	48(1)	-2(1)	-8(1)	-14(1)
C(1)	25(1)	31(1)	26(1)	-12(1)	9(1)	-12(1)

C(2)	25(1)	29(1)	28(1)	-12(1)	8(1)	-8(1)
C(3)	32(1)	34(1)	35(1)	-14(1)	7(1)	-13(1)
C(4)	47(1)	26(1)	46(1)	-11(1)	10(1)	-14(1)
C(5)	45(1)	31(1)	36(1)	-6(1)	3(1)	-2(1)
C(6)	35(1)	42(1)	33(1)	-13(1)	1(1)	-6(1)
C(7)	34(1)	32(1)	33(1)	-13(1)	7(1)	-12(1)
C(8)	29(1)	29(1)	21(1)	-5(1)	2(1)	-10(1)
C(9)	47(1)	34(1)	54(1)	-22(1)	3(1)	-11(1)
C(10)	32(1)	34(1)	25(1)	-9(1)	1(1)	-15(1)
C(11)	32(1)	44(1)	32(1)	-12(1)	7(1)	-14(1)
C(12)	28(1)	40(1)	42(1)	-14(1)	3(1)	-8(1)
C(13)	30(1)	35(1)	34(1)	-6(1)	-4(1)	-13(1)
C(14)	35(1)	41(1)	27(1)	-9(1)	4(1)	-19(1)
C(15)	29(1)	34(1)	28(1)	-12(1)	1(1)	-12(1)
C(16)	45(1)	50(1)	32(1)	-18(1)	12(1)	-13(1)

Table 5. Hydrogen coordinates (x 10^4) and isotropic displacement parameters (Å^{2}x 10^3)

	x	y	z	U(eq)
H(3)	2060(20)	960(20)	4590(20)	37(5)
H(4)	3100(20)	-1310(20)	6415(19)	39(5)
H(5)	4800(30)	-1430(30)	8190(20)	58(6)

H(6)	5460(20)	710(20)	8100(20)	49(6)
H(7)	4450(20)	2950(20)	6202(18)	33(5)
H(9A)	3010(30)	6820(20)	5440(20)	48(6)
H(9B)	1000(30)	7330(20)	5790(20)	44(5)
H(9C)	1710(30)	7780(30)	4240(20)	58(7)
H(11)	-620(20)	6130(20)	2950(20)	39(5)
H(12)	-1670(20)	8470(20)	1127(19)	48(6)
H(14)	1710(20)	6747(19)	-1479(19)	32(5)
H(16A)	5020(30)	3160(20)	-850(20)	53(6)
H(16B)	4500(20)	5000(20)	-1180(20)	50(6)
H(16C)	3300(30)	4240(20)	-1690(20)	52(6)

Table 6. Torsion angles [°]

C(10)-N(1)-C(1)-C(2)	176.19(14)
C(10)-N(1)-C(1)-C(8)	-6.5(2)
N(1)-C(1)-C(2)-C(7)	167.75(16)
C(8)-C(1)-C(2)-C(7)	-9.7(2)
N(1)-C(1)-C(2)-C(3)	-10.6(2)
C(8)-C(1)-C(2)-C(3)	171.92(15)
C(7)-C(2)-C(3)-C(4)	0.2(2)
C(1)-C(2)-C(3)-C(4)	178.58(15)
C(2)-C(3)-C(4)-C(5)	-0.9(3)
C(3)-C(4)-C(5)-C(6)	0.9(3)

C(4)-C(5)-C(6)-C(7)	-0.3(3)
C(5)-C(6)-C(7)-C(2)	-0.4(3)
C(3)-C(2)-C(7)-C(6)	0.5(2)
C(1)-C(2)-C(7)-C(6)	-177.95(15)
C(9)-O(1)-C(8)-O(2)	1.3(3)
C(9)-O(1)-C(8)-C(1)	-179.37(16)
N(1)-C(1)-C(8)-O(2)	-75.9(2)
C(2)-C(1)-C(8)-O(2)	101.57(19)
N(1)-C(1)-C(8)-O(1)	104.73(17)
C(2)-C(1)-C(8)-O(1)	-77.80(18)
C(1)-N(1)-C(10)-C(11)	-66.5(2)
C(1)-N(1)-C(10)-C(15)	117.43(18)
C(15)-C(10)-C(11)-C(12)	-2.1(3)
N(1)-C(10)-C(11)-C(12)	-178.15(17)
C(10)-C(11)-C(12)-C(13)	1.6(3)
C(11)-C(12)-C(13)-C(14)	-0.4(3)
C(11)-C(12)-C(13)-N(2)	-179.23(17)
O(4)-N(2)-C(13)-C(12)	-170.46(18)
O(3)-N(2)-C(13)-C(12)	9.7(3)
O(4)-N(2)-C(13)-C(14)	10.6(3)
O(3)-N(2)-C(13)-C(14)	-169.19(16)
C(12)-C(13)-C(14)-C(15)	-0.4(3)
N(2)-C(13)-C(14)-C(15)	178.50(16)

C(16)-O(5)-C(15)-C(14)	0.6(3)
C(16)-O(5)-C(15)-C(10)	-177.48(17)
C(13)-C(14)-C(15)-O(5)	-178.08(16)
C(13)-C(14)-C(15)-C(10)	-0.1(3)
C(11)-C(10)-C(15)-O(5)	179.44(15)
N(1)-C(10)-C(15)-O(5)	-4.4(2)
C(11)-C(10)-C(15)-C(14)	1.3(3)
N(1)-C(10)-C(15)-C(14)	177.44(16)

Symmetry transformations used to generate equivalent atoms:

X-ray crystal structure of *anti*-2.49d

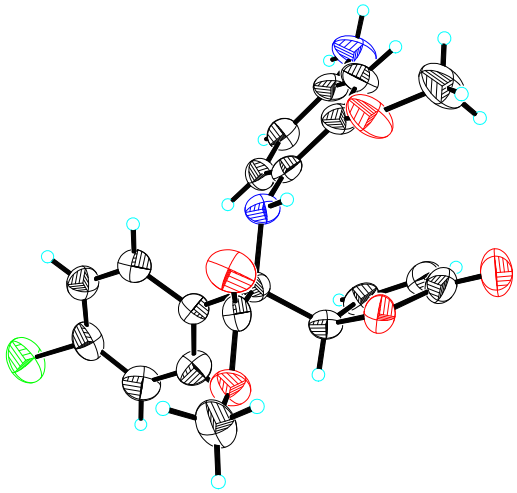

Table 1. Crystal data and structure refinement for reduced *anti*-**2.46d**

Identification code	emv01

Empirical formula	C20 H19 Cl N2 O5	
Formula weight	402.82	
Temperature	193(2) K	
Wavelength	0.71073 Å	
Crystal system	Orthorhombic	
Space group	P2(1)2(1)2(1)	
Unit cell dimensions	a = 8.8375(16) Å	α= 90°.
	b = 11.630(2) Å	β= 90°.
	c = 18.584(3) Å	γ = 90°.
Volume	1910.2(6) $Å^3$	
Z	4	
Density (calculated)	1.401 Mg/m^3	
Absorption coefficient	0.235 mm^{-1}	
F(000)	840	
Crystal size	0.1 x 0.1 x 0.05 mm^3	
Theta range for data collection	2.07 to 28.31°.	
Index ranges	-11<=h<=10, -11<=k<=15, -24<=l<=18	
Reflections collected	14569	
Independent reflections	4754 [R(int) = 0.0728]	
Completeness to theta = 28.31°	100.0 %	
Absorption correction	Empirical	
Max. and min. transmission	none and none	
Refinement method	Full-matrix least-squares on F^2	

Data / restraints / parameters	4754 / 0 / 329
Goodness-of-fit on F^2	0.995
Final R indices [I>2sigma(I)]	R1 = 0.0615, wR2 = 0.1043
R indices (all data)	R1 = 0.1139, wR2 = 0.1226
Absolute structure parameter	0.05(9)
Largest diff. peak and hole	0.247 and -0.171 e.$Å^{-3}$

Table 2. Atomic coordinates (x 10^4) and equivalent isotropic displacement parameters ($Å^2$x 10^3). U(eq) is defined as one third of the trace of the orthogonalized U^{ij} tensor

	x	y	z	U(eq)
Cl(1)	-66(1)	2810(1)	119(1)	70(1)
O(2)	6754(2)	5252(2)	2680(1)	41(1)
O(5)	3296(3)	5135(2)	2927(1)	46(1)
O(4)	3827(3)	6925(2)	2592(1)	56(1)
C(9)	5920(4)	4578(3)	2162(2)	38(1)
N(2)	5285(3)	6322(2)	1433(1)	36(1)
C(15)	3491(3)	4680(3)	1411(2)	33(1)
C(8)	4672(3)	5354(3)	1836(2)	33(1)
O(3)	9175(3)	5670(3)	2898(2)	65(1)
C(13)	3873(3)	5914(3)	2491(2)	35(1)
C(10)	7112(4)	4125(3)	1672(2)	42(1)

C(12)	8272(4)	5191(3)	2528(2)	46(1)
C(3)	6020(4)	5485(3)	255(2)	38(1)
C(20)	2579(4)	5263(3)	916(2)	42(1)
C(4)	6281(3)	6185(3)	841(2)	33(1)
O(1)	7816(3)	7506(2)	1442(1)	63(1)
C(6)	8558(5)	6842(3)	255(2)	50(1)
C(17)	2152(4)	2940(3)	1109(2)	50(1)
C(1)	8281(4)	6123(3)	-332(2)	43(1)
C(16)	3237(4)	3522(3)	1500(2)	45(1)
C(18)	1313(4)	3529(3)	618(2)	46(1)
C(5)	7588(4)	6862(3)	831(2)	42(1)
C(19)	1511(4)	4688(4)	516(2)	44(1)
C(14)	2593(5)	5574(5)	3577(2)	57(1)
C(11)	8438(4)	4475(3)	1895(2)	48(1)
C(2)	7014(4)	5451(3)	-320(2)	40(1)
N(1)	9333(4)	6057(4)	-887(2)	64(1)
C(7)	9313(6)	7873(5)	1603(3)	73(2)

Table 3. Bond lengths [Å] and angles [°]

Cl(1)-C(18)	1.745(3)
O(2)-C(12)	1.373(4)
O(2)-C(9)	1.445(4)

O(5)-C(13)	1.318(4)
O(5)-C(14)	1.451(5)
O(4)-C(13)	1.192(4)
C(9)-C(10)	1.489(5)
C(9)-C(8)	1.549(4)
N(2)-C(4)	1.418(4)
N(2)-C(8)	1.456(4)
C(15)-C(16)	1.375(5)
C(15)-C(20)	1.399(4)
C(15)-C(8)	1.526(4)
C(8)-C(13)	1.550(4)
O(3)-C(12)	1.192(4)
C(10)-C(11)	1.307(5)
C(12)-C(11)	1.448(5)
C(3)-C(4)	1.378(4)
C(3)-C(2)	1.385(4)
C(20)-C(19)	1.375(5)
C(4)-C(5)	1.398(4)
O(1)-C(5)	1.374(4)
O(1)-C(7)	1.423(5)
C(6)-C(5)	1.372(5)
C(6)-C(1)	1.396(5)
C(17)-C(18)	1.361(5)

C(17)-C(16)	1.381(5)
C(1)-C(2)	1.366(5)
C(1)-N(1)	1.391(5)
C(18)-C(19)	1.372(5)
C(12)-O(2)-C(9)	109.5(3)
C(13)-O(5)-C(14)	115.8(3)
O(2)-C(9)-C(10)	103.8(3)
O(2)-C(9)-C(8)	107.9(3)
C(10)-C(9)-C(8)	118.1(3)
C(4)-N(2)-C(8)	123.0(3)
C(16)-C(15)-C(20)	117.4(3)
C(16)-C(15)-C(8)	123.5(3)
C(20)-C(15)-C(8)	119.0(3)
N(2)-C(8)-C(15)	112.6(2)
N(2)-C(8)-C(9)	112.8(3)
C(15)-C(8)-C(9)	112.9(3)
N(2)-C(8)-C(13)	104.4(3)
C(15)-C(8)-C(13)	108.1(2)
C(9)-C(8)-C(13)	105.2(2)
O(4)-C(13)-O(5)	124.6(3)
O(4)-C(13)-C(8)	123.6(3)
O(5)-C(13)-C(8)	111.7(3)
C(11)-C(10)-C(9)	109.3(3)

O(3)-C(12)-O(2)	120.7(3)
O(3)-C(12)-C(11)	132.0(3)
O(2)-C(12)-C(11)	107.2(3)
C(4)-C(3)-C(2)	121.4(3)
C(19)-C(20)-C(15)	121.0(4)
C(3)-C(4)-C(5)	117.5(3)
C(3)-C(4)-N(2)	125.1(3)
C(5)-C(4)-N(2)	117.4(3)
C(5)-O(1)-C(7)	118.3(3)
C(5)-C(6)-C(1)	120.7(3)
C(18)-C(17)-C(16)	119.0(4)
C(2)-C(1)-N(1)	121.9(3)
C(2)-C(1)-C(6)	118.3(3)
N(1)-C(1)-C(6)	119.7(3)
C(15)-C(16)-C(17)	122.0(4)
C(17)-C(18)-C(19)	121.1(3)
C(17)-C(18)-Cl(1)	119.8(3)
C(19)-C(18)-Cl(1)	119.1(3)
C(6)-C(5)-O(1)	124.2(3)
C(6)-C(5)-C(4)	121.1(3)
O(1)-C(5)-C(4)	114.7(3)
C(20)-C(19)-C(18)	119.4(4)
C(10)-C(11)-C(12)	110.2(3)

C(1)-C(2)-C(3)	121.0(3)

Symmetry transformations used to generate equivalent atoms:

Table 4. Anisotropic displacement parameters ($Å^2 x\ 10^3$) for EMV01. The anisotropic displacement factor exponent takes the form: $-2\pi^2[\ h^2\ a^{*2}U^{11} + ...\ + 2\ h\ k\ a^*\ b^*\ U^{12}\ ]$

	U^{11}	U^{22}	U^{33}	U^{23}	U^{13}	U^{12}
Cl(1)	61(1)	85(1)	65(1)	-23(1)	-11(1)	-21(1)
O(2)	35(1)	52(2)	36(1)	-4(1)	-2(1)	5(1)
O(5)	50(1)	56(2)	33(1)	-1(1)	10(1)	-2(1)
O(4)	65(2)	42(2)	60(2)	-16(1)	18(1)	0(1)
C(9)	40(2)	38(2)	34(2)	2(2)	3(2)	-1(2)
N(2)	46(2)	29(2)	32(1)	-2(1)	1(1)	-1(1)
C(15)	35(2)	34(2)	30(2)	-4(1)	4(1)	4(2)
C(8)	35(2)	33(2)	31(2)	0(1)	-1(1)	0(1)
O(3)	42(1)	87(2)	66(2)	0(2)	-15(1)	-4(2)
C(13)	28(2)	38(2)	38(2)	-5(2)	-3(1)	0(2)
C(10)	53(2)	40(2)	34(2)	4(2)	2(2)	13(2)
C(12)	38(2)	54(2)	45(2)	9(2)	-3(2)	9(2)
C(3)	37(2)	40(2)	38(2)	-4(2)	-2(2)	-4(2)
C(20)	43(2)	41(2)	41(2)	-1(2)	2(2)	1(2)

C(4)	38(2)	30(2)	33(2)	6(1)	-2(1)	7(1)
O(1)	66(2)	68(2)	55(2)	-21(1)	10(1)	-28(2)
C(6)	52(2)	45(2)	52(2)	3(2)	7(2)	-16(2)
C(17)	59(2)	33(2)	56(2)	-8(2)	0(2)	-8(2)
C(1)	50(2)	44(2)	35(2)	8(2)	7(2)	-4(2)
C(16)	53(2)	37(2)	43(2)	-4(2)	-4(2)	4(2)
C(18)	39(2)	60(3)	38(2)	-17(2)	-2(2)	-5(2)
C(5)	52(2)	34(2)	39(2)	-2(2)	0(2)	-6(2)
C(19)	43(2)	52(2)	37(2)	2(2)	-1(2)	3(2)
C(14)	49(2)	84(4)	39(2)	-14(3)	6(2)	-8(3)
C(11)	39(2)	58(3)	46(2)	13(2)	11(2)	15(2)
C(2)	49(2)	41(2)	31(2)	-6(2)	-1(2)	1(2)
N(1)	76(2)	69(3)	46(2)	-4(2)	18(2)	-25(2)
C(7)	75(3)	84(4)	61(3)	-19(3)	-2(3)	-36(3)

Table 5. Hydrogen coordinates (x 10^4) and isotropic displacement parameters ($Å^2$x 10^3)

	x	y	z	U(eq)
H(3)	2730(30)	6080(30)	871(14)	27(8)
H(2)	5220(40)	5050(30)	230(14)	37(9)
H(1)	6850(30)	3650(30)	1272(16)	35(9)

H(8)	5650(30)	6840(30)	1769(17)	41(9)
H(11)	1940(30)	2170(30)	1207(14)	32(8)
H(5)	9780(40)	8290(30)	1244(19)	53(11)
H(9)	9380(40)	4290(30)	1758(17)	56(11)
H(10)	5460(30)	4010(30)	2463(15)	32(8)
H(6)	6780(30)	4970(30)	-706(16)	36(9)
H(7)	8990(50)	5630(40)	-1230(20)	73(15)
H(12)	3770(40)	3110(30)	1834(17)	46(10)
H(4)	9450(40)	7280(30)	287(15)	41(9)
H(14)	1710(50)	6120(40)	3450(20)	74(13)
H(16)	950(40)	5090(30)	229(16)	35(9)
H(13)	3220(40)	6160(30)	3807(19)	64(12)
H(15)	2450(60)	5030(40)	3850(20)	81(18)
H(17)	10080(50)	7180(40)	1690(20)	95(17)
H(18)	9240(50)	8280(40)	2100(20)	97(15)
H(19)	9810(50)	6720(40)	-1009(19)	73(14)

Table 6. Torsion angles [°]

C(12)-O(2)-C(9)-C(10)	-1.2(3)
C(12)-O(2)-C(9)-C(8)	-127.2(3)
C(4)-N(2)-C(8)-C(15)	-71.6(4)
C(4)-N(2)-C(8)-C(9)	57.7(4)

C(4)-N(2)-C(8)-C(13)	171.4(2)
C(16)-C(15)-C(8)-N(2)	150.1(3)
C(20)-C(15)-C(8)-N(2)	-31.8(4)
C(16)-C(15)-C(8)-C(9)	20.9(4)
C(20)-C(15)-C(8)-C(9)	-161.0(3)
C(16)-C(15)-C(8)-C(13)	-95.1(4)
C(20)-C(15)-C(8)-C(13)	83.0(3)
O(2)-C(9)-C(8)-N(2)	63.9(3)
C(10)-C(9)-C(8)-N(2)	-53.2(4)
O(2)-C(9)-C(8)-C(15)	-167.0(2)
C(10)-C(9)-C(8)-C(15)	75.9(4)
O(2)-C(9)-C(8)-C(13)	-49.3(3)
C(10)-C(9)-C(8)-C(13)	-166.4(3)
C(14)-O(5)-C(13)-O(4)	-1.2(5)
C(14)-O(5)-C(13)-C(8)	176.8(3)
N(2)-C(8)-C(13)-O(4)	0.3(4)
C(15)-C(8)-C(13)-O(4)	-119.9(3)
C(9)-C(8)-C(13)-O(4)	119.2(3)
N(2)-C(8)-C(13)-O(5)	-177.8(2)
C(15)-C(8)-C(13)-O(5)	62.1(3)
C(9)-C(8)-C(13)-O(5)	-58.8(3)
O(2)-C(9)-C(10)-C(11)	1.3(4)
C(8)-C(9)-C(10)-C(11)	120.6(3)

C(9)-O(2)-C(12)-O(3)	-178.6(3)
C(9)-O(2)-C(12)-C(11)	0.7(4)
C(16)-C(15)-C(20)-C(19)	-2.4(5)
C(8)-C(15)-C(20)-C(19)	179.4(3)
C(2)-C(3)-C(4)-C(5)	0.1(5)
C(2)-C(3)-C(4)-N(2)	176.3(3)
C(8)-N(2)-C(4)-C(3)	51.7(4)
C(8)-N(2)-C(4)-C(5)	-132.0(3)
C(5)-C(6)-C(1)-C(2)	0.5(5)
C(5)-C(6)-C(1)-N(1)	-175.5(4)
C(20)-C(15)-C(16)-C(17)	1.4(5)
C(8)-C(15)-C(16)-C(17)	179.6(3)
C(18)-C(17)-C(16)-C(15)	0.3(5)
C(16)-C(17)-C(18)-C(19)	-1.2(5)
C(16)-C(17)-C(18)-Cl(1)	-179.9(3)
C(1)-C(6)-C(5)-O(1)	177.1(3)
C(1)-C(6)-C(5)-C(4)	-1.4(5)
C(7)-O(1)-C(5)-C(6)	-21.4(6)
C(7)-O(1)-C(5)-C(4)	157.1(4)
C(3)-C(4)-C(5)-C(6)	1.0(5)
N(2)-C(4)-C(5)-C(6)	-175.5(3)
C(3)-C(4)-C(5)-O(1)	-177.5(3)
N(2)-C(4)-C(5)-O(1)	5.9(4)

C(15)-C(20)-C(19)-C(18)	1.6(5)
C(17)-C(18)-C(19)-C(20)	0.3(5)
Cl(1)-C(18)-C(19)-C(20)	179.0(3)
C(9)-C(10)-C(11)-C(12)	-1.0(4)
O(3)-C(12)-C(11)-C(10)	179.4(4)
O(2)-C(12)-C(11)-C(10)	0.2(4)
N(1)-C(1)-C(2)-C(3)	176.6(3)
C(6)-C(1)-C(2)-C(3)	0.6(5)
C(4)-C(3)-C(2)-C(1)	-0.9(5)

Symmetry transformations used to generate equivalent atoms:

Table 7. Hydrogen bonds for EMV01 [Å and °]

D-H...A	d(D-H)	d(H...A)	d(D...A)	<(DHA)
N(2)-H(8)...O(1)	0.93(3)	2.15(3)	2.627(4)	111(2)
N(1)-H(7)...O(2)#1	0.86(4)	2.36(4)	3.215(5)	169(4)
N(1)-H(19)...N(2)#2	0.91(5)	2.44(5)	3.322(5)	162(3)

Symmetry transformations used to generate equivalent atoms:

#1 -x+3/2,-y+1,z-1/2 #2 x+1/2,-y+3/2,-z

X-ray crystal structure of AgOAc-2.29 complex 2.53:

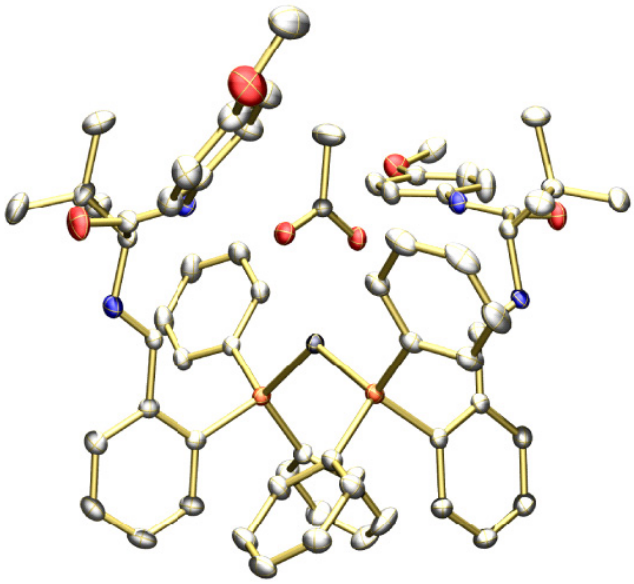

Table 1. Crystal data and structure refinement for AgOAc-**2.29** complex **2.53**.

Identification code	bc106	
Empirical formula	C70 H79 Ag N4 O7 P2	
Formula weight	1258.18	
Temperature	193(2) K	
Wavelength	0.71073 Å	
Crystal system	Orthorhombic	
Space group	P2(1)2(1)2(1)	
Unit cell dimensions	a = 17.451(4) Å	α= 90°.
	b = 17.675(5) Å	β= 90°.
	c = 21.505(6) Å	γ = 90°.
Volume	6633(3) Å^3	

Z	4
Density (calculated)	1.260 Mg/m^3
Absorption coefficient	0.406 mm^{-1}
F(000)	2640
Crystal size	0.12 x 0.10 x 0.10 mm^3
Theta range for data collection	1.49 to 25.00°.
Index ranges	-14<=h<=20, -18<=k<=21, -25<=l<=25
Reflections collected	42921
Independent reflections	11670 [R(int) = 0.0218]
Completeness to theta = 25.00°	100.0 %
Absorption correction	Empirical
Max. and min. transmission	0.9605 and 0.9528
Refinement method	Full-matrix least-squares on F^2
Data / restraints / parameters	11670 / 2 / 740
Goodness-of-fit on F^2	1.029
Final R indices [I>2sigma(I)]	R1 = 0.0316, wR2 = 0.0861
R indices (all data)	R1 = 0.0352, wR2 = 0.0895
Absolute structure parameter	-0.024(14)
Largest diff. peak and hole	0.936 and -0.350 $e.Å^{-3}$

Table 2. Atomic coordinates (x 10^4) and equivalent isotropic displacement parameters ($Å^2$x 10^3). U(eq) is defined as one third of the trace of the orthogonalized U^{ij} tensor

	x	y	z	U(eq)
Ag(1)	2286(1)	3664(1)	502(1)	32(1)
P(1)	1851(1)	2422(1)	838(1)	30(1)
P(2)	2558(1)	4084(1)	-551(1)	30(1)
O(1)	1963(1)	4614(1)	1264(1)	41(1)
O(2)	3193(1)	4342(1)	1256(1)	39(1)
O(3)	5525(1)	3198(1)	2099(1)	49(1)
O(4)	6799(2)	6206(2)	619(1)	66(1)
O(5)	-586(1)	5670(2)	933(1)	60(1)
O(6)	-1202(2)	4128(2)	3532(2)	80(1)
N(1)	4078(1)	2416(1)	1734(1)	33(1)
N(2)	4783(2)	4140(1)	1702(1)	39(1)
N(3)	574(1)	5452(2)	-70(1)	41(1)
N(4)	393(1)	5097(2)	1447(1)	40(1)
C(1)	2630(2)	4683(2)	1479(1)	37(1)
C(2)	2762(3)	5181(3)	2039(2)	86(2)
C(3)	2605(2)	1741(2)	655(1)	35(1)
C(4)	3338(2)	1822(2)	921(1)	34(1)
C(5)	3934(2)	1351(2)	725(1)	43(1)
C(6)	3812(2)	810(2)	270(2)	58(1)
C(7)	3098(2)	724(2)	17(2)	57(1)
C(8)	2495(2)	1187(2)	202(2)	47(1)

C(9)	3489(2)	2412(2)	1387(1)	31(1)
C(10)	4143(2)	3060(2)	2154(1)	33(1)
C(11)	4899(2)	3467(2)	1991(1)	35(1)
C(12)	4086(2)	2829(2)	2846(1)	39(1)
C(13)	3281(2)	2521(2)	2948(2)	55(1)
C(14)	4667(2)	2243(2)	3041(2)	52(1)
C(15)	4188(2)	3557(2)	3228(2)	59(1)
C(16)	5341(2)	4630(2)	1444(1)	40(1)
C(17)	5081(2)	5220(2)	1083(2)	46(1)
C(18)	5581(2)	5726(2)	813(2)	52(1)
C(19)	6355(2)	5658(2)	909(2)	47(1)
C(20)	6624(2)	5082(2)	1251(2)	63(1)
C(21)	6127(2)	4556(2)	1527(2)	64(1)
C(22)	7586(2)	6248(2)	773(2)	70(1)
C(23)	1603(2)	2256(2)	1649(1)	36(1)
C(24)	1721(2)	1563(2)	1931(2)	49(1)
C(25)	1472(2)	1456(2)	2542(2)	62(1)
C(26)	1120(2)	2025(3)	2858(2)	64(1)
C(27)	1000(2)	2714(3)	2579(2)	61(1)
C(28)	1254(2)	2836(2)	1977(2)	44(1)
C(29)	1020(2)	2075(2)	420(1)	35(1)
C(30)	842(2)	2404(2)	-152(1)	43(1)
C(31)	230(2)	2143(2)	-497(2)	53(1)

C(32)	-218(2)	1565(2)	-273(2)	49(1)
C(33)	-47(2)	1236(2)	284(2)	49(1)
C(34)	564(2)	1486(2)	638(2)	44(1)
C(35)	1692(2)	4137(2)	-1031(1)	32(1)
C(36)	1083(2)	4614(2)	-856(1)	31(1)
C(37)	441(2)	4671(2)	-1243(1)	40(1)
C(38)	390(2)	4236(2)	-1773(2)	46(1)
C(39)	964(2)	3732(2)	-1922(2)	50(1)
C(40)	1619(2)	3691(2)	-1559(1)	42(1)
C(41)	1113(2)	5043(2)	-268(1)	31(1)
C(42)	708(2)	5810(2)	530(2)	39(1)
C(43)	99(2)	5519(2)	982(2)	41(1)
C(44)	735(2)	6683(2)	478(2)	50(1)
C(45)	818(3)	7007(2)	1131(2)	70(1)
C(46)	37(3)	6998(2)	144(2)	73(1)
C(47)	1459(2)	6893(2)	110(2)	61(1)
C(48)	-9(2)	4836(2)	1977(2)	41(1)
C(49)	355(2)	4830(2)	2539(2)	56(1)
C(50)	-15(3)	4601(2)	3080(2)	63(1)
C(51)	-770(2)	4362(2)	3040(2)	57(1)
C(52)	-1130(2)	4344(2)	2470(2)	61(1)
C(53)	-764(2)	4585(2)	1945(2)	54(1)
C(54)	-902(4)	4230(3)	4120(2)	87(2)

C(55)	3205(2)	3482(2)	-996(1)	39(1)
C(56)	3590(2)	3728(2)	-1516(2)	50(1)
C(57)	4075(2)	3246(2)	-1839(2)	62(1)
C(58)	4165(3)	2522(2)	-1649(2)	68(1)
C(59)	3800(3)	2269(2)	-1129(2)	71(1)
C(60)	3310(2)	2742(2)	-800(2)	54(1)
C(61)	2956(2)	5042(2)	-623(1)	31(1)
C(62)	2806(2)	5503(2)	-1125(2)	43(1)
C(63)	3113(2)	6221(2)	-1153(2)	55(1)
C(64)	3570(2)	6478(2)	-673(2)	59(1)
C(65)	3718(2)	6031(2)	-172(2)	53(1)
C(66)	3411(2)	5306(2)	-146(2)	40(1)
O(1S)	6925(8)	3438(7)	3279(7)	314(6)
C(1S)	6727(6)	4760(5)	3235(4)	159(3)
C(2S)	6705(7)	4140(6)	3731(5)	198(5)
C(3S)	6820(9)	2876(8)	3890(6)	245(6)
C(4S)	6947(10)	2135(9)	3497(8)	299(8)

Table 3. Bond lengths [Å] and angles [°]

Ag(1)-O(1)	2.413(2)	Ag(1)-P(2)	2.4306(9)
Ag(1)-P(1)	2.4328(9)	Ag(1)-O(2)	2.562(2)

P(1)-C(29)	1.813(3)	P(1)-C(23)	1.820(3)
P(1)-C(3)	1.826(3)	P(2)-C(55)	1.824(3)
P(2)-C(35)	1.831(3)	P(2)-C(61)	1.836(3)
O(1)-C(1)	1.257(4)	O(2)-C(1)	1.248(4)
O(3)-C(11)	1.213(4)	O(4)-C(19)	1.389(4)
O(4)-C(22)	1.413(5)	O(5)-C(43)	1.229(4)
O(6)-C(51)	1.362(5)	O(6)-C(54)	1.381(6)
N(1)-C(9)	1.271(4)	N(1)-C(10)	1.457(4)
N(2)-C(11)	1.358(4)	N(2)-C(16)	1.416(4)
N(2)-H(2)	0.8800	N(3)-C(41)	1.260(4)
N(3)-C(42)	1.456(4)	N(4)-C(43)	1.349(4)
N(4)-C(48)	1.416(4)	N(4)-H(4)	0.8800
C(1)-C(2)	1.510(5)	C(2)-H(2A)	0.9800
C(2)-H(2B)	0.9800	C(2)-H(2C)	0.9800
C(3)-C(8)	1.396(4)	C(3)-C(4)	1.408(4)
C(4)-C(5)	1.397(4)	C(4)-C(9)	1.470(4)
C(5)-C(6)	1.384(5)	C(5)-H(5)	0.9500
C(6)-C(7)	1.368(6)	C(6)-H(6)	0.9500
C(7)-C(8)	1.391(5)	C(7)-H(7)	0.9500
C(8)-H(8)	0.9500	C(9)-H(9)	0.9500
C(10)-C(11)	1.543(4)	C(10)-C(12)	1.546(4)
C(10)-H(10)	1.0000	C(12)-C(14)	1.509(5)

C(12)-C(13)	1.521(5)	C(12)-C(15)	1.537(5)
C(13)-H(13A)	0.9800	C(13)-H(13B)	0.9800
C(13)-H(13C)	0.9800	C(14)-H(14A)	0.9800
C(14)-H(14B)	0.9800	C(14)-H(14C)	0.9800
C(15)-H(15A)	0.9800	C(15)-H(15B)	0.9800
C(15)-H(15C)	0.9800	C(16)-C(17)	1.377(5)
C(16)-C(21)	1.389(5)	C(17)-C(18)	1.377(5)
C(17)-H(17)	0.9500	C(18)-C(19)	1.372(5)
C(18)-H(18)	0.9500	C(19)-C(20)	1.340(5)
C(20)-C(21)	1.403(5)	C(20)-H(20)	0.9500
C(21)-H(21)	0.9500	C(22)-H(22A)	0.9800
C(22)-H(22B)	0.9800	C(22)-H(22C)	0.9800
C(23)-C(24)	1.382(5)	C(23)-C(28)	1.385(5)
C(24)-C(25)	1.396(5)	C(24)-H(24)	0.9500
C(25)-C(26)	1.361(6)	C(25)-H(25)	0.9500
C(26)-C(27)	1.373(6)	C(26)-H(26)	0.9500
C(27)-C(28)	1.387(5)	C(27)-H(27)	0.9500
C(28)-H(28)	0.9500	C(29)-C(34)	1.391(4)
C(29)-C(30)	1.395(4)	C(30)-C(31)	1.381(5)
C(30)-H(30)	0.9500	C(31)-C(32)	1.375(5)
C(31)-H(31)	0.9500	C(32)-C(33)	1.363(5)
C(32)-H(32)	0.9500	C(33)-C(34)	1.383(5)

C(33)-H(33)	0.9500	C(34)-H(34)	0.9500
C(35)-C(40)	1.388(4)	C(35)-C(36)	1.409(4)
C(36)-C(37)	1.398(4)	C(36)-C(41)	1.475(4)
C(37)-C(38)	1.378(5)	C(37)-H(37)	0.9500
C(38)-C(39)	1.378(5)	C(38)-H(38)	0.9500
C(39)-C(40)	1.386(5)	C(39)-H(39)	0.9500
C(40)-H(40)	0.9500	C(41)-H(41)	0.9500
C(42)-C(43)	1.530(5)	C(42)-C(44)	1.548(4)
C(42)-H(42)	1.0000	C(44)-C(45)	1.525(5)
C(44)-C(46)	1.519(6)	C(44)-C(47)	1.536(5)
C(45)-H(45A)	0.9800	C(45)-H(45B)	0.9800
C(45)-H(45C)	0.9800	C(46)-H(46A)	0.9800
C(46)-H(46B)	0.9800	C(46)-H(46C)	0.9800
C(47)-H(47A)	0.9800	C(47)-H(47B)	0.9800
C(47)-H(47C)	0.9800	C(48)-C(49)	1.366(5)
C(48)-C(53)	1.392(5)	C(49)-C(50)	1.390(5)
C(49)-H(49)	0.9500	C(50)-C(51)	1.387(6)
C(50)-H(50)	0.9500	C(51)-C(52)	1.378(6)
C(52)-C(53)	1.365(5)	C(52)-H(52)	0.9500
C(53)-H(53)	0.9500	C(54)-H(54A)	0.9800
C(54)-H(54B)	0.9800	C(54)-H(54C)	0.9800
C(55)-C(56)	1.374(5)	C(55)-C(60)	1.387(5)

C(56)-C(57)	1.388(5)	C(56)-H(56)	0.9500
C(57)-C(58)	1.351(6)	C(57)-H(57)	0.9500
C(58)-C(59)	1.363(6)	C(58)-H(58)	0.9500
C(59)-C(60)	1.390(5)	C(59)-H(59)	0.9500
C(60)-H(60)	0.9500	C(61)-C(62)	1.378(4)
C(61)-C(66)	1.380(4)	C(62)-C(63)	1.378(5)
C(62)-H(62)	0.9500	C(63)-C(64)	1.382(5)
C(63)-H(63)	0.9500	C(64)-C(65)	1.362(5)
C(64)-H(64)	0.9500	C(65)-C(66)	1.390(5)
C(65)-H(65)	0.9500	C(66)-H(66)	0.9500
O(1S)-C(2S)	1.622(13)	O(1S)-C(3S)	1.657(14)
C(1S)-C(2S)	1.530(11)	C(1S)-H(1S1)	0.9800
C(1S)-H(1S2)	0.9800	C(1S)-H(1S3)	0.9800
C(2S)-H(2S1)	0.9900	C(2S)-H(2S2)	0.9900
C(3S)-C(4S)	1.574(14)	C(3S)-H(3S1)	0.9900
C(3S)-H(3S2)	0.9900	C(4S)-H(4S1)	0.9800
C(4S)-H(4S2)	0.9800	C(4S)-H(4S3)	0.9800
O(1)-Ag(1)-P(2)	117.79(6)	O(1)-Ag(1)-P(1)	110.69(6)
P(2)-Ag(1)-P(1)	127.81(2)	O(1)-Ag(1)-O(2)	52.37(7)
P(2)-Ag(1)-O(2)	109.06(5)	P(1)-Ag(1)-O(2)	115.26(5)
C(29)-P(1)-C(23)	103.34(13)	C(29)-P(1)-C(3)	104.21(13)
C(23)-P(1)-C(3)	105.75(13)	C(29)-P(1)-Ag(1)	114.08(10)

C(23)-P(1)-Ag(1)	120.28(10)	C(3)-P(1)-Ag(1)	107.81(10)
C(55)-P(2)-C(35)	104.18(13)	C(55)-P(2)-C(61)	105.01(13)
C(35)-P(2)-C(61)	102.55(12)	C(55)-P(2)-Ag(1)	115.58(10)
C(35)-P(2)-Ag(1)	112.35(9)	C(61)-P(2)-Ag(1)	115.72(9)
C(1)-O(1)-Ag(1)	95.73(17)	C(1)-O(2)-Ag(1)	88.98(17)
C(19)-O(4)-C(22)	118.3(3)	C(51)-O(6)-C(54)	117.6(4)
C(9)-N(1)-C(10)	115.6(2)	C(11)-N(2)-C(16)	127.8(3)
C(11)-N(2)-H(2)	116.1	C(16)-N(2)-H(2)	116.1
C(41)-N(3)-C(42)	115.3(2)	C(43)-N(4)-C(48)	126.0(3)
C(43)-N(4)-H(4)	117.0	C(48)-N(4)-H(4)	117.0
O(2)-C(1)-O(1)	122.8(3)	O(2)-C(1)-C(2)	117.9(3)
O(1)-C(1)-C(2)	119.3(3)	C(1)-C(2)-H(2A)	109.1
C(1)-C(2)-H(2B)	110.7	H(2A)-C(2)-H(2B)	109.5
C(1)-C(2)-H(2C)	108.6	H(2A)-C(2)-H(2C)	109.5
H(2B)-C(2)-H(2C)	109.5	C(8)-C(3)-C(4)	118.6(3)
C(8)-C(3)-P(1)	121.0(2)	C(4)-C(3)-P(1)	120.0(2)
C(5)-C(4)-C(3)	119.6(3)	C(5)-C(4)-C(9)	119.6(3)
C(3)-C(4)-C(9)	120.8(3)	C(6)-C(5)-C(4)	120.6(3)
C(6)-C(5)-H(5)	119.7	C(4)-C(5)-H(5)	119.7
C(7)-C(6)-C(5)	119.9(3)	C(7)-C(6)-H(6)	120.0
C(5)-C(6)-H(6)	120.0	C(6)-C(7)-C(8)	120.6(3)
C(6)-C(7)-H(7)	119.7	C(8)-C(7)-H(7)	119.7

C(7)-C(8)-C(3)	120.6(3)	C(7)-C(8)-H(8)	119.7
C(3)-C(8)-H(8)	119.7	N(1)-C(9)-C(4)	123.4(3)
N(1)-C(9)-H(9)	118.3	C(4)-C(9)-H(9)	118.3
N(1)-C(10)-C(11)	106.8(2)	N(1)-C(10)-C(12)	112.6(2)
C(11)-C(10)-C(12)	113.4(2)	N(1)-C(10)-H(10)	107.9
C(11)-C(10)-H(10)	107.9	C(12)-C(10)-H(10)	107.9
O(3)-C(11)-N(2)	124.4(3)	O(3)-C(11)-C(10)	123.0(3)
N(2)-C(11)-C(10)	112.6(2)	C(14)-C(12)-C(13)	109.6(3)
C(14)-C(12)-C(15)	110.3(3)	C(13)-C(12)-C(15)	109.2(3)
C(14)-C(12)-C(10)	113.9(3)	C(13)-C(12)-C(10)	107.0(3)
C(15)-C(12)-C(10)	106.6(3)	C(12)-C(13)-H(13A)	109.5
C(12)-C(13)-H(13B)	109.5	H(13A)-C(13)-H(13B)	109.5
C(12)-C(13)-H(13C)	109.5	H(13A)-C(13)-H(13C)	109.5
H(13B)-C(13)-H(13C)	109.5	C(12)-C(14)-H(14A)	109.5
C(12)-C(14)-H(14B)	109.5	H(14A)-C(14)-H(14B)	109.5
C(12)-C(14)-H(14C)	109.5	H(14A)-C(14)-H(14C)	109.5
H(14B)-C(14)-H(14C)	109.5	C(12)-C(15)-H(15A)	109.5
C(12)-C(15)-H(15B)	109.5	H(15A)-C(15)-H(15B)	109.5
C(12)-C(15)-H(15C)	109.5	H(15A)-C(15)-H(15C)	109.5
H(15B)-C(15)-H(15C)	109.5	C(17)-C(16)-C(21)	117.9(3)
C(17)-C(16)-N(2)	117.2(3)	C(21)-C(16)-N(2)	124.8(3)
C(16)-C(17)-C(18)	121.4(3)	C(16)-C(17)-H(17)	119.3

C(18)-C(17)-H(17)	119.3	C(19)-C(18)-C(17)	120.2(3)
C(19)-C(18)-H(18)	119.9	C(17)-C(18)-H(18)	119.9
C(20)-C(19)-C(18)	119.6(3)	C(20)-C(19)-O(4)	125.4(3)
C(18)-C(19)-O(4)	114.9(3)	C(19)-C(20)-C(21)	121.2(4)
C(19)-C(20)-H(20)	119.4	C(21)-C(20)-H(20)	119.4
C(16)-C(21)-C(20)	119.6(3)	C(16)-C(21)-H(21)	120.2
C(20)-C(21)-H(21)	120.2	O(4)-C(22)-H(22A)	109.5
O(4)-C(22)-H(22B)	109.5	H(22A)-C(22)-H(22B)	109.5
O(4)-C(22)-H(22C)	109.5	H(22A)-C(22)-H(22C)	109.5
H(22B)-C(22)-H(22C)	109.5	C(24)-C(23)-C(28)	119.8(3)
C(24)-C(23)-P(1)	121.9(2)	C(28)-C(23)-P(1)	118.2(2)
C(23)-C(24)-C(25)	119.2(4)	C(23)-C(24)-H(24)	120.4
C(25)-C(24)-H(24)	120.4	C(26)-C(25)-C(24)	120.6(4)
C(26)-C(25)-H(25)	119.7	C(24)-C(25)-H(25)	119.7
C(25)-C(26)-C(27)	120.5(3)	C(25)-C(26)-H(26)	119.8
C(27)-C(26)-H(26)	119.8	C(26)-C(27)-C(28)	119.8(4)
C(26)-C(27)-H(27)	120.1	C(28)-C(27)-H(27)	120.1
C(23)-C(28)-C(27)	120.1(3)	C(23)-C(28)-H(28)	120.0
C(27)-C(28)-H(28)	120.0	C(34)-C(29)-C(30)	118.8(3)
C(34)-C(29)-P(1)	122.9(2)	C(30)-C(29)-P(1)	118.3(2)
C(31)-C(30)-C(29)	120.5(3)	C(31)-C(30)-H(30)	119.8
C(29)-C(30)-H(30)	119.8	C(32)-C(31)-C(30)	119.9(3)

C(32)-C(31)-H(31)	120.0	C(30)-C(31)-H(31)	120.0
C(33)-C(32)-C(31)	120.1(3)	C(33)-C(32)-H(32)	120.0
C(31)-C(32)-H(32)	120.0	C(32)-C(33)-C(34)	121.0(3)
C(32)-C(33)-H(33)	119.5	C(34)-C(33)-H(33)	119.5
C(33)-C(34)-C(29)	119.7(3)	C(33)-C(34)-H(34)	120.2
C(29)-C(34)-H(34)	120.2	C(40)-C(35)-C(36)	119.3(3)
C(40)-C(35)-P(2)	120.5(2)	C(36)-C(35)-P(2)	120.2(2)
C(37)-C(36)-C(35)	119.2(3)	C(37)-C(36)-C(41)	120.1(3)
C(35)-C(36)-C(41)	120.6(3)	C(38)-C(37)-C(36)	120.3(3)
C(38)-C(37)-H(37)	119.9	C(36)-C(37)-H(37)	119.9
C(39)-C(38)-C(37)	120.4(3)	C(39)-C(38)-H(38)	119.8
C(37)-C(38)-H(38)	119.8	C(38)-C(39)-C(40)	120.2(3)
C(38)-C(39)-H(39)	119.9	C(40)-C(39)-H(39)	119.9
C(35)-C(40)-C(39)	120.4(3)	C(35)-C(40)-H(40)	119.8
C(39)-C(40)-H(40)	119.8	N(3)-C(41)-C(36)	123.8(3)
N(3)-C(41)-H(41)	118.1	C(36)-C(41)-H(41)	118.1
N(3)-C(42)-C(43)	107.8(2)	N(3)-C(42)-C(44)	112.0(3)
C(43)-C(42)-C(44)	113.6(3)	N(3)-C(42)-H(42)	107.7
C(43)-C(42)-H(42)	107.7	C(44)-C(42)-H(42)	107.7
O(5)-C(43)-N(4)	123.6(3)	O(5)-C(43)-C(42)	123.2(3)
N(4)-C(43)-C(42)	113.1(3)	C(45)-C(44)-C(46)	111.9(3)
C(45)-C(44)-C(47)	107.7(3)	C(46)-C(44)-C(47)	109.2(3)

C(45)-C(44)-C(42)	108.1(3)	C(46)-C(44)-C(42)	112.1(3)
C(47)-C(44)-C(42)	107.7(3)	C(44)-C(45)-H(45A)	109.5
C(44)-C(45)-H(45B)	109.5	H(45A)-C(45)-H(45B)	109.5
C(44)-C(45)-H(45C)	109.5	H(45A)-C(45)-H(45C)	109.5
H(45B)-C(45)-H(45C)	109.5	C(44)-C(46)-H(46A)	109.5
C(44)-C(46)-H(46B)	109.5	H(46A)-C(46)-H(46B)	109.5
C(44)-C(46)-H(46C)	109.5	H(46A)-C(46)-H(46C)	109.5
H(46B)-C(46)-H(46C)	109.5	C(44)-C(47)-H(47A)	109.5
C(44)-C(47)-H(47B)	109.5	H(47A)-C(47)-H(47B)	109.5
C(44)-C(47)-H(47C)	109.5	H(47A)-C(47)-H(47C)	109.5
H(47B)-C(47)-H(47C)	109.5	C(49)-C(48)-C(53)	118.8(3)
C(49)-C(48)-N(4)	119.0(3)	C(53)-C(48)-N(4)	122.2(3)
C(48)-C(49)-C(50)	121.8(4)	C(48)-C(49)-H(49)	119.1
C(50)-C(49)-H(49)	119.1	C(51)-C(50)-C(49)	118.6(4)
C(51)-C(50)-H(50)	120.7	C(49)-C(50)-H(50)	120.7
O(6)-C(51)-C(52)	115.6(4)	O(6)-C(51)-C(50)	124.7(4)
C(52)-C(51)-C(50)	119.7(4)	C(53)-C(52)-C(51)	121.0(4)
C(53)-C(52)-H(52)	119.5	C(51)-C(52)-H(52)	119.5
C(52)-C(53)-C(48)	120.2(4)	C(52)-C(53)-H(53)	119.9
C(48)-C(53)-H(53)	119.9	O(6)-C(54)-H(54A)	109.5
O(6)-C(54)-H(54B)	109.5	H(54A)-C(54)-H(54B)	109.5
O(6)-C(54)-H(54C)	109.5	H(54A)-C(54)-H(54C)	109.5

H(54B)-C(54)-H(54C)	109.5	C(56)-C(55)-C(60)	118.8(3)
C(56)-C(55)-P(2)	123.0(2)	C(60)-C(55)-P(2)	118.2(2)
C(55)-C(56)-C(57)	120.7(4)	C(55)-C(56)-H(56)	119.7
C(57)-C(56)-H(56)	119.7	C(58)-C(57)-C(56)	120.0(4)
C(58)-C(57)-H(57)	120.0	C(56)-C(57)-H(57)	120.0
C(57)-C(58)-C(59)	120.4(4)	C(57)-C(58)-H(58)	119.8
C(59)-C(58)-H(58)	119.8	C(58)-C(59)-C(60)	120.5(4)
C(58)-C(59)-H(59)	119.8	C(60)-C(59)-H(59)	119.8
C(59)-C(60)-C(55)	119.6(3)	C(59)-C(60)-H(60)	120.2
C(55)-C(60)-H(60)	120.2	C(62)-C(61)-C(66)	119.4(3)
C(62)-C(61)-P(2)	122.7(2)	C(66)-C(61)-P(2)	117.8(2)
C(61)-C(62)-C(63)	120.4(3)	C(61)-C(62)-H(62)	119.8
C(63)-C(62)-H(62)	119.8	C(62)-C(63)-C(64)	119.7(3)
C(62)-C(63)-H(63)	120.2	C(64)-C(63)-H(63)	120.2
C(65)-C(64)-C(63)	120.6(3)	C(65)-C(64)-H(64)	119.7
C(63)-C(64)-H(64)	119.7	C(64)-C(65)-C(66)	119.6(3)
C(64)-C(65)-H(65)	120.2	C(66)-C(65)-H(65)	120.2
C(61)-C(66)-C(65)	120.3(3)	C(61)-C(66)-H(66)	119.9
C(65)-C(66)-H(66)	119.9	C(2S)-O(1S)-C(3S)	87.6(10)
C(2S)-C(1S)-H(1S1)	107.3	C(2S)-C(1S)-H(1S2)	109.8
H(1S1)-C(1S)-H(1S2)	109.5	C(2S)-C(1S)-H(1S3)	111.3
H(1S1)-C(1S)-H(1S3)	109.5	H(1S2)-C(1S)-H(1S3)	109.5

C(1S)-C(2S)-O(1S)	97.1(9)	C(1S)-C(2S)-H(2S1)	109.6
O(1S)-C(2S)-H(2S1)	117.3	C(1S)-C(2S)-H(2S2)	111.5
O(1S)-C(2S)-H(2S2)	112.7	H(2S1)-C(2S)-H(2S2)	108.1
C(4S)-C(3S)-O(1S)	93.3(11)	C(4S)-C(3S)-H(3S1)	111.3
O(1S)-C(3S)-H(3S1)	112.9	C(4S)-C(3S)-H(3S2)	113.1
O(1S)-C(3S)-H(3S2)	116.1	H(3S1)-C(3S)-H(3S2)	109.3
C(3S)-C(4S)-H(4S1)	107.8	C(3S)-C(4S)-H(4S2)	109.5
H(4S1)-C(4S)-H(4S2)	109.5	C(3S)-C(4S)-H(4S3)	111.1
H(4S1)-C(4S)-H(4S3)	109.5	H(4S2)-C(4S)-H(4S3)	109.5

Symmetry transformations used to generate equivalent atoms:

Table 4. Anisotropic displacement parameters ($Å^2 x\ 10^3$) for bc106. The anisotropic displacement factor exponent takes the form: $-2\pi^2[\ h^2\ a^{*2}U^{11} + ...\ + 2\ h\ k\ a^*\ b^*\ U^{12}\ ]$

	U^{11}	U^{22}	U^{33}	U^{23}	U^{13}	U^{12}
Ag(1)	37(1)	29(1)	30(1)	0(1)	0(1)	0(1)
P(1)	33(1)	30(1)	28(1)	0(1)	-4(1)	-2(1)
P(2)	33(1)	29(1)	28(1)	-1(1)	4(1)	0(1)
O(1)	35(1)	44(1)	45(1)	-6(1)	-2(1)	7(1)
O(2)	31(1)	44(1)	43(1)	1(1)	-3(1)	6(1)

O(3)	31(1)	57(1)	60(1)	14(1)	-4(1)	2(1)
O(4)	64(2)	70(2)	62(2)	12(1)	0(1)	-26(1)
O(5)	34(1)	87(2)	58(2)	11(1)	5(1)	16(1)
O(6)	76(2)	94(2)	70(2)	13(2)	11(2)	-18(2)
N(1)	33(1)	40(1)	26(1)	-1(1)	-2(1)	5(1)
N(2)	31(1)	44(1)	43(1)	4(1)	-3(1)	0(1)
N(3)	33(1)	51(2)	39(1)	-5(1)	-3(1)	8(1)
N(4)	30(1)	47(1)	42(1)	-4(1)	4(1)	6(1)
C(1)	42(2)	35(1)	33(1)	-3(1)	-1(1)	3(1)
C(2)	76(3)	109(4)	73(3)	-49(3)	-18(3)	14(3)
C(3)	44(2)	31(1)	30(1)	2(1)	-4(1)	1(1)
C(4)	42(2)	33(1)	28(1)	3(1)	-3(1)	1(1)
C(5)	46(2)	45(2)	39(2)	-3(1)	-6(1)	13(2)
C(6)	71(2)	52(2)	50(2)	-12(2)	-8(2)	23(2)
C(7)	75(3)	46(2)	50(2)	-20(2)	-14(2)	16(2)
C(8)	58(2)	39(2)	45(2)	-10(1)	-12(2)	4(1)
C(9)	29(1)	35(1)	30(1)	0(1)	3(1)	3(1)
C(10)	29(1)	37(2)	33(1)	-1(1)	-3(1)	3(1)
C(11)	34(2)	39(2)	32(1)	1(1)	-3(1)	1(1)
C(12)	41(2)	47(2)	29(1)	-7(1)	2(1)	2(1)
C(13)	51(2)	69(2)	45(2)	-3(2)	14(2)	-7(2)
C(14)	64(2)	58(2)	32(2)	9(1)	1(2)	9(2)
C(15)	72(2)	62(2)	43(2)	-19(2)	4(2)	3(2)

C(16)	37(2)	43(2)	39(2)	2(1)	-2(1)	-8(1)
C(17)	42(2)	47(2)	50(2)	5(2)	-12(2)	-7(2)
C(18)	59(2)	49(2)	48(2)	7(2)	-11(2)	-12(2)
C(19)	56(2)	45(2)	42(2)	-3(1)	-2(2)	-14(2)
C(20)	38(2)	69(2)	81(3)	7(2)	5(2)	-4(2)
C(21)	41(2)	63(2)	87(3)	26(2)	-6(2)	-1(2)
C(22)	53(2)	54(2)	104(3)	-12(2)	22(2)	-20(2)
C(23)	34(2)	44(2)	30(1)	-2(1)	-3(1)	-12(1)
C(24)	62(2)	47(2)	38(2)	4(1)	-2(2)	-16(2)
C(25)	77(3)	65(2)	44(2)	20(2)	-12(2)	-27(2)
C(26)	51(2)	110(4)	33(2)	1(2)	5(2)	-27(2)
C(27)	47(2)	95(3)	39(2)	-14(2)	0(2)	-4(2)
C(28)	39(2)	56(2)	38(2)	-5(2)	-5(1)	-2(2)
C(29)	36(2)	36(1)	34(1)	-4(1)	-5(1)	-1(1)
C(30)	43(2)	45(2)	40(2)	3(1)	-8(1)	-6(1)
C(31)	53(2)	65(2)	40(2)	-6(2)	-15(2)	-1(2)
C(32)	35(2)	63(2)	48(2)	-17(2)	-9(1)	-6(2)
C(33)	42(2)	52(2)	52(2)	-8(2)	2(1)	-14(2)
C(34)	46(2)	45(2)	40(2)	0(1)	-7(1)	-11(1)
C(35)	38(2)	29(1)	30(1)	2(1)	3(1)	-8(1)
C(36)	32(1)	29(1)	33(1)	2(1)	4(1)	-8(1)
C(37)	34(2)	45(2)	40(2)	4(1)	2(1)	-9(1)
C(38)	37(2)	64(2)	38(2)	2(2)	-6(1)	-13(2)

C(39)	51(2)	63(2)	36(2)	-12(2)	1(1)	-20(2)
C(40)	43(2)	46(2)	36(1)	-7(1)	3(1)	-8(2)
C(41)	27(1)	34(1)	33(1)	2(1)	-1(1)	-1(1)
C(42)	32(1)	48(2)	36(1)	-5(1)	0(1)	10(1)
C(43)	34(2)	50(2)	40(2)	-8(1)	1(1)	7(1)
C(44)	53(2)	44(2)	53(2)	-4(2)	9(2)	13(1)
C(45)	84(3)	56(2)	69(3)	-22(2)	16(2)	-1(2)
C(46)	74(3)	58(2)	88(3)	4(2)	5(2)	30(2)
C(47)	71(3)	52(2)	61(2)	0(2)	10(2)	1(2)
C(48)	38(2)	37(2)	48(2)	-5(1)	7(1)	3(1)
C(49)	51(2)	68(2)	50(2)	-2(2)	2(2)	-17(2)
C(50)	73(3)	71(3)	45(2)	4(2)	-2(2)	-10(2)
C(51)	59(2)	48(2)	64(2)	0(2)	24(2)	-4(2)
C(52)	54(2)	64(2)	65(2)	4(2)	5(2)	-8(2)
C(53)	44(2)	52(2)	66(2)	2(2)	0(2)	-4(2)
C(54)	131(5)	75(3)	56(2)	0(2)	4(3)	-16(3)
C(55)	37(2)	44(2)	34(1)	-5(1)	2(1)	5(1)
C(56)	54(2)	49(2)	47(2)	-2(2)	13(2)	6(2)
C(57)	54(2)	76(3)	55(2)	-9(2)	21(2)	6(2)
C(58)	64(3)	59(2)	80(3)	-22(2)	22(2)	11(2)
C(59)	87(3)	42(2)	83(3)	-2(2)	25(2)	15(2)
C(60)	68(2)	39(2)	56(2)	-2(2)	21(2)	8(2)
C(61)	26(1)	32(1)	35(1)	0(1)	4(1)	1(1)

C(62)	40(2)	45(2)	43(2)	8(1)	-5(1)	-6(2)
C(63)	45(2)	51(2)	68(2)	23(2)	-10(2)	-7(2)
C(64)	46(2)	40(2)	92(3)	14(2)	-11(2)	-12(2)
C(65)	49(2)	48(2)	62(2)	0(2)	-17(2)	-9(2)
C(66)	38(2)	38(2)	44(2)	5(1)	-5(1)	-2(1)

Table 5. Hydrogen coordinates (x 10^4) and isotropic displacement parameters (Å^{2}x 10^3)

	x	y	z	U(eq)
H(2)	4304	4289	1671	47
H(4)	880	4972	1418	48
H(2A)	3229	5016	2252	128
H(2B)	2327	5152	2326	128
H(2C)	2826	5704	1896	128
H(5)	4428	1401	906	52
H(6)	4223	500	133	69
H(7)	3013	344	-288	68
H(8)	2004	1125	17	57
H(9)	3127	2810	1431	38
H(10)	3711	3414	2062	40
H(13A)	3227	2036	2731	83

H(13B)	2905	2882	2784	83
H(13C)	3194	2447	3394	83
H(14A)	4583	2108	3478	77
H(14B)	5184	2450	2992	77
H(14C)	4611	1791	2781	77
H(15A)	3797	3926	3107	89
H(15B)	4698	3769	3150	89
H(15C)	4135	3440	3672	89
H(17)	4546	5279	1019	55
H(18)	5389	6123	559	63
H(20)	7161	5030	1308	75
H(21)	6326	4152	1768	77
H(22A)	7642	6299	1224	105
H(22B)	7815	6688	567	105
H(22C)	7845	5787	633	105
H(24)	1967	1165	1712	59
H(25)	1550	981	2739	75
H(26)	957	1945	3274	77
H(27)	742	3105	2799	73
H(28)	1189	3318	1789	53
H(30)	1145	2811	-304	51
H(31)	119	2363	-890	63
H(32)	-647	1394	-506	58

H(33)	-353	828	430	59
H(34)	672	1257	1028	52
H(37)	39	5011	-1140	48
H(38)	-43	4284	-2038	56
H(39)	910	3411	-2274	60
H(40)	2021	3356	-1673	50
H(41)	1565	5008	-24	38
H(42)	1219	5635	684	46
H(45A)	910	7553	1105	105
H(45B)	1251	6763	1341	105
H(45C)	347	6912	1367	105
H(46A)	56	7552	151	110
H(46B)	-429	6825	355	110
H(46C)	34	6820	-287	110
H(47A)	1420	6693	-313	92
H(47B)	1910	6675	316	92
H(47C)	1510	7445	95	92
H(49)	875	4987	2562	68
H(50)	244	4608	3469	76
H(52)	-1641	4161	2441	73
H(53)	-1024	4581	1558	65
H(54A)	-486	3868	4189	131
H(54B)	-1305	4149	4430	131

H(54C)	-703	4747	4158	131
H(56)	3523	4234	-1655	60
H(57)	4344	3424	-2194	74
H(58)	4483	2189	-1880	81
H(59)	3882	1765	-990	85
H(60)	3049	2559	-442	65
H(62)	2490	5326	-1454	51
H(63)	3010	6537	-1501	65
H(64)	3784	6972	-694	71
H(65)	4029	6213	158	64
H(66)	3515	4991	202	48
H(1S1)	7058	5164	3392	239
H(1S2)	6209	4959	3167	239
H(1S3)	6932	4568	2842	239
H(2S1)	6193	4130	3930	237
H(2S2)	7092	4228	4060	237
H(3S1)	7229	2943	4204	294
H(3S2)	6315	2892	4098	294
H(4S1)	6491	1817	3545	449
H(4S2)	7397	1864	3654	449
H(4S3)	7022	2254	3056	449

Table 6. Torsion angles [°]

O(1)-Ag(1)-P(1)-C(29)	106.45(12)
P(2)-Ag(1)-P(1)-C(29)	-51.05(11)
O(2)-Ag(1)-P(1)-C(29)	163.53(11)
O(1)-Ag(1)-P(1)-C(23)	-17.16(13)
P(2)-Ag(1)-P(1)-C(23)	-174.67(12)
O(2)-Ag(1)-P(1)-C(23)	39.92(13)
O(1)-Ag(1)-P(1)-C(3)	-138.34(10)
P(2)-Ag(1)-P(1)-C(3)	64.16(10)
O(2)-Ag(1)-P(1)-C(3)	-81.26(10)
O(1)-Ag(1)-P(2)-C(55)	152.20(12)
P(1)-Ag(1)-P(2)-C(55)	-51.67(12)
O(2)-Ag(1)-P(2)-C(55)	95.44(12)
O(1)-Ag(1)-P(2)-C(35)	-88.44(11)
P(1)-Ag(1)-P(2)-C(35)	67.70(10)
O(2)-Ag(1)-P(2)-C(35)	-145.20(11)
O(1)-Ag(1)-P(2)-C(61)	28.87(11)
P(1)-Ag(1)-P(2)-C(61)	-174.99(9)
O(2)-Ag(1)-P(2)-C(61)	-27.89(11)
P(2)-Ag(1)-O(1)-C(1)	-95.56(17)
P(1)-Ag(1)-O(1)-C(1)	104.42(17)
O(2)-Ag(1)-O(1)-C(1)	-2.13(16)
O(1)-Ag(1)-O(2)-C(1)	2.13(16)

P(2)-Ag(1)-O(2)-C(1)	113.02(16)
P(1)-Ag(1)-O(2)-C(1)	-95.30(17)
Ag(1)-O(2)-C(1)-O(1)	-3.9(3)
Ag(1)-O(2)-C(1)-C(2)	174.6(3)
Ag(1)-O(1)-C(1)-O(2)	4.1(3)
Ag(1)-O(1)-C(1)-C(2)	-174.3(3)
C(29)-P(1)-C(3)-C(8)	9.1(3)
C(23)-P(1)-C(3)-C(8)	117.7(2)
Ag(1)-P(1)-C(3)-C(8)	-112.4(2)
C(29)-P(1)-C(3)-C(4)	-178.1(2)
C(23)-P(1)-C(3)-C(4)	-69.5(2)
Ag(1)-P(1)-C(3)-C(4)	60.4(2)
C(8)-C(3)-C(4)-C(5)	0.1(4)
P(1)-C(3)-C(4)-C(5)	-172.8(2)
C(8)-C(3)-C(4)-C(9)	178.2(3)
P(1)-C(3)-C(4)-C(9)	5.3(4)
C(3)-C(4)-C(5)-C(6)	0.5(5)
C(9)-C(4)-C(5)-C(6)	-177.6(3)
C(4)-C(5)-C(6)-C(7)	-1.4(6)
C(5)-C(6)-C(7)-C(8)	1.6(6)
C(6)-C(7)-C(8)-C(3)	-1.0(6)
C(4)-C(3)-C(8)-C(7)	0.1(5)
P(1)-C(3)-C(8)-C(7)	172.9(3)

C(10)-N(1)-C(9)-C(4)	178.0(2)
C(5)-C(4)-C(9)-N(1)	-17.1(4)
C(3)-C(4)-C(9)-N(1)	164.8(3)
C(9)-N(1)-C(10)-C(11)	-120.4(3)
C(9)-N(1)-C(10)-C(12)	114.5(3)
C(16)-N(2)-C(11)-O(3)	3.7(5)
C(16)-N(2)-C(11)-C(10)	-174.5(3)
N(1)-C(10)-C(11)-O(3)	-70.0(4)
C(12)-C(10)-C(11)-O(3)	54.7(4)
N(1)-C(10)-C(11)-N(2)	108.3(3)
C(12)-C(10)-C(11)-N(2)	-127.0(3)
N(1)-C(10)-C(12)-C(14)	56.4(4)
C(11)-C(10)-C(12)-C(14)	-65.1(3)
N(1)-C(10)-C(12)-C(13)	-64.9(3)
C(11)-C(10)-C(12)-C(13)	173.6(3)
N(1)-C(10)-C(12)-C(15)	178.3(3)
C(11)-C(10)-C(12)-C(15)	56.8(3)
C(11)-N(2)-C(16)-C(17)	169.4(3)
C(11)-N(2)-C(16)-C(21)	-10.2(5)
C(21)-C(16)-C(17)-C(18)	-0.3(5)
N(2)-C(16)-C(17)-C(18)	-180.0(3)
C(16)-C(17)-C(18)-C(19)	-1.2(6)
C(17)-C(18)-C(19)-C(20)	2.1(6)

C(17)-C(18)-C(19)-O(4)	-179.2(3)
C(22)-O(4)-C(19)-C(20)	-11.2(5)
C(22)-O(4)-C(19)-C(18)	170.2(3)
C(18)-C(19)-C(20)-C(21)	-1.5(6)
O(4)-C(19)-C(20)-C(21)	179.9(4)
C(17)-C(16)-C(21)-C(20)	0.9(6)
N(2)-C(16)-C(21)-C(20)	-179.5(4)
C(19)-C(20)-C(21)-C(16)	0.0(7)
C(29)-P(1)-C(23)-C(24)	84.0(3)
C(3)-P(1)-C(23)-C(24)	-25.2(3)
Ag(1)-P(1)-C(23)-C(24)	-147.4(2)
C(29)-P(1)-C(23)-C(28)	-92.9(3)
C(3)-P(1)-C(23)-C(28)	157.9(2)
Ag(1)-P(1)-C(23)-C(28)	35.8(3)
C(28)-C(23)-C(24)-C(25)	1.1(5)
P(1)-C(23)-C(24)-C(25)	-175.8(3)
C(23)-C(24)-C(25)-C(26)	-0.1(6)
C(24)-C(25)-C(26)-C(27)	0.4(6)
C(25)-C(26)-C(27)-C(28)	-1.5(6)
C(24)-C(23)-C(28)-C(27)	-2.2(5)
P(1)-C(23)-C(28)-C(27)	174.7(3)
C(26)-C(27)-C(28)-C(23)	2.4(5)
C(23)-P(1)-C(29)-C(34)	-30.4(3)

C(3)-P(1)-C(29)-C(34)	80.0(3)
Ag(1)-P(1)-C(29)-C(34)	-162.7(2)
C(23)-P(1)-C(29)-C(30)	151.0(2)
C(3)-P(1)-C(29)-C(30)	-98.7(3)
Ag(1)-P(1)-C(29)-C(30)	18.6(3)
C(34)-C(29)-C(30)-C(31)	-0.8(5)
P(1)-C(29)-C(30)-C(31)	177.9(3)
C(29)-C(30)-C(31)-C(32)	1.3(5)
C(30)-C(31)-C(32)-C(33)	-1.6(5)
C(31)-C(32)-C(33)-C(34)	1.5(5)
C(32)-C(33)-C(34)-C(29)	-1.0(5)
C(30)-C(29)-C(34)-C(33)	0.6(5)
P(1)-C(29)-C(34)-C(33)	-178.0(3)
C(55)-P(2)-C(35)-C(40)	7.5(3)
C(61)-P(2)-C(35)-C(40)	116.7(2)
Ag(1)-P(2)-C(35)-C(40)	-118.4(2)
C(55)-P(2)-C(35)-C(36)	-174.6(2)
C(61)-P(2)-C(35)-C(36)	-65.3(2)
Ag(1)-P(2)-C(35)-C(36)	59.6(2)
C(40)-C(35)-C(36)-C(37)	-4.8(4)
P(2)-C(35)-C(36)-C(37)	177.2(2)
C(40)-C(35)-C(36)-C(41)	174.5(3)
P(2)-C(35)-C(36)-C(41)	-3.5(3)

C(35)-C(36)-C(37)-C(38)	3.3(4)
C(41)-C(36)-C(37)-C(38)	-176.0(3)
C(36)-C(37)-C(38)-C(39)	1.1(5)
C(37)-C(38)-C(39)-C(40)	-3.9(5)
C(36)-C(35)-C(40)-C(39)	2.0(4)
P(2)-C(35)-C(40)-C(39)	180.0(2)
C(38)-C(39)-C(40)-C(35)	2.4(5)
C(42)-N(3)-C(41)-C(36)	178.2(3)
C(37)-C(36)-C(41)-N(3)	2.6(4)
C(35)-C(36)-C(41)-N(3)	-176.7(3)
C(41)-N(3)-C(42)-C(43)	-118.4(3)
C(41)-N(3)-C(42)-C(44)	115.8(3)
C(48)-N(4)-C(43)-O(5)	-7.5(5)
C(48)-N(4)-C(43)-C(42)	171.1(3)
N(3)-C(42)-C(43)-O(5)	-67.3(4)
C(44)-C(42)-C(43)-O(5)	57.4(5)
N(3)-C(42)-C(43)-N(4)	114.1(3)
C(44)-C(42)-C(43)-N(4)	-121.2(3)
N(3)-C(42)-C(44)-C(45)	175.9(3)
C(43)-C(42)-C(44)-C(45)	53.4(4)
N(3)-C(42)-C(44)-C(46)	52.1(4)
C(43)-C(42)-C(44)-C(46)	-70.4(4)
N(3)-C(42)-C(44)-C(47)	-68.0(4)

C(43)-C(42)-C(44)-C(47)	169.5(3)
C(43)-N(4)-C(48)-C(49)	-141.3(3)
C(43)-N(4)-C(48)-C(53)	38.8(5)
C(53)-C(48)-C(49)-C(50)	-1.9(6)
N(4)-C(48)-C(49)-C(50)	178.2(3)
C(48)-C(49)-C(50)-C(51)	1.0(6)
C(54)-O(6)-C(51)-C(52)	-171.6(4)
C(54)-O(6)-C(51)-C(50)	9.0(6)
C(49)-C(50)-C(51)-O(6)	-179.5(4)
C(49)-C(50)-C(51)-C(52)	1.1(6)
O(6)-C(51)-C(52)-C(53)	178.1(4)
C(50)-C(51)-C(52)-C(53)	-2.4(6)
C(51)-C(52)-C(53)-C(48)	1.6(6)
C(49)-C(48)-C(53)-C(52)	0.6(5)
N(4)-C(48)-C(53)-C(52)	-179.5(3)
C(35)-P(2)-C(55)-C(56)	75.4(3)
C(61)-P(2)-C(55)-C(56)	-32.0(3)
Ag(1)-P(2)-C(55)-C(56)	-160.8(3)
C(35)-P(2)-C(55)-C(60)	-104.4(3)
C(61)-P(2)-C(55)-C(60)	148.1(3)
Ag(1)-P(2)-C(55)-C(60)	19.3(3)
C(60)-C(55)-C(56)-C(57)	0.0(5)
P(2)-C(55)-C(56)-C(57)	-179.8(3)

C(55)-C(56)-C(57)-C(58)	0.9(6)
C(56)-C(57)-C(58)-C(59)	-2.1(7)
C(57)-C(58)-C(59)-C(60)	2.4(7)
C(58)-C(59)-C(60)-C(55)	-1.4(7)
C(56)-C(55)-C(60)-C(59)	0.2(6)
P(2)-C(55)-C(60)-C(59)	-180.0(3)
C(55)-P(2)-C(61)-C(62)	83.8(3)
C(35)-P(2)-C(61)-C(62)	-24.9(3)
Ag(1)-P(2)-C(61)-C(62)	-147.5(2)
C(55)-P(2)-C(61)-C(66)	-97.4(2)
C(35)-P(2)-C(61)-C(66)	154.0(2)
Ag(1)-P(2)-C(61)-C(66)	31.3(3)
C(66)-C(61)-C(62)-C(63)	0.5(5)
P(2)-C(61)-C(62)-C(63)	179.3(3)
C(61)-C(62)-C(63)-C(64)	-0.2(6)
C(62)-C(63)-C(64)-C(65)	-0.3(6)
C(63)-C(64)-C(65)-C(66)	0.6(6)
C(62)-C(61)-C(66)-C(65)	-0.2(5)
P(2)-C(61)-C(66)-C(65)	-179.1(3)
C(64)-C(65)-C(66)-C(61)	-0.4(5)
C(3S)-O(1S)-C(2S)-C(1S)	-177.3(10)
C(2S)-O(1S)-C(3S)-C(4S)	175.0(12)

Symmetry transformations used to generate equivalent atoms:

Table 7. Hydrogen bonds for bc106 [Å and °]

D-H...A	d(D-H)	d(H...A)	d(D...A)	<(DHA)
N(2)-H(2)...O(2)	0.88	2.14	2.958(3)	155.2
N(4)-H(4)...O(1)	0.88	2.02	2.897(3)	173.4

Symmetry transformations used to generate equivalent atoms: